PROCEEDINGS OF THE THIRTEENTH ARCTIC AND MARINE OIL SPILL PROGRAM TECHNICAL SEMINAR

COMPTE RENDU: 13e COLLOQUE TECHNIQUE DU PROGRAMME DE LUTTE CONTRE LES DÉVERSEMENTS D'HYDROCARBURES EN MER ET DANS L'ARCTIQUE (AMOP)

JUNE 6-8, 1990
EDMONTON, ALBERTA

DU 6 AU 8 JUIN 1990
EDMONTON (ALBERTA)

Environment Canada
Environnement Canada

Canada

PROCEEDINGS

Thirteenth Arctic and Marine Oilspill Program Technical Seminar

June 6-8, 1990
Chateau Lacombe
Edmonton, Alberta

Seminar sponsored by

Technology Development Branch
Environmental Protection
Conservation and Protection
Environment Canada

COMPTES RENDUS

Treizième colloque technique de lutte contre les déversements d'hydrocarbures dans l'arctique

6 au 8 juin, 1990
Chateau Lacombe
Edmonton (Alberta)

Colloque commandité par

Direction du développement technologique
Protection de l'environnement
Conservation et Protection
Environnement Canada

90-05340/

© Minister of Supply and Services Canada 1990
Catalogue No. En 40-11/5-1990
ISBN 0-662-57535-0
BEAUREGARD PRINTERS LIMITED

© Ministre des Approvisionnements et Services Canada 1990
No de catalogue En 40-11/5/1990
ISBN 0-662-57535-0
IMPRIMERIE BEAUREGARD LIMITÉE

NOTICE

The materials and information contained herein are published in the exact form as presented to the sponsors by the conference speakers. Any statements or views presented here are totally those of the speakers and are neither condoned nor rejected by the sponsors. Mention of trade names or commercial products does not consitute endorsement or recommendation for use.

Inquiries related to the technical content of papers in this seminar should be directed to the author(s). Inquiries related to the **Arctic and Marine Oilspill Program Technical Seminar** in general should be directed to:

Technology Development
Branch
Environmental Protection
Conservation and
Protection
Environment Canada
Ottawa, Ontario
K1A 0H3

Phone: (613) 991-1956

Cover Photograph
- Oil slicks in Prince William Sound, April 1990
- photo courtesy of Exxon Corporation.

AVIS

Les textes et renseignements contenus dans le présent rapport sont publiés tels qu'ils ont été présentés par les conférenciers à l'occasion de la conférence. Toutes les déclarations et opinions paraissant dans ce rapport sont celles des conférenciers; elles ne sont ni approuvées ni rejetées par les organisateurs. La mention de marques de commerce ou de produits commercialisés ne constitut ni une approbation ni une recommandation d'emploi.

Toute demande d'information relativement au contenu des conférences devra être faite directement aux auteurs concernés. Toutefois, les demandes relatives au **Colloque technique de lutte contre les déversement d'hydrocarbures dans l'artique** devraient être adressées à:

Direction du
développement
technologique
Protection de
l'environnement
Conservation et protection
Environnement Canada
Ottawa, Ontario
K1A 0H3

Tél: (613) 991-1956

Photographie de la couverture - Nappe de pétrole à Prince William Sound, avril 1990
- gracieuseté d'Exxon Corporation.

TABLE OF CONTENTS
CONTENTS/MATIÈRES

PAGE

SESSION I — *Behaviour and Fate of Oil*

Propriétés physiques et chimiques déversées et comportement des hydrocarbures déversés

MEASUREMENT OF LARGE SCALE OIL SPILL BURNS — 1

D. Evans, W. Walton, H. Baum, R. Lawson *et al.*
National Institute for Standards and Technology
Gaithersburg, Maryland

A SIMULATION OF BUBBLE FORMATION DURING AN UNDERSEA OILWELL BLOWOUT — 39

J.D. Bugg and R.D. Rowe
University of Calgary
Calgary, Alberta

LONG-TERM WEATHERING OF HEAVY CRUDE OILS: EXPERIMENTAL MEASUREMENTS AND DEVELOPMENT OF MODELS — 49

S.C. Lee, W.Y. Shiu and D. Mackay
University of Toronto
Toronto, Ontario

THE EFFECTIVENESS OF FERROCENE IN REDUCING SMOKE EMISSION FROM BURNING CRUDE OIL — 75

J.B. Mitchell
University of Western Ontario
London, Ontario

A STUDY OF THE FORMATION OF WATER-IN-OIL EMULSIONS — 87

M.A. Bobra
Consultchem
Ottawa, Ontario

PAGE

CHARACTERIZATION OF CRUDE OILS FOR ENVIRONMENTAL PURPOSES 119

P.S. Daling and P.J. Brandvik
SINTEF - Group
Trondheim, Norway

D. Mackay
University of Toronto
Toronto, Ontario

MODELLING THE SPREAD OF OIL SPILLS IN ICE-INFESTED WATERS 139

S. Venkatesh
Atmospheric Environment Service
Downsview, Ontario

H. El-Tahan, G. Comfort and R. Abdelnour
Arctec Canada
Kanata, Ontario

AN INTERACTIVE OIL SPILL TRAJECTORY MODEL FOR ALASKAN WATERS 157

R.P. Britch and N.C. Shi
ENSR Consulting and Engineering
Anchorage, Alaska

NATURAL RECOVERY OF COLD WATER MARINE ENVIRONMENTS AFTER AN OIL SPILL 173

J.M. Baker
Shrewsbury, England

P.F. Kingston and R.H. Jenkins
Heriot Watt University
Edinburgh, Scotland

R.B. Clark
University of Newcastle upon Tyne
Newcastle upon Tyne, England

SESSION II ***Biological Fate and Effects***

Effets et incidences biologiques

SUMMARY OF THE ENVIRONMENTAL EFFECTS OF THE *ANTONIO GRAMSCI* OIL SPILL IN THE GULF OF FINLAND IN 1987 179

J-P Hirvi
National Board of Waters and Environment
Helsinki, Finland

PAGE

A STANDARDIZED APPROACH TO THE ECOLOGICAL MONITORING OF OIL SPILLS 197

C.J. Dobroski and R.B. Bogardus
Roy F. Weston Inc.
West Chester, Pennsylvania

EFFECT OF EXTERNALLY-APPLIED BUNKER FUEL ON BODY MASS, BODY TEMPERATURES, PLASMA CONCENTRATION AND WATER FLUX OF GLAUCOUS-WINGED GULLS, LARUS GLAUCESCENS 219

M.R. Hughes, C. Kassera and B.R. Thomas
University of British Columbia
Vancouver, B.C.

SESSION III ***Recent Spills and Spill Activities***
Déversements survenus dernièrement et expériences récentes

RISK ASSESSMENT OF OFFSHORE OIL SPILLS 231

R.P. Labelle
Minerals Management Service
Washington, D.C.

STATISTICAL EXPERIMENTAL DESIGN OPTIMIZATION OF DISPERSANT'S PERFORMANCE 243

P.J. Brandvik and P.S. Daling
SINTEF - Group
Trondheim, Norway

EMULSION FORMATION IN DISPERSANT-TREATED CRUDE OIL 255

H.M. Brown, D.K. Weiss and R.H. Goodman
Esso Resources
Calgary, Alberta

STUDY OF OIL SPILL DISPERSANTS - EFFECTIVENESS AND PHYSICAL STUDIES 265

M.F. Fingas, B. Kolakowski and G. Stoodley
Environment Canada
Ottawa, Ontario

PAGE

SESSION IV *Countermeasures*

Techniques d'intervention en cas de déversement

AIR JET ATOMIZATION AND BURNING OF OIL SLICKS 289

R. Belore and C. Seeley
S.L. Ross Environmental Research
Ottawa, Ontario

CONTAINED CONTROLLED BURNING OF SPILLED OIL DURING THE *EXXON VALDEZ* SPILL 305

A.A. Allen
Spiltec
Anchorage, Alaska

SESSION V *Remote Sensing and Spill Tracking*

Repérage et télédétection

IMPROVED AIRBORNE LASER FLUOROSENSOR FOR ASSESSMENT OF MARINE POLLUTION 315

R. Dick, R. Jackson, F. Kuja, A. Loveless, M. Paul and S. Wiles
Barringer Research
Toronto, Ontario

FIELD TEST OF SATELLITE-POSITIONED DRIFTERS FOR OIL SPILL SIMULATION AND TRACKING 329

M. Reed, C. Turner, A. Odulo and T. Isaji
Applied Science Associates
Narragansett, Rhode Island

REMOTE SENSING OF OIL SPILLS 361

M.F. Fingas
Environment Canada
Ottawa, Ontario

PAGE

SESSION VI ***Shoreline Cleanup***
Nettoyage du rivage

BIOLOGICAL REMEDIATION OF SHORELINE OILY WASTE FROM MARINE SPILLS 387

P. Labrie
Ultramar Canada
Montreal, Quebec

B. Cyr
Biogenie Inc
Montreal, Quebec

STRANDED OIL PERSISTENCE IN COLD CLIMATES 401

B. Humphrey
Seakem
Sydney, B.C.

E.H. Owens
Woodward-Clyde Consultants
Seattle, Washington

G. Sergy
Environment Canada
Edmonton, Alberta

SESSION VIa ***Special Session - Shoreline Cleanup Following the EXXON VALDEZ Spill***
Séance spéciale - Nettoyage du rivage suivi du déversement d'EXXON VALDEZ

SHORELINE CLEANUP FOLLOWING THE *EXXON VALDEZ* OIL SPILL - FIELD DATA COLLECTION AND THE S.C.A.T. PROGRAM 411

E. Owens
Woodward-Clyde Consultants
Seattle, Washington

A. Teal
Exxon
Anchorage, Alaska

SHORELINE CLEANUP FOLLOWING THE *EXXON VALDEZ* OIL SPILL - THE DECISION PROCESS FOR SHORELINE CLEANUP 423

A. Teal
Exxon
Anchorage, Alaska

SHORELINE CLEAN-UP TECHNIQUES: *EXXON VALDEZ* OPERATIONS 431

S.A. Nauman
Exxon
Anchorage, Alaska

PAGE

SUGGESTED IMPROVEMENTS TO OIL SPILL RESPONSE PLANNING FOLLOWING THE *NESTUCCA* AND *EXXON VALDEZ* INCIDENTS 439

E.H. Owens
Woodward-Clyde Consultants
Seattle, Washington

A BRIEF OVERVIEW AND INITIAL RESULTS FROM THE WINTER SHORELINE MONITORING PROGRAM FOLLOWING THE *EXXON VALDEZ* INCIDENT 451

E.H. Owens
Woodward-Clyde Consultants
Seattle, Washington

A. Teal
Exxon
Anchorage, Alaska

Poster Session Abstracts

Résumés de la séances d'affichage

THE UNITED NATIONS "GESAMP" REVIEW OF IMPACT OF OIL ON THE MARINE ENVIRONMENT: CURRENT PROGRESS 471

P.G. Wells
Environment Canada
Dartmouth, Nova Scotia

A STUDY OF THE UNDERWATER DISCHARGES OF CRUDE OIL AND GAS 473

R.J. Palczynski
Acadia University
Wolfville, Nova Scotia

General Session

Séance d'information générale

THE *EXXON VALDEZ* INCIDENT - ONE YEAR LATER 475

R.H. Goodman
Esso Resources Canada
Calgary, Alberta

REMOTE SENSING - WHAT DO YOU REALLY NEED 479

R.H. Goodman
Esso Resources Canada
Calgary, Alberta

Measurement of Large Scale Oil Spill Burns

D. Evans, W. Walton, H. Baum, R. Lawson, R. Rehm, R. Harris
National Institute of Standards and Technology
Gaithersburg, Maryland

A. Ghoniem
Massachusetts Institute of Technology
Cambridge, Massachusetts

J. Holland
Consultant
Wheaton, Maryland

ABSTRACT

Research has shown that burning can be an effective means to remove oil from the surface of the water. The combustion characteristics of crude oil have been measured in large laboratory tests using a nominal one meter diameter pool fire. This work reports on progress mid-way through a 2½ year research program. The objective of this research is to develop measurement equipment and calculations that can be used to characterize oil spill burning at operational scale during field trials of the technology. Field scale measurement techniques for fire radiation, smoke yield, particulate sampling, plume trajectory are described. Progress in the calculation of particulate deposition downwind of the burn site is presented.

INTRODUCTION

Response to oil spills includes considerations of oil containment, recovery, disposal and the logistics of delivering adequate response equipment quickly to the spill site. Particularly in remote areas, the use of burning as a oil spill response method is attractive. Burning requires a minimum of equipment, and because the oil is gasified during combustion, the need for physical collection, storage, and transport of recovered product is reduced to the few percent of the original spill volume that remains as residue after burning. The technology of oil spill burning and other response methods have been reviewed recently [1, 2, 3].

The technology of greatest interest is that designed to burn oil in-place. Present work is directed at burning spills under natural confinement such as within ice leads or with artificial confinement within fire-proof collection booms. Using the latter approach, approximately 15,000 gallons of oil from the recent Exxon Valdez spill were confined after nearly two days in the water and burned. The resulting fire lasting approximately 45 minutes consumed all but 300 gallons of residue that remained in the boom [4].

Burning oil spills in-place normally produces a visible smoke plume containing soot and other combustion products produced in the burning. The smoke plume produced by burning of crude oil spills and the possibility of undesirable combustion products carried in the plume have led to public concerns over the effects of burning large crude oil spills. Lack of knowledge about heat and radiation from large fires has also hampered application of burning to oil spills because of unresolved questions of personnel and equipment safety.

Burning may be thought of as an emerging technology for response to oil spills. The National Institute of Standards and Technology (NIST) is the U.S. National laboratory with the mission to aid industry in the development of new methods to improve productivity. In the area of technology for oil spill response, this includes providing the means to answer public concerns about the consequences of burning to provide a basis for evaluation of its use by industry. Under funding from the Minerals Management Service, U.S. Department of the Interior, with contributions from the United States Coast Guard, U.S. Department of Transportation, and unique technical assistance from the Technology Development and Technical Services Branch of Environment Canada, NIST has carried on a program of oil spill burning research since 1985.

BACKGROUND

In the five year research program, specialized large laboratory scale fire facilities at NIST have been used to investigate the fire dynamics and chemistry of the oil spill burning process. These studies have provided new quantitative information about the crude oil burning process. For example, laboratory measurements [5] have shown that the soot yield, the mass fraction of oil converted to soot during burning, is nominally 10 percent based on tests with Alberta Sweet crude oil. Other technical results about burning rate and combustion products are contained in previous papers [5, 6, 7, 8].

As with any large natural or accidental event that may impact the environment, opportunities to observe and measure the effects of large fires during emergency conditions are rare. Furthermore, permits to conduct large scale experiments that simulate oil spill burns at the appropriate scale and the large amount of funding needed to perform measurements at field scale are difficult to obtain. At best only infrequent opportunities will be available. Anticipating the sparsity of large scale test data, advanced calculations of plume dynamics have been part of the NIST research program since the beginning. These calculations provide a means to extrapolate laboratory measurements of burning conditions and combustion products through predictions of visible plume trajectory and deposition of products downwind of postulated large oil spill burns. Simply, these methods under development in the NIST research program will provide a means to perform hundreds of calculational experiments to add to the available experience from actual field tests. Examples of progress in the development of these calculation methods are contained in previous papers [5, 6, 7, 8].

The large accidental spill of crude oil from the tanker Exxon Valdez in Prince William Sound, Alaska focused national attention on oil spill response technology. In cooperation with a team of interested parties from industry and government planning has begun for operational tests of burning on an experimental oil spill at sea in 1991. In preparation for these tests, the NIST research program was expanded to develop means to measure the burning characteristic of these large fires. To accomplish this task, work was started to make laboratory methods and equipment used in previous studies at NIST robust enough for use in the field. In some cases, completely new measurement techniques were required because laboratory methods were inappropriate for field use or the measurements, such as plume trajectory, are only appropriate to large scale. This paper details the plans and progress to date in a 2½ year research program to move measurement of oil spill burning characteristics from the laboratory to the field using mid-scale 10 m to 15 m diameter fire tests to prove performance of the measurement equipment.

Mid-Scale Testing

As important to this research program as the eventual field tests, mid-scale tests will be performed to evaluate measurement techniques and provide personnel with the opportunity to gain working experience in the environment around large crude oil fires. As part of the interagency cooperation in this project, mid-scale tests are being planned for the summer of 1990 at the U.S. Coast Guard Fire and Safety Test Detachment located on Sand Island in Mobile Bay Alabama.

At this facility, oil pool fires up to 15 m in diameter can be burned in a tank welded to the deck of a 150 m surplus tanker which is used for fire testing. The tanker is moored in a lagoon of a 50 acre island in Mobile Bay, see Figure 1. As the ship is used routinely for fire testing, utilities and some measurement equipment are available on site.

MEASUREMENT PROGRAM

Fire Heat Release Rate (Burning Rate) History

Heat release rate is the primary burning characteristic of a fire. In the laboratory, oxygen consumption calorimetry [9] has been used to evaluate crude oil fire heat release rates [5, 6, 7,]. Estimations of heat release rate can be made also by multiplying the heat of combustion for a fuel times the mass loss rate. In the laboratory, mass loss rate can be determined easily by weighing the fuel.

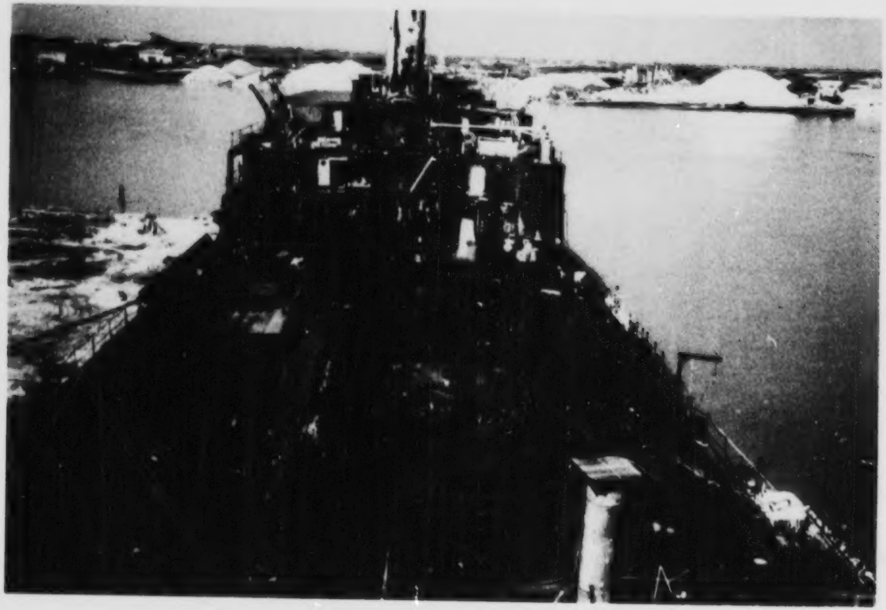

Figure 1 USCG fire test facility Mobile, Alabama.

In the field, there are no direct measurements for fire heat release rate. In a previous large scale oil burn test, [4] the average fuel consumption rate has been estimated by dividing the total mass of fuel consumed by the burning time. In that burn, 15,000 gallons of North Slope crude oil were consumed during 45 minutes of vigorous burning. The average fuel consumption rate during the vigorous burning was 330 gallons per minute. Thus, even in field burns the average burning rate is easily obtained if the amount of fuel consumed is known; and this average may be all that is needed when the fire is nominally constant in burning rate.

When the burning rate is not constant, more than an average rate is needed to characterize the combustion. It is possible that a technique can be developed for field use that uses measurements of surface thermal radiation, smoke plume trajectory, and burning area to calculate instantaneous fire heat release rate. Such a method will be developed and evaluated in mid-scale testing by correlating measurements of several fire diameters. Use of these correlations at field scale will be an extrapolation of the data beyond that correlated but within the same order of magnitude as the mid-scale tests.

Laboratory measurements of crude oil burning in pools up to 1.2 m in diameter have shown two distinct regions of burning, see Figure 2. After ignition there is a quiescent burning period with slightly decreasing heat release rate reflecting preferential depletion of high vapor pressure components from the fuel. The surface temperature of the burning oil maintains a temperature in the range of 250 to 350 °C. The hot oil below the burning surface eventually comes in contact with the water on which the oil is floating. In small scale tests with thick initial oil layers, the water boils, releasing vapor bubbles that burst at the surface and eject oil droplets into the flame. The increased flux of fuel causes the flame to flare up increasing the rate of heat release until extinction. In laboratory tests, Figure 2, the enhancement in burning rate by water boiling can be more than a factor of two. In large burns within booms being towed through the water [4] and large hydrocarbon pool fire tests conducted in Japan [10] enhanced burning due to water sublayer boiling has not been seen. There are two completely different mechanisms that could account for these observations.

In the case of oil burning while being moved over the water within a fire resistant confinement boom, ambient temperature water is continually being supplied below the oil layer. Thus, depending on the tow speed and current, the residence time for the burning oil over a given water mass may be insufficient to induce boiling. Figure 3 shows a schematic diagram of a laboratory apparatus built to measure oil burning characteristics under conditions simulating field conditions in which a contained burning oil mass is being moved on the water surface. For convenience, in this simulation the confined burning oil is kept stationary; and the water is flowed beneath it at selected speeds. Testing with this apparatus will provide insight into the effect of moving water layers on oil burning rate and residue remaining at flame extinction.

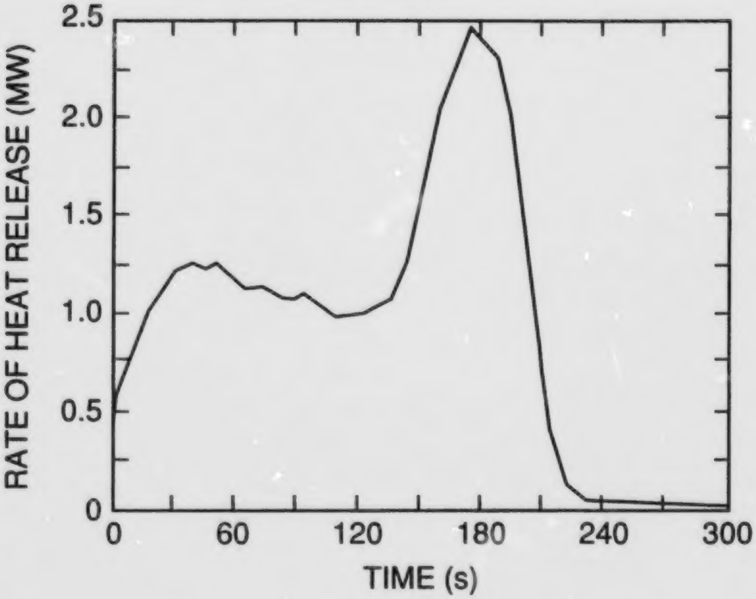

Figure 2 Measured heat release rate for 1.2 m diameter Alberta Sweet crude oil fire.

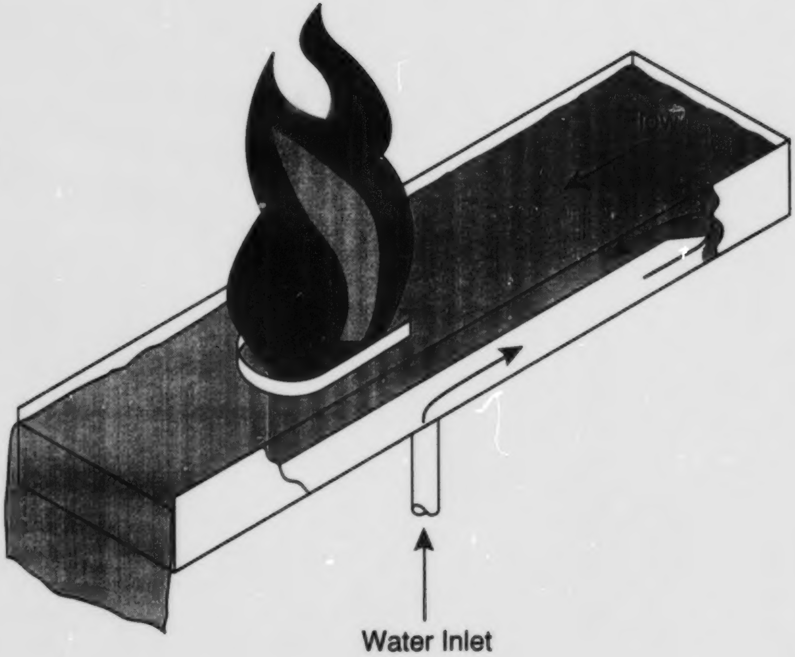

Figure 3 Schematic of boom simulation oil burning apparatus.

Maintaining a flow of cool water beneath the burning oil is only one factor in determining the conditions under which water sublayer boiling will occur during large scale burns in booms being towed through the water. Experiments in Japan at the Fire Research Institute have shown that there is an effect of scale as well. In their work for larger fires in which the fuel layer surface regression rate (or burning rate per unit area) was greater than that measured in smaller laboratory tests, no water sublayer boiling was seen. We postulate that in the larger pool fire tests conducted in Japan, up to 3 m in diameter, the onset of water sublayer boiling occurs when the burning oil layer is very thin. The onset of boiling for the larger scale fires may occur only for very thin layers representing the small depth that heat penetrates into the unburned fuel by thermal conduction from the hot surface because of increased fuel surface regression rate. The stirring of the shallow oil layer by boiling produces a sufficient temperature decrease to quench the burning. Therefore, in a large pool fire with increased burning rate per unit area as compared with small scale tests, the onset of water sublayer boiling produces flame extinction and not vigorous burning.

In field tests, both the large area and motion over the water of the burning oil will provide conditions unfavorable for water sublayer boiling. Mid-scale testing to be performed in this research program will provide greater insight into this effect.

Thermal Radiation

Measurements of thermal radiation from the burning oil are used to predict the potential hazard to personnel and equipment operating near the burn site. Thermal radiation measurements can also be used to predict the burning rate of the fuel. Correlations such as the ones developed by Shokri and Beyler [11] and Mudan and Croce [12] may be used to predict the radiative heat flux at a ground level target a given distance from the pool. These correlations are based primarily on gasoline, kerosene, JP-4 and JP-5 fires. Other large scale fire results which include data for crude oil have been reported by Koseki [10, 13]. Previous tests have shown the average surface emissive power of large sooty fires actually decreases with increasing diameter. This is probably a result of substantial radiation blocking by absorption in the thick black smoke carried around the flame by turbulent mixing. As a result, thermal radiation becomes a complex function of pool diameter. It remains to be seen whether this behavior can be quantified well enough to provide a measurement technique for the burning rate.

Thermal radiation to targets at various distances from the crude oil fires will be measured with Gardon type radiant heat flux gauges. These gauges are used routinely in fire safety research studies. The gauges measure the temperature difference between the center of a thin blackened surface and a thermal sink temperature at the edge. The radiant heat flux to the blackened surface is a function of the temperature difference.

Smoke Sampling

The sampling of smoke for chemical and yield analysis is a relatively easy task in the laboratory. This process consists of using an appropriate filter media such as PTFE with an 0.8 μm pore size for collecting the smoke particulates, a pump for drawing the smoke into the filter, and a constant flow rate controller. The mass of soot is determined by weighing the filter, and the filtered material is analyzed. In the laboratory, the equipment used for sampling can be of any reasonable size and weight, and is usually conveniently located on a test bench near the experiment. However, in the field with large fires, where the appropriate sample point in a smoke cloud may be several hundred feet in the air, this task of sampling becomes quite complex. With the need to sample well above ground level, the size and weight of an experimental package becomes critical. The efficiency of this experimental package takes on additional importance since sampling will be done in a constantly varying environment driven by the local weather conditions. Figure 4 shows the sampling system currently being used in this project. The largest part of this system is the sampling pump which is 15.7 cm long, 4.5 cm in diameter, and weighs 0.79 kg. This lightweight pump is identical to that flown as part of experiments on NASA Space Shuttle missions within the last year. The pump is operated from a simple 12 volt DC battery or power supply, and draws a constant flow rate of 10 liters per minute through a clean 47 mm filter. The filter holder is made of aluminum and is 5.5 cm long, 5.5 cm in diameter and weighs 0.16 kg. Clear plastic tubing is used to connect the system components. Filter media taken from this system during field tests will be returned to the laboratory so that PAH's and other important constituents may be measured.

Soot Production (Soot Yield)

Determinations of mass of soot produced per unit mass of fuel consumed has been done in laboratory tests using two methods [5]: stack particle flux sampling and the carbon balance method. Stack particle flux sampling is based on comparison of the mass of particulates collected from a known portion of the total smoke plume flow from the fire to the measured mass loss of the burning fuel during the same period of time. The carbon balance method determines the soot yield based on ratio of soot mass to the total mass of carbon found (soot plus mass of carbon contained in CO_2 and CO gases) in a sample of smoke plume combustion products. Of these two, only the carbon balance method is feasible for application to large fires.

A third method being investigated is isotopic tagging and tracing of particles by mass spectrometry [14]. This method also has the potential to measure soot deposition far downwind of a smoke source and therefore could be appropriate for use in the planned field tests.

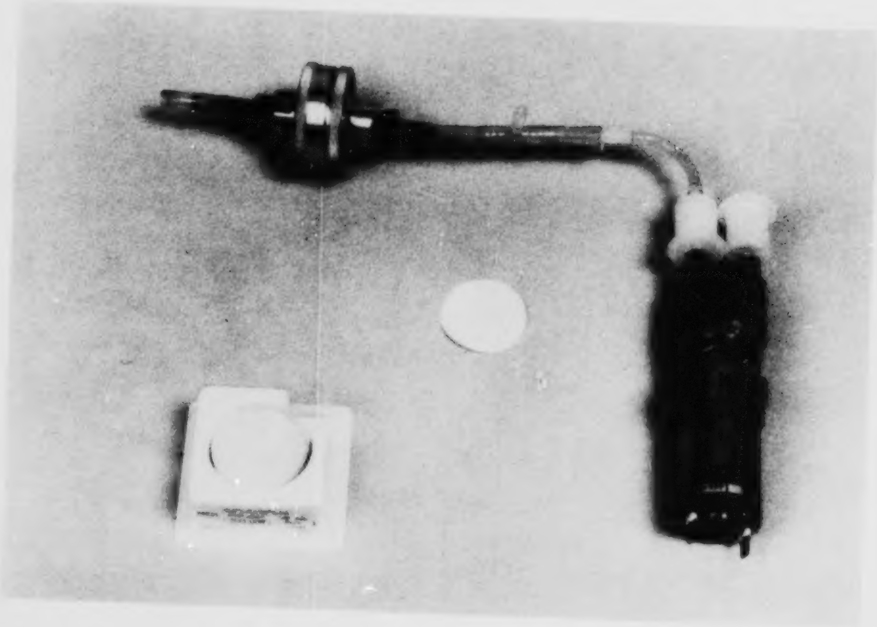

Figure 4 Pump and filter apparatus for smoke sampling.

The isotopic tagging technique involves addition of enriched isotopes of rare-earth elements into the fuel before combustion, and then measuring the perturbations in the natural isotopic ratios in aerosol particles collected downwind. In large scale oil burn tests being planned, particles collected downwind could be identified positively as originating from the oil spill burn and not other sources such as from ship engines. The isotopes used are nontoxic, chemically stable, nonradioactive, and relatively inexpensive, and can be detected with an ultimate sensitivity below 1 part in 10^{15} (mass/mass basis). This rivals or exceeds the sensitivity of the most sensitive inert tracer gases used to study the long-range transport of air masses and represents a more than 40,000-fold reduction in the amount of tracer material needed over previously-used tracer materials.

Since the tracer is added directly to the fuel before burning it is important to know if the tracer is liberated from the fuel during combustion proportionally with the crude oil consumed. Laboratory tests with the 0.6 m diameter pool fire and collection hood and soot sampling instrumentation used in previous studies [5] will be used to evaluate the liberation of the tracer into the combustion products during burning and determine the feasibility of the method for measurement of soot yield from crude oil burns. During these tests soot yield will be determined also by the stack particle flux sampling, a method developed by Mulholland, et al. [15] used in previous testing [5], for comparison with results from the new isotopic method. In these tests only 8 mg of enriched ^{150}Sm will be needed to treat 4 kg of oil needed in the test, a concentration of one part in 500,000. After collection the amount of tracer in the smoke particles will be determined by Inductive-Coupled Plasma Mass Spectrometry (ICP-MS) [14].

Smoke Concentration Measurements by Light Scattering

In order to measure the concentration of smoke in the fire plume rapidly and at many positions a small, light weight light scattering apparatus is being evaluated. The apparatus is shown in Figure 5. It uses a pulsed near-infrared light emitting diode source, a silicon detector, and collimating and filtering optics to sense the light scattered over a forward angle of 45 to 95 degrees by airborne particles passing through a open sensing volume. The airborne particles pass through the sensing chamber as a result of natural air currents. The device can accurately measure concentrations over a range of 0.01 to 100 mg/m^3 with a particle size range up to 10 μm. This instrument measures 10 x 10 x 5 cm and weighs 0.45 kg and is operated by a self-contained rechargeable battery. The meter has an analog output which is connected to a miniature data logger also shown in figure 5 to record measurements during flight. The combined weight of the meter and data logger is 1.05 kg. This meter system will be used at various known locations in the smoke plume with the mid-scale and large scale fire experiments. It is intended for measurement of smoke concentration along the near field plume trajectory.

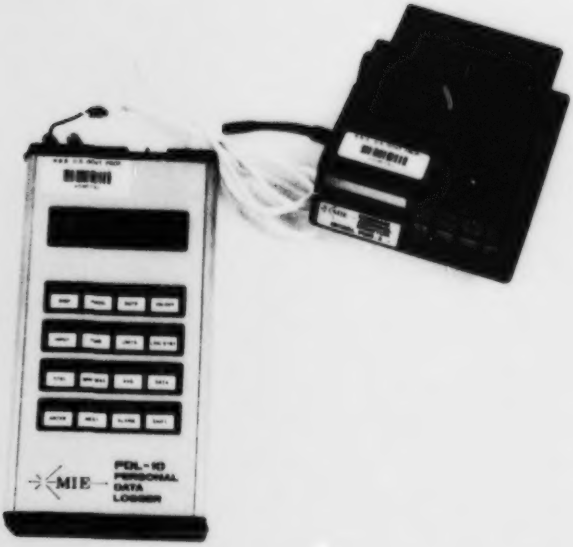

Figure 5 Light scattering apparatus for smoke concentration measurements.

Calibration Experiment

A series of calibration tests were conducted to evaluate smoke concentration measurements made with the light scattering apparatus described in the previous section. Louisiana and North Slope crude oils were used as test materials. The tests were conducted using the ASTM, E662 Smoke Density Chamber (Figure 6) so that the filter samples and the light scattering apparatus results could be evaluated and correlated with standardized optical density (OD) measurements made with the chamber. In addition, reduced data from the tests could be used to compare optical properties of smoke from crude oil with those from other combustibles. All tests were performed without supplemental radiant heating available from electric heating coils in the Smoke Density Chamber. The oils were burned in small crucibles positioned in the chamber at a point where the smoke plume had a clear path to chamber's ceiling. This was done to minimize soot particle deposition on hardware exposed directly to the smoke plume.

Results from the smoke chamber tests showed that smoke concentration measured with the scattering apparatus agreed within 6 percent with concentrations measured by filter collection and weighing, over the range of 55 to 92 mg/m^3. The scattering apparatus as supplied from the manufacturer has a useful measurement range from 0.01 to 100 mg/m^3. By decreasing the sensitivity of the apparatus broader measurement ranges are available. Mid-scale tests together with smoke plume calculations will provide information needed to select the sensitivity range of the scattering apparatus for the field scale tests.

Comparisons of optical density per meter as a function of mass concentration in air of the smoke from the crude oil fires to those of other combustibles are shown in Figure 7. Optical density is a logarithmic measure of light transmittance equal to $\log_{10}(I_0/I)$, where I_0 is the light intensity transmitted without obscuration and I is that for the obscuring sample. The data from both the Louisiana and North Slope crude oils are consistent with the correlation of data generated on a wide range of organic materials tested by King [16] and reported by Seader and Ou [17]. Thus smoke produced from burning crude oil is similar in optical characteristics to other common materials.

INSTRUMENT TRANSPORT AND POSITIONING

In both the mid-scale and field scale crude oil burn tests, measurements are to be made in the smoke plume emitted from the fire. Various means of positioning instruments within the smoke plume have been evaluated. These included: towers, manned aircraft, fixed winged and helicopter remotely piloted aircraft, and balloons or mini-blimps.

In the mid-scale tests, as much instrumentation as possible will be evaluated so that measurement methods of various levels of accuracy and performance may be

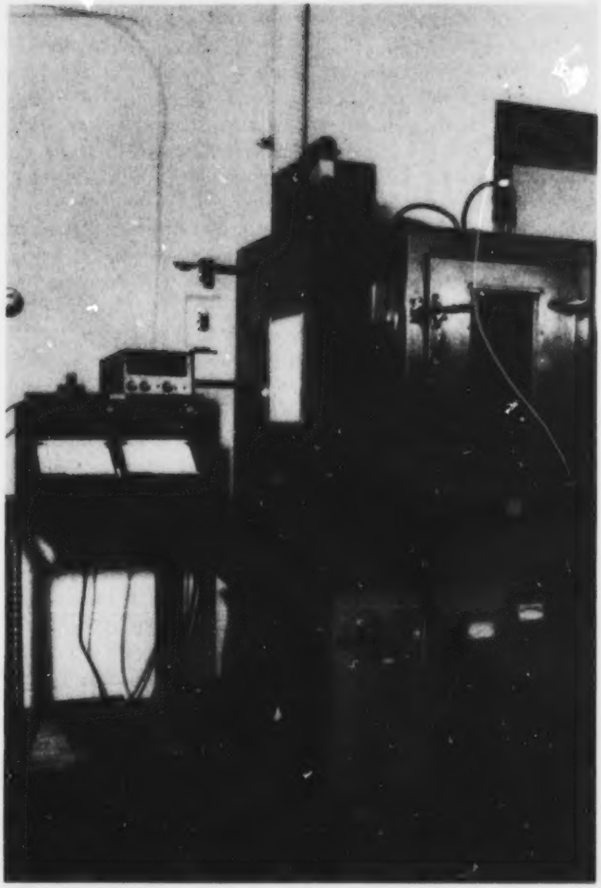

Figure 6 ASTM E662 Smoke Density Chamber.

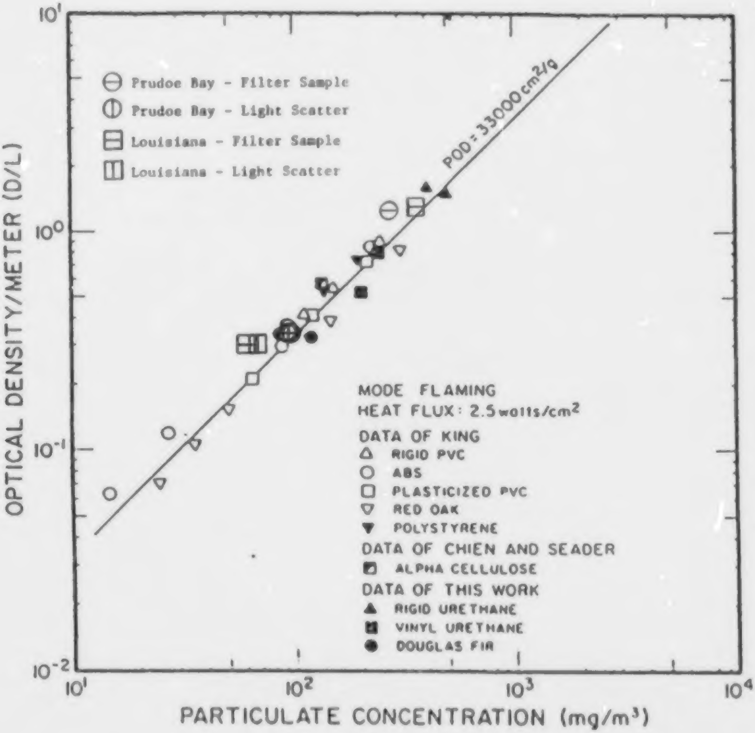

Figure 7 Optical Density versus smoke concentration for crude oils and other materials.

compared. This includes methods used in previous NIST laboratory tests and other field instruments in environmental air sampling.

Towers

Towers of useful height for fire plume measurements must be fixed or guyed for stability. The lack of mobility limits the usefulness of towers for plume measurements except for the area close to the source. Towers are projected for use in the mid-scale tests for mounting instruments near the edge of the crude oil pool and for supporting thermocouple arrays to obtain temperature measurements directly above the burning fuel.

Fixed-wing and Helicopter Remotely Piloted Aircraft

Two remotely piloted aircraft were evaluated for carrying instrument packages and providing video images during the mid-scale and field scales tests. A small light weight plane (Figure 8), developed for military surveillance, carries a black and white television camera and transmitting the video signal to a ground station for recording. The on-board camera is also used by the "pilot" on the ground to fly the craft by viewing a camera monitor. Even though the small aircraft could provide video images from above the fire, this type of support should be available with manned aircraft.

The capabilities of a larger aircraft (Figure 9) that carried a color camera and has capability to transport a 12 kg instrument package with a range of 25 km were examined. This aircraft was judged to be too difficult to launch and recover during the type of testing planned for this project. Also, the flight speed of the plane would severely limit the sampling time at any position. Finally, the large aircraft requires extensive training for the operator to become proficient with the controls for the craft.

A helicopter of the type used routinely by Environment Canada can be used for making measurements during both the mid-scale and field scale tests. This craft (Figure 10) is capable of carrying a video camera and a 9 kg instrument package and can hover at locations to collect samples. As with the large fixed-wing aircraft, operation of the small helicopter requires extensive training. It is planned to use this type of helicopter to gather data on smoke concentration at various positions within the smoke plume from the crude oil fires.

Balloons and Mini-Blimps

A tethered mini-blimp is being evaluated as the primary means of positioning instrumentation for soot collection in the smoke plume. Preliminary control and

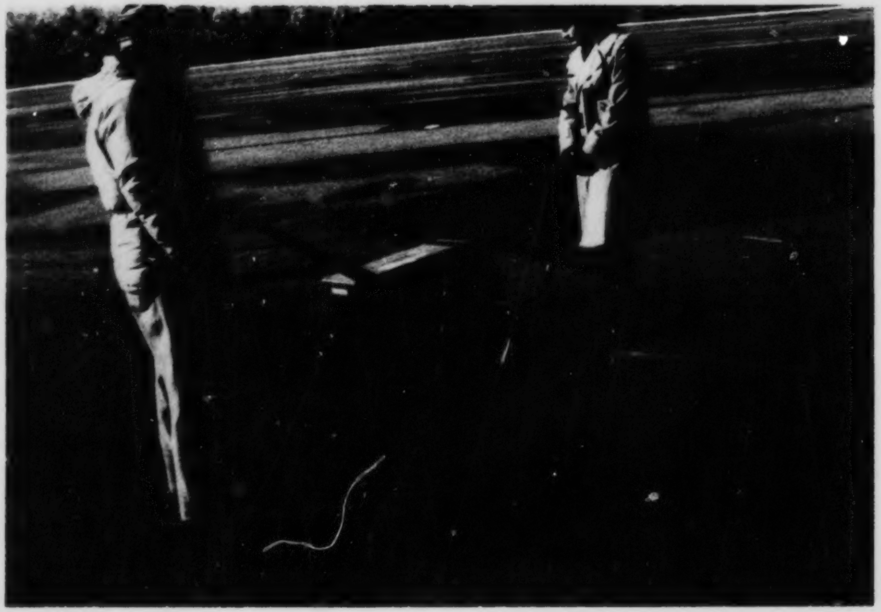

Figure 8 Small remote control aircraft.

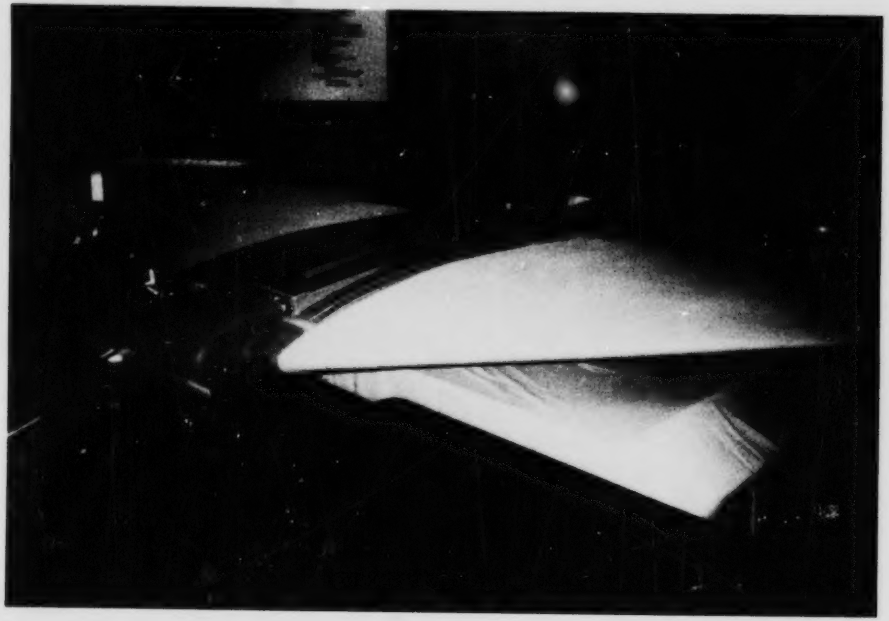

Figure 9 Large remote control aircraft.

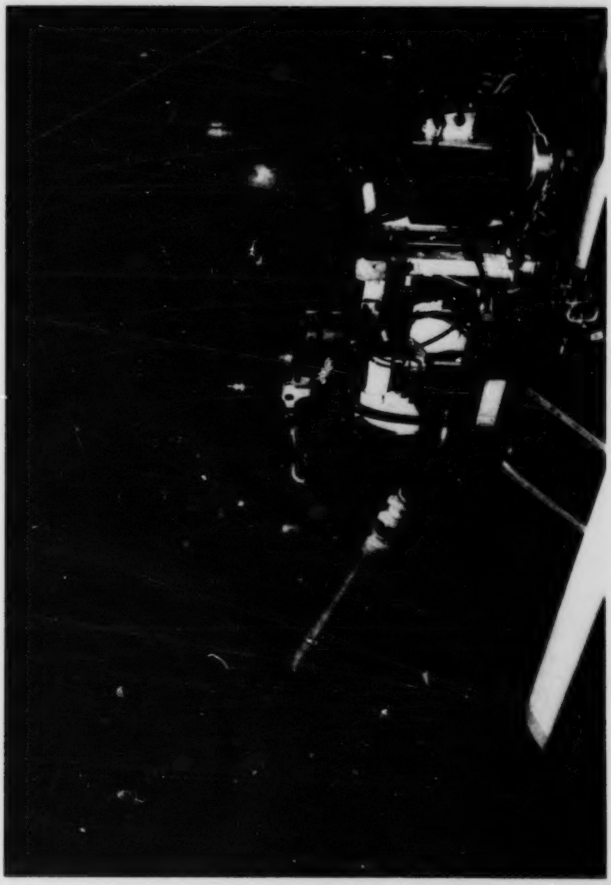

Figure 10 Environment Canada remote control helicopter.

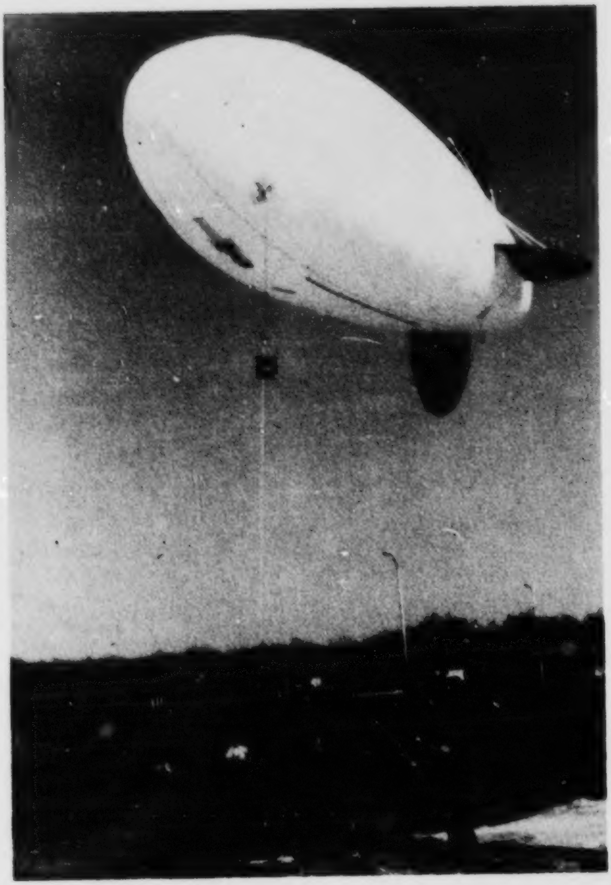

Figure 11 Mini-blimp.

instrument payload tests have been carried out to evaluate operational limits of the blimp, Figure 11. The blimp can carry a 4 kg instrument package to several hundred feet above ground level. It can be readily be moved from one location to another. Launch and recovery procedures are simple, and little time is needed to learn how to safely maneuver the blimp. Mini-blimps will be used in the mid-scale tests for positioning instrumentation packages. Experience in these tests will determine if the system is practical for the field scale tests.

Weather Station

In order to perform calculations on plume dispersion, data on local atmospheric conditions is needed. To measure these condition at the burn site two different types of weather stations have been acquired. One station provides a profile of conditions from the ground to 150 m altitude by transporting it on a tethered weather balloon. This instrument provides information on wind speed, direction, temperature and barometric pressure. At both the mid-scale and field scale tests this weather station will be deployed upwind of the burn site to measure atmospheric profiles prior to tests and continuously at one elevation during the test.

At both the mid-scale and field scale tests, a ground weather station will be deployed just up-wind of the test site. It will provide continuous weather information during the burn. The ground based station provides the same weather data as received from the station aloft.

SMOKE PLUME TRAJECTORY AND PARTICLE SETTLING MODELS

Observations During Mid-Scale Fire Tests

Mid-scale testing is a critical part of the measurement program in this project. In November, the research staff was given the opportunity to attend 15 m diameter pool fire burns of diesel fuel at the Farrier Firefighting Facility at Norfolk, Virginia. These large scale fires provided valuable experience that will be used in the design of practical instrumentation packages and safety plans for future crude oil burns. Observation from the tests are generally instructive and provide a specific case for comparison of classical predictive methods for smoke plume dispersion.

On the day of the tests the wind speed was approximately 3 m/s which is considered near the upper limit for effective measurement in mid-scale tests. This wind has a strong effect on the fire plume down to the base of the 15 m diameter fire (Figure 12a). The smoke moved generally upward and then turned sharply downwind (Figure 12b). The thermal radiation from the fires was such that one

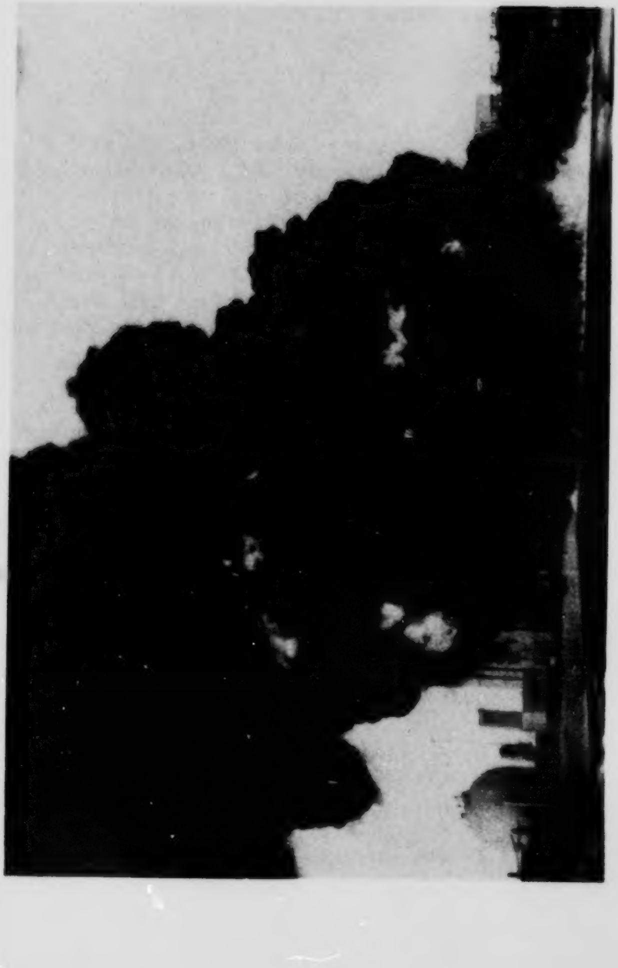

Figure 12a Mid-scale 15 m diameter diesel fuel fire during the first 30 seconds after ignition.

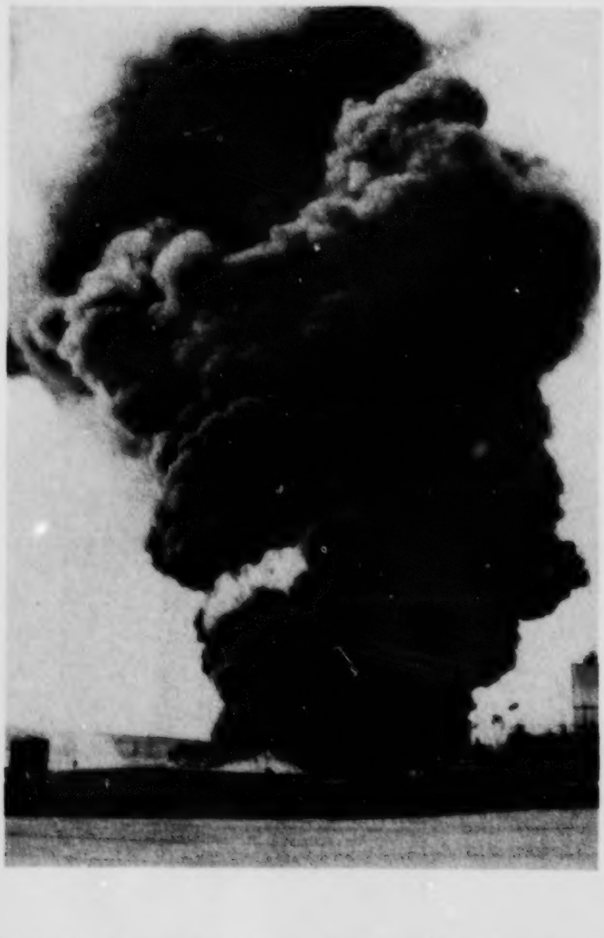

Figure 12b Smoke plume rises and turns downwind during peak burning period.

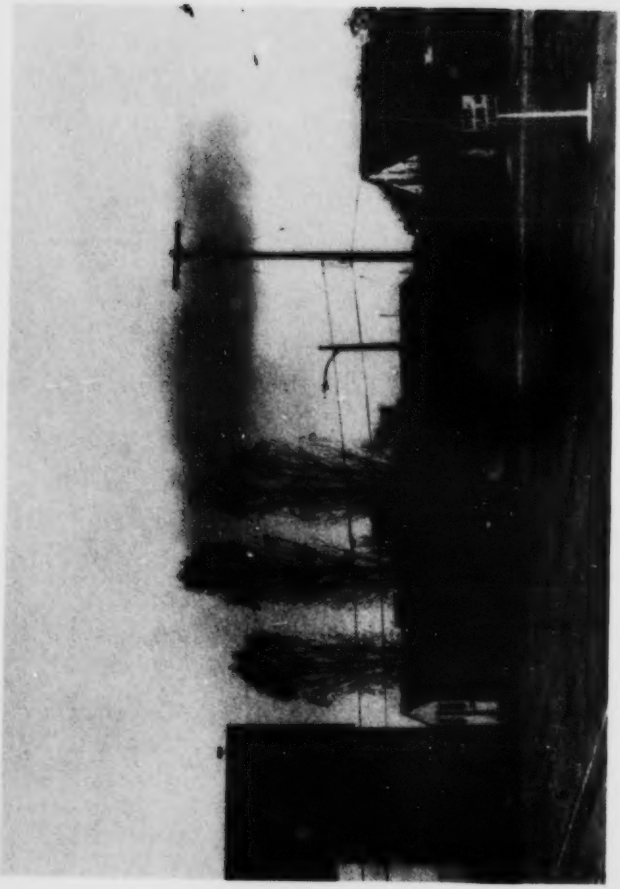

Figure 12c Smoke layer visible downwind 1/2 hour after test.

could easily approach to within approximately 1 to 2 fire diameters without feeling pain on bare skin. Most of the flame was obscured by the smoke. The smoke in the plume directly above the fires was sufficient to obscure the sun. As the smoke traveled away from the fire, it appeared to reach a constant stratification. The smoke was still visible downwind as a well defined cloud nearly a half-hour after the tests were terminated (Figure 12c).

Classical Analysis

Since the mid-1960s plume rise and dispersion from stacks has been an active area of research because of environmental concern about the dispersion of stack gases from manufacturing and power generation facilities [18]. To some extent this technology can be generalized to the dispersion of products from large diameter fires. For one of the 15 m diameter diesel fuel at the Farrier Firefighting Facility at Norfolk Virginia, an analysis of plume rise height, width, and depth as a function of distance from the burn was performed using classical correlations for plume dispersion. The predictions were compared with the video record of the test. The results given below indicate the sensitivity of plume rise height predictions to different assumed atmospheric conditions.

The plume height formulas given by Briggs [18] were used as the basis for the analysis. They are:

$$z_c - 1.6\, F_b^{1/3}\, x^{2/3}\, u^{-1} \tag{1}$$

for the period before atmospheric stability begins to limit plume rise, for example within a neutrally stable mixed layer, and

$$z_c - 2.6 \left(\frac{F_b}{u\ s}\right)^{1/3} \tag{2}$$

for the stabilization level in a stably stratified atmosphere, where

z_c is the height of the center of the cloud;

$F_b = g\, V_o\, (T_o - T_a)/T_o$, with

g = acceleration of gravity = 9.8 ms^{-2},

V_o = volume flux at the source = $\pi\, r_o^2 w_o$,

r_o = radius of plume at the level z_o, r_o taken as 7.5 m,

z_o = is a level where all heat has been added, z_o taken as 7.5 m,

w_0 = vertical velocity at z_0,

T_a = ambient temperature, taken as 286 K,

T_0 = average plume temperature at z_0,

x = distance downwind,

u = mean wind speed, taken as 4 ms^{-1},

$s = g(\partial T_a/\partial Z + \Gamma)/T_a$,

Γ = adiabatic lapse rate = 0.01 Km^{-1}

Determination of many of the values needed in these correlations depended on careful and detailed analysis of the video tape record of the test. At future mid-scale tests efforts will be made to measure as many as possible, but even analysis of near fire plume parameters and plume trajectory will always depend on analysis of video records. Parameters for this calculation were evaluated as follows.

To evaluate w_0 and T_0 a number of sequences of frames of the fires were examined and measurements were made of the coordinates of traceable features of the close-in smoke plume where the width of the pool (15 m) could be used as a scale reference. Two sets of smoke cloud element trajectories were analyzed. During period 1, about 40 seconds in duration immediately after fuel ignition, the fire had not reached full intensity. After 2.5 minutes of burning the fire reached peak intensity. During this period flames were visible up to at least 20 m height. Shortly thereafter the fire was extinguished by hose streams.

Smoothed coordinates (x,z) of cloud elements were calculated by 4-point running means for trajectories on which readings had been taken at intervals of 0.2 s, or 5-point running means for those with intervals less than 0.2 s. Horizontal (u) and vertical (w) velocity components were calculated from the least-squares linear trend in x and z over these same 4- or 5-point data samples. In this way 185 sets of x,z,u and w were obtained.

As parcel trajectories at levels below 7.5 m were significantly influenced by addition of heat, values were estimated for w_0 based on the video data samples above 7.5 m. These were 2.0 m/s for period 1 and 3.5 m/s for period 2. A typical effective flame temperature of 900 K was assumed to be the average at this level for period 2 ("mid-burn") while a more moderate 600 K was assumed for period 1 ("early burn"). These vertical velocities and temperatures are compatible with plume heating rates of the order of 1 and 0.5 MW/m^2 respectively.

The measured average value of u, 2.5 m/s perpendicular to the line of camera sight, for the trajectories above 7.5 m, implies a total speed of 3.5 m/s. This is consistent with the assumed ambient wind speed of 4 m/s based on recorded measurements at nearby weather stations, considering that the horizontal motion of the rising plume may not have been in equilibrium with the horizontal wind at that level.

Values for the stability parameter, s, were inferred from weather observations. Prior to the burn the sky was broken to overcast and as the tests were conducted near the end of November, the solar attitude, even at noon, was only 35° [19]. The wind was coming off the ocean with only a short fetch over land. The ocean and bay temperatures typically are slightly lower than the observed air temperatures,which showed very small diurnal increases of 1 to 3 °C from 10 a.m. to noon, the approximate time of the burn. Upper air soundings recorded by the nearest weather station were nearly isothermal conditions in the lowest kilometer at 7 a.m. and at 7 p.m. a near-adiabatic (neutral) mixed layer up to a height of only 500 m capped by an isothermal layer. Based on these observations, two values of vertical temperature gradient, 0.005 Km^{-1} ("half adiabatic") and zero ("isothermal") were adopted for the analysis to bracket the range of uncertainty in atmospheric conditions.

The calculated and observed smoke cloud heights versus distance from the burn are shown in Figure 13. It is evident that the cloud rise was limited by the stable stratification of the atmosphere.

To estimate cloud width and depth, the graphs of σ_y and σ_z versus distance and Pasquill-Gifford stability category in Turner's [20] manual were used. Following the reasoning above with regard to stability, two Pasquill-Gifford "types" were assumed: D (neutral) and E (slightly stable). Since 95% of the mass of a Gaussian distribution lies within the interval -2σ to $+2\sigma$, $4\sigma_y$ was chosen to estimate the width and $4\sigma_z$ to estimate the vertical depth of the visible cloud. Figures 14 and 15 show these estimates for the distances at which "observed" values were obtained from the videotape for smoke plume width and depth respectively. As with the height estimate, the more stable case fits the smoke cloud characteristics best.

Smoke Concentration

Order of magnitude estimates of smoke mass concentration in the plume downwind of the burn were calculated consistent with the above analysis. Assuming a mass loss rate of 35-40 g/m^2s [12] and 8% of this in the form of smoke [7] the smoke emission rate from the 15 m diameter pool would be about 500 g/s. Using Turner's [20] graphs for σ_y and σ_z versus distance, with the Gaussian distribution model, we can estimate the plume centerline concentration

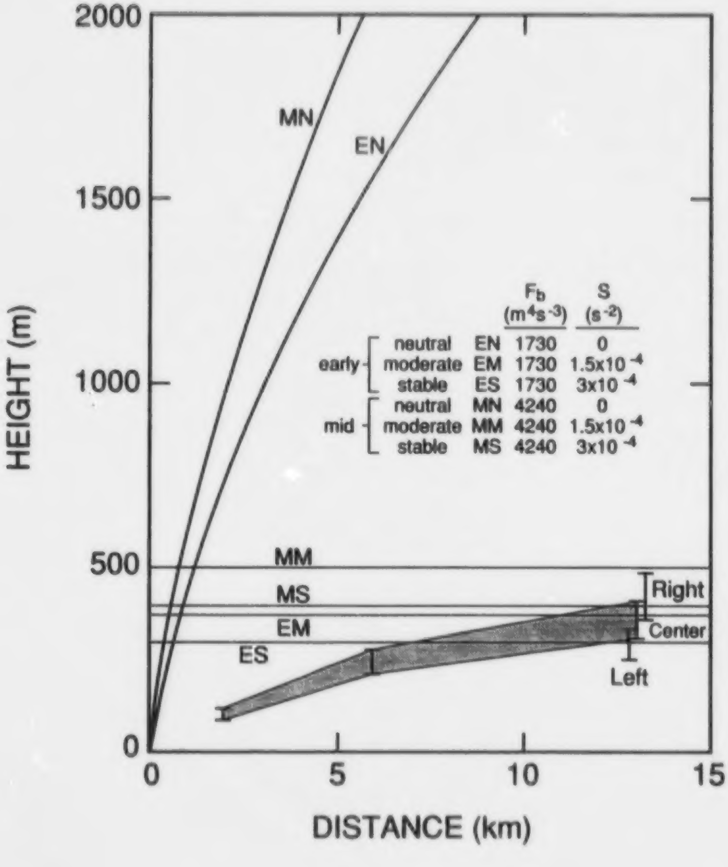

Figure 13 Smoke plume rise height versus distance from the burn.

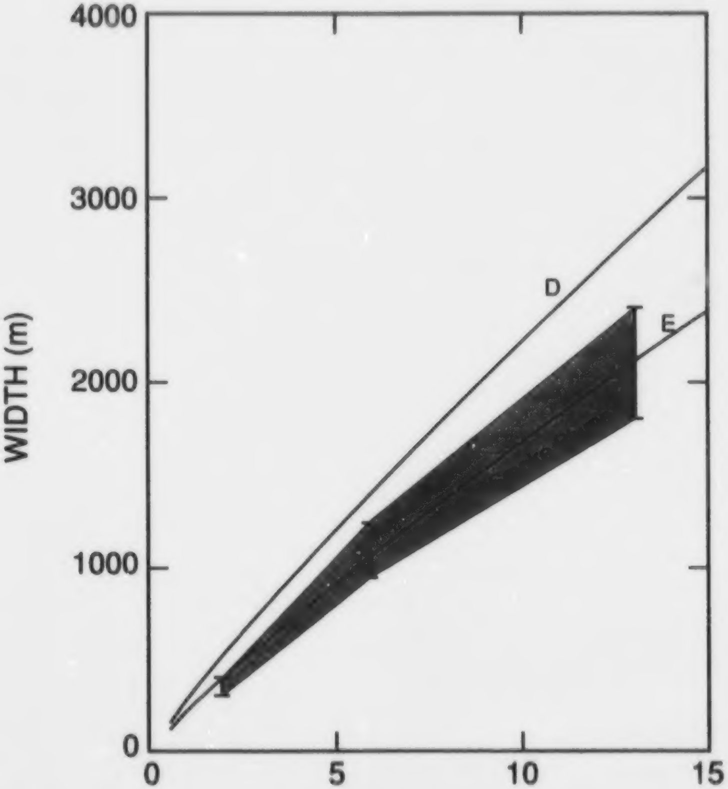

Figure 14 Smoke plume width versus distance from the burn.

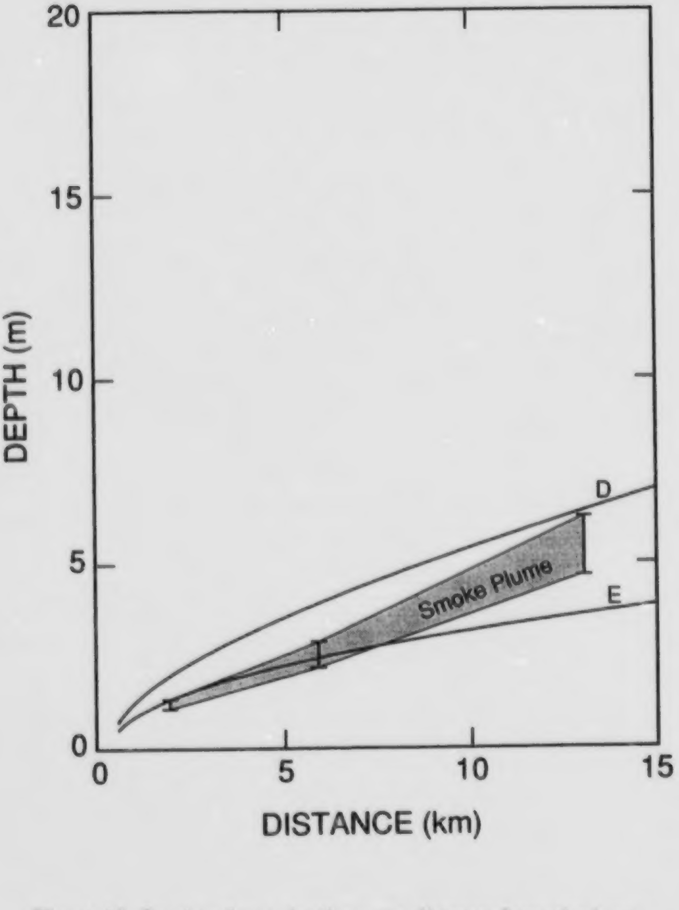

Figure 15 Smoke plume depth versus distance from the burn.

$$C\ (x,H) = Q/\pi\sigma_y\sigma_z u \quad (3)$$

and the ground-level concentration under the plume axis

$$C\ (x,O) = C\ (x,H)\ \exp\ (-H^2/2\sigma_z^2) \quad (4)$$

where

C (x,z) = concentration at distance x and height z,

Q = rate of emission, and

H = plume height

Calculated values for smoke mass concentration in the plume and in the air at ground level are shown in Figure 16 for Q = 500 g/s, H = 400 m and atmospheric stability type E (slightly stable).

For instrument package design, it is also necessary to know the nominal smoke mass concentration in the plume immediately downwind of the burning fuel. Using the same smoke emission rate as above (500 g/s) and a total speed of smoke flow in the plume of 3.5 m/s, from analysis of video data, the smoke concentration in the plume where the diameter is 30 m, (see Figure 12b), is 200 mg/m^3.

In view of the uncertainties and gaps in the available information it should be emphasized that the agreement or overlap between the ranges of observed and calculated parameters does not in itself confirm that the measurements, the assumed conditions, or the models are correct. Further analysis will be made of test records from future mid-scale tests in which more complete measurements particularly of atmospheric conditions will be made to determine the applicability of this model to smoke from crude oil burns.

These results are intended to illustrate the response of smoke transport to particular atmospheric conditions at the time and location of the burn at the Farrier Firefighting Facility at Norfolk, Virginia. Smoke plume dynamics are sensitive to local atmospheric conditions. For example, the temperature inversions typically occurring over Arctic ice surfaces would limit plume rise and vertical spread more severely, while the relatively vigorous convection over tropical waters would enhance buoyant rise and vertical mixing compared to the results obtained at Norfolk, Virginia.

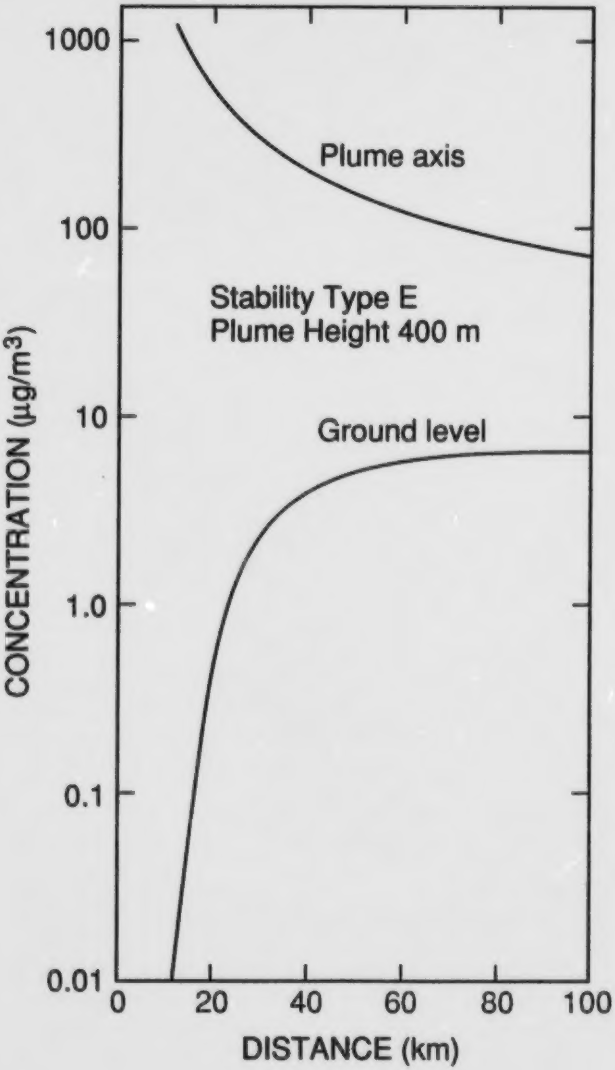

Figure 16 Calculated smoke concentration versus distance from the burn.

Vortex/Transport Element Method

The analysis in the previous section depends on information from experimental correlations of smoke dispersion from many studies. Another method to calculate smoke dispersion has become practical in recent years because of advances in computational methods and hardware. These methods make use of techniques to simulate numerically the turbulent mixing of smoke in the atmosphere.

The smoke plume model described in earlier paper from this research [8] has been implemented using a variant of the vortex element flow simulation technique developed by Ghoniem and his collaborators[21]. This technique, known as the transport element method [22, 23], has been applied to study the dynamics of turbulent shear layers, jets, and wakes. More recently, it has been extended to permit simulation of the Rayleigh-Taylor instability [24], a fundamental problem in gravity-driven flows. The code developed for this latter problem is the starting point for the calculations of the smoke plume settling displayed below. At the current stage of development, simulation capability is limited to consideration of the transport of a negatively buoyant plume of initially circular cross-section. The atmosphere is assumed to be unstratified, and the ambient wind is uniform. The research program currently under way will ultimately remove all of these restrictions.

Even at its current stage of development, the mathematical model exhibits many features of real turbulent mixing which are lost in models which assume prescribed forms for density and/or velocity profiles. These mechanisms are most readily explained by following the sequence of six frames from a simulation illustrated in Figures 17a-f. Each frame consists of a cross-sectional slice through the plume at successive stations downwind from the initial point. The uniform wind is coming out of the plane of the plots toward the viewer. Each curve represents a contour of constant particulate density as computed by the model. The innermost contour in the initial frame (Figure 17a) represents the maximum particulate density, which is then constant across the remainder of the interior. The outermost contour corresponds to zero particulate density. The ground is located at the bottom boundary of each plot. The numbers along the boundaries measure distance in units of the initial density gradient length, ℓ. This length specifies the initial particulate density profiles, ρ_P, as follows:

$$\rho_P = \rho_M \left[\frac{1 - \operatorname{erf}\left(\frac{r-\ell}{L}\right)}{2} \right] \qquad (5)$$

Here, ρ_M is the maximum particulate density, r is the radial coordinate measured from the center of the initial distribution, L is the nominal initial plume radius, and erf denotes the error function. The gradient length is physically significant in understanding the mixing process, as will be explained below.

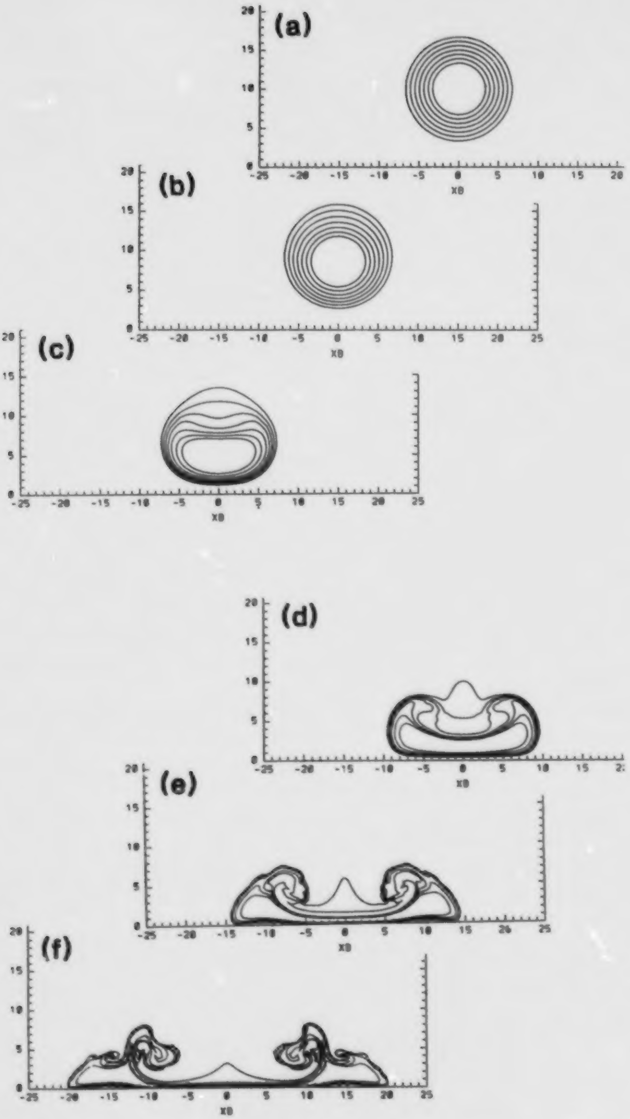

Figure 17 Plume vortex/transport element method output.

Now consider the sequence in detail. The first frame in Figure 17a shows the prescribed initial state of the plume, centered ten units above ground. Since horizontal density gradients induce vorticity fields opposite to the sign of the density gradient, positive vorticity is induced on the right side of the plume, and negative vorticity is induced on the left hand side. No vorticity is initially formed at the top or bottom of the plume. This pattern induces downward velocities everywhere in the plume, accompanied by the slight flattening seen in the second frame, Figure 17b. Note that the entire plume is displaced downward. The overall elliptical shape usually assumed in plume dispersion modeling is present for the first and only time in the simulation. The third frame, Figure 17c, shows the beginnings of the classical horseshoe shape widely observed in windblown plumes, modified by a flattening of the center portion caused by the presence of the ground.

The evolution is followed further in Figure 17d. This frame shows the further flattening of the plume as the opposite signed vorticity on each side of the plume interacts with the image vortices generated by the ground and are forced away from each other. This results in further distortion of the density contours, which generate strong secondary vorticity patterns. These secondary vortices act to entrain large amounts of clear air by sending out large tongues of particle laden air, engulfing volumes of surrounding atmosphere as shown in the fifth frame, Figure 17e. At each stage, the stretching and engulfing actions introduce smaller and smaller length scales into the problem. The horizontal density gradients become larger, inducing more intense vorticity, which further stretches and convolutes the density field, as shown in the final frame, Figure 17f. By this point in the simulation, the ratio of the maximum length scale, the overall geometric width, to the minimum gradient length, which generates the vorticity, is approaching 500.

These simulations which can be (and are) being performed on relatively modestly priced computer resources, permit the large scale turbulent mixing processes to be simulated directly without assuming anything about either the shapes of the velocity and density profiles, or the nature of the turbulence induced by the plume. When suitably extended to include more realistic scenarios and atmospheric phenomena, this methodology offers the promise of major improvements in predictive capability.

FUTURE RESEARCH

Many of the results reported here are ideas about how measurements and predictions will be made in both future mid-scale and field scale oil burn tests. During the following year, methods described here will be tested and evaluated in an extensive series of mid-scale test crude oil fires nominally 15 m in diameter. It is expected that these tests will identify needed improvements in the both the measurement and prediction methods being developed. Through this experience improvements will be introduced into the hardware and software being developed in this research program, so that the best possible measurements can be obtained in the field scale burned planned for 1991.

ACKNOWLEDGEMENTS

This work was largely supported by the Minerals Management Service, U.S. Department of the Interior. Recognition is gives to Mr. Ed Tennyson and Mr. John Gregory who organized and consulted in the development of this research program. Special technical assistance and cooperation was provided by Dr. Merv Fingas of the Technology Development and Technical Services Branch, Environment Canada. Dr. George Mulholland of the Center for Fire Research, NIST provided considerable guidance to the project on methods of soot measurement. Dr. William Kelly of the Center for Analytical Chemistry, NIST provided expertise in techniques of particle measurement with isotopic tracers. Mr. Jay McElroy provided the engineering design and construction of the model to simulate oil burning within a boom. Mr. Nelson Bryner, Mr. Richard Zile, Mr. Roy McLane, and Mr. Gary Roadarmel provided technical support in the large laboratory fire tests. We are all grateful for the opportunity provided by the fire fighters and instructors at Navy's Farrier Firefighting Facility in Norfolk VA to observe and measure large fuel oil fires as preparation for the crude oil fire measurement program. This provided all researchers with insight that can not be gained in any other way.

REFERENCES

[1] Jason, N. J., editor, Alaska Arctic Offshore Oil Spill Response Technology - Workshop Proceedings, November 29-December 1, 1989, Anchorage, Alaska, NIST SP 762, U.S. Government Printing Office, Washington, DC, April 1989.

[2] USCG R&D Center, Groton Connecticut, Report of the Interagency Planning Workshop on Oil Spill Research and Development, September 26-27, 1989, Groton, Connecticut, Conference Report 90-30-1509.2, November 1989.

[3] U.S. Congress, Office of Technology Assessment, Coping with an Oiled Sea: An Analysis of Oil Spill Response Technology, OTA-BP-O-63, Washington, DC, U.S. Government Printing Office, March 1990.

[4] Allen, A., "Contained Controlled Burning of Spilled Oil During the Exxon Valdez Oil Spill," submitted to Thirteenth Arctic and Marine Oilspill Program Technical Seminar, June 6-8, 1990, Edmonton, Alberta.

[5] Evans, D., Baum, H., McCaffrey, B., Mulholland, G., Harkleroad, M., and Manders, W., "Combustion of Oil on Water," Proceedings of the Ninth Arctic Marine Oilspill Program Technical Seminar, June 10-12, 1986, Edmonton, Alberta, Ministry of Supply and Services Canada Cat. No. En 40-11/5-1986E, pp. 301-336, 1986.

[6] Evans, D., Mulholland, G., Gross, D., Baum, H., and Saito, K., "Environmental Effects of Oil Spill Combustion," Proceedings of the tenth Arctic and Marine Oilspill Program Technical Seminar, June 9-11, 1987, Edmonton, Alberta, Ministry of Supply and Services Canada Cat. No. En 40-11/5-1987E, pp. 91-130, 1987.

[7] Evans, D., Mulholland, G., Gross, D., Baum, H., and Saito, K., "Burning, Smoke Production, and Smoke Dispersion from Oil Spill Combustion," Proceedings of the Eleventh Arctic and Marine Oil Spill Program Technical Seminar, June 7-9, 1988, Vancouver, British Columbia, Ministry of Supply and Services Canada, Cat. No. En 49-11/5-1988 E/F, pp. 41-87, 1988.

[8] Evans, D., Baum, H., Mulholland, G., Bryner, N., and Forney, G., "Smoke Plumes From Crude Oil Burns," Proceedings of the Twelfth Arctic and Marine Oil Spill Program Technical Seminar, June 7-9, 1989, Calgary, Alberta, Ministry of Supply and Services Canada, Cat. No. En 40-11/5-1989, pp. 1-22, 1989.

[9] Parker, W.J., "Calculations of the Heat Release Rate by Oxygen Consumption for Various Applications," Journal of Fire Sciences, 2, pp. 380-395, 1984.

[10] Koseki, H., Mulholland, G., Tadahisa, J., "Joint Study on Liquid Pool Fire Between NIST/CFR and FRI - Part 1 Study on Combustion Property of Crude Oil," Tenth Joint Panel Meeting of the UJNR Panel on Fire Research and Safety, October 19-24, 1989, Berkeley, CA, (in press)

[11] Shokri, M. and Beyler, C.L. "Radiation From Large Pool Fires", J. of Fire Prot. Engr., 1(4), pp. 141-150, 1989.

[12] Mudan, K., and Croce, P. "Fire Hazard Calculations for Large Open Hydrocarbon Fires", SFPE Handbook of Fire Protection Engineering, ED. P. DiNenno et. al., National Fire Protection Association, Quincy MA, Section 2, Chapter 4, pp. 45-87, 1988.

[13] Koseki,H. and Yumoto, T., "Air Entrainment and Thermal Radiation from Heptane Pool Fires," Fire Technology, 24, pp. 33-47, 1988.

[14] Kelly, W. R. and Ondov, J. M., "Isotopic Tagging and Tracing of Pollutant Particles by Mass Spectrometry," Atmospheric Environment, in press.

[15] Mulholland, G. W., Henzel, V., and Babrauskas, V., "The Effect of Scale on Smoke Emission," Fire Safety Science--Proceedings of the Second International Symposium, pp. 347-357, 1989.

[16] King, T.Y., "Empirical Relationships Between Optical Density and Mass Density of Smoke," Journal of Fire and Flammability, 6, p. 222, 1975.

[17] Seader, J.D. and Ou, S.S., "Correlation of the Smoking Tendency of Materials," Fire Research, 1, pp. 3-9, 1977.

[18] Briggs, Gary A., "Plume Rise and Buoyancy Effects," Atmospheric Science and Power Production, U.S. Dept. of Energy, Washington, DC, pp. 327-366, 1984.

[19] List, Robert J., Smithsonian Meteorological Tables, Smithsonian Institution, Washington, DC, p. 527, 1958.

[20] Turner, D. Bruce, Workbook of Atmospheric Dispersion Estimates, U.S. Dept. of Health, Education and Welfare, Cincinnati, OH, p. 84, 1967.

[21] Ghoniem, A.F., Heidarinejad, G., and Krishnan, A., "Numerical Simulation of a Thermally Stratified Shear Layer Using the Vortex Element Method," J. Comp. Phys., 79, p. 135, 1988.

[22] Ghoniem, A.F., Heidarinejad, G., and Krishnan, A., "On Mixing, Baro-Clinicity, and the Effect of Strain in a Chemically Reacting Shear Layer," AIAA 26th Aerospace Science Meeting, Reno, AIAA-88-0729, 1988.

[23] Ghoniem, A.F., and Krishnan, A., "Origin and Manifestation of Flow-Combustion Interactions in a Premixed Shear Layer," Twenty Second Symposium (International) on Combustion, The Combustion Institute, Pittsburgh, p. 675, 1988.

[24] Krishnan, A. and Ghoniem, A.F., "Simulation of the Rollup and Mixing in Rayleigh-Taylor Flow Using the Vortex/Transport Element Method," J. Comp. Phys., in press.

A Simulation of Bubble Formation During an Undersea Oilwell Blowout

J.D. Bugg and R.D. Rowe

Department of Mechanical Engineering
The University of Calgary
Calgary, Alberta, Canada

INTRODUCTION

This paper describes results of a numerical model of very large bubble growth at the exit of submerged pipes such as might occur during the blowout of an undersea oilwell. The model is a two dimensional, transient finite difference code capable of tracking material interfaces within the solution domain. This code solves the full Navier-Stokes equations in the liquid and is coupled to a gas pressure model in the gas filled regions through the free surface boundary condition.

This paper contains results for a postulated "full scale" blowout of an undersea oilwell. The conditions are those summarised by Meikle, 1981, namely 8.85m^3/sec gas flowrate (standard conditions) at up to 200 metres depth. The results show the initial formation of the bubbles and predict the type of flow behaviour expected. Appropriate scaling parameters are also investigated and the dominant dimensionless groups are discussed. It is illustrated that the numerical results appear to scale properly with these dimensionless groups.

THEORY

Numerical Model

The numerical model used in this work is a two dimensional, transient finite difference technique with the capability to track an interface through the interior of the solution domain by cataloging the volume fraction of fluid present in each cell as the solution progresses. The details of the liquid filled region velocity field calculation are available elsewhere and will not be presented here. The model has been used successfully to predict the initial motion of single cylindrical and spherical bubbles released from rest in quiescent liquids. This work, along with a more detailed discussion of the code, can be found in Bugg and Rowe, 1988 and Bugg and Rowe, 1989(a).

Gas Pressure Model

The technique used in this problem does not solve for the velocity field in the gas filled regions. These regions are coupled to the velocity field solution through the free surface boundary condition. The volume change experienced by each bubble during a time step is calculated from the liquid region velocity field as a result of the interface convection algorithm's movement of the surface. A model is required to update the pressure in each void region as a result of this volume change and the extra mass that enters the bubble during the time step.

The derivation of this model begins with the ideal gas law.

$$m = \frac{PV}{RT} \qquad \ldots 1$$

The total derivative with respect to time yields the mass flow as follows:

$$\dot{m} = \frac{1}{R}\left[PV\frac{d}{dt}\left(\frac{1}{T}\right) + \frac{P}{T}\frac{dV}{dt} + \frac{V}{T}\frac{dP}{dt}\right] \qquad \ldots 2$$

In discretised form, this expresses the updated pressure as,

$$P^{n+1} = P^n + \frac{T^n}{V^n}\left[\delta t R\dot{m} - \frac{P^n}{T^n}\delta V - P^n V^n \delta\left(\frac{1}{T}\right)\right] \qquad \ldots 3$$

The change in volume, δV, is given by the velocity field solution. The temperature change is derived from the first law as follows.

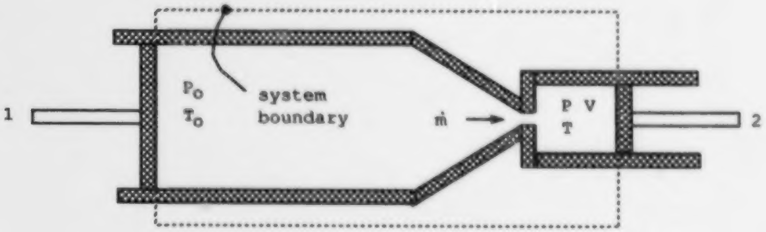

Figure 1: Hypothetical closed system model of gas flow into growing bubble.

Consider a hypothetical closed system as shown in figure 1 where piston 1 represents the air supply and piston 2 represents the bubble and any volume of piping beyond the choking location so that $V = V_l + V_{bubble}$. In general the first law can be written as, $Q = \Delta U + W$. It will be assumed that the system is effectively adiabatic because of the very short time scales involved. Work is done on the system (-) by the compressor and work is done by the system (+) due to the change in bubble volume. Letting the mass of air in the bubble be m^n and the temperature at the beginning and end of the time step be T^n and T^{n+1} respectively, this becomes:

$$0 = m^n C_v (T^{n+1} - T^n) + \dot{m}\delta t C_v (T^{n+1} - T_0) - P_0\delta V_0 + P^n\delta V \qquad \ldots 4$$

where the bubble work term has been explicitly approximated by $P^n\delta V$. Since $\delta V_0 = \dfrac{\dot{m}\delta t R T_0}{P_0}$ and $m^{n+1} = m^n + \dot{m}\delta t$ this can be written as,

$$T^{n+1} = \frac{m^n}{m^{n+1}} T^n \left(1 - \frac{\delta V}{V^n}(\gamma - 1)\right) + \frac{\dot{m}\delta t}{m^{n+1}}\gamma T_0 \qquad \ldots 5$$

giving the new temperature of the bubble. Equations 3 and 5 constitute a gas pressure model for a growing, adiabatic bubble with a volume change prescribed by the velocity field solution.

Dimensional Analysis

Since full scale blowouts are obviously difficult to reproduce in a laboratory, it is useful to investigate scaling laws which may be applicable to the problem. In this section a discussion of appropriate dimensionless groups will be presented. The scalability of the phenomena will be illustrated by presenting numerical results that are scaled according to the groups derived.

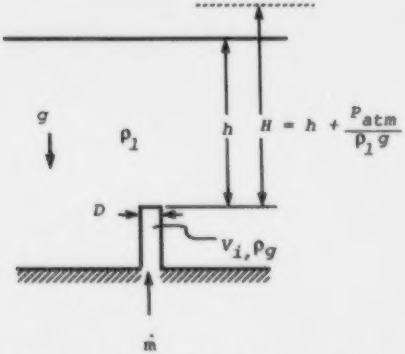

Figure 2: Schematic showing quantities of interest.

The first step in the analysis is to identify the quantities which have a significant influence on the behaviour of large bubbles growing at pipe exits. Consider the schematic shown in figure 2. All quantities considered important in the analysis are shown on this figure. Because of the large size of the bubbles, buoyancy and inertia effects will govern so surface tension and viscous effects have been neglected. The important variables are summarised in table 1 along with their dimensions in terms of mass (M), length (L) and time (T).

Symbol	Description	Dimensions
$\dot{m}$	Mass flowrate	M/T
D	Pipe diameter	L
H	Liquid depth	L
ρ_g	Gas density	M/L^3
ρ_l	Liquid density	M/L^3
g	Gravitational acceleration	L/T^2
V_i	Initial volume	L^3

Table 1: Quantities considered in dimensional analysis.

Since there are 7 quantities and 3 fundamental dimensions (M, L, T) there will be 4 dimensionless groups. Analysis yields H/D, V_i/D^3, ρ_l/ρ_g and $\dot{m}/(\rho_g\sqrt{gD^5})$ as one possible set of groups. The first two groups demand geometric similarity. The third is a liquid to gas density ratio and the final group is a type of Froude number. The Froude number could be expressed in terms of volume flowrate, $Q/(\sqrt{gD^5})$ but the volume flowrate must be adjusted for the depth of the orifice and not taken at standard conditions. If this analysis is valid, similar results should be obtained for any two runs of the model which have the same value for all of these groups.

Dimensional analysis does not indicate the functional relationship between these groups and bubble behaviour, so it remains to be determined which of these 4 groups are dominant and if any can be neglected. Since the Froude number (F) is the only group that involves the gas flowrate, it is undoubtedly very important.

If surface tension and viscosity were considered, their influence could be accounted for by two additional groups, a Reynolds number ($Q\rho_l/(\mu D)$) and a Weber number ($Q^2\rho_l/(D^3\sigma)$).

RESULTS

Full Scale Conditions

Typical full scale conditions during an undersea oilwell blowout were taken as those summarised by Meikle, 1981. This was a "worst case" scenario of 30,000 *barrels per day* of oil containing 900 *cubic feet* of gas per barrel. This yields a gas flowrate of 8.85 m^3/s at standard conditions. Water depths up to 200 *metres* were considered important.

For the purposes of the current simulation a 15 *cm* pipe was considered. Also, V_l was arbitrarily chosen to be equal to the volume of the protruding pipe. V_l is an important parameter in determining bubble behaviour. It is also one of the most difficult to quantify for an actual blowout. However, proceeding upon this assumption, these conditions represent a Froude number of $3350/H$ where H is the depth of the blowout plus 10.3 *metres* to account for atmospheric pressure. At the maximum depth of 200 *metres* this gives the following values for the 4 dimensionless groups:

$H/D = 1440, \quad V_l/D^3 = 2.62, \quad F = 16, \quad \rho_l/\rho_g = 41.$

Full Scale Results

The grid developed to model the full scale blowout is based on an axisymmetric coordinate system located on the pipe centerline. The pipe is assumed to protrude vertically 0.5 *metres* from the sea bed. The solution domain extends to a radius of 2.0 *metres* and to a height of 4.0 *metres* from the sea bed. The sea bed is modelled by a zero penetration, free slip boundary condition while all other boundaries allow inflow and outflow but restrict velocity gradients to zero. The grid is non-uniform so that control volumes can be concentrated near the pipe exit and still allow a reasonably large region to be modelled with a minimum number of control volumes. Both a coarse grid and a fine grid were developed for this problem. The coarse grid resolves the pipe diameter into 10 control volumes resulting in a total of 9750 control volumes. The fine grid is obtained by doubling the coarse grid and therefore has 4 times as many control volumes (39,000). The initial conditions for all runs are zero velocity in the liquid and a horizontal gas/liquid interface at the pipe exit. As well, the initial pressure in the pipe is set to the hydrostatic pressure at its exit.

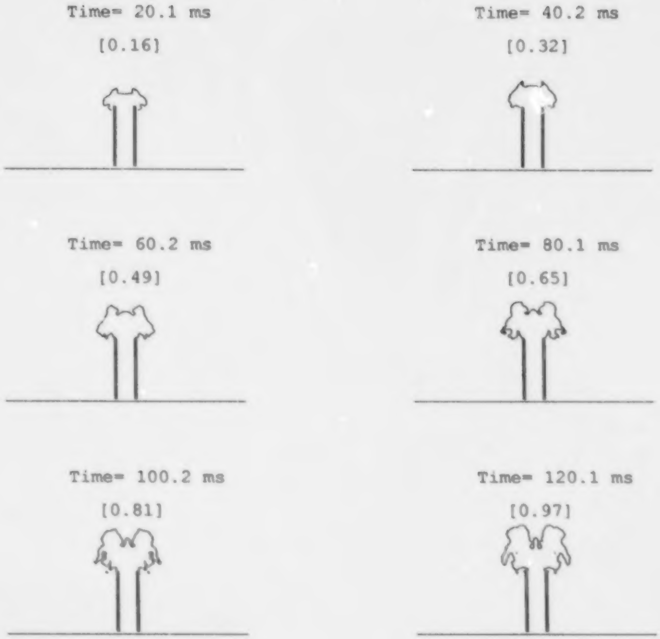

Figure 3: Bubble growth for $H/D = 1440$, $V_l/D^3 = 2.62$, $F = 16$, $\rho_l/\rho_g = 41$.

The results of the coarse grid simulation for the conditions described above are shown in figure 3. Both the real time and the dimensionless time (normalised by $\sqrt{g/D}$) are shown on each frame. The initial stages of growth show a toroid growing at the lip of the pipe. This is consistently observed in experiments (Bugg and Rowe, 1989(b)). As the bubble continues to grow it has a quite distorted surface. When its volume becomes appreciable (≈ 100 *ms*) the bubble's vertical motion becomes apparent and it begins to lift off of the pipe. The remainder of the simulation shows further vertical movement but a rather distorted lower surface on the bubble. The bubble appears to depart but the diffusive nature of the interface convection algorithm has left the control volumes between the lower surface of the bubble and the pipe exit with a small amount of void. The results is that the program interprets the bubble as still attached. Further development is required on the interface convection algorithm to correctly model the departure process.

Scaled Results

Although the code's results are only valid for a short time, it can still be used to investigate scaling laws. Scalability can be tested by running a 1/10 scale case with other physical parameters adjusted to keep all 4 groups constant. Geometric scaling alone ensures proper scaling of H/D and V_l/D^3. Because of the dependance of gas density on liquid density, through the hydrostatic pressure, scaling ρ_l/ρ_g demands

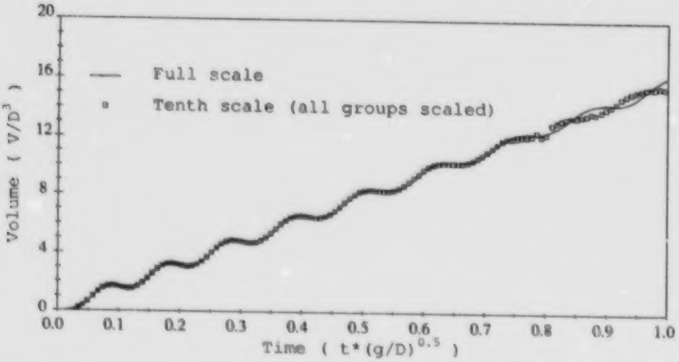

Figure 4: Volume versus time for full scale and tenth scale simulations.

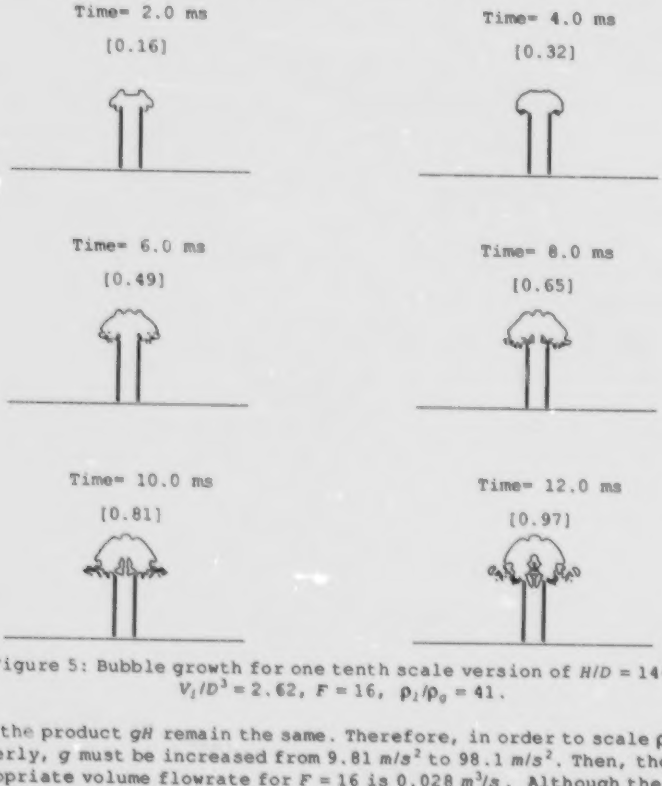

Figure 5: Bubble growth for one tenth scale version of $H/D = 1440$, $V_l/D^3 = 2.62$, $F = 16$, $\rho_l/\rho_g = 41$.

that the product gH remain the same. Therefore, in order to scale ρ_l/ρ_g properly, g must be increased from 9.81 m/s^2 to 98.1 m/s^2. Then, the appropriate volume flowrate for $F = 16$ is 0.028 m^3/s. Although the details of the surface distortion are not identical, the general

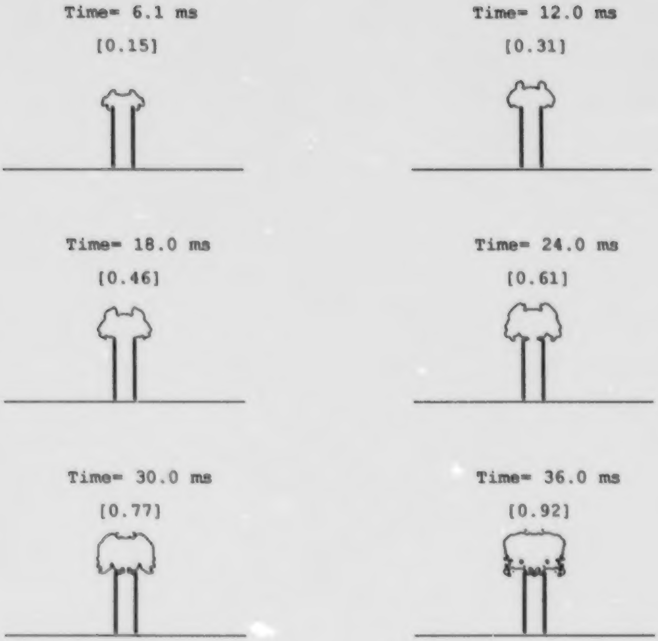

Figure 6: Bubble growth for $H/D = 1440$, $V_l/D^3 = 2.62$, $F = 16$, $\rho_l/\rho_g = 4.1$

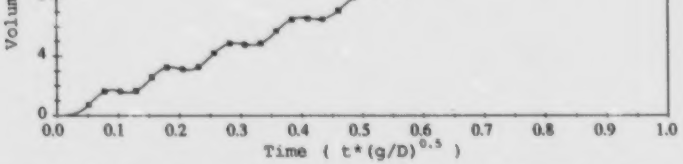

Figure 7: Volume versus time for full scale and $\rho_l/\rho_g = 4.1$ runs.

behaviour and growth rate is the same. Figure 4 shows the volume versus time for both the full scale and tenth scale runs. This indicates that these groups appear to scale large bubble growth properly. The bubble cross sections for this run are shown in figure 5.

The results shown in figure 4 merely indicate that if all 4 groups are scaled, bubble behaviour during the initial growth stage is essentially the same. A run will now be presented which illustrates that the ratio ρ_l/ρ_g has a very weak influence on behaviour. Figures 6 and 7 illustrate a run with H/D, V_l/D^3 and F as before but ρ_l/ρ_g decreases by a factor of 10. The results indicate that the initial bubble behaviour is a very weak function of ρ_l/ρ_g. Therefore, during the very early stages of growth, the set of important dimensionless groups can be reduced to the two geometric constraints and the Froude number. For any scale with geometric similarity, Froude number scaling should provide similar bubble behaviour. Later in the bubble's life, as it lifts off the pipe, ρ_l/ρ_g could become an important parameter.

Similar sensitivity studies where done with V_l/D^3 and H/D and they were found to have a profound influence on behaviour. In particular, they greatly affect the frequency with which the bubble volume (and pressure) oscillate as the bubble grows. Oscillations result from the momentum in the liquid overexpanding the bubble, causing its pressure to drop below that which the mass flow of gas can maintain. The rate at which the pressure in the bubble builds for a given mass flow is a strong function of V_l and the hydrostatic pressure surrounding the bubble, governed by H. The strong influence of V_l/D^3 and H/D on bubble behaviour while growing at a pipe exit indicates the importance of proper scaling.

CONCLUSIONS

It is apparent that the current model is able to predict some of the important features of large bubbles formed at the exit of submerged pipes. Dimensional analysis has been performed which indicates that a type of Froude number is a very important parameter. Also, scaling V_l/D^3 and H/D is necessary to ensure that the gas pressure model interacts with the velocity field solution in the proper way. The difficulty of estimating V_l for an actual blowout therefore becomes an important concern.

The limitations of the code become apparent when the departure process from the pipe must be modelled. This is due to deficiencies in the algorithm that convects the gas/liquid interface through the solution domain. Although it is reasonable to believe that improvements in the interface convection routine will lead to the proper modelling of the departure process, progressing the solution well beyond the first departure involves much more difficult processes. Firstly, the velocity field becomes much more turbulent and it will become necessary to model the effects of turbulence. Secondly, once a large bubble has detached, it will soon shatter, a process that at present is well beyond the capabilities of such a model to effectively predict. However, if the first departure can be effectively predicted and the initial growth of the second bubble can be started, it may be apparent whether the vital influence of the first bubble on the shape of the second is going to be properly modelled.

REFERENCES

Bugg, J.D., Rowe, R.D.: "A Numerical Study of Large Bubble Dynamics", Canadian Applied Mathematics Society Conference on Continuum Mechanics and its Applications, Hemisphere Publishing Corp., Vancouver, pp 611-620, May 30 - June 3, 1988.

Bugg, J.D., Rowe, R.D.: "Numerical Techniques for the Modelling of Large Gas Bubbles in Liquids", 6th International Conference of Numerical Methods in Turbulent and Laminar Flow, Swansea, U.K., July 11-15, 1989(a).

Bugg, J.D., Rowe, R.D.: "An Experimental Study of Large Bubble Dynamics", Proceedings of the Twelfth Arctic and Marine Oilspill Program Technical Seminar, pp 105-114, Calgary, June 1989(b).

Meikle, K.M., "Summary of Discussion", Proceedings of a Workshop on the Sub Sea Containment of Oil, Toronto, Canada, February 11-12, 1981.

THE LONG-TERM WEATHERING OF HEAVY CRUDE OILS: EXPERIMENTAL MEASUREMENTS AND DEVELOPMENT OF MODELS

S.C. Lee, W.Y. Shiu, D. Mackay
Department of Chemical Engineering and Applied Chemistry
University of Toronto
Toronto, Ontario

ABSTRACT

A research project is described in which observations and measurements are being made of the long term weathering processes to which heavy crude oils are subject. Experimental systems have been developed to expose the oil under controlled conditions to (i) evaporative weathering, (ii) dissolution weathering, and (iii) combined processes. The analytical systems are described, and an approach to modelling the data is suggested. Of particular interest is the formation of a weathered "crust" which appears to retard the weathering processes

INTRODUCTION

The Incentive

Numerous experimental studies and observations of real spill behaviour have shown that when conventional and heavy crude oils and petroleum products are spilled in the marine environment they are subject to a number of processes collectively termed "weathering", which cause profound changes in the oils' physical and chemical properties and composition. These processes include evaporation, dissolution, photolysis, formation of oil-in-water emulsions and water-in-oil emulsions, and adherence to the oil of organic matter and mineral particles present in the water column.

As weathering proceeds, the oils usually become denser, and their viscosity increases, and ultimately the oil masses may form semi-solid droplets or tar balls which float in a near-submerged state at the water surface. This material may persist indefinitely on the sea surface, or become stranded on shore, or sink and become incorporated into sediments. It is important to determine which types of oils, under which conditions, are subject to which type of behaviour. Whereas most experimental measurements are being made over the short-term, it is increasingly obvious that there is a need to predict long term behaviour of oil because this oil may drift appreciable distances from the source of the spill. A convenient review of these issues can be found in a recent report by Lee et al. (1989).

The purpose of this study is to design and test various methods by which long-term weathering phenomena can be investigated, observed and if possible quantified. The approach has been to isolate and quantify on an individual basis two weathering processes which are believed to be of particular importance.

Experimental Approach

First is evaporation which can cause appreciable density and viscosity increases. We have thus sought to devise an experimental approach, or protocol, for measuring the extent to which hydrocarbons will evaporate from oil, and in doing so identify the hydrocarbons which have evaporated. This is done in the hope that the protocol may be useful for routine characterization of oils which may be produced or transported in the marine or aquatic environment.

The second process is dissolution which is less important from the viewpoint of loss of mass by the oil, but is critically important for assessment of toxicity to aquatic or marine organisms. Again, we have sought to develop an experimental protocol whereby oils may be subjected to controlled dissolution conditions, and the dissolved and remaining oil identified and quantified.

A third aspect has been to devise a relatively simple laboratory system for measurement and observation of the long-term weathering of crude oils on a water surface. The oil is thus subjected to dissolution, evaporation and photolysis. The aim has been to simulate, as realistically as possible in the laboratory, conditions which occur at the ocean surface, and thus elucidate how a particular oil will be expected to behave as a result of combined weathering processes.

A problem inherent in this latter aspect is that it has been observed that as an oil weathers it may form a protective skin or crust consisting of high density, high viscosity material. This material, possibly altered chemically as a result of photolysis, protects the underlying or interior oil from further exposure to evaporation or dissolution. It is not clear which oils are susceptible to this phenomenon, and at which stage of weathering it occurs. Thus the simulation of evaporation, dissolution and photolysis simultaneously is necessary to gain an appreciation of each oil's characteristic behaviour.

A final aspect which is investigated in this study is the formation of water-in-oil emulsions. Previous reviews have been presented by Payne and Phillips (1985), and Mackay (1987). These emulsions are generally of high viscosity and high water content, and they profoundly affect oil behaviour and the feasibility of clean-up. Accordingly, a smaller experimental effort is being devoted to establishing the susceptibility of the oils to emulsion formation, and the stability of these resulting oils.

Models

Ultimately, it is desirable to develop some form of mathematical modelling approach to translate laboratory results to marine environmental conditions. The general sequence of events envisaged would be that standard laboratory tests would be conducted to obtain parameter values characteristic of the oil, and especially of its susceptibility to evaporation, dissolution, photolysis and emulsion formation. A mathematical model would be fitted to the experimental data. The same mathematical model would then be used under the different conditions of oceanic exposure, but with the same parameter values, in order to estimate the changes in oil composition and properties with time.

Ideally, it should be possible in a laboratory to "accelerate time", that is, undertake oil exposure experiments over a period of perhaps 20 days in the laboratory which will simulate exposure conditions in a marine environment for perhaps 200 days. There are obvious limitations in this respect; however, in the interests of economy, it is desirable to obtain oil characteristic data in as short a period of time as possible.

Any attempt to prepare a mathematical model of oil behaviour is rendered difficult by the very complex nature of crude oils, and especially the large number of components which are of unknown structure and properties. Accordingly in this study, we have attempted to develop a novel "matrix" approach for oil characterization during long-term weathering by modifying a procedure developed in our group for characterizing the long-term weathering behaviour of oils in a soil environment (Eastcott et al., 1987). The general concept is that the oil is divided up into a number of pseudo-components, each of which has defined properties such as volatility, solubility, density, and viscosity. As the oil is weathered, there is selective removal of these components caused by exposure to evaporation or dissolution. The result is a change in the proportion of the chemicals present in the matrix, and thus a change in the overall properties of the oil. In principle, it should be possible to characterize the changing properties of oil in terms of changes in the magnitude of the elements in the matrix.

Analyses

The key problem is the development of analytical techniques which will enable the composition of the original oil, and experimentally weathered oils, to be expressed in terms of matrix elements. Gas chromatography is very convenient as a method of characterizing the volatility of crude oils, thus one dimension of the matrix should obviously be a separation of oil into rows which consist of elements similar in volatility. It is desirable to separate the oil into matrix columns based on solubility, but this is more difficult. The first obvious approach is to subject a sample of the oil to dissolution under controlled conditions, and measure the amount of oil dissolved. This has been investigated as part of this project. A second approach is to separate the oil into classes of hydrocarbons such as alkanes, aromatics and polars which are known to have widely different solubility characteristics. If it was possible, for example, to assign a common solubility to the aromatics which lie in a specified volatility range then this approach can be used to provide a series of columns corresponding to oil components of different chemical structure. A third and attractive possibility, if it is feasible, is to subject oil fractions to HPLC analysis and separate the oil into solubility classes relying on the relationship between HPLC retention time and water solubility, or more precisely the water to stationary phase partition coefficient. This can be done using either conventional or reversed phase HPLC techniques. This HPLC approach has the advantage in that it is fast and routine, and could introduce considerable economies of time into the determination. However, it has not been to our knowledge successfully applied in this context although it has been used by various workers to estimate octanol-water partition coefficients for hydrophobic organic substances.

Accordingly, we have approached this problem by attempting all three methods with a view to establishing the preferred one.

In the balance of this paper, we describe the oils which are currently being tested, the experimental procedures which have been developed and are being used, and present some preliminary results. Full results will be published by Environment Canada in a forthcoming EE Series Report.

EXPERIMENTAL

The heavy crude oils were supplied by Environment Canada and the US Minerals Management Services. EPS standard oil was also used as to help develop an experimental protocol whereby heavy crude oils may be subjected to evaporation and dissolution conditions.

The physical-chemical properties of the heavy crude oils are listed in Table 1, and their gas chromatograms are shown in Figure 1. Table 2 gives the composition of the original oils using open column chromatography.

Table 1. Properties of Heavy Crude Oils and Residual Fuels

Property	California Crude API 15	California Crude API 11	Bunker C Fuel Oil	Cold Lake Bitumen	EPS
API Gravity	13.2	10.3	12.3	9.8	
Density (g/cm^3) @ 22 +/- 2°C	0.9681	0.9779	0.9712	0.9851	0.836
Viscosity (cp) @ 15°C	3.1e4	3.4e4	4.8e4	2.4e5	7.09*
Solubility (mg/L)					
d.d H_2O	25.7	11.3	4.23	0.26	34.5
salt H_2O**	14.7	9.74	1.95	0.13	

---

*3.0 % NaCl in salt H_2O.
**measured at 20°C.

Table 2. Hydrocarbon Analysis by Open Column Chromatography

Composition	California Crude API 15	EPS
Saturates	48.3	75.5
Aromatics	21.8	18.6
NSO compounds	5.1	3.63
Asphaltene	24.8	2.26

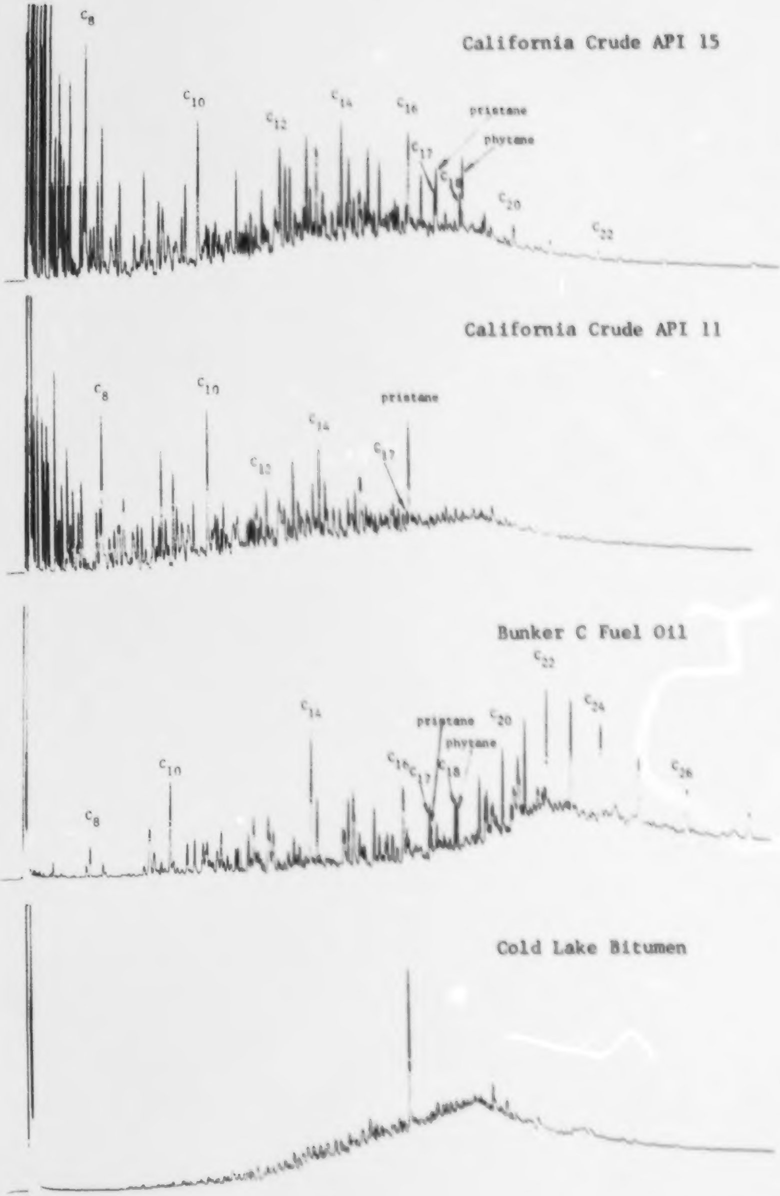

California Crude API 15

California Crude API 11

Bunker C Fuel Oil

Cold Lake Bitumen

Figure 1. Gas chromatograms of heavy crude oils and residual fuels.

Oil Weathering

Evaporation

There are several experimental methods for oil evaporation. One technique was to use a modified version of the gas stripping apparatus (Stiver and Mackay, 1984) which is shown in Figure 2A. A 250-mL graduated cylinder was fitted with a lid from which a glass tube was extended to the bottom of the container. The lower end of the inlet tube was enclosed except for several pinholes through which air was bubbled. Two gas traps were connected in series to the outlet of the cylinder. These vessels were similarly constructed, but the inlet tubes were open at the bottom. The gas traps were cooled with liquid nitrogen.

Air was supplied from the laboratory supply, and a Scientific Wet Test Meter was used to measure the cumulative air flow through the gas stripping system.

The graduated cylinder was filled with a known mass and volume of oil, and air was bubbled through the oil at a rate of 400 mL/min through the system. The air supply was periodically stopped, and at which time, the remaining mass and volume of the crude oil in the cylinder were measured as a function of the cumulative volume of air which flowed passed. In addition, oil samples were analyzed by gas chromatography to quantify the extent to which hydrocarbons were evaporated from oil. The compounds stripped from the oil were recovered by the gas traps and analyzed by GC. The recovery efficiency of the evaporated hydrocarbons averaged 90 %. Measurements were thus made of the weathered oils' changing composition, amount, and properties such as density.

A second more rapid method of weathering oil by evaporation was to use a rotating mesh disk apparatus which is illustrated in Figure 2B. Appropriate amounts of oil were applied to PeCap^R polyester mesh disks (Tetko Inc.) of 60 mm diameter. These oil-covered disks were secured to the rotating device in which the continuous circular movement of the apparatus prevented the loss of oil by dripping from the mesh disks. The entire system was placed in a dark fumehood, and subjected to turbulent air flow. The effective air flow rate for the system can be determined by comparison of oil composition data with those obtained from the air stripping experiment. With this method, there is a substantially increased rate of evaporation, and density measurements are easily made.

To further accelerate the evaporation process, distillation or tray evaporation can be used, but the distillation will give different compositional changes from the other methods because of the elevated temperature.

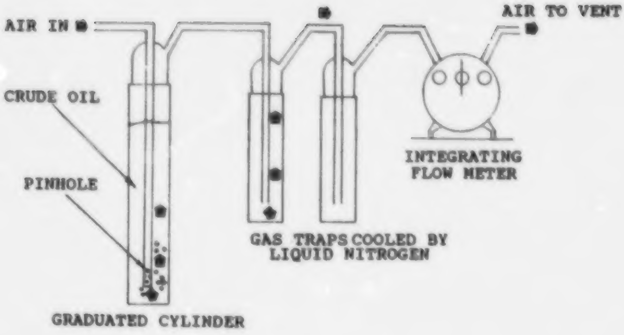

Figure 2A. Evaporation apparatus: air stripping.

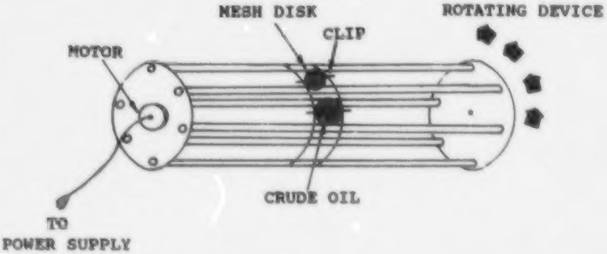

Figure 2B. Evaporation apparatus: rotating mesh disk.

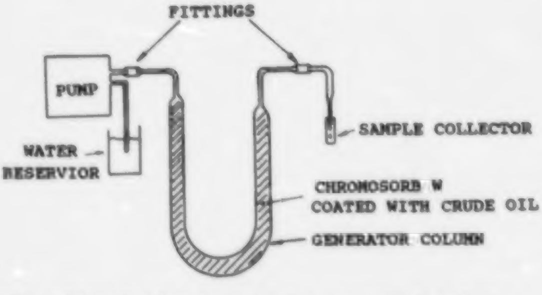

Figure 2C. Dissolution apparatus: generator column.

Dissolution

The generator column method was previously reviewed and discussed by Billington et al. (1988) and Shiu et al. (1988) for preparing solutions of single component systems and multicomponent oil systems such as crude oils. Here, we used this method to determine the identity of the dissolved hydrocarbons, and the extent to which they were dissolved as the water to oil volume was increased.

A U-tube generator column was packed with Chromosorb W (mesh size 80/100, Mansville Products Corp.) which was coated with 20 % by volume of oil. Glass wool was plugged into the ends to secure the Chromosorb W in the column. Double-distilled water was pumped with a Beckman solution metering pump through the column at a rate of 3.0 mL/min. Aqueous samples were collected at intervals and the soluble hydrocarbon concentrations analyzed by purge-and-trap GC as a function the water-to-oil volume ratio. The cumulative eluted water was measured by weighing. Two experimental runs were undertaken for each oil and were discontinued when the water-to-oil ratio reached 4100 and 10000. A schematic diagram of the generator column system is shown in Figure 2C.

After a water-to-oil volume ratio of 10000 was reached, 1.0 L of water was pumped through the remaining oil to obtain the less volatile, high-boiling point PAHs which were collected with a Waters C_{18} Sep-Pak (Waters Associates, Milford), and extracted from the cartridge with 5 mL ethyl ether. The eluent was concentrated, and analyzed by capillary GC.

The residual oils from the generator column experiments were extracted from the column with n-pentane and subjected to open column chromatography to determine the identity and amount of the undissolved hydrocarbons in the oil.

Long-term Weathering of Heavy Oils

To observe the long-term weathering of heavy crude oils on the water surface, a cylindrical container was filled with 5.0 L of distilled or salt water (3.0 wt% NaCl) on which oil was poured to form a thin slick. The water was continuously stirred with a magnetic stirrer to prevent the oil from adhering to the sides, and some of the water was replaced weekly. The apparatus was set up in the fumehood for a period of five months. Thus the oil was subjected to evaporation, and dissolution simultaneously. The changing physical characteristics of the oils were observed, and gas chromatographic analysis were performed on oil samples taken from the water surface, and eventually from denser-than-water oil globules in the water column.

Water-in-Oil Emulsion Formation

Attempts were made to form stable water-in-oil emulsions or "mousse" from California Crude API 15 with the Warren Spring apparatus using a water-to-oil volume ratio of 10:1. The water-oil mixture was rotated at 50 rpm for 6 hours. It was found that a large amount of the oil adhered to the sides of the apparatus, and any emulsion which formed proved unstable within 24 hours.

Another method of forming mousse was to use a Waring commercial blender. Approximately 15 mL of oil was added to 200 mL of water, and the mixture was blended at the low speed for 2 minutes. It was observed that an emulsion was formed, but it become unstable overnight, there being a clear separation of water from the oil. Further work is continuing to assess the stability of weathered oils.

Analysis

Gas Chromatography

Fresh and weathered oils, and their various fractions obtained from open column chromatography were analyzed by gas chromatography. The instrument used was a Hewlett-Packard GC model 5700A equipped with a flame-ionization detector. The column was a 0.75 mm ID x 50 m long glass capillary column coated with SE-30 which was supplied by Supelco Canada, Ltd. The operating conditions were as follows: the initial oven temperature was 50^{o}C for 8 minutes with a temperature programmed rate of 5^{o}C/min, and a final oven temperature of 220^{o}C for 30 minutes. The injection sample volume was 0.5 uL with a split ratio of 50:1. The peak areas were recorded by a Shimadzu Chromatopac C-R1A integrator using the area normalization method.

Open Column Chromatography

The crude oils were separated according to their structural class by open column chromatography. The fractions obtained by this method are saturates, aromatics, and polar compounds. This analysis facilitates identification and quantification of the hydrocarbons in the oil.

The pentane-insoluble asphaltene was precipitated from the oil by addition of n-pentane (Caledon Laboratories), filtered out and weighed. The de-asphaltened oil was separated into the three fractions using the procedure described by Cook and Westlake (1976). A column was packed with a 1:1 mass ratio of silica to alumina gel. The silica (28-200 mesh) and alumina gel (type F-20, 80-200 mesh) were obtained from Sigma Chemical Co. The order of elution was saturates with n-pentane, aromatics with benzene, and then soluble polar compounds with 1:1 mixture of benzene and methanol. The fractions collected were concentrated by distillation so that little of the volatile compounds were lost by evaporation. Analysis by capillary GC yielded information on the composition and amount of each fraction in the oil.

Liquid Chromatography

An alternative method for separating oil into solubility-related fractions was normal phase liquid chromatography. The HPLC system consisted of a Waters Scientific model 510EF solvent delivery system, an U6K injector with a 2-mL sample loop, a 6-port backflush valve, and a model 401 differential refractometer. The mobile phase was HPLC-grade n-pentane, and the stationary phase was NH_2 Bondapak which was packed in a semi-preparative 2.5 cm ID x 30 cm long stainless steel column. Samples of 100 uL were injected into the system and the fractions were eluted with a flow rate of 18.0 mL/min. The peak areas were recorded with a HP-3390 integrator. The polar compounds were eluted by backflushing the flow through the column. A liquid chromatogram of a typical crude oil is shown in Figure 3. The fractions were concentrated using a micro-distillation apparatus before injecting into the GC.

Purge-and-Trap Gas Chromatography

A Hewlett-Packard model 5840A GC with a flame-ionization detector and a HP-7675A purge-and-trap sampler was used to analyze, and thus quantify the soluble hydrocarbon concentrations in aqueous samples. The column was a 0.53 mm ID x 30 m long megabore fused silica capillary column coated with DB-1 (J&W Scientific, Inc.). The oven temperature was set at $50^{O}C$ for 10 minutes, and then programmed to increase at a rate of $5^{O}C$/min to a maximum temperature of $200^{O}C$ which was maintained for 20 minutes. The detector temperature was at $300^{O}C$. The sample volume used was between 2 to 8 mL, and the peak areas were integrated by a HP-5840A GC terminal.

The purge-and-trap technique was used to determine the aqueous solubility of crude oils. Saturated aqueous oil solutions were prepared by adding in a separatory funnel oil to water with a volume ratio exceeding 1:40. The funnel was shaken gently with a Burrell wrist action shaker for 24 hours and the mixture was allowed to settle for 48 hours before analysis.

RESULTS

A gas chromatogram of fresh EPS oil is depicted in Figure 4A. It has an abundance of low boiling, volatile hydrocarbons, and of highly water-soluble compounds such as benzene, toluene, ethylbenzene, xylenes, and

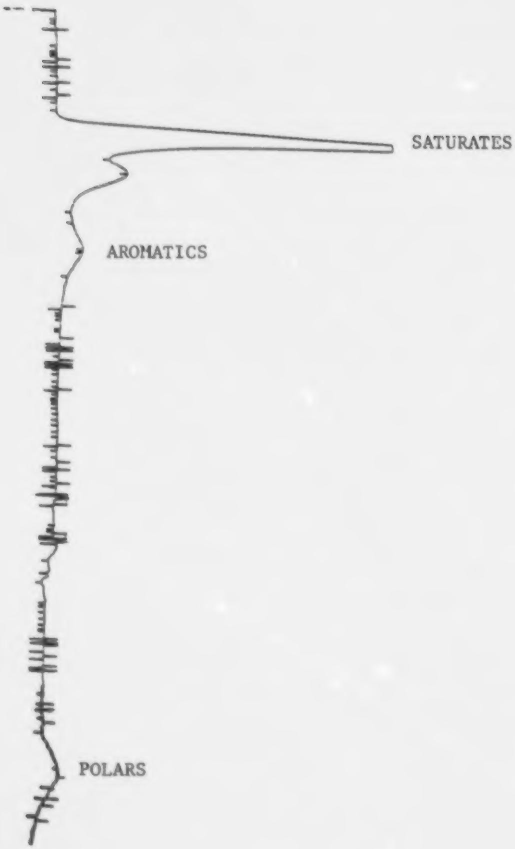

Figure 3. Liquid chromatogram of a typical crude oil.

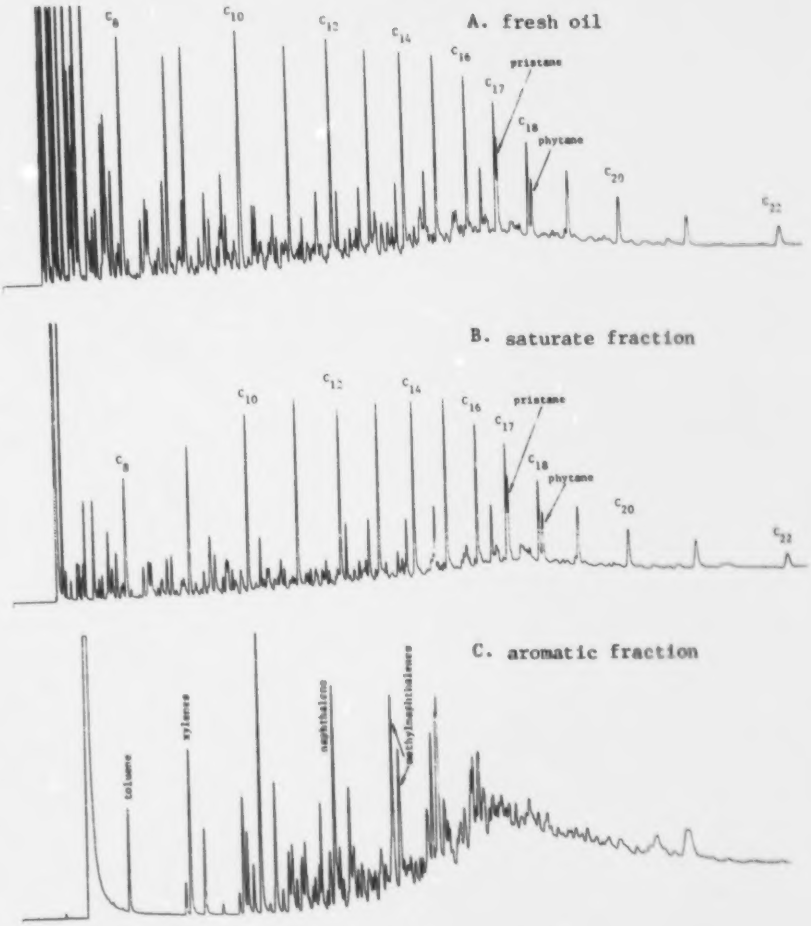
A. fresh oil

B. saturate fraction

C. aromatic fraction

Figure 4. Gas chromatograms of fresh EPS oil and its saturate and aromatic fractions.

naphthalene as shown by Figures 4B and 4C, respectively. The saturates and aromatics were separated from the oil using asphaltene precipitation and open column chromatography.

EPS oil was chosen as the crude oil on which we performed preliminary experiments because it is easily handled, and its changing properties and composition can be clearly observed.

This oil was subjected to evaporation with the gas stripping apparatus. Figure 5 shows the sample chromatograms of the saturate and aromatic fractions for an evaporative exposure Q_E of 8060 where Q_E is the ratio of air to initial oil volumes. The extent of weathering was 24 % by volume of oil evaporated, and its density increased by from 836 kg/m^3 to 883 kg/m^3 (Figure 6). Comparison with the gas chromatogram of the fresh oil revealed the loss of the highly volatile compounds in the saturate fraction.

The rotating mesh disk apparatus worked best for viscous and dense crude oils such California Crude API 15 because they are required to be coated on mesh disks before exposing them to evaporation. A result of this method is given by Figure 7. It shows the changing composition of California Crude API 15 after 3 days of exposure or an equivalent evaporative exposure Q_E. An advantage was the increased rate of evaporation over the gas stripping method by 100 times. The larger area of oil exposed to a greater volume of air enhanced the weathering process.

Fresh EPS oil was also contacted with water in a generator column, and thus subjecting it to dissolution only. The gas chromatograms of the saturates and aromatics for Q_D (the ratio of water to oil volumes) of 10000 are shown in Figure 8. Analysis by the purge-and-trap technique revealed that the aqueous solubility of the oil decrease from 34.5 mg/L to 1.0 mg/L. The WSFs of the fresh and weathered oil are given by Figure 9 which shows that most of the volatile, water-soluble hydrocarbons such as benzene, toluene, ethylbenzene and xylenes were depleted by dissolution. Figure 10 gives the trend of the solubility of EPS oil versus the water to oil volume ratio Q_D. The solubility decreased with the depletion of the soluble aromatics.

Figure 11A is a gas chromatogram of a fresh heavy crude oil, California Crude API 15. It has a high asphaltene and tar content which accounts for its high viscosity. Its saturate and aromatic fractions (Figures 11B and 11 C) reveal that the heavy oil contains large amounts of highly volatile and soluble compounds.

California Crude API 15 was subjected to evaporation and dissolution on a water surface in long term

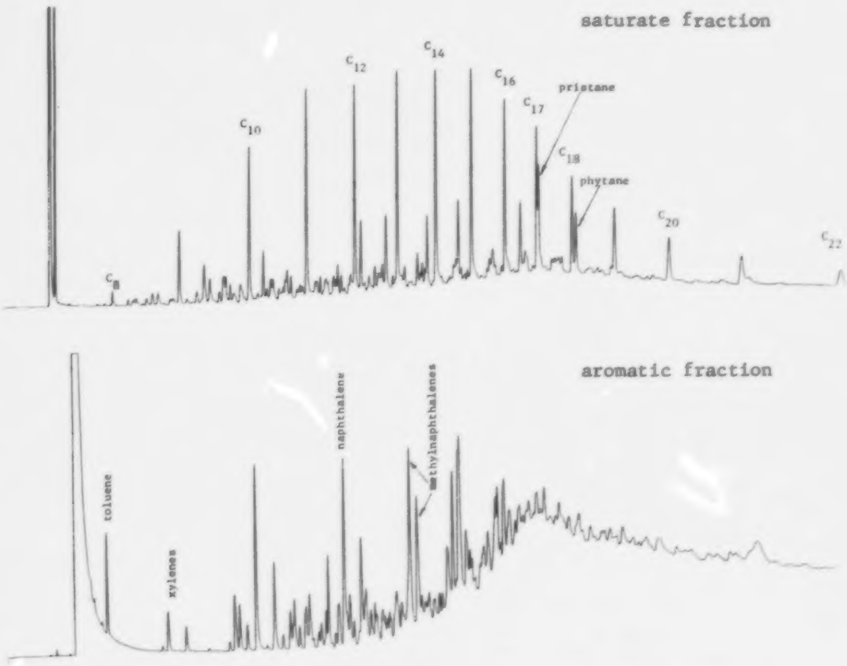

Figure 5. Saturate and aromatic fractions of EPS oil weathered using the air stripping method (Q_E=8060).

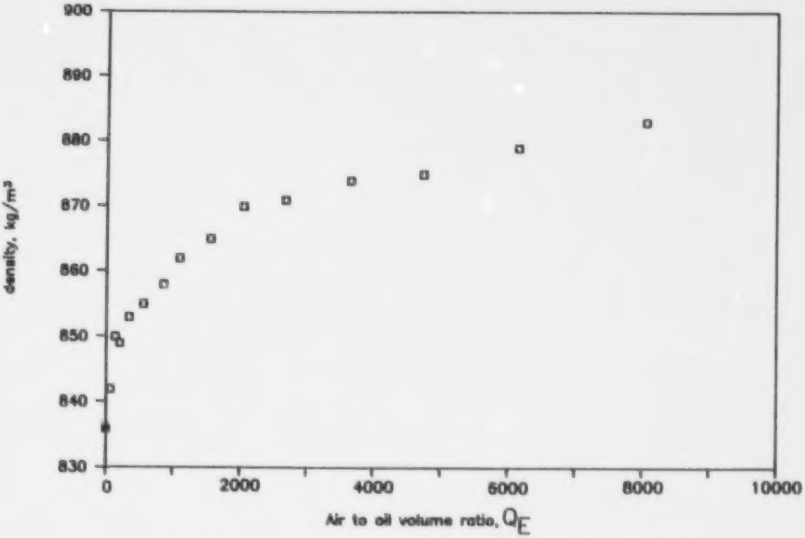

Figure 6. Density versus the air to oil volume ratio for EPS oil weathered using the air stripping method.

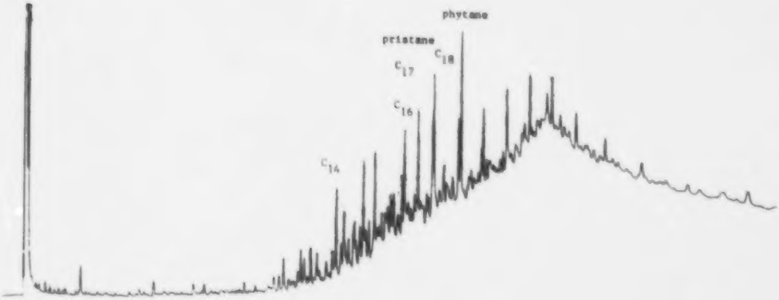

Figure 7. California Crude API 15 weathered using the rotating mesh disk method (after 3 days).

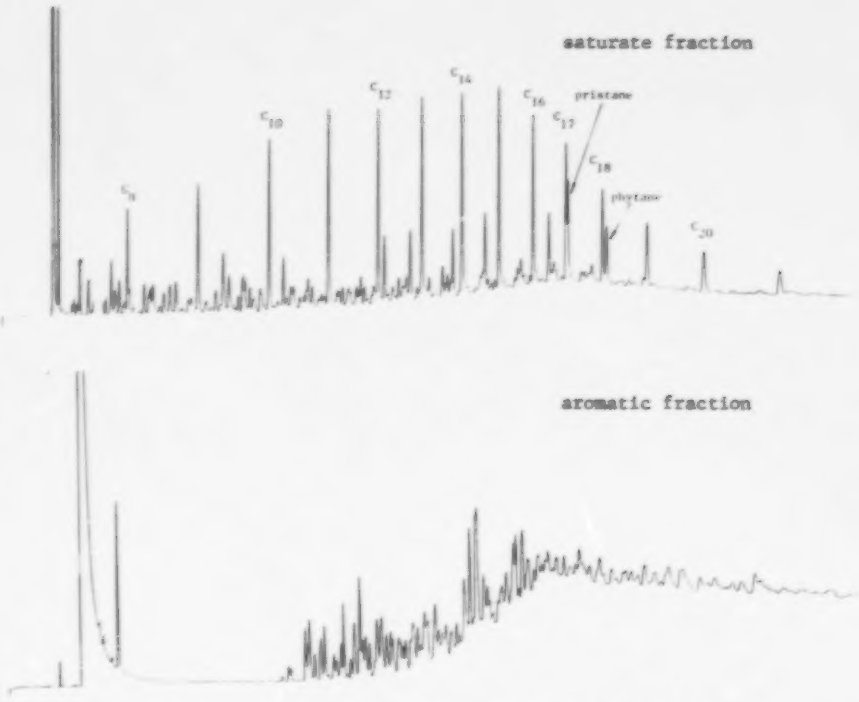

Figure 8. Saturate and aromatic fractions of EPS oil weathered using the generator column method (Q_D=10000).

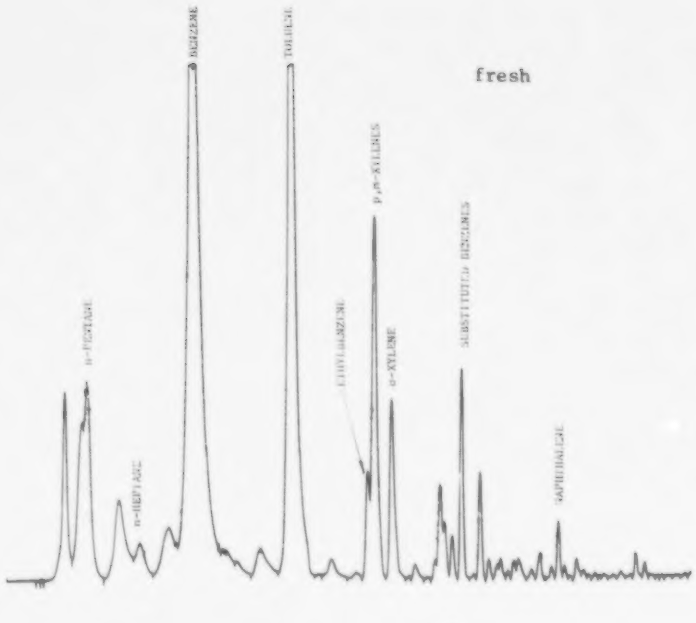

Figure 9. WSFs of fresh and weathered EPS oil.

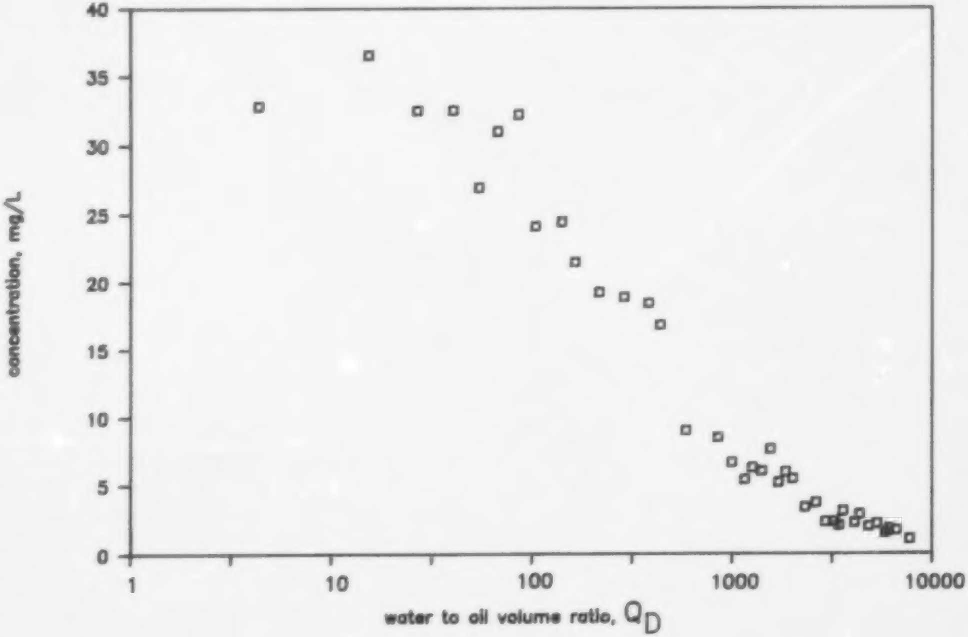

Figure 10. Aqueous solubility versus the water to oil volume ratio for EPS oil weathered using the generator column method.

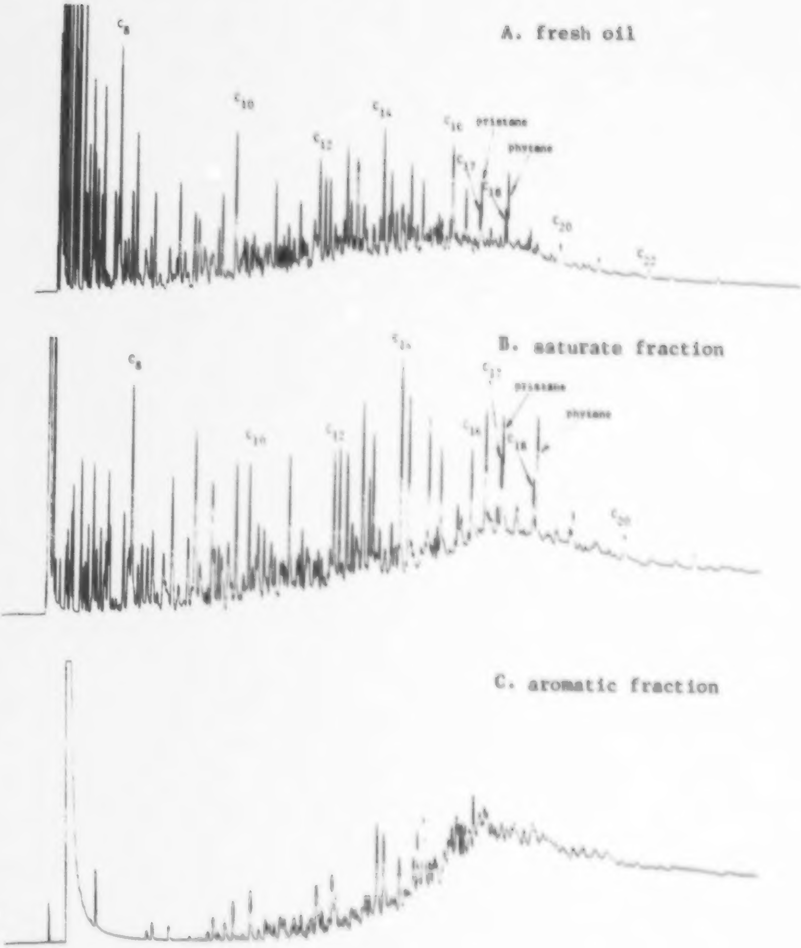

Figure 11. Gas chromatograms of fresh California Crude API 15 and its saturate and aromatic fractions.

weathering experiments. Spreading of the California Crude API 15 slick in distilled water occurred within several hours. In salt water, it spread to a lesser extent. The formation of a visible skin or crust was observed after two weeks. Tiny bubbles gradually appeared on the oil surface in both situations. After three months a 30-mm diameter oil droplet formed below the water surface and detached from the original mass in the distilled water experiment. This oil globule proved to be denser than the water because it sank into the water column. Further submergence of oil mass was observed in the next two months.

In the fifth month, an oil sample from the water surface was taken for gas chromatographic analysis. In addition, the first oil droplet was retrieved and frozen in the effort to obtain samples of the its skin/crust and interior for analysis. It proved difficult to obtain a crust sample because it was very thin, certainly less than 1 mm thick. Figure 12 illustrates the five-month weathering of the oil on the water surface and in the water column. The sunken oil was less weathered than the exposed oil on the water surface; the latter was depleted of all hydrocarbons up to C_{16}. Therefore, once submerged the oil was subjected to only dissolution which only causes a slight change in composition.

In the course of the experiments, there was no formation water-in-oil emulsions or "tar balls".

DISCUSSION

At this stage of the project, it is not possible to discuss the full results and develop conclusions, but it is useful to indicate the likely findings and the nature of the method by which the results can be modelled.

Clearly, reliable data on the extent of oil evaporation and dissolution can be obtained, but the results are specific to each oil and are not "generalizable". We envisage that the oil composition will be characterized as shown in the matrix in which the rows are of common volatility, or GC retention time, and the column classes of solubility or chemical structure. The elements to the top left will have the highest volatility and solubility. The amount in each element will be obtained by chemical analysis, that is, by GC or HPLC. Each row has a common air-oil partition coefficient K_{AO}, and each column has common solubility or water-oil partition coefficient K_{WO}. These partition coefficient are, of course, temperature dependent.

As discussed by Eastcott et al. (1987), the exposure to evaporation can be expressed as Q_E the ratio of air to oil volumes, and that to dissolution as Q_D the ratio of water to oil volumes. The fraction remaining of each element after exposure can then be approximated as

$$F = \exp(-Q_E*K_{AO}-Q_D*K_{WO})$$

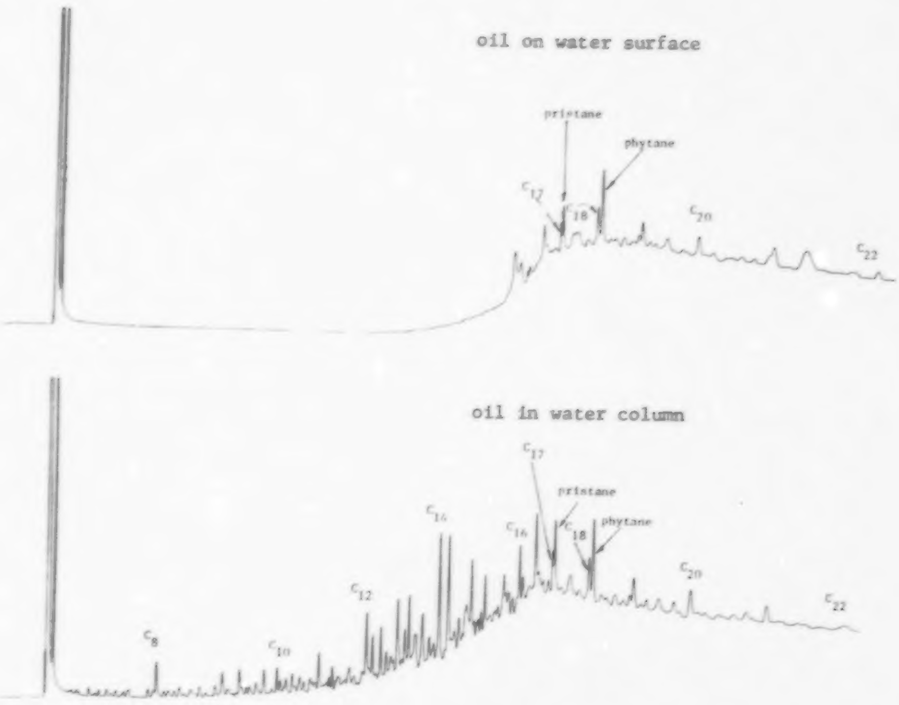

Figure 12. Long-term weathering of California Crude API 15 after 5 months.

The new oil matrix amounts can then be calculated and an overall composition deduced. The overall oil vapour pressure and solubility can be estimated. If densities and viscosities can be assigned to each element, the overall oil density and viscosity can be deduced.

The overall aims of the modelling effort are then to

- determine which element definition is most appropriate from the analytical and modelling viewpoints, and the optimal number of elements;
- express the initial oil composition in terms of element amounts;
- conduct weathering experiments to obtain changes in oil composition and properties;
- assign partition coefficients, densities and viscosities to each element;
- reconcile the model results with the experimental data, and in doing so develop appropriate "mixing rules", especially for viscosity.

A fascinating, important and difficult issue is that of "crust" formation. It should be straightforward to use the model to estimate weathering of the crust, although it may be necessary to include allowance for photolysis. The effect of the crust is believed to be to retard exposure of the interior oil, that is the oil is no longer well-mixed. We envisage that the model will calculate a changing viscosity as a function of time. As the viscosity increases, oil mixing becomes less rapid, surface-to-bulk exchange is reduced, and eventually a near-immobile surface layer forms. This could be described by a two-compartment model (Figure 13) in which the surface-interior exchange rate is a function of viscosity and diffusivity. At early stages of weathering the exchange will be sufficiently rapid that near homogeneous conditions will exist, but as viscosity increases a heterogeneity will develop and grow. A major unresolved issue is how to express this exchange rate reliably. We believe that it should be possible to formulate a model and calibrate it with experimental data.

It will then be possible to estimate the density of the oil mass from a knowledge of the relative proportions of the crust and interior volumes. Finally, the equations should be capable of being used for estimation of oil weathering at sea (preferably using real spill observed data) and for incorporation into oil spill models.

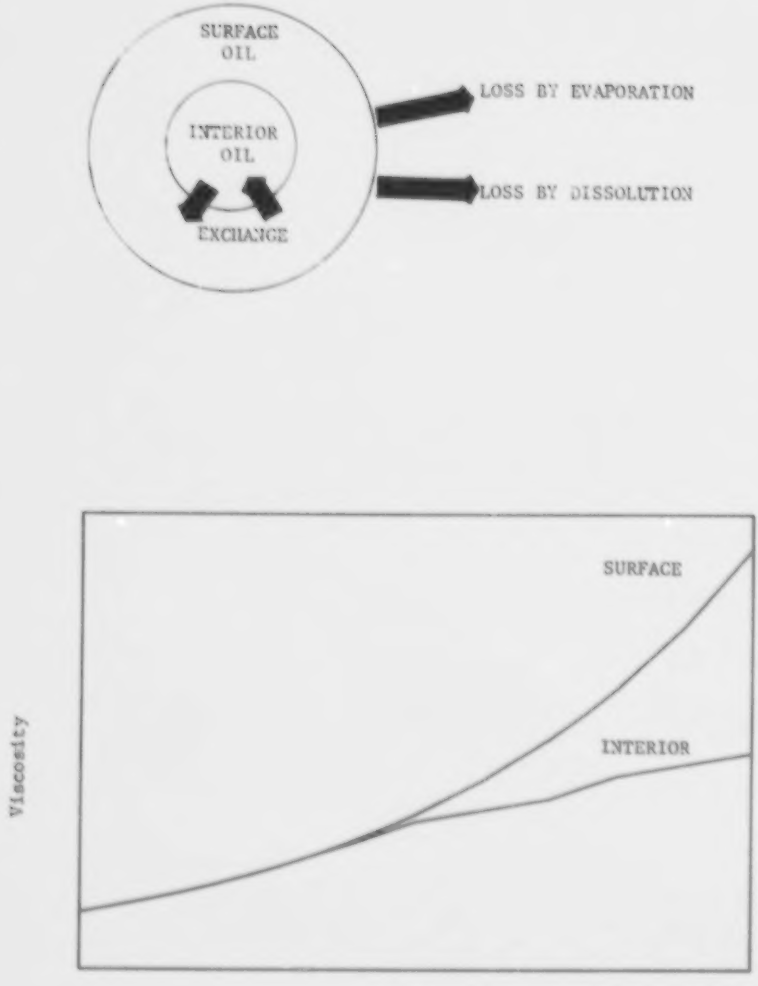

Figure 13. Two compartment model for "crust" formation.

CONCLUSIONS

The nature of the experimental program for determining the long-term weathering behaviour of heavy oils has been described and some illustrative results presented. The modelling approach by which the data will be processed has been outlined.

The first major unresolved issue is the optimal method by which the hydrocarbon mixture can be classified according to water solubility. When this is established it should be possible to estimate the magnitude of the matrix elements for each oil and test the models' validity against experimental data.

The second issue is the optimal treatment of "crust" formation, especially the crust thickness and exchange rates with the less-weathered interior oil.

ACKNOWLEDGEMENT

The authors are grateful for the financial support of Environment Canada and the US Minerals Management Services.

REFERENCES

Billington, J.W., G.L. Huang, F. Szeto, W.Y. Shiu and D. Mackay. 1988. Preparation of aqueous solutions of sparingly soluble organic substances: I. Single-component systems. Environ. Toxicol. Chem. 7:117-124.

Bobra, M.A. 1989. A Catalogue of Crude Oil and Oil Product Properties. Report EE-114. Environment Canada.

Cook, F.D. and D.W.S Westlake. 1976. Biodegradability of Northern Crude oil. Report No. QS-8116-000-EE-AI. Department of Indian and Northern Affairs, Ottawa.

Eastcott, L., W.Y. Shiu and D. Mackay. 1987. Weathering of Crude Oil in Surface Soils. Report from the University of Toronto for PACE (Petroleum Association for the Conservation of the Canadian Environment).

Lee, S.C., D. Mackay, F. Bonville, E. Joner and W.Y. Shiu. 1989. A Study of the Long-Term Weathering of Submerged and Overwashed Oil. Report EE-119. Environment Canada, Ottawa.

Mackay, D. 1987. Formation and Stability of Water-in-Oil Emulsions. Report EE-93. Environment Canada, Ottawa.

Payne, J.R. and C.R. Phillips. 1985. Petroleum Spills in the Marine Environment: The chemistry and formation of water-in-oil emulsions and tar balls. Lewis Publishers, Inc., Michigan.

Shiu, W.Y., A. Maijanen, A.L.Y. Ng and D. Mackay. 1988. Preparation of aqueous solutions of sparingly soluble organic substances: II. Multicomponent systems - hydrocarbon mixtures and petroleum products. Environ. Toxicol. Chem. 7:125-137.

Stiver, W. and D. Mackay. 1984. Evaporation rate of spills of hydrocarbons and petroleum mixtures. Environ. Sci. Technol. 18:834-840.

THE EFFECTIVENESS OF FERROCENE IN REDUCING SMOKE EMISSION FROM BURNING CRUDE OIL.

J.B.A. Mitchell
Dept. of Physics, University of Western Ontario, London, Ontario, Canada, N6A 3K7.

INTRODUCTION.

Oil spill cleanup is a difficult and expensive process that typically involves hundreds and even thousands of man-hours. It is frequently carried out under public scrutiny and has often prompted severe criticisms from environmentalists and concerned parties. An attractive method of clean-up is to simply ignite the oil and allow it to burn away. Such a technique would be rapid, would involve the minimum of personnel and be economical. A major concern would of course be to ensure that the conflagration would not represent a threat to personnel or property. This method is therefore best suited to spills occurring on open waters or in remote locations.

Studies by Brown and Goodman (1) have shown that oil spilled onto the ocean can be burned away efficiently provided that the combustion is initiated sufficiently soon after the spill has occurred and before wind and wave action have created an oil-water emulsion. A major problem however is the production of copious amounts of heavy smoke which is unsightly and in some cases environmentally damaging. This has mean't that oil combustion has been opposed by environmental groups as a viable clean-up method despite its efficiency.

Recent studies performed at the University of Western Ontario have shown that smoke emission from the combustion of crude oil can be reduced by as much as 90% by the addition of the compound ferrocene, to the fuel. These studies are described below.

PROPERTIES OF FERROCENE.

Ferrocene is the common name for bis-cyclopentadienyl iron which has the chemical formula $FeC_{10}H_{10}$ and the structure shown in figure 1. It is known as a sandwich compound for the iron atom is squeezed between two hydrocarbon rings. It was one of the first organometallic compounds to be synthesized and Wilkinson and Fischer received the Nobel Prize for Chemistry in 1973 for evaluating its structure. It is an orange, crystalline substance, insoluble in water but slightly soluble in hydrocarbon fuels to the extent of about 2% by weight. Most importantly for the application discussed here, it is

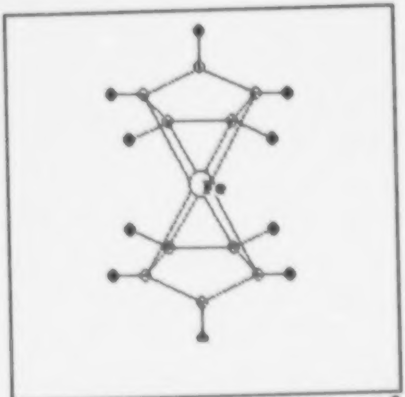

Figure 1. Structure of Ferrocene.

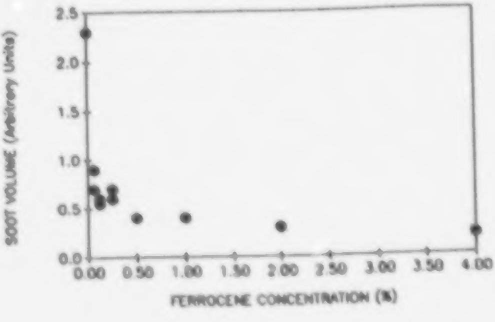

Figure 2. Collected soot volumes vs ferrocene concentration for samples of Norman Wells Oil.

non-toxic although, as with any other finely divided compound, precautions must be taken to avoid inhaling it.

Howard and Kausch, (2) have described a number of studies in which premixed ferrocene/fuel mixtures were burned in a variety of engines and combusters and generally it was found that ferrocene was a very effective smoke inhibiter. It does however have a serious drawback in these applications and that is that iron oxide deposits, left behind in the combustion chambers, can lead to engine fouling. As a result it has not seen widespread usage except in specialized military applications involving short duration use.

MECHANISM FOR SOOT INHIBITION.

The exact mechanism for soot formation is not well understood. The transition from the gaseous to the solid state, which takes place on a millisecond timescale, involves very rapid chemical reactions and surface catalytic processes which have not been specifically identified. The general picture, however, is that fast chemical reactions produce large precursor molecules which then act as nucleation centers onto which carbon growth occurs. The young soot particles thus produced, collide with each other and agglomerate, forming larger, mature particles. Since combustion necessarily takes place in an oxidizing environment, the immature soot particles are susceptible to oxidative attack producing gaseous carbon oxides. A number of fuel additives which inhibit soot formation are known. Some, such as alkali salts, when sprayed into flames, alter the electrical charge of the young soot particles and decrease the agglomeration rate so that larger soot particles, which are more resistant to oxidative attack, do not form. Others, such as barium salts, appear to enhance the oxidation process by means that are not clearly identified. (Mitchell and Miller, 3).

Ferrocene action however, is believed to be different. Studies by Ritrievi et al, (4), indicate that when a ferrocene/fuel mixture is burned, the ferrocene is rapidly oxidized to form small iron oxide particles which act as nucleation wntres. Carbon condenses out of the flame onto these particles to form young soot particles. The carbon is however, subsequently oxidized via reactions such as:-

$$FeO + C \rightarrow Fe + CO$$

In this way, the solid carbonacious particles are converted back to the gas phase and so smoke emission is reduced.

EFFECTIVENESS OF FERROCENE WITH CRUDE OIL.

As mentioned above, the main drawback to ferrocene usage is the fact that iron oxide particulates are formed during its combustion and these have deleterious effects on the operation of practical combustors. This, however, is not a problem for the oil spill application. Iron oxides are emitted into the atmosphere but they are non-toxic and are produced in much less quantities than soot particles. A series of studies was initiated therefore to determine the effectiveness of ferrocene addition in combatting smoke emission from crude oil combustion. The majority of these studies were conducted using Norman Wells Crude Oil supplied by ESSO Resources Canada Ltd.

A typical experiment involved burning a premixed ferrocene/crude oil sample in a ceramic crucible and collecting the emitted particulates on a glass-fibre filter attached to a vacuum pump. Following the burn, the soot volume was measured. All tests were conducted using equal weights of oil/additive samples and the results obtained are comparative, rather than absolute, in nature. Figure 2 shows a plot of soot volume collected versus ferrocene concentration. It can be seen that indeed, ferrocene is very effective, producing up to a 90% reduction in particulate emission. It is also evident that only small concentrations of ferrocene need be used.

Tests were also performed on other crude oils, supplied by Environment Canada and the tabulated results are shown in TABLE I.

TABLE I.

Soot production from the combustion of various oils with and without the addition of ferrocene.

Oil Sample	Ferrocene Concentration (% by Wt)	Soot Volume (ml)	% Reduction
Norman Wells	0	2.3	0
Norman Wells	4	0.2	91
Norman Wells	2	0.3	87

Oil Sample	Ferrocene Concentration (% by Wt)	Soot Volume (ml)	% Reduction
Norman Wells	0	2.3	0
Alberta Sweet Mix, (ASM).	0	1.2	0
ASM	2	0.2	83
ASM	0	1.2	0
ASM	2	0.35	71
Prudhoe Bay	0	1.6	0
Prudhoe Bay	2	0.1	94
Prudhoe Bay	0	1.6	0
Prudhoe Bay	2	0.25	84

These results show that ferrocene is a very useful soot inhibiter across the spectrum of crude oils. Since the intended application for this compound is the combustion of oil spills over water, tests were performed in which samples of oil and an oil/ferrocene mixture floating on water were burned in a crucible and the soot collected. This test is much less definitive for as is well known, Evans et al. (5), the combustion of oil floating in water involves a violent burning phase which terminates in extinction and so, in a small scale apparatus, it is difficult to control the burn time. Again however, our results, (shown in Table II), indicate that ferrocene produces very effective soot inhibition in this case.

TABLE II

Soot Volumes produced from the combustion of oil samples burned on their own and floating on water.

Sample	Soot Volume (ml)
15g Norman Wells Oil	2.3
15g Norman Wells Oil/4% Ferrocene	0.2
10g Norman Wells on Water	1

Sample	Soot Volume (ml)
10g Norman Wells/4% Ferrocene on Water	0.25

A STUDY OF OTHER IRON COMPOUNDS.

The tests described above were all performed using premixed ferrocene/oil samples. For use in an oil spill on water application, however, a method must be devised for introducing the additive into the spill. This is not straightforward for ferrocene does not dissolve rapidly in oil and, being more dense than seawater, if added directly in solid form, quickly sinks through the oil layer into the underlying water.

Since it is believed that iron is the active ingredient of ferrocene, it was postulated that perhaps other compounds with more suitable physical properties may be equally effective. A number of compounds were identified which were insoluble in water but soluble in oil. Two of these were examined. These were iron stearate and iron 2-ethylhexanoate. The former is a light powder which rapidly dissolves in oil, the latter is a liquid with a density less than that of water. Tests were performed on both these compounds but unfortunately, as indicated in Table III, neither was particularly effective in inhibiting soot emissions.

TABLE III.

Soot volumes collected from tests using different iron additives.

Additive.	Concentration (% by Wt).	Soot Volume (ml).
Oil only.	-	2.3
Ferrocene.	4	0.2
Iron Stearate.	4	1.4
Iron 2-Ethyl Hexanoate.	2	1.6

A number of surface analytical tests were performed on soot samples arising from the combustion of ferrocene/oil, iron stearate/oil and iron 2-ethyl hexanoate/oil samples. Energy dispersive x-ray analysis, (EDX) showed that in fact, while iron was a significant constituent of soot collected from a ferrocene/oil burn, it was entirely absent from soot collected in the other two cases, (See figure 3). This shows that ferrocene owes its effectiveness to its ability to introduce iron into the combustion environment. The reason for this is not well established but it could be due to the fact that ferrocene sublimes when heated. Auger Electron Spectroscopy, (AES), and X-ray Photoelectron Spectroscopy analyses were also performed on the soot samples arising from the ferrocene/oil and iron stearate/oil soot burns. During the Auger analysis, ion beam sputtering was used to remove outer layers of the samples and spectra were taken at different depths. This revealed that indeed, the iron resides in the interior of the soot particles, as expected from the model in which the iron oxide particles behave as nucleation centres, (see figure 4) and that much of the iron is in the oxide form. Again these tests showed that the soot produced from the iron stearate/oil combustion was iron deficient.

A METHOD OF INTRODUCING FERROCENE INTO AN OIL SPILL.

For the present it would appear that ferrocene is the most effective soot inhibiting additive that could be used for oil spill combustion. It therefore is important to find an appropriate method for introducing it into the spill. A search for good solvents for ferrocene found that toluene could be used to produce a concentrated solution. When added directly to oil and subsequently burned, however, it produced copious amounts of black smoke.

The ability of toluene to bring ferrocene into solution is however useful as demonstrated in the following test. The solution was absorbed in vermiculite and allowed to dry. The ferrocene soaked vermiculite was then added to the oil, upon which it floated,and after an hour or so, sufficient ferrocene was found to have dissolved in the oil to inhibit smoke emissions to the level experienced in premixed ferrocene/oil burns. It should be noted however that the best results were obtained when the vermiculite was removed prior to combustion. When the vermiculite was allowed to remain, combustion of the ferrocene itself produced considerable amounts of iron oxide particles.

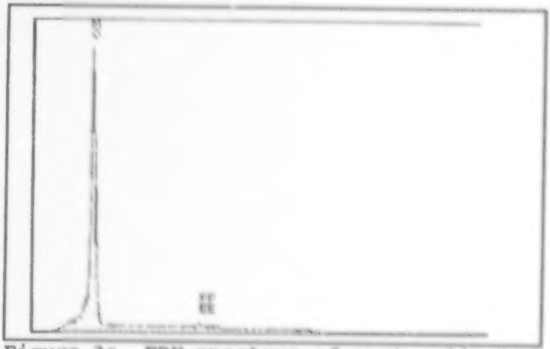

Figure 3a. EDX spectrum of soot collected from combustion of Norman Wells Oil/ferrocene mixture. Note the iron peak.

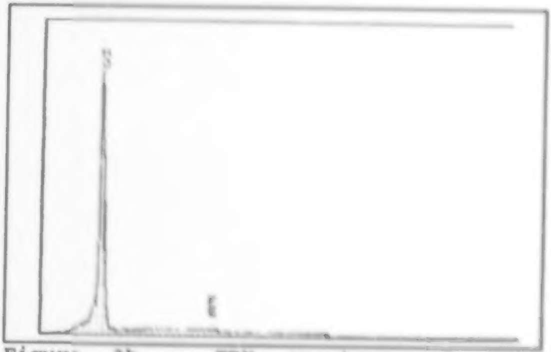

Figure 3b. EDX spectrum of soot collected from combustion of Norman Wells Oil/iron stearate mixture. Note the absence of iron peak.

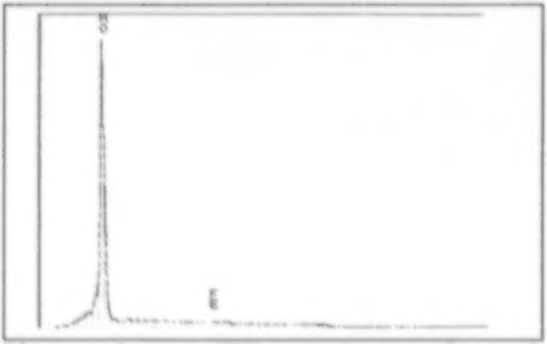

Figure 3c. EDX spectrum of soot collected from combustion of Norman Wells Oil/iron 2-ethyl hexanoate mixture. Note the absence of the iron peak.

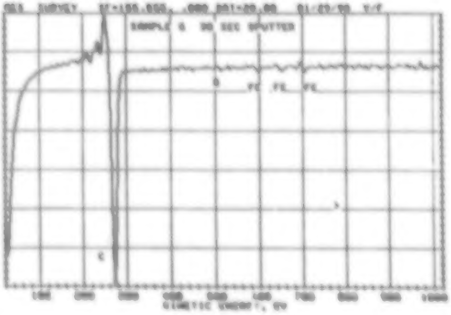

Figure 4a. Auger spectrum of soot collected from combustion of Norman Wells Oil/ferrocene mixture. 30 seconds sputter time, iron peaks very small.

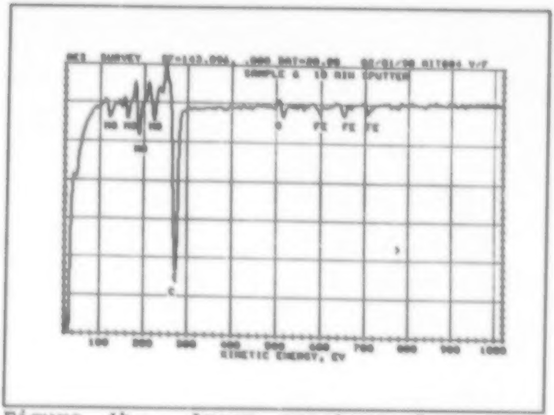

Figure 4b. Auger spectrum from same sample as shown in 4a, after 18 minutes of sputtering, (corresponding to a depth of 0.5 microns into sample). Note the three iron peaks.

CONCLUSIONS.

These findings are very exciting for they offer the promise of being able to burn crude oil spills with greatly reduced smoke emissions. Clearly there is room for improvement in the method of introducing ferrocene into the spill and work is progressing in this direction. It is intended that mesoscale tests will commence in the near future and that these will include realistic oil on water burns.

ACKNOWLEDGEMENTS.

I should like to gratefully acknowledge the generous support of ESSO Resources Canada Ltd. This research has greatly benefitted from many useful discussions with Dr Ron Goodman of that organization and with Mr. Mervin Fingas of Environment Canada. Thanks are also due to Dr. Tammy Chen and Mr. Ross Davidson of Surface Science Western for performing the surface analyses.

REFERENCES.

1. Brown, H.M. and Goodman, R.H. "In Situ Burning of Oil in Ice Leads," Proceedings of the Ninth AMOP Technical Seminar, June 10-12, 1986, Edmonton, Alberta, Canada, Environment Canada, Ottawa, K1A 0H3, 1986.
2. Howard, J.B. and Kausch, W.J. Soot Control by Fuel Additives. Prog. Energy and Combust. Sci. 6, 263, 1980.
3. Mitchell, J.B.A. and Miller, J.M. Studies of the Effects of Metallic and Gaseous Additives in the Control of Soot Formation in Diffusion Flames. Combustion and Flame 75, 45, 1989.
4. Ritrievi, K.E., Longwell, J.P. and Sarofim, A.F. The Effects of Ferrocene Addition on Soot Particle Inception and Growth in Premixed ethylene Flames. Combustion and Flame, 70, 17, 1987.
5. Evans, D. et al. Burning, Smoke Production and Smoke Dispersion from Oil Spill Combustion . NIST Report, 1989.

A Study of the Formation of Water-in-Oil Emulsions

by
Mark Bobra
Consultchem
P.O.Box 4472, Station 'E'
Ottawa, Ontario

Introduction

The formation of stable water-in-oil emulsions (mousse) has long been a source of problems for the oil industry. In the oil field, emulsions cause difficulties in production, storage and transportation. When oil is spilled in the marine environment, its emulsification behaviour will play a crucial role in determining the ultimate fate of the oil, and the effectiveness of countermeasure techniques.

Canevari (1982) pointed out that there are two possible mechanisms that are responsible for the formation of stable water-in-oil emulsions. The first mechanism is due to the action of naturally occurring surface active agents (surfactants) in petroleum and the second is due to the presence of solid particles. The mechanism by which surfactants stabilize emulsions is fairly well understood. Briefly, surfactants are amphipathic molecules which means that one section of the molecule is soluble in oil (lipophilic) and the other section is soluble in water (hydrophilic). Because of this molecular structure, surfactants tend to concentrate at the oil-water interface where they form interfacial films. This film reduces the interfacial tension between oil and water, thereby decreasing the amount of work required to introduce one phase into the other; and this film forms a barrier around droplets thus inhibiting coalescence. A general rule of thumb in surfactant chemistry is that surfactants with mainly lipophilic character (that is, predominantly oil soluble) form water-in-oil emulsions. Whereas, surfactants with mainly hydrophilic character (predominantly water soluble) produce oil-in-water emulsions. Examples of the latter are oil spill dispersants. (Rosen 1978, Becher 1983)

In the second mechanism of emulsion stabilization, the emulsifying agents are solid particles which in only a specialized sense can be considered to be surface active (Becher 1977). For solids to act as emulsifying agents, the particles must possess certain properties. The particles must be very small relative to the droplet size. The particles must collect at the interface and they must be 'wetted' by both the oil and water phases. Figure 1 shows three ways that particles may distribute themselves between an oil-water interface. If the particle is preferentially wetted by the oil, the contact angle between the oil-water-solid boundary, Θ is greater than 90° and a water-in-oil emulsion will form. If the particle is preferentially wetted by water, Θ is less than 90° and an oil-in-water emulsion will form. If the contact angle is much greater or lesser than 90°, the emulsion will be unstable. Stable emulsions form when the contact angle is near 90°.

It has long been recognized that indigenous petroleum emulsifying agents are concentrated in the higher boiling fractions (boiling point > 370°C) and particularly in the residuum (Lawrence and Killner 1948). Likewise, it is generally accepted that asphaltenes and waxes play key roles in the emulsion process (Birdie et al. 1980; Mackay 1987). These compounds are believed to be the main constituents of interfacial films which encapsulate water droplets within mousse. These films have been shown to have high mechanical strength and thus act as physical barriers which prevent droplet coalescence (Blair 1960, Hasiba and Jessen 1967). This in turn gives rise to the extreme stability of mousse. The phenomena of film formation has yet to be fully understood.

Although the role of solid particles in petroleum emulsification has been recognized for some time (van der Waarden 1958), the importance of this mechanism to mousse formation has not been completely appreciated. Eley et al. (1976) examined the interfacial surfaces of water-in-oil emulsions using an electron microscope. Their micrographs clearly showed particulate formations on the oil side of the interface. They isolated structures which they concluded to be asphaltene granules (dimensions: 10-30 nm) and plates of wax (<100nm). Thompson et al. (1984) showed that wax particles and associated solids exert considerable influence upon the emulsion stability of a waxy North Sea crude. They found that removal of particles reduced emulsion stability. They also showed that the emulsion behaviour of an oil can be changed dramatically by altering the size of the wax particles. The importance of this finding is that whether or not the oil formed a stable emulsion was dependent upon the physical form of the emulsifying agent (small versus large wax crystals) and not upon any changes in the oil's chemical composition or bulk properties. Similarly, Eley et al. (1988) demonstrated that by varying the aromatic/aliphatic ratio of a synthetic oil they could control the precipitation of asphaltenes and in turn, the extent of emulsification.

The aim of the work described in this paper was to elucidate the role that physiochemical factors play in determining an oil's susceptibility to emulsify. This was done by using model oils of known composition to examine the importance of oil chemistry in the emulsification process.

Oil Chemistry

The main constituents of any oil can be grouped into four broad classes of chemicals. These being: Alkanes (also sometimes called saturates or aliphatics); Aromatics; Resins; and Asphaltenes. Previous studies have identified that asphaltenes, resins and waxes (which are part of the alkane group) play a role in emulsification. It is important to realize how these components are defined and to have an understanding of their basic chemistry. Different methods of separating these fractions from oil are likely to produce different materials.

Waxes

Simple definitions of petroleum wax are: the material in an asphaltene/resin-free oil which are insoluble in the solvent methyl ethyl ketone or insoluble in dichloromethane at 32°C. Another definition for petroleum wax is the high molecular weight paraffinic substances which crystallize out from an oil when cooled below the pour point. Petroleum wax is normally divided into two sub-categories: paraffin wax and microcrystalline wax. Paraffin waxes are normal alkanes with 20 to 40 carbon atoms and melting points from 32 to 71°C. Microcrystalline wax mainly consists of iso-alkanes with 35 to 75 carbon atoms and has a melting point from 54 to 93°C (Clark 1988).

Resins

Resins are complex high molecular weight compounds containing oxygen, nitrogen and sulphur atoms. They are polar and have strong adsorption tendencies. The term "resins" has been defined in various ways but it is generally considered to be the material that remains in solution after the asphaltenes have been removed by precipitation and which will adsorb onto surface-active material (such as Fuller's earth).

Petroleum resins are often considered to be low molecular weight asphaltenes but usually contain a higher percentage of saturated aliphatic and naphthenic structures in their molecules. Molecular weights of resins are assumed to range from about 800 to 1500.

Asphaltenes

Asphaltenes are defined by their solubility behaviour; asphaltenes are soluble in aromatic solvents and insoluble in alkane solvents. Asphaltenes are generally considered to consist of condensed aromatic nuclei which carry alkyl and alicyclic systems with heteroatoms (nitrogen, oxygen, sulphur, metals, salts) scattered throughout in various locations. Asphaltene molecules can have carbon numbers from 30 to over 40, and molecular weights from 500 to 10,000 have been cited in the literature. Asphaltenes are characterized by a C-H ratio of close to one and a specific gravity near one. Relatively little is known about asphaltene structures and much of the data is inferred. Figure 2 shows a hypothetical structure of an asphaltene (Speight 1981).

The physical nature of asphaltenes as they exist in petroleum is still speculative. But it is now generally accepted that petroleum should be viewed as a colloidal system. Asphaltene molecules agglomerate to form clusters similar to micelles. These asphaltene micelles interact with the resins which in turn peptize the asphaltenes and enables a stable colloidal dispersion to exist. Since these colloids contain most of the polar material found in the oil, they essentially determine the interfacial properties (Clark 1988; Long 1979; Speight 1981; Neumann et al. 1981).

Solubility Theory

Griffith and Siegmund (1985) used the concept of solubility to describe the precipitation behaviour of asphaltenes from fuel oils. In this context, oil is viewed as being comprised of a solute and a solvent; the solute being the asphaltenes and the solvent being the rest of the oil. The Hildebrand-Scatchard equation (Barton 1983) is the basic equation that can be used to describe the solubility behaviour of asphaltenes in petroleum.

$$RT \ln (A_a/X_a) = \frac{M_a \phi_s^2 (\sigma_a - \sigma_s)^2}{p_a}$$

where:
A_a = activity coefficient of asphaltenes
X_a = mole fraction of asphaltenes
M_a = molecular weight of asphaltenes
ϕ_s = volume fraction of solvent
σ_a = Hildebrand solubility parameter of the asphaltenes
σ_s = Hildebrand solubility parameter of the solvent
p_a = density of asphaltenes
R = gas constant
T = temperature

It is assumed that asphaltenes can be treated as homogeneous material and that A_a = 1. The equation can be written in terms of the maximum amount of asphaltenes soluble in oil, X_a. If the amount of asphaltenes present in the oil exceeds X_a, the excess asphaltenes will precipitate.

$$\ln X_a = \frac{- M_a \phi_s^2 (\sigma_a - \sigma_s)^2}{p_a RT}$$

Figure 1 Three ways solid particles may be distributed in an oil/water interface. The particle on the left is more wetted by the water than the oil thus being situated primarily in the aqueous phase, whereas the particle to the right exists primarily in the oil phase. The center situation illustrates a solid particle equally wetted by both the oil and water phase.

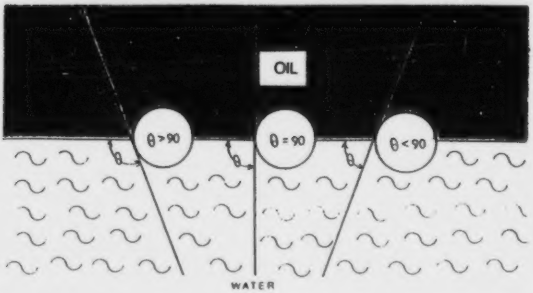

Figure 2 Hypothetical structure of a California crude oil asphaltene.

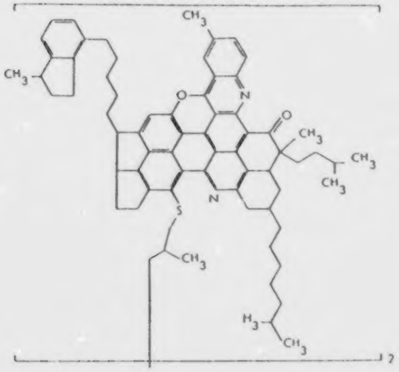

Experimental

The model oils used in these experiments consisted of three main components: 1. an alkane component; 2. an aromatic component; and 3. the potential emulsifying agent(s). The alkanes tested were n-octane, n-tetradecane, a light paraffin oil, and a heavy paraffin oil. The aromatics used were p-xylene, phenyl octane, dimethyl naphthalene, and diphenyl methane. Asphaltenes were precipitated from a California crude oil (API gravity: 11) using n-pentane at a pentane to oil ratio of 40:1 (Speight 1981). Asphaltenes and resins were precipitated together from the California crude using ethyl acetate (Neumann et al. 1981). Resins were precipitated from de-asphaltized oil using ethyl acetate. Precipitated materials were collected on a 0.45 micron filter, dried by a nitrogen purge, and stored in the dark under a nitrogen headspace. Other materials used were paraffin wax (Aldrich Chemical Company, melting point: 56-61°C) and graphite powder (Aldrich Chemical Company).

Model oils were prepared by adding the emulsifying agent to the aromatic component. The mixture was vigorously shaken for one hour on a shaker table. The alkane component was then added and the mixture was again shaken for one hour. 30 mL of the oil was poured into a 500 mL Fleaker containing 300 mL of artificial seawater. The Fleaker was sealed and allowed to stand for approximately 20 hours before undergoing the emulsion formation and stability test described by Bobra (1989). Briefly, the test involves rotating the Fleaker at 65 rpm for one hour and then allowing the mixture to rest for one-half hour before measuring the size of the emulsion and the fraction of oil that emulsifies, F. The rotation/rest cycle is repeated three more times. An indiction of an oil's tendency to emulsify is given by F_o, the fraction of oil that emulsifies when F is extrapolated to time zero. The stability of the emulsion is obtained by allowing the emulsion to rest for 24 hours and then measuring the fraction of oil that remains in the emulsion, F_f. The water content of stable emulsions were also measured. The following criteria set by Mackay et al.(1982) classify emulsion behaviour.

F_o	Emulsion formation tendency
0 to 0.25	not likely
0.25 to 0.75	fairly likely
0.75 to 1	very likely

F_f	Emulsion stability
0 to 0.25	unstable
0.25 to 0.75	fairly stable
0.75 to 1	very stable

The rheological properties of stable emulsions were measured using a Haake RV20 Rotoviscometer equipped with a M5/SV1 sensor. The programmed shear rate was 0 to 100 (s^{-1}) in 10 minutes and 100 to 0 (s^{-1}) in 10 minutes. The yield point values were determined from the increasing shear rate curves. The yield point can be considered to be an indiction of the "solid" character of the emulsion. It is the force required to change the emulsion from a "solid" to a flowing liquid. For the sake of comparison, under these same shear conditions mayonnaise has a yield point of 114 Pa and two samples of 18 day-old mousse from the Valdez spill had values of 17 and 121 Pa.

The size distribution of water droplets were determined using a Lab-Tec 1000 particle size analyser and a Zeiss Axioskop light/fluorescence microscope.

All experiments were conducted at 15°C.

Results and Discussion

Effect of Asphaltenes

Figures 3 to 6 show the influence of the alkane/aromatic ratio and the influence of increasing asphaltene content upon F_o, F_f, water content and yield point. The alkane component is heavy paraffin oil and the aromatic component is xylene. At an asphaltene concentration of 0.01 g/mL (1%), no stable emulsions are formed. At an asphaltene concentration of 0.025 g/mL (2.5%), the model oil has a tendency to emulsify (F_o=1) when the oil is 50% alkane and 50% aromatic, and this emulsion is only marginally stable (F_f=0.5). When the asphaltene content is increased to 0.05 g/mL (5%), stable emulsions are readily produced for oils containing 50 to 95% alkane component. Likewise, at an asphaltene concentration of 0.1 g/mL, stable emulsions form for oils containing 35 to 80% alkane. Figure 5 shows that the water content of stable emulsions are between 80 to 90%. The change in yield point as a function of alkane composition, Figure 6, clearly shows that there is a maximum value for each concentration of asphaltenes. For oils containing 5% asphaltenes this maxima occurs at 80% alkane, and for oils containing 10% asphaltenes this occurs at 70%.

The results illustrate several important points concerning the influence of the alkane/aromatic ratio upon an oil's emulsification behaviour. The amount of asphaltenes precipitated out of solution is determined by the alkane concentration. Figure 7 shows the percent of asphaltenes precipitated as a function of alkane concentration for an oil containing 5% asphaltenes. Clearly, the amount precipitated is important in determining the emulsification of the oil. But it would also appear that the alkane/aromatic ratio controls other factors which are involved in emulsification. The size of the asphaltene particles are determined by the alkane/aromatic ratio and this is particularly true given the method by which these model oils were prepared. Asphaltenes were first dissolved in the appropriate quantity of xylene and then the paraffin oil was added which causes the asphaltenes to precipitate out of solution. When the model oil is predominantly composed of paraffin oil, this precipitation mechanism does not occur and the asphaltene particles maintain their original dimensions (> 1 microns). These particles are too large to effectively stabilize water droplets. This was confirmed by microscopic examination of the oils. When model oils which were prone to emulsification were examined under the microscope, individual particle sizes could not be accurately determined because the particles were at the limit of resolution (<0.5 microns). But it could be seen that collectively the particles formed a continuous layer of finely dispersed particulates which are closely packed together. As the alkane content of the oil increased, the particles became more tightly packed and increased in size. An interesting phenomenon was observed when model oils with high aromatic content were viewed under the microscope. The actual precipitation of asphaltenes could be observed as the oil evaporated. Particles would precipitate out in a uniform distribution covering the slide with a film of submicron particles.

Figure 8 shows the interfacial tension, as measured by the duNuoy ring method, decreases as the aromatic content of the oil increases. It would appear that changes in interfacial tension have little to do with the emulsification behaviour of the model oils.

It would be expected that the alkane/aromatic ratio will have some effect on the contact angle between the particles and the interface, since oil composition will influence the wettability of particles. A simple experiment was performed which demonstrated the importance of the alkane/aromatic ratio on the contact angle. A series of oils of the same alkane/aromatic composition as previously tested were prepared and subjected to the emulsification test but instead of asphaltenes, graphite powder (0.05 g/mL) was used as the emulsifying agent. Graphite is insoluble in both xylene and paraffin oil. Therefore, there will be no changes in its physical form. The results from this experiment showed that stable emulsions only formed at an alkane/aromatic ratio of 1:1. Unfortunately, facilities to measure contact angle were not available and therefore, this effect of alkane/aromatic ratio upon contact angle, and in turn upon emulsification, could not be substantiated. The results from this experiment indicate that this influence upon contact angle is an extremely important determinant for emulsification by solid particles.

Figure 3: Fo versus % alkane
at different asphaltene concentrations

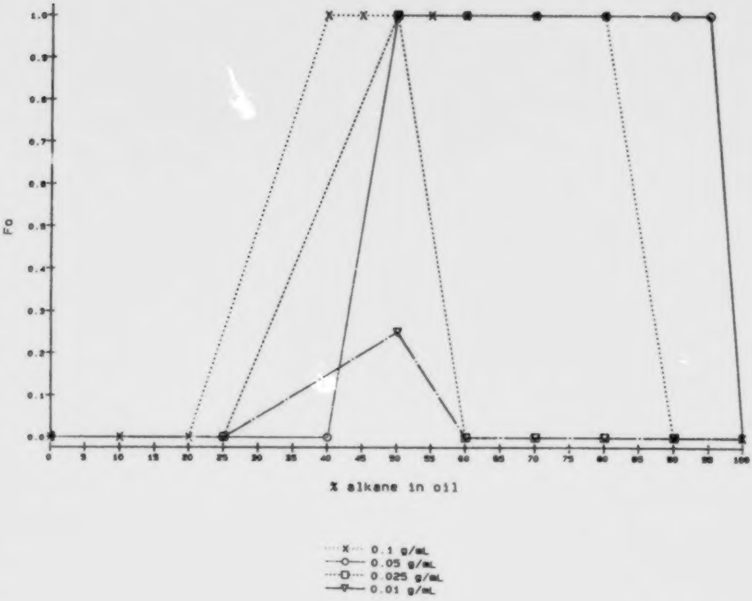

Figure 4: F final versus % alkane

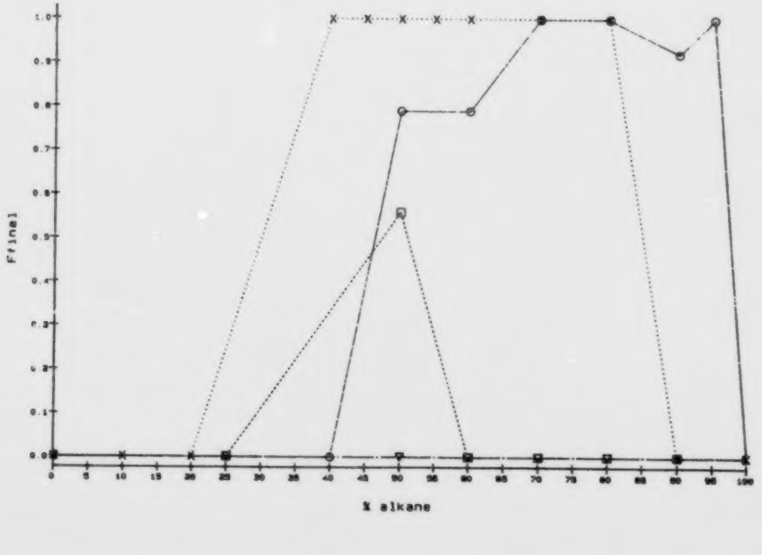

Figure 5: Water content vs % alkane

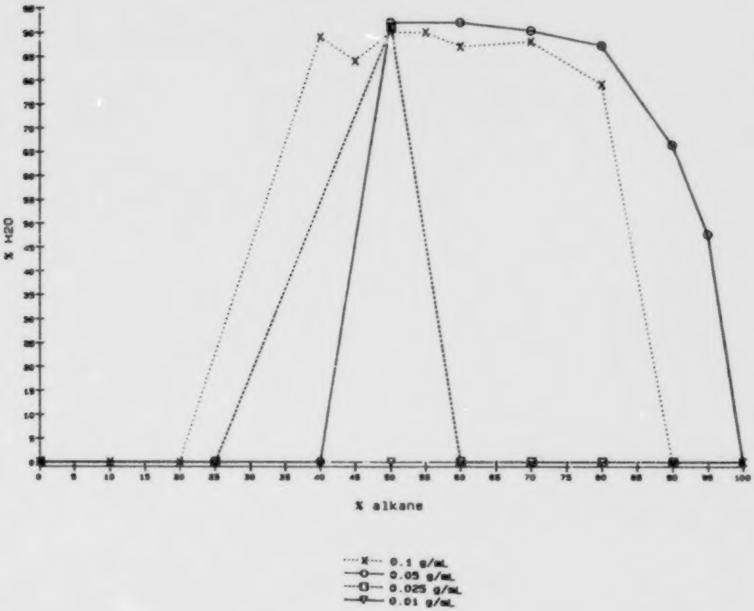

Figure 6: Yield point vs % alkane

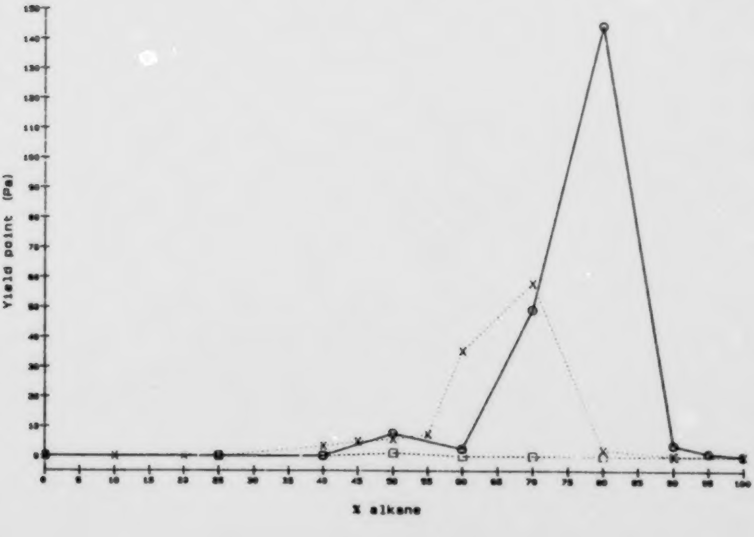

Figure 7: % asphaltenes precipitated versus % alkane in oil.
model oil: heavy paraffin oil/xylene containing 0.05 g/mL asphaltenes

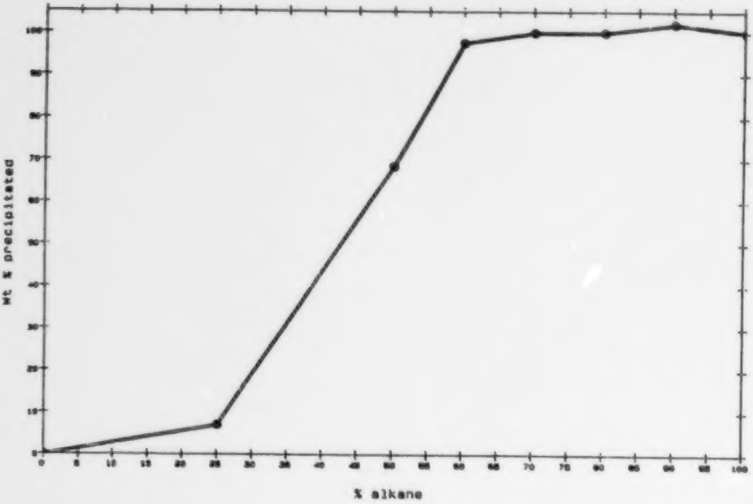

Figure 8: Interfacial Tension vs % alkane
for heavy paraffin oil/xylene model oil

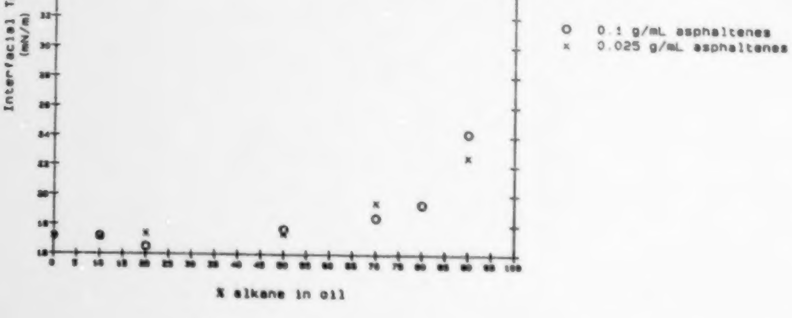

Effect of Aromatic Component

Figures 9 to 12 show F_o, F_f, water content, and yield point versus percent alkane for five different model oils consisting of heavy paraffin oil (HPO), 5% asphaltenes, and five different aromatic solvents. These being xylene; phenyl octane (PO); dimethyl naphthalene (DMN); diphenyl methane (DPM); and an equal volume mixture of the four solvents (MIX). As the results illustrate the aromatic component has a profound effect upon the emulsification behaviour of the oil. This can be best explained in terms of the Hildebrand solubility parameter, σ (units: $MPa^{1/2}$). These parameters can be either determined experimentally, calculated, or found in reference text (Barton 1983). The values for these parameters are 24.7 for the asphaltenes; 15.0 for heavy paraffin oil; 18.0 for xylene; 17.5 for phenyl octane; 21.0 for dimethyl naphthalene; 19.5 for diphenylmethane; and 19.0 for the mixture. From the Hildebrand-Scatchard equation, it can be seen that the amount of asphaltenes soluble in oil, X_a, is controlled by the term $(\sigma_a-\sigma_s)^2$. As $(\sigma_a-\sigma_s)^2$ increases, the amount of asphaltenes soluble in oil decreases, and any excess asphaltenes will precipitate. Therefore, the likelihood of producing a stable emulsion increases.

Figures 13 to 16 show F_o, F_f, water content, and yield point as a function of $(\sigma_a-\sigma_s)^2$ for the five model oils. It can be seen that most stable emulsions are formed when $(\sigma_a-\sigma_s)^2$ has a value between 60 and 90. Stable emulsions are not formed above a $(\sigma_a-\sigma_s)^2$ value of 90 in these experiments because, as previously mentioned, the asphaltene particles are too large to stabilize the water droplets. This is an artifact of the experimental design. It is expected that stable emulsions would form above this value if the chosen alkane/aromatic pairs allowed for the precipitation of asphaltenes to occur within the oil, thus providing particles which are an effective size.

The solvency power of the model oil, σ_s, controls the amount of asphaltenes that precipitate. If the solvency strength of the aromatic component is decreased, asphaltenes will be less soluble in the oil. This is shown in Figures 9 and 10, the oil containing phenyl octane (the lowest σ value of the aromatics tested) has the largest range over which stable emulsions are formed.

Figure 9: Fo vs % alkane
different aromatic components

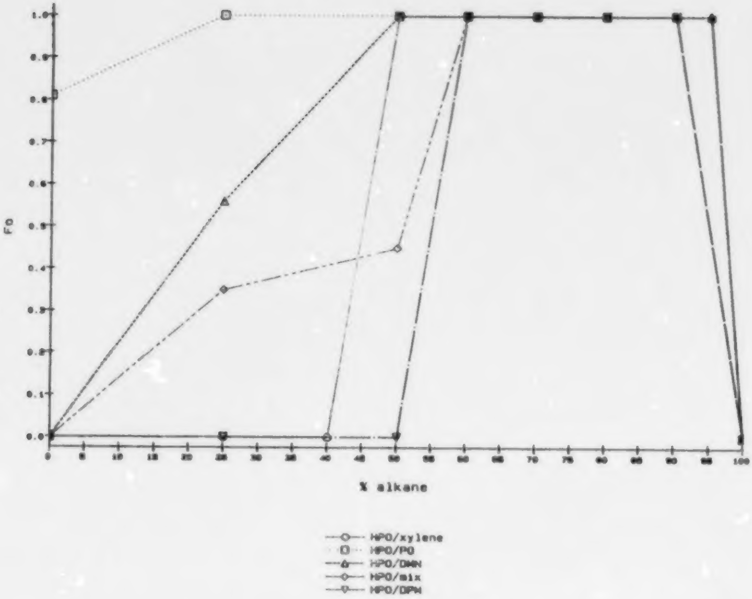

Figure 10: F final vs % alkane

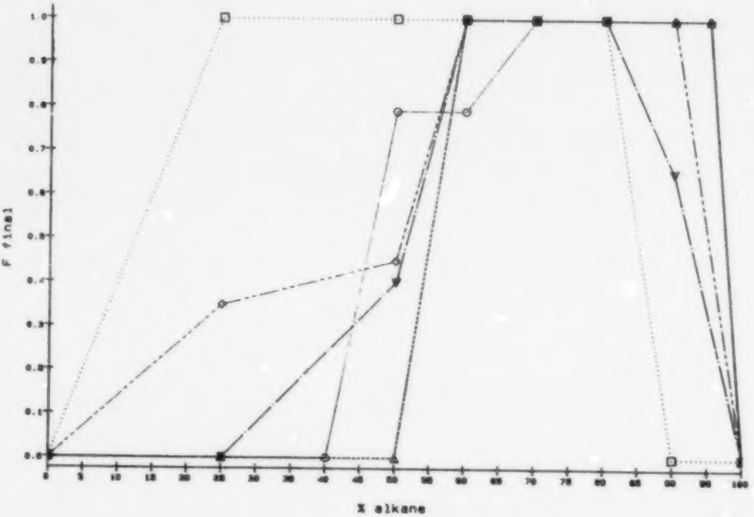

Figure 11: Water content vs % alkane

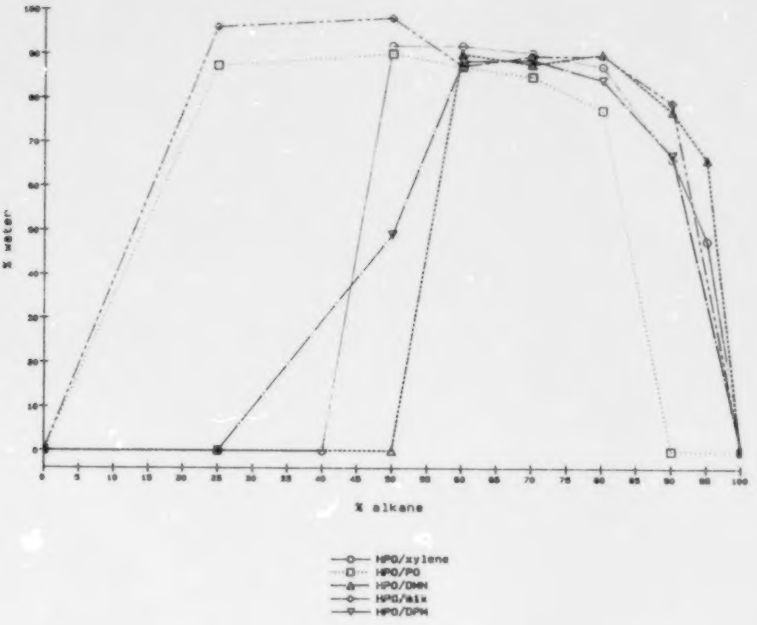

Figure 12: Yield point vs % alkane

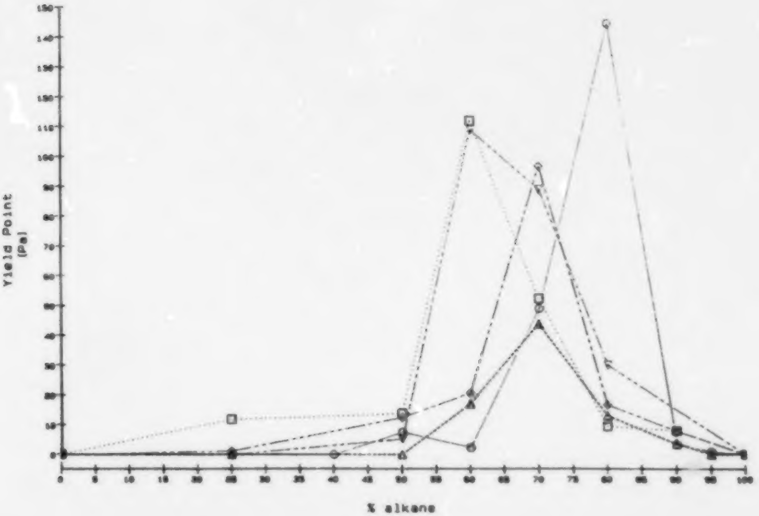

Figure 13: Fo vs (Oa-Os)^2
for different aromatic components

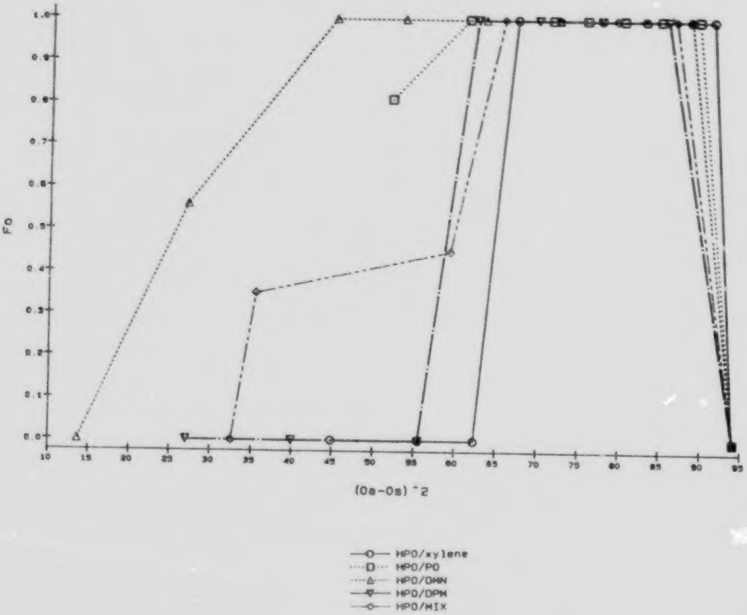

Figure 14: F final vs (Oa-Os)^2

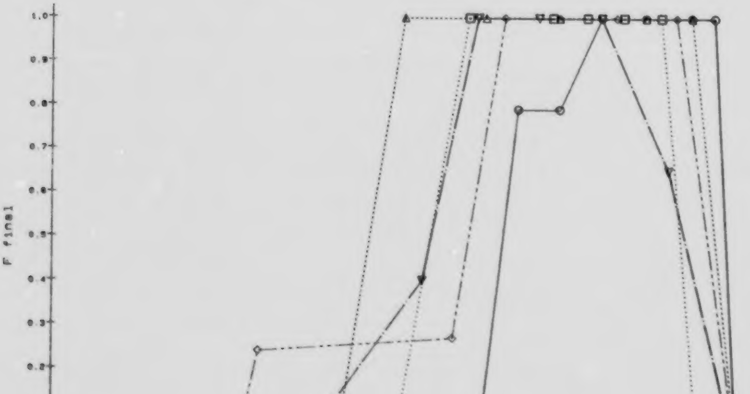

Figure 15: Water content vs (Oa-Os) ^2

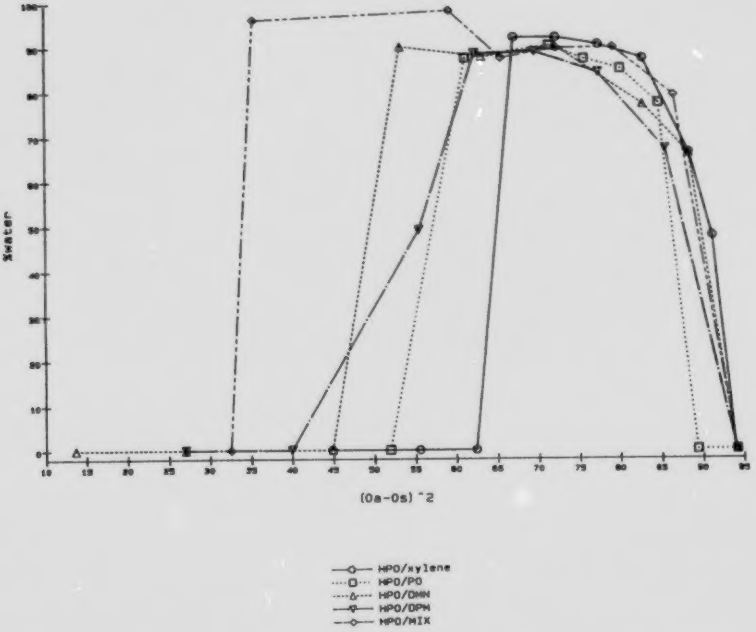

Figure 16: Yield point vs (Oa-Os) ^2

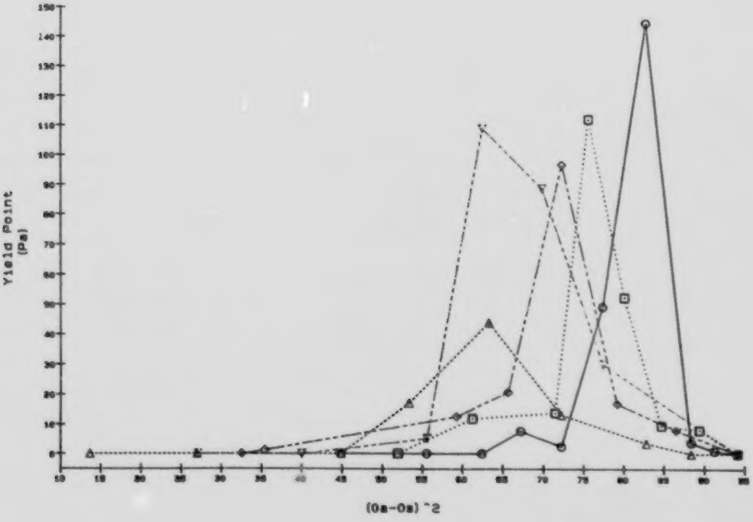

Effect of Alkane Component

The effect of using different alkane solvents as the precipitation medium for asphaltenes has been studied by Long (1979), Speight and Moschopedis (1979). Their findings indicate that as the carbon number of the alkane solvent increases, the amount of asphaltenes which precipitate decreases, and that the composition of the precipitated material also changes. Higher alkane solvents were shown to yield asphaltenes which have a higher degree of aromaticity, a higher proportion of heteroatoms, a higher degree of polarity, and higher molecular weights.

Figures 17 to 20 show F_o, F_f, water content, and yield point versus percent alkane for four different model oils consisting of xylene (XYL), 5% asphaltenes, and four different alkane components: n-octane (OCT)(σ=15.4), n-tetradecane (C14)(σ=16.3), light paraffin oil (LPO)(σ=14.7), and heavy paraffin oil (HPO)(σ=15.0). The results show that the model oils containing the paraffin oils (a complex mixture of alkanes) have a stonger tendency to form stable emulsions than do the oils made with the n-alkane solvents. The emulsions formed by oil containing the heavy paraffin oil are structurally stronger (higher yield points) than those formed by the light paraffin oil. When the emulsification behaviour of the model oils containing octane and tetradecane are compared, the tetradecane/xylene oil has a stronger tendency to form stable emulsions (higher F_f values), but these emulsions have less structural strength (lower yield point).

Comparison of Asphaltenes from Different Crudes

Asphaltenes from different oils will differ in elemental composition, structure and molecular weight. Therefore, the solubility/precipitation behaviour of asphaltenes from different sources could potentially differ. The experiments using the heavy paraffin oil/xylene oil containing 5% asphaltenes were repeated for asphaltenes extracted from Prudhoe Bay crude oil. Overall the emulsification behaviour was very similar to the California crude asphaltenes. The asphaltenes from the California crude were slightly more effective emulsifiers.

Figure 17: Fo versus % alkane
for different alkane components

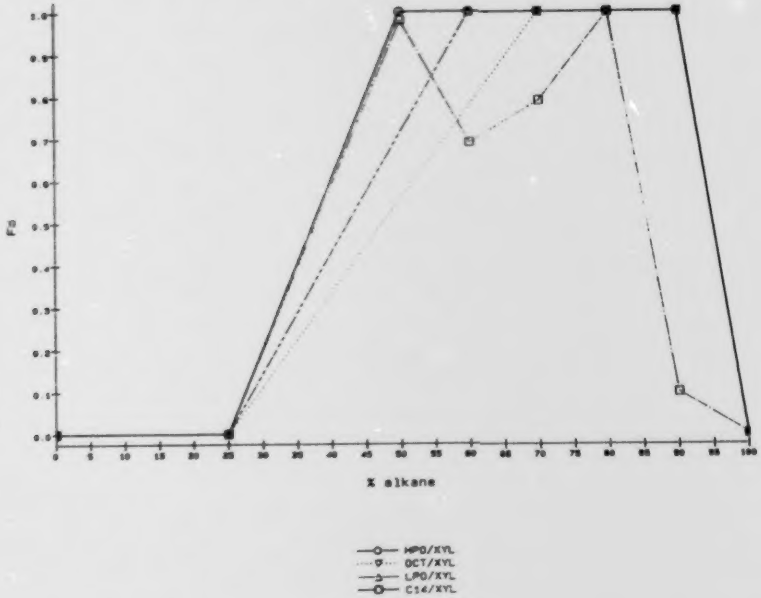

Figure 18: F final vs % alkane

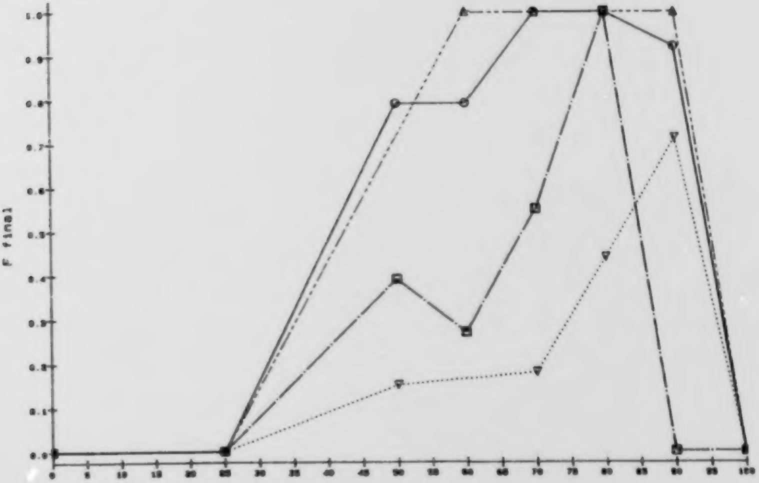

Figure 19: Water content vs % alkane

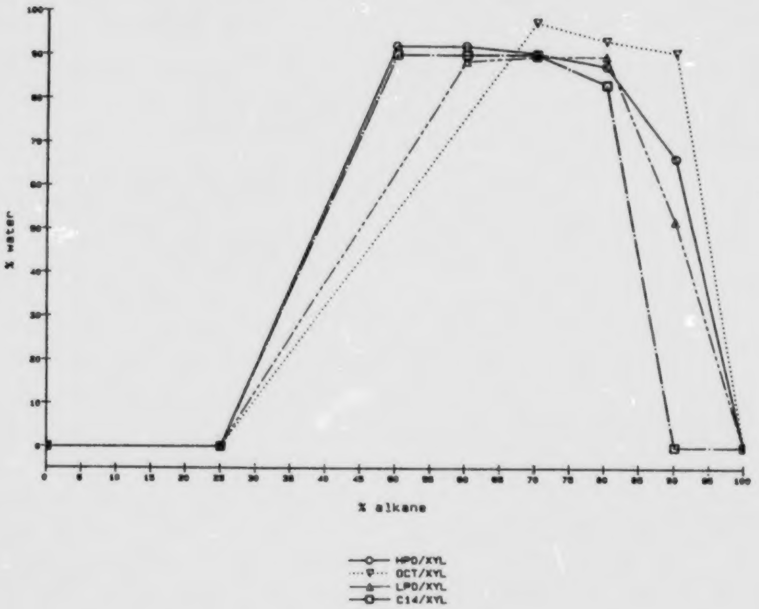

Figure 20: Yield Point vs % alkane

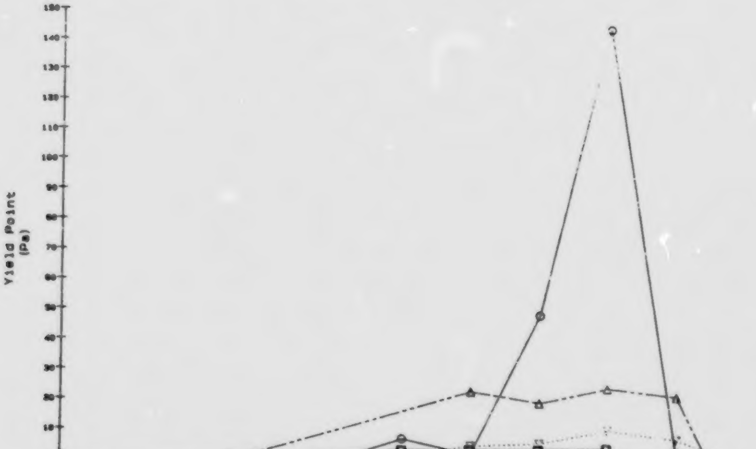

Effect of Resins

Figures 21 to 24 present the emulsification behaviour for model oils where the emulsifying agents are: 1. asphaltenes; 2. resins; and 3. asphaltenes and resins together. The results show that stable emulsions can be produced by resins alone. Although the range of alkane/aromatic ratios over which stable emulsions are produced is small, these emulsions have greater structural strength than emulsions stabilized by asphaltenes. When asphaltenes and resins are both present, the range over which stable emulsions are formed is larger than either resins or asphaltenes alone. But emulsions stabilized by the asphaltene/resin combination lack the maxima peak in yield point.

Effect of Wax

Figures 25 to 28 show the effect of adding 0.05 and 0.1 g/mL of wax to a model oil containing 1% asphaltenes. The model oil containing 1% asphaltenes has no tendency to form stable emulsions, but the addition of wax increases the emulsification tendency at all alkane/aromatic ratios. The range of alkane/aromatic ratios over which stable emulsions are produced increases as wax content increases. Increasing the wax content also increased the mechanical strength of the emulsions. Similar results were obtained when wax was added to the oil containing 2.5% asphaltenes.

The effect of adding 0.1 g/mL of wax to the model oil containing 5% asphaltenes is shown in Figures 29 to 32. The addition of wax has little effect upon F_o, F_f and water content but decreases the maxima yield point of the emulsions formed.

Figures 33 to 36 show the effect of increasing asphaltene content upon an oil containing 0.05 g/mL grams of wax. Model oils containing only wax as the emulsifying agent had no tendency to emulsify. As the Figures illustrate, the addition of asphaltenes results in the formation of stable emulsions. As the concentration of asphaltenes is increased, the oils have a greater tendency to produce stable emulsions.

Figure 21: Fo versus % alkane
effect of resins

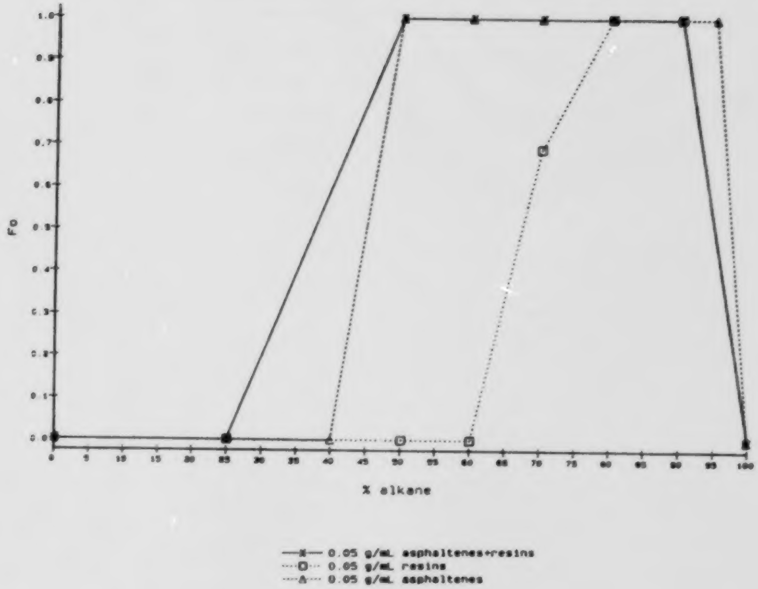

Figure 22 F final vs % alkane

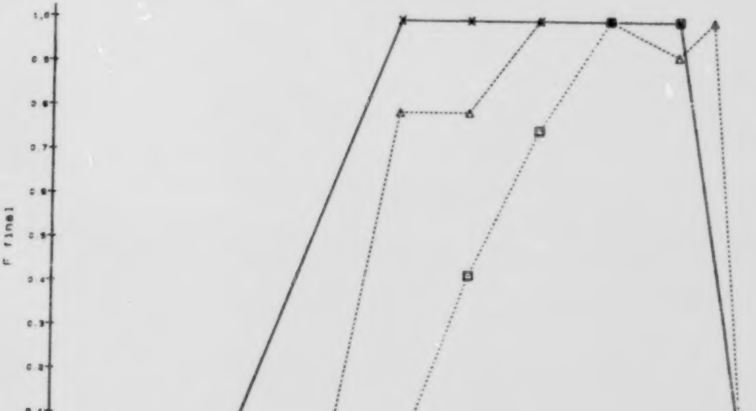

Figure 23: Water content vs % alkane

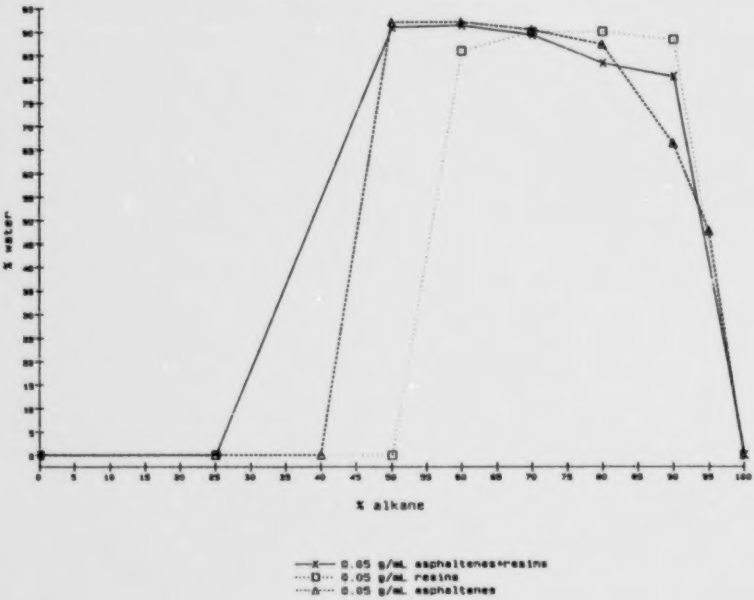

Figure 24: Yield Point vs % alkane

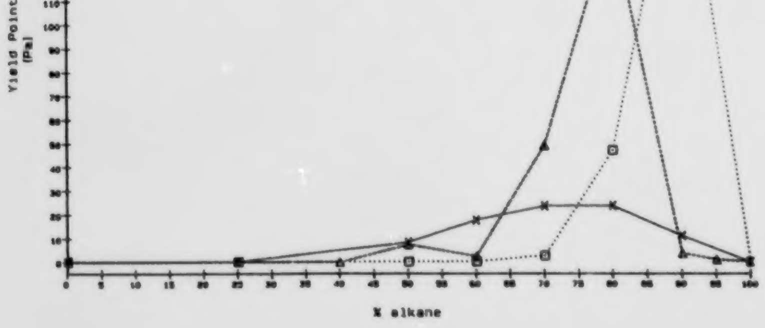

Figure 25: Fo vs % alkane
effect of increasing wax content

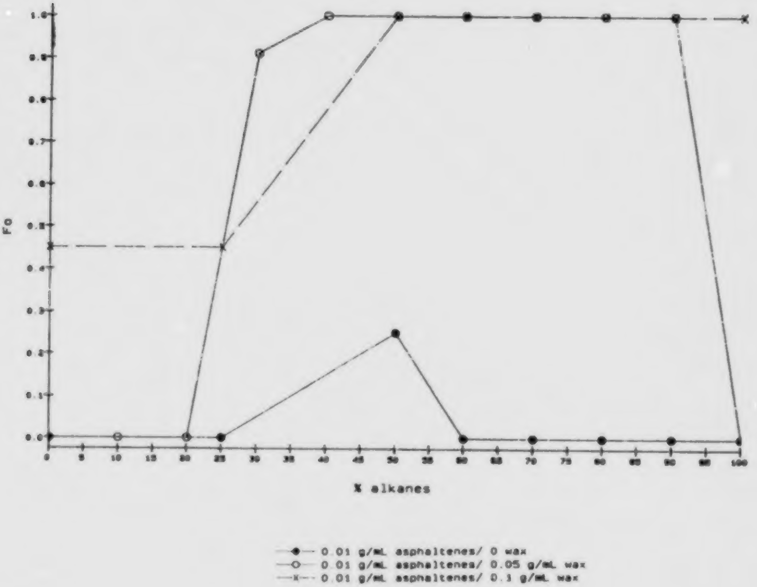

Figure 26: F final vs % alkane

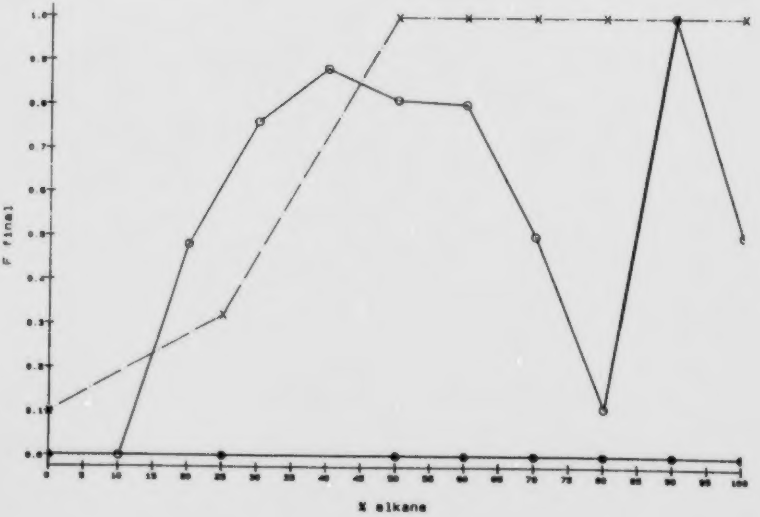

Figure 27: Water content vs % alkane

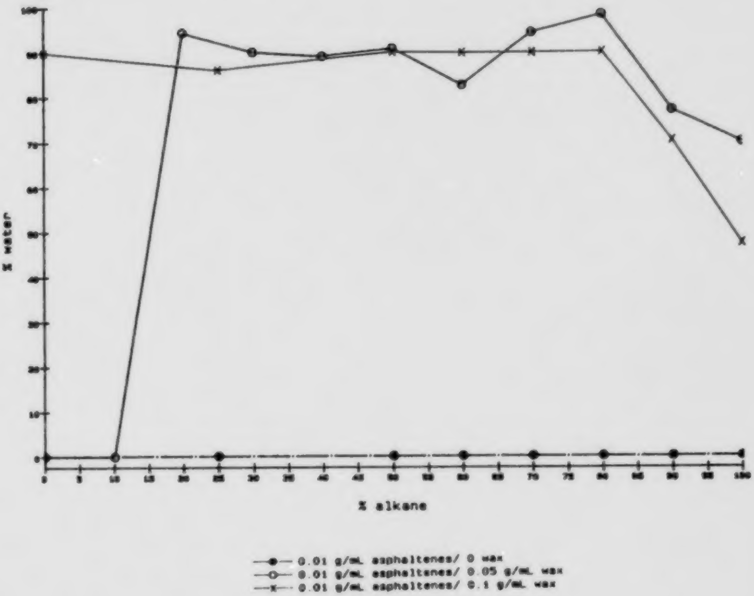

Figure 28: Yield Point vs % alkane

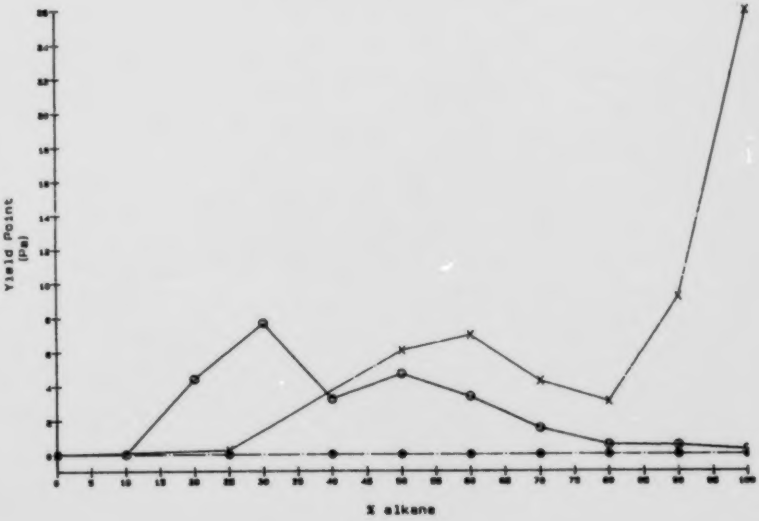

Figure 29: Fo versus % alkane
effect of adding wax

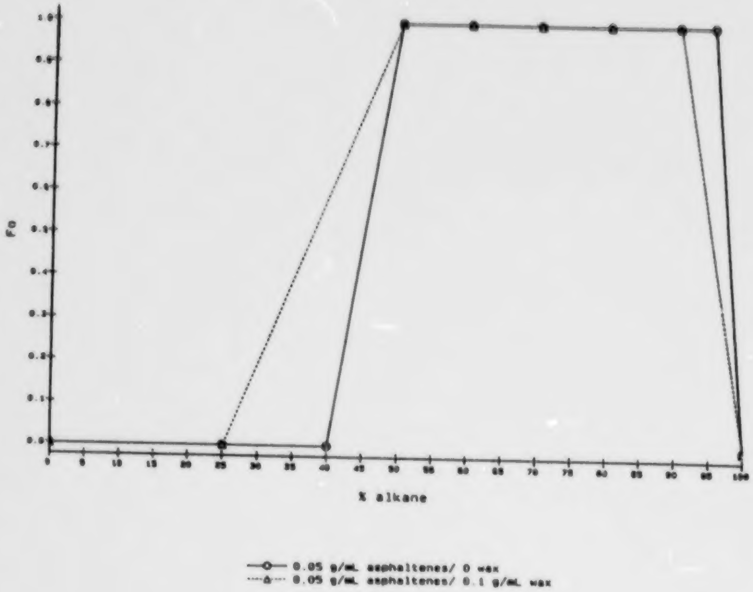

Figure 30: F final vs % alkane

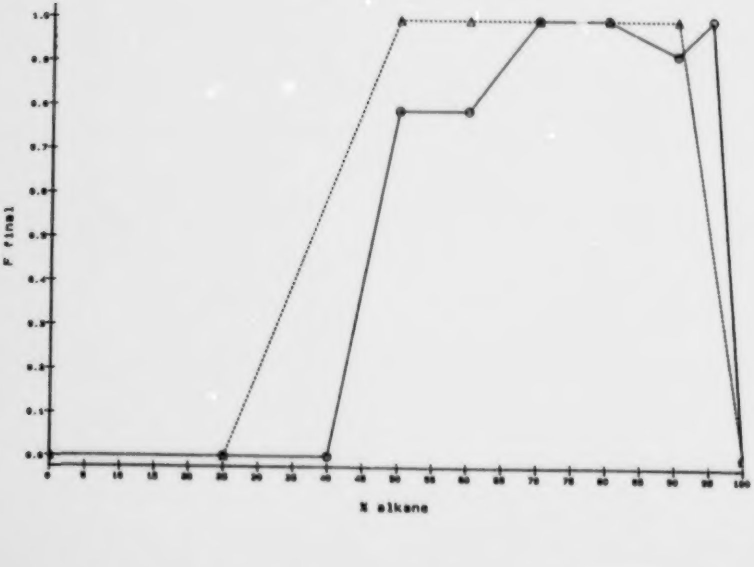

Figure 31: water content vs % alkane

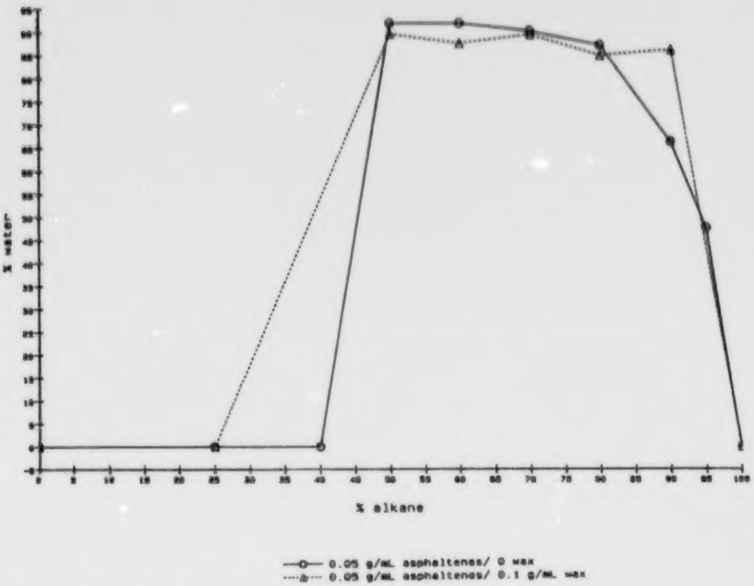

Figure 32: Yield point vs % alkane

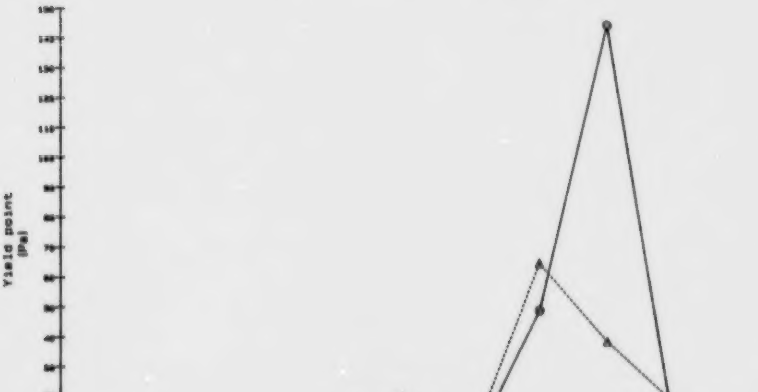

Figure 33: Fo versus % alkane
effect of increasing asphaltene concentration
in an oil having a wax concentration of 0.05 g/mL

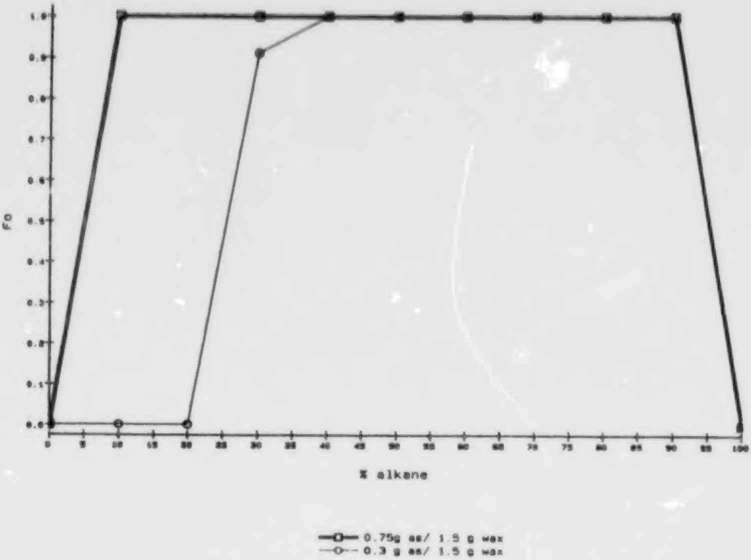

Figure 34: F final vs % alkane

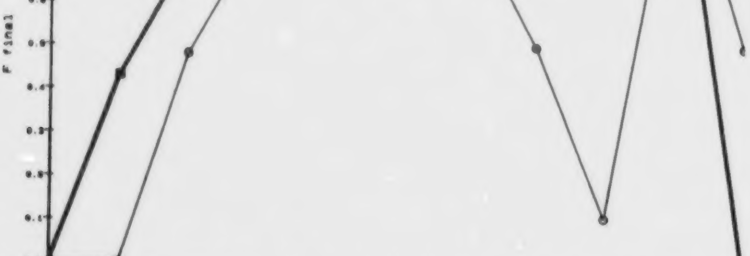

Figure 35: Water content vs % alkane

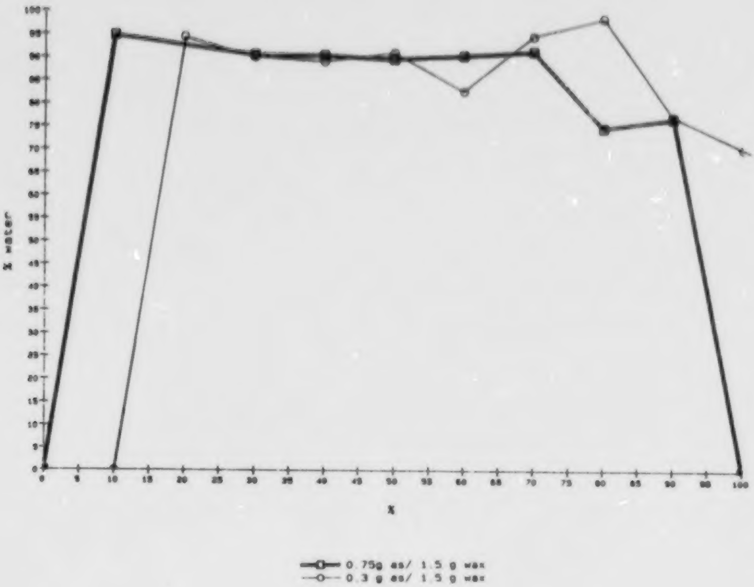

Figure 36: Yield point vs % alkane

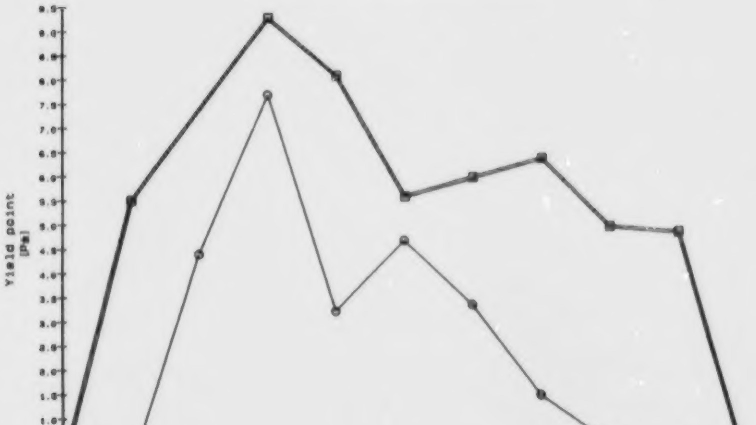

Rheological Properties

All the stable emulsions formed during this study exhibited non-Newtonian flow behaviour. Flow curves for mousse (Figure 37) indicate that they behave as pseudoplastic liquids which have a definite yield point and a thixotropic flow behaviour. This complex flow behaviour means that viscosity is extremely dependent upon shear conditions (shear rate and length of time shear is applied). Therefore, a single viscosity number can not properly characterize the fluidity of mousse. Figure 38 demonstrates this effect of shear rate on apparent viscosity.

Droplet Size Distribution

Figure 39 shows the droplet size distribution for a typical mousse formed by the model oils. The droplet diameters are very heterogeneous and appear to have at least a bi-modal distribution. This multi-modal size distribution means that the water content of emulsions can exceed the water content of uni-modal distributions which theoretically has a maximum value of 74%. In effect, this allows droplets of a smaller size to occupy the gaps between larger droplets, thus creating an extremely dense packing of droplets. The yield point of emulsions increases as the droplet size distribution shifts to smaller values.

Figure 37: Flow curve for mousse
Shear stress versus shear rate

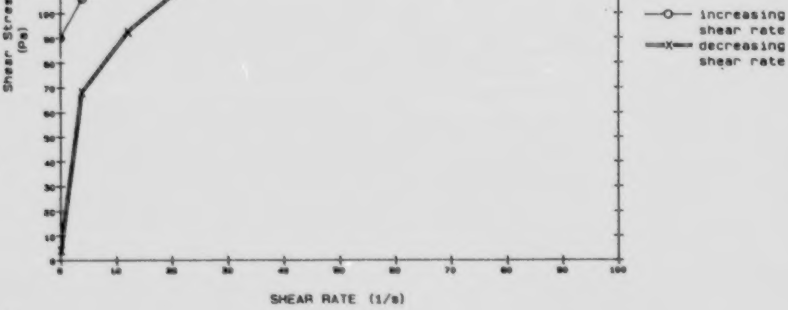

Figure 38: Effect of shear rate
on apparent viscosity of mousse

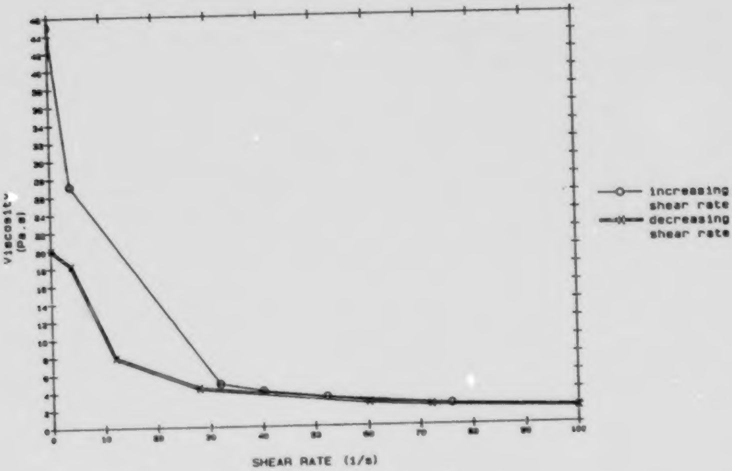

Figure 39: Droplet size distribution

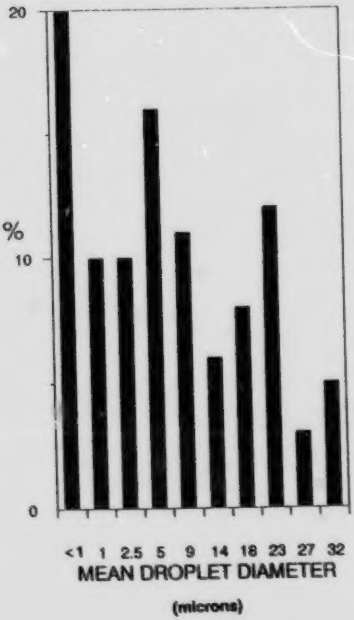

Conclusions

The results from this study demonstrate the importance that the physical state of an emulsifying agent has upon its ability to stabilize emulsions. It was found that to be effective emulsifiers, asphaltenes, resins and waxes must be in the form of finely divided particles. The chemical composition of the oil determines not only the amount and size of these particles but also their composition and their wetting properties. All these factors were shown to have an influence upon the emulsification process.

Asphaltenes and resins, by themselves and in combination, were effective emulsifying agents. Model oils containing only wax as the emulsifying agent did not form stable emulsions. But the addition of a nominal amount of asphaltenes, an amount insufficient by itself to produce emulsions, to oils containing wax lead to the formation of stable emulsions. This indicates that different emulsifying agents can synergically interact to stabilize emulsions.

The solubility/precipitation behaviour of asphaltenes in model oils follows the solubility theory as described by the Hildebrand-Scatchard equation. The use of solubility parameters can be applied to petroleum fractions and therefore, may be useful in predicting the physiochemical conditions which favour emulsification.

Acknowledgements

This study was co-funded by the United States Minerals Management Service and the Environmental Emergencies Technology Division of Environment Canada.

References

Barton A.F.M., Handbook of Solubility Parameters and Other Cohesion Parameters, CRC Press (1983).

Becher P., Emulsions: Theory and Practice, Kreiger Publishing, 2 (1977).

Becher P., Encyclopedia of Emulsion Technology, Marcel Dekker, 1 (1983).

Blair C. M., Chem. Ind. (London), (1960) 538.

Bobra M., A Catalogue of Crude Oil and Oil Product Properties, Envir. Canada, EE-114 (1989).

Bridie A. L., Wanders TH. H., Zegveld W. and Vander Heijde H. B., Marine Pollution Bulletin, 11 (1980) 343.

Canevari G. P., Marine Pollution Bulletin, 13 (1982) 49.

Clark G. H., Industrial and Marine Fuels Reference Book, Butterworth and Co., (1988).

Desmaison M., Desmarquest J.-P., Piekarski C. and Piekarski S., Revue de L'Institut Francais du Petole, vol 39, #5 (1984).

Eley D. D., Hey M. J. and Lee M. A., Colloids and Surfaces, 24 (1987) 173.

Eley D. D., Hey M. J. and Symonds J. D., Colloids and Surfaces, 32 (1988) 87/103.

Eley D. D., Hey M. J., Symonds J. D. and Willison J. H. M., J. Colloid Interface Sci., 54 (1976) 462.

Graham D. E., Crude Oil Emulsions: Their Stability and Resolution, 3rd Intl. Sym. on Chemistry in the Oil Industry, Northwest Region of the Industrial Division Royal Soc. of Chemistry, Special Pub. 67 (1988).

Griffith M. G. and Siegmund C. W., Controlling Compatibility of Residual Fuel Oils, Marine Fuels, ASTM STP 878, C. H. Jones, Ed., Amer. Soc. for Testing and Materials, Philadelphia (1985) 227.

Hasiba H. H. and Jessen F. W., Film Forming Compounds from Crude Oils, Interfacial Films and Paraffin Deposition, 18th Annual Tech. Meeting, Petrol. Soc. of CIM, (1967).

Lawrence A. S. C. and Killner W., J. Inst. Petrol., 34 (1948) 821.

Long R. B., The Concept of Asphaltenes, Sym. Division of Petrol. Chemistry Inc., Washington

(1979).
Mackay D., Formation and Stability of Water-in-oil Emulsions, Envir. Canada, EE-93 (1987).
Mackay D. and Zagorski W., Studies of Water-in-oil Emulsions, Envir. Canada, EE-34 (1982).
Neumann H. J., Paczynska-Lahme B. and Severin D., Composition and Properties of Petroleum, Geology of Petrol., H. Beckmann, Ed., Halsted Press, 5 (1981).
Rosen M. J., Surfactants and Interfacial Phenomena, John Wiley & Son, (1978).
Speight J.G., The Chemistry and Technology of Petroleum, Marcel Dekker Inc., (1980).
Speight J.G. and Moschopedis S.E., Some Observations on the Molecular Nature of Petroleum Asphaltenes, Sym. Division of Petrol. Chemistry Inc., Washington (1979).
Thompson D. G., Taylor A. S. and Graham D. E., Emulsification and Demulsification Related to Crude Oil Production, Sym. Formation of Liq-Liq Dispersions, Chemical and Engineering Aspects, Inst. of Chem. Engineers and Southeast Branch Fluid Mixing Process Subject Grp., (Feb. 1984).
Van der Waarden M., Kolloid Z., 156 (1958) 116.

CHARACTERIZATION OF CRUDE OILS FOR ENVIRONMENTAL PURPOSES

by

Per S. Daling and Per Johan Brandvik,
Continental Shelf and Petroleum Technology Research Institute (IKU),
SINTEF-Group, N-7034 Trondheim, Norway

Donald Mackay,
University of Toronto, Ontario, Canada

Øistein Johansen,
Oceanographic Company of Norway A/S (Oceanor),
P.O.Box 2514, N-7005 Trondheim, Norway

ABSTRACT

A new approach for predicting the behaviour of oil spilled on the sea has recently been developed at IKU, SINTEF-Group. The approach includes an extensive laboratory investigation of an oil's properties when exposed to weathering. Parameters especially tested are the tendency of the oil to form water-in-oil (w/o) emulsion (mousse), and the susceptibility of the w/o-emulsion or weathered oil to disperse using oil spill dispersants. The laboratory results are transformed to field conditions in a numerical model which predicts the rate of weathering processes at sea under different weather conditions. The computer system displays graphical charts for the development of each property with time, and estimates "time window" for e.g. effective application of dispersants under chosen set of sea conditions. The system may represent an important tool, for e.g. contingency planning and for "on-scene" commanders to facilitate decision-making concerning the use of different counter-measure techniques during oil spill combat operations. This approach may form the basis for a standard method for future characterization of the weathering properties of different oil types which may be spilled under a variety of environmental conditions.

BACKGROUND

As long as crude oils and petroleum products are transported across the seas by ships or pipelines there will be the risk of a spillage with the potential to cause significant environmental damage. The "EXXON Valdez" incident in Alaska, but also recent smaller ship accidents in e.g. Norway have again demonstrated the high level of public concern about the damaging effects of oil spills. These spills also demonstrated the need for a rapid decision-making process for assessing the feasibility and effectiveness of different countermeasures (mechanical recovery equipments, burning, dispersants etc.) during the oil spill combat operation.

When oil is discharged into sea water, it is subject to several processes including spreading, drifting, evaporation, dissolution, photolysis, biodegradation and formation of both oil-in-water and water-in-oil emulsions. Figure 1 gives a pictorial representation of the dominant oil spill processes. In principle, if the oil is well characterized and the environmental conditions of wind speed, sea state, currents, salinity, temperature and solar insolation are known, it should be possible to calculate the rates of many of these processes and thus establish how the oil changes in condition with time.

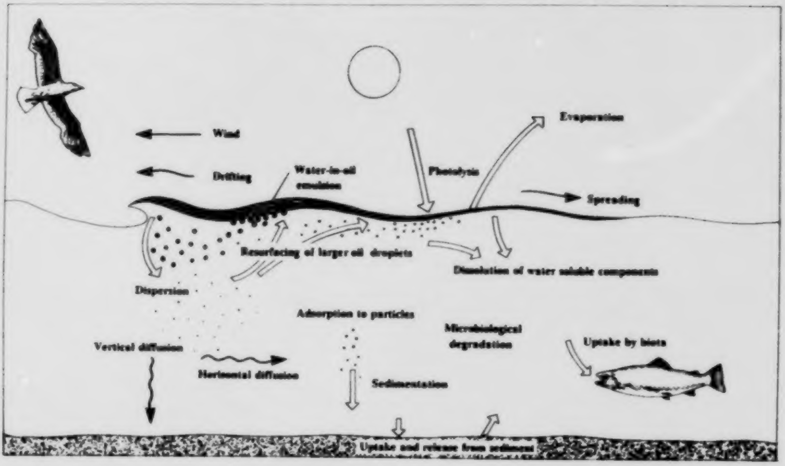

Figure 1. Oil spill processes.

The physical and chemical properties of crude oils play an important role in determining environmental fate and the effects of marine spills (National Academy of Sciences, 1985). Countermeasures can only be implemented effectively if the oils' condition is fully understood. Oils should therefore be subjected to analytical programs of property determinations which will help enable the fate of the oil to be predicted and the feasibility of various countermeasures to be better determined. Of particular interest are the extents to which the weathering processes of evaporation, dissolution and photo-oxidation alter the oil's properties and affect the tendency of the oil to form water-in-oil (w/o) emulsions, (mousses) and to disperse naturally (oil-in-water emulsions). Similar processes will also change the susceptibility of the oil to effective dispersion by chemical agents, i.e. chemical dispersants and to the effectiveness of burning the weathered oil.

The tendency for crude oil slicks to form w/o-emulsions on the sea surface results in substantial changes in behaviour and necessitates changes in countermeasure approaches. It is therefore desirable to understand, as fully as possible, the factors which cause an oil to emulsify, the rate at which the w/o-emulsification occurs and the w/o-emulsion viscosity and stability for a given oil under given environmental conditions. The chemical composition of the oil and the influence of weathering processes like evaporation and photolysis are especially important for the properties of the w/o-emulsions formed (e.g. Mackay, 1987).

The effectiveness of chemical treatment on different w/o-emulsions qualities has also been poorly investigated. Demulsifiers may be used to "break" w/o-emulsions (to separate the water from the oil) either during in-situ treatment on the sea surface or on mechanically recovered w/o-emulsions. W/o-emulsion inhibitors may be added in small amounts to fresh oil to inhibit or retard w/o-emulsification, thereby enhancing the dispersion of the oil by natural sea turbulence. Recent studies (e.g. Ross, 1986; Lichtenthaler and Daling, 1985) have showed that certain oil spill dispersants also may act both as w/o-emulsion breakers and as w/o-emulsion inhibitors.

The use of dispersants as a means of treating oil is being viewed with increasing favour as a result of the manufacture of more effective and less toxic dispersants and better application techniques. It is now widely accepted that chemical dispersants have an important role in oil spill countermeasures (e.g. National Research Council, NRC, 1989), especially in near-shoreline situations where most of the damage will result from the presence of a surface slick which may foul birds and/or shorelines.

Although much progress has been made the past 10 years, doubt still has remained concerning the actual effectiveness of dispersants at sea under different oil spill situations. From an operational viewpoint it is essential to identify the types of crude oils which will show the best response to dispersant use. Furthermore, it is still poorly understood how changes in physico-chemical composition due to weathering of an oil at sea (e.g. evaporation, w/o-emulsion formation, photolysis) affect the performance of dispersants. The weathering issue has been largely ignored and it is appropriate to devote more attention to it, as is intended in this paper.

As part of the four year project called "Application of Dispersants on Weathered Oils" (DIWO) undertaken by IKU, SINTEF-Group and funded by FINA Exploration Norway, available methods of oil characterization have been evaluated and a set of analytical procedures has been developed and applied to a number of crude oils and refined oil products. In this paper, we describe these methods, present illustrative laboratory results and we discuss briefly the utilization of these experimental data in numerical weathering models. It is hoped that these methods will be considered by other workers, thus improving consistency between measurements made by different groups and enabling more reliable prediction of an oil's environmental fate from knowledge of its characteristics.

LABORATORY PROCEDURES

The laboratory methodology for investigating the properties of each oil type consists of four parts. First is the preparation of 12 different weathered oil samples from the fresh oil as a result of exposure to a combination of evaporation, w/o-emulsification and photolysis. Second is the determination of the physical and chemical properties of the fresh and weathered oils samples. Third is an assessment of the susceptibility of the weathered (water free) oil samples to natural formation of w/o-emulsions ("chocolate mousses"). Finally, the susceptibility to chemical dispersion of totally 13 oil samples (12 weathered and 1 fresh) from each crude is extensively tested using different laboratory dispersant effectiveness test methods.

The laboratory methodology is briefly presented below. Full details of the laboratory methods have been described by Daling and Almås (1988).

Preparation of weathered oil samples

To isolate the influence of the different weathering processes (i.e. evaporative loss, photolysis and w/o-emulsification), the weathering of the fresh crude was carried out using a systematic, step-wise procedure. Figure 2 shows a schematic diagram of the weathering procedure. The first step involved three different degrees of evaporative loss by a modified ASTM D86/82 distillation (Stiver and Mackay, 1984): the crude was topped at 150°C, 200°C and 250°C (vapour temperature) which approximately (depending on weather conditions) simulates 0.5-1 hour, 0.5-1 day and 2-5 days evaporative loss at sea respectively. Secondly, the fresh crude was photolysed (artificial sunlight, cf. figure 3) for 20 hours. This caused an evaporative loss of the lightest components which was similar to the 250°C+ topped oil samples. Finally, the topped and the photolysed (water free) oil samples were emulsified with 50% and 75% sea water (by mechanical stirring and dropwise addition of sea water to the oil (Daling and Almås, 1988)).

Thus, 12 weathered oil samples were prepared from the fresh crude and each sample was subjected to physico-chemical analysis, w/o-emulsification studies and chemical dispersability tests.

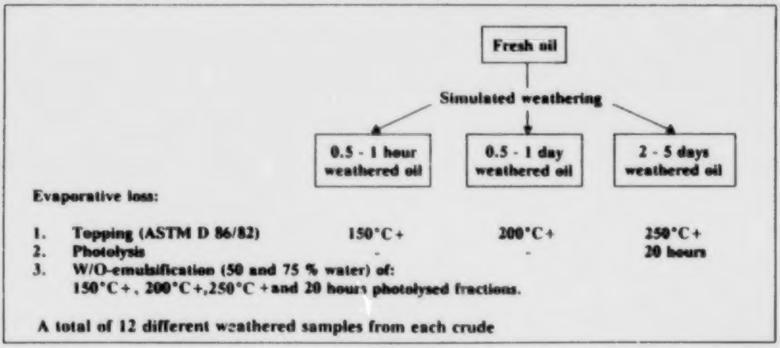

Evaporative loss:

1.	Topping (ASTM D 86/82)	150°C+	200°C+	250°C+
2.	Photolysis	-	-	20 hours

3. W/O-emulsification (50 and 75 % water) of:
150°C+, 200°C+,250°C +and 20 hours photolysed fractions.

A total of 12 different weathered samples from each crude

Figure 2. Schematic diagram of the oil weathering processes.

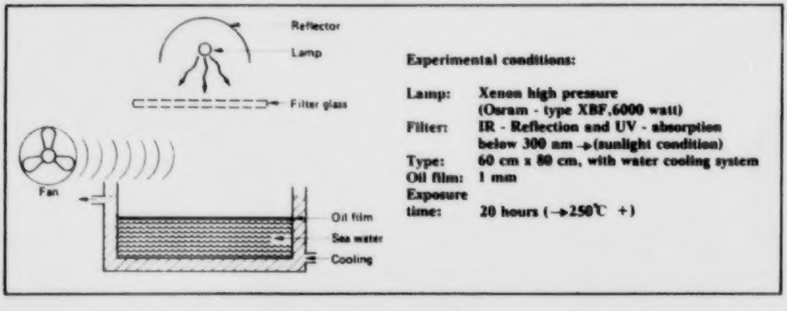

Experimental conditions:

Lamp:	Xenon high pressure (Osram - type XBF,6000 watt)
Filter:	IR - Reflection and UV - absorption below 300 nm →(sunlight condition)
Type:	60 cm x 80 cm, with water cooling system
Oil film:	1 mm
Exposure time:	20 hours (→250°C +)

Figure 3. Schematic diagram of photolysis of the oil film.

Physico-chemical analysis

The physico-chemical properties of the fresh, topped and photolysed oil samples were characterized by the analytical methods listed below:

- **Specific gravity:**	ASTM-method D4052-81
- **Viscosity (dynamic):**	Haake Rotovisco RV3
- **Pour point:**	ASTM-method D97-66 (IP-method 15/67)
- **Flash point:**	ASTM-method D93-80 (IP-34/85)
- **Interfacial tension:**	a) Pendant drop tensiometer b) de Nouy ring method (ASTM-method 971-82)
- **"Soft" asphaltene content:**	n-pentane insoluble (Daling and Almås, 1988)
- **"Hard" asphaltene content:**	IP-method 143/84
- **Wax content:**	Precipitation of deasphalted oil in 2-butanone/dichlorometane (1/1 vol) at -10°C (Bridié et al., 1980)
- **Saturate, aromatic and resin content:**	Iatroscan TLC/FID

Examples of the changes in the physico-chemical properties of crudes with increased weathering are given in Tables 1 and 2.

Table 1:
Chemical properties of fresh and weathered crude oils used in the experiments.

Oil type	Saturates[1] (wt.%)	Aromatics[1] (wt.%)	Resins[1] (wt.%)	Asphaltenes (wt.%)[2] "hard"	"soft"	Waxes[3] (wt.%)
GULLFAKS:						
Fresh	-	-	-	0.02	0.49	1.60
150°C+	-	-	-	0.02	0.52	1.72
200°C+	-	-	-	0.03	0.58	1.90
250°C+	52.1	40.0	6.8	0.03	0.65	2.14
20. h. ph.ox (250°C+)	45.3	37.8	15.3	0.24	1.11	-
STATFJORD:						
Fresh	-	-	-	0.01	0.39	4.14
150°C	-	-	-	0.01	0.47	4.78
200°C+	-	-	-	0.02	0.54	5.77
250°C+	56.2	34.8	7.8	0.02	0.63	6.68
20. h. ph.ox (250°C+)	59.5	25.6	13.7	0.29	1.14	-
ARABIAN HEAVY:						
Fresh	-	-	-	4.33	7.38	4.62
150°C+	-	-	-	4.89	8.34	5.22
200°C+	-	-	-	5.31	9.05	5.67
250°C+	23.2	49.0	18.4	5.80	9.89	6.19
20. h. ph.ox (250°C+)	23.6	41.4	23.6	7.21	10.42	-

[1] Quantification by Iatroscan TLC/FID
[2] Asphaltene content is calculated from data of the 250°C+ fraction. "hard" asphaltenes: IP-143 method, "soft" asphaltenes: n-pentan insoluble.
[3] Wax content is calculated from data of the maltene fraction of 250°C+ (after the "hard" asphaltene separation)

Table 2:
Physical properties of fresh and weathered crude oils used in the experiments.

Oil type	Evapor. loss (Vol.%)	Density (g/ml) (15.5°C)	Pour point (°C)	Interf. tension (mN/m)	Viscosity of oil and w/o-emulsions 1) (cP at 13°C) 0% Water	 50% Water	 75% Water
GULLFAKS:							
Fresh	-	0.882	<-34	13	20	-	-
150°C+	8	0.893	-26	13	33	440	1780
200°C+	18	0.905	-15	15	72	800	4980
250°C+	28	0.914	-9	17	241	1780	6760
20. h. ph.ox (250°C+)	28	0.916	-	1.1	282	2300	14000
STATFJORD:							
Fresh	-	0.834	-15	23	7	-	-
150°C+	20	0.867	7	16	20	160	1200
200°C+	32	0.882	11	15	57	490	3560
250°C+	42	0.895	16	16	221	1800	4600
20. h. ph.ox (250°C+)	42	0.896	17	1.0	314	2850	18500
ARABIAN HEAVY:							
Fresh	-	0.887	-28	20	41	-	-
150°C+	15	0.920	-23	14	241	~800	- 2)
200°C+	23	0.935	-18	18	700	6000	- 2)
250°C+	30	0.951	-5	17	2344	7350	- 2)
20. h. ph.ox (250°C+)	30	0.954	-8	1.1	4350	11500	- 2)

1) Measured at a shear rate = $10s^{-1}$
2) Emulsion not possible to prepare

Formation and properties of water-in-oil emulsions

The method used for studying w/o-emulsion properties of a crude were based on the rotating flask apparatus of Mackay and Zagorski (1982). The method involves rotation of centrifuge bottles containing sea water and oil (ratio 10 to 1) for a 1 hour or 24 hours period of time at a rotation speed of 65 rpm. After the mixing period, both the formation tendency and the stability of any w/o-emulsions formed were assessed (see Fig. 4a). Some modifications have been made to the original procedure of Mackay and Zagorsky for the present study (Daling and Brandvik, 1988).

Using this rotating flask method, it is possible to study the following:

- **the relative rate of w/o-emulsion formation** ($t_{1/2}$-value)
- **the maximum water content in a w/o-emulsion** (%, Em_1)
- **the stability of w/o-emulsions** ($R_{2/1}$-value, untreated or treated with chemicals, e.g. demulsifiers)
- **the inhibition effectiveness of chemicals** (e.g. dispersants or emulsion inhibitors) **on w/o-emulsion formation.**

Figure 5 shows an example of the experimental curves for the water uptake of three different crudes (200°C+ topped samples). Both the relative water uptake rate and maximum water uptake ability seem to depend strongly on the physical and chemical properties of the crudes. To express the rate for the water uptake, a theoretical exponential curve is fitted to each experimental curve. A $t_{1/2}$-parameter can then be calculated, which is the mixing time elapsed when the water content is half of the maximum water uptake ability. Figure 6 shows the close correlation which appears to exist between the viscosity of an oil (water-free) and the ability of the same oil to take up water.

By measuring the water-to-oil ratio of a w/o-emulsion before (R_1-value) and after a 24 hour settling time (R_2-value), we can calculate the $R_{2/1}$-value (defined as the R_2-value divided by the R_1-value). The $R_{2/1}$-value (between 0 and 1) is used as a parameter for the relative

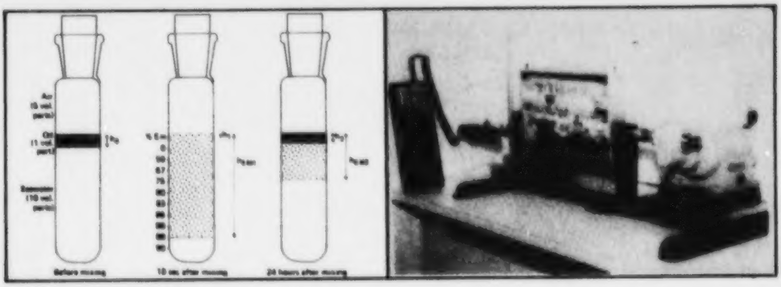

Figure 4. Schematic diagram of the rotating bottles (a) and the set up of the rotating flask apparatus used in this study (b).

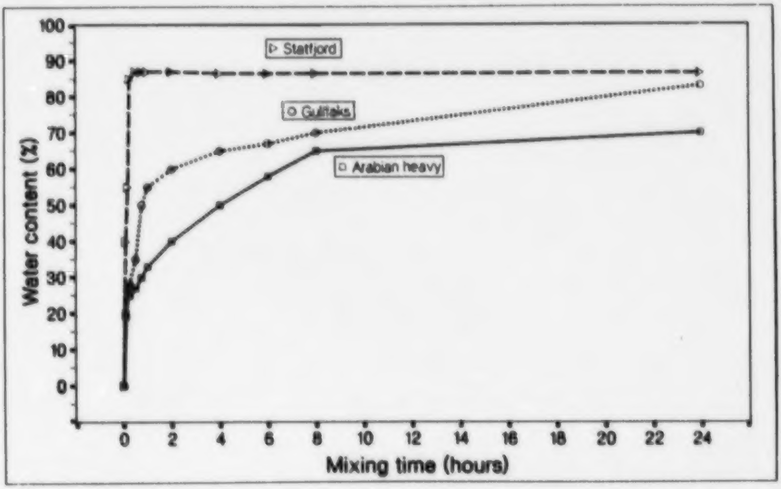

Figure 5. Formation of w/o-emulsion (water uptake for the 200°C+ topped samples of three crudes (Gullfaks, Statfjord and Arabian Heavy).

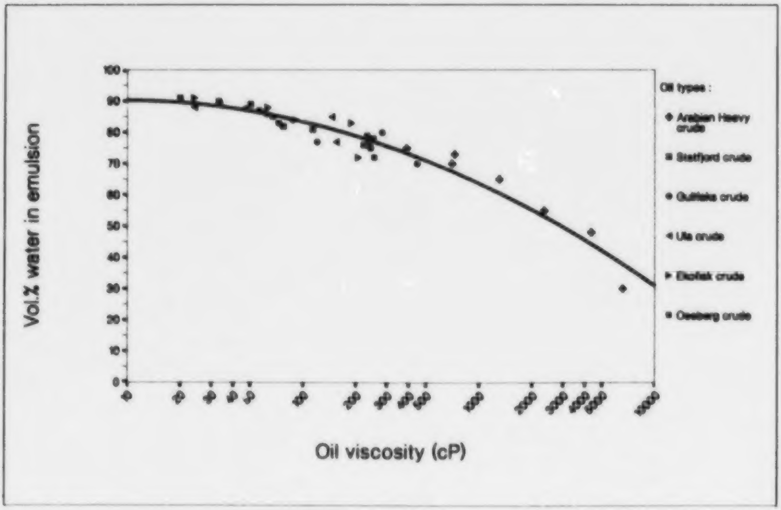

Figure 6. Maximum water uptake ability (based on 24 hours mixing period) for different crudes plotted against the viscosity of the parent (water free) oil.

stability of the w/o-emulsion formed. For example, $R_{2/1}=0$, means that all the water has been settled out from the w/o-emulsion during the settling time, while $R_{2/1}=1$ means that the w/o-emulsion is stable. Figures 7a-b show that the stability of w/o-emulsions depends highly on type of crude, weathering degree and the mixing time for the preparation of the w/o-emulsions.

When adding chemicals (e.g. emulsion-breakers) to the prepared w/o-emulsions, the $R_{2/1}$-value can be used to obtain information concerning the relative effectiveness of the chemicals on different w/o-emulsion qualities (see figures 7c-d). Photolysis of the oils has a marked influence on the stability of the w/o-emulsion and on the effectiveness of the emulsion-breaking chemicals (Figures 7a-d).

The influence of the mixing time on w/o-emulsion stability may reflect the relatively large amount of smaller water droplets in w/o-emulsions mixed over a 24 hour period relative to those mixed over a 1 hour period (Figures 8a-b).

Testing of chemical dispersability

There has been some controversy as to which is the best laboratory method for dispersant effectiveness testing. From an assessment of the literature and the results of various studies in this field, it is clear that the various laboratory tests give different effectiveness results even for the same oil/dispersant combination because each test measures different phenomena. Variations in experimental parameters like turbulence (energy input), settling time and oil-to-water ratio in various test apparatus, are found to be very important for the effectiveness value (e.g. Fingas et al.,

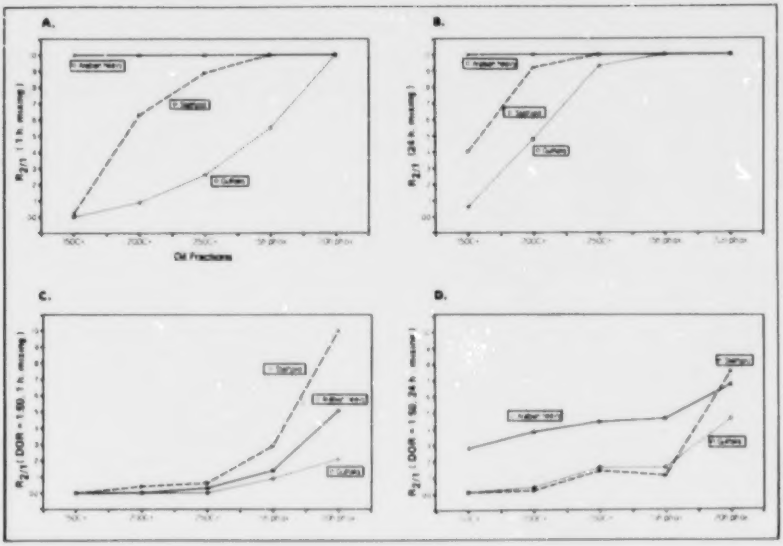

Figure 7. Relative w/o-emulsion stability ($R_{2/1}$-values) for:
A: 1 hour mixed w/o-emulsion (untreated).
B: 24 hours mixed w/o-emulsion (untreated).
C: 1 hour mixed w/o-emulsion treated with emulsion breaker.
D: 24 hours mixed w/o-emulsion treated with emulsion breaker.

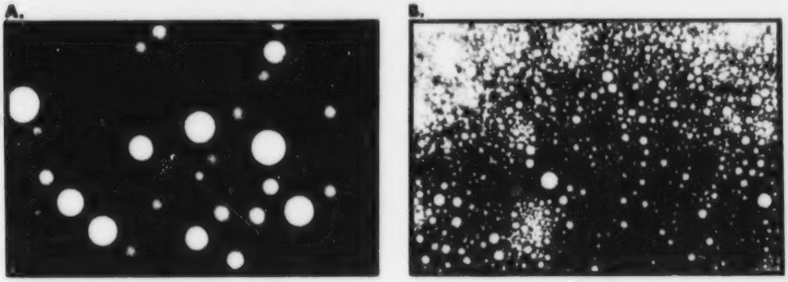

⊢—⊣ = 100 microns

Figure 8. The influence of mixing time on the water droplet size in the w/o-emulsion (Arabian Heavy 150°C+).
A: 1 hour mixing, B: 24 hours mixing.

1989; Daling, 1988; Gillot et al., 1987).

Since different test methods may give divergent results, it is valuable to conduct tests with different methods. From considerations of the scale, speed of testing and cost, we have evaluated three laboratory tests. Their basic principles and designs for producing mixing energy are very different. This implies that they will simulate different "sea states" or conditions of use:

- In the **Mackay-Nadeau-Steelman test (MNS-test**, Mackay and Szeto, 1980) energy is applied by blowing air across the oil/water surface, producing a circular wave motion. The energy input in this system corresponds more to a medium to high sea-state condition. One sample of the oily water is taken under dynamic conditions and a second sample is taken after a settling period of 5 minutes (static conditions).
- In the **Labofina/Warren Spring Laboratory test (WSL-test**, Martinelli, 1984) mixing energy is supplied by revolving flasks which gives a relatively higher specific energy input compared to the MNS-test. The mixing period is followed by a settling period of 1 minute before sampling (static sampling).
- **The IFP-test** (Bocard et al., 1984) is a low energy input test (compared to the MNS-test) and is probably a more realistic approach because of the introduction of the dilution concept. The sampling is taken under dynamic conditions.

The chemical dispersability of all the 13 oil samples (1 fresh and 12 weathered and w/o-emulsified samples, see fig. 2) from each crude were tested using the three laboratory test methods (MNS-, WSL- and IFP-tests). Additionally, the size distribution of oil droplets present in the dispersions produced by the test methods was measured.

The dispersability testing was carried out under the following conditions:

- **Dispersants:**	Finasol OSR-5 (concentrate, type 3) Finasol OSR-12 (conventional, type 1)
- **Dispersant-to-oil ratio (DOR):**	1/25 for type 3 dispersants 1/2.5 for type 1 dispersants
- **Temperatures (water and air):**	6°C and 13°C (North Sea winter and summer conditions)

The dispersion results presented in this paper deals mainly with the 13°C test results with Finasol OSR-5. However, it is thought that the same approach can be used for other commercial dispersants.

Figures 9a and b show an example on the effectiveness of Finasol OSR-5 at 13°C on different North Sea crudes with the IFP and MNS methods respectively. The figures summarize the effectiveness results of both fresh, topped, photolysed and emulsified samples (13 samples from each crude totally), all plotted as a function of the oil or w/o-emulsion viscosity (shear rate = $10s^{-1}$).

Due to the different design of the two test apparatus, the effectiveness results become somewhat different. However, the main trends agree fairly well with the two methods. Both Figure 9a and b clearly demonstrates that the type of crude is an important factor in determining the performance of a dispersant at sea. Furthermore, there is a significant change in chemical dispersability with increased weathering of the different crudes. The viscosity limit for the dispersability of w/o-emulsions seems to be specific for the different

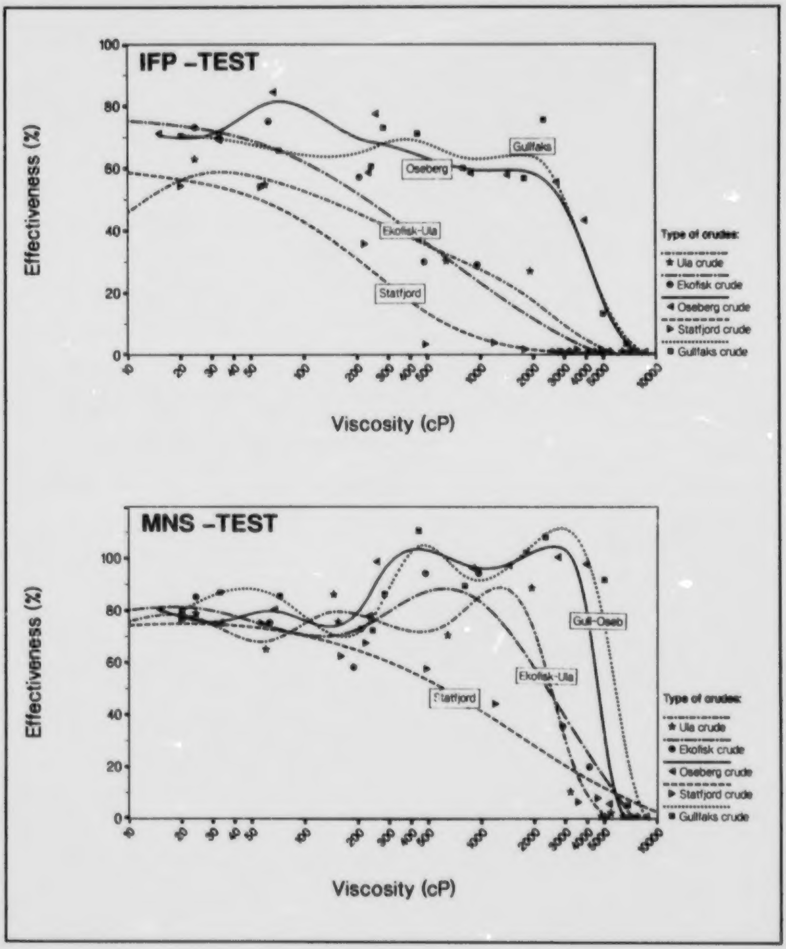

Figure 9. Dispersability of weathered North Sea crudes tested on two test methods:
a) IFP-test
b) MNS-test (1st sampling)
Dispersant: OSR-5 (DOR=1:25), Temperature 13°C).

crudes. This prevents the formulation of a general rule concerning the upper viscosity limit for dispersability of w/o-emulsions. This kind of information represents crucial input to numerical weathering models for estimating the "time window" for chemical dispersion of specific crudes under different weather conditions. This issue will be discussed further in the next chapter.

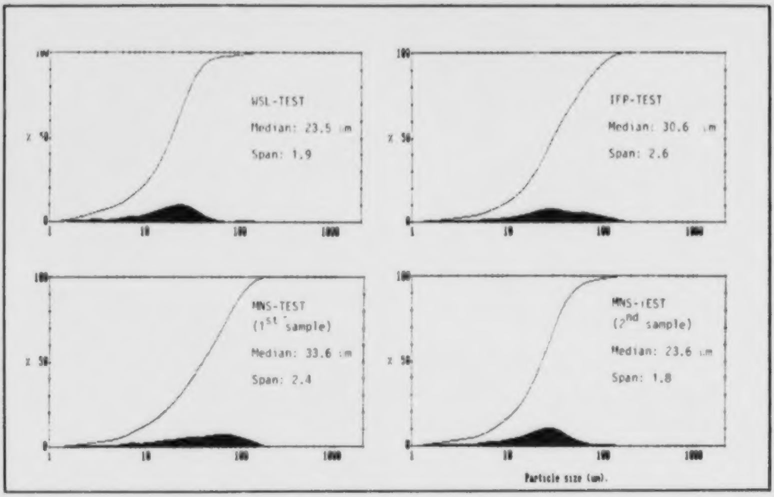

Figure 10. Example of the median droplet size (µm) and droplet size distribution (span) in the different test methods (Gullfaks 150°C+, treated with Finasol OSR-5 at 13°C).

The Malvern particle size analyzer has been used to characterize the oil droplet size distribution in all the dispersions produced by the 13 oil samples in the 3 test methods. The droplet size measurements gave valuable information about the effectiveness of dispersants in addition to the mass balance of dispersed oil. Earlier work by Lewis et al. (1985) has shown that considerable insight can be obtained about dispersant performance by making such droplet size measurements. The median droplet size (D_{50}, defined as the droplet diameter at which 50 vol% of the oil consists of droplets less than D_{50}) and the droplet size distribution (expressed by the Span = $(D_{90}-D_{10})/D_{50}$) are significantly different in the 3 tests (Figure 10). This reflects the different design (particularly the energy input and the sampling procedure) of the methods. In the systems with static sampling (WSL and 2nd MNS), the settling time allows the largest oil droplets to float up and out of the sample zone in accordance with Stokes law. This results in smaller values for both the D_{50} and the Span.

Both the dispersant effectiveness measurements (mass balance of dispersed oil) and droplet size measurements of the dispersed oil have clearly demonstrated that the three test methods are measuring different phenomena. The IFP-method appears to be the most selective and most sensitive of the three laboratory methods according to type of dispersant, oil quality and weathering effects (see fig. 9a). Due to the low surface energy and turbulence, the IFP-method is especially sensitive to oils that are unusually viscous or close to their pour points. Also the MNS tends to give good selective results between the different crudes particularly in the higher viscosity area. Due to the higher energy level, the MNS-method (1st sampling) tends to give higher effectiveness values compared to the IFP-results.

Due to the settling time before sampling, the WSL-test results become very sensitive to the resurfacing velocity of oil droplets and thus tends to give high performances for dense oils and low effectiveness values for light crudes. The high relative volume of oil used in this test system may be an other important negative factor, causing interaction and coalescence of oil droplets giving low and unreliable results (Daling, 1988). The WSL-method is therefore not so suitable laboratory method as the MNS- and IFP-tests in studying chemical dispersability with respect to different oil qualities and effect of weathering and w/o-emulsification.

USE OF EXPERIMENTAL DATA IN NUMERICAL WEATHERING MODELLING

The efficiency of various marine oil spill combat methods is known to depend to a large extent on the physical properties of the oil. As discussed above, this is particularly true for chemical dispersants, where increased viscosity due to weathering and w/o-emulsion formation may make the oil resistant to dispersants within hours (or days) after the oil is spilled. Hence, reliable predictions of the changing properties of the oil during variable sea conditions may be of great value in determining the "time window" for efficient application of dispersants. It is to believe that similar limitations exist also for e.g. the efficiency of burning.

Different approaches to the oil property prediction problem have been established. One approach is to derive a set of "mixing rules", where the various physical properties of the oil are derived on the basis of the changing composition of the weathered oil. Simple mixing rules may be relevant for prediction of some of the properties, e.g. the density of the oil, while this type of approach may be less relevant for other properties, such as viscosity and pour point. As a consequence, we have chosen a more direct, empirical approach, where the laboratory measurements discussed in the previous serve as the basis for the predictions.

The laboratory data described in the previous concerns the properties of crude oils at different stages of weathering with reference to fraction distilled (topped). A link between these data and weathering properties in field conditions may be established on the basis of computations of evaporative loss and w/o-emulsion formation. The basic assumptions providing this link are:

1) The product remaining after a given fraction is topped by distillation corresponds to the product remaining after an equal amount is removed by evaporation at sea.
2) The w/o-emulsification process studied in the laboratory corresponds to the process taking place at sea.

Evaporative loss

The first assumption implies that in general a one to one relation exists between the properties of the oil after evaporation of a certain fraction of the crude, and the properties measured in the laboratory after an equal fraction has been topped by distillation. However, corrections for temperature are made for the viscosity, based on a standard ASTM temperature relationship.

The fraction evaporated is computed by a pseudo-component concept, with the original composition defined in terms of the boiling point curve (Reinhart and Rose, 1982). Parameters such a equilibrium vapour pressure, molweight and specific density are derived from empirical relations related to the mean boiling point of each boiling point cut and the ambient temperature. The other parameters taken into account include the oil film thickness and a wind speed dependent mass transfer coefficient (Smith, 1989). The evaporative loss is obtained by numerical integration of the evaporation rate equation with variable time steps, adjusted on the basis of stability consideration related to the most volatile component remaining in the mixture.

The weathered oil properties, predicted by interpolation of the experimental data (table 2) on the basis of the computed evaporative loss, include the following, referred to non-emulsified (water free) oil: oil density, oil viscosity, flash point and pour point.

W/o-emulsion formation

For w/o-emulsions, the viscosity is known to depend on the viscosity of the parent oil and the water content. To establish the water content in field conditions, the following procedure is utilized (ref. assumption 2):

The rate of w/o-emulsion formation is known to depend on the mixing energy applied. Based on the rotating flask experiments, this rate may be expressed in terms of the parameter $t_{1/2}$, i.e. the mixing time elapsed when the water content is half of the maximum water content obtained after 24 hours of mixing. To establish a link between the laboratory experiment and sea conditions, the laboratory values of $t_{1/2}$ must be related to a given sea state, and the sea state dependence of the rate of w/o-emulsion formation must be known.

Presently, this link has been established on the basis of laboratory measurements on Ekofisk crude and field data on the same crude published by Cormack (1983). The comparison between these set of data, indicate that the rate of water uptake obtained with the rotating flask corresponds to field conditions with wind speed of 20 m/s. This comparison was based on a wind dependence of the rate of w/o-emulsion formation proposed by Mackay et al. (1980), i.e.

$$t_{1/2}(U_2) = t_{1/2}(U_1)\,(1 + U_1)^2/(1 + U_2)^2 \qquad (1)$$

where U_1, U_2 represent different wind speeds.

The maximum water content obtained after 24 hours of mixing in the rotating flask experiment was found to depend on the stage of weathering of the parent oil, as shown previously in figure 6. The method used implies and exponential increase in the water content towards these maximum values, with a rate determined by the $t_{1/2}$ values adjusted to the actual sea state.

The viscosity of the w/o-emulsion (μ) depends, as indicated above, on the viscosity of the parent oil (μ_{oil}), and the water content. A relationship proposed by Hossain and Mackay (1980) is applied for this purpose:

$$\mu = \mu_{oil}\,\exp[a\,W/(100 - b\,W)] \qquad (2)$$

where a and b are empirical constants; $a = 2.5$, $b = 0.654$, W, water content in the w/o-emulsion (%).

However, results from the viscosity measurements of w/o-emulsions formed in the laboratory procedure indicate that the empirical constant a in Eq. (2) is dependent on the stage of weathering, and the type of crude under investigation. For this reason, we have chosen to use an empirically determined factor a in the predictions, adjusted to fit the viscosity ratio obtained from the laboratory measurements on the different weathered oil samples.

Applications

The method described above implies in short terms that the properties of weathered oils are obtained from a standardised laboratory investigation of the crude oil. These data are then transferred to sea conditions by computations of evaporative loss and w/o-emulsion formation related to a chosen set of initial conditions (sea state, sea temperature, oil film thickness).

Figure 11 gives a schematic diagram of the experimental data that are put into the model, and the predicted properties that comes out of the model.

This procedure is presently applied in Norway for production of manuals on weathered properties of selected North Sea crude oils, including graphical charts for the development of each property with time under a chosen set of sea conditions (wind speeds) both at summer and winter sea temperatures. Examples of such standard charts are given in figures 12a and b, including evaporative loss, pour point, water content and viscosity of the w/o-emulsion in terms of time for a set of wind speeds. Corresponding charts are produced for the other properties of concern, i.e. density, flash point and viscosity of the parent oil. Criteria related to the effectiveness of dispersants are included in the charts, based on the results from the laboratory investigation (e.g. figure 9). This implies threshold values for viscosity of the w/o-emulsion, and limitations resulting from the increase in the pour point of the oil. This means that the "time window" for chemical treatment operations can be estimated for the specific crude under chosen set of sea conditions (Figure 12b).

The prediction model is presently running on a VAX-main frame computer, however, to make this model generally available, we aim in the near future at implementing the model on IBM compatible personal computers.

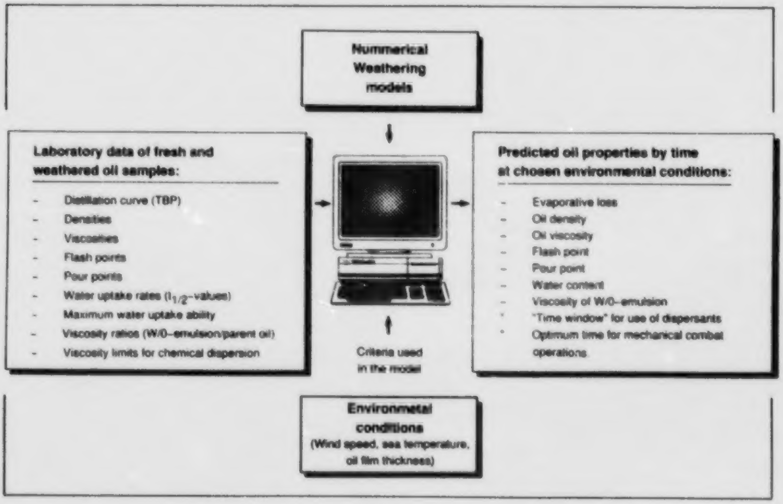
Nummerical
Weathering
models
Laboratory data of fresh and
weathered oil samples:
- Distillation curve (TBP)
- Densities
- Viscosities
- Flash points
- Pour points
- Water uptake rates ($t_{1/2}$-values)
- Maximum water uptake ability
- Viscosity ratios (W/O-emulsion/parent oil)
- Viscosity limits for chemical dispersion
Criteria used
in the model
Predicted oil properties by time
at chosen environmental conditions:
- Evaporative loss
- Oil density
- Oil viscosity
- Flash point
- Pour point
- Water content
- Viscosity of W/O-emulsion
* "Time window" for use of dispersants
* Optimum time for mechanical combat operations
Environmetal
conditions
(Wind speed, sea temperature,
oil film thickness)

Figure 11. Schematic diagram of the input data to the model and the predicted output oil properties.

Property: **EVAPORATIVE LOSS**

Oil Type: Oseberg Crude (30/9-T1, Etive Formation)

Data Source: IKU (Sintef group), Oceanor A/S Date: 7 Feb. 1989

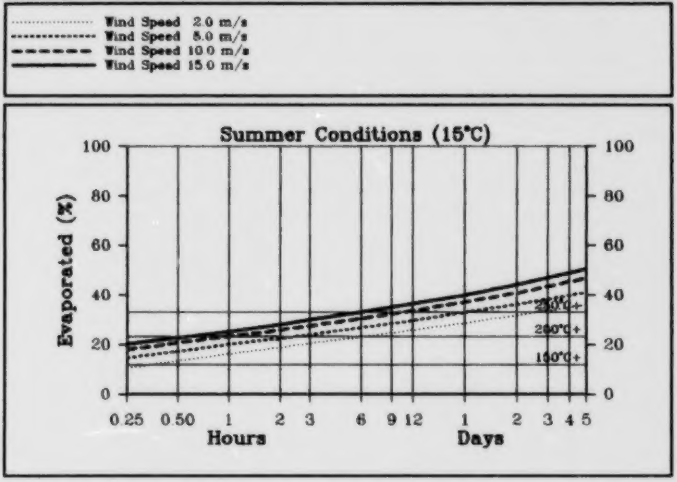

Property: **POUR POINT**

Oil Type: Oseberg Crude (30/9-T1, Etive Formation)

Data Source: IKU (Sintef group), Oceanor A/S Date: 7 Feb. 1989

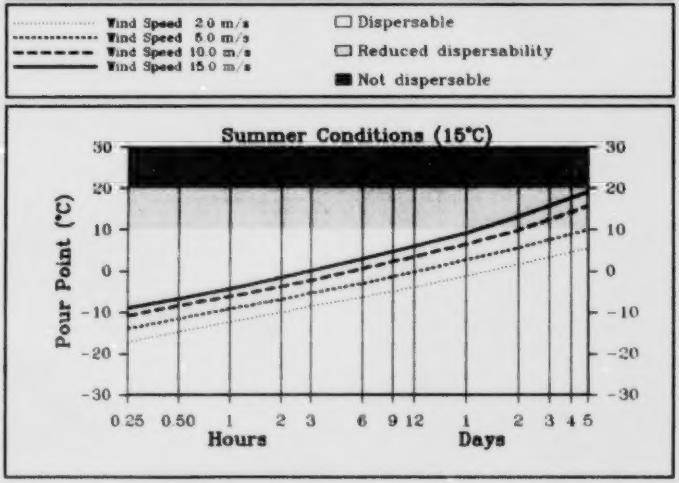

Figure 12a. Examples of standard charts on predicted oil properties (evaporative loss and pour point) of Oseberg crude under a chosen set of sea conditions (wind speeds).

Property: **WATER CONTENT**

Oil Type: Oseberg Crude (30/9-T1, Etive Formation)

Data Source: IKU (Sintef group), Oceanor A/S Date: 7 Feb. 1989

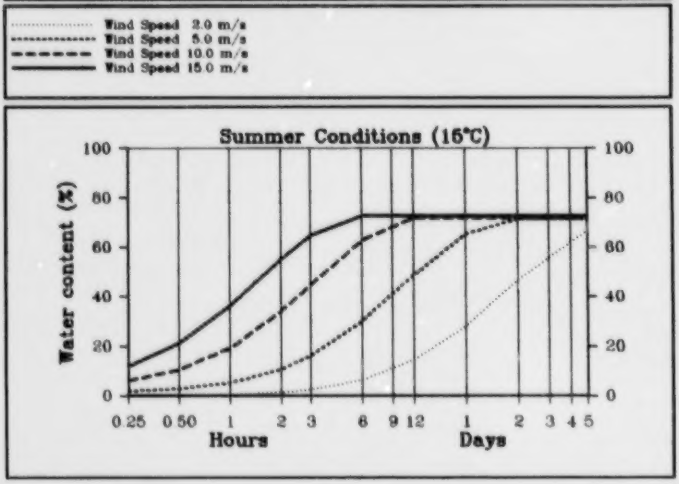

Property: **VISCOSITY OF EMULSION**

Oil Type: Oseberg Crude (30/9-T1, Etive Formation)

Data Source: IKU (Sintef group), Oceanor A/S Date: 7 Feb. 1989

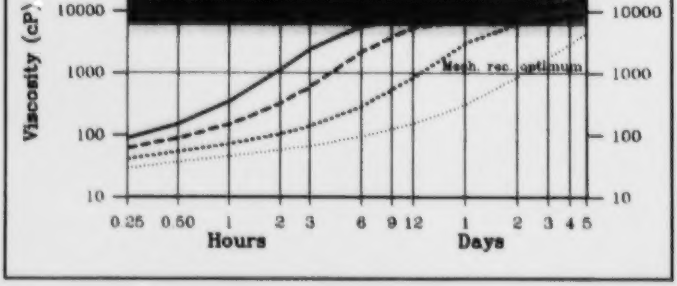

Figure 12b. Examples of standard charts on predicted oil properties (water content and viscosity) of Oseberg crude under a chosen set of sea conditions (wind speeds).

CONCLUSIONS AND RECOMMENDATIONS

Extensive laboratory investigations of crude properties combined with numerical modelling have been used for predicting the behaviour of oils spilled on the sea. The new approach has clearly demonstrated that the type of crude is essential for the rate of the weathering processes (water uptake, viscosity increase etc.) under different sea conditions. The method reveals that even for the North Sea crudes, where variation in the physico-chemical parameters are relatively small (same oil-class according to EPA, 1982), the weathering behaviour and the effectiveness of dispersants at sea may vary greatly.

It is hoped that the approach used here will be considered by other laboratories and used in a similar way on a large number of crude oils. This kind of investigations will provide valuable data input which later may be used for extending present prediction models.

With experimental weathering data available for a wide range of oils, correlations may be derived for reliable predictions of oil weathering properties on the basis of only generally available crude assay data (e.g. true boiling point curves, density, pour point, wax and asphaltene content etc.). It is also hoped that such oil property predictions can form basis for reliable evaluations of the "time window" for effective use of other countermeasures (including mechanical recovery equipment, burning and other oil spill chemicals) on various oil qualities which may be spilled under a variety of environmental conditions.

ACKNOWLEDGEMENTS

The work reported here is part of the research program presently running at IKU called "Application of Dispersants on Weathered Oils (DIWO)". The DIWO program is funded by Fina Exploration Norway Utenl. A/S. Special gratitude goes to Halfdan Akre-Aas (Akre-Aas Miljøkjemi A/S) and Alain Charlier (FINA Research) for their extensive engagement in the research program.

REFERENCES

BOCARD, C., CASTAING, G., GATELLIER, C.: "Chemical oil dispersion in trials at sea and in laboratory tests: the key role of dilution processes". In: Oil Spill Chemical Dispersants: Research, Experience and Recommendations, STP 840, Tom E. Allen, Ed., American Society for Testing and Materials, Philadelphia, pp.125-142, 1984.

BRIDIÉ, A.L., WANDERS, TH.H., ZEGVELD, W., v. DEN HEIJDE, H.B., "Formation, Prevention and Breaking of Sea Water in Crude Oil Emulsions, Chocolate Mousse", Marine Poll. Bull., vol.11, pp.343-348, 1980.

CORMACK, D.: Response to oil and chemical marine pollution, Applied Science Publishers Ltd., Essex, England, ISBN 0-85334-182-6, pp.36, 1983.

DALING, P.S.: A study of the chemical dispersability of fresh and weathered crude oils. Proceedings of the eleventh Arctic and Marine Oil Spill Program Technical Seminar, Environment Canada, Ottawa, Ontario, pp.481-499, 1988.

DALING, P.S., ALMÅS, I.K.: Description of laboratory methods in the DIWO-project. DIWO-report no. 2. IKU, Trondheim, Norway, 1988.

DALING, P.S., BRANDVIK, P.J.: A study of the formation and stability of water-in-oil emulsions. Proceedings of the 11th AMOP-seminar, Environment Canada, Ottawa, pp.153-170, 1988.

ENVIRONMENTAL PROTECTION AGENCY (EPA), Manual of practice - Chemical Agents in Oil Spill Control, EPA-report no. 600/8-82-0/0, Washington D.C., 1982.

FINGAS, M., DEBRA, L.M., WHITE, B., STOODLEY, R.G., CRERAR, I.D.: Laboratory testing of dispersant effectiveness: The importance of oil-to-water ratio and settling time. Proceedings of the 1989 Oil Spill Conference, API, Washington D.C., pp.365-373, 1989.

GILLOT, A., CHARLIER, A., VAN ELMBT, R.: "Correlation results between IFP and WSL laboratory tests of dispersants". In: Oil and Chemical Pollution. Vol. 3, no. 6, pp.445-453, 1987.

HOSSAIN, K., MACKAY, D.: "Demulsifiers - a new chemical for oil spill countermeasures". Spill Technology Newsletter, Vol. 5, No. 6, pp.154-156, 1980.

LEWIS, A., BYFORD, D.C., LASKEY, P.R.: "Significance of dispersed oil droplet size in determining dispersant effectiveness under various conditions". In: Proceedings of the 1985 Oil Spill Conference, API, Washington D.C., pp.433-440, 1985.

LICHTENTHALER, R.G., DALING, P.S.: Aerial application of dispersants - comparison of slick behaviour of chemically treated versus non-treated slicks. In: Proceedings of the 1985 Oil Spill Conference, API, Washington D.C., pp.471-478, 1985.

MACKAY, D., BUIST, I., MASCARENHAS, R., PATERSON, S.: Oil spill processes and models. Report EE-8, Environment Canada, Ottawa, Ontario, 1980.

MACKAY, D., SZETO, F.: Effectiveness of oil spill dispersants - development of a laboratory method and results for selected commercial products. Institute of Environmental Studies, University of Toronto, Publ. no. EE-16, 1980.

MACKAY, D., ZAGORSKY, W.: Studies of water-in-oil emulsions. Report EE-34: Environment Canada, Ottawa, Ontario, 1982.

MACKAY, D., CHAU, A., POON, Y.C.: A study of the mechanism of chemical dispersion of oil spills. Environment Canada report, March, 1985.

MACKAY, D., CHAU, A.: A study of oil dispersion. The role of mixing and weathering. Environment Canada report, March, 1987.

MACKAY, D.: Formation and stability of water-in-oil emulsions. DIWO-report no. 1, IKU, Trondheim, Norway, 1987.

MARTINELLI, F.N., LYNCH, B.W.J.: Factors affecting the efficiency of dispersants, Warren Spring Laboratory, Report :LR363, 1980.

MARTINELLI, F.N.: "The status of the Warren Spring Laboratory's Rolling flask test". In: Oil Spill Chemical Dispersants: Research, experience and recommendations. STP 840. Tom E. Allen, Ed. American Society for Testing and Materials, Philadelphia, pp.55-68, 1984.

MORRIS, P.R., MARTINELLI, F.N.: A specification for oil spill dispersants. Warren Spring Laboratory. Report LR448B(OP), 1983.

NATIONAL ACADEMY OF SCIENCES: Oil in the sea: Inputs, fates and effects. National Academy Press, Washington D.C, 1985.

NATIONAL RESEARCH COUNCIL (NRC): Using oil spill dispersants on the sea. National Academy Press, Washington D.C., 250pp, 1989.

REINHART R., ROSE, R.: "Evaporation of crude oil at sea". Water Res. Vol. 16, pp.1319-1325, 1982.

ROSS, S.L.: An experimental study of the oil spill treating agents that inhibit emulsification and promote dispersion. Report EE-87, Environment Canada, Ottawa, Ontario, 1986.

SMITH, S.D.: "Coefficients for sea surface wind stress, heat flux, and wind profiles as a function of wind speed and temperature". J.Geophys.Res. Vol.93, No.C12, pp.15467-15472, 1987.

STIVER, W., MACKAY, D.: "Evaporation rate of spills of hydrocarbons and petroleum mixtures". Environ. Sci. Technol., Vol.18, no.11, pp.834-840, 1984.

MODELLING THE SPREAD OF OIL SPILLS IN ICE-INFESTED WATERS

S. Venkatesh
Atmospheric Environment Service
4905 Dufferin Street
Downsview, Ontario, Canada M3H 5T4

H. El-Tahan*, G. Comfort, R. Abdelnour
Fleet Technolgy Limited
311 Leggett Drive
Kanata, Ontario, Canada K2K 1Z8

ABSTRACT

This paper describes methodologies developed for predicting the spread of oil spills in ice-infested waters. Particular emphasis is placed on oil spills in medium and high ice concentrations. Empirical methods are used to determine the spread of oil in ice of different concentrations. The study showed that the equilibrium oil thickness in slush or brash ice is nearly four times that on cold water which is itself very different from that on warm water. Comparisons with limited available data show good agreement.

1.0 INTRODUCTION

The potential development of the oil fields in the Arctic and on the Grand Banks off the Canadian east coast has brought into focus the need for the development of effective countermeasures for oil spills in cold ocean environments. While the problem of oil spills on open water has been extensively studied (see reviews on the subject by Stolzenbach (1977), Huang and Monastero (1983), Spaulding (1988) and recent work by Venkatesh (1988) and Venkatesh et al. (1988)), the cold ocean presents some unique problems in dealing with oil spills.

The presence of ice further complicates an already complex problem in understanding the behaviour and fate of oil released under various cold ocean environmental conditions. In response to this concern, several field and laboratory studies have been conducted over the past decade. Most of these studies were concerned mainly with oil spilled on the water surface and on, or under, continuous static ice. Some studies have recently been carried out to study the behavior and fate of oil spills in open leads.

The behaviour and fate of oil spills under the above-mentioned conditions are at the point of being reasonably well understood and numerical models have been developed for prediction purposes. While the knowledge base for the behaviour of oil spills in open water and under solid ice cover has been building, there is a conspicuous absence of data on oil spills that occur in broken ice cover. The experience of the Kurdistan spill (Reimer (1980), Dawe et al. (1981)) provides an example of oil spills in non-continuous ice cover. Understanding the spread of oil in broken ice fields that may consist of various types of ice such as floes, pancakes, grease ice, slush, brash ice, etc., (See Armstrong et al. (1966) for definitions) becomes very important in dealing with oil spills that take place before or during the Arctic ice buildup/breakup seasons. A brief review of literature related to oil spills in cold ocean environments can be found in Venkatesh et al. (1990).

---

*Present affiliation: Crescent Consulting Ltd., P.O. Box 2638, Stn. C, St. John's, Nfld., A1C 6K1

This paper describes a model developed to predict the behaviour of oil spills in broken ice fields with intermediate to high ice concentrations (behaviour in low ice concentration is expected to be similar to that in open water). The model is intended to emphasize accidental oil spills in cold ice- infested oceans, rather than well blowouts where a large quantity of gas may be present. Also emphasized is the physical behaviour, rather than the chemical fate of the oil. The model is evaluated against the very limited data available.

2.0 MODELLING OF OIL SPILLS IN BROKEN ICE

The work to date has identified a number of processes and parameters which significantly affect the fate and behaviour of oil released in broken ice and lead conditions. These processes include:

a) the physical motion of oil in broken ice which would be a function of ice concentration, floe sizes and thicknesses, presence of deformed ice, and other parameters whose influences are not clearly understood;

b) oil storage in under-ice roughnesses;

c) oil spreading under gravity forces and containment provided by the ice floes and brash (broken) ice;

d) oil entrainment in ice in freezing situations and oil absorption in snow and slush mixtures;

e) oil particle adherence to brash and pancake ice;

f) oil chemical property changes (e.g. weathering), the formation of emulsions and the formation of oil globules.

The overall interaction of the above-mentioned processes is complex and a detailed model would involve a large number of input parameters which are not likely to be known in a field situation and/or are likely to be highly variable. Except for the storage of oil under sheet ice (eg. Comfort, 1986; Wotherspoon et al., 1985), models have not been developed to adequately parameterize most of the processes.

Therefore at this stage one requires a simplified modelling approach which makes use of basic input data that are likely to be available in a field situation. In this paper the model development is limited to consideration of the spreading of oil in ice of medium to high concentrations. It is also assumed that the spill consists only of oil and not an oil and gas mixture.

2.1 QUANTIFYING OIL SPREADING IN BROKEN ICE

There are two aspects to the spreading of an oil spill. One is the thickness of the oil as it spreads and the other the areal extent of the oil-contaminated zone (see Figure 1). The spreading of oil in the presence of ice may be quite different from that on open water.

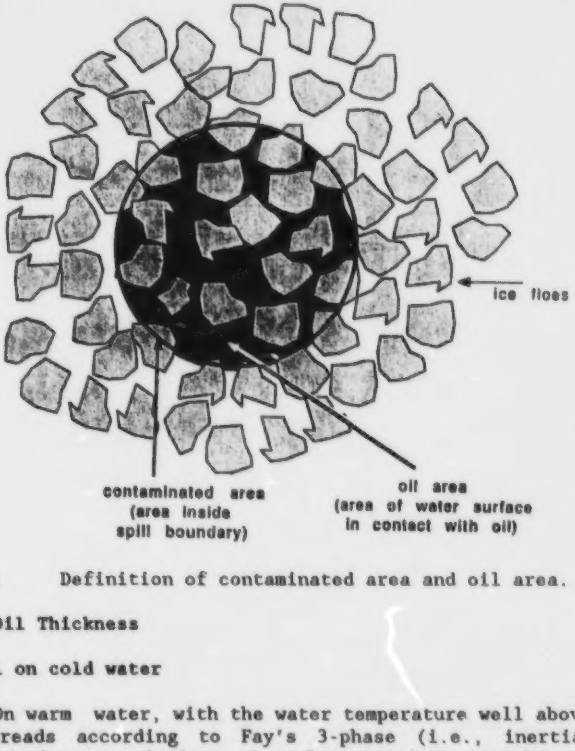
ice floes
contaminated area (area inside spill boundary)
oil area (area of water surface in contact with oil)

Fig. 1: Definition of contaminated area and oil area.

2.1.1 Oil Thickness

(a) Oil on cold water

On warm water, with the water temperature well above freezing, oil spreads according to Fay's 3-phase (i.e., inertia/ gravity, gravity/ viscous and viscous/ surface tension) equations (Fay (1969, 1971), see also Venkatesh(1988)). In the third phase where viscous and surface tension forces are in balance, the radius of the spill at any time t is given by

$$r = \frac{K\sigma^{1/2}}{(\rho_w^2 \nu_w)^{0.25}} t^{0.75} \qquad (1)$$

Table 1: Data from oil spills in cold and/or ice-infested waters

REFERENCE	TEST	OIL TYPE	OIL VOL.	AIR	WATER	OIL THIC.	ICE	TIME TO	REMARKS
			(LITRES)	TEMP °C	TEMP °C	(mm)	CONCENT	EQLBRM	
TASK FORCE'83	FIELD	PRUDHOE B	136	1.7	0.5	2.8	3/8-5/8	2-3 MIN.	WIND 5-7 KNTS
TASK FORCE'83	FIELD	PRUDHOE B	1090	2.2 TO 3	0.5	3	3/8-5/8	3-3.5 MIN.	WIND 5-7 KNTS
TASK FORCE'83	FIELD	PRUDHOE B	1090	2.2 TO 3	0.5	3.3	3/8-5/8	3-3.5 MIN.	WIND 16-18 KNTS
GETMAN&SCHULTZ'76	LAB	PRUDHOE B	90.8	0	0	7.3	0	"VERY FAST"	
GETMAN&SCHULTZ'76	LAB	PRUDHOE B	90.8	0	0	25-37	90%	"VERY FAST"	ICE AFFECTED SPREADING
GETMAN&SCHULTZ'76	LAB	#2 FUEL	3.8	0	0	< 0.2	0	"VERY FAST"	SPREADING LIMITED BY TANK
GETMAN&SCHULTZ'76	LAB	#2 FUEL	3.8	0	0	SEE REM	90%	"VERY FAST"	SPREADING AS IN OPEN WATER
METGE & TELFORD '79	LAB	PRUDHOE B	0.05	-6 TO -9	1.3	1.3	0	< 1 MIN.	
METGE & TELFORD '79	LAB	PRUDHOE B	0.05	-6 TO -9	1.3	SEE REM	SLUSH	SEE REM	OIL WAS RELEASED UNDER
METGE & TELFORD '79	LAB	ATKINSON	0.05	-6 TO -9	1.3	< 0.04	0	< 1 HR	30 mm SLUSH, PERCOLATED
METGE & TELFORD '79	LAB	ATKINSON	0.05	-6 TO -9	1.3	1	SLUSH	< 1 HR	THROUGH SLUSH AND SPREAD
METGE & TELFORD '79	LAB	NORMAN W.	0.05	-6 TO -9	1.3	1.3	0	< 1 MIN.	OVER SLUSH EXCEPT PRUDHOE B
METGE & TELFORD '79	LAB	NORMAN W.	0.05	-6 TO -9	1.3	1.6	SLUSH	< 1 HR	OIL REMAINED UNDER SLUSH
ROSS & DICKINS '87b	FIELD	ALBERTA	1000	-8	-1.5	0.03-1	40-60 %	> 3 HRS	OIL REL. ON OPEN WATER
ROSS & DICKINS '87b	FIELD	SWEET MI-	1000	-14	-1.5	28	60-70 %	15 MIN.	OIL REL. ON 35 CM BRASH ICE
ROSS & DICKINS '87b	FIELD	XED BLEND	1000	-11	-1.5	28	30-50 %	1MIN	OIL REL. ON 35 CM BRASH ICE
BUIST ET AL '87	LAB	M.S.W.	1	-3 TO -8	1.5	1	OPEN W.	N/A	MIXED SWEET WESTERN OIL
BUIST ET AL '87	LAB	M.S.W.	1	-3	0	2.52	SLUSH	3 MIN.	MIXED SWEET WESTERN OIL
BUIST ET AL '87	LAB	86%BUNK.C	1	-3	0	10.4	SLUSH	N/A	86 % BUNKER C, 14% DESIL
BUIST ET AL '87	LAB	45%BUNK.C	1	-3	0	1.38	SLUSH	N/A	45 % BUNKER C, 55% DESIL
BUIST ET AL '87	LAB	86%BUNK.C	1	-3	0	39.2	SEE REM	N/A	CONSOLIDATED GREASE ICE
BUIST ET AL '87	LAB	M.S.W.	1	-3	0	2.85	SEE REM	N/A	CONSOLIDATED GREASE ICE
BUIST ET AL '87	LAB	M.S.W.	1	3	0	1.1	SLUSH	14 HR	3.5 m/s WIND
									(7 m/s FOR ABOVE TESTS)
MACNEIL&GOODMAN'8	OD	ADGO OIL	10	-3	-0.5	5-10	SLUSH	N/A	LEAD HAS SLUSHY WATER
MACNEIL&GOODMAN'8	BASIN	ADGO OIL	5	-2	-0.5	2	OPEN W.	N/A	OPEN LEAD HAS NO SLUSH

where

ρ_w = density of water
ν_w = kinematic viscosity of water

K = 2.3
σ = spreading coefficient for a specific type of oil.

According to Fay (1971), the radius r_{max} at maximum spread is given by the dimensional relationship

$$\pi r^2_{max} = 10^5 V^{0.75} \qquad (2)$$

where r_{max} is in m and the volume V of oil is in m^3. Fay also suggests that the cessation of spread is caused by the evaporation of certain oil fractions which reduces the spreading coefficient to zero.

However, on 'cold' water where the water temperature is near freezing, the equilibrium thickness of oil is observed to be much higher than that suggested by Fay's theory and is reached much sooner than the time indicated by Fay's 'warm' water equations. Schultz (1984) noted that in a cold environment the surface tension spreading (the third phase) is absent. The gravity/viscous (referred to as viscous) spreading is given by (Fay, 1971)

$$r = K_v(\Delta g V^2 t^{3/2} \nu_w^{-1/2})^{1/6} \qquad (3)$$

where

K_v = 1.45
Δ = Ratio of density difference between water and oil to density of water
g = Acceleration due to gravity.

Based on spreading experiments conducted with a range of oil viscosities, Ross and Energetex Engineering (1985) suggested a correction factor to be applied to Eq.(3). The corection in effect replaced the water viscosity in Eq.(3) with the viscosity of the oil ν_o. Therefore the modified Fay's equation for viscous spreading is

$$r = K_v(\Delta g V^2 t^{3/2} \nu_o^{-1/2})^{1/6} \qquad (4).$$

Plots of the area attained at the time of cessation of spreading of each of the spills in open cold water listed in Table 1 show that the points lie on the curve defined by Fay's equation for surface tension spreading (Eq.(1)) and/or the modified equation for viscous spreading (Eq.(4)). Figure 2 is a plot of the data from the spills of Industry Task Group (1983). The density and viscosity of the oil used in this study were 914 kg m^{-3} and 500 mPa s (milli-Pascal seconds) respectively. (See Ross and Dickins (1987b) for a plot of the data from that study.) In Figure 2 the radius of the spill at cessation of spreading (and hence the time taken to reach that stage at which spreading ceased) was not that obtained by using Eq.(2). In fact all spills listed in Table 1, except one, followed the viscous spreading curves and the spreading ceased before entering the surface tension phase. Therefore, while Fay's equations can be used to determine the initial rate of oil spreading in cold water, they cannot be used to predict the time of maximum spread and hence the equilibrium area or equilibrium thickness. For comparison Figure 2 also shows the equilibrium area attained by spills 2 and 3 (spills in brash ice) from the Ross and Dickins (1987b) study. (In the field tests carried out by Ross and Dickins (1987b) there were three separate oil releases the locations of which are shown in Figure 3. In spill 1 the oil was released in the open water area of a 40-60% concentration ice cover. Spills 2 and 3 were released on 35 cm brash ice.) In these cases the observed area is several orders of magnitude less than that predicted by Fay's equations.

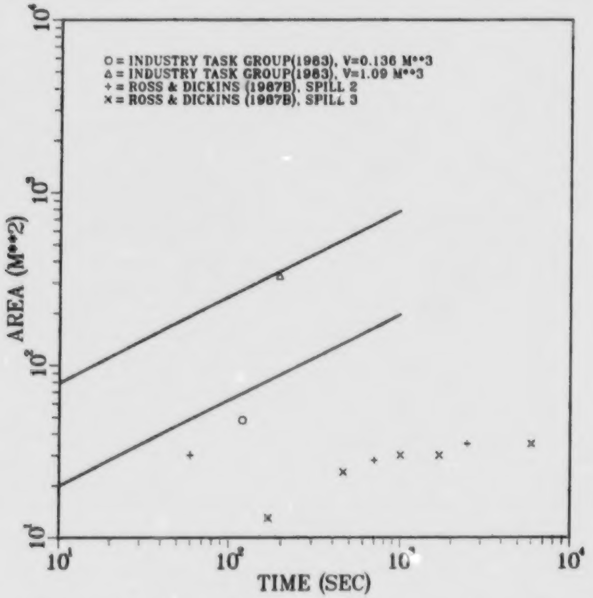

Fig. 2: Observed areas of oil from Industry Task Group (1983) spills (see Table 1). Solid lines represent plots of Eq.(4) for oil volumes of 1.09 m^3 (upper curve) and 0.136 m^3. Figure also shows observed areas from Spills 2 and 3 of Ross and Dickins (1987b).

In view of the non-applicability of Fay's equations to determine the equilibrium thickness of oil spills in cold water, an empirical approach was taken. For liquids, viscosity is a parameter that usually increases with decreasing temperature (Bird et al., 1960). But viscous forces come into play only when there is relative motion and hence viscosity may not be an appropriate factor to control equilibrium oil thickness which implies no motion. However, in the absence of any other obvious choice of parameter or an understanding of the physical reasons for the higher equilibrium oil thicknesses in cold water, a correlation between viscosity and oil thickness was attempted. The observed thicknesses (assumed to be at or near equilibrium since no appreciable changes beyond this time were noted) from Table 1 were plotted against oil viscosity (Figure 4) and the oil thickness is indeed seen to increase with viscosity. With the limited number of data points, a linear fit was assumed. From Figure 4, for oil spills in cold water, the equilibrium thickness T_w (mm) can be related to the viscosity of the oil, μ (mPa s), by

$$T_w = \mu/125 \qquad (5)$$

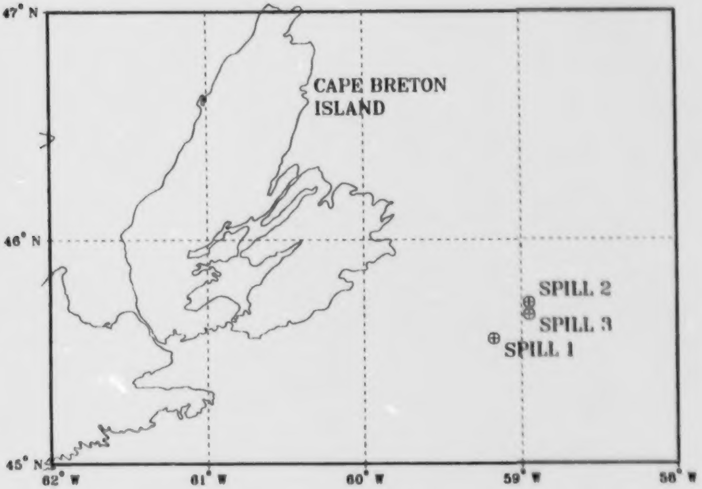

Fig. 3: Locations of oil releases in the Ross and Dickins study (Adapted from Ross and Dickins, 1987b).

where the line is constrained to pass through the origin. (The intercept is small even without this constraint.) Figure 4 includes data from the study of Schultz (1984) where the oil thickness was "estimated" to be about 5 mm (data not shown in Table 1 due to measurement uncertainties). The slope of the line in Figure 4 is, however, not very different with or without this data (slope difference of about 4%). The data for the open water spill from Ross and Dickins (1987b) will be used as an independent test case for evaluation purposes.

(b) Oil spreading in particle ice

The term "particle ice" includes slush, frazil ice, brash ice or grease ice (see Armstrong et al. (1966) for definitions). Ross and Dickins (1987b) carried out field tests where 1 m^3 of oil were spilled in brash (broken) ice of thickness 30-40 cm (Spills 2 and 3 in Table 1). In both spills 2 and 3 the oil reached a near equilibrium thickness of about 28 mm in less than 15 minutes and as indicated in Figure 2 did not follow Fay's equations. Ross and Dickins (1987b) found that this thickness can be predicted by the equation developed by Kawamura et al. (1986) for spreading of oil in snow. The final area A_f of a spill in snow is given by

$$A_f = \frac{0.45\ V^{0.2}\ d^{0.2}\ \rho_o^{\ 0.0675}\ g^{0.4125}\ \mu_o^{\ 0.05}}{(\varphi\ \rho_s)^{0.48}\ \delta^{0.4375}} \qquad (6)$$

where

V = spill volume (m^3)
d = snow depth (m)
φ = snow crystal factor
  = 1.0 for crystalline snow
  = 0.1 for spherical snow
ρ_o = oil density (kg/m^3)
ρ_s = snow density (kg/m^3)
μ_o = oil viscosity (Pas)
δ = surface tension of spilled substance (N/m)
g = accelaration due to gravity (m/s^2)

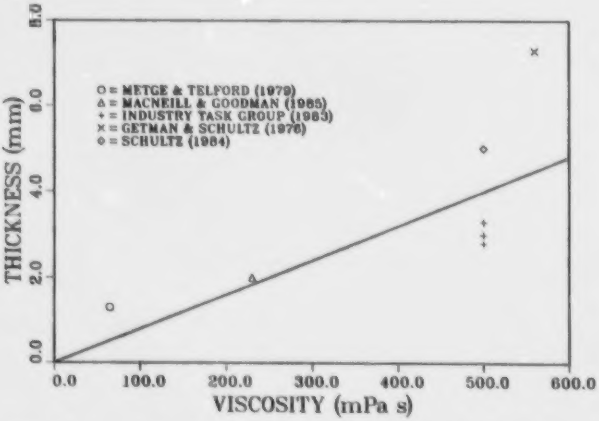

Fig. 4: Oil thickness as a function of oil viscosity for spills on cold water (Water temperature -1.5°C to +1.3°C). The line is defined by Eq.(5).

After making some assumptions for the equivalent thickness of the snow layer and crystal structure of the snow, they arrived at a computed thickness of 28.8 mm, which is very close to the observed value. However, the computed time of spreading, using an equation proposed by Kawamura et al., was found to be several orders of magnitude greater than that observed.

The applicability of the Kawamura et al. (1986) formulation to the rest of the oil in ice data from Table 1 was examined (Table 2).

Table 2: Observed and computed oil thicknesses of spills on brash ice or slush. Computed thicknesses are obtained using the spill-on-snow equation of Kawamura et al. (1986)

REFERENCE	OIL TYPE	OIL VOLUME (m^3)	OIL DENSITY kg/m^3	OIL VISC. (Pas)	OIL SIGMA (N/m)	SNOW DEPTH (m)	COMPUTED OIL AREA m^2	COMP. THICK (mm)	OBSERVED THICKNESS (mm)
ROSS&DICK '87b	ALBERTA S.M.B.	1	857	0.0437	0.032	0.05	34.678	28.8	28
BUIST ETAL'87	M.S.W.	0.001	857	0.0437	0.032	0.003	0.050	20.2	1.1 & 2.9
BUIST ETAL'87	BUNKERC 45%	0.001	917	0.074	0.02	0.003	0.066	15.1	1.38
BUIST ETAL'87	BUNKER C 45%	0.001	981	1.481	0.04	0.003	0.060	16.6	39.2
MACNEIL&GD'85	ADGO OIL	0.01	952	0.234	0.021	0.025	0.796	12.6	5-10

SNOW DENSITY = 800 KG/M^3 CRYSTAL FACTOR = 1

As seen from Table 2 the equation of oil spreading in snow could not be used to predict the observed oil thicknesses except for the Ross and Dickins (1987b) spills. The observed and computed thicknesses differ by at least a factor of 2 and as much as a factor of 20. Furthermore, the Kawamura et al. formulation predicts that (for a given oil-water surface tension) the equilibrium thickness decreases as the oil viscosity increases while observations seem to indicate otherwise.

Once again an empirical approach was adopted to obtain a better estimate of the oil equilibrium thickness in the presence of particle ice. The relevant data from Table 1 are used. Again, given the scarcity of data a linear fit was assumed in the curve fitting process. Figure 5 shows a plot of the data. Note that the data from the Ross and Dickins study are excluded from Figure 5, but are used as independent cases for testing the proposed model. From Figure 5, through a least squares fit, the equilibrium thickness, T_s (mm) in particle ice can be related to the viscosity, μ, (mPa S) by:

$$T_s = 0.0316\,\mu \qquad (7)$$

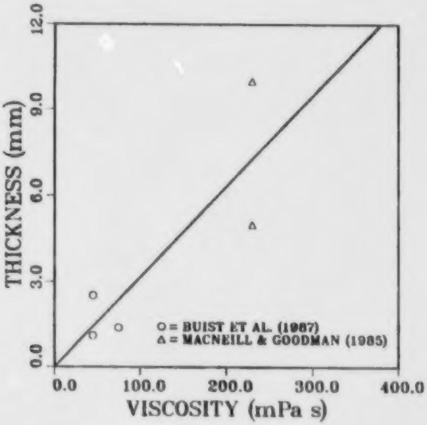

Fig. 5: Oil thickness as a function of oil viscosity for spills on water covered by slush. The line is defined by Eq.(7).

2.1.2 Area of oil-contaminated zone

This area will obviously be a function of the ice concentration since the latter defines the amount of open water available and hence a path for the oil to spread. For the sake of convenience the ice concentration C will be divided into three broad classes:

i)	$C < 30\%$	Low Concentrations
ii)	$30\% < C < 80\%$	Medium Concentrations

iii) $C > 80\%$ High Concentrations.

While the border between low and medium ice concentrations is somewhat arbitrary, the reasons for the choice of 80% as the border between medium and high concentrations is discussed later.

In examining the spread of oil in various ice concentrations a point source (for the oil) below the ice is considered. The source is assumed to be close enough to the bottom of the ice that the oil is assumed not to spread laterally as it rises to meet the ice. A point source below the ice is chosen so that the trapping of the oil on the underside of the ice can also be described and evaluated. A spill at the surface is a subset of this scenario.

(a) Low ice concentrations

An oil spill in ice of low concentrations ($C < 30\%$) is treated as being similar to that in cold open water. It is also assumed that no appreciable quantity of oil will be trapped under the ice. Under such low concentration conditions, the surface area covered with ice will generally be small enough for this assumption to be valid (see section on sensitivity studies). Ice concentration affects only the extent of the oil-contaminated zone.

If T_w is the equilibrium thickness of a given oil on cold open water and V is the volume of oil spilled, then the area A_s of the oil-contaminated zone is given by

$$A_s = V/(T_w(1-C)) \qquad (8).$$

In the absence of ice, of course, the area would be given by V/T_w.

(b) Medium ice concentrations

There are two main features that distinguish the spread of oil in ice of medium concentration from that in low ice concentration. They are (i)some of the oil is trapped on the underside of the ice floe that the oil encounters as it rises to the surface, and (ii)a portion of the oil is trapped by slush or brash (broken) ice. A quantitative estimate of the amount of oil accounted for by these two factors is given below.

(i) Oil under ice

As stated earlier we are using, for the spill, a point source a short distance below the underside of the ice. Assuming no lateral spreading of the oil as it rises to the surface, the oil will contact the underside of a single ice floe. If A_{fl} is the horizontal area of an average floe and T_{ui} the under-ice storage volume per unit area (i.e. thickness units), the volume of oil trapped on the underside of the average floe is given by

$$V_{ui} = A_{fl} * T_{ui} * C \qquad (9).$$

The factor C is included in the above equation as a measure of the probability that the oil will encounter the average floe. Here the probability is assumed to be the same as the ice concentration.

The work of Comfort (1987) (see also Kovacs(1981) and Comfort(1986)) is used to estimate T_{ui}. The under ice storage volume is derived as a linear function of ice thickness for ice thickness greater than 0.5 m. The storage volume per unit area was taken as 30% of the ice thickness standard deviation when the depressions were filled to the mean thickness level. From observations the ice thickness standard deviations were found to vary from about 0.7% to 15.8% of the ice thickness for continuous ice sheets. In the present study the ice thickness standard deviation is assumed to be 7% of the ice thickness, a value near the middle of the range. Thus

$$T_{ui} = 0.3(\text{Ice thickness S.D.}) = 0.3*0.07(\text{Ice thickness}),\ \text{or}$$

$$T_{ui} = 0.021(\text{Ice thickness}). \qquad (10)$$

(ii) Oil in slush

The volume V_s of oil trapped by slush or brash ice is given by

$$V_s = T_s * A_s \qquad (11)$$

where A_s is the area covered by slush and is obtained from observations. T_s is computed from Eq.(7).

The remaining oil is then available for spreading. The volume of oil remaining is

$$V_r = V - (V_{ui} + V_s) \qquad (12)$$

and the area covered by this volume can be obtained from Eq.(8).

(c) High ice concentrations

The next category comprises ice concentrations of 80% or greater. The behaviour of oil in such concentrations will be very different from that in ice of lower concentrations. If one considers circular ice floes, the area of a circle of diameter d is approximately 80% of that of a square of side d. Thus at 80% concentration the circular ice floes will be touching each other and the oil once trapped in the space between ice floes will not be able to spread laterally. (The concentration at which the ice floes touch each other is a function of the shape of the floes and can vary from location to location within the ice pack. Thus the 80% value, appropriate for circular floes, is used here as one (perhaps the most likely) possibility. Therefore, while the concentration at which the ice floes touch each other may vary, the behaviour of spilled oil under such ice conditions can be expected to be similar.) The oil accumulating in the gaps will have thickness much greater than the equilibrium thickness defined by Eq.(5). The oil will either flow over the ice or seep under the ice depending on the ratio of oil and ice densities (see Figure 6). While for high ice concentrations the volume of oil trapped under a floe can be determined by using equation (9), the volume of oil trapped in the spaces between floes within an area A is given by

$$V_{fl} = (1-C)*A*h_o \qquad (13)$$

where h_o is the thickness of the oil filling the closed gaps (computation is presented in Figure 6).

If the concentration exceeds 95% the ice is assumed to be a solid ice cover and all oil will be stored under the ice.

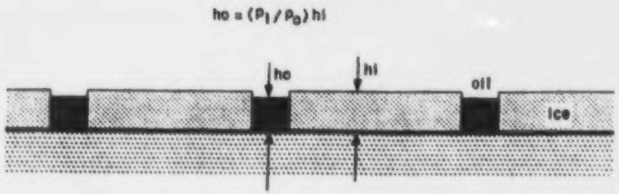

A) OIL DENSITY, ρ_o, IS HIGHER THAN ICE DENSITY, ρ_i

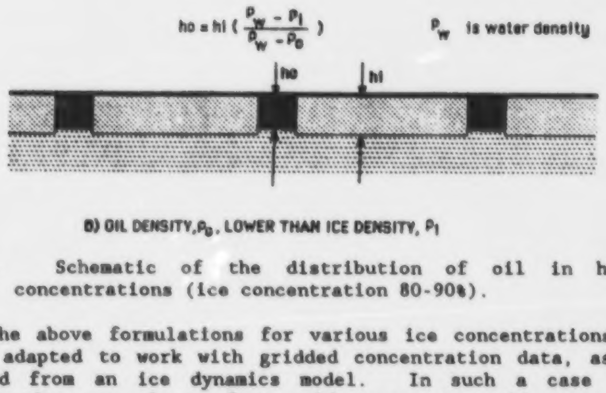
$ho = hi\left(\frac{\rho_w - \rho_i}{\rho_w - \rho_o}\right)$
ρ_w is water density
ho
hi

B) OIL DENSITY, ρ_o, LOWER THAN ICE DENSITY, ρ_i

Fig. 6: Schematic of the distribution of oil in high ice concentrations (ice concentration 80-90%).

The above formulations for various ice concentrations can be easily adapted to work with gridded concentration data, as may be obtained from an ice dynamics model. In such a case the ice concentration may change from grid square to grid square. The details of the spread of oil from one grid square to the next under these changing concentration conditions are given in El-Tahan et al. (1988). A detailed discussion of the sensitivity of the spreading model to various parameters is given in Venkatesh et al. (1990).

2.1.3 Evaluation of the Spreading Model

To carry out a comprehensive evaluation of any model one needs several complete sets of data that cover most of the possible scenarios and conditions which the model is designed to handle. An ideal data set for the evaluation of the present model should contain reasonably accurate measurements of oil spreading, drift of oil and ice, and ice/oil interactions made for a large oil spill over a long period of time. The data set should also include all the corresponding environmental data.

The extensive review carried out as part of this study indicated that available quantitative field data on oil spills in broken ice is extremely limited. Accidental oil spills in broken ice are rare and the information gathered from them are usually of a general qualitative nature. For example, spill of Bunker C oil from the tanker KURDISTAN in Cabot Strait in 1979 is considered to be one of the best documented investigations of a spill in a broken ice field. However, even in this spill no systematic measurements were made of the spreading of oil, the contaminated area or oil drift.

The only controlled quantitative field study designed to investigate the interaction of oil with broken ice is that by Ross and Dickins (1987b). They carried out three experimental spills each of $1m^3$ of Alberta Sweet Mixed Blend crude oil in pack ice off Cape Breton island on the Canadian east coast (Figure 3). The ice conditions ranged from 40-60% dynamic open pack ice (for spill 1) to more than 90% packed ice in a state of moderate compactness (spills 2 and 3). Each spill was monitored for a period of about 5 hours. Measurements were made of oil thickness, contaminated area, the drift of oil and ice and weathering of oil. In addition, currents were measured during spill 1 only while wind data, wave conditions and air temperatures were reported for spills 1, 2 and 3.

For Spill 1, where the oil was released in open water, some of the oil formed a thin layer that spread under gravity/surface tension forces while the rest of the oil was about one order of magnitude thicker and spread under gravity-viscous forces (see Ross and Dickins ,1987b). The thick part of the spill contained most of the oil. The contaminated area of the thin portion was observed to be about 100,000 m^2 while that of the thick portion was about 3,000 m^2. The other two spills, where the oil was released on 35 cm brash ice, spread substantially less than did Spill 1. The equilibrium areas for Spills 2 and 3 were observed to be 36 and 35 m^2, respectively.

In the present model the equilibrium thickness of oil is determined based on data collected from field and laboratory experiments that indicated viscous spreading of oil in most of the cases. Therefore it can only simulate the spreading of the thick portion of the oil in Spill 1. Since the spreading of Spills 2 and 3 were almost identical we decided to carry out the simulation for Spill 2 only in addition to Spill 1. The spreading and contaminated areas were obtained using the formulations described in section 2.1.

Ross and Dickins (1987b) reported that the spreading rate of spill 1 was described by Fay's equation for surface tension spreading, Eq.(1), for the thin portion of the slick and by the modified Fay's equation for viscous spreading, Eq.(4), for the thick portion of the slick. Since the oil was released on the surface of the open water (there was 50% ice cover nearby) there was, of course, no trapping of the oil underneath the ice. The oil had a density of

857 kg m^{-3} and a viscosity of 43.7 mPa S. From Eq. (5) the thickness of the thick portion of spill 1 is 0.35 mm and hence will occupy an area of 2857 m^2. This compares very well with the observed value of 3000 m^2.

Fay's equations failed to predict the spreading of spill 2 or spill 3 (that was spilled on compact brash ice). Given the small volume of oil spilled the spreading behaviour will very much depend on ice characteristics in the immediate vicinity of the spill. Ross and Dickins (1987b) state that the ice was in a state of moderate compression at the time of these spills. (Conditions surrounding the spill consisted of 3-3/10 medium first-year ice floes, and 3/10 pancakes. The remaining area was covered with a compressed slush layer.) One can therefore expect spreading behaviour to be similar to that of oil in ice of high concentration. With an ice concentration near 90% (including the compressed slush) the ice floes are touching each other and hence the oil is not free to spread laterally. The thickness of oil accumulating in the gaps between floes (Figure 6) is much larger than the equilibrium thickness on open water or in particle ice. Since the oil spill is at the surface there is no accumulation of oil under the ice. The ice thickness in the area was 0.35 m and the ice density was 910 kg m^{-3}. Accordingly, the predicted contaminated area, using the model developed here (see Figure 6b), is 42 m^2 (the corresponding area in particle ice, Eq.(7), will be 724 m^2). This compares very well with observed values of 36 m^2 and 35 m^2 respectively for spills 2 and 3.

The above comparison could be considered a fairly good but limited validation of the spreading mechanism presented in Figure 6. However, additional data sets are required for a more complete and accurate evaluation of the model.

3.0 SUMMARY AND CONCLUSIONS

In this paper methodologies have been developed for computing the spread of oil spills in broken ice. The spread of oil in ice fields of different concentrations is based on new parameterizations of the equilibrium thickness of the oil derived from observed data.

The study has reiterated that the equilibrium thickness of an oil spill in cold water is different from that in warm open water. The oil thickness in particle ice is nearly four times that in cold water. The oil-contaminated area increases with ice concentration upto about 80% at which point the oil is trapped between floes as there is no clear path for it to move laterally between floes. For oil spilled in ice concentrations greater than 80% the thickness of the oil layer is a function of the relative oil, water and ice densities. The oil-contaminated area at these higher ice concentrations is several orders of magnitude smaller than that in lower concentrations.

The spread models have been evaluated with data from the field study carried out by Ross and Dickins (1987b). The areal spread of the oil, i.e. the oil-contaminated area, in both open water and slush computed using the parameterizations developed in the present study are found to be in good agreement with observations.

While the models developed as part of this study show good promise in dealing with oil spills in ice-infested waters, it is clear that more data are needed to fully evaluate the different aspects of these models. It is therefore recommended that controlled laboratory and field experiments be carried out to collect the necessary data to evaluate these models. There is also a need for a better understanding of variation of surface tension effects with temperature. The empirical relationships developed here could serve as a base for developing a more physically based theoretical framework for describing the behaviour of oil in ice-infested waters. It is also recommended that in the event of future accidental oil spills detailed quantitative data be collected as early as possible and for as long a period as possible.

ACKNOWLEDGEMENTS

The authors would like to acknowledge the assistance of Dr. V.R. Neralla and Dr. D.J. Lawrence during the course of this study. Financial support for the study was provided by the Canadian Federal Panel on Energy Research and Development.

REFERENCES

Armstrong, T, Roberts, B. and Swithinbank, C., 1966. Illustrated Glossary of Snow and Ice, Published by The Scott Polar Research Institute, Cambridge, U.K., pp60.

Bird, R.B., Stewart, W.E. and Lightfoot, E.N., 1960. Transport Phenomena, John Wiley & Sons, Inc., New York, pp780.

Buist, I.A., Joyce,S.P. and Ross, S.L., 1987. Modelling Oil Spills in Leads: Wind/Wave Tank Testing and Preliminary Results. Proc. Tenth Arctic and Marine Oilspill Program Technical Seminar, Edmonton, Alberta, June 9-11, 1987, pp131-148.

Comfort, G., 1986. Under-Ice Roughness Measurements. Arctec Canada Limited Report No. 2041-II submitted to the Environmental Studies Revolving Fund, Dept. of Energy, Mines and Resources, Ottawa, Ontario.

Comfort, G., 1987. Analytical Modelling of Oil and Gas Spreading Under Ice, Environmental Studies Revolving Fund Report 077, Dept. of Energy Mines and Resources, Ottawa, Ontario.

Dawe, B.R., Parashar, S.K., Ryan, J.P. and Worsfold, R.D., 1981. The Use of Satellite Imagery for Tracking the Kurdistan Oil Spill. Environment Canada Report No. EPS 4-EC-81-6, Ottawa, Ontario. pp1-31.

El-Tahan, H., Comfort, G. and Abdelnour, R., 1988. Development of a Methodology for Computing Oil Spill Motion in Ice-Infested

Waters. Report submitted by Fleet Technology Limited, Kanata, Ontario to Atmospheric Environment Service, Downsview, Ontario, pp85.

Fay, J.A. 1969. The Spread of Oil Slicks on a Calm Sea. In Oil on the Sea, D.P. Hoult (Ed.), Plenum Press, pp. 53-63.

Fay, J.A. 1971. Physical Processes in the Spread of Oil on a Water Surface, Proc. Joint Conference on Prevention and Control of Oil Spills. American Petroleum Institute, Washington, D.C., pp. 463-467.

Getman, J.H. and Schultz, L.A. 1976. Tests of Oil Recovery Devices in a Broken Ice Field. Paper No. 2695, Proc. Offshore Technology Conference, Houston, Texas, May 3-6, 1976.

Huang, J.C. and Monastero, F.C., 1982. Review of the State-of-the-Art of Oil Spill Simulation Models. American Petroleum Institute, Washington, D.C.

Industry Task Group, 1983. Oil Spill Response in the Arctic, Part 2, Field Demonstrations in Broken Ice. Shell Oil Company, Sohio, Alaska Petroleum Company, Exxon Company, USA and AMOCO Production Company, Anchorage, Alaska.

Kawamura, P., MacKay, D., and Goral, M. 1986. Spreading of Chemicals on Ice and Snow. Report submitted to Environment Canada, Environmental Emergencies Technology Division, Ottawa, Ontario.

Kovacs, A., 1981. Pooling of Oil Under Sea Ice. Proc. Conference on Port and Ocean Engineering Under Arctic Conditions, Quebec City, Quebec, July 27-31, 1981.

MacNeill, M.R. and R.H. Goodman. 1985. Motion of Oil in Leads. Proc. Eighth Arctic Marine Oilspill Program Technical Seminar, Edmonton, Alberta, June 18-20, 1985.

Metge, M. and A.S. Telford. 1979. Oil in Moving Pack Ice Study. Proc. Conf. Port and Ocean Engineering Under Arctic Conditions, Oslo, Norway, August 13-18, 1979, pp255-264.

Reimer, E., 1980. Oil In Pack Ice: the Kurdistan Spill. Proc. Third Arctic Marine Oilspill Program Technical Seminar, Edmonton, Alberta, June 3-5, 1980, pp529-544.

Ross, S.L. and Dickins, D.F., 1987b, Field Research Spills to Investigate the Physical and Chemical Fate of Oil in Pack Ice, Environmental Studies Revolving Fund Report No. 062, Dept. of Energy Mines and Resources, Ottawa, Ontario. pp118.

Ross, S.L. and Energetex Engineering, 1985. In-situ Burning of Uncontaminated Oil Slicks. Environment Canada - C&P, Ottawa, Ontario, K1A 0H3, Report No. EE-60.

Schultz, R., 1984. A Field Guide for Arctic Oil Spill Behaviour. Arctec Inc., Columbia, Maryland. U.S.A.

Spaulding, M.L., 1988. A State-of-the-Art Review of Oil Spill Trajectory and Fate Modeling. Oil and Chemical Pollution, Vol.4, pp39-55.

Stolzenbach, K., Madsen, O., Adams,E., Pollack, A. and Cooper, C., 1977. A Review and Evaluation of Basic Techniques for Predicting the Behaviour of Surface Slicks. Report No. 222, Ralph M. Parsons Laboratory, Massachusetts Institute of Technology, Cambridge, MA.

Venkatesh, S. 1988. The Oil Spill Behaviour Model of the Canadian Atmospheric Environment Service, Part I: Theory and Model Evaluation. Atmosphere-Ocean, Volume 26, No. 1, pp. 93-108.

Venkatesh, S., El-Tahan, H., Comfort, G. and Abdelnour, R., 1990. Modelling the Behaviour of Oil Spills in Ice-infested Waters. Atmosphere-Ocean (In Press).

Venkatesh, S., Neralla, V.R., Hume, W., Parker, N. and Thomson, B., 1988. The Oil Spill Behaviour Model of the Canadian Atmospheric Environment Service, Part II: Evaluation of Model Guidance for Emergency Response. Atmosphere-Ocean, Volume 26, No. 1, pp. 109-117.

Wotherspoon, P., Swiss, J., Kowalchuk, R., and Armstrong, J., 1985. Oil in Ice Computer Model. Environmental Studies Revolving Fund Report 019, Dept. of Energy, Mines and Resources, Ottawa, Ontario.

AN INTERACTIVE OIL SPILL TRAJECTORY MODEL FOR ALASKAN ARCTIC WATERS

by

Robert P. Britch, P.E.,[1]
Nungjane C. Shi, Ph.D., and[2]
Richard V. Shafer, P.E.[3]

ABSTRACT

An oil spill trajectory model has recently been developed to help petroleum operators with contingency planning for operations in the Alaskan Beaufort and Chukchi Sea area. The model, which runs on MS-DOS based equipment, facilitates prediction of oil movement and weathering, using graphic as well as tabular presentations of output information. The presence of sea ice can be taken into account, and the model will predict the movement of oil spilled beneath the ice. A special feature of this model is its ability to simulate the effect of countermeasures, including mechanical recovery, in situ combustion, and chemical dispersion. The model includes a database containing 10 years of weather data for the area, permitting operators to make groups of model runs based on past statistics.

INTRODUCTION

ENSR Consulting and Engineering (ENSR), with funding by Alaska Clean Seas (ACS), developed an interactive computer model to predict oil spill transport and spreading in the Chukchi and Beaufort Seas. The primary objective of the model is to provide ACS and its member companies a tool for planning spill response efforts.

The computer model OSP is menu-driven and is designed to run on 286 or 386 IBM compatible microcomputers. The program is constructed from a number of discrete models. This allows the user considerable flexibility in the OSP model application, and it will reduce the effort required to upgrade the model in the future. The model is written in Microsoft C (Version 5.1).

The OSP model organization is depicted on Figure 1 and model input are summarized on Table 1. The main menu provides the operator options for conducting actual model runs with user either specified input or statistical model runs. HELP and QUIT menus are also available in the main menu. For actual model runs, data required to run the model are input through data screens. The model will then either run to completion or it may be interrupted at any point in the

---

[1] ENSR Consulting and Engineering; Anchorage, Alaska

[2] IPC; Woodenville, Washington

[3] Alaska Clean Seas; Anchorage, Alaska

Table 1. Summary of model input.

Parameter	Actual Simulation	Statistical Analysis
Time of Spill	User specifies date	User specifies month
Location	User specifies latitude and longitude	User specifies latitude and longitude
Boundaries	User specifies screen display boundaries	User specifies screen display boundaries and statistical grid size and boundaries
Ice Conditions	User specifies	Computed based on month and location or use specifies
Type of Product	Crude, diesel, or user specified	Not applicable
Type of Spill	User specifies if continuous or instantaneous	Model assumes instantaneous
Duration of Run	User specifies	User specifies
Wind Information	User specifies	Model extracts data for user specified month
Cleanup Options	User specified burning, dispersants, or skimming	Not applicable

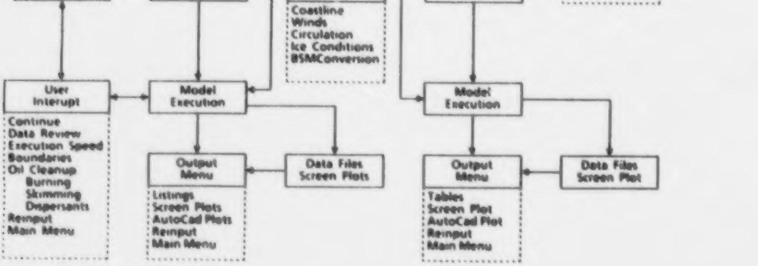

Figure 1. OSP model overview.

model to provide new input data, adjust graphical display boundaries, change model execution speeds, provide for cleanup action (e.g., skimming, burning and chemical dispersion), or review the data (screen or printer output of listings or plots).

Output from both the actual and statistical runs may be obtained in the form of data listings and screen plots. Actual runs may also be saved in AutoCAD files.

The model operates in a geographic coordinate system (latitude and longitude) rather than in a traditional grid system. Within this system, data interpolation between data points is accomplished within the program. The resolution of the coastline is governed primarily by the pixel resolution of the computer screen.

MODEL DESCRIPTION

The model operation domain encompasses an area extending from 138°W longitude (near Herschel Island in the Canadian Beaufort Sea) to 172°W longitude in the Siberian Chukchi Sea) and from 65°40'N latitude (at the Bering Straits) to 74°N latitude in the Arctic Ocean (see Figure 2). Model boundaries include all U.S. Outer Continental Shelf (OCS) lease areas currently planned for the Arctic.

A geographic coordinate system was used over the entire model domain. In this approach, the x-coordinate for computations is measured in degrees longitude, and the y-coordinates is measured in degrees latitude. Since longitudes converge at the poles, the x-coordinate based on a geographic coordinate system varies with latitude.

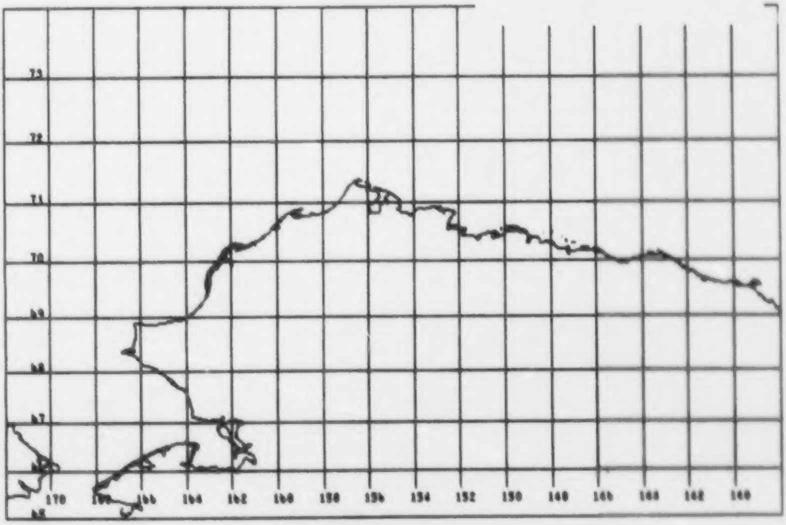

Figure 2. OSP model area.

While the use of the geographic coordinate system complicates computational procedures, it offers a number of specific advantages. These include:

- Any spill information is tied to a latitude and longitude rather than an internal grid system.
- The shoreline can be represented as an actual (digitized) boundary rather than by a grid approximation of the boundary.
- Databases of varying spatial density may be used.

The latter point is particularly important in that the model runs using data at the same resolution as the database.

Transport Equations

Oil spilled on the sea surface is typically assumed to move under the combined effect of a net circulation current component, a surface wind drift current and a tidal current (Waldman et al., 1973; Stolzenbach et al., 1977). Tides and tidal currents in the Beaufort and Chukchi Seas are relatively low (generally less than 1 ft and 0.1 knot, respectively; NORTEC 1981, Britch et al., 1983); consequently, these effects were not considered for these analyses.

From a computation standpoint, open water and ice-infested water spills are treated similarly. For spills in ice-infested water, the spill is assumed to be in part subjected to entrapment or have its movement retarded by the presence of ice floes. Similarly, the presence of ice will tend to retard surface wind drift and net circulation currents because of the reduced area available for transfer of wind energy across the air-sea interface. In addition, because ice has 90 percent of its volume below the water surface, its transport is assumed to be primarily a function of the net circulation current rather than surface wind drift currents. Consequently, for the case of ice-infested waters, spill transport is calculated in accordance with NORTEC (1983) as:

$$\vec{Us}_i = (1-I)^2(\vec{Uw}) + (1-I)^2(\vec{Uc}_{i-1} + \ldots + \vec{Uc}_{i-12})/12 + I(1-I)(\vec{Uc}_{i-1} + \ldots + \vec{Uc}_{i-12})/12 \qquad (1)$$

where I is the ratio of ice area to total area in the vicinity of the spill, Us is the mean spill velocity, Uw is the wind drift current, and Uc is the net circulation current. The subscript i represents time (in hours) and all currents are in common units. As calculated, the net circulation component is time varying and is affected by wind conditions for the preceding 12 hours.

Although it is recognized that in shallower nearshore waters (particularly in the Beaufort Sea), response to wind effects may occur over a shorter period of time (possibly in the order of 2 to 4 hours), the 12-hour period was assumed to be more representative of "average" conditions over the entire model area.

Calculations of below-ice transport are somewhat more complex as driving forces for below-ice Arctic currents are poorly understood. Based on an analysis of below-ice current data (NORTEC, 1981), currents below the ice occur in pulses which appear to be random in magnitude. Although data are by no means conclusive, there appears to be a tendency, at least for larger pulses, for directions of these currents to be a function of the wind direction. Similarly, there appeared to be a distinct relationship between the speed of the current pulse and the duration of its persistence.

Based on these observations, oil spilled below the ice was assumed to be transported by sequentially occurring current pulses in which the magnitude of the pulse is randomly generated, the pulse duration is a function of the current magnitude and the direction is a function of the wind direction. For this model, the pulse is treated as a rectangular element whose magnitude is given as:

$$Up = 0.95e^{3.36R} \tag{2}$$

where Up is the magnitude of the pulse (in cm/s) and R is a random number between 0 and 1. Similarly, the pulse duration is defined as:

$$tp = 4.5-0.087Up \tag{3}$$

where tp is the pulse duration in hours. The direction of the current pulse is assumed to be the same as the time-averaged (for the preceding 12-hour period) net circulation component as discussed for both the open water and ice-infested water cases.

Based on laboratory tests reported by Uzuner et al. (1979) oil spilled below the ice will move at a reduced velocity from the current due to shear between the ice-oil interface. Results of these tests suggest that for crude oil, the following equations apply:

Current Velocity (Up)	Spill Velocity (Us)	
< 8 cm/s	$Us = 0$	(4)
8-28 cm/s	$Us = 8.6\text{x}10^{-6}Up^{4.20}$	(5)
> 28 cm/s	$Us = 1.10Up-16.60$	(6)

Similarly, equations were also developed for below-ice spills of No. 2 diesel fuel:

Current Velocity (Up)	Spill Velocity (Us)	
< 3.3 cm/s	$Us = 0$	(7)
> 3.3 cm/s	$Us = 0.38Up-1.26$	(8)

Equations (4) through (8) above were used for calculation of velocities for transport of the spill.

Wind drift currents result as a wind blows over the water surface. Resulting surface currents are typically in the order of 2 to 5 percent of the wind speed. For this study, it was assumed that the wind drift current would be 3 percent of the near surface wind speed. Corrections to wind drift current direction due to Coriolis forces were also considered.

Spreading Equations

From a theoretical standpoint, spills have traditionally been treated either as instantaneous or continuous spills, and equations to describe spreading under both conditions are available in the literature. In the OSP model, continuous spills are represented by spillets at 1-hour intervals. The spillet is assumed to occur instantaneously and contain the volume spilled over a 1-hour period.

Spreading of oil spills in open water or ice-infested water is calculated in accordance with general relationships provided by Fay (1969), Waldman et al. (1973), and Osamor et al. (1981). In these equations, spreading occurs in three phases: (1) gravity-inertial phase, (2) gravity-viscous phase, and (3) surface tension-viscous phase. Designations for these phases are based on the forces controlling spreading in each phase.

In calculations for spill thickness, it was also assumed that if a spill reached a minimum thickness of 0.25 cm for crude oil (Amoco et al., 1983) and 0.0025 cm for diesel fuel (Schwartzberg, 1970), then spreading would cease.

Computations for spreading of oil spills in ice-infested waters are similar to those used for open water spills. The notable difference is that the thickness of the spill in ice-infested water is increased by a factor of 1/(1-I) in order to account for the area occupies by ice floes. The radius or width of the spill, however, remains unaffected by the percent of ice cover.

Equations for radial spreading of oil spills below the ice used methods as summarized by Uzuner et al. (1979) and Cox et al. (1980). For below-ice spills, spreading is assumed to be dominated by the gravity and viscous forces. The volume of the spill represents the volume of oil which is not trapped by ice roughness rather than the total initial volume of the spill. For below-ice spills, oil must first fill volumes created by below-ice roughness (a user input value) before spreading and transport is allowed to occur. For both the case of instantaneous and continuous below-ice spills, the average thickness of the spill is determined as the untrapped spill volume divided by the spill area.

Spill Partitioning

When crude oil or diesel fuel is spilled on the water surface; evaporation, dissolution and settling will all tend to reduce the volume of the spilled substance present on the water surface. These effects have been incorporated into the model cases for spills in open water and in ice-infested water. Since many of these factors are either not present or present at a significantly reduced level in below-ice spills, the model only considers trapping of oil (or diesel fuel) in this spill case.

Spill partitioning for the cases of open water and ice-infested water spills was derived primarily from data presented by Dome Petroleum Ltd. et al. (1982), which was assumed to be representative of arctic conditions. In this reference, portions of crude oil spill going into the atmosphere, remaining on the sea surface (or beached), entering in the water column and settling to bottom are provided as a function of time.

In the modeling efforts, it was assumed that partitioning of diesel fuel was similar to that for crude oil (in absence of cold water data for diesel). Although it is recognized that evaporation and dissolution will occur at a higher rate than for crude oil, the model should provide "conservative" estimates for volumes remaining on the sea surface.

Spill Response Efforts

The OSP model provides three options for removal of oil from a variety of spill response options. These include removal by skimming, burning, and use of dispersants. In all cases, the response efforts are directed to an individual user specified spillet. Actual calculations of product removed are based on the condition of the spillet (e.g., dimensions, volume remaining on the water surface, etc.) at the time in which the cleanup activities occurred. As an example, the amount of product removed (1) cannot be greater than the amount on the water surface, and (2) the efficiency of removal is predicated on input/calculated environmental conditions and on physical properties of the spillet.

Skimming. The model allows for use of any one of three general types of skimmers with assumed coverage rates or alternatively allows for the user to input of a rate of coverage. The three general types of skimmer include small, medium, and large skimmers. A small skimmer includes portable over-the-side systems with recovery rates of 100 gal/min or less. Medium skimmers are those moderately sized, self-propelled units or over-the-side skimming systems where small towed diversion booms could be employed to extend operating swaths; recovery rates are typically 100 to 300 gal/min. Large skimmers have relatively high throughput units (up to 600/gal/min) and would normally be used in conjunction with large V-boom configurations and auxiliary storage containers such as towed bladders or barges. Assumed areal coverage rates for these three skimmer classes are as follows:

Areal Coverage Rate (Acres/min)		
Size	Range	Average
Small	0.004-0.044	0.024
Medium	0.058-0.233	0.150
Large	0.349-1.163	0.760

The efficiency of mechanical cleanup is dependent on the spillet thickness and on wave activity. Wave heights (H) are first calculated using the following equation:

$$H = 7.553 \times 10^{-3} U^2 \qquad (9)$$

where U is the wind speed in ft/s. This equation assumes a fully developed sea which is neither fetch or depth nor duration limited (CERC, 1984). As this computation is used only to determine whether waves are 3 feet or less; fetch, depth, and duration considerations are assumed to be unimportant. In the presence of ice, wave heights are reduced by a factor of (1-I) where I is the fraction of ice cover. For wave heights less than 3 feet, the efficiency is calculated. For wave heights greater than 3 feet, an efficiency of 5 percent is assumed.

Burning. In developing the model, it was recognized that the spillet may be neither discrete nor contiguous, particularly in broken ice conditions where spillets could occur as patches of oil separated by ice or open water. As a first step in the model computation, the area to be burned is input by the user. The model then calculates the percentage of the spillet on which burning will be used (up to a maximum of 100 percent). The spillet area not burned will continue unaffected by burning activities.

Burning is assumed to be an effective means of removal when the spill thickness is greater than 0.1 inch and when wind speeds are less than 16 knots. If both of these conditions occur, an efficiency of 90 percent removal is assumed. If a fire boom is being used, an efficiency of 90 percent removal is also assumed. For all other situations, an efficiency of 10 percent is assumed.

Chemical Dispersion. The OSP model allow for three levels of preset dispersant application rates as well as for a user-specified application rate. Fixed dispersant application rates are provided for application by vessels, small fixed wing aircraft or helicopters, and large fixed wing aircraft as indicated below:

Areal Coverage Rate (Acres/min)		
Operation	Range	Average
Vessels	0.465- 2.326	1.400
Small FW Aircraft/Helicopter	3.721-14.884	9.300
Large FW Aircraft	29.070-81.395	55.000

The average areal coverage rate is assumed in the OSP model.

The efficiency of dispersant use is dependent on the wind speed and spill thickness (t). For spill thickness less than 0.006 inches, the efficiency is calculated. In all cases if wind speeds are less than 4 knots or greater than 27 knots, dispersants are only expected to be 5 percent efficient.

Model Databases

The OSP model contains a number of databases to describe environmental conditions within the model domain.

Net Circulation Currents. The OSP model uses two current databases for approximating the net circulation component. For the nearshore Beaufort Sea area current data from the Beaufort Sea Model (BSM) previously develop by NORTEC (1983) are used. The remainder of the study area, net circulation data are derived from available literature, notably Lissauer et al. (1984).

BSM data are contained in 80 data files created using a 2-dimensional hydrodynamic computer model for the nearshore Alaskan Beaufort Sea. These data files were developed using steady state wind condition for eight directions (N, NE, E, SE, S, SW, W, and NW) and five speeds (5, 10, 20, 30 and 40 knots). In the

BSM, x and y current components are provided on an unique one-nautical-mile by one-nautical-mile grid. These databases are contained in the OSP model, but have been converted to a binary form to reduce storage requirements and increase computational speed. In the OSP model computations, geographic coordinates are converted to grid coordinates and appropriate current data are extracted. The OSP model also provides an interpolation subroutine to account for winds from 360 degrees as opposed to the 8-point compass used in the BSM. The OSP model also maintains the time-dependent function for determining the net circulation component within the BSM area.

Outside the BSM area, the net circulation component is determined from direct access to data files of current speeds and directions at fixed geographic coordinates as determined from available literature. Interpolation of currents at other points in the OSP model domain is accomplished within the OSP model.

Ice Databases. The OSP model contains three separate files containing ice data which are used primarily in conjunction with statistical simulations. Data files are digitized contours of probabilities of 5-tenths ice concentration boundaries for June 15 and August 15. These data are as described by LaBelle et al. (1983).

In the OSP model, the probabilities of 5-tenths ice cover are assumed to be actual percentage of ice cover, primarily because of the limited availability of summarized ice data. As an example, the 0 percent ice probability contour is assumed to be equivalent to the 0 percent ice cover contour. Based on a review of normal ice edge maps (also as presented by LaBelle et al., 1983) this approximation is fairly realistic. As another example, the 50 percent ice probability contour would represent the exact location of the 50 percent (average) ice concentration contour.

Meteorological Database. The OSP model contours a 10-year record of meteorological data from Barrow, Alaska. Data are provided for wind speed, wind direction, and air temperatures at 3-hour intervals for the years 1978 through 1987.

The statistical analyses for the OSP model, accesses the wind database once per day for the first 20 days of the month. Assuming a 10-day spill, the entire month would be covered by this analysis. For spills with durations greater than 10 days, data from the subsequent month are used in calculations.

Coastline Database. The coastline for the model was obtained primarily by digitizing NOAA Nautical Chart 16003 which is at a scale of 1:1,587,870. Digital data for a portion of the central Beaufort Sea (approximately 142° to 158°W longitude) was obtained directly from NOAA digital coastline data. The entire NOAA digital database was not used as there are gaps in portions of that database in the vicinity of major bays and inlets in the western portions of the Beaufort Sea.

MODEL OPERATION

The OSP model documentation includes a detailed users guide which describes each menu. Figure 3 provides a logic diagram for the menus which illustrates the various pathway or options a user may take while operating the OSP model. In general, the program has been structured to allow the user to either return to the next highest level of the program menu structure or break out of the program. Each option is identified with a specific designation such as B1 or E14; and each is described in the model documentation (e.g., example of the screen display, options the user has to proceed, and any relevant comments).

Sample Output

Model output is generally controlled by three menus. These include a main output menu for the actual real time conditions (D1), a main output menu for the statistical run (D3), and a data view menu associated with the user interrupt functions for the actual runs (E7). The D1 and E7 output menus contain options for obtaining listings, screen plots and AutoCad plot files. With the statistical runs, only listings (tables) and screen plots are available.

Examples of the various types of output available for the actual and statistical runs. In all simulations, the user has the flexibility to control the geographic area for display on the screen and output.

Figures 4 and 5 provide corresponding sample output for an instantaneous spill of 5,000 barrels in the Harrison Bay area. Figure 4 provides the tabular output including hour, wind history input, spillet coordinates a volume balance during the first 24 hours of a spill for the spillet and the spill dimensions. In this example, skimming was used in hours 10, 12 and 16 and resulted in removal of 73 barrels of oil from the water surface. During hour 22, dispersants were used and 189 barrels went from the water surface to the water column.

The screen plot (Figure 5) provides trajectory of the spillet during the first 24 hours. For continuous spills, the plot of the individual spillets are saved at user specified intervals. Saving the entire time hourly history for each spillet for the continuous spill was not deemed possible due to storage limitations in most microcomputer systems.

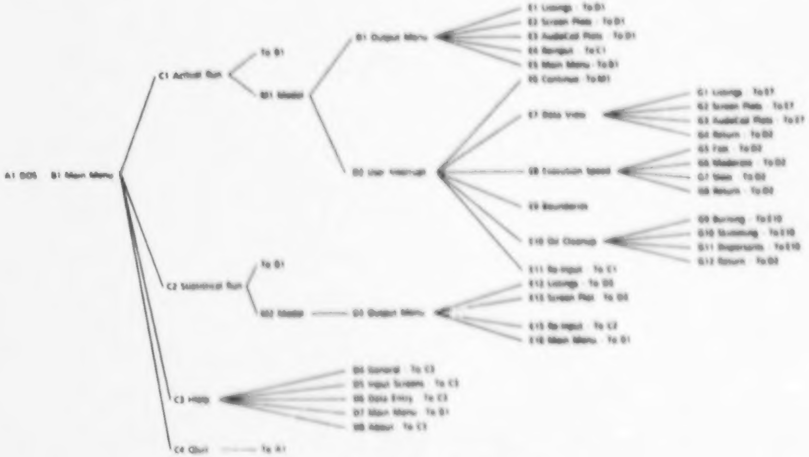

Figure 3. User logic diagram.

```
---------------------------------------------------------------------------------------------
Beaufort and Chukchi Seas Oil Spill Model
Run Time  : 17:16:47        Run Date : 05/03/90
Spill Date:  9/ 1/90        Spill Hour : 00
Spill Location:  150.50000 W    70.80000 N
Type of Spill:   Instantaneous spill in open water
Spill Volume :   5000     Barrels
---------------------------------------------------------------------------------------------
Hourly Spill Status

     Wind      Coordinate       Volume of Oil (Barrel)                                 Spill
    Spd Dir   Long     Lat           Water  Water   Sea    Clean    Amount              Size   Thick
 Hr Kts  T                      Atm   Surf Column Floor   Action   Removed    Total     Ft     Inch
---------------------------------------------------------------------------------------------
  0  12  25 150.500 70.800        0   5000      0     0                  0     5000       0  0.000
  1  12  25 150.514 70.796      155   4677    168     0                  0     5000    1020  0.072
  2  12  25 150.528 70.791      159   4663    178     0                  0     5000    1213  0.051
  3  12  25 150.542 70.787      164   4649    187     0                  0     5000    1342  0.042
  4  12  25 150.558 70.784      169   4634    196     1                  0     5000    1442  0.036
  5  12  25 150.574 70.781      173   4620    206     1                  0     5000    1525  0.032
  6  12  25 150.587 70.777      178   4606    215     1                  0     5000    1596  0.029
  7  15  45 150.611 70.775      183   4592    224     1                  0     5000    1659  0.027
  8  15  45 150.634 70.773      187   4577    234     1                  0     5000    1766  0.024
  9  15  45 150.654 70.769      192   4563    243     2                  0     5000    1929  0.020
 10  15  45 150.674 70.766      197   4510    253     2 Skimmed         39     5000    2088  0.017
 11  15  45 150.693 70.762      201   4496    262     2                  0     5000    2242  0.014
 12  15  45 150.712 70.757      206   4460    271     2 Skimmed         21     5000    2394  0.013
 13  18  65 150.737 70.755      211   4446    281     3                  0     5000    2542  0.011
 14  18  65 150.764 70.753      215   4432    290     3                  0     5000    2687  0.010
 15  18  65 150.791 70.752      220   4418    300     3                  0     5000    2830  0.009
 16  18  65 150.821 70.751      225   4390    309     3 Skimmed         13     5000    2970  0.008
 17  18  65 150.848 70.750      229   4376    318     3                  0     5000    3108  0.007
 18  18  65 150.875 70.748      234   4362    328     4                  0     5000    3244  0.007
 19  22  70 150.908 70.746      239   4347    337     4                  0     5000    3379  0.006
 20  22  70 150.941 70.743      243   4333    347     4                  0     5000    3511  0.006
 21  22  70 150.973 70.741      248   4319    356     4                  0     5000    3642  0.005
 22  22  70 151.014 70.742      253   4116    354     4 Dispers        189     5000    3771  0.005
 23  22  70 151.055 70.742      257   4101    364     5                  0     5000    3899  0.004
 24  22  70 151.087 70.740      262   4087    373     5                  0     5000    4026  0.004
```

Figure 4. Sample data listings for an instantaneous spill in Harrison Bay during the first 24 hours.

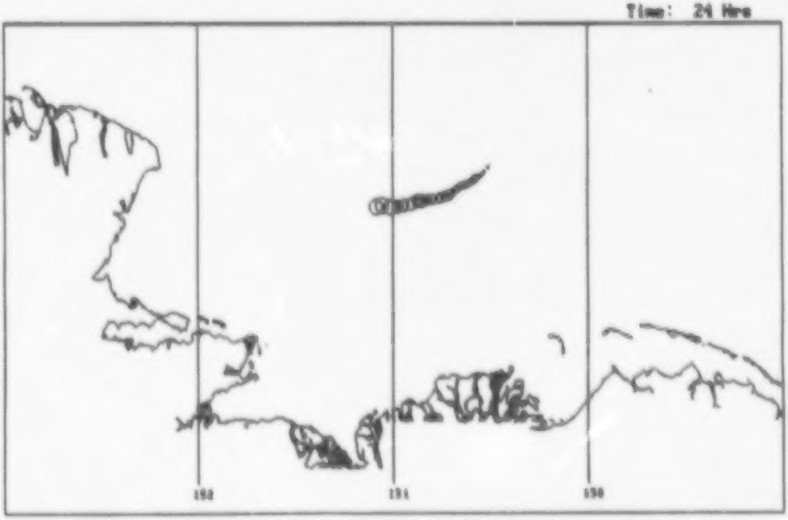

Figure 5. Sample screen plot for an instantaneous spill in Harrison Bay during the first 24 hours.

Computer listings provided from the statistical run include cumulative percent frequencies of impact. Both the grid size and location for accumulating statistics can be modified for each simulation.

Examples of screen plots from statistical runs in the Chukchi Sea are provided on Figures 6 through 8 for 10 years of open water simulations during the month of August. Each figure represents a total of 200 overlapping simulations using historical wind data. Individual simulations are initiated at 165°30' longitude and 70°30'N latitude and allowed to run for 1-, 3- and 10-day durations. Figure 9 shows the corresponding June 10-day duration simulation assuming a 25 percent ice coverage.

SUMMARY

The OSP model is designed primarily for flexibility. Various modules containing individual algorithms may be modified as new or more appropriate computational procedures are developed. Similarly, the current and ice databases are also such that they may be easily modified to incorporate new data. Finally, the entire model may be easily adapted to other areas by modification of coastline and current databases.

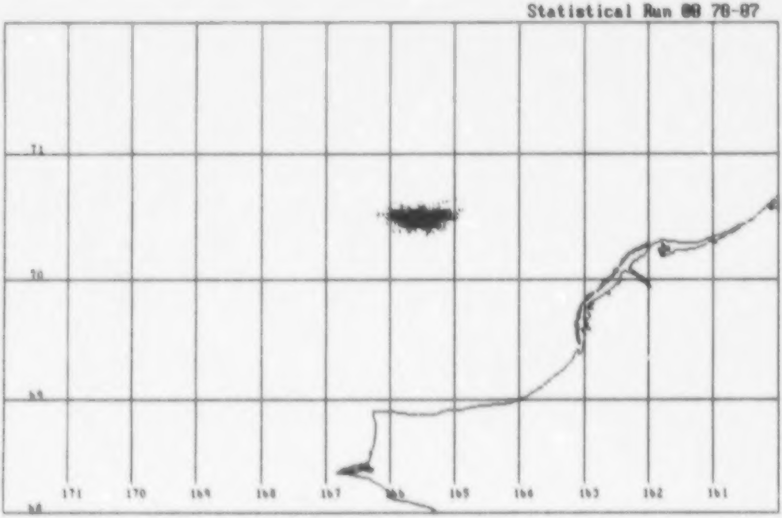

Figure 6. Statistical screen plot during August for 10 years of 24-hour (1 day) simulations with no ice.

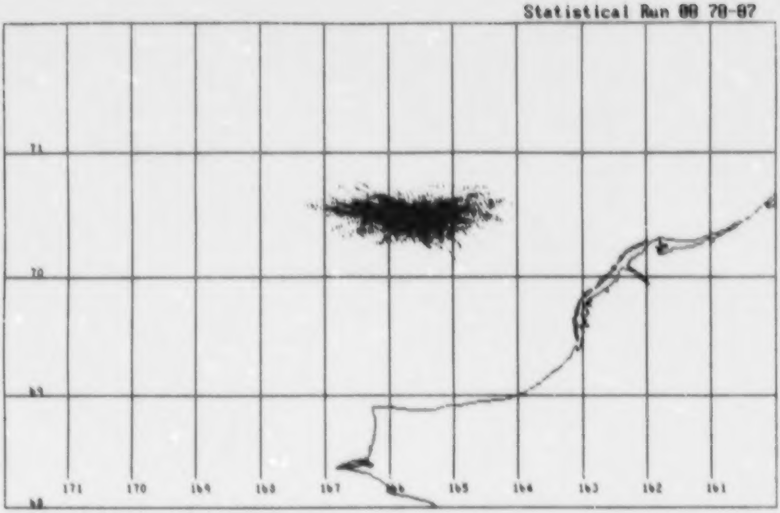

Figure 7. Statistical screen plot during August for 10 years of 72-hour (3 day) simulations with no ice.

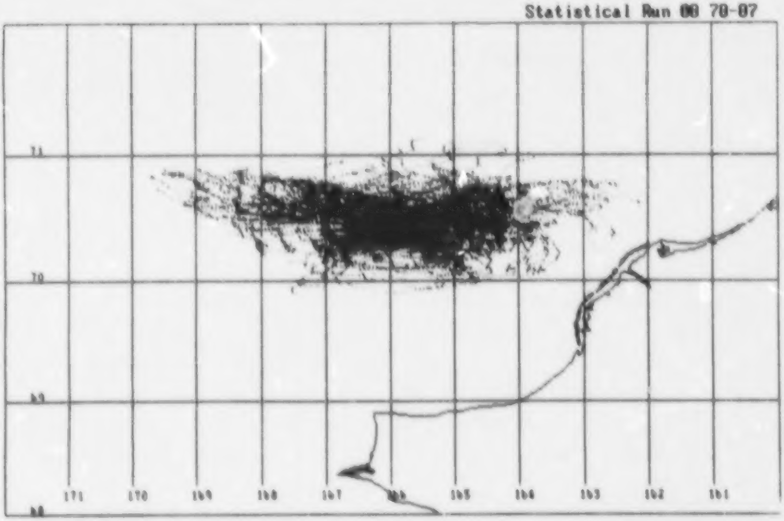

Figure 8. Statistical screen plot during August for 10 years of 240-hour (10 day) simulations with no ice.

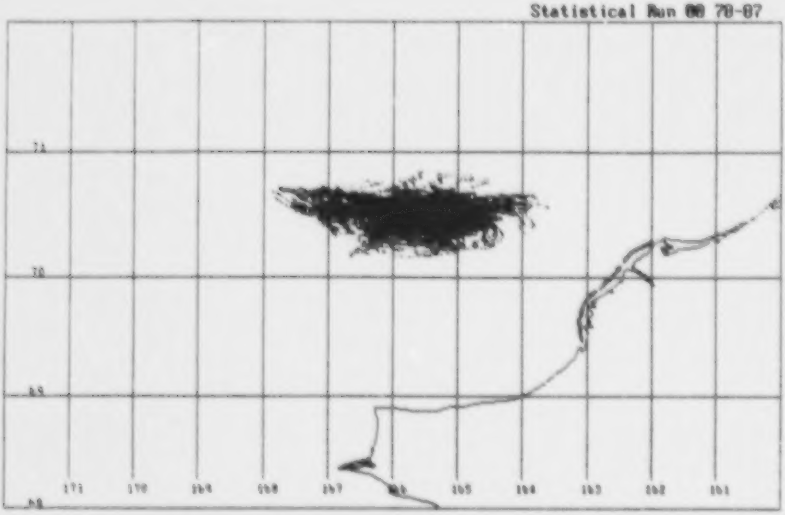

Figure 9. Statistical screen plot during August for 10 years of 240-hour (10 day) simulations with assumed 25 percent ice coverage.

REFERENCES

Britch, R.P., R.C. Miller, J. Downing and M. Veit. Volume II - Physical Processes. In Gallaway, B. and R. Britch (eds). In Gallaway, B. and R. Britch (eds). Environmental and Ecological Studies for the Endicott Development - Summer, 1982. Prepared for Sohio Alaska Petroleum Company, Anchorage, AK. 219 p., 1983.

Coastal Engineering Research Center (CERC). Shore Protection Manual. U.S. Army Corps of Engineers, Waterways Experiment Station, in 2 volumes. 1984.

Cox, C., L.A. Schultz, R.P. Johnson and R.A. Shelsby. The transport and behavior of oil spilled in and under sea ice. NOAA/OCSEAP, Research Unit 568, Final Report, 170 p. 1980.

Dome Petroleum Ltd., Esso Resources Canada Ltd. and Gulf Canada Resources Inc. Beaufort Sea-Mackenzie Delta Environmental Impact Statement. Vol 6 - Accidental Spills. Prepared for Environment Canada. 1982.

Fay, J.A. The spread of oil slicks on a clam sea. Mass. Inst. of Technology, Dept. of Mech. Engr., 14 p. 1969.

Lissauer, I.M., L.E. Hackmeister, and B.J. Morson. Atlas of the Beaufort Sea. U.S. Coast Guard Report No. CG-D-33-84. 1984.

Northern Technical Services (NORTEC). Beaufort Sea drilling effluent disposal study. Prepared for the Reindeer Island Stratigraphic Test Well Participants, 329 p. 1981.

Northern Technical Services (NORTEC). Alaska Beaufort Sea Oil Spill Trajectory Analyses. Prepared for Alaska Clean Seas, 159 p. 1983

LaBelle, J.C., J.L. Wise, R.P. Voelker, R.H. Schulze, G.M. Wohl. Alaska Marine Ice Atlas. Arctic Environmental Information and Data Center, Univ. of Alaska, 302 p. 1983.

Osamor, C.A. and R.C. Ahlert. Oil slick dispersal mechanics. Environmental Protection Agency, Report EPA-600/2-81-199, 238 p. 1981

Stolzenbach, K.D., O.S. Madsen, E.E. Adams, A.M. Pollack and C.K. Cooper. A review and evaluation of basic techniques for predicting the behavior of surface oil slicks. Mass. Inst. of Technology, Report MITSG 77-8, 323 p. 1977

Uzuner, M.S., F.B. Weiskopf, J.C. Cox and L.A. Schultz. Transport of oil under smooth ice. Environmental Protection Agency, Report EPA-600/3-79-0412, 49 p. 1979.

Waldman, G.D., R.A. Johnson and P.C. Smith. The spreading and transport of oil slicks on the open ocean in the presence of wind, waves and currents. prepared for U.S. Coast Guard, Contract DOT-CG-20617-A, 70 p. 1973.

Wiegel, R.L. Oceanographic engineering. Prentice-Hall, New Jersey, 532 p. 1964.

NATURAL RECOVERY OF COLD WATER MARINE ENVIRONMENTS AFTER AN OIL SPILL

by

J. M. Baker[1], R. B. Clark[2], P. F. Kingston[3],
and R. H. Jenkins[3]

1 Consultant, Shrewsbury, England

2 Dept. of Biology, University of Newcastle upon Tyne,
Newcastle upon Tyne, England

3 Institute of Offshore Engineering, Heriot-Watt University,
Edinburgh, Scotland

INTRODUCTION

This review of published literature examines natural cleaning and natural recovery of ecosystems and biological communities following oil spills in cold water regions of the world.

The objectives of this paper are, in the context of an oil spill, to provide:

- Practical working definitions of the terms "clean" and "recovery"
- A framework for understanding natural cleaning and recovery processes and their duration in cold water environments

The review draws on over 350 published scientific studies relating to oil spill incidents and relevant field trials and excludes the tropical environment. A total of 25 previous spills are referenced. The Valdez spill was not included in this review due to the lack of published scientific literature to-date. The complete paper also includes a discussion of the concepts and definitions for natural cleaning and natural recovery.

SUMMARY OF FINDINGS

The following is a list of major findings from our review, grouped according to the primary subject areas covered by the complete paper. The scientific literature permits generalisations to be drawn; but oil spills in exceptional circumstances may produce exceptional effects. In a number of cases, long-term studies of recovery processes are incomplete, and recovery time scales suggested involve some extrapolation.

Basic Concepts

- Consideration of the overall, long-term impact of a particular spill must take into account the relative proportions of oiled- and unoiled-habitats in the area of interest; and, in the case of oiled habitats, to consider the relative proportions of different habitat types. Some areas may have a high percentage of habitats likely to recover relatively quickly, whereas other areas may have a high percentage of habitats likely to recover more slowly.

- For many cases, recovery of the availability of human services of a system impacted by oil is not closely related to biological recovery and is generally more rapid than biological recovery.

- Current evidence indicates that hydrocarbons are present in all environments. They originate from both natural and human sources and serve to define background levels of petroleum hydrocarbons.

- Clean, in the context of an oil spill, is defined here as the return to levels of petroleum hydrocarbons that have no significant detectable impact on the function of the ecosystem. The size of the ecosystem is obviously an important consideration. It is not microscopic, but is large enough to include the major plant and animal communities. Practical application of this definition requires taking into account the relative proportions of oiled- and unoiled-habitats. It does not necessarily require a return to some pre-existing background level or the complete removal of petroleum hydrocarbons from the environment.

- Recovery of an ecosystem damaged by petroleum hydrocarbons begins as soon as the toxicity or other adverse property of the oil has declined to a level that is tolerable to the most robust colonising organisms. Recovery processes can begin in the presence of residual oil.

- Recovery of an ecosystem is marked by the re-establishment of a healthy biological community in which the plants and animals of the community are functioning normally. It may not have the same composition or age structure as that which was present before the damage and will continue to show further change and development. It is difficult or impossible to say whether an ecosystem that has recovered from an oil spill is the same or different from that which would have developed in the absence of the spill.

- Ecosystems are in a constant state of flux due to natural causes. These fluctuations can be as great as, or even greater, than those caused by the impact of an oil spill.

Natural Cleaning

- Most of the toxic components in a fresh oil spill on the surface of the sea rapidly evaporate. After evaporation, these toxic components disperse into the atmosphere and are rapidly diluted to background levels. Most of the remaining toxic components that do not evaporate, dissolve and disperse in the water column to low concentrations.

- Generally, the higher the aromatic content of an oil, the higher the toxicity. Weathered crude is less toxic than fresh crude because most of the toxic components have evaporated. Most of the toxic compounds are readily degradable.

- Oil concentrations in the water column below oil slicks are very low.

- The persistence of oil slicks on the sea surface is dependent upon the type of oil spilled and sea state conditions. Some slicks can be removed by natural processes within a few days. Other oils can form stable, highly viscous emulsions (mousses), which may persist for weeks or months in the open ocean. Eventually these slicks will form tarballs that are relatively harmless to biological systems.

- Microbial degradation is an important process in the eventual disappearance of oil from the marine environment. Degradation rate is controlled by oxygen and nutrient availability, temperature, chemical composition and surface area of the oil, and in some cases the activities of other organisms.

- Degradation is oxidative, and therefore the rate is reduced when oxygen concentrations are low as is sometimes the case in fine sediments.

- Although some oxidation products resulting from biodegradation or photolysis are toxic, their rates of generation are slow at the surface of spilled oil because they are controlled by diffusion. If these products are leached from the surface of the oil and enter the water column, they are rapidly diluted to low concentrations. Therefore, they are not likely to have significant ecological impact.

- High-energy rocky shores usually do not accumulate oil, but if impacted are subjected to rapid cleaning by wave action.

- Oil does not penetrate easily into fine sediments in the intertidal zone, but can sink into shingle, gravel, and coarse sand. In some cases oil may penetrate to the water table, which forms a natural barrier to further penetration.

- On sheltered shores with high biological productivity, oil can penetrate down biological pathways, e.g., worm burrows and plant root systems. Oil may persist for many years in the sediments, especially if oxygenating biological activity (e.g., new burrow formation) is depressed.

- Large accumulations of oil or mousse may incorporate beach material and harden to form asphalt pavements; these are gradually eroded but may persist for many years on the upper shore and on sheltered beaches.

- Physical '"removal" of oil by natural processes itself does not eliminate oil from the environment; it redistributes it. This redistribution can be beneficial, e.g., when wave action cleans the shoreline, it facilitates dispersion of the oil in the water column, and increases the surface area of the oil droplets, thereby encouraging other degradation processes. However, such redistribution may also involve sediment-bound oil being transported to the seabed.

- The toxicity of hydrocarbons on the seabed can vary widely depending on the composition of the oil, the organism exposed to it, the transport pathways, and the extent to which the hydrocarbons can be degraded in the bottom sediments.

Natural Recovery

- Diving seabirds suffer heavy mortalities from oil. However, the mortalities arising from a single oil spill are not significantly different from natural mass mortalities experienced from time to time and are significantly less than annual mortalities from fishing activities.

- There is no evidence that seabird populations are declining as a result of oil spills. In fact, North Atlantic populations of most species have been increasing in recent years despite heavy annual losses from oil pollution.

- Kills of adult fish from exposure to oil are rare. The only important casualties from oil spills are rockfish and shellfish in near-shore waters, and fish in mariculture installations.

- Loss of pelagic eggs and fish larvae, if these are present at the time of an oil spill, has had no detectable impact on the fish stocks available to the fishing industry.

- Annual recruitment of fish stocks fluctuates naturally, and the size of the catchable stocks is more determined by the activities of the fishing industry (e.g., over-fishing) and by climatic changes, than by any other factor.

- Although the toxic components of petroleum hydrocarbons kill planktonic organisms, there is no evidence that these effects have any ecological significance in open waters. In closed waters, effects may persist for several months.

- To date, there are insufficient data in the scientific literature on marine mammal mortality and recovery to assess impact on breeding populations.

- Estimates of recovery times vary depending upon the environment. Past experience has shown that exposed, rocky shores usually recover in 2 to 3 years. Other shorelines show substantial recovery in 1 to 5 years with the exception of sheltered, highly productive shores (e.g., salt marshes) which may take 10 years or more to recover.

- Subtidal sand and mud systems recover in recognisable successions. Usually, recovery times are 1 to 5 years, but they can be 10 years or longer in exceptional cases.

- Biological recovery of low-energy soft-substrate (sand, mud, etc.) ecosystems follows a generally well-defined course; but there are several alternative recovery routes for hard substrate (rock, boulder, etc.) ecosystems, and the restored community may not be the same as that before the damage.

- Sublethal effects have been shown to occur after an oil spill and have been considered in the estimate of recovery times stated here. There is no evidence that sublethal effects are of any longer-term ecological significance.

- The early colonisers, once the physical and toxic effects of the oil ameliorate, play an active role in the breakdown of the remaining hydrocarbons.

- Removal of oil using drastic cleaning methods, beyond initial bulk oil removal, can actually delay recovery because the cleanup also removes living organisms and damages the habitat.

AVAILABILITY OF COMPLETE PAPER

For a copy of the complete paper which includes over a 100 pages of text, tables, figures, and references, please write the Environmental Emergencies Technology Division of Environment Canada or contact the authors.

SUMMARY OF THE ENVIRONMENTAL EFFECTS OF THE ANTONIO GRAMSCI OIL SPILL IN THE GULF OF FINLAND IN 1987.

Juha-Pekka Hirvi
National Board of Waters and the Environment of Finland

ABSTRACT

In early 1987 the Soviet tanker MT Antonio Gramsci ran aground in the Gulf of Finland and about 570 tons of crude oil were spilled into the ice-covered sea. The spill situation was acute for several months and the oil spread over an estimated sea area of 2500 km^2.

Fortunately, the time factor, physical conditions and natural processes were able to decrease the reactivity of the oil and pollution damage was limited to individual cases of oil-contaminated birds and fish traps.

Unfortunately, the oil did affect fish and sea-floor fauna. This conclusion is supported by the lower-than-normal vitamin C concentrations, clear changes in the relative sizes of the liver and the sexual glands in fish and occurrence of certain types of damage in young fish. The oil-contamination was evident in the samples of the sea-floor fauna and population densities had dropped a year after the spill incident. Recovery of these parts of the marine ecosystem is still continuing in the Gulf of Finland.

INTRODUCTION

The grounding of MT Antonio Gramsci on February 6, 1987 and the ensuing crude oil spill (570 tons) became as famous as other spill incidents in the Baltic Sea. But this case differed in one point from the others. The acute phase of the spill situation lasted several months because of the severe ice-conditions in the Gulf of Finland. The oil remained firmly in the grip of the ice and oil drifted uncontrolled at sea constituting a serious environmental hazard. It threatened birds and their important nesting islets. Pups born to ringed seal in March - April were at risk. Fishing in the coastal waters was also threatened. Environmental studies were needed and asked for.

On 12 March 1987 the Finnish State Council decided to set aside a research grant (2.1 million FMK) for the purpose of studying possible environmental effects of the oil spill. Thereafter, a research project was initiated by the National Board of Waters and the Environment.

The environmental studies were conducted in collaboration with the Water and Environment Research Institute, the Game and Fisheries Research Institute, the Institute of Marine Research and the Environment Research Group Ltd. The field studies were mainly carried out in 1987 and 1988, but sampling of biota for chemical analysis was continued into 1989 to study the recovery of the sea-floor fauna.

The following paper summarizes the main results of the environmental follow-up studies. All references are made to the final report which will be published in June this year (Hirvi 1990). It is expected that some of the research results will be discussed more profoundly in different scientific papers.

ORIGIN OF OIL

On 6 February 1987 the Soviet tanker **MT Antonio Gramsci** carrying a full cargo of crude oil (39 000 tons) ran aground in the vicinity of the Porvoo lighthouse (60° 05,8'N : 25° 35,8'E) in the Gulf of Finland (**FIGURE 1**). The incident resulted in an oil spill of about 570 tons into the ice-covered sea. The spilt oil was of the type "Soviet Export Blend -crude oil (SEB -oil). The oil spill appeared to become a large incident. It involved so many potential risk factors that could produce severe damage to the natural systems in this shallow basin of the Baltic Sea.

OCCURRENCE OF OIL

The extent of the area into which oil drifted and in which it was present in the Gulf of Finland during winter and spring 1987 can be estimated at 2 500 km^2 (**FIGURE 1**). The spreading area would have been larger had the drifting of oil to the Soviet territorial water zone also been taken into account.

In early May after a period of intensive ice melting in the Gulf of Finland the oil was finally released to the sea. Oil film, emulsion drops and clumps (tarballs) were widely observed at sea. No concentrated oil slicks were formed at sea, only oil film. In mid-May the oil started to drift ashore in the archipelagos of southern Finland. Oil was detected on almost every outer island in the coastal zone over a length of about 100 km (**FIGURE 2**). It may be interesting to note that the oil was present under the water surface in the form of large emulsion drops (5 - 20 mm). This indicated the formation of near buoyant water-in-oil-in-water particles, consisting of large water spheres surrounded by a thin oil film. This is an interesting but probably unimportant process as stated by Mackay (1982). However, the emulsion formations lasted for weeks and spread over a large sea-area. The last observation of an extensive oil film (3 x 15 km) was made on 3d June in the open sea-area off Helsinki to the Söderskär islands in the east. The next day the oil film had disappeared under the effect of the swell of the sea. The last observation of stranded oil was reported in late June 1987.

COMBATTING AND CLEAN-UP ACTIONS

In the winter of 1987 the ice-conditions were difficult and unfavorable to all oil combatting work. E.g. the measures for collecting oily ice blocks from the sea didn't produce results, and it turned out to be impossible to control the spreading and drifting of oil with those

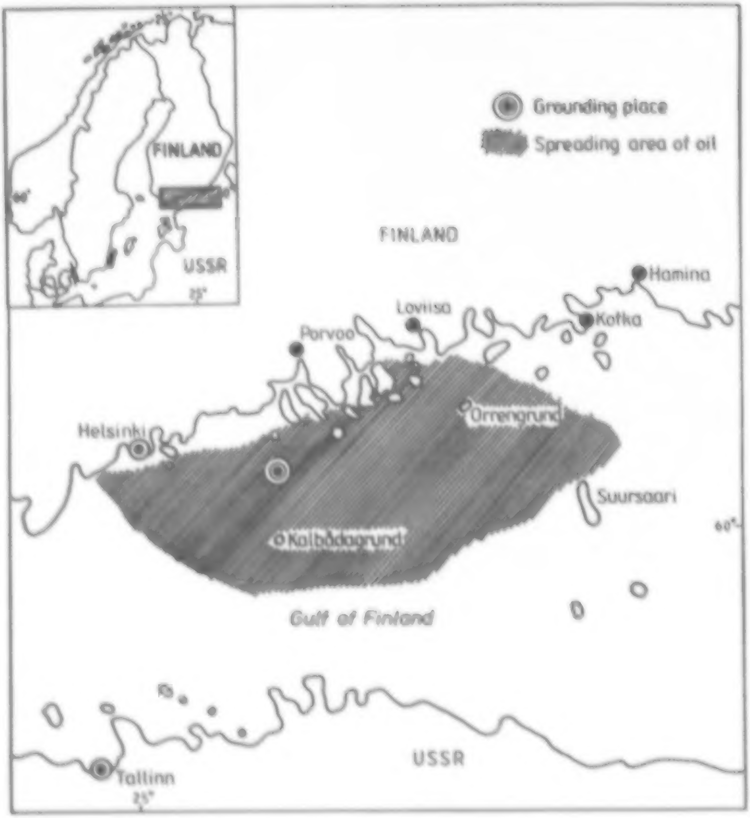

FIGURE 1. The grounding place of MT Antonio Gramsci in the Gulf of Finland on February 6, 1987 and the total spreading area of oil during the period from 6 February to 3 June 1987.

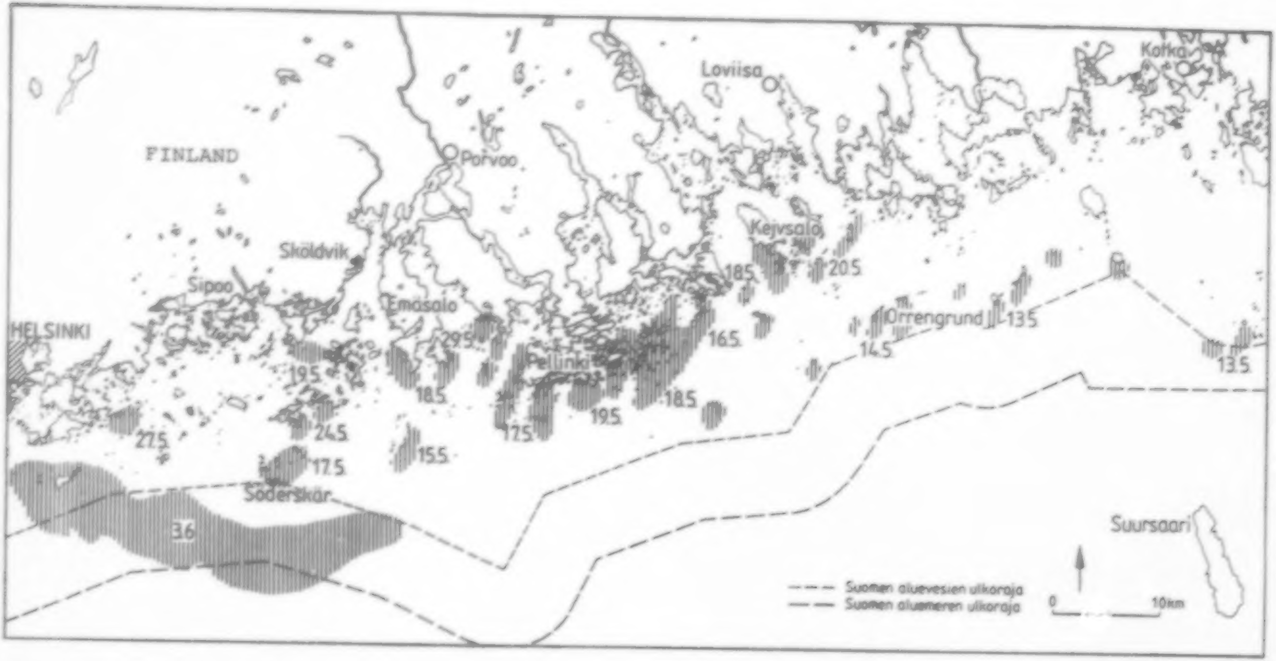

FIGURE 2. The dated observations of oil film and oil clumps in the surface water and on the shores within the coastal sea area of southern Finland during May and June 1987. [Symbols: ▥ oil, --- inner boundary - - - outer boundary of the territorial water zone of Finland].

massive closed ice-fields in the Gulf of Finland. All attempts to collect oil among the ice blocks were stopped on 27 February 1987. Only about 100 tons of oil were collected from the sea in February. In May 1987 the oil was finally released from the ice and large oil film formations occurred at the sea. Because of small amounts of oil spread over large surface areas the oil combatting operations didn't succeeded in collecting oil from the sea surface. In mid-May the operations in the open sea area were stopped but in the archipelagos the work continued. The cleaning-up of the Finnish shorelines resulted in the collection of 38 tons of oily waste as summarized in **TABLE 1**.

TABLE 1. The results of the clean-up actions performed on the shores within the coastal sea area of southern Finland in May and June 1987.

District	Islands (No)	Places (No)	Length of shoreline (km)	Oily waste (tons)
Hanko	3	3	2.0	0.1
Kirkkonummi	47	101	-	0.5
Sipoo	14	87	5.1	0.3
Porvoo	57	77	40.3	28.9
Loviisa	26	26	21.2	8.0
Total	147	294	68.6	37.8

THE FATE OF THE OIL

In late 1987, some laboratory experiments were carried out in the Technical Research Centre of Finland for the purpose of studying the behavior of the Soviet export blend crude oil in cold brackish water (Hirvi et al. 1988). The fate of the Antonio Gramsci oil spill in the Gulf of Finland could be estimated according to the results of these laboratory experiments and other known facts.

Of the total amount of 570 tons of spilled crude oil, about 110 tons were recovered by oil combatting measures and 185 tons were eliminated by natural processes (mainly by evaporation). The approximately 270 tons of oil were remained in the marine environment. Analysis of petroleum hydrocarbons in sea water and bottom sediments didn't give any clear indication on oil contamination. However, the laboratory experiments confirmed the indication that "the crude oil of the Soviet export blend type has a fairly strong tendency to disperse and to form emulsions in cold brackish water". It could be concluded that the rest of the oil dispersed and mixed effectively into the water column of the Gulf of Finland.

PRESENCE OF OIL IN THE WATER COLUMN AND SEDIMENTS

Water: The presence of oil-derived hydrocarbons in seawater was charted both in the open sea and the coastal sea -area of southern Finland in 1987 and 1988.

In 1987 the concentrations of the total petroleum hydrocarbons (PHCs measured by UV/F) in the sea-water remained on the average within the range 0.7-2.1 µg/l (**TABLE 2**). Such values are typical of the Gulf of Finland as reported by Poutanen and Tervo (1987). However, high PHC concentrations were present only in individual samples of water, especially in the samples collected from the vicinity of the oil-contaminated shores where PHC concentrations up to 12 µg/l were measured in June. But already in September these had dropped to the normal level; from this it can be concluded that the oil which had been on the rocks on the shore had been rinsed off.

TABLE 2. The petroleum hydrocarbon (PHC) concentrations in the surface water (1 m depth) in the coastal sea area of southern Finland in 1987 and 1988. Monthly means (µg/l SEB crude oil equivalence). PHCs obtained by UV/F 310/400 nm.

MONTH		**N**	**mean**	**SD**	**range**
1987					
FEBRUARY		7	1.7	0.7	0.7-2.6
MARCH		8	1.3	1.1	0.3-3.3
MAY		20	1.2	0.4	0.6-17.0
JUNE	sl.w.	5	4.8	4.3	1.6-12.2
		18	0.7	0.3	0.5-1.5
JULY	sl.w.	1	0.6	-	-
		9	0.6	0.2	0.3-1.0
AUGUST		13	0.4	0.1	0.3-0.5
SEPTEMBER	sl.w.	5	0.8	0.7	0.3-2.1
		12	0.9	0.8	0.2-2.9
OCTOBER	sl.w.	2	0.9	0.3	0.7&1.1
		2	0.8	0.2	0.7&1.0
1988					
MARCH		6	1.8	0.5	1.1-2.4
MAY		3	0.8	0.06	0.8-0.7
SEPTEMBER		6	0.9	0.5	0.4-1.9

sl.w. = shoreline water

Sediment: PHCs (measured by UV/F) in the sediment samples showed that extensive, clearly oil-contaminated sea-floor areas were not found in the Gulf of Finland. The predominant type of sea-floor in the studied area is an erosion-type floor of rock, gravel and silt-clay. If petroleum hydrocarbon has sedimented on such sea-floor, locating it is difficult and haphazard. Oil binds poorly to an erosion-type sediment, and the mobility of oil on the surface of such a sea-floor is expected to be considerable. PHCs in the sediments clearly correlated with the content of dry matter (dm %). The PHC concentrations were as general between 55 and 350 µg g^{-1} in the samples with low content of dry matter (2 -> 14 %) and between 7 and 175 µg g^{-1} in the samples with higher content of dry matter (15 -> 70 %), (**TABLE 3**).

The measurements of PHCs gave poorly comparative results because the sediment quality (dry matter %) differed considerably between the samples collected from the same sea area in 1987 and 1988.

TABLE 3. Mean concentration ($\mu g\ g^{-1}$ dw) of the petroleum hydrocarbons (PHCs) in the sediment samples (0->2 cm) collected from the coastal sea area of southern Finland in 1987 and 1988. PHCs obtained by UV/F. DM % = content of dry mater.

		1987			1988		
	DM %	**N**	**mean**	**range**	**N**	**mean**	**range**
PHCs	2-14	11	165	55-354	12	181	95-288
	15-70	11	72	7-175	5	56	8-123

The qualitative analyses of sediments showed that the mean sum of the normal alkanes from C15 to C30 was slightly increased in the samples of 1988, (**TABLE 4**). This depended mostly on the higher concentrations of the n-alkane C17 and the isoprenoid alkane pristane in the second-year samples. The presence of these hydrocarbons indicated a biogenic source associated with planktonic detritus, probably from the heavy algal blooms observed in the Gulf of Finland in 1987. Ratios typical of the SEB -crude oil composition were not found in the sediment samples of 1987 and 1988 (**TABLE 4**).

TABLE 4. Summary of the aliphatic hydrocarbon composition in the sediment samples (0->2 cm) collected from the coastal sea area of southern Finland in 1987 and 1988. Mean concentration ($\mu g\ g^{-1}$ dw) obtained by GC/FID. SEB = Soviet Export Blend -crude oil.

	1987	1988	SEB
	mean ± SD	**mean ± SD**	
nC17	2.35 ± 2.10	4.37 ± 2.47	3040
Pristane	0.46 ± 0.20	1.13 ± 0.30	1760
nC18	0.37 ± 0.39	0.44 ± 0.23	2680
Phytane	0.20 ± 0.10	0.32 ± 0.17	1730
Odd-n-alkanes[1]	6.66 ± 2.55	11.86 ± 5.79	16780
Even-n-alkanes[1]	2.35 ± 0.77	3.05 ± 1.45	15640
SUM	9.01 ± 3.30	14.91 ± 7.00	32420
UCM	37.00 ±19.00	35.00 ±32.00	-
nC17/pristane	4.7 ± 2.3	4.0 ± 2.4	1.7
nC18/phytane	1.5 ± 0.8	1.4 ± 0.5	1.5
Prist/phyt	2.3 ± 0.6	4.5 ± 2.9	1.0
CPI[2]	3.1 ± 0.5	4.0 ± 1.4	1.1

1 = including n-alkanes from C15 to C30

2 = ratio of Σ nC15-nC29 and Σ nC16-nC30

The most interesting results were obtained from the measurements of the 16 polyaromatic hydrocarbons (PAHs) in the sediments. The mean of the total concentration of PAHs was elevated in the samples of 1987 (**TABLE 5**). This was related to the presence of a naphthalene fraction in concentrations between 0.4 and 1.1 µg/g dw. Naphthalene was not found in the sediment samples of 1988 which led to the conclusion that petroleum hydrocarbons had sedimented in small amounts over a wide sea-area.

TABLE 5. Mean sum and range of the polyaromatic hydrocarbons in the sediment samples collected from the coastal sea area of southern Finland in 1987 and 1988. PAHs obtained by HPLC.

		1987			1988		
	dm %	n	mean	range	n	mean	range
PAHs[1]	2-14	4	3.2	2.2-4.7	5	1.3	0-2.2

1 = see Farrington et al. 1986 and Uthe et al. 1986.

IMPACT ON SEA-FLOOR FAUNA

Studies of the sea-floor fauna were carried out both in the open sea and the coastal sea area of southern Finland in 1987 and 1988. The results showed that the oil did contaminate and locally affect the sea-floor fauna. Oil contamination: Oil was observable to the naked eye in the first-year samples of the amphipod Pontoporeia sp. collected from the vicinity of Kalbådagrund in the **open sea area** (Andersin 1990).

In **the coastal sea area** the oil contaminated individuals of the amphipods Pontoporeia sp. and Gammarus sp. were encountered in frequencies between **2 and 13 %**. Contaminated individuals of Gammarus sp. were also found in the second-year samples collected from the Fucus-belts and it was surprising that the frequencies were as high as in the samples of 1987. Also gastropods e.g. Lymnaea sp. which had been moving in patches of oil on rocks on the shore, were contaminated.

The petroleum hydrocarbons (PHCs), aliphatic hydrocarbons (AHCs), unresolved complex mixture (UCM) and the 16 polyaromatic hydrocarbons (PAHs) were analyzed in the samples of the isopod Mesidotea entomon, the shoreline living gastropod Lymnaea sp. and the bivalves, Baltic clam (Macoma balthica) and common blue mussel (Mytilus edulis). The PHC, AHC, UCM and PAH concentrations in the studied organisms have been summarized in **TABLE 6**. Only a few clearly oil-contaminated samples of biota could be found in 1987. But in 1988 the concentrations of PHCs and the aliphatic UCM were elevated in all samples of the sea-area. Althought, the oil contamination couldn't be proved in the sediment samples of 1988, the Macoma samples collected from the same sampling sites as the sediments showed that the oil has been present in the system still

TABLE 6. The mean concentrations of petroleum hydrocarbons in the samples of the isopod *Mesidotea entomon*, the gastropod *Lymnaea* sp. and the bivalves of baltic clam (*Macoma balthica*) and common blue mussel (*Mytilus edulis*) collected from the coastal sea area of southern Finland in 1987, 1988 and 1989. PHCs obtained by UV/F, aliphatic fraction ($\Sigma nC15-nC30$) and UCM obtained by GC/FID and polyaromatic hydrocarbons (PAHs) obtained by HPLC. Concentrations given as $\mu g\ g^{-1}$ dry tissue weight.

PHCs

	1987			1988			1989		
Sample	N	mean	SD	N	mean	SD	N	mean	SD
Mesidotea	7	77	38	2	215	7	-		
Lymnaea sp.	12	286	203	18	468	111	-		
Macoma	12	302	84	11	1423	460	6	2360	275
Mytilus	3	278	43	3	2142	637	-		

UCM (aliphatic)

	1987			1988			1989		
Sample	N	mean	SD	N	mean	SD	N	mean	SD
Mesidotea	2	29	17	-			-		
Lymnaea sp.	3	43	8	5	276	146	-		
Macoma	4	63	9	10	630	446	6	1815	328
Mytilus	3	49	5	3	680	210	-		

ALIPHATIC FRACTION

	1987			1988			1989		
Sample	N	mean	SD	N	mean	SD	N	mean	SD
Mesidotea	2	6.2	5.6	-			-		
Lymnaea sp.	3	8.7	4.6	5	4.0	1.6	-		
Macoma	4	3.9	1.3	10	4.8	1.9	6	4.1	2.0
Mytilus	3	2.3	0.4	3	4.2	2.1	-		

PAHs

	1987			1988			1989		
Sample	N	mean	SD	N	mean	SD	N	mean	SD
Mesidotea	2	2.85	2.27	-			-		
Lymnaea sp.	3	4.89	4.24	5	0.48	0.46	-		
Macoma	4	5.70	2.69	10	1.37	1.31	6	0.40	0.29
Mytilus	3	1.15	0.62	3	1.79	1.55	-		

during the winter of 1987/88. Unfortunately, no samples were collected during this winter period. Some Macoma samples were also collected in 1989. The PHC and UCM concentrations were still high. However, the composition of the resolved alkanes showed that the normal alkanes between C22 and C26 dominated in the Macoma samples of both 1988 and 1989 which indicates that no more new oil had been introduced to the ecosystem after 1987 or 1988.

This indication is confirmed by the measurements of polyaromatic hydrocarbons (PAHs) which were present in higher concentrations in the samples of 1987 but in lower concentrations in the samples of 1988 and 1989 (**TABLE 6**). The composition of PAHs in the Macoma samples were similar to that of the sediment samples. However, no naphthalene fraction could be analyzed from the clam tissue. The most interesting PAHs found in the Macoma samples were **fluorene**, **phenanthrene**, **fluoranthene**, **pyrene** and **krysene**. These compounds were clearly elevated only in the samples of 1987. The PAHs in Lymnaea sp. collected from shoreline waters clearly showed differences between the samples of different years. Fluorene, **phenanthrene**, **anthracene**, **krysene** and **benzo(b)fluoranthene** were present in the concentrations between 0.07 to 1.4 in the samples of 1987 but absent in the samples of 1988.

Quantitative effects: The oil moved forth and back in the middle of the Gulf of Finland during the winter of 1987. Quantitative changes in macrozoobenthos of the open sea-area could be observed only in one station which is in a shallow water zone in the vicinity of Kalbådagrund. The oily ice moved through this sea-area several times. In the area the oil had affected the 1987's reproduction of the amphipod Pontoporeia sp. This was confirmed by the abundance and size distribution of the Pontoporeia populations in the second-year samples which clearly differed from that of the first-year samples (Andersin 1990).

The quantitative changes on the macroscopic (>0.5 mm) sea-floor fauna were also proved in the coastal sea-area. The study is based on data collected during the summers of 1987 and 1988 in the archipelago of Porvoo (Kalliola 1990). Quantitative samples were collected from six stations in rather deep water (15-23 m), from four shallow water (4-5 m) stations and from seven sites in the Fucus-belt. In some of the deep zone stations the abundances of the amphipod Pontoporeia affinis had decreased a year after the oil spill. Also the densities of Ostracods had declined significantly in the second-year samples. In the shallow water zone the population densities didn't show any differences between the samples of 1987 and 1988. But in the Fucus-belt (bladder-wrack zone) where the degree of oil-contamination was evidently high, the population densities of the amphipod Gammarus sp. had significantly decreased in the samples of 1988, a year after the oil spill (Kalliola 1990). However, this effect couldn't be observed in two stations in the western part of the study area in which the densities had slightly increased a year after the oil spill.

IMPACT ON SEA BIRDS

In 1987 the nesting bird fauna of a total of 45 outer islands was investigated in the coastal sea-area of southern Finland. Oil didn't cause any visible damage on sea-bird communities while it drifted among the ice from February to April 1987. The massive solid ice-cover along the coasts prevented the oil from reaching the shorelines and oil never caused severe pollution damage in the archipelagos. However, in May 1987 the effects of possible oil contamination were observed on 7 islands, mostly tree-covered large islands of the inner archipelagos.

On May 13th, the oil began to strand on the islets of the study areas. The arrival of the oil lasted only a few days. Certain bird sanctuary islets off the coast of Loviisa were contaminated the worst. Almost all of the oil came to the **east-side and south-side shores** of the islets. This saved, for example, the rocky areas favored by the razor-bill on the northern and western shores of islets (Hario 1990).

The arrival of the oil occurred in a phase in which most of the eider females were already hatching on the islets; no information was obtained regarding the oil-contamination of the males which were out on the water at that time. The eider females returned with their young ones to the water only after the oil had stopped coming. They thus avoided the oil drifting on the water. In the follow-up squares in the outer islets, the eider fledglings evaded all patches of oil. They did not avoid oily shores but "knew" how to avoid oil slicks.

The oil-contamination of birds was limited to individual cases and was not significant at the population level.

IMPACT ON SEALS

In the aerial reconnaissances carried out in spring 1987, no ringed-seal pups were seen on the Finnish side of the Gulf of Finland (Hario 1990). The woolly hair of seal cubs is sensitive to oil. By contrast, adult seals can withstand oil-contamination better. However, oil was not present on the outer islets on the Finnish side to such an extent that it would have constituted a hazard to seals.

IMPACT ON FISH AND FISHERIES

The oil (spill) from MT Antonio Gramsci caused no heavy pollution-damage to the shores of the vulnerable sea-areas, e.g. important nesting islands of birds. But 270 tons of oil was dispersed in the water column and this phase lasted for weeks in the Gulf of Finland. It was expected that possible effects might be detected in fish in the oil-influenced sea-areas.

The effects of oil on the health status of perch and flounder were studied in 1987 and 1988. Fish caught in 1987 from the oil-affected sea areas had higher content of aliphatic hydrocarbons in liver tissue than fish from the reference area (**TABLE 7**). The content of aromatic hydrocarbons was > 10 µg/g (ww) in liver tissue of perch caught from the Pellinki archipelago in May 1987, but the content of aromatics had already decreased in the samples caught in September 1987 (Tana & Lehtinen 1990).

The oil spill probably affected the state of health of the fish. This conclusion is supported by the lower-than-normal vitamin C concentrations in caudal fin of perch and flounders caught from the oil-influenced sea areas (**TABLE 7**). Furthermore, the increased frequencies of certain diseases and parasites in the fish were detected in the actual oil-spill area (Tana & Lehtinen 1990). Flounders caught in September 1988 showed already a better state of health. It must be pointed out that there are no earlier studies on fish populations carried out in the Gulf of Finland with which to compare the present results. That is why it is difficult to confirm whether the differences in petroleum hydrocarbon and vitamin C concentrations detected in fish between the oil-spill areas and the reference area are due to the Antonio Gramsci oil spill or whether they are typical of fish in the charted sea areas.

TABLE 7. Mean concentrations of aliphatic and aromatic hydrocarbons in liver tissue and vitamin C in caudal fin of perch and flounder caught from the oil-influenced sea areas (1-3) and the reference area (ref.) in 1987 and 1988, (modified from Tana & Lehtinen 1990).

	month/year	Sea area[1]	Aliph. µg/g ww	Arom.[2] µg/g ww	Vitam C µg/g
Perch	May 1987	ref.	6.5	1.76	37
	May 1987	2.	18.4	10.78	15
		3.	57.8	0.15	13
	Sept.1987	ref.	19.5	-	56
		1.	12.0	-	54
		2.	22.1	3.73	19
Flounder					
	May 1987	ref.	-	-	19
		1.	137.0	0.43	6
	Sept.1987	ref.	40.3	2.10	27
		2.	126.5	3.50	12
	Sept.1988	ref.	100.2	0.01	8
		1.	91.0	0.05	6

1) Ref. = the Tvärminne archipelago, 1. the Söderskär, 2. the Pellinki and 3. the Loviisa archipelagos.

2) Mean Σ: phenanthrene + naphthalene + anthracene + dibenzothiophene

Possible effects of oil were also confirmed by the changes in relative sizes of liver and sexual glands of fish when a comparison was made between the fish stocks from the different sea areas (Urho & Ahvonen 1990). In the herring females caught in April and May 1987 from the sea-area of Helsinki -> Kalbådagrund, the gonad somatic indexes (GSI) were lower and the liver somatic indexes (LSI) higher than in females from the sea area of Emäsalo -> Pellinki. Comparisons of the next-year samples showed that the differences in GSI and LSI values had decreased between the studied herring populations (**FIGURE 3**). These changes were not natural and could only have been caused by an external environmental factor such as oil and petroleum hydrocarbons to which herring fish probably were exposed but only for a short time (Urho & Ahvonen 1990). In addition, certain types of damage in young fish were more common in the oil spill area than elsewhere in the Gulf of Finland, as reported by Urho & Ahvonen (1990). Furthermore, odour and flavour of oil was proved in some catches of herring and salmon. Also oil-damage on fish traps or nets was documented in the oil-influenced sea area as shown in **FIGURE 4**.

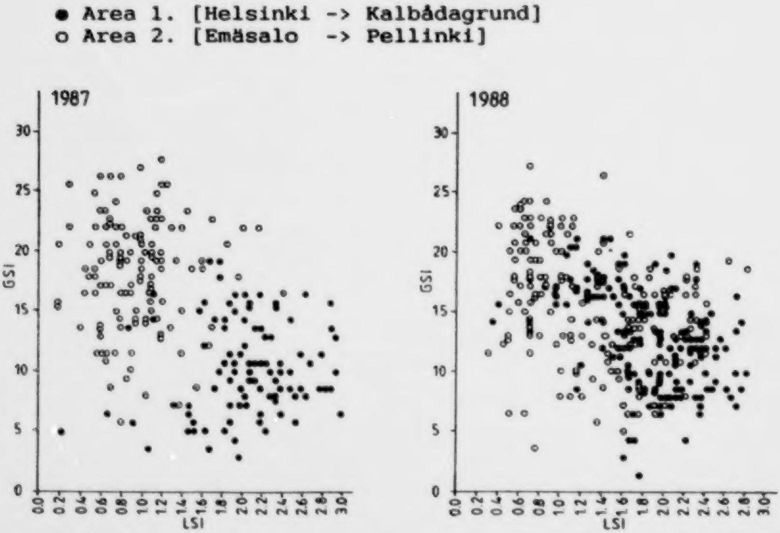

FIGURE 3. Distribution of GSI (gonad somatic index) and LSI (liver somatic index) in herring females caught from two different sea-areas in the Gulf of Finland in 1987 and 1988 (Urho & Ahvonen 1990).

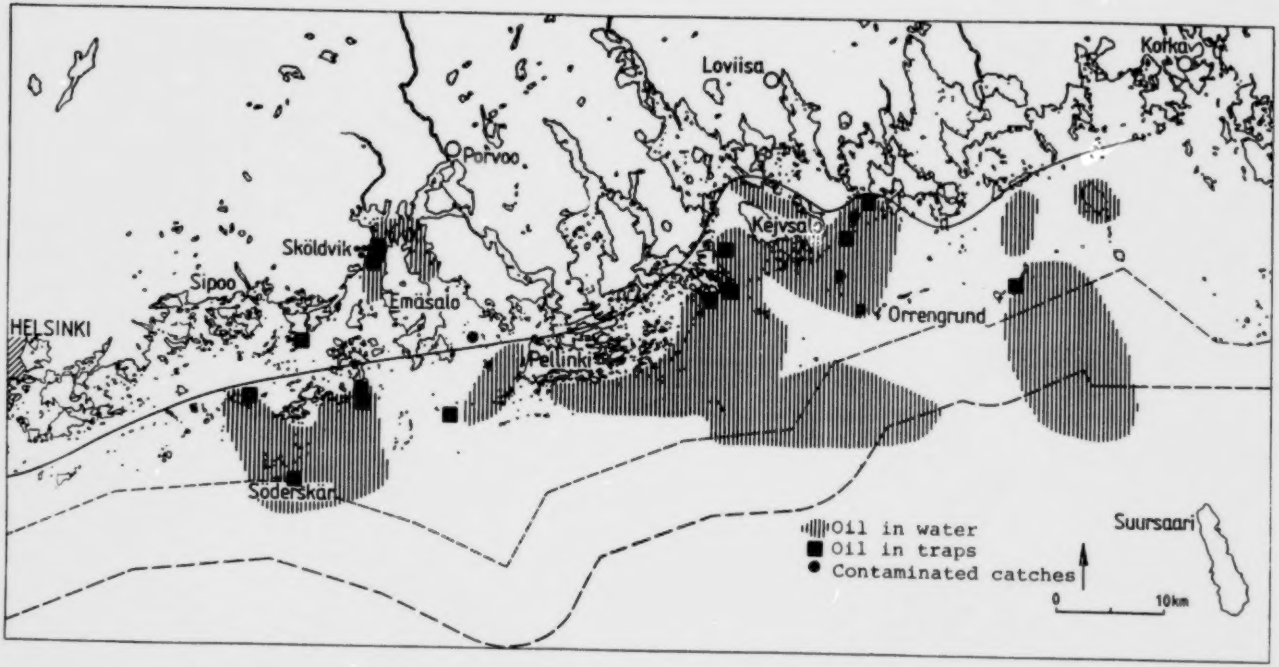

FIGURE 4. The observations of oil made by the local fishermen at the coastal sea area of southern Finland during May 1987. The location of the damaged traps and contaminated catches (after Urho & Ahvonen 1990).

In 1987 the salmon catches in the oil spill area were poor compared with the previous fishing season (Kuikka 1990). The analyses of data on the catch per unit effort of salmon and trout in the oil-influenced area showed that the trout catches of trapnets were not influenced by the oil. However, the catches of salmon dropped, especially at the beginning of the fishing season. Catches seemed to be uninfluenced in the western part of the Gulf of Finland. It is likely that the oil affected the behaviour of the salmon stock. Because the mean catches had dropped in 1987 it could be expected that the catches of some individual fishermen had fallen significantly.

The Antonio Gramsci oil spill in the Gulf of Finland caused no drastical economical effects on fisheries. Some biological effects were detected but seemed to be only momentary.

WHAT WAS THE LEARNING OF THIS OIL SPILL

All oil spill incidents at sea have been different. It is difficult at the time of spillage to predict how severe an oil-spill can become. Development of an oil spill to a serious one depends on season and prevailing meterological conditions, type and amount of oil, effectiveness of oil combatting measures etc.

Biological effects are related to degree of oil pollution damage in the vulnerable areas e.g. in important nesting islands and foraging waters of sea birds, breeding zones and herding sherries of seals, important fishing zones and nursery areas of fish. There is always need for up-to-date information on seasonal changes in sensitivity of the natural systems. However, there is seldom plenty of time to try to collect such information after an oil spill incident but in the case of the Antonio Gramsci the time was long enough to do it.

There are always special problems connected with oil spills in ice-covered sea areas during the winter. E.g. available combatting measures are inefficient for controlling and collecting oil in ice-conditions. Oil will decompose slightly among ice. It may drift with ice from place to place and split into small spills. So an oil-spill situation will be prolonged and be acute for several months. The factum is that an oil spill constitutes an environmental hazard until oil (waste) can be eliminated through clean-up actions by man and at last by natural processes as in this case.

The Antonio Gramsci oil spill involved many potential risk factors that could produce severe damage to the marine environment and its natural systems. Fortunately, the time factor, physical conditions and natural processes were able to decrease the reactivity and toxicity of the oil.

But unfortunately, as this case proved, there are always some parts of the marine ecosystem which couldn't avoid to be affected. Recovery of the sea-floor fauna and the fish stocks in the coastal waters of southern Finland is still continuing and these are the targets for further studies.

REFERENCES

Andersin, A-B. 1990. Effects of oil on macrozoobenthos in the open sea area of the Gulf of Finland. In: Hirvi, J-P. (ed.). Suomenlahden öljyvahinko 1987. (The oil spill in the Gulf of Finland 1987). Publications of the Water and Environment Administration A 51. Helsinki. ISBN 951-47-3675-3. ISSN 0786-9592. (In Finnish). (in print).

Farrington, J. W., David, A. C., Livramento, J. B., Clifford, C. H., Frew, N. M. & Knap, A. 1986. ICES/IOC intercomparison exercise on the determination of petroleum hydrocarbons in biological tissues (mussel homogenate) - ICES 2/HC/BT. Coop. Res. Rep. int. Coun. Explor. Ser., 141, 75 p.

Hirvi, J-P. 1990. Suomenlahden öljyvahinko 1987. (The oil spill in the Gulf of Finland 1987). Publications of the Water and Environment Administration A 51. Helsinki, Finland. ISBN 951-47-3675-3. ISSN 0786-9592. (in Finnish). (in print).

Hario, M. 1990. Effects of oil on birds and seals. In: Hirvi, J-P. (ed.). Suomenlahden öljyvahinko 1987. (The oil spill in the Gulf of Finland 1987). Publications of the Water and Environment Administration A 51. Helsinki. ISBN 951-47-3675-3. ISSN 0786-9592. (in Finnish). (in print).

Kalliola, I. 1990. Effects of oil on macrozoobenthos in the coastal sea area of southern Finland. In: Hirvi, J-P. (ed.). Suomenlahden öljyvahinko 1987. (The oil spill in the Gulf of Finland 1987). Publications of the Water and Environment Administration A 51. Helsinki. ISBN 951-47-3675-3. ISSN 0786-9592. (in Finnish). (in print).

Kuikka, S. 1990. Analysis of data on the catch per unit effort of salmon and trout in the oil-influenced sea area. In: Hirvi, J-P. (ed.). Suomenlahden öljyvahinko 1987. (The oil spill in the Gulf of Finland 1987). Publications of the Water and Environment Administration A 51. Helsinki. ISBN 951-47-3675-3. ISSN 0786-9592. (in Finnish). (in print).

Mackay, D. 1982. Fate and behaviour of oil spills. In: Sprague, Vandermaulen & Wells. Oil and dispersants in Canadian seas - Research appraisal and recommendations. Environment Canada. Environmental Protection

Service Reports. Economic and Technical Review, Report EPS 3-EC-82-2. ISBN 0-662-11995-9. p. 7 - 27.

Poutanen E.-L. & Tervo, V. 1987. Meriveden öljyhiilivedyistä. (Petroleum hydrocarbons in sea water). Kemia-Kemi, vol. 14, no. 5, p. 441 - 444.

Tana, J. & Lehtinen, K-J. 1990. Effects of oil on the state of health of fish. In: Hirvi, J-P. (ed.). Suomenlahden öljyvahinko 1987. (The oil spill in the Gulf of Finland 1987). Publications of the Water and Environment Administration A 51. Helsinki. ISBN 951-47-3675-3. ISSN 0786-9592. (in Finnish).(in print).

Urho, L. & Ahvonen, A. 1990. Effects of oil on fish and fisheries. In: Hirvi, J-P. (ed.). Suomenlahden öljyvahinko 1987. (The oil spill in the Gulf of Finland 1987). Publications of Water and Environment Administration A 51. Helsinki. ISBN 951-47-3675-3. ISSN 0786-9592. (in Finnish). (in print).

Uthe, J. F., Musial, C. J. & Sirota, G. R. 1986. Report on the intercomparative study 03/HC/BT on the determination of polycyclic aromatic hydrocarbons in biological tissue. Coop. Res. Rep. int. Coun. Explor. Ser., vol. 141, 10 p.

A STANDARDIZED APPROACH TO THE ECOLOGICAL MONITORING OF OIL SPILLS

by

Charles J. Dobroski and Raymond B. Bogardus
Roy F. Weston, Inc.

Introduction

This paper provides a scientific framework for standardizing the ecological monitoring of oil spills in the arctic marine environment. In response to oil spills not only in the arctic, but also in other climatic regions, there appears to be a need for a concerted strategy for assessing their effects.

One of the greatest concerns in the current approach to monitoring the impact of oil spills and to determining their overall effect on the exposed populations is the lack of a reference by which the insult can be measured. Currently, the environmental monitoring associated with oil spills and the data collected by the regulatory and scientific community is conducted and are obtained as a "post hoc" exercise in which a mad scramble of activity is undertaken to define the potential threat or effects of the spill. Consequently, much of the data collected is in response to a condition which already exists. Facing the difficult questions posed in the arena of ecological risk assessment and natural resources damage assessments, the scientific community is required to answer questions that are not easily addressed by post-mortem assessments. To determine if, and by how much, environmental conditions have changed (if that, in fact, is the equivalent to impact), there must be a point of reference from which we proceed; we must know what conditions were like before the impact occurred. Establishing a difference is the essential element in demonstrating an adverse ecological effect.

The premise of this paper, therefore, is that there is a need for the scientific community to establish reference monitoring sites and a continuous monitoring program both in those areas where the greatest potential for spills exists, and where habitats are sufficiently noteworthy and representative that their rehabilitation to pre-spill conditions will be requisite.

Goals and Objectives

The approach discussed herein is a proposal to establish an Ecological Monitoring Network for Oil Spills (EMNOS). The network and its ancillary studies provide a monitoring program that would continuously monitor the ecological status of potentially affected habitats in the arctic marine environment. The goals and objectives of this monitoring network are presented in Table 1. By way of summary, we believe that this long-term, integrated, multi-habitat program distinguishes itself from most of the current monitoring programs, which are "reactive" instead of "proactive" exercises, by:

- Identifying the existing environmental conditions of coastal areas most likely threatened by the accidental release of oil,
- Improving the resolution of the extent and magnitude of the ecological impact of the oil spill,
- Providing confirmatory rather than predictive results.
- Providing a solid technical baseline by which the efficacy and accuracy of other monitoring scenarios may be judged.
- Providing a benchmark for evaluating the success of any rehabilitation program.
- And although the approach is not predictive in and of itself, the empirical data derived from this approach will provide the bases upon which predictive models of ecological effects and the efficacy of cleanup can be developed and validated.

Although proposed for a somewhat different set of objectives in mind, the monitoring network presented herein is conceptually similar to the U.S. EPA's recently conceived "Environmental Monitoring and Assessment Program (EMAP)." Affirming the absence of sufficient ecological data to determine community trends and recognizing the broad base of support for better

Table 1

Goals and Objectives of the Ecological Monitoring Network For Oil Spills

---

Goals

- To develop and initiate a comprehensive inventory of ecological points of reference.
- To provide meaningful information about the effect of oil spills on the arctic coastal ecosystem.
- To reduce the uncertainty associated with predicting adverse impacts of oil spills.

Objectives

- To identify the existing condition of coastal areas most likely threatened by the accidental release of oil.
- To improve the resolution of the extent and magnitude of ecological impact of oil spills.
- To provide a confirmation of the effect of a spill rather than a prediction of that effect.
- To provide a solid technical baseline by which the efficacy and the accuracy of other monitoring scenarios may be judged.
- To provide the bases upon which predictive models of ecological effects can be developed and validated.
- To incorporate all data into an arctic marine databank to promote the dissemination of data to management agencies and the scientific community.
- To evaluate the effectiveness of oil spill cleanup strategies within reference coastal areas in the marine arctic system.

environmental monitoring, the EPA's Science Advisory Board recommended a program that would monitor the ecological status and trends as well as develop innovative methods for anticipating emerging problems (USEPA 1989a). We have proposed the Ecological Monitoring Network for Oil Spills (OMNES) to reduce the uncertainty associated with predicting adverse impacts from oil spills, however, we also believe that this network will provide additional benefits from the quantitative and scientific assessment of the status of ecological resources in the arctic marine environment.

Such an endeavor, we think, will best enable the formulation of cost-effective regulatory actions and cleanup strategies. Moreover, we believe that the establishment of a formal monitoring network such as the one proposed herein, will encourage the analysis and review that not only foster the discovery of unanticipated results but also promote the dissemination of scientifically sound information.

Obviously, there is a political debate to be entered as to the allocation of costs to begin and maintain an EMNOS program. As scientists, we believe "a priori" sampling of habitats in oil-lease and development areas is overdue.

The Design of the Ecological Monitoring Network for Oil Spills

To address the goals and objectives of the proposed ecological monitoring network, a plan of action that defines four principal tasks and a number of subtasks is presented in Table 2.

Selection of Reference Monitoring Sites

The EMNOS program is designed to provide a mechanism to monitor the existing condition of the coastal environments potentially affected by an accidental release of oil in the arctic waters. The purpose of this exercise is to select those coastal sites that have both a reasonable probability of being subjected to an accidental release and a habitat, which is of special or

Table 2

A FRAMEWORK FOR THE ECOLOGICAL MONITORING FOR OIL SPILLS

SEQUENCE OF TASKS

Task 1 - Collect and Analyze Existing Information

Collect, Review and Analyze Information Which Would Assist the Identification of High Risk Areas

- Identify magnitude of ship traffic volume, port and transfer terminal activity, past accident history, etc
- Identify hydrographic conditions that would contribute to risk - channel morphology, current characteristics, others
- Identify the presence of noteworthy and representative habitats, sensitive receptors

Task 2 - Select Reference Monitoring Sites

- Based on information obtained in Step 1, determine the need for reference monitoring site(s)
- Compare information on traffic volume and coastal hydrograph to define the potential for accidental release
- Compare the likelihood of release with ecological significance of the area
- Select as reference monitoring sites those locations with greatest potential for major disturbance

Table 2

A FRAMEWORK FOR THE ECOLOGICAL MONITORING FOR OIL SPILLS

SEQUENCE OF TASKS

(continued)

Task 3 - Design Ecological Monitoring Plan for the Reference Monitoring Site

- Review existing data, where available
- Define habitats to be monitored
- Review available data for each habitat type
- Select key ecological endpoints that measure "structural base" of the habitat
- Select key ecological endpoints that measure system "functions"
- Define schedule of baseline activity

Task 4 - Review and Refinement of Monitoring Strategy

- On a periodic basis, data will be reviewed to assess the need to refocus the current monitoring strategy.

noteworthy ecological significance. Tasks 1 and 2 of the preliminary framework provide a sequence of subtasks for the selection of reference monitoring sites.

Information that would assist the assessment of high risk areas such as, the magnitude of ship traffic, channel/depth characteristics, hydrographic data on currents, and others, would be compiled and evaluated in a coordinated effort with the Canadian Ministry of Environment, the U.S. Coast Guard, NOAA, and others to establish those coastal water bodies where the potential for an oil spill is highest. Information collected herein would be geographically compared with available ecological and habitat data for the area. To assist in the management and use of possibly large volumes of environmental data needed to develop both the network design and the criteria for the selection of the reference monitoring sites, we propose that all data be assembled, managed, and kept current using a data management system such as the Geographic Information System (GIS) format.

Certain components of the coastal ecosystem are recognized as ecologically vital and in need of protection. These components serve one or more of three major functions: maintaining ecosystem productivity stabilizing community structure, and providing essential habitat. The maintenance of critical habitat is requisite to the survival and well-being of biological communities, to the functioning of the ecosystem, and thus to the maintenance of biological carrying capacity. Some of the vital habitats that are anticipated for incorporation in EMNOS and their principal functions are provided in Table 3 (USFWS, 1978a).

It is important that the reference monitoring sites in the ecological monitoring network incorporate as many habitats as possible because the type of habitat can ultimately affect the nature and magnitude of the environmental impact. For example, the release of oil onto a rocky shoreline will probably be less persistent because of the wave action than the same release into a tidal marsh where little tidal energy is available to help dissipate the spill.

Table 3

A Summary of Vital Shoreline and Near Shore Aquatic Habitats and Their Functions for Use in the Selection of Reference Monitoring Sites, (USFWS, 1978)

HABITAT	VALUE
Rocky Shorelines	Act as buffers to upland habitat. They represent exceptional habitat for a variety of benthic and floral species that require hard substrate. They are important habitats for diverse associations of marine species.
Salt Marsh	Buffer between tideflats and upland areas, tidally inundated areas, support numerous plant species, provide nursery areas for fish, as well as exceptional habitat for birds. Functions include primary productivity and nutrient storage.
Submerged Aquatic Vegetation Beds	SAV beds play a major role in providing nursery habitat to various fish and invertebrate species. Supply general habitat, primary productivity, and nutrient storage.
Tideflats	Provide feeding areas for fish and shore and wading birds. May produce high yield of shellfish and marine worms. Functions as an important storage element for energy and nutrients.
Shellfish Beds	Provide an important economic resource and food source for fish, birds, and mammals. Are important habitats for diverse associations of marine species.
Kelp Beds	Provide dampening effect of storm and tidal surge on shorelines. Provide food and favorable habitat for many fish, as well as nursery areas for juveniles.
Convergence Areas	Includes areas of high concentrations of species due to critical functions, such as, breeding areas, migration pathways, nurseries, feeding basins, etc.

The development of criteria for and the ultimate selection of the reference monitoring sites will require a coordinated effort of the regulatory, scientific, political, and industrial communities. Criteria could be developed to provide a ranking which would incorporate the likelihood of an oil spill with the proximity of ecologically vital habitats or sensitive receptors. The assessment of all relevant information and the selection of reference sites will be a collective effort of those deemed expert. Specialists, possibly in the form of an expert panel, will be consulted to ensure that all important habitats are addressed.

Design of the Ecological Monitoring Plan for Reference Monitoring Sites

The ability to assess the ecological effect of an oil release to a marine ecosystem requires an understanding of the ecological structure and function of that affected system. The multitude of organisms inhabiting the coastal marine systems are numerous and their interrelationships complex (Figure 1). Consequently, field efforts at the reference monitoring sites will be directed at collecting quantitative information about the structure and dynamics of biotic communities that may be potentially threatened. In order to do this, a multi-media and multi-level monitoring program that incorporates several tasks is envisioned.

Review of Existing Data and Expertise

An effective ecological assessment for the monitoring network will require a design that is tailored to specific characteristics of each reference monitoring site. Choosing which of the many possible variables to investigate in the study will depend on the nature of the site, the types of habitats present, and the objectives of the study. All too often, the direction of the study and the level of effort are a function of the investigators' interests and capabilities. Although that may strengthen a particular aspect of the study, it also represents some obvious limitations.

In selecting the assessment methodologies for which monitoring will be conducted at each of the reference monitoring sites, the input of a good mix

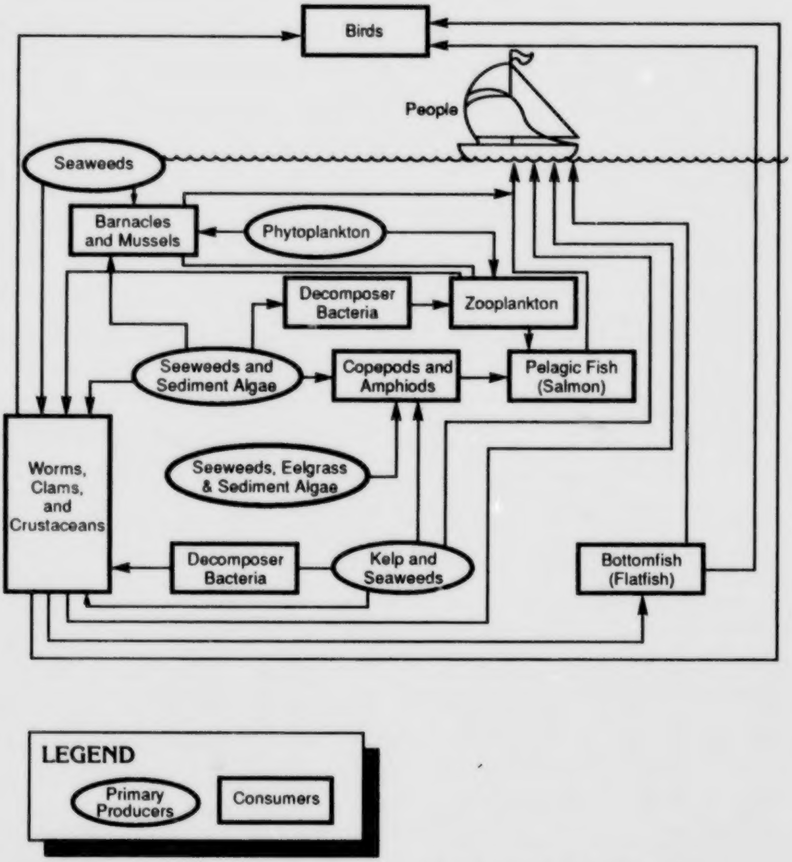

Source: Puget Sound Water Quality Authority, The State of the Sound 1986 (Seattle, WA, July 1986)

233-1424

GENERALIZED MARINE FOOD WEB

of ecological expertise in the research team and a level of judgement of interpreting data from complex systems are needed.

Just as importantly, a review of the literature to obtain site and impact specific data on past spills will increase the efficiency of the monitoring program by providing additional perspective. Previous studies may provide important information not only on habitat characterizations, but also on environmental responses to various perturbations. The use of these data can help optimize time and expense when shaping the monitoring protocol by taking advantage of information accrued from previous experiences in monitoring oil spills.

Selection of Ecological Endpoints

In order to establish a causal link between the release of hazardous materials and an ecological perturbation, in this case oil into the ecosystem, it is necessary to establish a point of reference from which changes can be assessed. The following narrative discusses these references points in terms of "ecological endpoints". Ecological endpoints are defined as those environmental attributes, which when monitored, give the best picture of the community response to a disturbance, whether it be an oil spill or an industrial discharge.

Suter, with Oak Ridge National Laboratories (1990) suggests that two types of endpoints exist in the context of ecological assessments. An "assessment" endpoint is an expression of the actual environmental values, as perceived by society, that are to be protected. This type of endpoint is a societal value in which its importance is influenced by political, economic, and philosophical considerations. An example of an "assessment value" would be the reduced quality of life resulting from an oil spill as perceived by the local citizenry. Such a judgmental evaluation would incorporate perceptions of lost economic, recreational, and aesthetic value.

The second type of ecological endpoint, and the one with which this paper is most concerned, is termed a "measurement" endpoint. Measurement endpoints are quantitative expressions of an observed or measured effect of an environmental insult. We generally recognize them as parameters that may be measured in the field or in the laboratory. To aid in the selection of ecological parameters for an environmental assessment, Suter (1990) offers a few characteristics of good measurement endpoints (Table 4).

In establishing the ecological endpoints for the EMNOS, several logistical and technical questions must be addressed, including:

- At what ecological level should reference data be collected (e.g., cellular, organism, population, community)?
- What suite of ecological endpoints should be monitored?
- Of the available methods, which are best suited to conditions of the individual reference monitoring sites?
- Over what time scale and area should baseline or reference data be collected?
- Will all endpoints be measured at all sites, or can a cost effective compromise for some sites be made?

Suggestions as to which endpoints are most appropriate for ecological assessments have been offered by numerous researchers (Suter 1990, 1989; Harwell and Harwell, 1989; US EPA, 1989; Cairns et al., 1981, and others). As previously noted, the ecological endpoints selected for EMNOS will necessarily be site-specific. However, a minimum list of endpoints for each site may be

Table 4

Characteristics of Good
Measurement Endpoints
(Suter, 1990)

1.	Corresponds to or is predictive of an assessment endpoint	The perceived importance of the research is enhanced if it has social relevance, e.g., bald eagle protection
2.	Readily measured	Consideration of time and cost
3.	Appropriate to scale of disturbance	
4.	Appropriate to route of exposure	
5.	Appropriate temporal dynamics	Should reflect life stage compound and seasonal differences
6.	Low natural variability	Should attempt to limit variables (principle of Occam's razor)
7.	Diagnostic	The measurement should reflect the known or potential impact
8.	Broadly Applicable	To allow comparison between reference sites and other habitats
9.	Standard	To allow precise comparisons between sites
10.	Existing data series	To allow an estimate of temporal trends

suggested (Cairns, 1981). In general, taxonomic surveys, estimations of population size, and data on system dynamics should be obtained. Information should be collected on the

- degree of diversity
- biomass and productivity
- nutrient and energy flow
- population dynamics, and
- physiological state of selected species.

Structural Endpoints

Table 5 presents a matrix of ecological endpoints recommended for the evaluation of some of the structural components of biological communities expected to occur at the reference monitoring sites. For the most part, these structural endpoints presented meet the requirements for good ecological endpoints as previously described by Suter (1990). Methods for collecting and analyzing these components are fairly standard, are applicable, and are readily measured. Moreover, these endpoints are believed to be appropriate to the routes of exposure (water column and sediments) and will be diagnostic of the impact.

We recognize, however, that for certain community endpoints, the required characteristics are less-suited. For example, benthic infauna have a tendency to be patchy; their distribution is largely determined by sediment type. Consequently, the community variability tends to be high. Similar circumstances occur for fish populations where density is dependent on the schooling behavior of certain species.

Table 5
Ecological Endpoints for the Structural Evaluation of Biological Communities at the Reference Monitoring Sites

Community	Distribution	Abundance	Biomass	Diversity	Evenness	Juvenile Index	Age Structure	Biotic Index
1. Microflora	x	x						
2. Periphyton	x	x		x	x			
3. Macrophytes	x	x	x					
4. Macroinvertebrates								
infauna	x	x	x	x	x			x
epifauna	x	x	x	x	x			x
5. Fish	x	x	x	x	x	x	x	x
6. Birds	x	x		x				
7. Mammals	x	x						

Functional Endpoints

In addition to monitoring the ecological endpoints that define the "structure" or organization of populations and communities occupying a specific habitat, the monitoring of reference sites should also be directed toward understanding the dynamics or "function" of those habitats. For this discussion, habitat "functions" are defined as those processes that regulate the interactive flow of mass, energy, nutrients, and pollutants, between structural components within those habitats. Although not as easily defined or measured as the population or community characteristics of the habitat, functional processes provide the linkage between the structural components of the system. Ecological endpoints that measure changes in mortality, reproduction, or nutrient and energy exchange may provide the best assessment of the more subtle effects of oil and other pollutants in the marine environment. That is to say, the effects occurring at the function level represent the causes for changes at the structural level. Therefore, if we wish to have explanations for what is observed in the community composition, we should look at the processes that govern or are diagnostic of community change, e.g., productivity, fecundity. Table 6 represents a list of ecological endpoints for the evaluation of functions for some of the habitat types anticipated to occur at the reference monitoring sites.

Again, while we recognize the importance of these ecological endpoints in interpreting observed changes in population or community structure, a lack of standard approach as well as some of the other characteristics of good ecological endpoints may limit their usefulness (LaPoint and Fairchild, 1989).

Abiotic Factors

Although the narrative has purposefully focused on biological monitoring, we

Table 6

Ecological Endpoints for Evaluating Functions in Habitats of the Reference Monitoring Sites

---

Primary Production

Fecundity

Reproductive Capacity

Biological Integrity

Guild Structure

Tissue Analysis

Overt Symptomology

Microbial Tests

Nutrient Cycling

- carbon, nitrogen, sulphur, and phosphorus transformation

---

fully recognize the importance of characterizing the physical and chemical environment of the habitats of the reference monitoring sites. Marine communities exist within the physical and chemical constraints of their habitats and as such, they are affected by and react with a broad spectrum of physical and chemical factors (States *et al.*, 1978). Consequently, it is essential that any monitoring of ecological endpoints in the OMNES program be coincident with the monitoring of various physical and chemical attributes of the habitat. Table 7 presents some of the more common physio-chemical parameters that are proposed as part of the Ecological Monitoring Network.

Summary

In summary, we have presented a scientific framework for standardizing the ecological monitoring of oil spills. This framework is based on the need for the scientific community to establish an Ecological Monitoring Network for oil spills. This network would establish reference monitoring sites in those areas having not only the greatest potential for the accidental release of oil, but also critical marine habitat value. Reference monitoring sites would incorporate a diversity of ecological habitats potentially affected in the coastal marine environment.

At each of the reference monitoring sites, a monitoring program would be designed and ecological endpoints selected. The ecological endpoints would represent key ecological attributes that would provide an elucidation of the status and trends of target population and community structure, as well as an explanation of the "functions" of that system. For each of the reference sites, at least four sets of seasonal data would be collected each year to coincide with periods of seasonal significance, such as spawning runs, spring overturn, etc.

We suggest that the development of criteria for and the ultimate selection of the reference monitoring sites, as well as the monitoring program, will be best served by a coordinated effort of the regulatory, scientific, political, and industrial communities.

Table 7
Abiotic Parameters to be Collected at Each of the Reference Monitoring Sites

Surface Water	Sediments
Physical	
Tidal cycle	
Tidal amplitude	Substrate type
Current velocity	Composition and
Circulation	Quality
Turbidity	Grain Size
Temperature	
Duration of Ice Cover	
Protectiveness	
Suspended Load	
Depth	
Chemical	
Salinity	
pH	Major Ions
Hardness	Trace Elements
Dissolved Oxygen	Total Organic Carbon
Biochemical Oxygen Demand	Select Target Chemicals
Major Ions	Sediment Oxygen Demand
Trace Elements	
Nutrients	
Select Target	
Chemicals	

The Ecological Monitoring Network for Oil Spills will provide the critical long-term ecological data required not only for evaluating the effectiveness of present monitoring and cleanup programs in achieving their goals, but also in supporting the science upon which they are based.

BIBLIOGRAPHY

Cairns, J. Jr. et al. Testing for Effects of Chemicals on Ecosystems. National Academy Press. Washington, DC. 100 pp. 1981.

Harwell, M. A. and Harwell, C. C. Environmental Decision Making in the Presence of Uncertainty. in Ecotoxicity: Problems and Approaches. Springer-Verlag. pp 517-540. 1989.

LaPoint, T. W. and Fairchild, J. F. Field Assessments in Ecological Assessment of Hazardous Waste Sites: A Field and Laboratory Reference, USEPA. Env. Res. Lab. Corvallis, Or. 1989.

Office of Technology Assessment. Wastes in Marine Environments. U.S. Congress. Wash. DC. 1987.

States, J. B. et al. A Systems Approach to Ecological Baseline Studies. U.S. Fish, and Wildlife Service, U.S. Dept of Interior, Wash. DC. 1978.

Suter, G.W. II. Ecological Endpoints in Ecological Assessment of Hazardous Waste Sites: A Field and Laboratory Reference, USEPA. Env. Res. Laboratory. Corvallis, OR. 1989.

Suter, G. W. II. Endpoints for Regional Ecological Risk Assessments. Journal of Environmental Management. Vol 14. No. 1: 9-23. 1990.

U.S. Environmental Protection Agency. Ecological Assessment of Hazardous Waste Sites: A Field and Laboratory Reference. Environmental Research Laboratory. Corvallis, OR. 1989.

U.S. Environmental Protection Agency. Environmental Monitoring and Assessment Program (EMAP). Office of Research and Development. Wash. DC. 1989.

U.S. Environmental Protection Agency. Risk Assessment Guidance for Superfund: Environmental Evaluation Manual. Interim Final. Office of Emergency and Remedial Response. Wash. DC. 1989.

U.S. Fish and Wildlife Service. Environmental Planning for Offshore Oil and Gas. Vol III. Effects on Living Resources and Habitats, U.S. Dept of Interior. Wash. DC. 1978.

EFFECT OF EXTERNALLY APPLIED BUNKER FUEL ON BODY MASS, BODY TEMPERATURE, PLASMA CONCENTRATION, AND WATER FLUX OF GLAUCOUS-WINGED GULLS, LARUS GLAUCESCENS

M. R. Hughes, C. Kasserra, and B. R. Thomas
Department of Zoology
University of British Columbia
6270 University Blvd.
Vancouver, B.C. Canada V6T 2A9.

Abstract___ Coating the feathers of Glaucous-winged Gulls, *Larus glaucescens*, with bunker fuel reduced ($P < 0.001$) food intake, body mass, water flux, body temperature, and plasma sodium and chloride concentrations.

INTRODUCTION

Every year much time, energy, and money is spent rehabilitating seabirds contaminated by oil spills, yet our understanding of how oil affected their physiology, especially water and ion regulation, is fragmentary. Oil appears to increase basal metabolic rate (BMR) (Lambert *et al*. 1982) and body heat loss (McEwan and Koelink 1973). In nestling seabirds oil increased plasma sodium concentration ($[Na]_{pl}$) suggesting dehydration (Miller *et al*. 1978; Peakall *et al*. 1982). Since seabirds produce free water by secreting intestinally absorbed Na^+ via the salt glands in less water than was absorbed with it (Schmidt-Nielsen *et al*. (1958), increased plasma concentration could reflect impaired Na^+ uptake in the gut (Crocker *et al*. 1974). Based on these observations oiled seabirds are often treated for dehydration and elevated plasma concentration (Burridge and Kane 1985), although neither condition has been experimentally demonstrated in mature birds under controlled conditions. In the present study we evaluated the effects of severe external oil contamination on body mass, body temperature, total food intake, water usage, total body water (TBW), water efflux, and plasma concentration of full grown gulls.

MATERIALS AND METHODS

Twenty-four nestling Glaucous-winged Gulls, *Larus glaucescens*, from a rookery at Christie Islet, B. C. (49° 30'N, 123° 18'W) were kept 5 months on *ad libitum* freshwater and vitamin supplemented bait herring, *Clupea palasii*, in an outdoor enclosure at the University of British Columbia Animal Care unit. They were fasted overnight, weighed, leg banded, and randomly divided into four equal groups, each housed in a 4' x 4' x 2' elevated metal cage. The mean holding room temperature (degrees Centigrade, °C) and mean relative humidity (RH, %) throughout the experiment were: Day 0, 19 °C, 64%; Day 2, 17.8 °C, 62%; Day 3, 16.7 °C, 65%; Day 4, 16.7 °C, 65%. Twice daily they were fed weighed pieces of herring (water content, 73.2% ± 0.5%) and three liters of water in a partially covered 6-inch deep container. Food and water intake were monitored until they appeared to be stabilized (three weeks after the gulls were placed in the cages) and throughout the experimental period. Mean total water usage per gull (mLs.day-1) was calculated by summing (mLs in waterer start - end 24 h) + (food water content) + (metabolic water derived from the food, 0.61 $\text{mL} \cdot \text{g food}^{-1}$ (assuming fish to be 80% protein and 20% fat, Schmidt-Nielsen 1975, p. 418) and dividing this sum by the number of gulls (6) in each cage. The birds were fasted overnight and water was removed for one hour. Then each gull was weighed, a blood sample (3.5 mL) was taken into a heparinized syringe from the brachial vein, and 12 uCi ^3H_2O were intravenously injected in 1.0 mL sterile isotonic saline (time 0). The exact volume was determined by weighing the syringe before and after loading. A continuous timer (Casio electronic clock, Chromatographic Specialities Ltd. Brookline, Ont) was activated for timing subsequent blood samples. After a 1 - 1.5 hour equilibration period with no water available (Hughes *et al* 1987), a blood sample (0.3 mL) was taken for determination of plasma chloride concentration ($[Cl]_{pl}$) and ^3H_2O concentration ($[^3H_2O]_{pl}$, which was corrected for water content (94.1%, Hughes *et al*. 1987). Total body water (TBW) was determined by isotope dilution. Then about 150 mLs Marine Bunker fuel (Esso Petroleum Canada, corresponding to #6 grade Canadian Government specifications) was applied uniformly over the feathers of 12 gulls. The marine bunker fuel had a density of 0.991 maximum, a typical viscosity of 400 centiStokes at 50°C, and a maximum sulfur content of 4.5% by weight. The remaining 12 birds served as controls. Control gulls were weighed before each blood sampling; oiled gulls were reweighed when completely dry after the first washing. Blood samples

(0.3 - 0.5 mL) were taken from oiled gulls on Days 2, 3, and 4 or 5 and from control gulls on 3 of the next 9 days. The water efflux of control gulls was calculated by equation #3 of Nagy and Costa (1980). Oiled gulls lost body mass during the study period. After the last blood sample was taken, each gull was injected with 12 uCi ^3H_2O and TBW was redetermined. Their water influx and efflux were calculated by equations #4 and #6 of Nagy and Costa (1980). Body temperature was measured during blood sampling (about 5 minutes) using a probe (Tele-Thermometer, Yellow Springs Instrument Company Inc.) inserted 5-6 cm into the vent. At the end of the water flux study each oiled gull was wiped with cloths moistened with stove oil or diesel fuel (Esso Petroleum Canada) to facilitate the removal of the crude oil and washed with Dawn (Proctor and Gamble, Cincinnati OH) or Joy 2 (Proctor and Gamble, Toronto, Ont), following procedures suggested by Williams (Burridge and Kane 1985). Two days later all gulls received a second washing (Joy 2). They were kept in a warm room (mean temperature 23 oC, RH 43%) between washings and for 7 - 10 days afterwards. The first four days they were force fed 2 - 3 times daily with a slurry of blended catfood, liquid vitamins, raw eggs and sucrose (Burridge and Kane 1985) in which the [Cl] was adjusted to 130 mM. Small pieces of herring and fresh water were available *ad libitum*. On the fourth day, they were given water ([Cl], 117 mM) in which to swim. Most gulls began to eat well voluntarily before the seventh day, at which time they were returned to their outdoor enclosure which had a heat lamp suspended over a bed of wood chips. Because of their weakened condition (they had eaten almost nothing for 5 days), no blood samples were taken from the oiled gulls after they were washed.

Eleven days after the end of the water efflux study the effects of sham oiling were measured in six of the original control gulls. The gulls were weighed, blood samples were taken for determination of residual isotope concentration, 12 uCi $3H_2O$ were injected for TBW determination (see above) and the gulls were held and rubbed to simulate application of oil. Blood samples were taken on days 1, 4, and 5 after sham oiling.

All blood samples were treated in the following manner. Triplicate Strumia microhematocrit tubes were immediately filled with blood and centrifuged simultaneously with the remaining blood for 3 mins at 15,600 g. The plasma was promptly decanted and duplicate aliquants immediately apportioned for the following determinations: 10 - 50 uL into a scintillation vial containing 10 mL Aquasol[2] (New England Nuclear, Lachine, Quebec) for tritium, using a

LKB Wallac 1214 Rackbeta Excel Liquid Scintillation Counter (Turku, Finland); 50 uL into 10 mL 15 mM LiCl for sodium and potassium concentration, using an Instrumentation Laboratory Inc. Model 143 flame photometer; and 10 uL for chloride concentration, using a Buchler digital chloridometer. The remaining plasma was frozen for next day determination of osmotic pressure (OP), using a Wescor Vapour Pressure Model 5500 osmometer. A correction factor of +3.5% (determined by measuring plasma OP immediately after centrifugation and after overnight freezing in 10 samples) was applied to OP values. Data are given as mean ± standard error and analyzed by analysis of variance and Tukey's HSD post-hoc test on pairs of means (Wilkinson 1988). Significance was assumed if $P < 0.05$.

RESULTS

Body Mass.

During the three week acclimation period, the mean body mass of the 24 gulls decreased from 1117 ± 150 g to 938 ± 106 g ($P < 0.001$) and the initial mean body masses of control gulls and gulls that were oiled were the same. The mean body mass of control and sham oiled gulls did not change during the five days of the water efflux study; oiled gulls lost 10% of their body mass (Table 1).

Table 1. Percentage change in body mass and total body water in oiled gulls.

	Body Mass grams	Total Body Water % body mass
CONTROL (n = 12)	+0.1% ±1.4%	
OILED (n = 12)	-10.1%[a,b] ±1.8%	+19.6%
SHAM OILED (n = 6)	+3.7% ±1.1%	

[a] P < 0.001 oiled gulls compared to control gulls

[b] P < 0.05 oiled gulls compared to sham oiled gulls

Food Consumption and Water Usage.

Initial food consumption was the same in control gulls and gulls subequently oiled (Table 2). Routine capture and blood sampling of control and sham oil gulls did not affect food intake, food consumption was markedly reduced by the oil treatment ($P < 0.001$), Mean total water usage was same in all groups (Table 2). The total water intake derived from food (Table 2; as % water efflux) was 70% in sham oiled gulls and 10% in oiled gulls.

Table 2. Mean food consumption and water usage by control and oiled gulls.

	Grams or milliliters, bird· day^{-1}			
	Food	Drinking water	Water Intake (Calc)	Water[a] Efflux
CONTROL				
before expt[b]	94.6 ±6.7	247.1 ±36.5	331.8 ±38.8	
during expt	84.4 ±8.7	276.3 ±32.8	352.0 ±38.1	122.3 ±6.9
OILED				
before expt	105.8 ±13.6	301.2 ±65.4	395.8 ±75.3	
during expt	5.4* ±1.2	318.5 ±42.1	344.8 ±29.21	48.1* ±3.2
SHAM OILED	74.0 ±16.8	388.0 ±46.6	454.2 ±56.8	110.7 ±5.9

*$P < 0.001$ Oiled gulls compared to all other groups.

Total water intake includes free water from drinking and eating and metabolic water derived from the fish.

[a] Water efflux, mL(kg· day)$^{-1}$, measured by disappearance of injected tritiated water from the body.

[b] before expt = daily record for 3 weeks prior to isotope injection.

Body Temperature.

On Day 0 the mean body temperatures (MBT, °C) of control (38.1 ± 0.3) and gulls to be oiled (38.0 ± 0.3) were the same. On Day 2 the MBT of control gulls was unchanged (37.1 ± 0.3, $P < 0.3$); MBT of oiled gulls was significantly decreased (36.2 ± 0.2, $P < 0.001$) and remained lowered on Day 3 (36.4 ± 0.1, $P < 0.01$, $n = 6$) and Day 4 (36.8 ± 0.2, $P < 0.06$, $n = 12$). On Day 5, the MBT of control gulls was unchanged from Day 0 (38.2 ± 0.1, $n = 6$) and higher than MBT of oiled gulls (36.9 ± 0.2, $n = 6$; $P < 0.05$).

Hematocrit (Hct) and Plasma Ionic and Osmotic Concentrations.

The initial Hct, $[Na]_{pl}$, $[Cl]_{pl}$, $[K]_{pl}$ or osmotic concentrations were the same among gulls that served as controls and those that were subsequently oiled (Table 3). Control gulls showed no change in Hct over the five days of the water efflux study; Hct of oiled gulls was significantly reduced by Day 4. The $[Na]_{pl}$, $[Cl]_{pl}$ and plasma OP of control gulls did not change during the water efflux experiment; there was a transient increase ($P < 0.05$) in $[K]_{pl}$ on Day 2. Among oiled gulls $[Na]_{pl}$ and $[Cl]_{pl}$ were significantly ($P < 0.001$) decreased and $[K]_{pl}$ was significantly ($P < 0.01$) increased by Day 2 of the water efflux experiment. By Day 4 plasma OP was significantly ($P < 0.001$) decreased. These decreases persisted through Day 5.

Total body water, water influx and efflux.

The mean initial TBW of control and gulls later oiled was the same. Relative to body mass, TBW increased ($P < 0.001$) during the period when the gulls had oil on their feathers. The water efflux (mean, $mL(kg \cdot day)^{-1}$) of oiled gulls, 48.1 ± 3.3, was significantly ($P < 0.001$) lower than that of control gulls, 122.3 ± 6.9. Water influx, 56.5 ± 5.3, and water efflux were the same in oiled gulls.

DISCUSSION

The gulls had been held in outdoor runs and fed to satiety for several months prior to the experiment. Their body mass was much greater then usual for captive gulls of this species. When caged in groups of six, their body mass decreased 16%, but they were still larger than gulls used in previous studies from this laboratory (Walter and Hughes, 1978; Roberts and Hughes 1984; Goldstein et al. 1986). Food consumption, water usage and body mass were unaffected by experimental handling (Table 1) and further decreases in body mass were insignificant.

Table 3. Hematocrit and plasma concentration of control and oiled gulls during the water efflux study.

Treatment (day)	Hct, %	Plasma Concentration		
		Na, mM	Cl, mM	OP, mOsm·kg^{-1}
CONTROL				
0	47.7 ±1.0	153.5 ±0.8	114.9 ±0.6	309.1 ±1.5
2	44.4 ±0.9	150.4 ±1.2	111.2 ±0.9	314.7 ±1.7
5	43.8 ±0.9	152.2 ±0.4	110.8 ±1.0	310.6 ±1.7
OILED				
0	50.3 ±0.9	155.7 ±1.4	113.4 ±0.8	309.1 ±0.8
2	48.8 ±0.8	146.9* ±1.4	101.5* ±0.8	303.2 ±2.9
4	46.4*[a] ±0.9	141.0[b] ±2.4	97.6[b] ±2.0	295.5*[b] ±7.5

Twelve gulls in each group except Control day 5 (n=6)

*$P < 0.001$, compared to Day 0 oiled gulls

[a] $P < 0.05$; [b] $P < 0.001$, Day 4 oiled gulls compared to Day 5 control gulls.

Fat is hydrophobic. Since body water content is expressed relative to total body mass, lean gulls have proportionately greater TBW than fat birds. The lower initial TBW (52.9% and 50.2% in control and gulls later oiled, respectively, Table 1) compared to TBW previously measured in this species (76.5% (recalculated for protein-free plasma from data of Walter and Hughes, 1978; 66.0% (Hughes *et al*. 1987) is probably due to a greater proportion of fat in the birds we used in this study. The oiled gulls ate very little (Table 2) and lost about 10% of their body mass over the 4 -5 days exposure to oil (Table 1). The decrement in body mass, assumed due to fat utilization, which should account for increase in percentage body water.

Young birds may be more susceptible to the effects of ingested oil than adults. Body mass gain was impaired in nestling gulls given oil (Butler and Lukasiewicz 1979), but adult male Mallard Ducks (*Anas platyrhynchos*) given crude oil (2.5 $mL \cdot kg$ body mass^{-1}) in their food did not decrease either food intake or body mass (Gorsline and Holmes 1982). However, adult Mallard Ducks forced to swim in water contaminated with PBC did increase BMR 10% (Lambert *et al*. 1982), which might be due to an increase in plasma thyroxine concentration induced by oil ingestion (Peakall *et al*. 1981). If oiling did increase BMR of the gulls, the increased metabolism was unable to maintain body temperature (Erasmus *et al*. 1981; present study). Low salt intake (resulting in low $[Na]_{pl}$) has been associated with decreased body temperature in chickens (Arad and Skadhauge 1986). We found that body temperature and $[Na]_{pl}$ fell in parallel in oiled gulls. A relationship between $[Na]_{pl}$ and body temperature is inferred, but not validated, by our data. We did not determine how much crude oil the gulls ingested, but autopsy of a bird that died on Day 5 showed a small amount of oil in the small intestine and none in the hindgut. Our findings do not discriminate between effects of externally applied and ingested oil.

Apparent water intake of control and oiled gulls was the same (Table 2), however, water influx, determined by isotopically labelled water, was only 16% of water usage of oiled gulls, compared to 44% in control gulls. The gulls could only insert their beaks into the water containers, but, if they shook their beaks forcefully through the water, spillage would have occurred. The discrepancy between apparent water usage and actual water influx is likely due to greater spillage of drinking water amongst oiled gulls. Measurement of water usage was an invalid method for determining water influx in these birds. The mean decrease in Hct among oiled gulls was small and its physiological importance is uncertain. It was probably due to blood sampling, since a statistically insignificant decrease in Hct also occurred among control gulls (Table 3). Decreased Hct has, however, been seen after oil exposure in ducks (Hartung and Hunt 1966), Herring Gulls, *Larus argentatus*, and Atlantic Puffins, *Fratercula arctica*, (Leighton *et al*. 1985). Changes in Hct might also be related to changes in erythrocyte enzymatic reactions and membrane permeability noted in Herring Gulls following oil ingestion (Leighton *et al*. 1983; 1985). In control and oiled gulls we observed a transient, but significant increase in $[K]_{pl}$ one or two days after isotope injection, which we can not explain. It may reflect stress imposed by handling the gulls. Among oiled gulls plasma OP decreased less than was expected from the large decreases in $[Na]_{pl}$ and $[Cl]_{pl}$, indicating accumulation of other osmotically active substances in the plasma. The salt glands produce free water by secreting NaCl absorbed from ingested seawater in a smaller volume of water than was absorbed with it (Schmidt - Nielsen *et al*. 1958). Oil components are absorbed and accumulate in tissues (M^{c}Ewan and Whitehead 1980) without significant impairment of extrarenal NaCl excretion (McEwan 1978). In young birds crude oil may suppress the changes in the intestinal mucosa associated with saline acclimation (Crocker *et al*. 1974; Crocker *et al*. 1975), decreasing gut Na^+ (and, therefore water) uptake, resulting in dehydration (Crocker *et al*. (1974). The gut ion transport capacity of accidentally oiled mature seabirds would be completely competent, so that oiling should not produce dehydration. The observations on young birds have led to the use of fresh water and a low salt diet during rehabilitation of oil contaminated marine birds (Burridge and Kane 1985). Our results show freshwater therapy may, in fact, be counterproductive, because oiled gulls were not dehydrated (Table 1). They lost body mass (Table 1) and plasma NaCl (Table 3) and the proportion of the body which was water actually increased during oil exposure. The large decreases in plasma NaCl among oiled gulls indicate ongoing ion losses for which the noneating gulls could not compensate when drinking fresh water. Nestling gulls denied food did not alter $[Na]_{pl}$ (Jeffrey *et al*. 1985) or when given oil (Miller *et al*. 1978; Peakall and Hallett 1980; Peakall *et al*. 1982) increased $[Na]_{pl}$. Cardiovascular function is dependent upon the maintenance of extracellular fluid volume, especially the blood volume, which in turn depends upon maintenance of plasma osmolality. The reduced $[Na]_{pl}$ and $[Cl]_{pl}$ observed in oiled gulls indicate that these gulls might be more vulnerable to cardiovascular failure.

In summary, oiled adult gulls markedly reduced food intake, lost body mass, and decreased water efflux and plasma concentration. The decrease in plasma concentration is likely due to ion losses not balanced with ion intake, although oil contamination may affect the renal and/or extrarenal salt excreting systems, possibly through inappropriate hormonal activity. They also suggest that freshwater rehabilitative therapy (derived largely from studies of domestic ducks and nestling seabirds) may be inappropriate for oiled adult seabirds. Reduced drinking might diminish the rate of elimination of toxic metabolites or oil derivatives. Further investigations of salt and water balance of oiled gulls (or other more marine species) are required to verify the effect of oil contamination on body fluid content and concentration in order to develop better osmotic regimes for rehabilitating oil contaminated seabirds.

Acknowledgements Grants from the Imperial Oil Company, Ltd and the Natural Sciences and Engineering Council of Canada Grant (A- 3442, MRH) supported this work. We thank Gail Kermode for technical assistance; Arthur VanDerHorst for excellent animal care; Dr. Peter Hochachka for use of the scintillation counter and Chris Moyes for help in its use; Esso Petroleum Canada for petroleum products; Esso Sr. Technical Specialist L. J. Hart for advice; Liz Thunstrom and Susan Dougans of the Wildlife Rescue Association for their practical advice on cleaning birds and gift of Dawn detergent; and Dorothy Hill, Lorne Gould, Joel Hughes, Michael Tiu, and Mike Hedrick for help with the birds.

REFERENCES

Arad, Z. and Skadhauge, E., Body temperature and plasmaarginine vasotocin in fowls adapted to high- and low-NaCl diets. Br. Poult. Sci. 27:115-121, 1986.

Burridge, J. and Kane, M., Rehabilitating Oiled Birds: A field manual. American Petroleum Institute Publication no. 4407. American Petroleum Institute, Washington, D. C., 1985.

Butler, R. G. and P. Lukasiewicz., A field study of the effect of crude oil on Herring Gull (Larus argentatus) chick growth. Auk. 96:809-812, 1979.

Crocker, A. D., Cronshaw, J., and Holmes, W. N., The effect of a crude oil on intestinal absorption in ducklings (Anas platyrhynchos). Environ. Pollut. 7:165-177, 1974.

Crocker, A. D., Cronshaw, J., and Holmes, W. N., The effect of several crude oils and some petroleum distillation fractions on intestinal absorption in ducklings (Anas platyrhynchos). Environ. Physiol. Biochem. 5:92-106, 1975.

Erasmus, T., Randall, R. M., and Randall, B. R., Oil pollution, insulation and body temperatures in the Jackass Penguin, Spheniscus demersus. Comp. Biochem. Physiol. 69A:169-171, 1981.

Goldstein, D. L., Hughes, M. R., and Braun, E. J., Role of the lower intestine in the adaptation of gulls (Larus glaucescens) to sea water. J. Exp. Biol. 123:345-357, 1986.

Gorsline, J. and Holmes, W. N., Suppression of adrenalcortical activity in mallard ducks exposed to petroleum-contaminated food. Arch. Environ. Contam. Toxicol. 11:497-502, 1982.

Hartung, R., and Hunt, G. S., Toxicity of some oils to waterfowl. J. Wildlife Manag. 30:564-570, 1966.

Holmes, W. N., Gorsline, J., and Cronshaw, J., Effects of mild cold stress on the survival of seawater-adapted mallard ducks (Anas platyrhynchos) maintained on food contaminated with petroleum. Environ. Res. 20:425-444, 1979.

Hughes, M. R., Roberts, J. R., and Thomas, B. R., Total body water and its turnover in free-living nestling Glaucous-winged Gulls with a comparison of body water and water flux in avian species with and without salt glands. Physiol. Zool. 60:481-491, 1987.

Jeffrey, D. A., Peakall, D. B., Miller, D. S., and Herzberg, G. R., Blood chemistry changes in food-deprived Herring Gulls. Comp. Biochem. Physiol. 81A:911-913, 1985.

Lambert, G., Peakall, D. B., Philogene, B. J. R., and Engelhart, F. R., Effect of oil and oil dispersant mixtures on the basal metabolic rate of ducks. Bull. Environ. Contam. Toxicol. 29:520-524, 1982.

Leighton, F. A., Lee, Y. Z., Rahimtula, A. D., O'Brien, P.J., and Peakall, D. B., Biochemical and functional disturbances in red blood cells of herring Gulls (Larus argentatus) ingesting Prudhoe Bay [Alaska, USA] crude oil. Toxicol. Appl. Pharmacol. 81:25-31, 1985.

Leighton, F. A., Peakall, D. B., and Butler, R. G., Heinz-Body hemolytic anemia from ingestion of crude oil: A primary toxic effect in marine birds. Science. 220:871-873, 1983.

McEwan, E. H., The effect of crude oils on salt gland sodium secretion of orally imposed salt loads in glaucous-winged gulls, Larus glaucescens. Can. J. Zool. 56:1212-1213, 1978.

McEwan, E. H. and Koelink, A. F. C., The heat production of oiled mallards and scaup. Can. J. Zool. 51:27-31, 1973.

McEwan, E. H. and Whitehead, P. M., Uptake and clearance of petroleum hydrocarbons by the glaucous-winged gull (Larus glaucescens) and the mallard duck (Anas platyrhynchos). Can. J. Zool. 58:723-726, 1980.

Miller, D. S., Peakall, D. B., and Kinter, W. B., Ingestion of crude oil: Sublethal effects in herring gull chicks. Science. 199:325-317, 1978.

Nagy, K. A. and Costa, D. P., Water flux in animals: analysis of potential errors in the tritiated water method. Am. J. Physiol. 238:R454-R465, 1980.

Peakall, D. B. and Hallett, D., Effects of ingested crude oil on Black Guillemots: a combined field and laboratory study. Ambio. 9:28-30, 1980.

Peakall, D. B., Hallett, D. J., Bend, J. R., Foureman, G. L. and Miller, D. S., Toxicity of Prudhoe Bay crude Oil and its aromatic fractions to nestling Herring Gulls. Environ. Res. 27:206-215, 1982.

Peakall, D. B., Tremblay, J., Kinter, W. B., and Miller, D. S., Endocrine dysfunction in seabirds caused by ingested oil. Environ. Res. 24:6-14, 1981.

Roberts, J. R. and Hughes, M. R., Exchangeable sodium pool size and sodium turnover in freshwater- and saltwater-acclimated ducks and gulls. Can. J. Zool. 62:2142-2145, 1984.

Schmidt-Nielsen, K., Animal Physiology, Adaptation and Environment. Cambridge University Press, New York., p. 418., 1975.

Schmidt-Nielsen, K., Jorgensen, C. B., and Osaki, H., Extrarenal salt excretion in birds. Am. J. Physiol. 193:101-107, 1958.

Walter, A. and Hughes, M. R., Total body water volume and turnover rate in fresh water and sea water adapted Glaucous-winged Gulls, Larus glaucescens, 1978.

Wilkinson, L., SYSTAT: The system for statistics. Evanston, IL: SYSTAT, Inc., 1988.

Data presented were abstracted from a paper by these authors to appear in the Canadian Journal of Zoology in early 1990.

RISK ASSESSMENT OF OFFSHORE OIL SPILLS

by

Robert P. LaBelle
U.S. Department of the Interior
Minerals Management Service
381 Elden Street
Herndon, Virginia 22070

ABSTRACT

Assessing the risk from potential oil spills offshore Alaska is a controversial and complex task. A major benefit of a formal approach to risk assessment is its objectivity, since the way in which risks are perceived is strongly correlated with the way in which they are calculated. The goal of formal risk assessment is to enlighten decisions, rather than to create the perfect model of a system. Calculations, including uncertainty, must be open to public scrutiny, thus allowing the basis of the analysis to be evaluated. In addition, the process of conducting and defending risk analysis methods highlights the uncertainties of risk estimates, which in turn leads to direction for research to improve the assessment method.

A formal approach is outlined to assessing risks of potential oil spills from oil development and transportation offshore Alaska. Risk estimates discussed include those related to oil-spill occurrence and contact. The assessment method assumes that the risk of spill occurrence is related to the amount of oil produced and transported, as well as to previous spill history. Current information is updated on rates of spill occurrence for activities such as production on platforms and transport of oil via pipeline and tankers. Both numbers and sizes of past major spill events are compared.

Also addressed are current efforts to upgrade oil-spill trajectory analysis to better estimate the chance of spill contact, given occurrence. These efforts include techniques to incorporate field observations in models and to improve model verification and error estimates. The assessment method described is currently used by the U.S. Department of the Interior to support its analysis of environmental impacts associated with oil production scenarios on the Outer Continental Shelf (OCS).

INTRODUCTION

The Oil Spill Risk Analysis (OSRA) model was developed in 1975 by the U.S. Department of the Interior as a tool to assist in evaluating oil-spill risks to the environment from offshore oil and gas lease sales and related activities. The model is used primarily to provide environmental impact analysts with probabilistic estimates of oil-spill occurrence and contact with biologic and economic resources located on the OCS and the adjoining coasts.

As shown in Figure 1, model results are also used by other agencies as part of their evaluation of risk to endangered species. In addition, the OSRA has been used by joint State/Federal task forces concerned with oil-spill issues and in State and public review of Federal decision documents. Model results may influence decisions on the location and timing of lease offerings; potential mitigating measures, such as placement of cleanup equipment on shore; or potential stipulations, such as a seasonal restriction on drilling activity due to risk of oil-spill contact to migratory species or hazardous ice conditions.

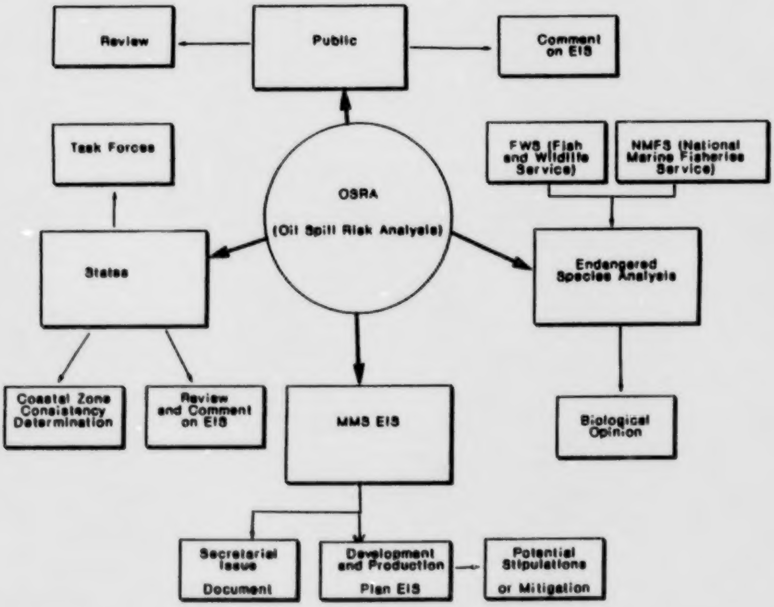

Figure 1.
Users of Oil Spill Risk Analysis (OSRA) results.

Review
Public
Comment on EIS
Task Forces
FWS (Fish and Wildlife Service)
NMFS (National Marine Fisheries Service)
OSRA
(Oil Spill Risk Analysis)
States
Endangered Species Analysis
Coastal Zone Consistency Determination
Review and Comment on EIS
MMS EIS
Biological Opinion
Secretarial Issue Document
Development and Production Plan EIS
Potential Stipulations or Mitigation

Oil-spill occurrence rates have been calculated based on historic production, transportation, and accident experiences. Separate rates, expressed in terms of the estimated mean number of oil spills per billion barrels of oil handled, have been calculated for U.S. OCS platform spills, U.S. OCS pipeline spills, and worldwide tanker spills.

The OSRA process combines the risk of spill occurrence with the chance of spill contact to sensitive resources, for an overall estimate of potential risk. The spill contact estimate is derived from trajectory simulation and analysis which incorporate the best information available on ocean and wind physics from field sampling and circulation models.

Only oil spills greater than or equal to 1,000 barrels in size are considered in the model. The model was designed to address spills large enough to persist over several days, lending themselves to accurate reporting and trajectory analysis. These large spills represent less than 1 percent of all spill events on the OCS. Potential impacts from smaller spills must be addressed separately.

FORMAL RISK ASSESSMENT

The OSRA follows an objective, quantitative approach to oil-spill risk assessment, the elements of which are charted in Figure 2. Much detailed work, supported by a high level of funding for research, goes into making and using these assessments. A formal approach entails an objective methodology that generates reproducible results through accepted scientific principles. A major benefit of a formal approach to risk assessment is its objectivity. Calculations, including uncertainty, are open to public scrutiny, and the basis of the analysis or decision can therefore be evaluated.

The process of conducting and defending the method of risk analysis highlights the uncertainties of risk estimates. This has led to a beneficial direction for future research to improve the assessment method. It should be noted that uncertainty does not imply lack of knowledge, per se. The overall goal is not certainty, but to improve information available to decisionmakers (Hance et al., 1988).

It is well known that the way in which risks are perceived is strongly correlated with the way in which they are calculated. The use of historical observations to assess future risks is the well-accepted approach OSRA employs to estimate the chance of future oil spills.

Figure 2.
Flowchart of major elements in the
Oil Spill Risk Analysis (OSRA) process.

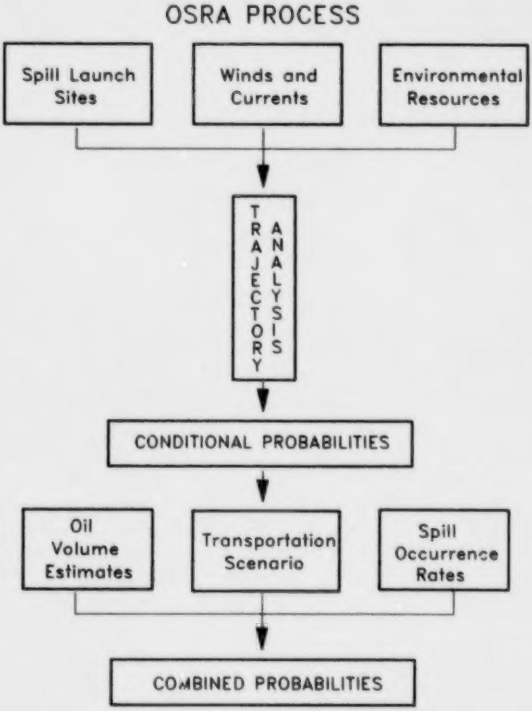

ESTIMATING SPILL OCCURRENCE

As described in Anderson and LaBelle (1990), the OSRA model estimates the chance of spills occurring during the production and transportation of a specific volume of oil over the lifetime of the scenario being analyzed. Spill occurrence has been shown to conform to a Poisson process (Smith et al., 1982), with volume of oil handled as the exposure variable.

Each spill event record was examined, verified if possible, and classified based on its size, product spilled and source. Platform and pipeline spill analyses are limited to U.S. Outer Continental Shelf events so that the calculated spill rates best reflect the magnitude of spill occurrence under U.S. regulation and operational controls. The updated record shows 11 platform spills and 9 pipeline spills over the period 1964-1989. The tanker spill record is based on worldwide data for crude oil carriers from 1974-1989. Prior to 1974, international spill occurrences were recorded on an irregular basis. Inland spills and spills from barges are excluded from the calculations.

With the exception of tanker spills, the limited number of observations precludes cross-sectional analysis of possible spill rate variations that may exist between Alaskan waters vs. the Gulf of Mexico (where the vast majority of oil production and oil spills have occurred). The rates, therefore, are based on U.S. OCS-wide information and should not be adjusted based on the intuition that more hostile environments are riskier. The more hostile environments, such as Alaska, have more stringent engineering and procedural regulations, which may offset or even reduce the risk of a spill occurring relative to historic OCS experience.

The estimation process uses a spill rate constant, expressed as a mean number of spills per billion barrels of produced or transported oil, based on historic accidental spills greater than or equal to 1,000 barrels. The mean spill occurrence estimate is obtained by multiplying the rate constant by the volume of oil projected to be handled. This results in the "mean number of spills estimated to occur" due to a hypothetical volume of oil being handled. The mean number of spills may also be expressed, through the Poisson distribution, as the "probability of one or more spills occurring."

Oil-spill occurrence rate constants for U.S. platforms and pipelines and worldwide tankers have been calculated (Anderson and LaBelle, 1990) on data available through 1987 (1985 for tankers). Using spill and production data now available through 1989, these rate constants have been revised as shown in Table 1. While platform rates have declined somewhat, both pipeline and tanker spill rates appear to have increased.

While the above deals with spill occurrences as integer events, it is equally important to consider spill size or volume. Using the newly available data through 1989, Table 2 lists the relative average and median spill sizes for each spill source. Medians are shown since one or two enormous spills can easily influence the "average" spill size.

Table 1
OSRA Model Oil Spill Occurrence Rates*
Current Rates and Preliminary Revisions
Spills of 1,000 Barrels and Greater

Spill Source	Current Spill Rates Thru 1987	Preliminary Revisions Thru 1989
OCS Platforms	0.60	0.53
OCS Pipelines	0.67	0.78
Worldwide Tankers	1.30 (thru 1985)	1.39

* Expressed as spills per billion barrels of oil handled.

Table 2
Comparison of Spill Size by Source
Spills of 1,000 Barrels or Greater
Thru 1989

Spill Source	Number of Spills Observed	Average Spill Size	Median Spill Size
OCS Platforms	11	18,000	7,000
OCS Pipelines	9	25,000	6,000
Tankers--Worldwide	190	97,500	17,000
Tankers--U.S. Waters	35	27,000	9,000
Tankers--Alaskan Waters	6	47,500	11,500

OCS platform and pipeline data, 1964–1989; worldwide tanker data, 1974–1989.

SPILLS IN ALASKAN WATERS

For visual comparison, the spill size information from Table 2 is graphed in Figure 3. It is obvious that worldwide tanker spills show the largest spill volumes of all the sources. A subset of this data set is tanker spills in U.S. waters, which show roughly half the median spill size of worldwide tankers. A further subset of the U.S. data, tanker spills in Alaskan waters, represents 17% of the U.S. tanker spills and has a substantially higher median spill size. It is not clear from the available data whether this is due to chance, environmental conditions, or cargo capacity differences of tankers in Alaskan waters. The average tanker spill volume in Alaskan waters is of course heavily influenced by the 250,000 barrel Exxon Valdez spill in 1989.

Figure 3.

Comparison of Spill Size by Source

Spills of 1,000 Barrels or Greater

Thru 1989

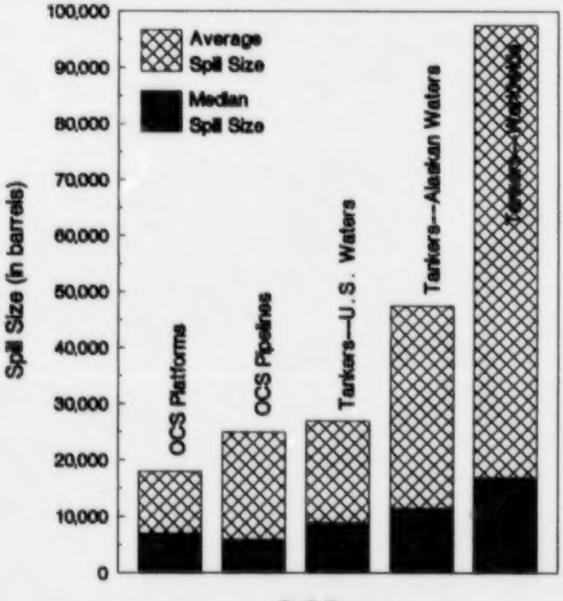

(OCS platform and pipeline data, 1984–1989; worldwide tanker data, 1974–1989.)

Using the OSRA method, it is possible to calculate a spill occurrence rate constant based on the record of oil transported through the Trans-Alaska Pipeline System (TAPS). From 1977 through the present, more than 7.35 billion barrels of crude oil from TAPS have been handled at the port of Valdez. As shown in Figure 4, at least 8 tanker spills of 1,000 barrels or more have occurred as a result of this activity. The "TAPS spill rate constant" would thus be calculated as 8/7.35, or 1.09 spills per billion barrels handled. This compares somewhat closely to the OSRA worldwide tanker spill rate constant of 1.39 spills per billion barrels handled.

OIL SPILL TRAJECTORY ANALYSIS

Through simulation modeling, the OSRA process attempts to define the likely pathways of oil spilled on the sea surface. Spill movement is modeled in Monte Carlo fashion with a sample of 500 spills per season, each transported by surface current and wind vectors. The locations and monthly vulnerabilities of specific environmental resources are digitized and represented within the study area. Model output is presented in tables of conditional contact probabilities (i.e., the probability of contacting an environmental resource, given that a spill has occurred), as well as probability distributions for oil spills both occurring and contacting resources over specific seasons and times. The latter are referred to as "combined probabilities," as shown in Figure 2.

The trajectory component of the model accesses appropriate data bases to simulate oil-spill trajectories. This involves using data which are essentially Eulerian, such as surface current fields provided by general circulation models (GCM's). In theory, it is possible to simulate the tidal, tidal residual, wind-induced, density-induced, barotropic, and nonlinear interactions of the fields of motion using this type of model. In reality, the limitations of modeling large coastal regions require simplifications. There are constraints imposed by the need to specify large open-boundary conditions and initial conditions, and to include sufficient resolution to simulate the first-order features of the circulation. A more difficult problem is to provide adequate temporal resolution in the simulation when the data to specify the boundary conditions are available on a seasonal basis.

The Minerals Management Service is presently funding modeling projects where the objective is to run the GCM in a prognostic mode to produce dynamically consistent

Figure 4.
Spills of 1,000 barrels (BBL) and greater of Trans-Alaska Pipeline System (TAPS) crude oil transported from Valdez.

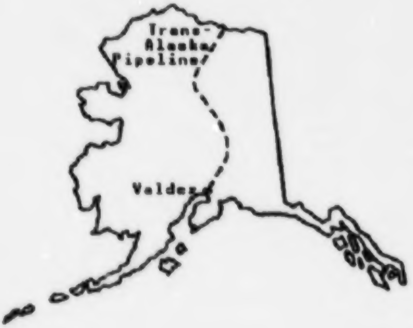

The transportation of oil through the TAPS began in 1977. To date, more than 7.35 billion barrels of oil have been handled at Valdez.

SPILLS OF 1,000 BARRELS (BBL) AND GREATER OF TAPS CRUDE OIL TRANSPORTED FROM VALDEZ

VESSEL NAME	DATE	VOLUME SPILLED	SPILL LOCATION	DESTINATION
TEXACO CONNECTICUT	06/07/80	4,047 BBL	PANAMA CANAL	PORT NECHES, TX
ARCO ANCHORAGE	12/21/85	5,690 BBL	PUGET SOUND	CHERRY POINT, WA
STUYVESANT	01/06/87	15,000 BBL	GULF OF ALASKA	PUERTO ARMUELLES PANAMA
GLACIER BAY	07/02/87	3,096 BBL	COOK INLET, AK	NIKISKI, AK
STUYVESANT	10/04/87	14,286 BBL	OFF BRITISH COLUMBIA	PUERTO ARMUELLES PANAMA
THOMPSON PASS	01/03/89	1,700 BBL	PORT VALDEZ, AK	PANAMA
EXXON VALDEZ	03/24/89	261,905 BBL	PRINCE WILLIAM SOUND	LONG BEACH, CA
AMERICAN TRADER	02/07/90	7,000 BBL	HUNTINGTON BEACH, CA	LONG BEACH, CA

Sources: MMS Arctic Summary Report, 1983; MMS Alaska Summary/Index, 1987; Washington Post, 3/25/89, 3/29/89; Oil Spill Intelligence Report, 3/20/89; Los Angeles Times, 3/[illegible]/90; MMS Branch of Environmental Modeling Worldwide Tanker Spill Database representations of the currents, including the wind-driven currents, on short time scales. The goal is to run such models for sufficiently long time periods to create trajectories to satisfy the need for a statistical (probabilistic) analysis.

MODELING OFF ALASKA

The present study effort by Greenhorne & O'Mara, Inc., has the goal of developing a high-resolution model system capable of calculating large- and small-scale atmospheric flows, oceanic circulation patterns in both deep and shallow waters, ice motion and ice coverage, and oil-spill trajectories reflecting the presence of sea ice. Potential products include accurate surface motion fields through numerical simulation of representative years, which capture a significant portion of the atmospheric and oceanic variability.

The status of major accomplishments to date for this study effort are as follows:

* Development and validation of a regional mesoscale wind model which accounts for topographic and land- and sea-breeze effects, covering an area extending from the Gulf of Alaska to the Beaufort Sea.

* An interannual (1981-1983) study of the ice drift and ice compactness for the Bering and Beaufort Seas, using a dynamic-thermodynamic ice model.

* An investigation of the tidal regime in the Gulf of Alaska, Bering Sea, and Beaufort Sea, using a primitive equation 3-D model.

* Initial study of wind-driven and density-driven currents in the Bering Sea, using a primitive equation 3-D ocean model.

* Development of a comprehensive data base containing Alaska OCS atmospheric and oceanographic data to be used as forcing fields for the models, as well as for validation purposes.

Over the next year, it is anticipated that the study will result in the completion and validation of a fully coupled ice-ocean model with variable grid resolution; the generation of 3 years of sea-surface winds using the mesoscale wind model; and 3 years of surface motion fields using the coupled ice-ocean model. Efforts are ongoing to assess model skill and sensitivity. Intermediate products are checked for skill using field data, and statistical analyses are employed to select modeled years and to use the output correctly to assure statistical representation.

OSRA MODEL VERIFICATION

Before the outputs of the OSRA model are used by environmental impact analysts, the results go through quality control and verification tests. The attempt to verify that thousands of trajectories simulated over wide ranges of environmental conditions are reasonable is a challenging task. Similar to weather forecasting, the task is to simulate events that are stochastic in nature. A formal error analysis (i.e., one in which the expression of error in the end result is a function of the error in the input quantities) is seldom possible with model systems such as these. In oil-spill modeling, the error of the input quantities (the circulation model output, wind-field data, etc.) may not be known or calculable.

It is difficult to attach a "standard error," in the statistical sense, to the results of a model run when the output takes the form of a probability distribution. However, methods do exist to assess the reliability of the model results. These include: assessing individual model components to ensure that they are performing correctly; investigating the sensitivity of model results to particular assumptions; and comparing model results with appropriate actual observations. These steps are taken in review of the OSRA process.

Currently under development is a system of storing, comparing, and using field observations with model products. Graphics workstations will make it possible to scan results of GCM runs for consistency and "reasonable" behavior. Future study is needed to investigate observational data assimilation into models as part of the overall strategy to improving oil-spill trajectory analysis.

REFERENCES

Anderson, C.M. and LaBelle, R.P., "Estimated Occurrence Rates for Analysis of Accidental Oil Spills on the U.S. Outer Continental Shelf", Oil & Chemical Pollution, Vol. 6, pp. 21-35, 1990.

Hance, B.J., Chess, C., and Sandman, P.M., Improving Dialogue with Communities: A Risk Communication Manual for Government, Environmental Communication Research Program, Rutgers University, 83 pp., 1988.

Petak, W.J. and Atkisson, A.A., Natural Hazard Risk Assessment and Public Policy, Springer-Verlag, New York, 467 pp., 1982.

Smith, R.A., Slack, J.R., Wyant, T. and Lanfear, K.J. The Oil Spill Risk Analysis Model of the U.S. Geological Survey, USGS Professional Paper 1227, USGS, Reston, VA., USA, 1982.

STATISTICAL EXPERIMENTAL DESIGN IN THE OPTIMIZATION OF DISPERSANT'S PERFORMANCE

Per Johan Brandvik
and
Per S. Daling

Continental Shelf and Petroleum Technology Research Institute (IKU)
SINTEF-Group
N-7034 Trondheim, Norway

ABSTRACT

The variation in performance of commercial dispersants is large. Furthermore, the performance of a specific dispersant can also show a large variation among different crudes and petroleum products. When a decision has been made to use dispersants in a given oil spill situation, it is crucial to select a dispersant that is formulated to give high effectiveness for the actual oil type.

To enhance the optimization of the dispersant and to reduce the number of experiments needed for development of new products, statistical experimental design has been used together with multivariate analysis. This combined technique has proved to be very powerful in the optimization of dispersants. The optimized formulation has been effectively worked out for different surfactant combinations tested on a wide range of oil qualities. As a result, IKU has developed a new dispersant that is specially formulated for high effectiveness on weathered North Sea crudes.

The optimization technique used is presented here together with the measured performance of the new dispersant on both fresh and weathered evaporated (or "topped"), photo-oxidized and w/o-emulsified crudes and petroleum products. The effectiveness of the new dispersant is also compared to commercial products.

INTRODUCTION; MAPPING THE EFFECTIVENESS OF DISPERSANTS

Dispersants consist of different surface active components (surfactants) dissolved in a solvent or a blend of solvents. These surfactants are the active components which reduce the interfacial tension between water and oil. Due to the complex synergistic effects between the surfactants, the optimization of dispersants is complicated.

The dispersant optimization work presented here has been one activity in a four year project called "Application of Dispersants on Weathered Oils" (DIWO) undertaken at IKU, SINTEF-Group and funded by Fina Exploration Norway.

In this study the dispersants blended and tested have consisted of three different surfactants. The relative composition of the three surfactants in the dispersants can be visualized in a triangle-shaped plot. Each position inside this triangle corresponds to a mixture of the three surfactants x_1, x_2 and x_3. For example, a position in the middle of the triangle corresponds to a dispersant consisting of equal amounts of the three surfactants. Since the effectiveness of a dispersant is dependent on the types of surfactants used and their relative concentrations, the effectiveness can be plotted as contours in the previously mentioned triangle-plot. An example of such a contour plot is given in figure 1.

When a contour plot like the one in figure 1 is established, it makes the optimization of the dispersant easier, because the surfactant composition which gives the highest effectiveness can be read

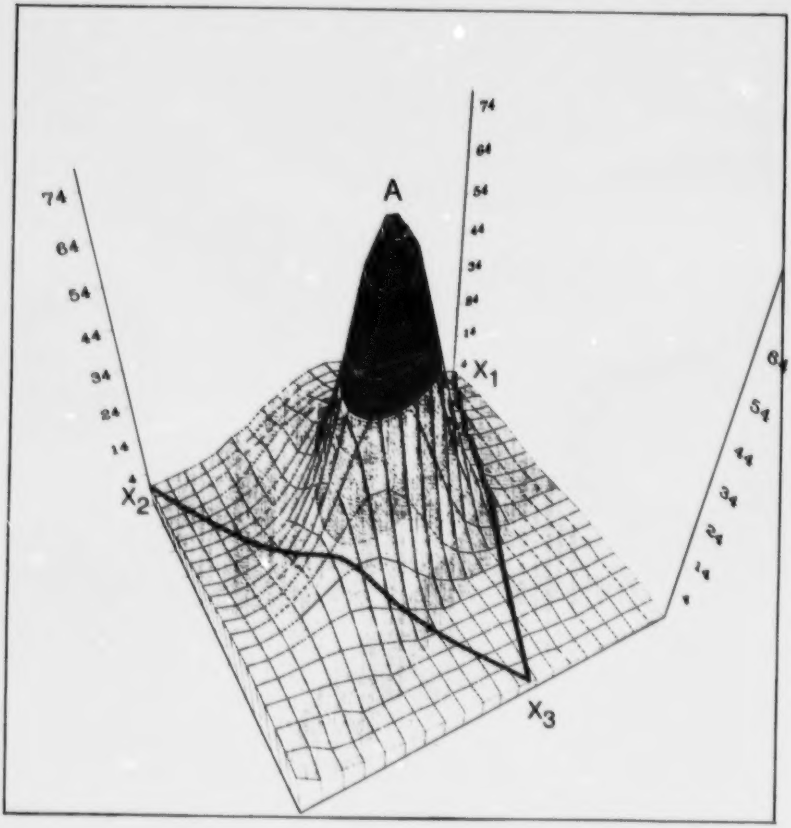

Figure 1: Three-dimensional contour plot showing the effectiveness of the different mixtures of the surfactants x_1, x_2 and x_3. The height of the response surface over the triangle in the figure illustrates the effectiveness, while the positions in the triangle gives the relative composition of the surfactants. The highest point in the response surface represents the optimum composition (point A).

directly from the figure (point A). The way in which these contour plots are obtained with as little laboratory experimentation as possible is explained in the next two sections.

EXPERIMENTAL DESIGN

The basic problem when optimizing a chemical product is to decide which constituents (eg. surfactants in a dispersant) to change and to determine the intervals and resolution for this variation. When this problem has been solved, another problem arises; finding the pattern of the experimental points that will best reveal the aspects of interest. The aim is to discover the optimum composition and to understand the interaction of the constituents on the quality-describing variable (eg. the dispersant effectiveness) by using as few experiments (as low cost) as possible.

The classical approach is to vary the content of only one constituent at a time, in order to keep track of which variable causes the changes in the response. The disadvantages with this classical one-variable-at-a-time strategy are several and important and are described in the literature (Box et al., 1978). Today, other experimental designs are available. The main advantage with these new experimental designs is that the interaction effect (synergistic or antagonistic) among the constituents can also be calculated, with relatively few experiments.

In mixture experiments, the constituents are ingredients of a mixture, and their levels are not independent. For example, a dispersant that consists of a mixture of surfactants dissolved in a solvent, the total amount of surfactants and solvent has to add up to 1.0 (or 100%). If the amount of one surfactant is changed, then the relative ratio of all surfactants is changed. When mixture design is used to optimize dispersant formulation, the measured response (effectiveness) is assumed to depend only on the relative proportions of the components in the dispersant. The mixture design used in this work is called a simplex-centroid design (Khuri and Cornell, 1987) and is shown in figure 2. The ten experiments can be used to build a model which describes the influence of the relative proportions of the three surfactants on the amount of oil dispersed by the dispersant. The ten experiments limit the complexity of the estimated model, so that only 10 parameters or coefficients for the model equation describing the dispersability of the oil can be estimated (see next section).

The design in figure 2 is constructed so that a minimum of 10 percent of all three surfactants is present in all mixtures. This was done because all three surfactants were expected to be important for the dispersion process. Dispersants consisting of only one or two surfactants (located along the outer side of the triangle in figure 2) were expected to show a very low effectiveness. For further reading about experimental design with mixtures, the following literature are recommended: Khuri and Cornel, 1987 and Deming and Morgan, 1987.

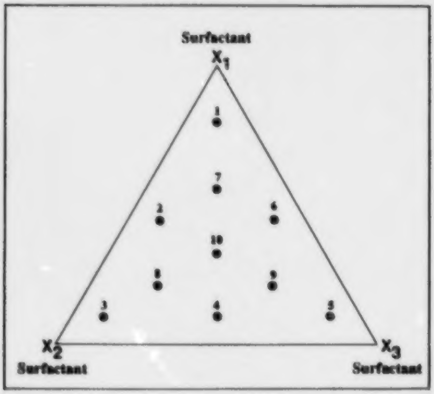

Figure 2: Statistical experimental design for optimization of mixtures with three constituents (simplex-centroid design).

RESPONSE SURFACE METHODS

If we limit this brief introduction to response surfaces to experimental data from mixture designs, we have three original variables, the contents of the three surfactants x_1, x_2 and x_3. The mixture design gives effectiveness measurements from each of the 10 experimental points in the triangle plot (figure 2). This data set and response surface techniques were used to estimate the distribution of dispersant effectiveness as a function of composition. This estimated distribution is also called a response surface and can be illustrated as a surface in the previous mentioned triangle plot. A region with high dispersability, will be represented by a surface far above the "floor" of the triangle, while a region with low dispersability will be located near the "floor" of the triangle. In this way the response surface will have "hills" and "valleys" which describe the changes in the dispersant effectiveness as a function of surfactant composition (see figure 1).

The response function

How do we calculate this response surface from the measured data? If the response surface is dependent on the surfactant composition, then there should exist a function of x_1, x_2 and x_3, that expresses the response surface:

$$y = f(\beta_0, x_1, x_2, x_3) \qquad \text{Equation 1.}$$

This function is called the true response function and is assumed to be a continuous function of x_1, x_2, and x_3. β_0 is a vector of constants. By using response surface techniques we try to approximate a response function based on the experimental data to this unknown true function (Martens and Næs, 1989). To estimate this approximate function multiple linear regression was used with first order terms (eg. x_1), interaction terms (eg. $x_1 \cdot x_2$) and second order terms (eg. x_1^2) (Massart et al., 1988; Mardia et al., 1982; Montgomery, 1984).

EXPERIMENTAL CONDITIONS

Effectiveness testing

The effectiveness of the dispersants were tested in the laboratory with the Labofina/Warren-spring laboratory test (WSL), The Makcay-Nadeau-Steelman (MNS) test and the IFP-dilution test (IFP). Further details concerning the test methods are presented elsewhere in this proceedings by Daling et al., 1990.

The IFP test was used for all the optimization experiments and all three test methods were used for verification testing of the final optimized dispersant. The main test conditions used in these IFP-measurements were:

Dispersant/oil ratio:	1:25
Temperature:	13°C
Sea water salinity:	3.3%

Malvern droplet size analyzer

In addition to measuring the mass-balance (percent of oil dispersed) the droplet size of the dispersed oil-in-water emulsion was also measured. The Malvern droplet size analyzer is described by Daling et al., 1990.

RESULTS AND DISCUSSIONS

In this optimization work several types of surfactant combinations were tested. These included surfactants with rather large structural differences and surfactants with only smaller HLB modifications. The oils used were different North Sea crudes (eg. Statfjord, Gullfaks and Oseberg) together with a medium bunker fuel (IF-30). The oils had previously been artificially weathered to different degrees. This involved both photo-oxidation, topping and w/o-emulsion formation (Daling et al., 1990).

Optimized dispersant for waterfree oils

For each of the surfactant combinations we wanted to optimize, the experimental design shown in figure 2 where used. After the ten experiments in the design were performed, these data points were used to estimate a response surface by multivariate analysis. Two examples of these response surfaces are shown as ordinary two-dimensional contour maps in figures 3 a-b. The identities of the surfactants are not revealed due to ongoing patent registration.

Figure 3 a-b shows the estimated response surface for IF-30 bunker fuel (150°C+) with two different surfactant combinations. Both figures show the power of this technique in exploring the effectiveness of a dispersant as a function of surfactant composition. The most effective surfactant combination can be estimated from the response surface (the highest point). The estimated optimum compositions were verified by experiments to be true optimum.

Only when the estimated response surfaces showed a sufficient fit to the experimental data, the response surfaces were used for chemical interpretation of the surfactant composition's influence on the effectiveness. The degree of fit of the estimated response surface to the experimental data was measured with an ordinary Fisher test (Box et al., 1978). The fit was sufficient for most of the surfactant combinations tested.

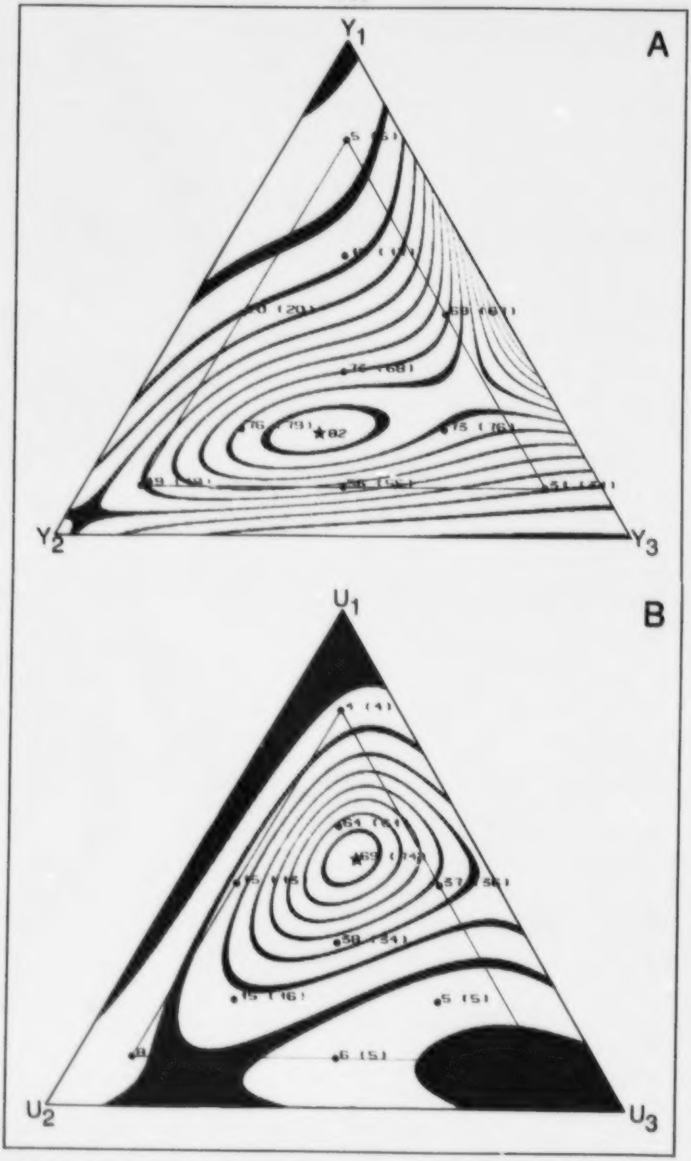

Figure 3 a-b: Response surfaces (distribution of dispersant effectiveness) for IF-30 bunker fuel (150°C+) with two different surfactant combinations. The estimated optimum points are marked (*) and the measured effectiveness are noted. For each experimental point both the measured and estimated effectiveness are given, estimates are in brackets.

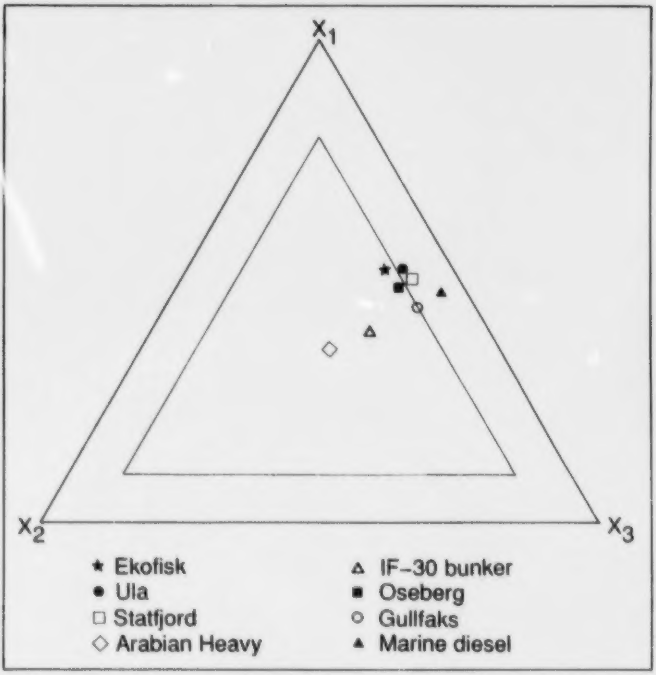

Figure 4: Estimated optimum surfactant compositions for one combination of surfactants tested on eight different oil types (250°C+, photo-oxidated oils).

Figure 4 Shows the estimated optimum points for a specific surfactant combination tested on a wide range of oil types. The optimal dispersant formulation depends strongly on the physico-chemical composition of the oils. The optimum points for the North Sea crudes are in the same area however, which made it possible to end up with one compromise formulation for the North Sea crudes.

Optimized dispersant for w/o-emulsions

Similar optimization experiments as described in the previous section were also done with w/o-emulsions. The w/o-emulsions were mixed with a specified water-to-oil ratio for 24 hours (Daling et al., 1990). In order to compare the optimized surfactant composition for a waterfree oil and the corresponding w/o-emulsion, similar optimization experiments were done. Figure 5 a-b shows that the optimum composition for both a waterfree oil (Statfjord 150°C+) and a corresponding w/o-emulsion (50% water) are quite similar. This implies that a dispersant which is optimized for a waterfree oil seems also to be optimal for the corresponding w/o-emulsion.

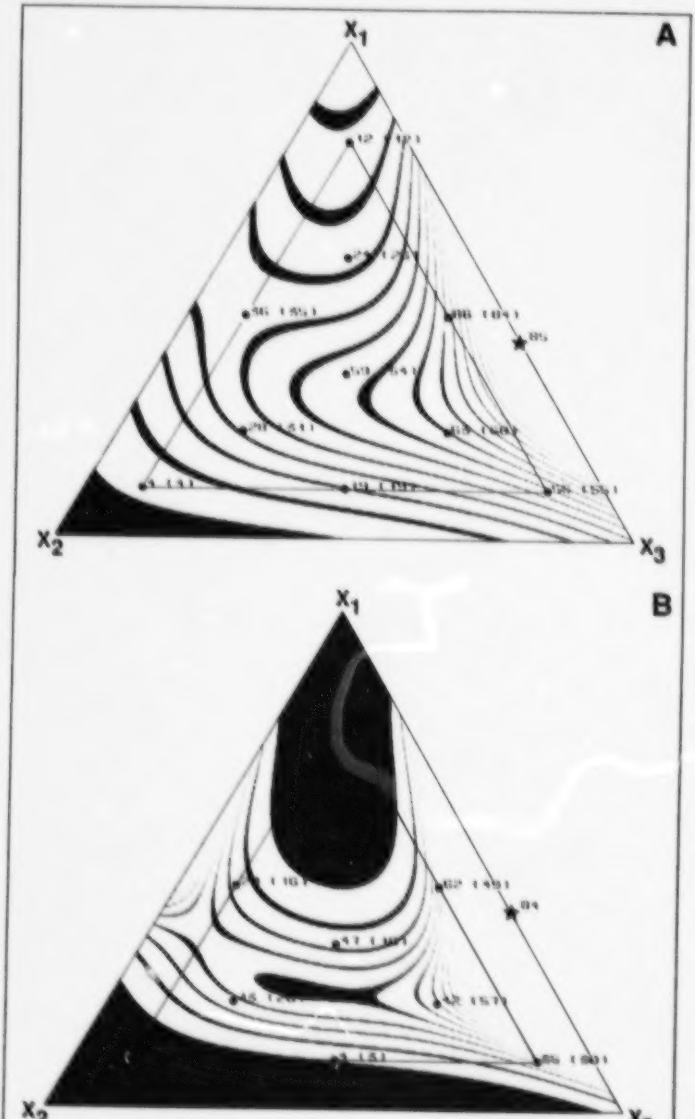

Figure 5 a-b: Comparison of the response surfaces with the same surfactant combinations for both waterfree oil and w/o-emulsion. The waterfree oil is a Statfjord 150°C+ (A) and the w/o-emulsion from the same oil contains 50% water (B).

Final effectiveness testing

The final optimized product called IKU-9 was formulated for high performance on a broad selection of weathered North Sea crudes. Other criteria taken into account were low toxicity and low viscosity (at low temperature (-20°C) and also high effectiveness under brackish water condition (salinity: 1.0-0.5%). This dispersant (IKU-9) was tested on different waterfree oils and w/o-emulsions.

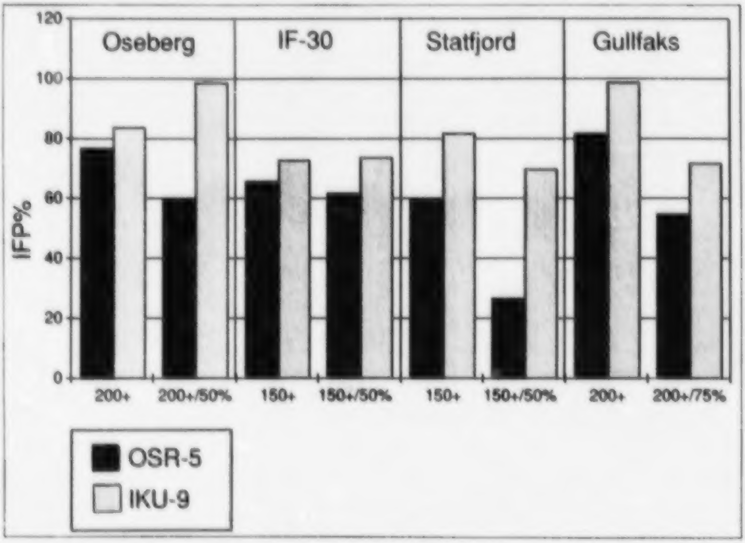

Figure 6: Measured effectiveness (IFP-method) of the optimized dispersant (IKU-9) compared to the commercial product, Finasol OSR-5, on four different oils, both waterfree and emulsified. The term 200+ corresponds to an oil topped at 200°C and the term '50% water' corresponds to a w/o-emulsion containing 50% water.

Figure 6 shows that the new optimized dispersant (IKU-9) has a higher effectiveness than Finasol OSR-5 for all the weathered oils in both waterfree and emulsified forms. The increase in effectiveness over the commercial product is especially large for the w/o-emulsions. The viscosities for the w/o-emulsions used were:

Oiltype	**Topping temperature (°C)**	**Water content (%)**	**Viscosity and Shear rate (cP)**	**(s^{-1} at 10°C)**
Oseberg	200	50	1000	10
IF-30	150	50	5400	10
Statfjord	150	50	200	100
Gullfaks	200	75	4100	10

To compare the effectiveness of the optimized dispersant when determined by other test methods than the IFP-test, tests were also made with the WSL and the MNS test methods. The effectiveness results from the three methods and the mean droplet sizes measured are presented in figure 7.

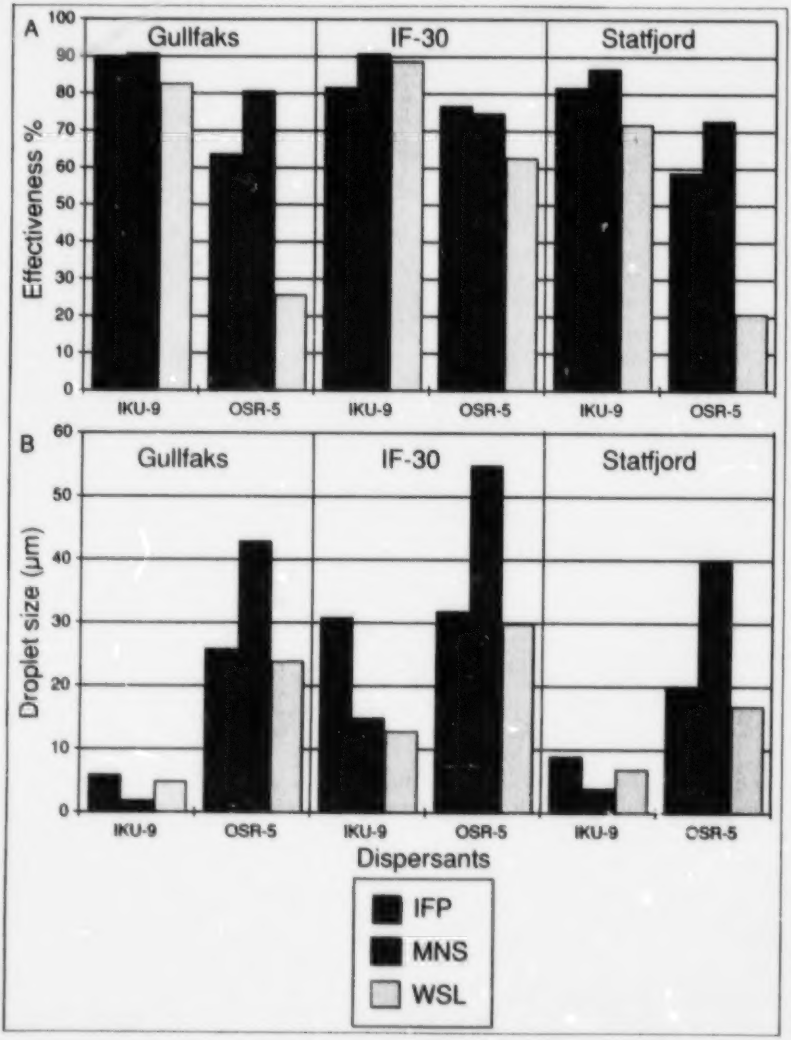

Figure 7: Effectiveness (%) and mean droplet size (µm) for the optimized dispersant (IKU-9) and Finasol OSR-5 measured with the three different test methods (IFP, WSL and MNS). The oils used (Gullfaks, IF-30 and Statfjord) were all topped at 150°C.

From figure 7a it can be seen that the effectiveness of the new optimized dispersant called IKU-9 is higher than Finasol OSR-5 for all three test methods. The difference in effectiveness among the three test methods are relatively small for IKU-9 compared to the differences among the test methods when OSR-5 was used. This can be explained by the extremely small oil droplets formed with IKU-9. The mean droplet size is in the range of 2-7 µm for all three test methods (Gullfaks 200°C+), whereas the corresponding droplet size for OSR-5 is in the range of 25-40 µm (see figure 7b). These small droplets formed decreases the influence on the effectiveness of the different energy inputs and sampling procedures used in the three test methods.

To compare the effectiveness of the optimized dispersant with other commercially available dispersants, tests were done with the WSL apparatus used for government approval in both the UK and Norway. These results are presented in figure 8.

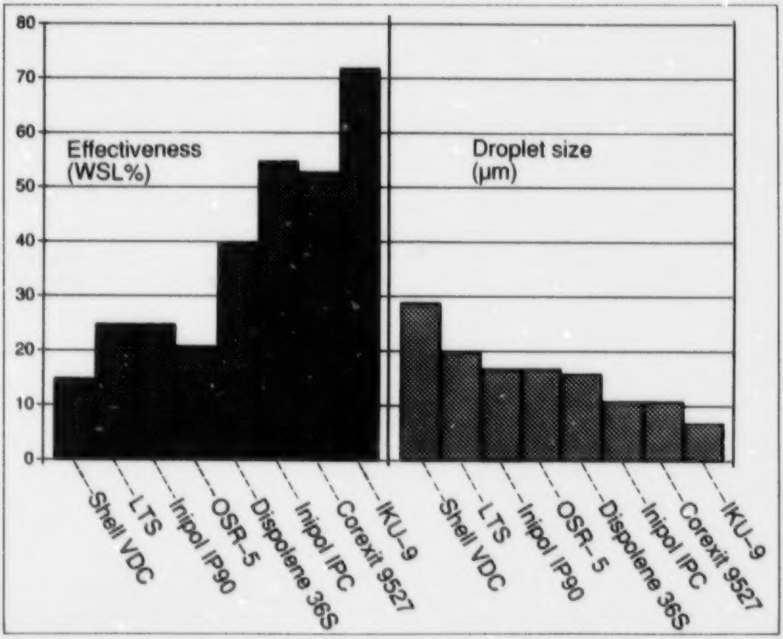

Figure 8: Effectiveness (%) and mean droplet size (µm) for the optimized dispersant (IKU-9) and other commercially available dispersants.

From figure 8 it can be seen that in this collection of dispersants, the new developed dispersant (IKU-9) formed the smallest oil droplets and had the highest effectiveness.

CONCLUSIONS

This work shows the importance of using proper statistical experimental designs in product development. In this case the technique has been used in the development of a dispersant with three constituents, but the technique can easily be used also for more complex products as well. As a matter of fact, as the complexity of a product increases the need for a statistical experimental design will increase even more.

The use of such response surfaces are especially useful when optimizing a dispersant for several oil types and degrees of weathering. Not only the optimum point is obtained, but a total distribution of the effectiveness as well. This knowledge of how the effectiveness is distributed helps the experimenter to select a suitable compromise composition when other variables eg. different oil types, viscosity and toxicity must also be taken into account.

AKNOWLEDGEMENTS

Fina Exploration Norway for the funding for this research project at IKU.

Alain Charlier, Fina Research Brussels, Belgium and Halfdan Akre-Aas, Akre-Aas Miljøkjemi a/s, Norway for valuable assistance and discussions.

Inger Kjersti Almås, Leif Husvik and Oddveig Bakken, staff technicians at IKU's Laboratory for Dispersant Testing.

REFERENCES

BOX, G.E.P., HUNTER, W.G., HUNTER, J.S., Statistics for experimenters, An introduction to design, data analysis and model building, John Wiley & Sons, New York, 1978.

DALING, P.S., BRANDVIK, P.J.: Characterization of crude oils for environmental purposes. Proceedings of the 13th AMOP-seminar, Environment Canada, Edmonton, 1990.

DEMING, S.N., MORGAN, S.L., Experimental design: a chemometric approach, In: Data handling in science and technology - Volume 3, 1987.

KUHRI, A.L., CORNELL, J.A., Response surfaces, Designs and analyses, Marcel Dekker Inc. ASQC Quality Press, New York, 1987.

MARDIA, K.V., KENT, J.T., BIBBY, J.M., Multivariate analysis, A volume in "Probability and mathematical statistics", editors: Z.W.Birnbaum and E.Lukacs, Academic Press, Inc., london, 1982.

MARTENS, H., NÆS, T. Multivariate Calibration, John Wiley and Sons, Chichester, 1989.

MASSART, D.L., VANDEGINSTE, B.G.M, DEMING, S.N., MICHOTTE, Y., KAUFMAN, L., Chemometrics: a textbook, in: Data handling in science and technology - vol. 2, Elsevier, Amsterdam, 1988.

MONTGOMERY, D.C. Design and analysis of experiments, Second edition, John Wiley and Sons, New York, 1984.

EMULSION FORMATION IN DISPERSANT TREATED CRUDE OIL

by
H.M. Brown, D.K. Weiss, and R.H. Goodman
Esso Resources Canada

INTRODUCTION

Crude or refined oil products which have been spilled offshore are subject to natural processes which will eventually degrade and disperse them. These processes include evaporation, dissolution, dispersion, emulsification, sinking, photooxidation, and biodegradation. Among these processes only emulsification, that is the incorporation of water drops into the oil through wave action, measurably impedes the general dispersal of the floating oil. Emulsification results in an increase in the oil viscosity and density which generally inhibits the other processes of dispersal. Emulsions may contain up to 80% by volume of water and can be stable over periods of months.

The longevity of such emulsions was especially evident after the March 1989 grounding of the tanker Valdez in Prince William Sound. The oil from this spill was initially carried by ocean currents through the islands of the sound and into the Gulf of Alaska where much of the slick dispersed naturally. Some weathered and emulsified windrows were observed in late April (one month after the spill) as far south and west as Shelikof Strait between the Alaska Peninsula and Kodiak Island. This oil apparently washed onto the Katmai coast of the Alaska Peninsula approximately 650 km from the spill site. Subsequently, no floating oil on open water was again observed until late June when emulsion patties began appearing well within Cook Inlet (north of Kodiak Island) and again in Shelikof Strait. This was probably emulsified oil refloated by high Spring tides from heavily oiled shores in Prince William Sound and from some coves along the Kenai Peninsula. This phenomenon of emulsified oil persisting on the ocean surface for long periods and resisting the natural dispersal processes has been observed in some previous spills but the mechanisms involved have received little study.

The literature on emulsion formation and properties is sparse but has been reviewed by Payne and Phillips (1985). The incorporation of water drops into floating oil is apparently enhanced by natural surfactant molecules although the identification of these compounds or compound families has not been made. Usually oils high in asphaltenes or waxes and with high viscosities are more susceptible to emulsion formation. The stability of the emulsions probably also depends on the nature of the indigenous surfactants, asphaltenes, and higher molecular weight waxes. The two oils used in this study, Alaska North Slope and Drift River, are known to form stable emulsions (Mackay and Chau (1986)).

A number of studies have been made on the effect of dispersants and emulsion breaking chemicals on emulsion formation and stability (eg: Bocard and Gatellier (1981), Bridie et al.(1980)). Usually demulsifiers are successful in preventing formation when applied to fresh oil but do not break an emulsion (or 'mousse') once it is formed. Dispersant chemicals generally do not disperse mousse very successfully and in one laboratory test did not prevent emulsion formation when added to fresh oil. The effect of dispersants on the oil remaining from a partially dispersed slick has not been studied.

The formation of water-in-oil emulsions by North Slope oil and its long term persistence has added significantly to the cleanup problems from the Valdez incident. This study investigates the effect of dispersants on the formation of emulsions in oil remaining from dispersant treated slicks of Drift River and North Slope crude oils.

EXPERIMENTAL PROCEDURE

Tests were conducted in a wave basin to determine the effect of dispersants on the formation and properties of emulsions of the non-dispersed oil. During the test series two Alaskan oils, North Slope and Drift River, were each treated with two dispersants, Corexit 9550 and Corexit 9527. Emulsion properties were determined by measuring the viscosity and water content of the oil slick as the tests progressed.

Experimental Set-up

Three floating booms, each 10 m in diameter, were placed side by side in the wave basin midway along its length to contain the oil slicks. A stationary crane at the basin edge was used as a camera platform 15m above the water surface. Both a colour video camera and a remotely triggered 35mm camera were used from this vantage point to record surface phenomena during the experiments. Fifty tonnes of NaCl were added to the water to imitate sea water with a salinity of 30ppt. Seventy-five (75) litres of Drift River oil were spilled in each of the three booms and weathered for 16 hours. After the oil had weathered, 3.75 *l* of Corexit 9550 and 3.75 *l* of Corexit 9527 was applied to the middle boom and to the northern-most boom respectively using a hand sprayer. This represents an application rate of 1:20 dispersant to oil ratio. The southern boom was left untreated as a control. Twenty centimetre regular waves with a period of 1.6 seconds were generated during each day of the test from 8:00 to 16:00 hours. The test continued for four days and then was repeated using North Slope oil which had been weathered 40 hours before the dispersants were applied.

Sampling

Samples of the oil within each boom were taken immediately after the dispersant was applied and at intervals of 4, 8, 16, 24, 32, 48, 56, 72, and 80 hours. The samples were taken manually using one litre jars and care was taken to obtain only the oil and as little water as possible. An aliquot of about 20-30 ml was taken from each sample and put into a graduated centrifuge tube to determine the stability of the emulsion. These samples were kept for 1 month and the amount of water which settled out was measured periodically. All samples were analyzed for viscosity and water-in-oil as soon as possible after the samples were taken but were stored at 6°C if any delay occurred. The viscosity was measured with a vibrating ball viscometer at 20°C on samples decanted from any free water. Water-in-oil determinations were made on the same samples as those prepared for the viscometer using a modification of the standard Bottom Sediment and Water Test (BS & W Test). The samples were diluted 50/50 w/w with toluene and warmed to 90°C, then centrifuged at 1450 rpm for 20 minutes. Corexit 7652 (2 drops) was added before centrifuging to aid in breaking the emulsion. The water always separated cleanly using this procedure and was measured in graduated centrifuge tubes.

At the end of each experiment the remaining oil or emulsion was recovered from the water with a skimmer and put into 50 litre carboys to allow the free water to separate. The total oil recovered was measured at this time.

RESULTS AND DISCUSSION

Initial Observations

An example of the change in viscosity and water content during the experiment is shown in Figures 1 and 2 for Drift River oil. There are two interesting features of these graphs: both the viscosity and the water content increase more rapidly in the slicks treated with dispersants compared to the control and there is a loss of water from the emulsions (and corresponding change in viscosity) during the night when the slick is not subject to wave action. Similar results were obtained with North Slope oil except that the viscosity and water content were higher in the untreated slick. For this oil,

FIG. 1 DRIFT RIVER - VISCOSITY

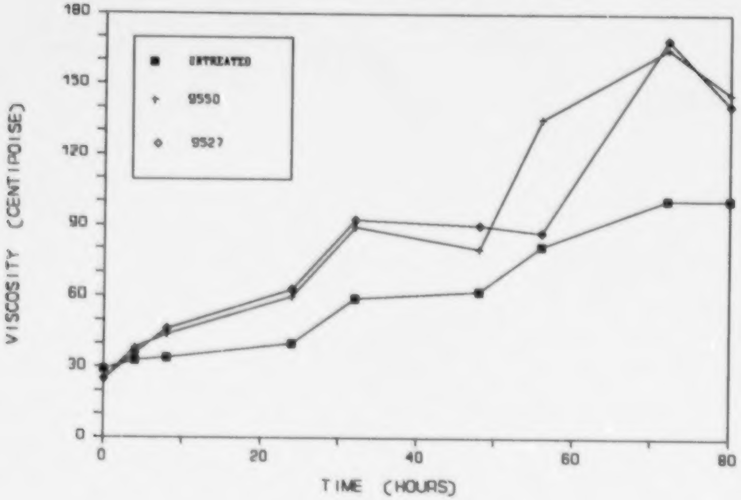

FIG 2 DRIFT RIVER - WATER CONTENT

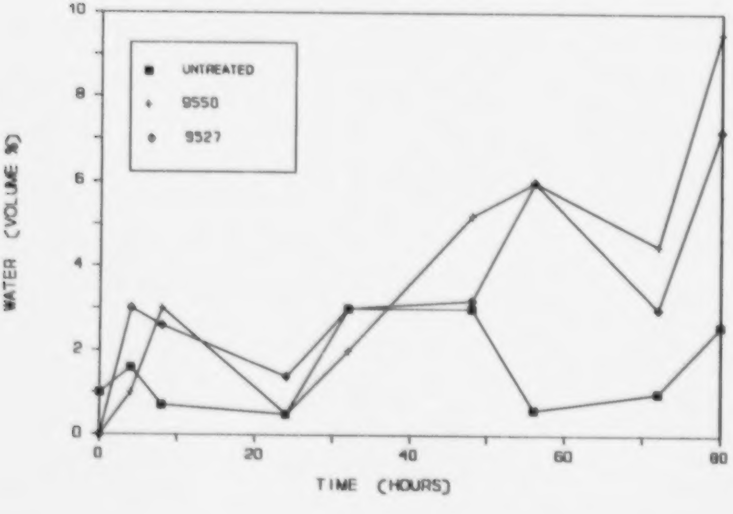

which was weathered for 40 hours before dispersant application, it appears that both dispersants inhibited the emulsion formation. For both of the untreated oils, the measured viscosity and water content agree with similar measurements of Mackay and Chau (1986).

Emulsion Formation

The raw viscosity and water content data described above was reworked to determine if more information on the processes which were occurring could be obtained. In Figure 3 the water content as a function of time for the Drift River experiment is shown for both the control slick and for the 9550 treated slick. Two best fit, first order curves have been drawn for each slick - one curve through points measured during wave agitation (at 4, 8, 32, 56, and 80 hours) and one curve through points measured after the slick had settled overnight (at 0, 24, 48, and 72 hours). Because of the small number of measured points there is no justification in attempting a higher order curve fit nor is there any physical model available which would suggest a reason for doing so. During the day with wave agitation, water is being incorporated into the oil; at night with the waves off some phase separation occurs. If the water gain to the emulsion during the day is corrected for the water loss on phase separation at night, then a graph such as Figure 4 can be drawn, where the abscissa represents continuous wave activity.

FIG. 3 DRIFT RIVER - WATER CONTENT

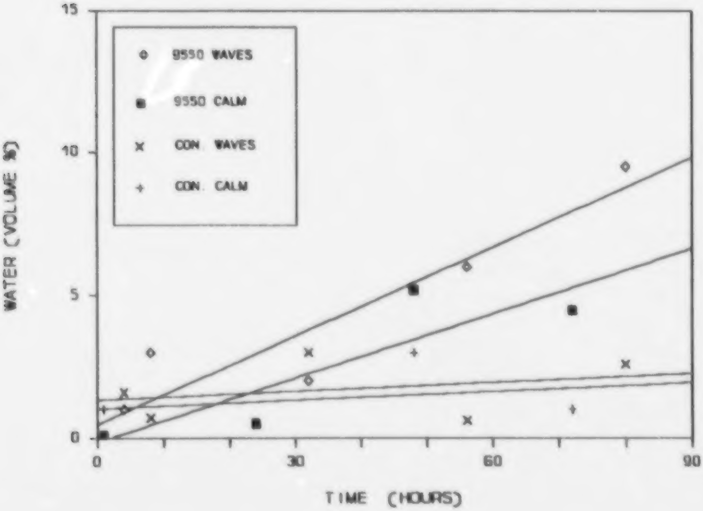

FIG. 4 DRIFT RIVER - WATER UPTAKE (9550)

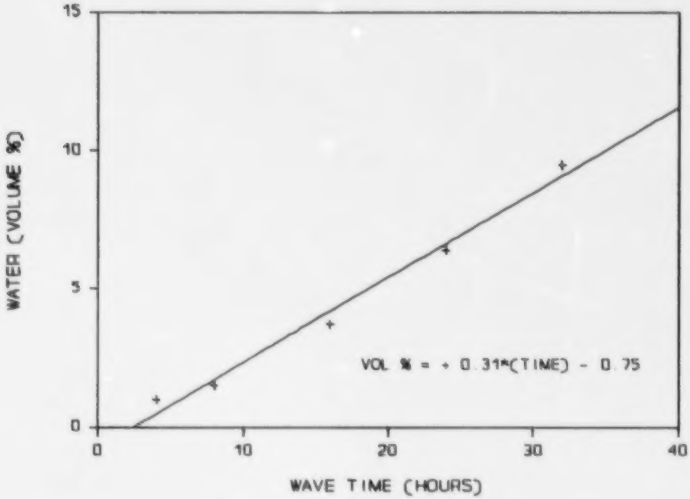

The expression in the figure gives the water uptake as a function of time for the best fit. A similar analysis for the slick treated with 9527 and for the untreated slick was made. The expressions obtained were:

With 9550: WATER (Vol %) = + 0.31*(TIME) - 0.75

With 9527: WATER (Vol %) = + 0.25*(TIME) - 0.70

Untreated: WATER (Vol %) = + 0.03*(TIME) + 1.20

These equations clearly show that for the first two days after either Corexit 9550 or 9527 was applied to the Drift River oil, emulsions would form more rapidly than with the untreated oil.

A similar analysis can be made on the data from the test with North Slope oil, starting with curve fitting to the water uptake measured with and without wave agitation. The data for the untreated slick and for the slick treated with 9527 is shown in Figure 5. Again there is some scatter in the points measured and only a first order fit can be justified. After correcting for the water loss during phase separation when no waves were present, the water content as a function of time is given by:

With 9550: WATER (Vol %) = + 1.0*(TIME) - 0.7

With 9527: WATER (Vol %) = + 1.1*(TIME) + 3.4

Untreated: WATER (Vol %) = + 1.5*(TIME) + 19.2

FIG. 5 NORTH SLOPE - WATER CONTENT

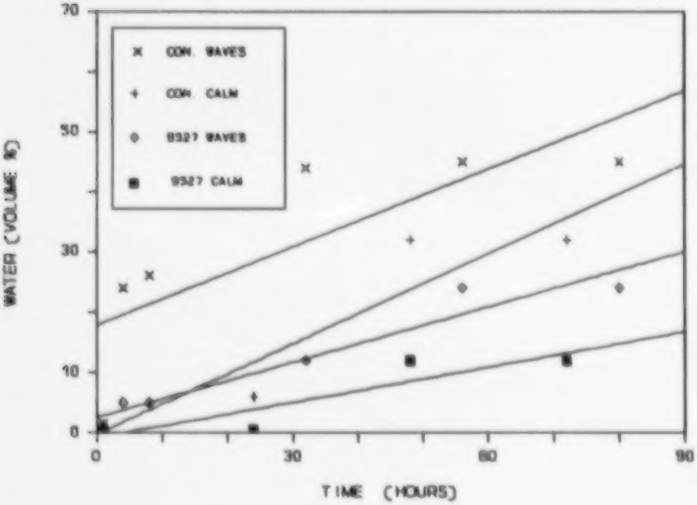

Unlike the case with Drift River oil, these expressions show that water is incorporated into North Slope oil more slowly when it has been treated with either Corexit 9550 or 9527. Note however, that North Slope oil forms emulsions much more readily than Drift River oil whatever the treatment.

Payne et al.(1983) studied the weathering processes of North Slope oil in an outdoor flow-through tank system with wave agitation and found that the water content of the oil increased rapidly to about 50% in the first four days. It then increased more slowly. This appears to be a similar rate of water uptake to what has been measured in the current tests although we are not able to compare the relative wave energies used. Rates of emulsion formation for

Drift River oil have not been previously measured although Mackay and Chau (1986) did produce emulsions with weathered samples of the oil in their laboratory experiments.

Oil viscosity is altered by weathering processes and thus is a less useful indication of emulsion formation than is the water content of oils. However, Mackay et al.(1980) did adapt equations which describe the rheological properties of suspensions of rigid particles to relate the viscosity of an emulsion to its water content. They determined that

$$Vis/Vis_0 = \exp\{2.5w/(1-kw)\}$$

where Vis is the apparent emulsion viscosity
Vis_0 is the apparent oil viscosity
k is a constant with a value of about 0.65
w is the emulsion fractional water content.

FIG. 6 NORTH SLOPE - VISCOSITY RATIO

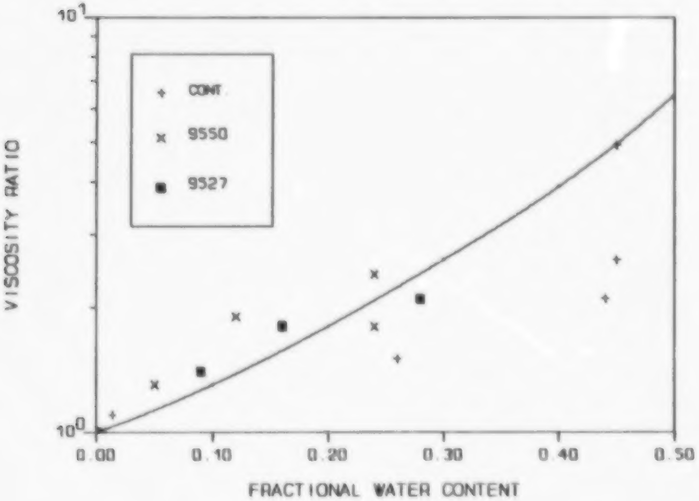

In Figure 6, the viscosity ratio is plotted against the water content measured for the North Slope test. The apparent oil viscosity was taken to be that of mildly weathered oil (viscosity of 350 cp). The solid curve is the viscosity ratio calculated from the expression above. Although there is some scatter, the results are similar to those reported by Mackay et al. and suggest that the expression has some validity especially below 0.30 water content. Given a knowledge of emulsion viscosity, an estimate of the expected water content can be made. The measured values of viscosity and water content for the Drift River test also fall along the solid line but are not shown for clarity as they all cluster below 0.10 water content.

CONCLUSIONS

Measurements of the water content and viscosity of oil slicks treated with either Corexit 9550 or Corexit 9527 have been made. For the non-dispersed portion of slicks of Drift River oil, the application of these dispersants appears to enhance the incorporation of water and increase the viscosity compared to an untreated control slick. The opposite effect was observed for slicks of North Slope oil. The untreated control slick formed water-in-oil emulsions more readily than the oil remaining in slicks treated with either of the dispersant chemicals. The viscosity increased more slowly in the treated slicks as well. The rate of water uptake for North Slope oil during these wave basin tests is consistent with the earlier reported work of Payne et al. and the viscosities measured for both oils are similar to those reported by Mackay and Chau. The relation between viscosity and water content developed by Mackay et al. appears to have some validity and provides a method of determining emulsion water content if viscosities are known.

ACKNOWLEDGEMENTS

This study was carried out by Esso Resources Limited under the auspices of The Cook Inlet Resource Organization. We wish to thank Barry Eldridge, the Manager of CIRO, for his kind cooperation and encouragement during the study. The authors wish to thank R.A. Paterson who was responsible for the operation of the wave basin, and Harm Reuver and Chris Bianchi who assisted with the sampling of the oil.

REFERENCES

Bocard, C. and C. Gatellier (1981), "Breaking of fresh and weathered emulsions by chemicals", Proc. 1981 Oil Spill Conf., API, Washington, pp 601-607.

Bridie, A.L., Th.H. Wanders, W. Zegveld, and H.B. Van der Heijde (1980), "Formation, prevention and breaking of sea water in crude oil emulsions 'Chocolate Mousses'", Mar. Poll. Bull. 2 pp 343-348.

Mackay, D., I. Buist, R. Mascarenhas, and S. Patterson (1980), "Oil spill processes and models", Report EE-8 Environmental Emergencies Technolgy Division, Environment Canada, Ottawa.

Mackay, D. and A. Chau (1986), "The dispersion characteristics of selected Alaskan crude oils", A Report to the Cook Inlet Resource Organization.

Payne, J.R., B.E. Kirsten, G.D. McNabb Jr., J.L. Lambach, C. de Oliveira, R.E. Jordan, and Wilson Ham, "Multivariate analysis of petroleum hydrocarbon weathering in the subarctic marine environment", Proc. 1983 Oil Spill Conference, API.

Payne, J.R. and C.R. Phillips (1985), "Petroleum spills in the marine environment; the chemistry and formation of water-in-oil emulsions and tar balls", Lewis Publishers, Chelsea, USA.

STUDY OF OIL SPILL DISPERSANTS EFFECTIVENESS AND PHYSICAL STUDIES

Merv F. Fingas and Beata Kolokowski
Environmental Emergencies Technology Division
Environment Canada
Ottawa, Ontario

E.J. Tennyson
U.S. Minerals Management Service
Herndon, Virginia

INTRODUCTION

Dispersants continue to be a lively topic of discussion twenty years after the TORREY CANYON incident. Little has changed in the way of documentation. There is still no undisputed documentation on large-scale experiments or use to show whether dispersants are effective or not. Similarly, no large scale biological experiments have convinced all environmentalists that the use of dispersants is safe in all conditions, although the evidence is becoming increasing clear that dispersants cause little ecological damage above that by untreated oil and that they could, in fact, minimize ecological damage if they were effective. The current focus on dispersants is now more on the effectiveness than on the toxicity. The current emphasis on joint Environment Canada-U.S. Minerals Management Service work is on mechanism studies. These are intended to discover the variables involved in dispersant action so that insights will be found on how effectiveness can be improved.

The active ingredients in dispersants are surface active agents or surfactants. Surfactants have varying solubility in water and have varying actions toward oil and water. One parameter that has been used to characterize surfactants is the HLB or the hydrophillic-lipophilic balance.[1] A surfactant with an HLB of about 1 to 8 promotes the formation of water-in-oil emulsions and one with an HLB in the range of 12 to 20 promotes the formation of oil-in-water emulsions. Dispersants have HLB's in the range of 9 to 11. The HLB range as defined is only applicable to non-ionic surfactants, however ionic surfactants can be rated using an expanded scale and often have HLB's ranging from 25 to 40. They are strong water-in-oil emulsifiers, very soluble in water, relatively insoluble in oil, and generally work from the water to any oil present. Such products have little applicability to oil on water because they rapidly disappear in the water column, having little effect on oil. However, because of their commonality and cheapness, many ionic-surfactants are proposed as dispersants. Many of these agents would be better classed as surface-washing agents.

Surface-washing agents are surfactant-containing mixtures with high HLB's and are best suited to removing oil from solid surfaces such as shorelines, roads and parking lots. EETD has developed an effectiveness test for such agents and results of these tests are reported in the literature. Many surfactant-containing agents of all types come onto the market each year, many are re-packaged industrial cleaners and have little utility in spills.

DISPERSANTS - FIELD EFFECTIVENESS TRIALS AND ACTUAL USE

Over the past 12 years, 107 test and control spills have been laid out to test the effectiveness of oil spill dispersants.[2] The results achieved during these tests show clearly that dispersants are not highly effective, even under highly controlled experimental situations. Of greater concern than this is the methodology used to estimate effectiveness. Some experimenters simply estimated effectiveness but most based their measure on integrations of water column concentrations relative to surface slick dimensions. This is not a correct means to perform the measure because the underwater concentrations have little positional relationship to the surface slick. Underwater dynamics of the ocean are very different than surface dynamics. Extreme cases of the positional variances between surface and sub-surface slicks have been illustrated by Brown and Goodman in controlled tank testing.[3] Their work has shown that the underwater plumes move in highly random fashions with respect to the surface slick and even two trials conducted on the same day will not have similar movement patterns. Furthermore, all of the experimenters who used underwater concentrations to estimate field effectiveness also used the method of dividing the water into different compartments and averaging concentrations. Mathematically this is not appropriate and can result in effectiveness values that are much larger than the actual values. In fact, because dispersion only occurs from the thicker portions of the slick and because these only constitute about 10% of the slick surface area, the error in measurement can be as great as a factor of 10 in two dimensions and as great as 10 times 10 or 100-fold in three dimensions or overall! Other errors in the opposite direction compensate for this somewhat, but the overall result is a large exaggeration of effectiveness.

Surface measures are also inadequate. Remote sensing does not provide a thickness measure and thus calculating volume is impossible. Numerous surface phenomena also interfere with the process of estimating slick volume. These have been detailed in a paper by Goodman and Fingas.[4] A new technique for measuring surface thickness is currently under development by Esso Resources Canada, Minerals Management Service, Environment Canada and the American Petroleum Institute. This instrument offers potential to measure effectiveness on the open ocean.

In summary, field trials of dispersant effectiveness have not shown any quantitative or qualitative proof of high (>50%) dispersant effectiveness. Analytical means do not exist at this time to accurately quantify dispersant effectiveness in field trial situations.

Dispersant usage during some notable large spills has been reviewed by a number of authors.[5,6] The problem with actual spill data is that some observers may have reported seeing evidence of effectiveness and others directly the opposite. In none of the cases were any analytical means tried to quantify effectiveness or even to provide better estimates. Dispersants are used more frequently in countries like Great Britain and in many Arabic counties. Again, no quantitative results are available to show effectiveness nor lack of such.

DISPERSANTS - LABORATORY STUDIES OF EFFECTIVENESS

A number of laboratory studies have been performed to compare the test results from different apparatus and procedures. A review of these results shows that there is poor correlation in effectiveness results between the various test methods.[7] A recent study by the present author has shown that lack of correlation is primarily a function of settling time allowed between the time that the energy is no longer applied and the time that the water sample is taken from the apparatus.[8] Another important factor is that of the oil-to-water ratio in the apparatus. When these two parameters are adjusted to be the same and to larger values test results from most apparatus are similar. Results from more energetic dispersant effectiveness tests, such as the Mackay test and the Labofina or Warren Springs test, are somewhat higher but, when corrected for natural dispersion, these results are nearly identical to those from less energetic apparatus. Results from a series of tests including corrected results, are shown in Table 1. The effectiveness results from all tests are nearly identical even though the errors for measurement in the Mackay and Labofina tests are 10 percent or more. The fact that these values are nearly identical may imply that they have some meaning. Just the fact that this phenomena occurs also indicates that energy plays a lesser role than was previously thought. The high energy in the Mackay and Labofina tests only increases the dispersant effectiveness for those oils that disperse naturally.

Early studies were used to help to come to an understanding of laboratory effectiveness tests. It had been found that the existing tests yield different results for different dispersant-oil combinations. This was especially true when the oil type was varied, rather than the dispersant type. Dispersants which appeared to be effective on one oil were often quite ineffective on that same oil in another apparatus or test protocol. Additionally, the main test then in the literature, the Labofina (or Warren Springs or Rolling Flask) test and the Mackay (or MNS or Mackay-Nadeau-Steelman) test produced results that quite different. The former test uses a separatory funnel with 250 mL of water and 5 mL of oil to test the dispersant. The resulting oil-water ratio is 1:50, a factor that shall later be shown to be of

TABLE 1 EFFECTIVENESS IN FOUR APPARATUS

OIL	DISPERSANT	DISPERSABILITY IN PERCENT			
		SWIRLING FLASK	FLOWING CYLINDER	LABOFINA	MNS
ADGO	9527	61	52	78	64
	CRX-8	42	40	77	87
	EN 700	67	59	76	93
AMAULIGAK	9527	48	38	86	44
	CRX-8	56	46	73	85
	EN 700	54	39	59	73
ASMB	9527	22	21	31	39
	CRX-8	28	31	34	61
	EN 700	43	43	62	76
ATKINSON	9527	7	18	67	17
	CRX-8	9	10	47	19
	EN 700	8	18	55	22
BENT HORN	9527	29	46	29	29
	CRX-8	27	37	27	51
	EN 700	44	51	19	42
FEDERATED	9527	39	35	51	35
	CRX-8	23	31	35	76
	EN 700	38	42	70	76
GEAR OIL	9527	29	18	18	12
	CRX-8	40	25	27	10
	EN 700	10	6	15	30
HIBERNIA	9527	6	12	23	6
	CRX-8	9	10	19	9
	EN 700	7	8	23	14
ISSUNGNAK	9527	24	22	61	41
	CRX-8	42	76	35	100
	EN 700	42	60	75	100
LAGO MEDIO	9527	7	8	29	16
	CRX-8	11	15	19	19
	EN 700	10	23	24	27
LUBE OIL	9527	13	19	40	44
	CRX-8	14	24	40	53
	EN 700	13	23	40	80
MOUSSE MIX	9527	9	15	27	30
	CRX-8	11	25	18	26
	EN 700	24	32	23	43
NORMAN WELLS	9527	41	55	65	47
	CRX-8	60	47	70	65
	EN 700	63	53	74	89
PANUK	9527	100	100	89	100
	CRX-8	93	100	85	100
	EN 700	100	100	87	100
PRUDHOE BAY	9527	7	13	47	27
	CRX-8	5	16	38	23
	EN 700	17	14	48	37
SYNTHETIC CRUDE	9527	57	50	78	83
	CRX-8	69	55	40	91
	EN 700	61	39	76	86

LEGEND 9527 = COREXIT 9527, CRX-8 = COREXIT CRX-8, EN 700 = ENERSPERSE 700 significance. The separatory funnel is rotated at 33 rpm for 10 minutes and then a sample taken after a settling time of 2 minutes and analyzed colorimetrically. The Mackay apparatus, on the other hand, employs 10 mL of oil and 6 L of water to yield an oil-to-water ratio of 1:600. Energy is supplied by a high velocity stream of air. Sampling is done dynamically - no settling time is allowed. The results of the two tests differ with oils - the Mackay test consistently gave higher numbers for heavier oils and especially for very viscous oils. The Mackay effectiveness numbers were also very noisy and had a tendency to be very high or very low. The Labofina effectiveness values tended to only appear in the mid-range of values - that is around 50%. Attempts to correlate both results with field values were futile. The first effort of EETD was to generate a good data set with both devices to determine what the variances indeed were. The second effort was to test other concepts to see if every device or test yields unique effectiveness values. An oscillating hoop test which employs an oil-to-water ratio of 1:200 using the given protocol was tried. The values produced using this apparatus and test protocol showed values more similar to the Mackay test than to the Labofina, however the data was also noisy like that from the Mackay test. Early conclusions from these study were that lab tests produced unique results based on their protocols and test features. This offered no hope for further understanding of dispersants effectiveness.

EETD continued research despite the pessimistic conclusions noted above. The first effort was the development of a rapid and simple test. The purpose of this was to speed research. About 10 tests per day could be done with the Labofina apparatus then in use and about 6 for the Mackay apparatus. It was obvious that to perform tests for many oils and dispersants in many different conditions, that a faster test was needed. The development resulted in the Swirling Flask test which employs a standard 125 mL flask with a bottom spout for decanting the sample. Depending on the type of test, 30 to 50 runs could be conducted in one day. The protocol chosen for the test was an oil to water ratio of 1:1200 and a settling time of ten minutes. The first results achieved with this new test did not correlate well with either the Mackay or Labofina tests results and there was almost no correlation with the oscillating hoop test results. What was dramatically different from all three tests was that results were repeatable within 5%. Results from other tests were often ten times this value!

Testing continued using the new apparatus. The effectiveness of many oils and several dispersants were measured. Values appeared to be correct but low compared to those for other tests. Variation of effectiveness with settling time was measured extensively and it was found that the effectiveness changes as an exponential function with settling time settling from 0 to 10 minutes and then only changes a small amount after 10 minutes. This settling time was also measured in the Labofina and Mackay tests and found to be the same. Some of the "noise" in both the latter tests can then be explained by the settling time. In the case of the Labofina, sampling is done at the 2-minute mark, a time at which particles are rapidly rising to the surface. Any small error in timing can result in significant variation in amount of oil sampled and subsequently effectiveness. Test results using the swirling flask apparatus are presented in Table 2.

MECHANISM STUDIES

The first round of mechanism studies focused on changing variables in the laboratory tests and observing the effect on dispersant effectiveness. Long-term settling (or rising, depending on the point of view) experiments using the swirling flask apparatus were the first round of experiments to be conducted. It was found that there were about 3 classes of dispersants, those that showed good stability over 48 hours (effectiveness only went down about 20%), those that showed medium stability over the same time period (effectiveness went down about 50%) and those that had poor stability (effectiveness went down about 75%). Most commercial products showed good stability characteristics. The tests showed that dispersed oil could be somewhat stable in water over a 48-hour period.

Tests conducted on the oscillating hoop, Labofina, Mackay and the Swirling Flask test showed one very disturbing finding. All of the first three tests were insensitive to whether the oil was placed in the water or on the oil. Only the swirling flask tested showed no trace of this tendency. In fact, in the case of the three offending apparatus, it only made a small difference in effectiveness on where the dispersant was placed, with the Labofina showing the least difference, and the Mackay the most. This finding would imply at first glance, that in the case of the first 3 apparatus, the dispersant can work from the water to the oil rather than vice versa which is the way it would be in nature or in the swirling flask apparatus. This was the first strong indication that the protocols or apparatus were deficient in measuring dispersant effectiveness.

Because the dispersant worked almost as well from the water to the oil in these apparatus, experiments were conducted to see the effect of two main differences between the four apparatus mentioned above, oil-to-water ratio and settling time. As the oil-to-water ratio was increased, the effectiveness went down in all the tests, however became more similar to that of the swirling flask. Similar results were observed for the settling time. When the four apparatus were run using an oil-to-water ratio of about 1:1000 and a settling time of ten minutes, nearly identical results were produced for many oils, but not for all. Examination of the properties of the deviant oils

Table 2 DISPERSANT EFFECTIVENESS			EFFECTIVENESS PERCENT		
OIL	DISPERSANT	AVERAGE	% PREMIXED	% 1 DROP	% 2 DROPS
ADGO	C 9527	61	61	82	41
ADGO	CRX-8	39	61	31	26
ADGO	ENER 700	59	76	53	47
ADGO	DASIC	8	11	7	5
AMAULIGAK	C 9527	45	50	36	49
AMAULIGAK	CRX-8	50	61	51	37
AMAULIGAK	ENER 700	62	65	62	58
AMAULIGAK	DASIC	28	23	40	22
AMAULIGAK	DREW	0	TL	TL	TL
AMAULIGAK	C 9550	0	TL	TL	TL
AMAULIGAK	BQ	60	72	52	57
AMAULIGAK	II	0	22	TL	TL
ARABIAN LIGHT	C 9527	17	31	16	3.3
ARABIAN LIGHT	CRX-8	9	15	8.6	4.8
ARABIAN LIGHT	ENER 700	22	16	27	23
ARABIAN LIGHT	DASIC	33	24	36	40
ARABIAN LIGHT	BQ	42	28	54	43
ASMB	C 9527	33	42	28	28
ASMB	CRX-8	45	57	43	36
ASMB	ENER 700	51	68	51	35
ASMB	DASIC	24	16	27	28
ASMB	DREW LT	0	TL	TL	TL
ASMB	C 9550	0	TL	TL	TL
ASMB	BQ	79	81	82	73
ASMB	II	18	49	5	0
ASMB	WELLAID 3315	14	8	12	21
ASMB	BP1100WD	12	6	14	17
ASMB	BP1100X	7	1	10	11
ATKINSON	C 9527	39	59	31	27
ATKINSON	CRX-8	31	67	19	7
ATKINSON	ENER 700	73	79	75	66
ATKINSON	DASIC	49	33	61	53
AVALON J-34	C 9527	11	18	7.5	8
AVALON J-34	CRX-8	5	7.6	5.3	3.3
AVALON J-34	ENER 700	11	15	12	7
AVALON J-34	DASIC	16	8	18	21
AVALON J-34	BQ	10	11	11	7.1
AVALON ZONE 4	C 9527	10	14	10	5.7
AVALON ZONE 4	CRX-8	7	14	4.2	3.1
AVALON ZONE 4	ENER 700	26	25	27	27
AVALON ZONE 4	DASIC	30	12	40	38
AVALON ZONE 4	BQ	13	16	14	10
BENT HORN	C 9527	17	12	17	21
BENT HORN	CRX-8	20	15	18	27
BENT HORN	ENER 700	23	10	18	42
BENT HORN	DASIC	35	14	43	48
BUNKER C	C 9527	1	2.3	1.1	1
BUNKER C	CRX-8	2	3.8	1.3	0.9
BUNKER C	ENER 700	1	0.9	1.9	0.8
BUNKER C	DASIC	2	2.1	2.8	0.6
BUNKER C	BQ	1	1.4	1.4	0.8
BUNKER C LIGHT	C 9527	1	0.6	1	0.4
BUNKER C LIGHT	CRX-8	1	0.7	0.8	0.7
BUNKER C LIGHT	ENER 700	1	0.7	2	1.5
BUNKER C LIGHT	DASIC	1	0.8	1.7	1.3

Table 2 DISPERSANT EFFECTIVENESS			EFFECTIVENESS PERCENT		
OIL	DISPERSANT	AVERAGE	% PREMIXED	% 1 DROP	% 2 DROPS
BUNKER C LIGHT	BQ	2	1.6	2.6	0.8
CALIFORNIA CRUDE (11.0)	C 9527	1	0.5	1.1	0.9
CALIFORNIA CRUDE (11.0)	CRX-8	1	2.3	1.2	0.8
CALIFORNIA CRUDE (11.0)	ENER 700	1	0.4	2.7	0.8
CALIFORNIA CRUDE (11.0)	DASIC	1	0.2	2.2	0.8
CALIFORNIA CRUDE (11.0)	BQ	1	0.4	2.2	1.7
CALIFORNIA CRUDE (15)	C 9527	1	1.3	0.7	0.3
CALIFORNIA CRUDE (15)	CRX-8	1	0.4	0.8	0.6
CALIFORNIA CRUDE (15)	ENER 700	1	0.9	0.9	1
CALIFORNIA CRUDE (15)	DASIC	2	0.8	3	3.3
CALIFORNIA CRUDE (15)	BQ	1	1.4	1.3	0.8
COHASSET	C 9527	95	88	100	98
COHASSET (11.2% W)	C 9527	96	88	99	100
COHASSET (25.6% W)	C 9527	88	75	92	97
COHASSET (28.1% W)	C 9527	90	74	97	100
COLD LAKE BITUMEN	C 9527	2	1.9	2.3	0.4
COLD LAKE BITUMEN	CRX-8	1	1.1	2.1	0.6
COLD LAKE BITUMEN	ENER 700	1	0.9	1.4	0.4
COLD LAKE BITUMEN	DASIC	1	1	1	0.3
COLD LAKE BITUMEN	BQ	1	1.1	1.5	0.3
ENDICOTT	C 9527	7	17	2.3	2.8
ENDICOTT	CRX-8	8	20	1.3	2.4
ENDICOTT	ENER 700	6	10	2.4	6.4
ENDICOTT	DASIC	14	8.1	15	18
ENDICOTT	BQ	13	18	6.9	13
ENDICOTT (7.5% W.)	C 9527	3	3	3	3
ENDICOTT (7.5% W.)	CRX-8	4	5	3	3
ENDICOTT (7.5% W.)	ENER 700	6	4	6	9
ENDICOTT (7.5% W.)	DASIC	4	1	1	11
ENDICOTT (7.5% W.)	BQ	6	4	6	7
ENDICOTT (11.7%W.)	C 9527	2	2	2	2
ENDICOTT (11.7%W.)	CRX-8	2	2	3	2
ENDICOTT (11.7%W.)	ENER 700	6	2	9	6
ENDICOTT (11.7%W.)	DASIC	3	1	3	4
ENDICOTT (11.7%W.)	BQ	4	1	6	6
FEDERATED	C 9527	25	41	24	11
FEDERATED	CRX-8	31	50	26	16
FEDERATED	ENER 700	40	41	58	22
FEDERATED	DASIC	38	23	55	36
FEDERATED	BQ	64	66	85	42
HIBERNIA	C 9527	6	13	1.9	1.8
HIBERNIA	CRX-8	6	14	2.6	2
HIBERNIA	ENER 700	10	7.3	10	14
HIBERNIA	DASIC	14	8.6	18	16
HIBERNIA	BQ	9	7.8	12	8
HIBERNIA	WELLAID 3315	4	3	4	4
HIBERNIA (15.4% W)	C 9527	4	6.1	2.3	2.5
HIBERNIA (15.4% W)	CRX-8	3	5.8	1	2
HIBERNIA (15.4% W)	ENER 700	8	5	11	7.5
HIBERNIA (15.4% W)	DASIC	7	1	8	11
HIBERNIA (15.4% W)	BQ	5	4	6	4
ISSUNGAK	C 9527	66	70	93	36
ISSUNGAK	CRX-8	60	58	75	47
ISSUNGAK	ENER 700	62	51	79	57
ISSUNGAK	DASIC	51	31	60	61
ISSUNGAK	BQ	77	77	69	84

Table 2 DISPERSANT EFFECTIVENESS			EFFECTIVENESS PERCENT		
OIL	DISPERSANT	AVERAGE	% PREMIXED	% 1 DROP	% 2 DROPS
LAGO MEDIO	C 9527	**5**	9.5	3.6	1.5
LAGO MEDIO	CRX-8	**5**	13	1.8	1.4
LAGO MEDIO	ENER 700	**13**	11	21	5.9
LAGO MEDIO	DASIC	**15**	4.1	16	24
LAGO MEDIO	BQ	**18**	22	25	8.3
MOUSSE MIX	C 9527	**6**	9	5	3
MOUSSE MIX	CRX-8	**9**	15	6	5
MOUSSE MIX	ENER 700	**14**	10	19	13
MOUSSE MIX	DASIC	**17**	9	22	20
MOUSSE MIX	BQ	**18**	25	17	12
MOUSSE MIX	II	**6**	15	3	0
NORMAN WELLS	C 9527	**36**	51	40	17
NORMAN WELLS	CRX-8	**43**	60	38	30
NORMAN WELLS	ENER 700	**51**	73	26	53
NORMAN WELLS	DASIC	**26**	19	33	27
NORMAN WELLS	DREW LT	**0**	TL	TL	TL
NORMAN WELLS	C 9550	**0**	TL	TL	TL
NORMAN WELLS	BQ	**77**	83	80	68
NORMAN WELLS	II	**0**	33	TL	TL
PANUK	C 9527	**96**	95	95	97
PANUK	CRX-8	**78**	100	62	71
PANUK	ENER 700	**96**	93	97	99
PANUK	DASIC	**40**	44	36	37
PANUK	BQ	**100**	100	100	99
PANUK (47.4% W)	C 9527	**99**	98	100	100
PANUK (53.2% W)	C 9527	**99**	98	100	100
PRUDHOE BAY	C 9527	**13**	19	13	7
PRUDHOE BAY	CRX-8	**13**	23	9	6
PRUDHOE BAY	BQ	**32**	43	29	24
PRUDHOE BAY	ENER 700	**35**	48	26	31
PRUDHOE BAY	DASIC	**11**	14		18
PRUDHOE BAY (1989)	C 9527	**7**	13	5.6	2.5
PRUDHOE BAY (1989)	CRX-8	**7**	15	3.2	3.9
PRUDHOE BAY (1989)	ENER 700	**10**	15	3.1	13
PRUDHOE BAY (1989)	DASIC	**14**	11	18	13
PRUDHOE BAY (1989)	BQ	**15**	25	4.8	16
PRUDHOE BAY (1989)	WELLAID 3315	**4**	3	5	3
PRUDHOE BAY (89) (7.6% W)	C 9527	**6**	9	3	5
PRUDHOE BAY (89) (7.6% W)	CRX-8	**6**	13	3	3
PRUDHOE BAY (89) (7.6% W)	ENER 700	**16**	8	25	16
PRUDHOE BAY (89) (7.6% W)	DASIC	**16**	12	19	18
PRUDHOE BAY (89) (7.6% W)	BQ	**19**	29	18	10
PRUDHOE BAY (89) (14.5% W)	C 9527	**4**	5	4	3
PRUDHOE BAY (89) (14.5% W)	CRX-8	**4**	6	2	3
PRUDHOE BAY (89) (14.5% W)	ENER 700	**8**	4	6	14
PRUDHOE BAY (89) (14.5% W)	DASIC	**10**	2	14	13
PRUDHOE BAY (89) (14.5% W)	BQ	**9**	7	15	6
SOUTH LOUISIANA CRUDE	C 9527	**31**	53	19	21
SOUTH LOUISIANA CRUDE	CRX-8	**36**	55	33	19
SOUTH LOUISIANA CRUDE	ENER 700	**48**	31	75	37
SOUTH LOUISIANA CRUDE	DASIC	**42**	27	50	50
SOUTH LOUISIANA CRUDE	BQ	**62**	71	80	35
SYNTHETIC CRUDE	C 9527	**63**	77	88	25
SYNTHETIC CRUDE	CRX-8	**41**	49	41	34
SYNTHETIC CRUDE	ENER 700	**61**	89	89	48
SYNTHETIC CRUDE	DASIC	**25**	23	30	21

Table 2 DISPERSANT EFFECTIVENESS			EFFECTIVENESS PERCENT		
OIL	**DISPERSANT**	**AVERAGE**	**% PREMIXED**	**% 1 DROP**	**% 2 DROPS**
SYNTHETIC CRUDE	BQ	**55**	89	42	34
TERRA NOVA CRUDE	C 9527	**16**	29	13	6.5
TERRA NOVA CRUDE	CRX-8	**11**	22	5.2	6.5
TERRA NOVA CRUDE	ENER 700	**28**	21	38	24
TERRA NOVA CRUDE	DASIC	**40**	19	58	44
TERRA NOVA CRUDE	BQ	**40**	40	53	27
TRANSMOUNTAIN BLEND	C 9527	**8**	14	6	3.1
TRANSMOUNTAIN BLEND	CRX-8	**8**	13	5.3	6.6
TRANSMOUNTAIN BLEND	ENER 700	**28**	17	43	25
TRANSMOUNTAIN BLEND	DASIC	**27**	11	40	31
TRANSMOUNTAIN BLEND	BQ	**19**	25	18	15
USED MOTOR OIL	C 9527	**33**	42	31	27
USED MOTOR OIL	CRX-8	**31**	39	31	23
USED MOTOR OIL	ENER 700	**36**	47	32	30
USED MOTOR OIL	DASIC	**29**	29	27	31
USED MOTOR OIL	BQ	**36**	42	41	24

EXPLANATION OF TESTS

PREMIXED - REFLECTS THE LARGEST AMOUNT DISPERSED
WHEN DISPERSANT MIXED INTO OIL AT RATI 0 1:25
1-DROP - REFLECTS LARGEST AMOUNT DISPERSED AT
A DISPERSANT TO OIL RATIO OF 1:10
- TEST MEASURES HOW OIL/DISPERSANT COMBINATION
FUNCTIONS WITH REAL APPLICATION
2-DROP - REFLECTS LARGEST AMOUNT DISPERSED AT
A DISPERSANT TO OIL RATIO OF 1:10 BUT DELIVERED IN
TWO DROPS
- TEST MEASURES THE HERDING EFFECT OF THE
OIL/DISPERSANT COMBINATION WHEN COMPARED
TO THE ONE DROP TEST

BQ AND II ARE EXPERIMENTAL DISPERSANTS MADE BY EETD

TL = TO LOW TO MEASURE

revealed that all were naturally dispersable. Blanks (samples without dispersants) were run in the respective apparatus and blank values subtracted from the value run with dispersant. In other words, dispersant effectiveness values were corrected for natural dispersion. This finding is very significant in that all tests can be related and furthermore, the constant result produced by these tests would appear to be a universal effectiveness value. Perhaps this value is the maximum effectiveness which could be expected with the oil-dispersant combination.

At the same time as the above tests were under way, a new test was developed to confirm the effect of oil-to-water ratio. This test is different in concept than any of the other tests and is unique to tests around the world. The test, known in EETD labs as the flowing-cylinder test, employs a measuring cylinder with a top and bottom side-spout. Water is circulated from the bottom side-spout through a filter to catch dispersed oil and returned to the cylinder via the top spout. The only dispersing energy supplied to the system is the small amount of energy resulting from the fall of the chemical from the top spout to the oil layer (a distance of about 3 cm). Dispersed oil is continuously removed from the system so that there is no interference of dispersed oil with any processes that may be on-going. The height between the surface of the oil and the withdrawal spout is about 30 cm. This ensures that only more stable droplets which do not resurface are withdrawn from the system. Other droplets will rise to re-form a slick. The test was developed for two reasons, to have a system which could measure oil-to-water ratios to very high values (as large as 1:1,000,000) and to have a system which was not analogous to those others tested so that variables did not include modes of adding energy or operation. The flowing cylinder apparatus yielded the same results as the other four devices or tests when they are operated at high oil-to-water ratios and 10 minute settling times. This confirms that the previous findings was independent of apparatus mode of operation and that an additional device could produce the same results. The device was used to measure the effect of oil-to-water ratio on dispersant effectiveness. It was found that effectiveness was constant with oil-to-water ratio from about 1:800 up to 1:1,000,000 and that effectiveness peaked at 1:600 then slowly fell as the ratio decreased to 1:100. This was confirmed by performing the same experiment in the other three apparatus. It was concluded that this effectiveness was due to a change in mechanism of dispersant action between high oil-to-water ratios and low. In the case of low ratios, the surfactant may interact to form agglomerates and micelles, thus interfering with the main process by removing surfactant. This would account for the lower effectiveness at the lower ratios. Because dispersion at sea would involve high ratios, laboratory equipment should strive to do the same.

The next round of experiments focused on the measurement of dispersed oil droplet sizes produced in the different apparatus. After several hundred measurements, it was found that in all apparatus, all oils with all dispersants resulted in the same droplet size of 30 microns VMD. This occurs when the apparatus are operated at the optimal settling time and with the optimal oil-to-water ratio, as noted above. The meaning of VMD should be explained at this point. In performing particle analysis, two measurements are obtained, particle number and size. The distribution may change from one sample to another. A distribution is a very difficult way to understand test results. For this reason scientists developed the concept of VMD, or volume mean diameter, which is a single number and is the only way to simplify the interpretation of a complex distribution. It is calculated by summing the volume of particles until the mid-point of the total volume is reached. It is the size at which half the volume of the particles are represented. Because the volume of particles goes up as the cube of particle diameter, averages or numbers of particles are meaningless. One 50 micron diameter oil particle contains more oil than 100,000 - 1 micron droplets.

The significance of the droplet-size finding is that there exists a distribution size of oil droplet sizes, 30 microns VMD as found in the experiments, which are stable and to which all oil spill dispersions will tend. The significance of this finding is two-fold. First, further measurement of sizes is meaningless since the same number is the result and second, most oil dispersions are relatively stable. The only variance noted in stability is caused by the dispersant.

Analysis of remote sensing data showed additional problems with dispersants including, herding of the oil and the direct passage of dispersant into the water column. Initial thinking was that rendering dispersants more oleophilic would cure both of these problems. Studies also began in EETD labs to examine possible formulation changes for dispersants. Early work focused on "doping" existing dispersant formulations with surfactants that would render the mixture more oleophilic. This did not result in success because, as can be seen later, dispersant technology is very critical in terms of oil/water solubility.

Investigations into the basics of surfactant technology has brought some revelations into the whole issue of dispersants and their effectiveness. Existing dispersants consist of three active ingredients or surfactants - a high HLB one typically around 15, a low HLB one, typically around 5 HLB, and an ionic surfactant whose HLB would be about 40. All of the commercial dispersants produced since 1968 have had a very similar formulation, only the solvents and specific choices of these surfactants vary. The formulation is sometimes even provided in general terms by surfactant suppliers. The formulation was first developed as a low-toxicity domestic degreasing or oil-removing formula. The logic behind choosing the two surfactants with HLB of 5 and 15 was that the different geometric configurations would cause tighter packing than would occur by the use of one surfactant alone. The second presumption is that mixing surfactants of high and low HLB can be done to produce a stable product with an average HLB of around 10. The ionic surfactant is present to give even tighter packing but its HLB is difficult to consider in designing a formulation. As later studies show, each of these assumptions is incorrect in open systems such as in the use of dispersants at sea.

One of the problems examined by a number of researchers was the herding, or pushing aside, of the oil by the dispersant. This was observed at a number of field trials and during actual applications. Before 1980 or so, most people believed that this phenomena was actually dispersants working very rapidly. Unfortunately, some people still cling to the belief. The only research on herding on open systems was done by Brown of Esso Resources who was able to quantify herding rates and velocities. Tests in the EETD laboratory showed that herding occurred at all times on thin slicks with most dispersants. Once waves were increased from 2 to 3 cm. herding ceased. Literature on the phenomenon is scarce, however early work by E. Nagy has also shown that tests of herding agents showed similar limitations. The finding is logical in that the spreading energy of a chemical is weak compared to gravity and that the two forces would be equal at a gravitational difference of 2 to 5 cm. This also explains why herding was not universally observed at spill scenes. Work done by Betcher on herding has shown that surfactants with HLB's greater than 10 do herd and that this effect increases as the HLB increases. This indicates that either the dispersant has high HLB's or that the surfactants are separating to cause herding. The latter is largely confirmed by analysis of remote sensing data at the Beaufort Sea trials which shows surfactant on the sea surface slowly separating from the slick. To confirm these hypothesis, the formulator of a major dispersant recently revealed that their herding agent has an identical surfactant as the high HLB one in the dispersant!

The solvents in the old dispersant mixtures were aromatic petroleum solvents and were quite toxic to aquatic life. After the TORREY CANYON incident, this was changed to less toxic petroleum solvents. The generation of "no mix" dispersants saw this change to butyl cellosolve and polyols. Butyl cellosolve is now regarded as a chemical with potential health problems. Improvements in dispersants could also include solvent change because the current solvents have a tendency to move the surfactants into the water rather than accommodate them to the oil.

Investigation into dispersant formulation continued with work on simple mixtures. Rendering the existing mixtures more oleophilic resulted in only slightly improved performance for lighter oils.

Significant lessons were learned about dispersant action mechanisms: that surfactant HLB is much more critical than originally thought (one surfactant family showed a high effectiveness with an HLB of 10.2, whereas the member with one more methylene group showed no effectiveness and caused the oil to form emulsion); that only surfactants with HLB of 10 showed promise, that mixtures of surfactants to yield an average HLB of 10 using high and low HLB products were not as effective as single surfactants nor did their group effectiveness indicate as high an effectiveness as would be expected; that ionic surfactants by themselves had no effectiveness and simply went into the water; and that most solid surfactants did not work , largely because they would not mix with the oil.

In 1989, a joint study with the U.S. MMS was begun to examine another phenomenon, that of the accelerated weathering caused by dispersants.[9] It was known that dispersants caused accelerated weathering of the oil, but the extent to which this might occur was not. Two series of experiments were run, the first phase using standard dispersant laboratory effectiveness apparatus, the Mackay, the Labofina and the Swirling Flask test. The method of performing the experiment was to measure oil in the water column and left on the surface so that a mass balance could be achieved. In oils not treated with dispersant all mass could be accounted for within the experimental error of about 5%. For dispersant-treated oils the loss of mass was taken as the amount lost due to accelerated weathering. This round of experiments resulted in the findings that the amount of weathering was dependent on the oil type. The amount lost from the treated oil was about half of the maximum amount lost through normal weathering on exposure for long periods of time. For a series of common oils, this averaged about 10%, but could be as much as 20% for a very light oil.

The second phase of the experiment involved analysis of both the oil in the water and the oil remaining on top by gas chromatography and compare this to the starting oil. Using chromatographic analysis, it was found that accelerated weathering again occurred to about the same percentage as found before. In addition to this, a very important discovery was made, that the composition of the oil in the water column and on the surface had compositional changes other than those caused by weathering alone. It was found more n-alkanes were taken into the water column for those chain lengths corresponding to the same chain length of the oleophilic portion of the surfactant. Surface oil was deficient in these same compounds, confirming the hypothesis that this was absorption to the oleophilic portion of the surfactant. The oil on the surface contained a higher amount of n-alkanes of longer chain lengths than did the starting oil, showing that separation of the oil does occur to a certain extent and that certain portions, eg. longer molecules, are less dispersable. These findings are significant, showing that longer-chain surfactants may be necessary to achieve greater dispersion, that surface means of measuring dispersant effectiveness means must compensate for the accelerated weathering and that there are lesser dispersable components of the oil.

The findings of the mechanism studies conducted up to 1990, can be summarized as follows:

1. That separation of mixed surfactant systems occurs,
2. That herding is limited to low wave heights, <2 to 3 cm,
3. Herding in existing dispersants is largely due to the high HLB fractions of mixed surfactant systems currently in use,
4. Dispersant use results in accelerated weathering of the oil,
5. Dispersants draw more of the oils compounds that correspond to their oleophilic chain lengths into the water,
6. That long chain lengths and perhaps other components of the oil, are dispersed less than shorter chain lengths.
7. That the droplet sizes produced by most dispersants and most oils in most apparatus may have the same size distribution

EFFECT OF TEMPERATURE, SALINITY, AMOUNT OF DISPERSANT AND MIXING TIME

The effects of a number of basic parameters on dispersant effectiveness were tested using the swirling flask apparatus operated in a normal configuration and using standard procedures except for the variance in the parameter of interest.[9] Dispersant was pre-mixed with the oil to ensure a higher degree of repeatability. All experiments were performed with Alberta Sweet Mixed Blend (ASMB) crude oil and the dispersant Corexit 9527, except where noted.

Figure 1 shows the effect of temperature on effectiveness. The temperature refers to both the temperature of the oil and the seawater. The graph shows that effectiveness rises significantly with increasing temperature. There is approximately a two-fold rise in effectiveness with a three-fold rise in temperature. A large part of this variation is due to the decreasing viscosity of the oil with temperature rise.

Figure 2 shows the effect of salinity on dispersant effectiveness. Both ASMB and Norman Wells crude oils were used with Corexit 9527 and Enersperse 700. Polynomial curves with two variables are fit to the data using a least-squares procedure. The results are consistent between the different oil/dispersant combinations. Dispersant effectiveness is at a maximum at a salinity of 40 to 45 ppt (parts-per-thousand or degrees salinity) and falls down very sharply with a decrease or increase in salinity. Freshwater effectiveness is nearly 0 for all four combinations. Separate experiments were conducted with other dispersants, including those designed for freshwater with similar results. This indicates that ionic interaction is necessary to the dispersion process, at least for the dispersants

VARIATION OF EFFECTIVENESS WITH TEMPERATURE

FIGURE 1

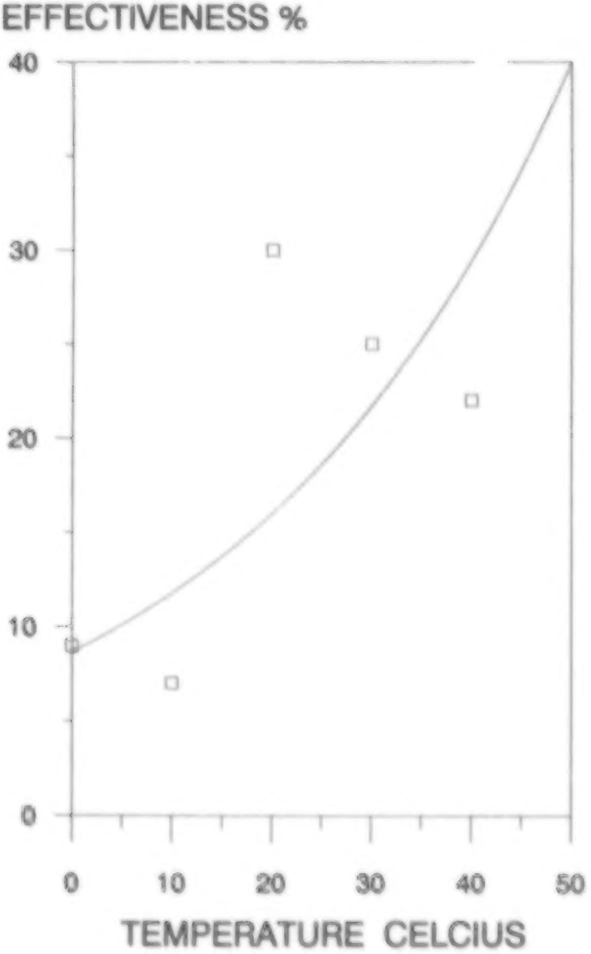

VARIATION OF EFFECTIVENESS WITH SALINITY

FIGURE 2

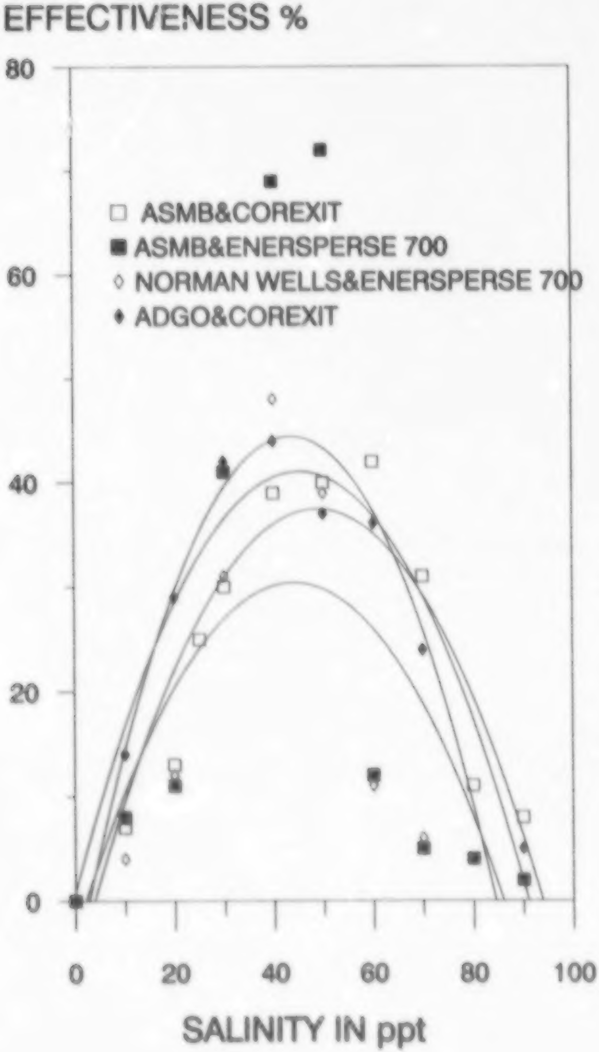

tested. The decrease in effectiveness with salinity increase above 40 ppt was unexpected, but is easily explained by the fact that the main surfactants in the products tested are non-ionic. These formulations are optimal at a moderate ionic strength.

The effect of the amount of dispersant was studied by conducting a series of experiments using differing amounts of dispersant in the oil, ASMB in every case. The ratio of dispersant to oil was varied from 1:5 to 1:60 in steps of 5 parts of oil. Results of this experiment are shown in Figure 3. The curves are logarithmic and are fitted using a least-squares methodology. The correlation coefficients for the values are very high and range between 0.90 and 0.99. The behaviour of the various dispersants are consistent, the effectiveness rapidly falls off with decreasing dispersant amount. Effectiveness approaches 0 at dispersant to oil ratios of about 1:40 to 1:60 for three commercial dispersants. Some experiment dispersants display a slightly better performance. The sharpness of the curves is somewhat a surprise and can explain the variances in observed dispersant effectiveness both in the lab and in the field. A doubling of dispersant can easily result in a doubling of effectiveness and vice versa. Loss of dispersant in an experiment can result in a very significant difference.

The effect of mixing time was investigated by running the standard swirling flask experiment for times different than the usual 20 minutes. Results of this are shown in Figure 4. Straight lines were fit to the data with high correlation coefficients. The results show that, contrary to expectations, there is no increase in effectiveness but the results are not entirely consistent. The results appear to indicate that there is probably little change in effectiveness, but that increased evaporation over the time period removes some of the oil. The conclusion is that there is little effect with increased mixing time. It is mixing energy, as has been shown by other experiments, that will increase dispersant effectiveness.

METHODS OF PREPARING CALIBRATION CURVES

The results of some tests conducted in the past year appeared to be in error and the problem was investigated. It was found that some surfactants, in particular an experimental dispersant known as BQ, produced a high degree of coloration in the extraction process. This coloration, because of the methodology used to measure effectiveness, interferes and cause the values to appear quite high.

The traditional method of measuring laboratory dispersant effectiveness is to take a small aliquot of the dispersion test water, extract the oil, usually with methylene chloride and then measure the colour at a specific wavelength. This value is compared to a standard curve and an effectiveness assigned. The preparation of the standard curve was traditionally done by injected the appropriate amount of oil directly into the methylene chloride and measuring

VARIATION OF EFFECTIVENESS WITH DISPERSANT QUANTITY

FIGURE 3

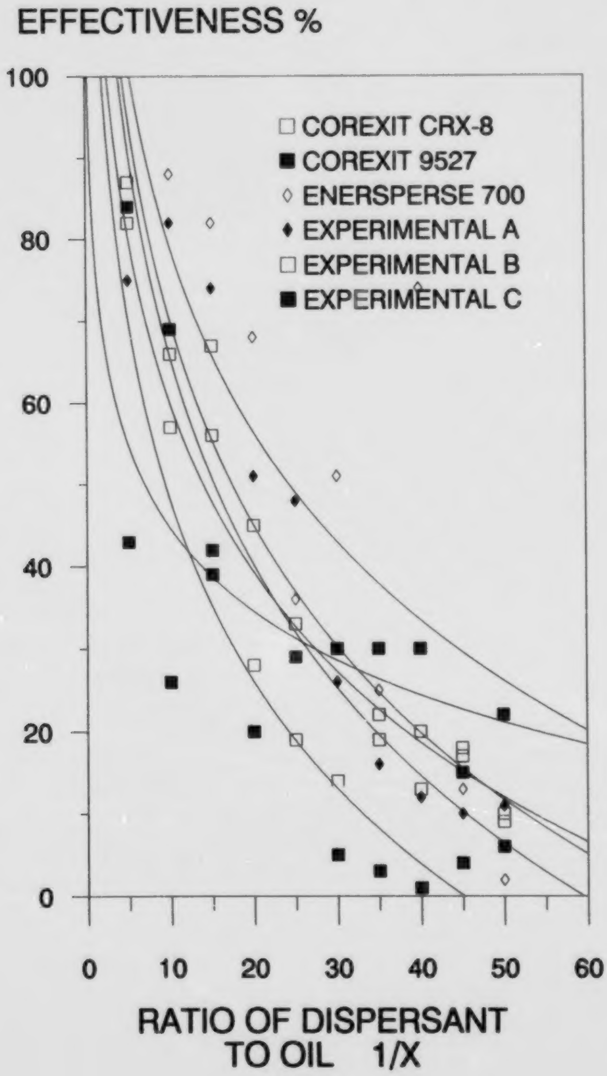

VARIATION OF EFFECTIVENESS WITH MIXING TIME

FIGURE 4

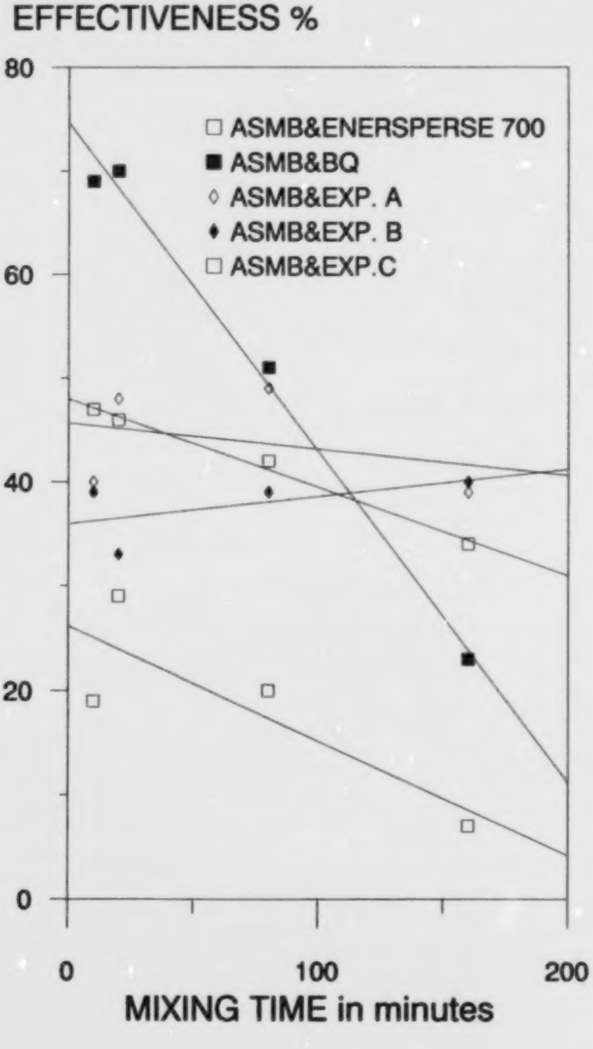

colour density. When the swirling flask test was developed, it was found that the traditional approach of preparing standard curves was somewhat in error because the simple addition of water to the extraction process produced some coloration in the methylene chloride. This results in inflated effectiveness values. The protocol for the swirling flask effectiveness overcomes this error by using a standardization procedure that is directly analogous to the actual extraction procedure. This cancels the effect that sea water alone can have on the results.[8] Also, the protocol calls for colorimetric measurements at three separate wavelengths (340, 370 and 400 nm) to overcome errors caused by the lack of resolution of the spectrometer.

The effect of the dispersant on the calibration procedure was tested but was not included because the commercial dispersants tested did not show a significant effect. However, the reinvestigation of this in recent times has shown that some surfactant mixtures will result in high colorations of the methylene chloride causing high and incorrect dispersant effectiveness. Table 3 gives summary values of some experiments conducted to investigate calibration procedure.

Table 3 EFFECT OF CALIBRATION PROCEDURES ON EFFECTIVENESS VALUES

Oil/Dispersant	EFFECTIVENESS IN PERCENT AS GIVEN BY EACH CALIBRATION PROCEDURE			
Combination	TRADITIONAL (direct oil)	STANDARD (water corrected)	STANDARD + (water & dispers.)	CORRECTION (dispersant alone)
ASMB + BQ	60	46	29	27
ASMB + Corexit		33	31	33
Issungnak + BQ	65	46	21	22
Issungnak + Corexit			22	22
Norman Wells + BQ	75	57	31	33
Syncrude + BQ		40	27	30

The means for performing each form of calibration is as follows. The "traditional" method, not generally used by Environment Canada, consists of adding the correct amount of oil directly to the extract, usually methylene chloride. The method does not compensate for coloration caused by the sea water or the dispersant. The "standard" method refers to the method published for the swirling flask apparatus in which the standard curves are prepared in a manner analogous to the actual extraction procedure. This method compensates for the coloration caused by the water and losses incurred during the extraction procedure. The next method given in Table 3 is referred to as "standard +" and consists of applying the standard procedure plus adding the dispersant premixed in proportion to the actual test (1:25, dispersant to oil). This method directly compensates for dispersant coloration but would require that a complete calibration curve be prepared for every oil/dispersant combination. The final method is to correct the standard curve by compensating for the dispersant. This is accomplished by running a calibration experiment without oil but with the dispersant.

Colorimetric readings are taken and subtracted from the ultimate experimental results. This method has the advantage that a correction is achieved for each dispersant without having to draw up an entire calibration curve. As can be seen from the table, this method yields results similar to the procedure of preparing an entire calibration curve but is much simpler.

The results in Table 3 show that the dispersant BQ yields much higher dispersant effectiveness than is correct. The dispersant BQ requires correction for the coloration it produces by itself. The dispersant Corexit 9527 does not appear to yield such errors. The few values done by the traditional method indicate that this does not yield satisfactory results because large amounts of coloration are not compensated for.

Given that a dispersant itself can be run through the calibration procedure and a correction value derived, this procedure should be followed with all new dispersants to ensure that true effectiveness values are measured.

SUMMARY RESULTS OF RECENT STUDIES

The recent studies can be summarized as follows:

1. The effect of temperature is largely the result of changing viscosity. The higher the temperature, the greater the effectiveness,

2. Dispersants are most effective at a salinity of about 40 ppt. Dispersant effectiveness rapidly decreases when salinity is increased or decreased. Freshwater effectiveness of present-day dispersants is very low,

3. The amount of dispersant is very important to effectiveness. Effectiveness falls to nearly 0 for a light oil at a dispersant to oil ratio between 1:40 and 1:60,

4. Mixing time has little effect on effectiveness, and

5. Calibration procedure for laboratory dispersant effectiveness tests is important. Calibration procedure must include contact with water in a manner analogous to the extraction procedure itself. Failure to include this procedure results in inflated effectiveness values. Compensation for the coloration produced by the dispersant alone is important for some dispersants only. A separate calibration curve for each oil/dispersant combination is an accurate way of performing the compensation but is very time-consuming. Compensation can by performed simply by running a dispersant blank through the calibration procedure.

REFERENCES

1. Fingas, M., "Dispersant Effectiveness at Sea: A Hypothesis to Explain Current Problems With Effectiveness", Proceedings of the Eleventh Annual AMOP Technical Seminar, Environment Canada, Ottawa, Ontario, p. 455-479, 1988.

2. Fingas, M.F., "Field Measurement of Effectiveness: Historical Review and Examination of Analytical Methods", Chemical Dispersants - Countermeasures For the 90's, M. Flaherty, Ed., ASTM 1084, American Society for Testing and Materials, Philadelphia, pp. 157-178, 1989.

3. Brown, H.M. and Goodman, R.H., "Dispersant Tests in a Wave Basin", Proceedings of The Eleventh AMOP Technical Seminar, Environment Canada, Ottawa, Ontario, p. 501-514,1988.

4. Goodman, R.H. and Fingas, M.F., "The Use of Remote Sensing in The Determination of Dispersant Effectiveness", Proceedings of The Eleventh AMOP Technical Seminar, Environment Canada, Ottawa, Ontario, p. 377-384, 1988.

5. Nichols, J.A. and Parker, H.D., "Dispersants: Comparison of Laboratory Tests and Field Trials with Practical Experience at Spills", Proceedings of the 1985 Oil Spill Conference, American Petroleum Institute, Washington, D.C., p. 421-427, 1985.

6. Burke, E., and R. Golob, "Dispersant Usage in Historic Oil Spills", Proceedings of the Conference on Oil and Chemical Spills, Hazardous Material Research Institute, Rockville, Maryland, p.75-83, 1980.

7. Fingas, M.F., M.A. Bobra and R.K. Velicogna, "Laboratory Studies on the Chemical and Natural Dispersability of Oil", Proceedings of the 1987 Oil Spill Conference, American Petroleum Institute, Washington, D.C., p. 241-246, 1987.

8. Fingas, M.F., D.L. Munn, B. White, R.G. Stoodley and I.D. Crerar, "Laboratory Testing of Dispersant Effectiveness: The Importance of Oil-to-Water Ratio and Settling Time", Proceedings of the 1989 Oil Spill Conference, American Petroleum Institute, Washington, D.C., pp. 365-363, 1989.

9. Fingas, M.F., M. Di Fruscio, B. White and E. Tennyson, "Studies on the Mechanism of Dispersant Action: Weathering and Selection of Alkanes", in Proceedings of The Twelfth Arctic and Marine Oil Spill Seminar, Environment Canada, Ottawa, Ontario, pp. 61-89, 1989.

AIR JET ATOMIZATION AND BURNING OF OIL SLICKS

R.C. BELORE AND CHRIS SEELEY
S.L. ROSS ENVIRONMENTAL RESEARCH LIMITED

ABSTRACT

This paper describes laboratory scale evaluations of air jet atomization of oil slicks and the testing of a full scale burner provided by the Environmental Emergencies Technology Division. The original work statement included the testing of ultrasonic oil atomization transducers but initial testing revealed that the transducers provided could not handle the power input required to effectively atomize oil. The project was then modified to address only the use of air jet atomization of oil.

The small scale testing of air jet atomizers revealed that the air jets must operate at or above the water-oil interface to eliminate excessive water uptake. The nozzle type (blunt or conical) had little effect on the oil atomization rate. Maximum oil uptake was achieved using the larger nozzle diameters.

A total of 27 full scale burn tests were completed which evaluated the effect of air pressure, nozzle position and oil type on burn rates and cleanliness. The results indicate that a clean burn is possible only if the air nozzles are placed at or above the water-oil interface. Burn rate was not affected by the nozzle pressure or air flow rate but the burns were clean only at the highest air flows used.

SMALL SCALE TESTING OF AIR JET ATOMIZATION

Figure 1 illustrates the experimental set up used to evaluate the air jets. The tank used was 1.9 m in diameter and 0.3 m deep. Oil was contained on the water surface above the air jets with a floating containment ring 0.5 m in diameter. The air jet nozzles were held in place using a simple stand placed in the tank which allowed for vertical adjustment of the nozzle position. Air was provided to the nozzle via a (560 watt 3/4 horsepower) compressor, pressure tank and pressure regulator. The most difficult aspect of this phase of the study was the collection of the product generated by the air jets. After several failed

FIGURE 1 Small Scale Test Apparatus

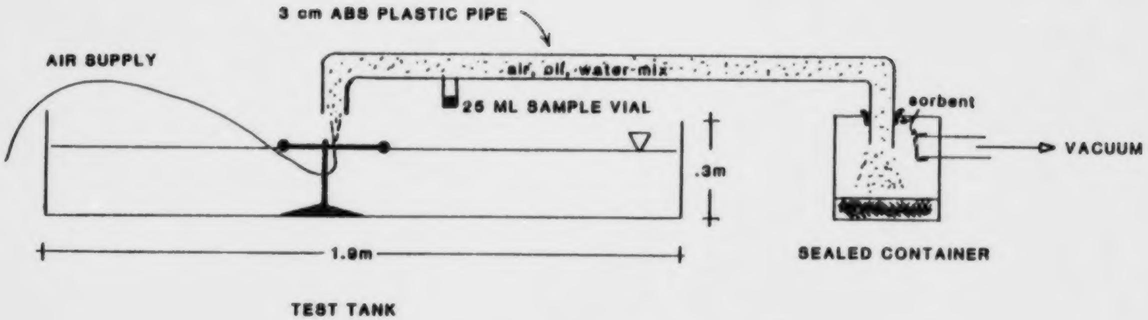

attempts the arrangement seen in Figure 1 was finally used in the testing. The primary problem encountered in collecting the liquid product was in venting the high volume of air being pushed by the atomizing nozzles without losing the atomized oil entrained in the air.

Forty-one tests were conducted using various combinations of 4 nozzles (2 blunt, 2 conical), 3 nozzle depths, three oil depths and 3 air pressures. The results seen in Table 1 indicate the following basic trends.

i) For nozzle depths greater than 2 cm below the water surface atomization of oil was impractical since the water content of the product was frequently greater than 90%. Little "atomization" occured; instead, a spout of water was formed regardless of nozzle type or diameter.

ii) When the nozzles were positioned 2 cm below the water-oil interface atomization occurred but water contents were again generally in the 80-100% range for the collected product. Oil recovery rates were significant in this position but it would appear that for an effective burn to occur the nozzles would have to be operating at the oil water interface to eliminate excessive water uptake.

iii)When the nozzles were operated at the oil-water interface water uptake was about 50% for 0.5 mm slicks dropping to 10% or less for the 2 and 4 mm slicks. Changing the nozzle type (conical vs. blunt) appeared to have little effect on oil recovery rate. Larger diameter nozzles increased the recovery rate as did a drop in pressure from 275 to 200 to 140 kPa. This is likely due to a lower velocity air jet and its ability to "pull" oil to the main air stream rather than just "punch a hole" through the oil/water interface. Maximum oil uptake rates, with the tested configuration, were about 54 l of oil per hour per nozzle.

Based on these tests it appeared that the air atomization technique would have greatest merit for thick oil slicks where the air jet nozzle could be held within the thick oil.

TABLE 1:
AIR ATOMIZATION LAB SCALE EXPERIMENTAL RESULTS

Nozzle Data	Test #	Pressure (kPa)	Depth of Nozzle (mm)	Depth of Oil (mm)	Height Spray (cm)	Water in Product (%)	Total (g/s)
#4C*	1	275	20.5	0.5	>195	91.67	9.743
ID=3mm	2	275	22.0	2.0	>195	89.58	11.763
OD=5mm	3	275	24.0	4.0	>195	40.91	64.671
#4C	5	275	0.5	0.5	>195	45.83	3.519
ID=3mm	6	275	2.0	2.0	>195	7.14	18.350
OD=5mm	7	275	4.0	4.0	>195	2.40	6.318
#1B+	8	275	0.5	0.5	>195	50.00	5.072
ID=2mm	9	275	2.0	2.0	>195	43.75	4.191
OD=8-12mm	10	275	4.0	4.0	>195	6.52	6.472
#1B	11	275	80.5	0.5	35	96.00	
ID-2mm	12	275	82.0	2.0			
OD=8-12mm	13	275	84.0	4.0			
#1B	14	275	40.5	0.5	80		
ID=2mm	15	275	42.0	2.0			
OD=8-12mm	16	275	44.0	4.0			
#1B	17	275	20.5	0.5			
ID=2mm	18	275	22.0	2.0			
OD=8-12mm	19	275	24.0	4.0			
#1B	20	275	10.5	0.5	>140	95.83	2.582
ID=2mm	21	275	12.0	2.0	>165	47.83	28.966
OD=8-12mm	22	275	14.0	4.0	>165	40.00	39.344
#3C	23	275	0.5	0.5	>195	65.38	4.053
ID=3mm	24	275	2.0	2.0	>195	30.43	25.805
OD=7mm	25	275	4.0	4.0	>195	6.25	41.747
#3C	26	275	0.0	0.5	>195		
ID=3mm	27	275	0.0	2.0	>195		
OD=7mm	28	275	0.0	4.0	>195	0.00	1.000
#3C	29A	275	20.5	0.5	>195	96.00	6.058
ID=3mm	29B	275	22.0	2.0	>195	96.00	4.785
OD=7mm	29C	275	24.0	4.0	>195	84.00	21.020
#2B	30	275	0.5	0.5	>190	52.17	3.956
ID=6mm	31	200	0.5	0.5	>165	55.00	4.941
OD=9mm	32	140	0.5	0.5	>165	27.78	12.418
#2B	33	275	2.0	2.0	>195	4.35	19.941
ID=6mm	34	200	2.0	2.0	>180	7.89	12.725
OD=9mm	35	140	2.0	2.0	>165	3.75	14.347
#2B	36	275	4.0	4.0	>195	27.78	11.038
ID=6mm	37	200	4.0	4.0	>195	5.79	16.794
OD=9mm	38	140	4.0	4.0	>195	1.09	24.683
#2B	39	275	20.5	0.5	>195	100.00	0.000
ID=6mm	40	275	22.0	2.0	>165	80.00	20.793
OD=9mm	41	275	24.0	4.0	>190	65.38	28.058

* conical nozzle

+ blunt nozzle

FULL-SCALE BURNS

Experimental Set-up

The full-scale burn experiments were conducted in a 10 metre x 5 metre above ground swimming pool filled with approximately .75 metres of water. The burner was held above the tank using two 50 mm x 75 mm x 5 mm steel box beams. The air jets were mounted on a submerged frame which was suspended from the sides of the burner. Photos 1 and 2 show the general experimental setup. Oil was held under the burner using a square retaining ring (1.4 m x 1.4 m) constructed from 10 cm x 10 cm and 5 cm x 15 cm lumber. Oil was placed inside the ring by pouring it onto a small spill plate floating inside the ring. Ignition was accomplished by simply igniting the atomized oil with a propane torch attached to the end of an extension handle. This torch was initially mounted in the throat of the burner chimney and ignited remotely via a standard propane barbecue piezo-electric sparking device but this system proved to be unreliable so it was abandoned after the first test. Air was supplied to the atomization nozzles via a large diesel powered air compressor capable of delivering approximately 1 m^3/s at 690 kPa. The air line from the compressor was fed to a manifold connected to five pressure regulators and electronically controlled valves (see Photo 3). From these valves 6 mm diameter air lines were passed underwater to the air nozzles mounted below the burner. The nozzles used were 6 mm diameter brass tubes fitted into the flexible hosing. The cleanliness of the burns was measured by videotaping each test and by taking light measurements of a standard grey card (18% reflectance) and the smoke plume. The reflectance technique was adapted from Comfort, 1989.

The reflectance of the smoke plume was measured using a hand held light metre and a Gray Card (of 18% reflectance). The luminance of both the plume and the card were measured for each test. The reflectance of the plume was then calculated as follows:

Photo #1: Burner assembly mounted above tank

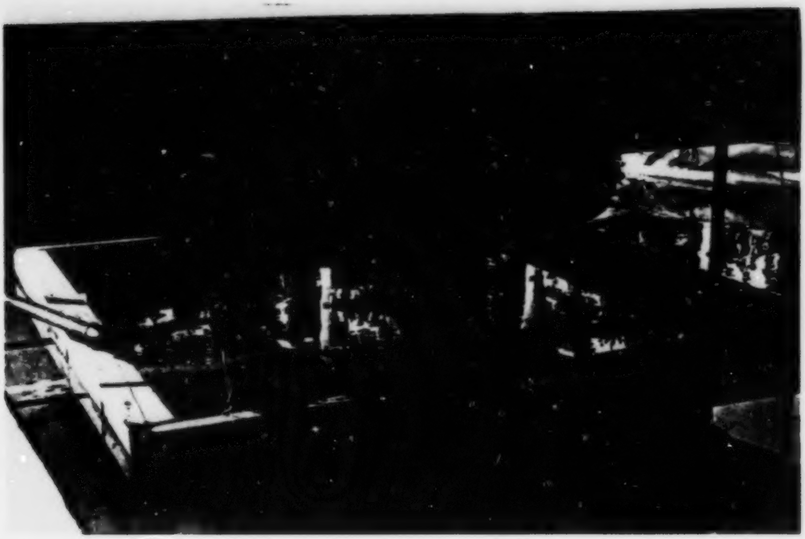

Photo #2: Air Jet array and oil containment zone

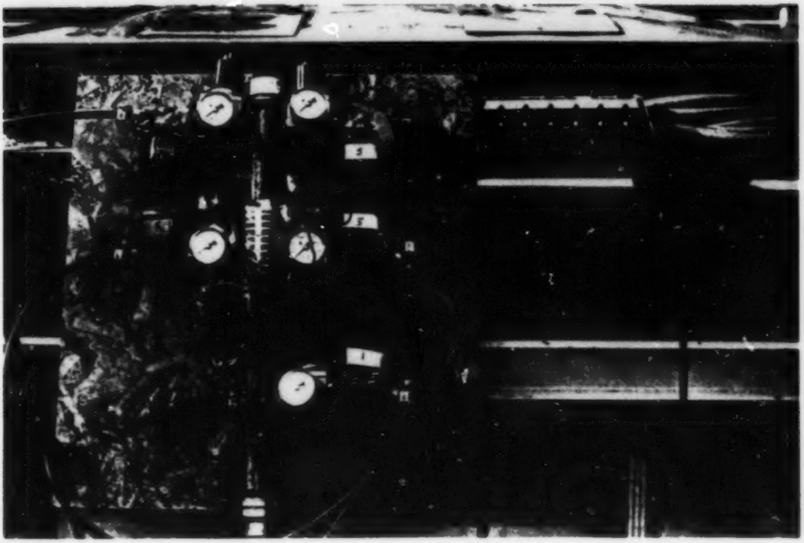

Photo #3: Pressure regulators, electric valves and control box

$$\text{Plume Reflectance} = \frac{\text{Grey Card Reflectance (18\%) x Plume Luminence}}{\text{Card Luminance}}$$

These data were then related to standard smoke densities by measuring the reflectance of the grey shades from the standard density chart. These data are summarized in Table 2 from Comfort, 1989.

TABLE 2
REFLECTANCE OF SMOKE DENSITY CHART

Density	Spotmeter Reading		Reflectance
	#	EV (Foot-Lamberts)	Luminance
	1	10.5	5068%
	2	9.9	4055%
	3	9.5	2940%
	4	8.7	1824%
	5	8.1	1115%

Experimental Procedure

The general method followed for each test was as follows:

i) the air pressure was adjusted to the required setting with the nozzles in operation to account for un-equal pressure distribution and pressure drops in the distribution manifold;

ii) the appropriate quantity of oil was placed in the retaining ring;

iii)a grey card reflectance light reading was taken;

iv) the video camera and timer were started;

iv) the video camera and timer were started;

v) the air jets were turned on;

vi) the oil was ignited and time of ignition recorded;

vii)the reflectance of the resultant smoke plume was measured;

viii)35 mm photos of the burn were taken;

ix) the time of extinction of the burn was recorded; and

x) the air jets and video camera were turned off.

Test Results

The primary objective of the burning tests was to identify operating parameters which would result in clean burns. Burn rates and burn efficiency (visual only) were also recorded throughout the testing. A total of 27 tests were completed; the test conditions and results are summarized in Table 3; smoke density estimates are summarized in Table 4. A video tape of all tests has been provided to the scientific authority.

TABLE 3

FULL SCALE BURNER TEST RESULTS

Test	Oil Type	Oil Volume (litres)	Thick	No. Nozzles	Height of Nozzle Above Water (mm)	Nozzle Diameter (mm)	Air Pressure kPa	Start Burn	Stop Burn	Length	Comments
1	fresh crude	50	2	5	0	6	varied	1:13	7:55	6:42	chimney didn't function; pool burned out of control
2	fresh crude	5	2	5	0	6	200	2:43	4:03	1:20	started clean; turned dirty
3	fresh crude	5	2	5	0	6	200	0:49	1:45	1:04	clean 1st half then dirty
4	fresh crude	5	2	3	0	6	200	1:15	2:14	:59	dirty burn
5	fresh crude	5	2	5	0	6	200	1:26	2:30	1:04	cleaner than run #4
6	fresh crude	5	2	0	0	– –	– –	8:30	9:34	1:04	dirty but with flames out top
7	fresh crude	5	2	5	0	6	140	1:15	2:12	:57	camera not on
8	fresh crude	5	2	5	0	6	140	1:48	2:48	1:00	very dirty
9	fresh crude	5	2	5	0	6	275	1:37	2:25	:48	cleaner burn
10	fresh crude	10	4	5	0	6	275	6:55	8:12	1:17	very dirty
11	fresh crude	5	2	5	0	6	600	1:45	2:40	:55	initial white plume then cleaner; no video
12	fresh crude	5	2	5	0	6	600	1:06	1:56	:60	initial white plume then cleaner
13	fresh crude	5	2	5	– 10	6	600	1:55	N/A	N/A	incomplete burn, emulsion and dispersion formed
14	burn residue from above										
	fresh crude	4		5	0	6	600	1:23	N/A	N/A	incomplete burn again
15	fresh crude	5	2	5	0	1 x 8	275	1:21	2:16	:55	still poor burn; nozzles moved to 4 mm above water
16	fresh crude	5	2	5	4	1 x 8	275	1:15	2:30	1:15	cleaner with periods of white smoke
17	fresh crude	5	2	5	4	1 x 8	600	1:29	2:30	:56	very clean orange flame
18	fresh crude	5	2	5	4	1 x 8	415	1:05	1:47	:42	clean with a few puffs of black smoke
19	diesel	5	2	5	4	1 x 8	415	1:15	2:20	1:05	clean orange flame
20	diesel	5	2	5	4	1 x 8	600	1:10	2:10	1:00	very clean
21	diesel	5	2	5	4	1 x 8	275	1:08	2:20	1:12	dirty burn
22	weathered crude	5	2	5	4	1 x 8	275	1:45	3:10	1:25	clean with slight trace of smoke
23	weathered	5	2	5	4	1 x 8	415	1:48	2:55	1:07	very clean
24	weathered	5	2	5	4	1 x 8	600	1:58	2:53	:55	same as 60 psi test
25	weathered	10	4	5	4	1 x 8	600	1:50	3:20	1:30	clean burn
26	weathered	15	6	5	4	1 x 8	600	2:40	4:40	2:05	clean burn
27	weathered	15	6	5	4	1 x 8	600	2:25	4:00	1:35	clean burn; chimney glowed red

TABLE 4

SMOKE DENSITY ESTIMATES BY LIGHT METER READINGS

Test	18% Reflectance Grey Card		Plume		Plume Reflectance %	Smoke Density	Smoke Observations
	Spotmeter	Luminance	Spotmeter	Luminance			
1	Not Taken						
2	Not Taken						
3	20	1067	20	1067	18	5	initially clean then very dirty
4	19.5	754	19.25 – 20	634 – 1067	15 – 25	4 – 5	very dirty
5	19.33	670	20	1067	29	4	cleaner than run #4
6	17.66	211	19	533	46	2 – 3	dirty with flames out top
7	20.33	1341	18.33 – 19	335 – 533	4.5 – 7	5	very dirty
8	19.33	670	16.33 – 19	84 – 533	2 – 14	5	very dirty
9	18.5	377	19 – 19.5	533 – 754	25 – 36	3 – 4	cleaner burn
10	Not Taken						very dirty
11	18.33		19 – 20	533 – 1067	29 – 57	2 – 4	initial white smoke then cleaner
12	19	533	20	1067	36	3	initial white smoke then cleaner
13	Not Taken						
14	Not Taken						
15	Not Taken						
16	17	133	17.5 – 18.5	189 – 377	25 – 51	2 – 4	clean with periods of white smoke
17	17.33	168	19	533	57	2	very clean: orange flame
18	16.5	94	17.5 – 18.3	189 – 328	36 – 63	1 – 3	clean with few puffs of black smoke
19	14.66	26	18	267	180	1	clean orange flame
20	14.33	21	17	133	114	1	very clean
21	14.33	21	14 – 15.5	16.7 – 47	14 – 40	3 – 5	dirty burn
22	17.5	189	19	533	51	2	clean with slight trace of smoke
23	17.6	211	19.5	754	64	1	very clean burn
24	18	267	19.33	670	45	3 – 4	very clean: same as 23
25	18	287	19	533	36	3	very clean
26	18	267	19	533	436	3	very clean
27	18	267	19	533	436	3	very clean: chimney glowed red

* by manufacturers calibrations luminance $= 266.7 \times 2^{(\text{Spotmeter Value} - 18)}$

In the first test the bottom of the chimney was located approximately 0.3 metres (1 ft.) from the water's surface and 50 litres of oil were placed in the containment zone (this resulted in a slick thickness of 2.5 cm). The atomized oil was ignited with the propane torch mounted inside the throat of the chimney but the fire rapidly spread to the entire pool. The chimney did not function properly in this orientation and the fire simply burned out the downwind side of the burner platform. The extensive heat generated by this burn eventually resulted in the melting of a portion of the pool liner to the waterline and more significantly in the failure of the downwind steel support. This steel beam became pliable with the heating and bent under the weight of the burner resulting in the downwind side of the burner dropping approximately .15 metres (6 inches) as seen in Photo 4. This beam was replaced and the chimney base lowered to within 0.15 metres (6 inches) of the water surface for the remaining burns. In this configuration the chimney operated properly and funnelled all flames up the chimney. For the remaining tests a smaller oil volume was also used to reduce the risk of support failure.

Tests 2 through 6 were carried out to determine the effect of the number of nozzles on burn cleanliness. Oil thickness (2 mm), type (fresh crude) and nozzle operating pressure (200 kPa) were kept constant. Reducing the number of nozzles operating (from 5 to 3 to zero) resulted in a progressively dirtier burn. The burn duration and quantity of burn residue were essentially identical for all of these tests regardless of the air jet nozzles.

Tests 7 to 9 investigated the effect of nozzle pressure on the burn cleanliness by operating at 140 and 275 kPa and keeping all other parameters constant. It was evident from these burns that the higher pressure resulted in cleaner burns. In test 10 the oil volume was doubled and the jet pressure set to 275 kPa. The burn was essentially the same as test 9 with the exception of a slightly longer burn time as would be expected. The oil thickness did not appear to affect the cleanliness of the burn.

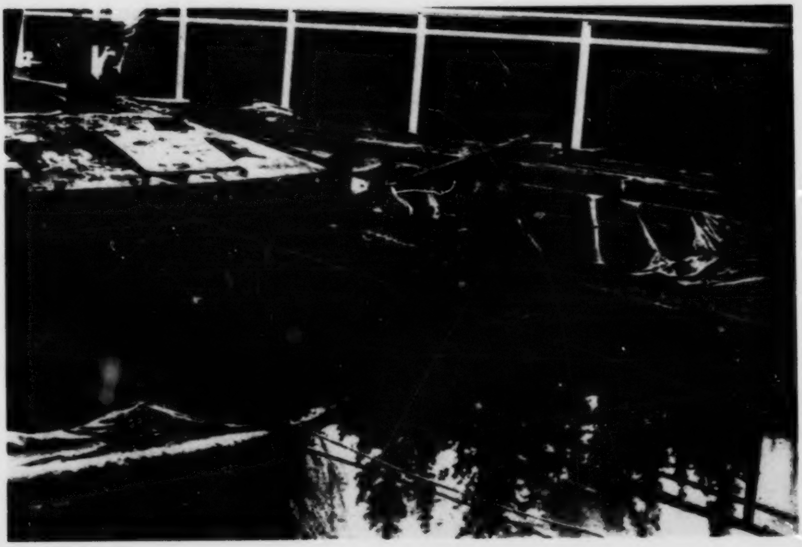

Photo #4: Test facility after first burn

In tests 11 and 12 the jet pressure was increased to the maximum possible (550-620 kPa depending on nozzle) with the compressor being used. The resulting burn was essentially smoke free.

For test 13 the nozzles were submerged to a position about 1 cm below the water/oil interface and the jets operated at the maximum pressure. This resulted in a very dirty burn and the formation of a water-in-oil emulsion which did not burn fully. Considerable product remained after the fire extinguished.

The nozzles were then moved back to the water surface and four litres of fresh crude were added to the burn residue. Again the burn was not efficient (test 14) and left considerable residue. This residue was then removed, the nozzles pinched to increase the jet velocity at a given pressure and fresh oil added. Test 15 again was inefficient so the nozzles were moved up slightly above the water surface (4 mm) for test 16 which burned much cleaner. The primary observation to be made from tests 13 through 15 is that it is very critical that the air jet nozzles be mounted slightly above the water surface to eliminate excessive water uptake and oil emulsification.

Tests 16, 17 and 18 investigated the burn efficiency of the modified jets (brass tubes were pinched to a 1 mm wide by 8 mm long slot and mounted slightly above the water surface) with variation in air supply pressure. This increased the average air velocity at the orifice by a factor of 3.3. At 275 kPa the burn was generally clean with periodic puffs of dark smoke . At 600 kPa the burn was very clean with light orange flames eminating from the chimney. At 415 kPa the burn was clean but the flames were a darker orange in colour indicating a cooler burn.

Tests 19 to 21 were a repeat of the operating conditions of tests 16 to 18 with diesel fuel. The results were essentially identical to the fresh crude oil tests.

Tests 22 to 24 used Ontario light crude oil weathered by bubbling air through a diffuser, placed in the bottom of a 1/3 full barrel, at 270 kPa for 4 hours. The viscosity of the weathered oil was 27 cp compared to 23 cp for the fresh crude. Again the burns behaved very similar to the fresh crude and diesel with the exception that the 415 kPa burn was generally as clean and hot as the 600 kPa test.

The final three tests (25-27) investigated the effect of oil thickness on the burn efficiency. The burns were conducted at maximum pressure for 2 and 3 times the oil thickness of the previous tests. Burn cleanliness and efficiency were not affected by the oil thickness. In the final burn (test #27) the burner chimney glowed red indicating the hottest burn of all the tests which were conducted.

The results of the spotmeter readings of the grey card and smoke plume indicate that the method has some merit for estimating smoke plume density. In general, lower smoke densities were recorded by this method for those runs where the burn was observed to be cleaner. Unfortunately, the method also estimated smoke densities of up to level 3 for very clean "smokeless" burns; see tests 24 to 27.

CONCLUSIONS

i) Submerged air jets resulted in high water:oil ratios in the small scale testing and poor burns in the large scale testing.

ii) Nozzle shape appeared to have little effect on oil atomization rates in the small scale testing.

iii)Larger diameter nozzles and lower pressures increased the oil atomization rates in the small scale testing. These conditions also reduced the burn cleanliness in the large scale tests. This may suggest that higher oil volumes were being supplied to the burner under these conditions thus resulting in an incomplete combustion. However, this theory is not supported by the burn durations which were essentially identical for all tests with similar initial oil volumes.

iv)The burner did not function properly when positioned 0.6 metres above the water. In this position the chimney was not able to draw in enough air to direct the flames and smoke through the burner.

v) Clean burns were achieved using the large scale burner when it was placed within .15 metres of the water surface, all 5 air jets were operated at supply pressures of 415 kPa or greater, and the nozzles were placed at or slightly above the water's surface.

vi) Only a small quantity of burn residue was left at the end of each burn (approximately 50 mLs) with the exception of the test with the submerged air jets. When the jets were submerged, a dirty, incomplete burn resulted along with the formation of a water-in-oil emulsion.

vii)The oil pool immediately under the burner ignited and burned during the testing. Fire can spread to areas outside the influence of the burner if oil thicknesses in its vicinity exceed about 1 mm. This would cause severe safety problems and result in unclean burning around the burner. If the oil in the vicinity of the burner is less than 1 mm very little oil would be removed by the burner.

viii)The burner could be placed at the apex of a fireproof boom for clean burning of collected oil at a burn rate of 5 L/min.

ACKNOWLEDGEMENTS

This work was funded by the United States Department of the Interior, Minerals Management Service and Environment Canada, Environmental Emergencies Technology Division.

REFERENCES

Comfort, G. 1989. Tests to Evaluate the Effect of a Waterjet Barrier on the Burning Efficiency of a Floating Oil Slick. Environment Canada Report EE-112.

CONTAINED CONTROLLED BURNING OF SPILLED OIL DURING THE EXXON VALDEZ OIL SPILL

By

Alan A. Allen
Spiltec
Anchorage, Alaska

ABSTRACT

During the evening of the second day following the Exxon Valdez oil spill, an estimated 15,000 to 30,000 gallons (57,000 to 114,000 liters) of North Slope crude oil were eliminated using in-situ combustion techniques. The oil was collected with 3M's FIRE BOOM towed in a U-configuration behind two fishing boats. Working with 500-foot- (152-meter-) long tow lines, a 450-foot - (137-meter-) long boom was moved at about 1/2 to 1 knot (0.26 to 5.2 meters/second) through slightly emulsified oil patches in the downwind region of the spill. Once oil had filled the downstream portion of the "U", and the boats were clear of any surrounding slicks, a gelled-fuel igniter was released from one of the tow boats. Shortly after ignition, flames gradually spread out over the entire area of the contained oil. As flames reached 200 to 300 feet (61 to 91 meters) into the air, the area of the contained oil layer (and therefore the size and intensity of the fire) could be controlled by adjusting the speed of the vessels. The total burn time was approximately 1 hour and 15 minutes; however, the intense part of the burn lasted for about 45 minutes. Using several methods to estimate the volume of oil collected, this volume (likely between 15,000 and 30,000 gallons) resulted in approximately 300 gallons (1,136 liters) of stiff, taffy-like burn residue that could be picked up easily upon completion of the burn. The controlled elimination of crude oil therefore resulted in an estimated 98% or better efficiency of burn.

OIL COLLECTION

During the afternoon of Saturday, March 25, 1990, 500 feet (152 meters) of 3M FIRE BOOM were loaded aboard two fishing vessels, the Midnight Sun and the Sea Ruby. Both vessels left the dock at the Alyeska Valdez Marine Terminal at approximately 1423 and headed south out of the Port Of Valdez Alaska. Shortly after the vessel left the terminal, word was received over the radio that permission had been granted to conduct a burn test in the area generally off the mouth of Fidalgo Bay. At approximately 1800, a spotter helicopter from Alyeska Pipeline Service Company flew over and directed the operations to a location approximately 5 to 7 miles (8 to 11 kilometers) west of Goose Island (Figure 1). It was felt that thick oil patches could be intercepted there and that clear open waters could also be found nearby so that the contained oil could be burned at a safe distance from any surrounding oil layers.

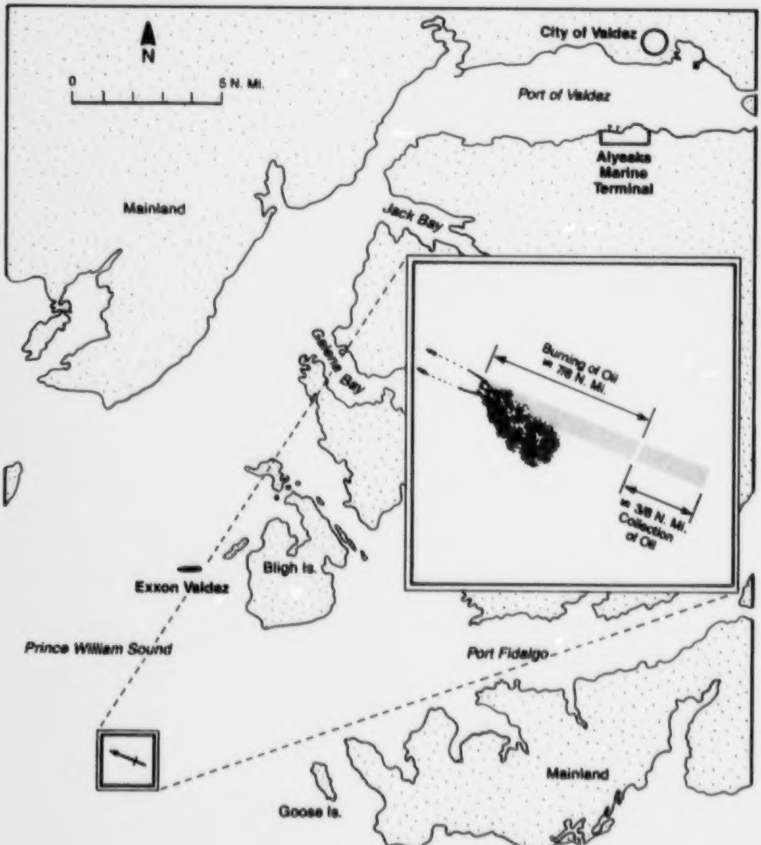

FIGURE 1 Approximate Location of Test Burn

At about 1845 the FIRE BOOM was deployed and taken under tow behind one of the fishing boats. The boom was accidentally jerked into motion, causing damage to one of the leading boom sections. Within minutes, one 50-foot (15.3-meter) section of boom had been removed, leaving 450 feet (137 meters) of boom for containment of oil in the designated collection area. After the boom was placed in a U-configuration, it was towed at about 3/4 knot with an opening between the two tow boats of approximately 100 to 130 feet (30 to 40 meters). Figure 2 illustrates the 3M FIRE BOOM configuration and the nature of the oil during the oil collection phase of the test burn.

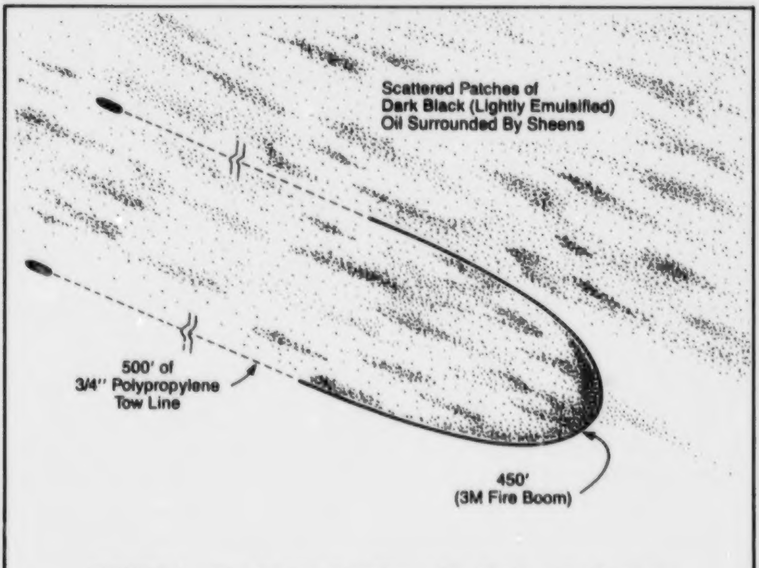

FIGURE 2 Fire Boom Configuration During Collection

After the boom was towed through scattered oil slicks for about 1/2 hour (about 2010), a decision was made to attempt a burn of the collected oil. It was dark upon completion of the oil collection phase; however, it could be seen with the vessel's spot lights that the waters forward of the towing boats were relatively free of any oil.

During the oil collection phase, sorbents were dipped periodically into the oil passing between the tow boats to assist with a very rough approximation of the average thickness of the oil It was felt that the average oil thickness was probably on the order of a hundredth to several hundredths of an inch (0.3 to 1 mm). In places, the patches of oil nearly filled the space between the tow boats and appeared to be close to a tenth of an inch (2 to 3 mm) in thickness (or more). Before any ignition of the oil was attempted, it was estimated that the oil encounter rate could easily approach several hundred gallons/minute (i.e., well over 1,000 liters/minute). Since oil had been collected for about 1/2 hour, it was believed that the volume of oil contained within the boom could be on the order of 10,000 gallons (approximately 38,000 liters) or more.

OIL IGNITION

Plans had been made to ignite any captured oil using a Helitorch (inset of Figure 3). However, because of darkness, it was felt that ignition should be attempted using a hand-held igniter. A small plastic bag of gelled gasoline (approximately 1/2 liter of fuel and a handful of Sure Fire gelling mix) was prepared and ignited, and then allowed to float back into the oil within the boom. The ignition of the contained crude oil required several minutes because of the single point-source igniter. Had the Helitorch been used, numerous ignition points could have been spread throughout the contained oil, thus providing a much more efficient heating and ultimate ignition of the oil.

Samples of the oil prior to ignition were not retained; however, the crude oil did have the color and consistency of a lightly emulsified oil layer (perhaps 20% to 30% water-in-oil). The floating patches of oil collected with the FIRE BOOM had been on relatively calm seas for an estimated 30 to 40 hours.

The gradual spread of flame over the entire surface area of the contained oil was very slow at first. Within approximately 10 to 15 minutes, however, the fire was big enough to accelerate the breakdown of emulsions and the release of volatile vapors over most of the contained oil. By the time the fire reached the entire region of contained oil, flames were already reaching more than 150 to 200 feet (45 to 60 meters) into the air. At the stern of each towing vessel (approximately 650 feet, or 200 meters, from the fire), the heat from the fire was noticeable, but not uncomfortable.

BURN PHASE

The entire burn period (including ignition) lasted about 1 hour and 15 minutes. The intense portion of the burn lasted about 45 minutes. The entire burn was conducted shortly after dark -- the photo in Figure 3, however, helps to provide a similar day-time view of what the burning oil and FIRE BOOM looked like. The test burn in Figure 3 was conducted off Spitsbergen in July 1988 in cooperation with 3M and various government, academic and industry groups from Norway. The Spitsbergen burn involved 300 feet (91 meters) of 3M FIRE BOOM and approximately 500 gallons (1,893 liters) of Statfjord crude oil.

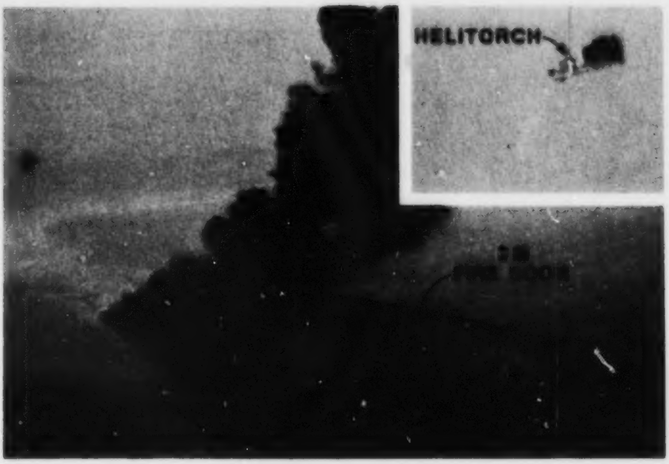

FIGURE 3 **In-Situ Burning Of Crude Oil --Spitsbergen, July, 1988**

During the test burn involving crude oil from the Exxon Valdez, it was noted that the area of burning oil could be controlled quite easily by adjusting the speed of the towing vessels. If the vessels slowed down to a near standstill, the burning oil would move forward toward the leading ends of the FIRE BOOM. If the vessels speeded up, the leading edge of the burning oil could be moved back toward the apex of the U-configuration. Throughout most of the test burn, a slow towing speed of about 1/2 knot (0.26 meters/sec) was maintained while keeping the burning oil back in the downstream 1/3 to 1/2 of the boom's containment area. Based on the approximate oil holding capacity of a 450-foot boom held in a U-configuration (Figure 4), the oiled region about 1/3 of the way toward the leading ends of the boom could hold about 100 barrels (15,900 liters) per inch of oil depth. A total containment volume of 20,000 to 30,000 gallons (76,000 to 114,000 liters) could therefore be accounted for with an average oil depth of 5 to 7 inches (13 to 18 centimeters). This potential holding capacity can be compared with the observed oil encounter rate (previous section) and the oil burn rate (next section) to provide a reasonable estimate of the volume of oil eliminated during the test burn.

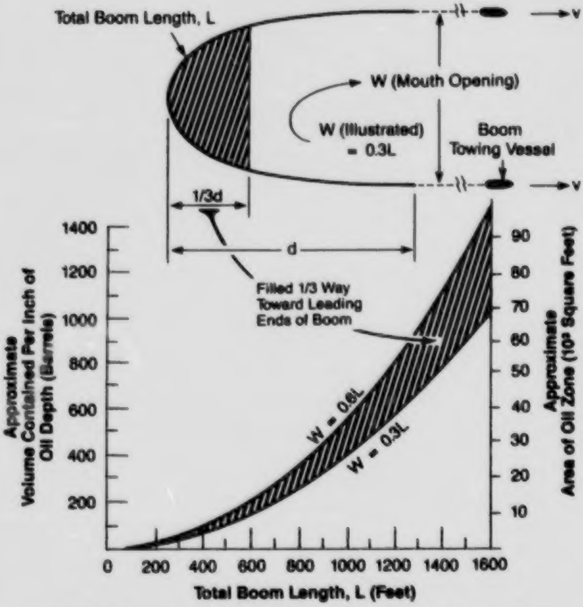

FIGURE 4 Typical Oil Volume Holding Capacity

The seas during the test burn remained calm, with only a light breeze out of the west, northwest. The direction of tow during collection and burning of the oil was maintained into the wind (Figure 1). After approximately 45 minutes of very intense burning with flames sometimes reaching 200 to 300 feet (61 to 91 meters) into the air, the fire began to subside. This reduction took another 10 to 15 minutes, resulting in an obviously smaller and less dramatic burn. At about 2130, 1 hour and 15 minutes following ignition, the fire went out . The boom was then allowed to go slack; one of the towing vessels held on to both tow lines; and the second boat moved back to inspect the boom and burn residue.

BURN RESULTS

Inspection of the 3M FIRE BOOM revealed an expected amount of thermal stress to certain components of the boom resulting in a slight loss of freeboard and some embrittlement of the fabric between flotation segments. These effects of the burn were not surprising since the boom used was the last of an earlier boom design. Modifications to the design and materials used in the boom have significantly enhanced the retention of freeboard and the durability of the boom's thermal protection components. The sacrificial PVC covering on the outside of the boom had melted off to the waterline as it is designed to do. The forward-most leading ends of the boom were still unaffected by the fire, as were the polypropylene towing lines. The boom was in satisfactory condition to be used for additional oil collection and burning operations.

Upon inspection of the remaining oil residue, it was discovered that there was no free-floating (unburned) crude oil inside or immediately outside the FIRE BOOM. The remaining oil residue was of a taffy-like consistency, covering an estimated area of approximately 100 square feet (9.3 square meters). The residue had been swept back by the boom's forward motion to an average thickness of about 4 to 5 inches (10 to 13 centimeters), representing a total volume of about 300 gallons (1,136 liters). There was no apparent burn residue floating downstream of the boom; however, some residue had managed to build up and cling to the boom on its outside, downstream side. One of the towing vessels remained with the boom and residue, while the other returned to the Port of Valdez The burn residue was to be picked up at first light, and a sample of the residue returned to the Exxon Command Center.

Upon completion of the burn test, boom deployment charts (Figures 4 & 5) were examined and used to estimate that the burn area during the previous night's test could have varied between 5,000 and 10,000 square feet (465 and 929 square meters). Combined with the fact that most relatively fresh, thick crude oil layers burn at about 0.07 gallons/square foot/minute (i.e., about 0.1 inch/minute or 2 to 3 mm/minute regression rates), the volume elimination rate could be estimated at about 350 to 700 gallons/minute (1,325 to 2,650 liters/minute). Uncertainties exist involving the actual burn rates of emulsions and the actual burn areas experienced throughout the test burn. However, the elimination rates of from 350 to 700 gallons/minute should reflect reasonable approximations for the total amount possibly burned. A conservative estimate of the total volume of oil burned, based on 45 minutes of intense burn only, would range from 15,750 to 31,500 gallons (approximately 60 to 120 cubic meters).

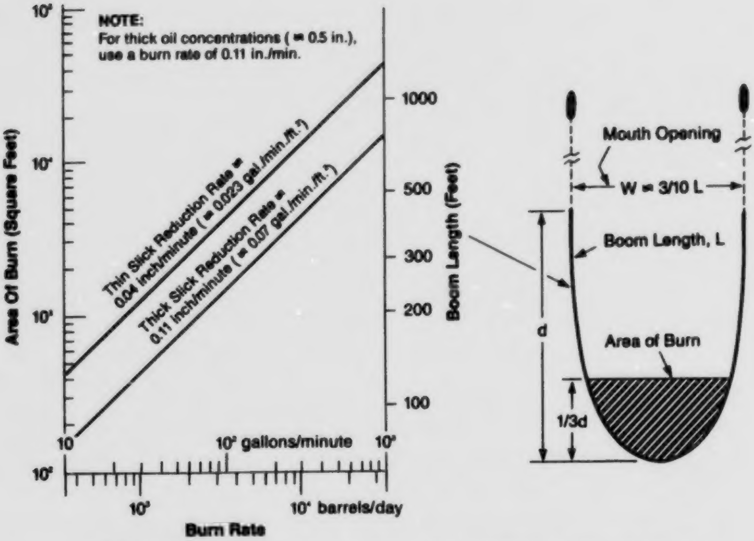

FIGURE 5 Approximate Burn Rate Versus Boom Length

SUMMARY

The above oil volume estimates can be summarized as follows:

Oil Encounter Rate -- on the order of 10,000 gallons (38,000 liters) or more
Boom Holding Capacity -- 20,000 to 30,000 gallons (76,000 to 114,000 liters)
Burn Rate -- 15,750 to 31,500 gallons (60,000 to 120,000 liters).

It is evident from these estimates that the total amount burned on the evening of the second day following the Exxon Valdez spill could conceivably be between 15,000 and 30,000 gallons (57 to 114 cubic meters). Using the lower estimate of 15,000 gallons, the 300 gallons of burn residue would suggest that approximately 2% of the original oil was left upon completion of the burn. If the 30,000-gallon figure was used, the burn residue would represent only 1% of the original oil. The achievement of a 98% to 99% efficiency of burn is consistent with numerous other controlled burns involving floating crude oil contained within a barrier. This burn, however, is very likely the first time that oil has been eliminated through combustion involving an actual accidental oil spill contained within a fire containment boom.

AUTHOR'S NOTE

It should be recognized that the elimination of spilled oil using in-situ burning must be considered in light of the full range of potential impacts (safety, air quality, etc.) associated with the burning of oil on water. The mechanical removal of spilled oil is by far the preferred cleanup technique whenever possible. Burning, on the other hand, may provide a safe, efficient and logistically simple method for eliminating oil under certain conditions. As a backup for mechanical cleanup techniques, in-situ burning can provide a useful means of eliminating large quantities of oil quickly, while avoiding the need for recovered oil storage containers. Anyone considering the use of burning should be sure that all regulatory controls have been satisfied, that the ignition and burning operations can be carried out safely, and that the temporary reductions in local air quality represent the lower of all other environmental impacts should the spilled oil not be burned.

Improved Airborne Laser Fluorosensor for Assessment of Marine Pollution.

by

R. Dick, R. Jackson, F. Kuja, A. Loveless, M. Paul and S. Wiles

Barringer Research Ltd.,

304 Carlingview Dr, Rexdale, Ontario M9W 5G2

ABSTRACT

Coastal waters represent a major source of food, recreation and energy, and conservation of this resource requires monitoring systems which provide both synoptic data and the real-time information required to deal with emergencies. Airborne laser fluorosensors, pioneered in Canada for the detection and identification of floating oil, can contribute to both tasks. As part of a programme sponsored by Environment Canada, US Coastguard, US Minerals Management Service and Fisheries & Oceans Canada, an improved fluorosensor has been built and bench tested. This system uses XeCl excitation at 308nm and measures fluorescence from 330 to 630nm, with 5nm spectral resolution and 12-bit amplitude, 1.5m range and 1 x 3mrad spatial resolutions. Provision has been made for rapid change of spectral coverage and for the use of other lasers. Adjustable range gating allows for detection of submerged oil and depth profiling.

Introduction

The Earth's coastal and inland waters represent a major source of food, recreation and energy. Conservation of this resource requires monitoring systems which can provide both synoptic data on water quality and the real-time information required to deal with spill emergencies. Airborne laser fluorosensors are suited to both tasks. Pioneered in Canada [1], [2] for the detection and identification of floating oil, they have been used around the world to measure oil [3], [4], [5] and, on an experimental basis, other pollutants [2],[4], marine biological pigments [6], and ocean temperature profiles [7].

The major effects involved in the operation of an airborne laser fluorosensor over the ocean are illustrated in Fig.1. Traversing the atmosphere, the laser beam is absorbed, scattered and may excite fluorescence in the aerosol. In a clean area (Fig 1a), about 2% is specularly reflected at the sea surface, and the remainder is transmitted and refracted into the water. In the water, there is particulate scattering, Raman scattering, and absorption, with some of the absorbed photons re-emitted as fluorescence. In an oil-polluted area (Fig.1b), the surface film of oil increases the specular reflectance, to about 3.5%, and attenuates the transmitted beam with an absorption coefficient ranging from a few microns, in the UV, to several mm., in the visible. The film also attenuates the upward flux from the bulk water and augments it with oil fluorescence. The curves in Fig. 2a, (re-drawn, in part, from data in [3], [4] and [5]), illustrate the spectral shapes of fluorescence for 'pure' materials (i.e. clean ocean, thick oil). Observed spectra are, in general, combinations of these. Fig.2b shows low-resolution spectra of a slick in the North Sea, obtained by the BRL/BP 'FLUOROSCAN' system. The oil spectrum is calculated from the spectra of the slick and the clean ocean, using the relation

F{Oil} = F{Slick} - F{Ocean}*Raman{Slick}/Raman{Ocean}

This assumes that a) attenuation by the oil is only significant at the laser wavelength (308nm) and b) the oil does not fluoresce significantly at the Raman wavelength (344nm). Oil spectra calculated in this manner are similar to laboratory spectra of thick samples, but we, and others [5], have also observed point-to-point changes in slick spectra which are not explainable, simply, as changes in thickness, but appear to indicate changes in composition, presumably due to differential evaporation, dissolution and spreading of the fluorescent components of the oil.

The history of laser fluorosensors in Canada begins with the pioneering work of Measures and co-workers at UTIAS [1] and the testing of the first Canadian airborne fluorosensor by this group using the facilities of the Canada Centre for Remote Sensing [2]. This was followed by the CCRS MkII and MkIII [3] 16-channel, range-gated systems, the BRL/BP FLUOROSCAN$^{(R)}$ 5-channel system, (which has flown over 20,000 line kilometers of oil exploration), and the CCRS MkIV programme, which was to have produced a 64-channel system, but was halted by Federal expenditure cut-backs.

Currently, a co-operative programme, sponsored by Environment Canada, US Coastguard, US Minerals Management Service, and Fisheries & Oceans Canada, is pursuing the following objectives:-

a) the construction, using the experience and some of the hardware from the MkIII, MkIV and FLUOROSCAN$^{(R)}$ projects, of a 64-channel, range-resolved, fluorosensor system, a system optimized for pollution monitoring, but with the potential for retrofit of other lasers and receiver wavelengths;

b) the installation of this system in an aircraft and the gathering of data on situations associated with oil-spills, e.g.

- oil on water
- oil on/in ice
- oil on shorelines

c) the use of this data to optimize a Laser Environmental Airborne Fluorosensor (*LEAF*) system which can be rapidly deployed to provide real-time data in support of the containment and clean-up of spills;

d) extension of the capabilities of the *LEAF* system to other environmental tasks e.g.

- measurement of biomass
- tracking of fish migration
- mapping of chronic pollution.

This report describes the progress to date toward objective a), namely, the fabrication of a 64-channel, gated, receiver and its integration with the transmitter and control and data-logging sub-systems from FLUOROSCAN$^{(R)}$. Table 1 summarizes the evolution of the *LEAF* system from its precursors.

Table 1:- Fluorosensor Evolution

Function	***LEAF***	**FLUOROSCAN**	**Mk. III**
Gating	**Adjustable**	**N/A**	**Fixed**
Resolution	**4.7nm @ 400 OR 2.7 @ 550**	**5 bands, 50 to 150nm**	**20nm**
Spect. range	**320 - 635nm OR 525 -696nm**	**344 - 700nm**	**380 - 700nm**
Laser	**XeCl @ 308nm OR Dye* @ 490-520nm**	**XeCl @ 308nm**	**N_2 @ 337nm**
Display	**Video of target ID* + strip-chart**	**Strip-chart**	**Video, Corr. Fn.**
Scanning	**Conical, 15°***	**N/A**	**N/A**

***** ***Future up-grade***

The 64-channel Fluorosensor

The system assembly of the 64-channel fluorosensor is shown in Fig.3. The shaded items have been made or modified under the current programme; the excimer laser and the TN6132/TN6130-1 gated diode array come from the MkIV project, courtesy of CCRS; the remaining items are on loan from BRL. The Block Diagram of the 64-channel flurosensor is shown in Fig.4a and the general arrangement in an Aerocommander in Fig.4b. Functionally, the system resembles the FLUOROSCAN$^{(R)}$, but an entirely new Gated Diode Array Spectrometer has replaced the 5-channel dichroic unit, an in-flight calibration facility has been added, and substantial upgrades have been made to the software for control, data-logging and real-time display. As is evident from Table 1, the array gives the system much better spectral resolution than earlier units, and the adjustable gating feature gives strong rejection of scattered sunlight and allows sampling at different depths. While depth sampling, as such, is of limited utility in the pollution mission, due to the small penetration depth of the UV wavelengths which are required to excite oil fluorescence, it will be most useful in future water-quality, water temperature and biomass measurements, which will use longer wavelengths.

In flight, the system operator controls the system by means of commands entered into the DATAPAK via a hand-held, RS-232 terminal. The DATAPAK is an STD-buss data-logging and control system, designed for airborne remote sensing. Having entered the desired conditions, the operator sets the DATAPAK 'ON-LINE', and it sends a set-up message to the System Controller, followed by a stream of trigger messages at a 10Hz rate. Communication between the units is via an IEEE-488 link, using slave processors, with Direct Memory Access, at each end. On receipt of each trigger, the System Controller sets up the conditions (gain, gate-width etc.) requested by the message, and proceeds to fire the laser 10 times, at a 100Hz rate. A fraction of the laser photons goes to the Laser Monitor and generates the START pulse, which starts the Lidar Altimeter. After a suitable delay, calculated from the last measured altitude and the desired penetration depth, the Altimeter gates the intensifier of the diode array 'ON' in anticipation of the arrival of the fluorescence excited by the laser. When the backscattered laser photons return to the telescope, the Backscatter Monitor issues the STOP pulse, which stops the Altimeter and starts the sequence which reads the analogue video from diode array. This video, which represents the spectrum of the laser-excited fluorescence plus the scattered sunlight, is then digitized (12-bits) by the System Controller. The read-out and digitization of the video takes about 5ms, half the period between laser shots. By this time, all fluorescence has died out, so that,when the array is again gated 'ON', the spectrum acquired is that of the scattered sunlight background. In this way, a 'SIGNAL+BACKGROUND' and a 'BACKGROUND' are acquired for each laser shot.

Table 2:- SYSTEM CONTROLLER

Function	Triggers laser; digitizes and pre-processes data; communicates with Datapak via GPIB
System	STD-BUSS with 7909A Termination
Master CPU	RLC SBC-188
Slave CPU	ZT-8830
Datapak I/O	SBX-20 GPIB Interface
Panel I/O	PL7605-1 32-bit parallel
GDAS I/O	2 x RS422 Interface Boards
A/D	2 x RTI 1260 (12-bit; 12msec/conv)

In the intervals of servicing the video digitizer, the System Controller (Table 2) does a substantial amount of processing; it examines the data and flags overflows and other doubtful values; applies background correction; calculates the spectral and temporal averages used for the real-time display; digitizes the altitude, laser energy, and other housekeeping data; and, finally, formats everything pertaining to the previous group of ten laser shots into a data message, which it returns to the DATAPAK. The DATAPAK combines the fluorosensor data with navigation and aircraft attitude data, a listing of the current value of all the system variables (gain, gate-width etc.), and a time-stamp, and records them on 1/2 inch cassette tapes. One cassette holds about 20megabytes, which is about 20 minutes' worth of data. The DATAPAK also drives the operator's real-time display.

If a fluorosensor is to assist emergency containment and clean-up efforts on a routine basis, it is essential that real-time data be made available to those directing the operation, and it must be in a standardized and easily assimilated format. A number of algorithms have been developed, by BRL, for the post-time interpretation and mapping of fluorosensor data from natural oil seeps. Preliminary estimates have been made of the computing speed, and data storage, required to implement these algorithms in real-time. These indicate that it is feasible to do this in a small aircraft, with the results presented as dynamic video displays, and, via telemetry, as hard-copy printouts at surface command centres, provided that the DATAPAK is replaced by a modern high-speed microcomputer with several slave processors added to the buss. Fig.5a shows the data flows involved, and Fig. 5b shows a possible display format. Area A is the history of the fluorescence spectrum over the past 20 seconds. Areas B and C are plan plots, of selected quantities, for the area scanned by the sensor during this period, and area D shows the colour image from the ground-track camera, to the same scale. All these displays scroll down the screen as the aircraft advances.

These are the types of displays required in a fully operational system. However, while flight testing any new airborne system, the primary concern, because of the high cost of flying time, is that the data display for the system operator be optimized for his critical role in minimizing both unproductive flying and ground maintenance time. While it should be possible, for calibration and diagnosis, to access the numeric value of any quantity in the the system, the routine, in-flight display must be simple and easily read, even when conditions are less than ideal. Error messages should be clearly visible, informative, and limited to significant events. There should be a hard copy to allow rapid post-flight assessment of data quality. Hard-copy is also useful as a scratch-pad for operator comments, though it is preferable that these be entered via the terminal, so as to appear in the archival tape record. The operator display which has been implemented for the 64-channel fluorosensor consists of a strip chart printer/plotter and an alphanumeric annotation on the display from the ground-track camera. Data on the strip-chart are classified as "ALARM" or "STANDARD". Standard data are, starting at the right margin,

Stripe1: (0.1 inch)
- Time hh:mm:ss

Stripe 2: (3 inch)
- Lidar Alt. @ 50ft/inch,'wrapped' @ 150ft.,300ft., ...
- Laser Energy
- Gain @ 5step/inch
- Gain Change as Gxx
- Warning messages hh:mm:ss Wnn *text*
- B'kgnd Correction Status as Bx, (x = 0,1,2)
- Normalization Status as Dx, (D = 0,1)

Stripe 3 .... Stripe 7 (7.2 inch)

-Fluoresence; 5 spectrally averaged bands of 1/10sec-group-average data,(which may be normalized) displayed with maximum amplitudes of 1.6in. and an offset of 1.2in. between zeros; a grid line, in a distinctive format, is drawn continuously at each zero.

Stripe 8: (1.2 inch)
- Laser B'scatter

Stripe 9: (0.6inch)
- Spectral Av. (Solar) B'kgnd

Stripe 10: (0.6inch)
- Peak Fluorescence (the largest value in the 64 group-averages of raw data)

The spacings have been chosen to minimize the possibility of traces crossing, while maintaining reasonable amplitudes. Zero reference lines are included to aid in reading signal amplitudes. The Peak Fluorescence channel allows the operator to set the gain to maintain signal in the upper third of the dynamic range of the A/D convertor. The 5 spectral bands are selectable by the operator, but will normally correspond to Raman, UV, Blue, Yellow and Red. If data is being gathered from more than one depth, the operator can select which depth is displayed. Normalized data is corrected for solar background and variations in aircraft altitude and laser output, and shows the operator the true changes in the fluorescent efficiency of the ocean. Non-normalized data, which may be chosen as signal, signal+background, or background only, will be used during alignment and calibration, and for fault diagnosis. Warning messages are printed as a matter of record; conditions requiring operator intervention cause an 'ALARM'.

Alarm is an eye-catching string displayed at the left chart margin as long as any of the following remain TRUE:-

2 MIN. TAPE REMAINING
OVER TEMPERATURE
LASER FAN STOPPED
HIGH VOLTAGE OFF
TOO MANY OVERFLOWS
NEXT LINE ID REQUIRED
WARM-UP DELAY
NO COOLANT FLOW
INTENSIFIER GATE FAILURE
COM or SYS ERROR

These were selected because they represent conditions requiring operator action: either there is something the operator should do, (e.g., change the tape), or, there is a strong possibility that the equipment is unserviceable, or the data unuseable, and she should consider going home.

Table 3:- Fluorosensor Calibration

Function	Freq.	Cal. Reference	Shutter
Dark Current	10Hz	none	X
Laser EMI	10Hz	none	X
CW Gain	10Hz	Internal LED	X
	End-of-Line	Internal LED	X
CW Response	Pre-flight	Ext. std.lamp	O
	Monthly	Ext. std.lamp	O
Pulse Response	Pre-flight	Std. tgt @50m	O
Laser/Rx. Align't	Pre-flight	Std. tgt @50m	O
Laser Monitor	Pre-flight	Calorimeter	X
Altimeter	Monthly	Std.tgt.30-150m	O
Gate Offset	A/R	Std tgt	O
Range law	A/R	Std. tgt.	O
Receiver F-O-V	A/R	Point Source	O
System F-O-V	A/R	Pt. fluor. tgt.	O

The first task for the 64-channel system will be to gather experimental data which will be used to optimize algorithms for the discrimination of oil from complicated backgrounds, such as ice and shoreline. To do this, it is essential that data taken at different times, under a variety of conditions, be compatible, and therefore the system must be comprehensively calibrated and the stability of this calibration monitored. A comprehensive schedule of calibrations has been compiled, and is shown in Table 3. A shutter and a LED source have been built into the new spectrometer to permit in-flight calibration of the responsivity and dark-current of the diode array. While the shutter and source are capable of inserting twenty calibration points per second, it is anticipated that flight experience will show that a much lower rate is adequate, perhaps as low as once/flight-line, i.e. every 10 - 20 minutes.

The major new hardware items completed thus far are, the Gated Diode Array Spectrometer (GDAS), an analogue Lidar Altimeter capable of range-gating the GDAS, and a new structural frame to unite the GDAS with the FLUROSCAN telescope, laser beam-expander optics, Laser Monitor and Backscatter Monitor, to form a new Receiver sub-system. The GDAS consists of a spectrograph, a Tracor Northern TN1632/TN6130-1 gated intensified diode array, and an electronics package, whereby the array communicates with the System Controller. The TN1632 consists of an EG&G, 'S'-series, 1024-elment, silicon diode array, optically coupled to the output phosphor of an ITT S-20 proximity-focussed image intensifier, which can be gated 'ON', for as little as 20nsec, via the TN1630-1 pulse amplifier. The spectrograph, (Table 4) is a catadioptric, out-of-plane, unsymmetrical, Czerny-Turner arrangement. The grating mount is kinematic, allowing the grating, and hence the spectral range and resolution, to be rapidly changed, without re-alignment or calibration. The entrance aperture and f/# are chosen to match the FLUOROSCAN telescope, and the output focal-length, and the grating dispersion(s), are chosen to match the resolution(s), and spectral range(s), with the 25x2.5mm active area of the array. Since the output is f/2.2, with an 11deg. total field, two elements are needed for acceptable aberration levels. A lens was chosen as the second element because it provides two degrees of freedom for aberration correction and allows a more compact layout. Since each colour comes to its own focus, the only ill effect of chromatic aberration is to tilt the focal plane, slightly increasing the angles of incidence at the intensifier faceplate. The direction of dispersion is set perpendicular to the conventional direction because this reduces the off-axis angle at the second concave mirror. The spectral resolution and efficiency have been measured, and meet the design goals.

Table 4:- SPECTROMETER

Optics Type	Out-of-plane Czerny-Turner
F - Ratio	Entrance, f/3.1 ; Exit, f/2.2
Grating	600g/mm; blazed @ 400nm, 1st order OR 923g/mm; blazed @ 500nm, 1st order
Detector	Gateable, intensified diode array 1024 diodes, read in pairs.
Gate Width	≥20nsec
Spectral Range	320 - 635nm OR 525 - 696nm
Channels	32 to 64, user-selectable
Resolution	4.7nm @ 450nm (64 channels) OR 2.8nm @ 600nm (64 channels)

The GDAS electronics consist of a Sequence Controller and an Interface Card. The Sequence Controller times the operation of the diode array. Following the intensifier gate, there is a delay of about 3ms while emission from the intensifier output phosphor is completed, then the analogue video from the diode array is clocked into a gated integrator, which sums the pulses, in groups of 16, to give 64 (time multiplexed) analog levels. This spectrum goes to the System Controller for digitization. The Sequence Controller also includes a digital Lidar Altimeter using a 100MHz crystal clock, and several Test Sequence Generators, which allow it to conform with a design principle, applied throughout the system to simplify fault diagnosis, namely, that any major sub-system should be able to function even if some or all of the other sub-systems are disconnected.

Table 5:- ANALOGUE ALTIMETER

Range	100 to 1000ft
Cal. constant	10mv/ft
Resolution	± 0.5ft RMS (single shots)
Temp. coeff.	0.013 ft/C
Accuracy	± 0.5ft @ 25C (after calibration)
Gate Offset Range	Surface ± 30ft in 5ft steps
Gate Width	20 to 180nsec in steps of 10nsec
Self-check	On command; uses internal crystal

The (analogue) Lidar Altimeter (Table 5) measures altitude from the interval between START and STOP, i.e. the time for the laser pulse to travel to the surface and be scattered back to the aircraft. It also generates the delay between START and the intensifier gate pulse, as well as the length of the gate. These functions were implemented in analogue because, using a minimum of high-speed components, this gives time resolution which would be difficult to achieve digitally, even with ECL logic. The altimeter converts voltage to time, and time to voltage, by charging or discharging a capacitor via a current source. The only high-speed components are the transistors which turn the current on and off, the majority of the circuitry, which is concerned with the long term accuracy of the current source, consists of low speed servos. There is also a self-calibrate facility, using a crystal clock.

Acknowledgment

The work reported herein was supported, in part, by Environment Canada, US Coastguard, US Minerals Management Service, and Oceans and Fisheries Canada, under Contracts KW203-7-1300/02-OSC and KE144-9-6319/01-SS, and by Canada Centre for Remote Sensing, under Contract 17SR.23413-4-4379.

References

[1] Measures, R.M. and M. Bristow, *Can. Aeron. Space J.*, 17, 421-422 (1971)
[2] Measures, R.M., W.R. Houston and M. Bristow, *Can. Aeron. Space J.*, 19, 501-506 (1973)
[3] O'Neil, R.A., L. Buje-Bijunas and D.M. Rayner, *Appl. Optics*, 19, 863-870 (1980)
[4] Hoge, F.E. and R.N. Swift, *Appl. Optics*, 19, 3269-3281 (1980)

[5] Diebel-Langhor, D,, T. Hengstermann, and R.Reuter, "Laser Remote Sensing of the Marine Environment: etc. " In:- Proc. 3rd Int. Coll. on Spectral Signatures in Remote Sensing, Les Arcs, France (Dec1985)

[6] Bristow, M.P.F., D.H. Bundy, C.M. Edmonds, P.E. Ponto, B.E. Frey and L.F. Small, Int. J. Remote Sensing, **6**, 1707-1734 (1985)

[7] Leonard, D.A., B. Caputo, and F.E. Hoge, *Appl. Optics*, **18**, 1732-1745 (1979)

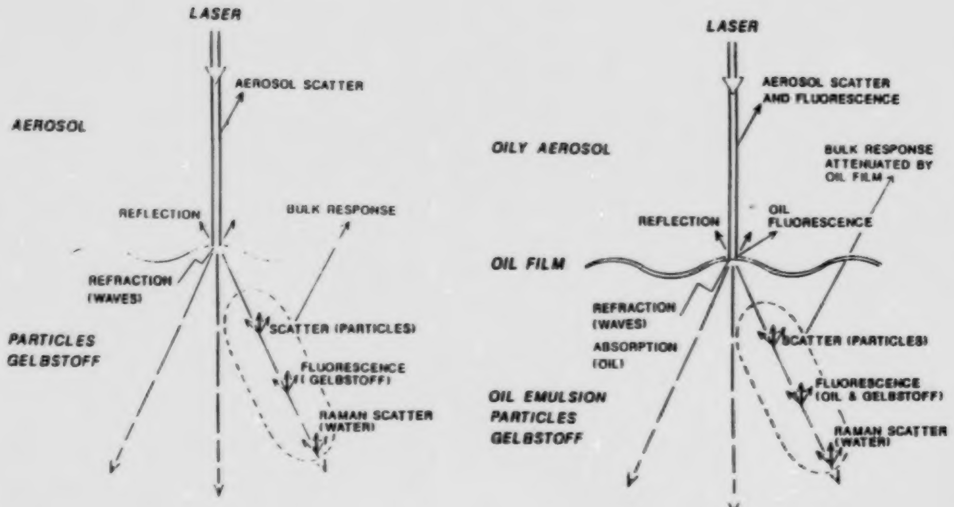

a) LASER INTERACTIONS IN BACKGROUND AREA b) LASER INTERACTION IN SEEPAGE AREA

FIGURE 1

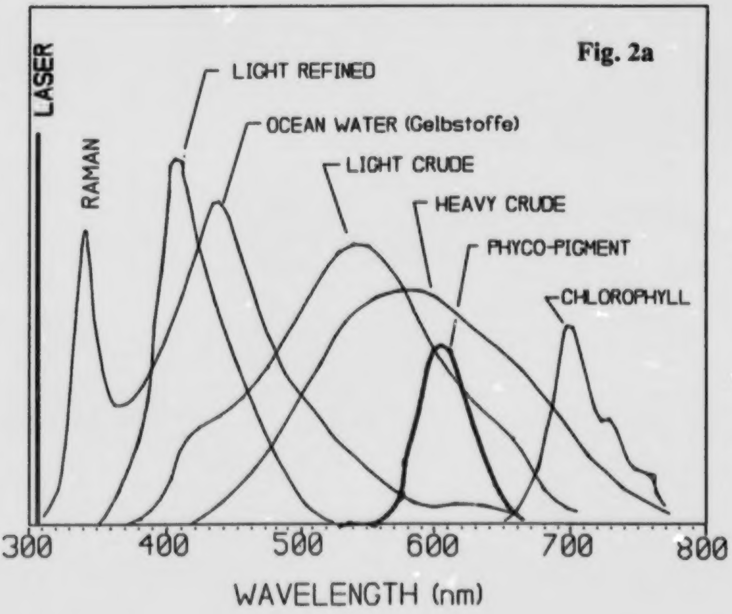

Fig. 2a

LASER
RAMAN
LIGHT REFINED
OCEAN WATER (Gelbstoffe)
LIGHT CRUDE
HEAVY CRUDE
PHYCO-PIGMENT
CHLOROPHYLL
300
400
500
600
700
800
WAVELENGTH (nm)

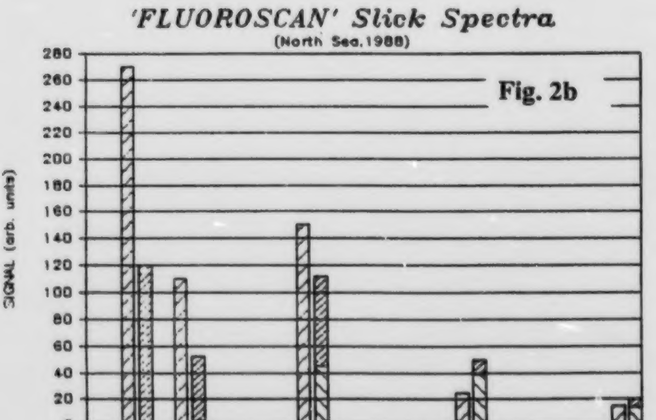

Fig. 2b

'FLUOROSCAN' Slick Spectra
(North Sea.1988)
SIGNAL (arb. units)
280
260
240
220
200
180
160
140
120
100
80
60
40
20
0
344
365
440
540
680
WAVELENGTH (nm)
ocean
oil (calc.)
slick

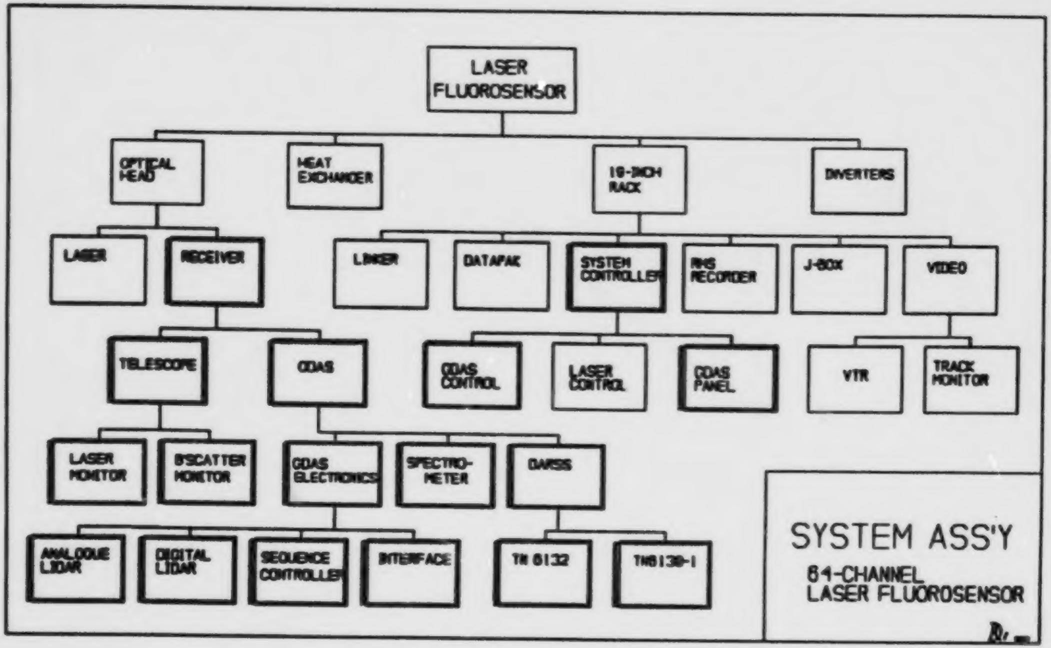
LASER FLUOROSENSOR
OPTICAL HEAD
HEAT EXCHANGER
19-INCH RACK
DIVERTERS
LASER
RECEIVER
LINKER
DATAPAK
SYSTEM CONTROLLER
RMS RECORDER
J-BOX
VIDEO
TELESCOPE
CDAS
CDAS CONTROL
LASER CONTROL
CDAS PANEL
VTR
TRACK MONITOR
LASER MONITOR
B'SCATTER MONITOR
CDAS ELECTRONICS
SPECTRO-METER
DARSS
ANALOGUE LIDAR
DIGITAL LIDAR
SEQUENCE CONTROLLER
INTERFACE
TM 6132
TM6130-I
SYSTEM ASS'Y
64-CHANNEL LASER FLUOROSENSOR

Fig. 3

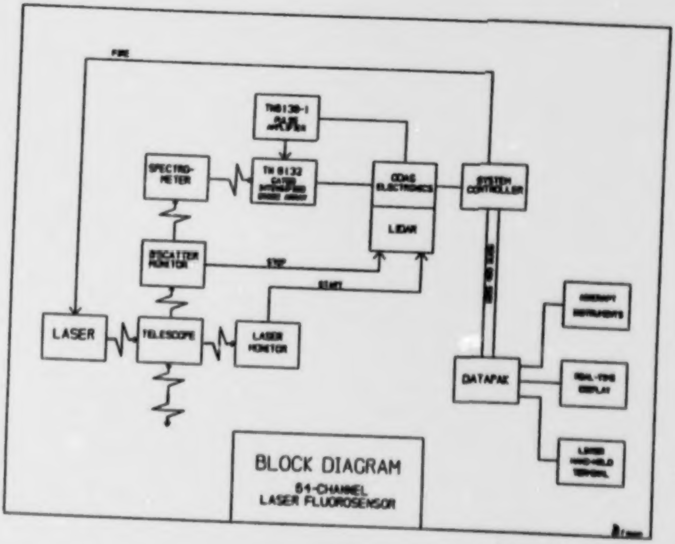
FIRE
SPECTRO-METER
TH 8132
CCAS ELECTRONICS
SYSTEM CONTROLLER
LIDAR
BSCATTER MONITOR
STOP
START
LASER
TELESCOPE
LASER MONITOR
DATAPAK
AIRCRAFT INSTRUMENTS
REAL-TIME DISPLAY
HAND-HELD TERMINAL
BLOCK DIAGRAM
64-CHANNEL
LASER FLUOROSENSOR

Fig. 4a

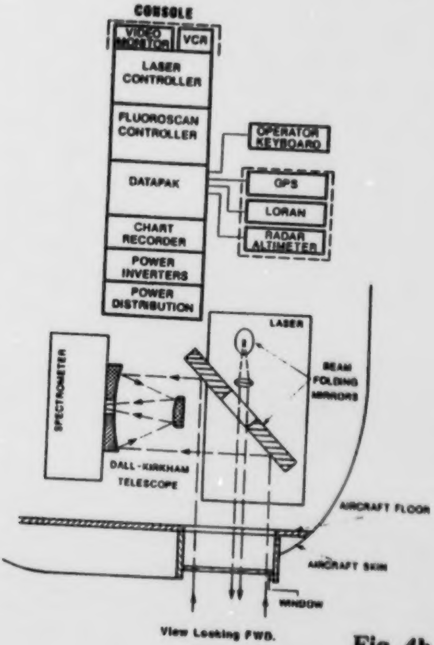
CONSOLE
VIDEO MONITOR
VCR
LASER CONTROLLER
FLUOROSCAN CONTROLLER
DATAPAK
CHART RECORDER
POWER INVERTERS
POWER DISTRIBUTION
OPERATOR KEYBOARD
GPS
LORAN
RADAR ALTIMETER
LASER
BEAM FOLDING MIRRORS
SPECTROMETER
DALL-KIRKHAM TELESCOPE
AIRCRAFT FLOOR
AIRCRAFT SKIN
WINDOW
View Looking FWD.

Fig. 4b

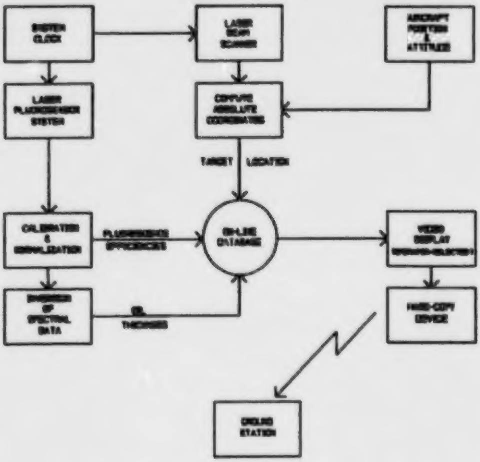
SYSTEM CLOCK
LASER BEAM SCANNER
AIRCRAFT POSITION & ATTITUDE
LASER FLUOROSENSOR SYSTEM
COMPUTE ABSOLUTE COORDINATES
TARGET LOCATION
CALIBRATION & NORMALIZATION
FLUORESCENCE EFFICIENCIES
ON-LINE DATABASE
VIDEO DISPLAY (OPERATOR-SELECTABLE)
INVERSION OF SPECTRAL DATA
OIL THICKNESS
HARD-COPY DEVICE
GROUND STATION

Fig. 5a - DATA FLOW

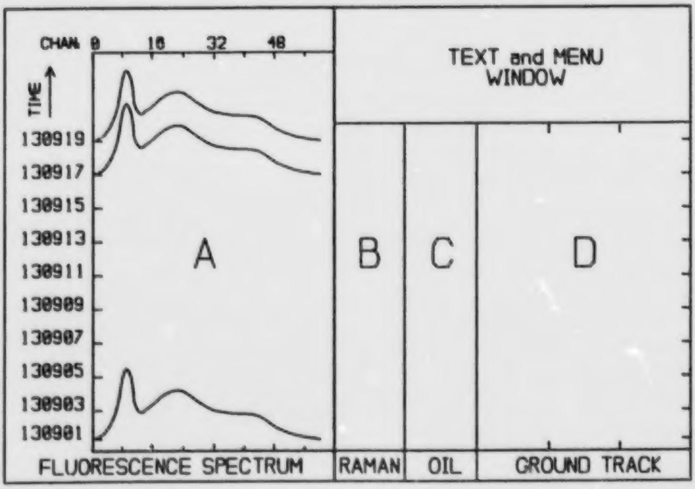

Fig. 5b - PRIMARY OPERATIONAL VIDEO DISPLAY

FIELD TEST OF SATELLITE-POSITIONED DRIFTERS FOR OIL SPILL SIMULATION AND TRACKING

by

Mark Reed, Chris Turner, Anatoly Odulo, and Tatsu Isaji

Applied Science Associates, Inc.
70 Dean Knauss Drive
Narragansett, Rhode Island 02882-1143

ABSTRACT

The U.S. Department of the Interior, Minerals Management Service, is interested in the use of satellite-tracked surface-drifting buoys to simulate the movement of spilled oil on the sea surface. A field test of candidate buoys was performed in the Norwegian Sea in June-July, 1989. The test involved the release of 30 tonnes of Oseberg crude oil, and 26 drifters equipped with Argos transmitters.

The experiment lasted approximately four days, at which time the oil had dissipated from the sea surface. During the experiment, Eulerian wind, wave and current data were recorded. A horizontal array of Stokes drifters was also deployed, to establish a Lagrangian record of the horizontal variability averaged over the top meter of the water column. Airplane overflights recorded the location, shape, and size of the surface slick using visual, ultra-violet, infra-red, and radar imagery.

Analysis of sequential oil and drifter locations resulted in development of a transfer function with which to compute oil trajectories from drifter trajectories. Ballast corrections were necessary to achieve good similitude between drifter and oil motion. Results of this test should be applicable to other offshore, wind-driven oceanic regimes. Other ballast corrections and transfer functions must be developed for other oils, and regimes in which non-wind-driven currents contribute significantly to surface transport.

1. INTRODUCTION

This project, an experimental oil spill and associated analyses, initiates the second phase (field portion) of a three phase program. Phase I was a theoretical review of surface drifting buoys (Reed et al., 1988), and resulted in a ranking of candidate drifters for their ability to track oil slicks. The first stage of Phase II, described here, involved field testing the two top-rated buoys, a disk and a sphere, recommended as a result of Phase I and analysis of the results. The final (Phase III) goal of this program is the acquisition and deployment of large numbers of drifting buoys in the various Outer Continental Shelf (OCS) planning areas. The trajectories of these buoys can then be used as measures of potential oil spill trajectories, and as test data for hydrodynamic and trajectory models.

Historically, one goal of the Minerals Management Service (MMS) OCS Environmental Studies Program has been to estimate the probability of oil spill occurrence, and to compute oil spill trajectories. Using this information, the likelihood of oil contacting sensitive marine and coastal resources as a result of petroleum exploration, development, production, and transportation on the OCS can be estimated. The MMS uses an Oil Spill Risk Analysis (OSRA) model to estimate the probability of spill occurrence, and to model potential spill movement (Smith et al., 1982; Labelle and Anderson, 1985). A critical input to the oil spill trajectory component of the OSRA model is the surface current representation which incorporates the influences of major surface and subsurface circulation features.

The possibility exists, due to recent technological developments and reductions in cost, to use satellite-tracked surface drifting buoys to simulate the movement of spilled oil on the ocean surface. If a buoy can be used to simulate economically the movement of spilled oil, then the MMS intends to use a large number of them to test the deterministic or predicted results of ocean circulation models, to test the physics affecting spill movement represented in the OSRA and other circulation models, and to test specified OSRA run(s) using measured winds and currents as input. The buoys would also be useful in complex, nearshore circulation regimes which are not readily modeled, and for assessing the probability of oil contacting sensitive resources.

The Norwegians were planning an experimental oil spill and appeared to be good partners for this field test because of their considerable experience with experimental oil spills as well as satellite-tracked surface drifters. In 1978, four surface drifters equipped with Argos and DECCA positioning systems were released with oil off northern Norway (Audunson et al., 1979). Two subsequent experiments were performed on Haltenbanken in 1982 and 1985 (Audunson et al., 1984; Sørstrøm and Johansen, 1985). The 1982 experiment, with 100 tonnes of Statfjord crude oil, focused on the drift and spread of the oil, microbial degradation, effects on fish eggs, larvae, and other zooplankton, and practice with oil response equipment. In 1985, four 10 tonne slicks of Statfjord crude were released, two as controls, one with dispersant, and one with demulsifier. The purposes were to assess differences in horizontal and vertical spread of treated and untreated oil, and to collect data for testing of simulation models. These experiments are reviewed in some detail in the Phase I report (Reed et al., 1988). This background of experience was seen as contributing significantly to the probable success of this project.

This project had three specific objectives:

(1) field test selected buoys during a planned oil spill, and evaluate their motion relative to that of the surface slick;
(2) during the field test, measure physical forces moving the oil and the drifters;
(3) based on analysis of drifter and oil motions and forcing functions, make appropriate recommendations to MMS regarding future operational use of these drifters in the various OCS planning areas.

Specific components of the experiment included:

(1) a spill of 30 tonnes of crude oil;
(2) deployment of 11 copies each of two types of satellite-tracked surface drifting buoys;
(3) a moored meteorological buoy recording residual current at 3 m depth, wave period and height, wind velocity, air and sea surface temperatures, and air pressure;
(4) a moored wave-riding buoy recording wave height, direction, and period;
(5) a moored current string with acoustic meters at 3, 10, and 20 m below the surface;
(6) a horizontal array of satellite-tracked flooded volume Stokes (Argostars) drifters to produce a record of the mean surface current field;
(7) time series of oil properties (density, viscosity, evaporation, water content);
(8) three hydrographic surveys (one before, during, and at the end of the test) recording salinity, temperature, density (STD) and acoustic Doppler current profiler (ADCP) measurements;
(9) an acoustic surface velocity profiler (RINO), supplied and deployed by Woods Hole Oceanographic Institute (WHOI) personnel;
(10) airplane overflights with vertical photographic, ultraviolet (UV), infra-red (IR), and side-looking airborne radar (SLAR) instrumentation.

The results of these various components were used to achieve project objectives as outlined in Figure 1. The field components of Phase II took place in late June/early July, 1989 over Haltenbanken on the Norwegian Shelf (Figure 2). The location and timing of the spill were selected to coincide with low biological activity, minimum probability of coastal impacts, and the window of mildest wind/wave/storm activity in the statistical weather record.

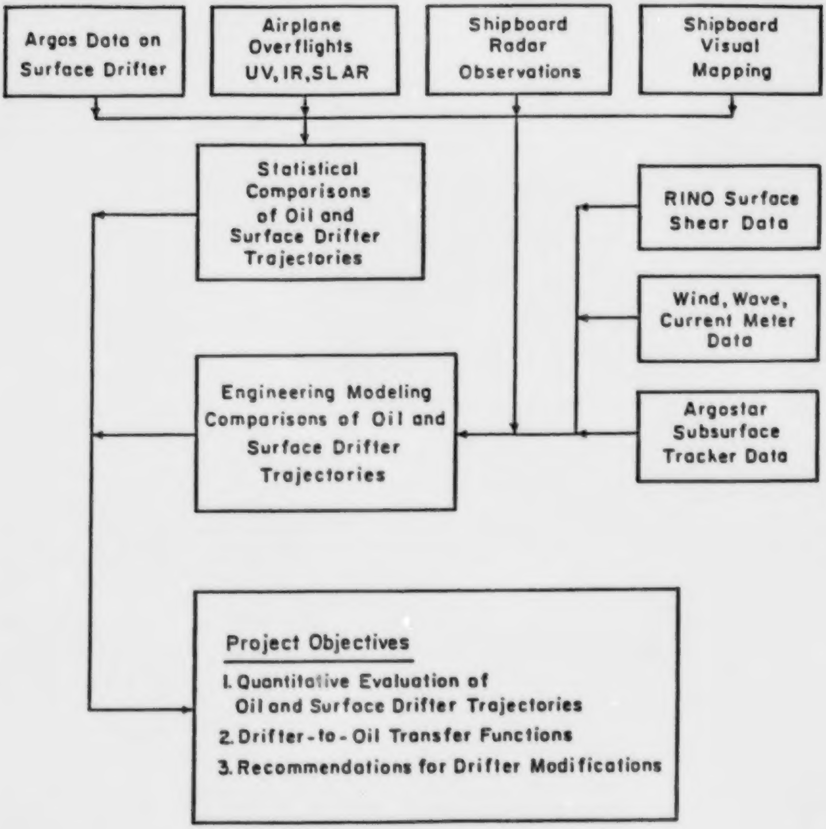
Argos Data on Surface Drifter
Airplane Overflights UV, IR, SLAR
Shipboard Radar Observations
Shipboard Visual Mapping
Statistical Comparisons of Oil and Surface Drifter Trajectories
RINO Surface Shear Data
Wind, Wave, Current Meter Data
Engineering Modeling Comparisons of Oil and Surface Drifter Trajectories
Argostar Subsurface Tracker Data
Project Objectives
1. Quantitative Evaluation of Oil and Surface Drifter Trajectories
2. Drifter-to-Oil Transfer Functions
3. Recommendations for Drifter Modifications

Figure 1 Schematic overview of project components for field evaluation of drifters.

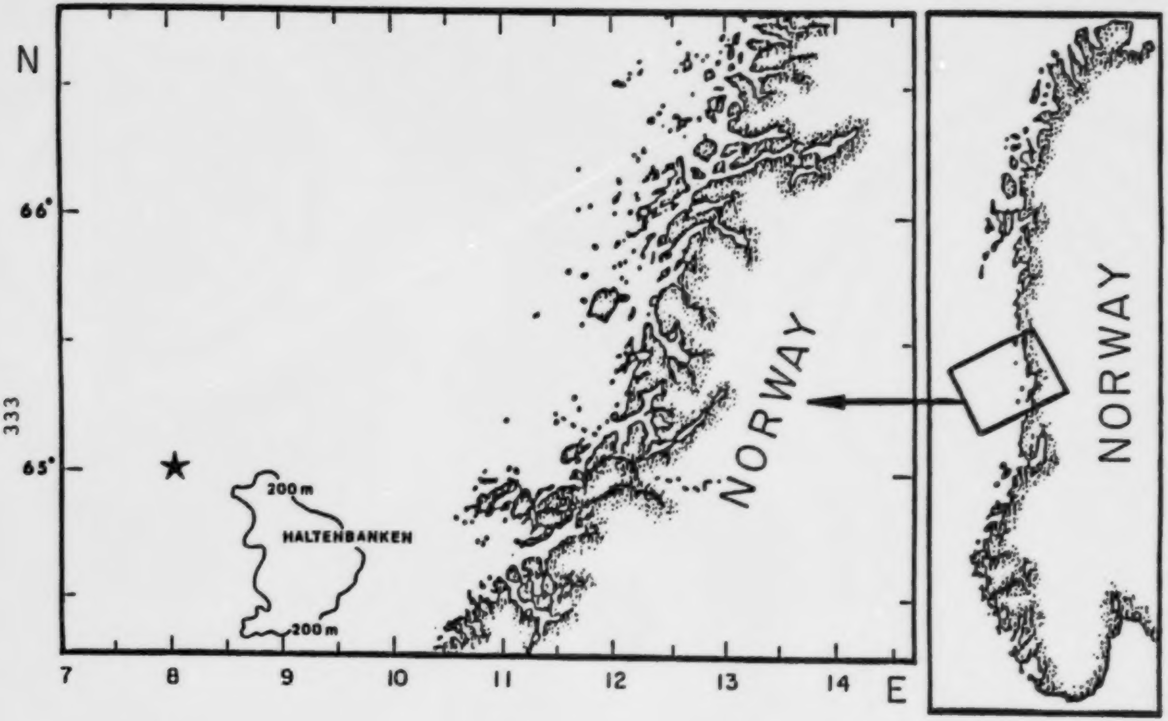

Figure 2 Map showing the geographical location of the experimental oil spill on Haltenbanken.

From the standpoint of the probability of success for Phase II, we were of course interested in the oceanographic and meteorological climatology of the area. The actual spill site, at 65° N, 8° E, was slightly northwest of the bank, about 200 km off the Norwegian coast, in about 240 meters of water. Table 1 gives some background climatological statistics for the area and the same parameters for the actual time of the experimental spill.

The schedule of activities during the field cruise is shown in Table 2. [Times throughout the report are Greenwich Mean Time (GMT) unless Norwegian Time (NT) is specified. During the experiment, NT was 2 hours later than GMT.] From the 26th to the morning of the 29th of June, time was spent deploying the moored instruments, readying the on-board equipment for the actual spill, and completing the first hydrographic survey. The 29th and 30th were spent in waiting out a storm front, and the actual release of oil took place on July 1. The oil was tracked until July 4. On July 5, the slick could no longer be found by aerial reconnaissance.

Characteristics of the Oil

The oil spilled was Oseberg medium light North Sea crude oil, with a viscosity at room temperature of about 12 cSt, a pour point of -9°C, and a density of 0.85 kg/l. Oseberg crude emulsifies rapidly on the ocean, reaching a maximum water content of 70-80% within about 12 hours. De-emulsification takes place over a period of several days in the laboratory at room temperature (Daling and Johansen, 1986).

Table 1 Climatological statistics for Haltenbanken in July, compared with mean values during the experiment.

Parameter	Climatological	July 1-4, 1989
Min. Air Temperature	- 3°C	+ 6°C
Min. Sea Temperature	+ 2°C	+ 10°C
Mean Air Temperature	+ 12°C	+ 8°C
Mean Sea Temperature	+ 12°C	+ 10°C
Mean Wind Speed	6 m/sec	6 m/sec
Max. Wind Speed (+2σ)	16 m/sec	17 m/sec
Mean Wind Direction	240° (met. conv.)	230°
Typical Salinity above 50 m	34.7 ppt	34.5 ppt
Typical Salinity below 50 m	35.2 ppt	35.1 ppt
Mean Significant Wave Height	2 m	2.5 m
Mean Significant Wave Period	8 sec	8 sec
Mean Current Velocity	6 cm/sec NNE	4 cm/sec NE
Max. Tidal Current Velocity	20 cm/sec	20 cm/sec

Table 2 Schedule of activities.

Date	Time (GMT)	Activity
89-06-26	10:00	Mobilization of primary vessel and equipment (Trondheim)
	15:00	Departure
89-06-27	01:00	Arrive at spill site
	01:00 - 04:30	Deployment of moored equipment
	05:00	Deployed Stokes drifter 9819 at spill site
89-06-27	07:00	First hydrographic survey begun
89-06-29	06:00	Took on full scientific staff from second vessel; review of Norwegian and English weather forecasts; decision to delay oil release
	08:00	Vessels head to shelter at Frøya Island
	14:00	Arrived Frøya
89-06-30	06:00	Test deployment of RINO; ballast corrections made
89-07-01	00:30	Deployed RINO at spill site
	01:30 - 06:30	Deployed Stokes Drifters 9812-9817
	07:00	Return to spill site
	08:00 - 08:16	Oil released
	08:10 - 08:20	Drifters released in oil slick
	09:00 - 10:15	First reballasting and redeployment
	09:00	Release of Stokes drifter 9820 at slick
	10:30	First airplane overflight
	12:00	Deployed last Stokes drifter 9818
	17:00 - 19:00	Second reballasting and redeployment
	18:30	Second airplane overflight
89-07-02	12:15 - 13:30	Third reballasting and redeployment
	10:30	Third overflight
89-07-02	18:40	Fourth overflight; second hydrographic survey
89-07-03	10:00	Return to slick
	10:30	Fifth overflight
89-07-04	14:00	Relocated slick; sixth overflight
	14:00 - 24:00	Retrieval of drifters
89-07-05	04:00	Began final hydrographic cruise
	10:00	Final overflight fails to locate slick
	24:00	Recovered RINO, moored instruments
89-07-07	04:00	Completed final hydrographic survey
	13:00	Returned to Trondheim
	15:00	Demobilization of vessel complete

Oil and Surface Drifter Deployment

Two types of surface drifters (Figure 3) were deployed under direct funding from MMS. The Low Cost Drifter (LCD) is manufactured by the Charles Stark Draper Laboratory in Cambridge, Massachusetts. The Argosphere is a spherical drifter manufactured by Technocean, Inc. of Del Mar, California. We released 11 of each type. Argos transmitters in the drifters were programmed to transmit at 90 second intervals for 20 days, at which point they would turn off automatically if not recovered.

Three drifters developed by the Continental Shelf Institute (IKU) in Trondheim were also deployed. These drifters (Figure 3) are larger and heavier than the U.S. drifters, but have been tested previously with reasonable success in tracking of oil spills (Audunson et al., 1984; Sørstrøm and Johansen, 1985). An ice drifter developed by Oceanor was also deployed, for purposes of comparison.

Environmental Measurements

The purpose of measuring the oceanographic forces moving spilled oil and drifters was to isolate cause and effect relationships with trajectories. Specifically, we sought to obtain measures of:

(1) surface current velocities and shears as near as possible to oil and buoy locations;
(2) the wave field;
(3) the wind field;
(4) the current field and hydrography.

Moored instruments were deployed to measure

- wind speed and direction;
- air temperature and pressure;
- wave height, period, and direction;
- water current speed and direction at 3, 10, and 20 m below the sea surface.

Lagrangian Stokes drifters were deployed to give spatial information on surface current structure. Three hydrographic surveys were undertaken, one each before, during, and after the experiment, with measurements of temperature, salinity, density, and vertical current structure at each station.

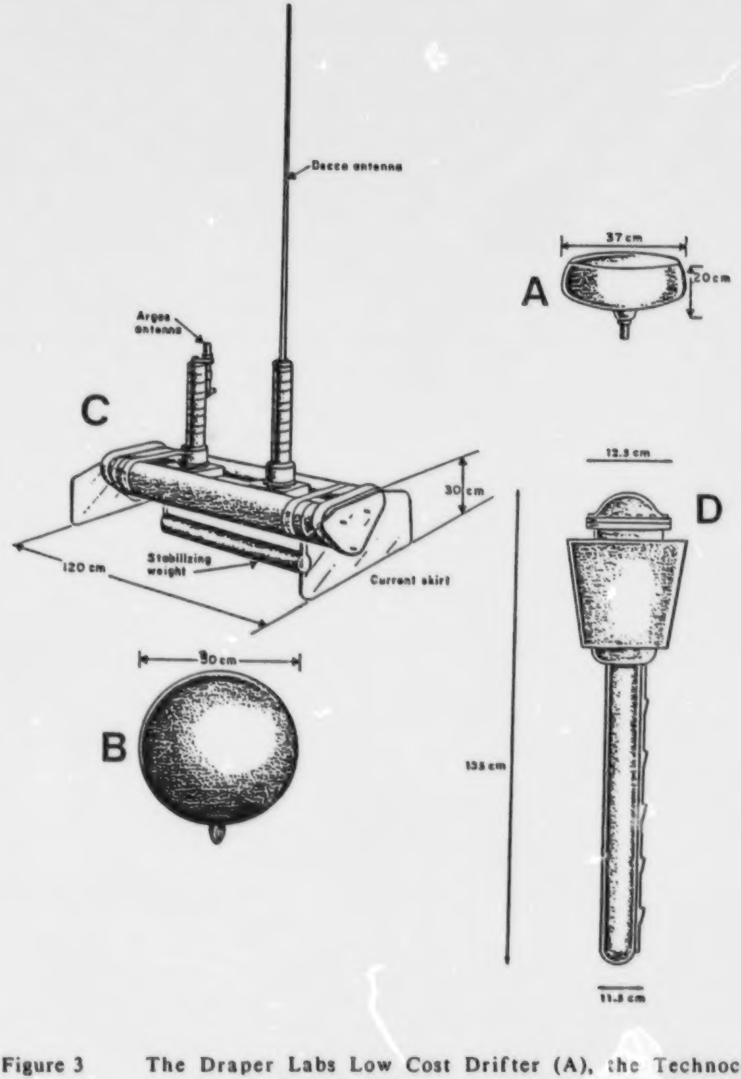

Figure 3 The Draper Labs Low Cost Drifter (A), the Technocean Argosphere (B), the IKU Oil Tracking Drifter (C), and the Oceanor Ice Drifter (D).

Locations of Drifting Buoys

Drifting buoys were tracked using the Argos satellite system. This system consists of two satellites, each equipped with onboard data collection and location systems which receive, process and re-transmit data to ground stations. The platform transmitter terminal (PTT) in each drifter sends a signal periodically, typically once every 60 to 90 seconds. The PTT's transmit their messages periodically on the same frequency, independently of each other, and without satellite interrogation. Messages from PTT's within view of a satellite reach the receiver onboard the satellite at random. The position of each buoy is determined by measuring the Doppler shift on the carrier frequency of incoming messages. Sensor data, if any, transmitted from the oceanographic measurement buoys, are stored together with determined positions in computer files at Argos telemetry stations in Toulouse, France and Landover, Maryland, USA. About 3 hours after transmission from the PTT's to the satellite, the data were available for access at these ground stations.

Locations of Surface Oil

Surface slicks were located visually from onboard ship and recorded intermittently by hand. Several airplane overflights were also carried out with two specially equipped aircraft, supplied by the Norwegian Pollution Authority and the Netherlands North Sea Directorate. Both planes carried photographic, infra-red/ultraviolet (IR-UV), and side-looking airborne radar (SLAR) imaging equipment coupled to their DECCA navigational systems. Synchronized locations and distributions were recorded whenever weather and slick characteristics permitted. Table 3 shows the overflight schedule, weather, and images recorded.

Table 3 Aerial overflight schedule, weather, and images recorded.

Date/Time	Hrs. After Oil Release	Weather	Images Recorded
89-07-01/10:30	2.5	Clear	Visual, IR-UV, SLAR
89-07-01/18:00	10.0	Clear	Visual, IR-UV, SLAR
89-07-02/10:40	26.5	Clear	Visual, IR-UV, SLAR
89-07-02/18:50	34.9	Clear	Visual, IR-UV, SLAR
89-07-03/10:40	50.5	Overcast	SLAR
89-07-04/14:40	78.5	Overcast	SLAR
89-07-05/10:30	96.5	Overcast	No slick found

2. RESULTS: THE DESCRIPTIVE VIEW

The core scientific and technical team left Trondheim on board the 50 m fishing vessel *Endre Dyrøy* at 15:00 on the 26th of June, 1989. We deployed the moored instruments at the proposed spill location (65°N, 8°E), then completed the first hydrographic survey. During the night of June 30-July 1, we deployed the Argostar Stokes drifters in an approximate 3 by 3 grid pattern centered on the spill site, with 10 km separating deployment points.

The actual release of oil took place at 08:00 on the morning of July 1. At 07:00, the ship's work skiff was lowered with the chemistry team and equipment. At 07:15, a 14 foot motorized rubber raft was set in the water, and the Argospheres and LCD's were loaded on board. At 08:00, with both work boats in position, the oil tanker was instructed to begin releasing the oil. Using a high volume pump, the tanker released the entire 30 tonnes of oil in 16 minutes, then departed. Chemical sampling began immediately, a control sample having been taken directly from the tanker an hour earlier. Approximately 10 minutes into the oil release process, when a clearly identifiable surface slick had formed, we activated the surface drifters (removed external magnets) and released them at the downwind edge of the slick.

We then took the work skiff around to the upwind side of the slick to observe drifter behavior. At 08:40 we returned to the *Endre Dyrøy* to pick up the last Argostar Stokes drifter, #9820, which we deployed with a dye packet at the leading edge of the slick. The drifter appeared to slip relative to the surface water at about 2 to 4 cm/sec, or 2 m/min.

It soon became apparent that all but the unballasted surface drifters, #9821 and 9822, were rapidly falling behind the slick. We collected the lagging drifters (08:50-09:20), removed between 0.5 and 2 kilograms of ballast, and repositioned the drifters at the leading edge of the slick (09:45). Total movement of any one drifter during this redeployment was estimated to be less than 100 m.

The first overflights by the Norwegian and Netherlands surveillance aircraft took place between 10:00 and 11:15 (Table 3). The overflight photographs at this time show that many of the drifters had again begun to lag behind the slick. We decided to wait a few hours before making further alterations, to allow the differences in drifter behavior to become more evident.

Figure 4 shows the IR/UV imagery of the oil slick about 3 hours after the release (11:00 GMT). The cross-wind width of the slick at this time was about 120 m; the upwind-downwind length is about 300 m. The images in Figure 4 are taken with west at the top. There appears to be a shear zone in the middle of the slick, such that the southern portion is moving faster than the northern portion. The wind at this time was light (2-5 m/sec) and almost directly out of the west. During the afternoon the wind rose to about 7

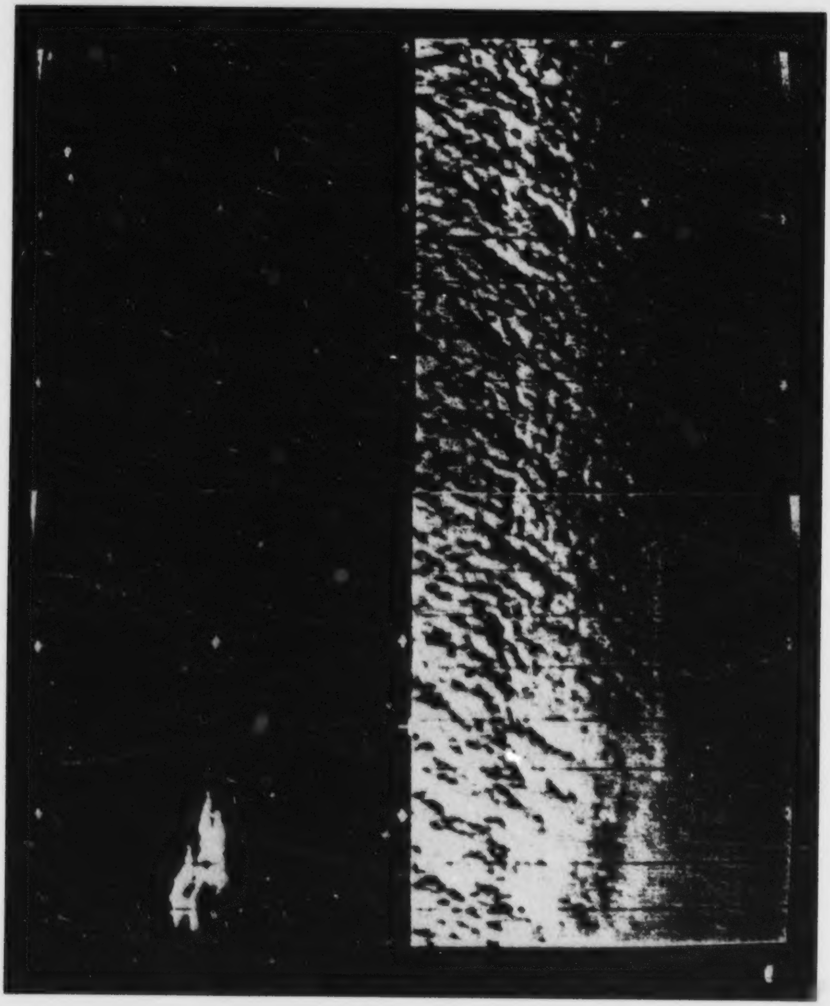

Figure 4 IR (left) and UV (right) images of the oil slick at 10:30 on July 1. Distance between reference ticks in the photograph is 280 m. The lighter areas in the IR photo show location of thicker oil. The top of the picture is almost due west.

m/sec, and then dropped during the late evening/early morning of the next day.

Most of the Argospheres were still carrying in excess of 3 kg of ballast on the afternoon of July 1. It soon became apparent that the Argospheres were falling behind the slick considerably faster than most of the LCD's. At this time one of the IKU drifters and the two symmetric LCD's, #9821 and #9822, were still within a hundred meters of the leading edge of the slick. The IKU drifters had been released after the others, and behind the slick, so this one (#4059) appeared to be moving faster than the other drifters and the oil. (An empty egg carton, discarded through a porthole by the chef on the tanker during discharge of the oil, was also very close to the leading edge, and was repeatedly sighted there over the next 24 hours.)

We recorded on video-tape a survey from the ship of the distribution of drifters between 16:50 and 17:10 on the afternoon of July 1. We began at the upwind (western) end of the slick, and recorded orally the locations of drifters and drifter types along with the telephoto video of the slick. From this information, we constructed a rough map of the distribution of drifters (Figure 5). We then went out in the rubber raft (17:45-18:30) and associated individual drifter numbers with the recorded positions, collected the lagging drifters, reballasted them, and redeployed them at the leading (eastern) edge of the slick (19:30). Maximum displacement due to redeployment computed subsequently from aerial photographs, was under 1500 m. The recorded locations (Figure 5) are actually the ship locations when the ship was abeam of each drifter, and are therefore offset to the north by 100 to 200 m. Figure 6 shows the composite infrared/ultra-violet (IR/UV) images of the slick at 18:21 on July 1. The IR image is on the left, the UV is on the right.

The slick had now elongated, such that the heavy oil was concentrated in an area about 25-50 m wide, and 500 m in length. The UV image (Figure 6, right) shows the sheen area increasing in width in the wake of the leading edge, with a mean width of about 150 m. At this time, the slick appears as a classical plume, except that the source (leading edge) is moving relative to the underlying fluid.

At 05:00 on the morning of July 2, the wind remained light, 3 to 4 m/sec out of the WNW. Several Argospheres, LCD's and one IKU drifter remained within 200 m of the leading edge of the slick. At 10:30, we initiated a second survey from the ship of the distribution of drifters along the east-west axis of the slick. This survey was timed to coincide with the first aerial overflights of the day, with the ship traveling parallel to the long axis of the slick. The ship-board survey was completed at 11:10. The IR/UV imagery from this overflight is shown in Figures 7. At this time the wind had shifted towards the northwest, producing a series of "fingers" angling off from the east-west axis of the slick.

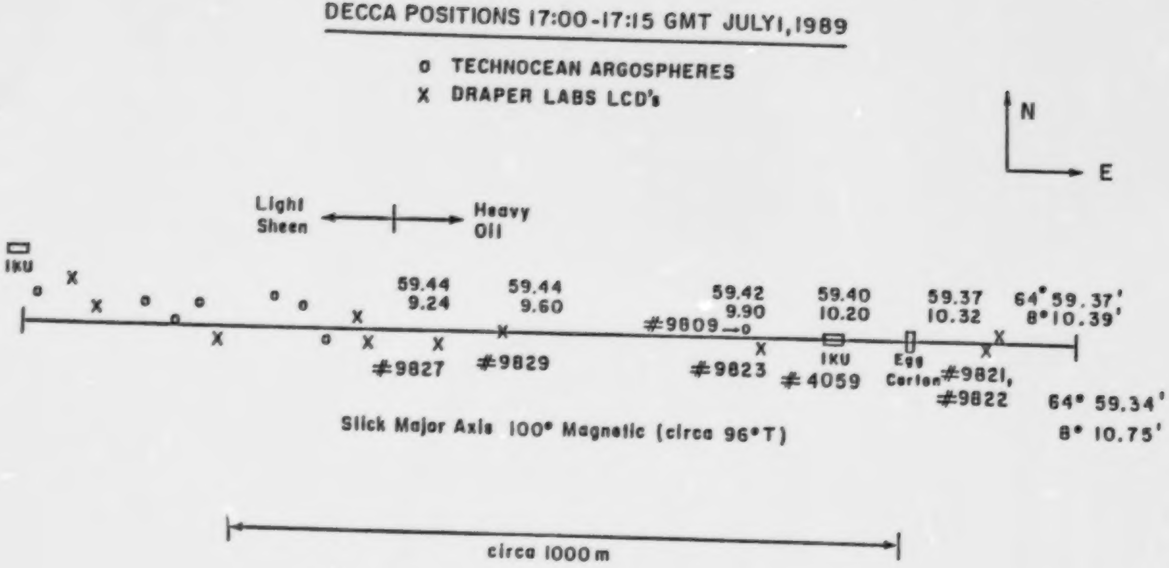

Figure 5 Field sketch of drifter locations in slick at about 17:00 (±10 min) GMT. Decca positions shown are actually ship positions at the time, and are therefore approximately 150 m north of actual drifter positions. Drifters for which positions are given were actually in the heavy oil at the time of observation. Others were in the region of light sheen to the west. Direction of drift is towards the east.

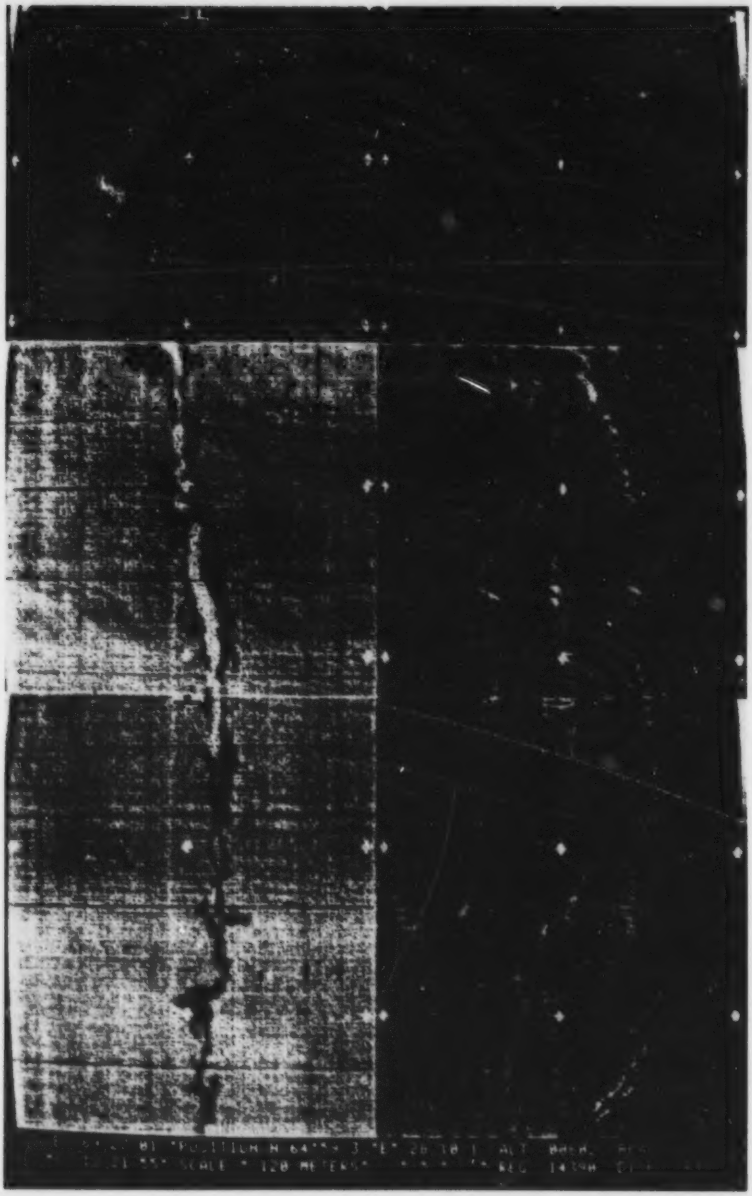

Figure 6 IR (left)/UV (right) image of the slick at 18:21 GMT on July 1. The downwind (leading) edge of the slick is at the top (east). Distance between cross-hairs is about 120 m.

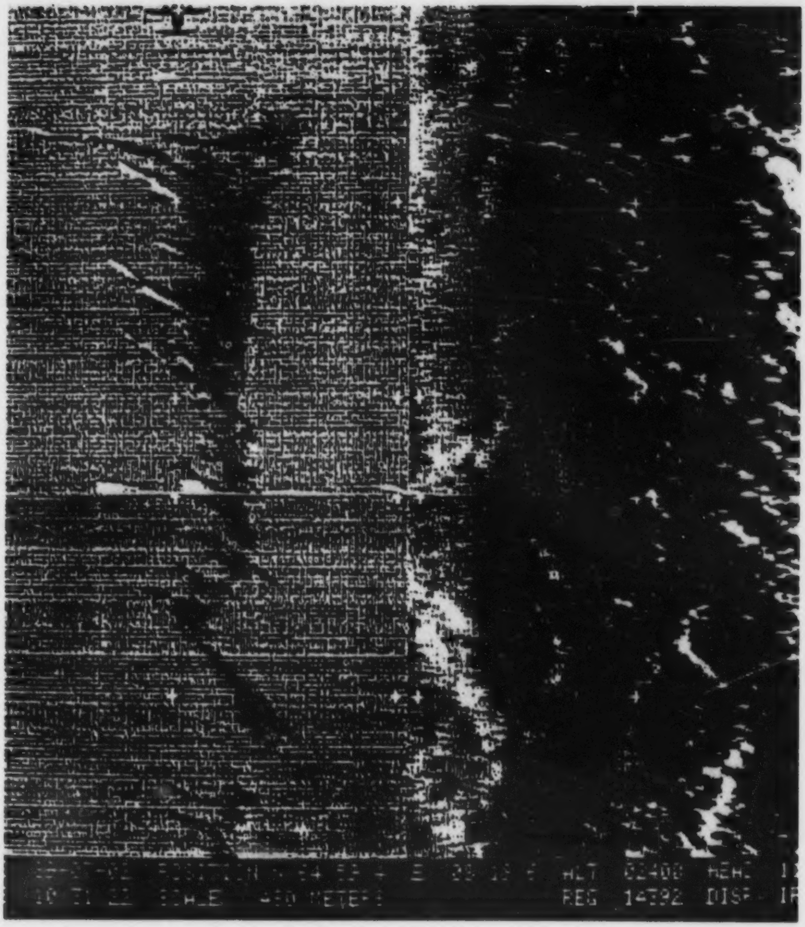

Figure 7 IR/UV images of the slick at 10:22 GMT on the morning of July 2, 26 hours after release. The wind has shifted from west (bottom of picture) to south-southwest.

At 12:15 we again went out to collect and reposition lagging drifters for the final time. Although some LCDs were repositioned nearer the eastern end of the slick, no ballast changes were made. Maximum displacement of drifters during this operation was about 1500 m, from the western to the eastern end of the slick. Since the wind had now swung around to the south, and remained out of the south and southwest for the remainder of the experiment, this displacement of drifters improved the probability that drifters would be subject to similar environmental forcing without directly affecting their locations relative to the slick in the direction of the wind.

The second set of overflights on July 2 took place between 18:20 and 19:00. The IR/UV imagery for this time is shown in Figure 8.

By the morning of July 3, the wind had increased to about 10 m/sec, and the slick had thinned significantly. A heavy overcast allowed only limited visual imagery. The thinness of the oil slick precluded useful IR/UV imagery, and combined with the stronger surface wind effects, also made the SLAR imagery useful only for establishing a mean location for the slick. With the assistance of the aircraft, we were able to locate a few patches of emulsified oil (circa 100 m^2). Heavy seas precluded safe use of the work skiff, so sampling was performed with a bucket on a rope from the ship. The emulsified oil had a viscosity of about 10,000 centipoise at this time, similar to heavy roofing tar at room temperature.

The *Endre Dyrøy* departed from the oil slick at this time to continue hydrographic surveys. On the morning of July 4, neither the ship nor the aircraft was able to relocate the oil slick. We then accessed the most recent Argos data for the drifters, and radioed the central coordinates to the aircraft, which then quickly located the slick. As on July 3, no aerial images were useful. From the ship, the slick appeared thin and patchy, covering a total area of about 2 km? Since we anticipated considerable difficulty in locating the slick the following day, and since we had already stretched the project budget because of the two-day weather delay, we decided to recover as many drifters as possible and then proceed with the final hydrographic survey.

3. RESULTS: THE ANALYTIC VIEW

Drifters were activated and released with the oil at about 08:15 on July 1; the majority were recovered, cleaned, and deactivated between 15:30 and 23:00 on July 4. Based on the timing of overflight windows by the two TIROS satellites during this time, there were 81 available windows for reporting of drifter locations over the 80-90 hours of the experiment.

Figure 8 IR (left)/UV (right) images of the slick at 18:52 GMT on July 2. North is at the right.

The first step in data processing was to compute velocities inferred by subsequent location updates. When the distance and time interval between two successive points inferred a velocity in excess of 1 m/sec, the lower quality of the two data points was eliminated. (The 1 m/sec threshold was selected based on discussions with the Quality Review Board. Argos reports the quality of location data on a sliding scale to reflect accuracy.)

Locations of surface drifters and oil were recorded intermittently during the experiment using aerial and shipboard Decca, to supplement the Argos location data for the drifters. The surveys from on board ship were intended to augment the overflight data, and provide additional opportunities for cross-checking navigational accuracies. It was never possible to identify by Argos number each drifter sighted during a shipboard survey, nor was it feasible to locate visually all the drifters. In addition, locations recorded during these shipboard surveys reflect ship location at the time the ship was abeam of a drifter, with physical offsets of 100-300 m.

Table 4 summarizes the distances of individual drifters from the spill center at seven specific times following release of the oil. Locations of the spill surface slick were based on Decca navigation, and are probably accurate within ± 100 m. Locations of drifters are interpolated linearly between successive Argos fixes, and are typically accurate to approximately ± 1000 m. Individual entries in Table 4 are unreliable. However, the general trend, that the Argospheres tended to behave more uniformly and tracked the slick better than the LCDs, is consistent with visual observations.

Table 4 Summary of distances of individual drifters from spill center at various times. Locations of drifters were interpolated between Argos fixes. Locations of the slick were determined by the more accurate DECCA system. Navigational errors associated with individual distances are on the order of 1000 m.

Date	July 1	July 1	July 2	July 2	July 3	July 4	July 4
Time (GMT)	10:37	18:08	10:41	18:52	10:40	14:42	18:30
Time since spill (hrs)	2	10	26	34	50	78	82
Spill size (km)	0.3	1.5	1.9	2.5	---	---	---
Distance traveled (km)	0	5.3	12.3	15.7	32.6	57.	62.
Linear speed (km/h)	0.66	0.66	0.43	0.42	0.94	0.94	0.62
Argos ID #	Distance from Spill Center (meters)						
Argospheres							
9802	528	351	911	751	1990	2030	---
9803	214	495	1010	618	1630	2070	---
9804	204	709	1030	709	1330	1340	---
9805	120	610	768	871	1650	1710	---
9806	229	345	998	1700	1740	2100	---
9807	84	96	961	563	1750	2360	---
9808	325	318	1130	349	1640	2050	---
9809	360	2010	439	423	1240	950	---
9810	260	1590	961	976	1480	1980	---
9811	450	343	550	634	1360	2330	610
9834	129	1100	407	660	1890	1890	---
Mean	358	724	840	841	1470	1730	610
LCDs							
9821	147	805	1810	1021	1120	2300	---
9822	257	545	1220	1050	462	3800	921
9823	175	176	277	550	3160	5580	7140
9824	192	767	265	176	2820	4060	4170
9825	443	563	305	1240	4120	3860	5570
9826	587	460	191	445	3250	5160	8130
9827	883	1510	2640	1970	2160	1720	1240
9828	327	522	1340	342	1660	491	480
9830	754	1110	1140	443	---	---	---
9831	890	1110	837	816	3100	6070	8710
Mean	514	688	911	733	2420	3670	4330

Actual trajectories of the Argospheres and LCDs are shown in Figure 9, with successive positions of the oil slick. Between 10:37 on July 1 and 18:52 on July 2, most of these drifters were redeployed at least once in an easterly direction, but with displacements typically less than 1 km (0.02° or 1.3' long. at 65° lat). Such redeployments would have negligible effects on the large scale behaviors shown here.

The trajectories reflect the two distinct environmental states evident during the trial. From the start time at 08:00 on July 1 through mid-day of July 2, winds were light and mostly easterly. Winds shifted towards the north and increased in magnitude, coming back around towards the northeast on the morning of July 3. The increased separation of trajectories following the overflight at 18:52 on July 2 reflects in part the spread of drifters along the east-west axis of the slick during the previous wind regime. The apparent spread is increased somewhat by missing intermediate location updates for some drifters.

The wind shifted from north to north-easterly at about 07:00 on July 3 (Section A-A, Figure 9). Thereafter the trajectories of the Argospheres and LCDs bifurcate, with the latter moving more slowly and about 20° further to the right. The reduction in speed and shift to the right are both consistent with increased subsurface drag and more subsurface Ekman effect. The symmetric LCDs, #9821 and #9822, and the unballasted #9828, are the three exceptions, and tracked the slick trajectory well. The Argospheres, on the other hand, moved virtually downwind, consistent with a larger sail area. The Argosphere trajectories appear a few degrees to the left of the oil.

It is also possible that the LCDs are more subject to wave rectification than the Argospheres. As discussed later, the net Stokes drift at the surface appears to have been about 6° to the right of the wind, and could have contributed to the observed divergence between the Argospheres and ballasted LCDs. That the unballasted LCDs did not behave in this way, however, weakens this argument somewhat.

Figure 10 shows the positions of the drifters and surface slick relative to the release point after approximately 80 hours. The Argospheres are clustered in a relatively tight pattern, compared to either the LCDs or the IKU drifters. The LCDs separated into two distinct groups, with those carrying external ballast falling further behind and to the right.

Figure 11 shows the trajectories of the LCDs alone. The three northerly trajectories are those of the unballasted drifters, #9821, #9822, and #9828. These drifters differ substantially in weight, and bracket the total weights of each of the LCDs which traveled more slowly and further to the right. This appears to lend strong support to the theory that, at least in long-wave, wind-dominated oceanic regimes, behavior of the LCDs is only weakly dependent

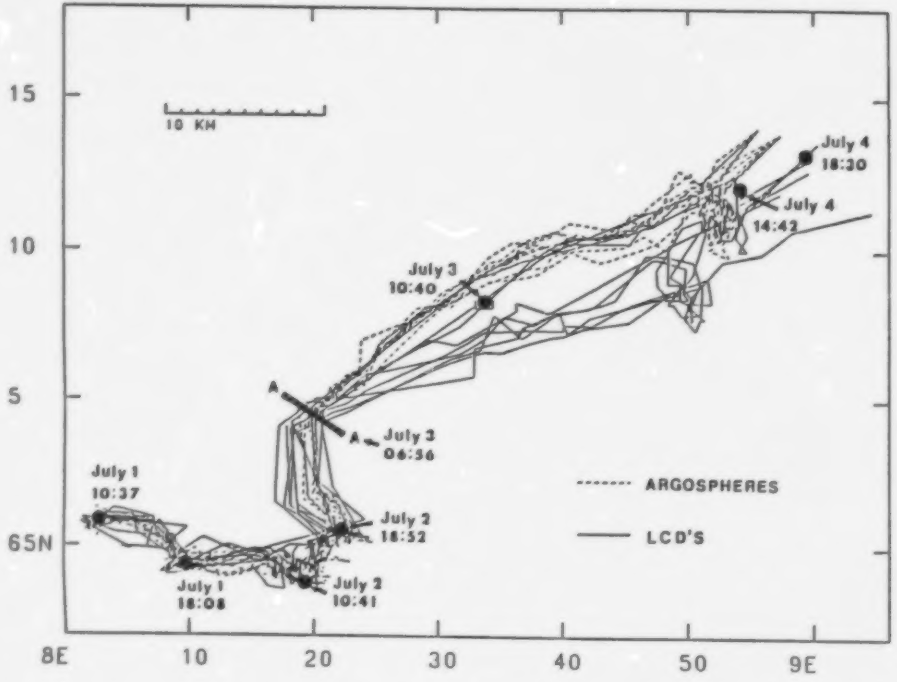

Figure 9 Trajectories of Argospheres and LCDs, and successive locations of oil slick. Line A-A differentiates the earlier, relatively quiet, and later, higher wind energy portions of the trajectories. No re-deployments of drifters took place after about 19:00 on July 2.

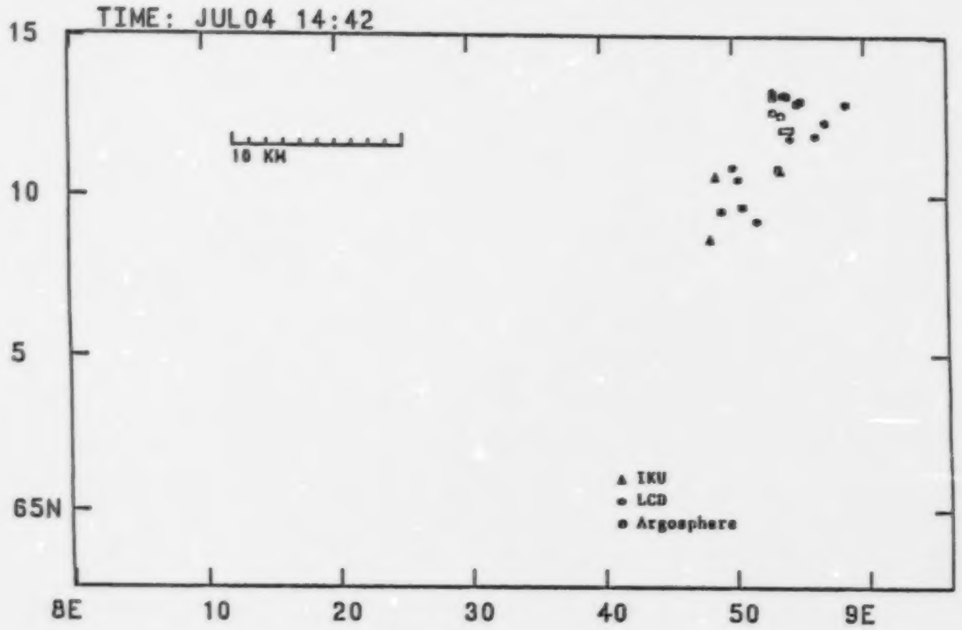

Figure 10 Position of drifters and oil relative to release point (65°N, 8°E) 80 hours after release. The rectangle locates the area covered by oil at this time.

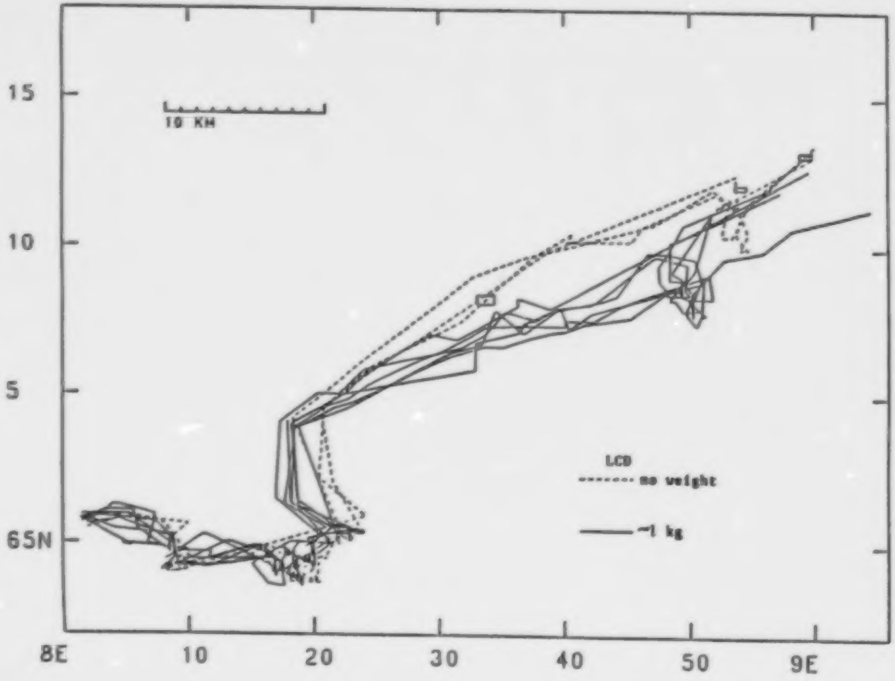

Figure 11 Trajectories of unballasted and ballasted LCDs, and successive locations of oil slick.

on their total mass, and is dominated by the relative drag forces of water and wind. Accordingly, it is not the added mass of the ballast which alters behavior (i.e. by further submerging the drifter), but the drag induced by the physical presence of the ballast weights themselves under the drifters.

Figure 12 shows the Argosphere trajectories alone. Differences in behavior are apparently not correlated with ballasting. The complete symmetry of these drifters appears to work in their favor in producing consistency. In the environment of this test, a small amount of additional ballast (and drag) might have served to further improve performance of these drifters.

Modeled and Observed Trajectories

The purpose of this section is to compare modeled and observed behaviors of oil and surface drifters. Determination of best fit models will allow us to identify transfer functions, to improve estimates of oil drift based on observed motions of surface drifters. The basic approach used here is the usual parameterization for surface drift problems:

$$\vec{u} = A\vec{W} + b\vec{C} \tag{1}$$

where the drift velocity, $\vec{u}$, is a function of the wind velocity, $\vec{W}$, and the non-wind-driven surface current velocity, $\vec{C}$. Here the Stokes drift has been included implicitly as a linear function of the wind speed. As discussed further below, this approach is only useful when the contribution from long period swell is closely aligned with the wind, or is negligible.

The rotational matrix A is

$$A = a \begin{bmatrix} \cos\theta & \sin\theta \\ -\sin\theta & \cos\theta \end{bmatrix} \tag{2}$$

where a is a dimensionless drift factor, and θ is a deflection angle. The coefficient for the surface current, b, is taken as unity. We varied the values of a and θ to produce best fit trajectories based on the observations. We also evaluated the usefulness of including various representations of the surface current versus using only the wind.

Best fit simulations for both oil and drifter trajectories were achieved by neglecting available estimates of the near-surface current in Equation (1). This result is not surprising to the extent that surface currents and waves were primarily wind-driven during this field trial. The parameter values found here (Table 5) are all at the high end of other sets of data in the literature. A major difference, however, between this and most previous studies with undrogued surface drifters, is that we were trying to define the drift rate of surface slicks, not the surface current (e.g. averaged over the top

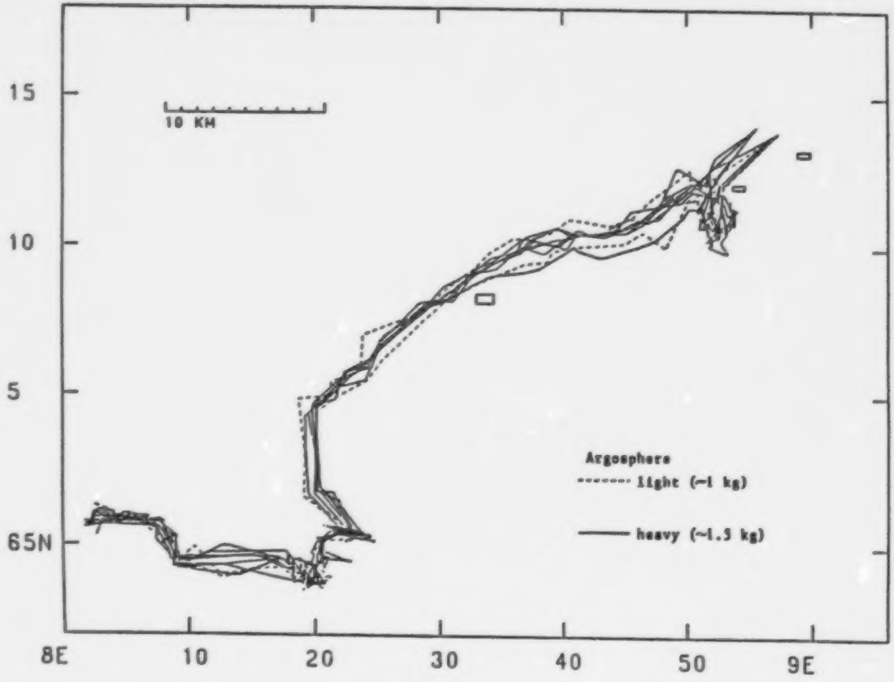

Figure 12 Trajectories of light (1 kg) and heavily (1.5 kg) ballasted Argospheres, and successive locations of oil slick.

1 m of the water column). The surface current drift factor found here, based on the Stokes drifters, is nearer the classical 3%. It would appear that thick surface slicks may drift considerably faster, and observations with dye studies suggest the differential velocity to be about 1.1%, for a total on the order of 4.1% of the wind speed.

Table 5 Summary of wind drift factors and deflection angles for the 1989 experiment on Haltenbanken.

	Oil	Argospheres	LCDs (unballasted)
Overall	4.6% @ 2°	4.2% @ 3°	4.2% @ 3°
Light Winds (2-5 m/sec)	4.7% @ -7°	4.2% @ 3°	4.2% @ 6°
Medium Winds (6-12 m/sec)	4.3% @ 7°	4.2% @ 3°	4.2% @ 3°

Figure 13 shows the computed best fit trajectory for the oil, compared with successive positions of the surface slick recorded by ship and aircraft. The mean error of the computed slick positions is about 2000 m.

Based on the work described above, an optimal correction or transfer matrix was derived to convert observed (satellite tracked) drifter trajectories to inferred oil trajectories:

$$A_D = \begin{bmatrix} 0.0040 & -0.0006 \\ 0.0006 & 0.0040 \end{bmatrix} \tag{3}$$

This matrix represents a stepwise correction to be applied to successive displacements of drifters to improve the simulation of oil trajectories.

4. SUMMARY AND RECOMMENDATIONS

1. A transfer matrix was derived to convert drifter velocities to oil velocities for future physical simulation work. This matrix is applicable for wind-dominated open ocean (long wave) conditions only. In oceanographic regimes with significant currents unrelated to local winds, other matrices must be derived from future experimental results. Three significant figures are necessary if the present matrix is to be non-zero, indicating that within the confidence of the navigational systems used, trajectories of Argospheres and unballasted LCDs were nearly indistinguishable from that of the oil.

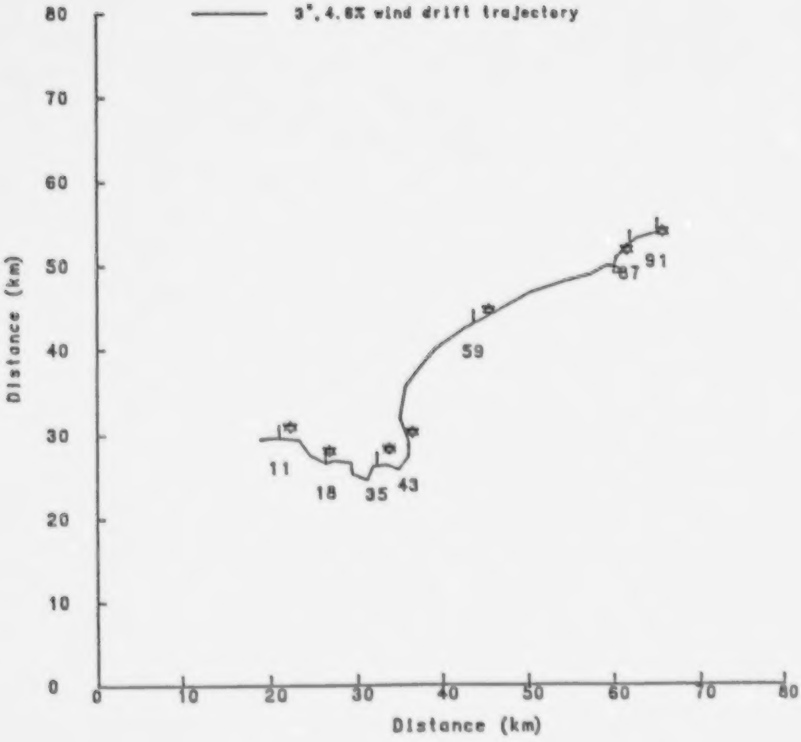

Figure 13 Best fit computed trajectory for surface oil, using wind only (a = 0.046; θ = 3°). Stars locate positions of oil; associated times are hours after midnight, July 1. Vertical lines locate associated positions along the computed trajectory.

2. Tests of PTTs performed prior to the field release of drifters reported here consisted primarily of checking PTTs against a hand-held receiver. In future tests, the frequency stability and signal strength of PTTs should be tested prior to deployment. A reasonable methodology would be to set the drifters out in an open field or on a rooftop, activate them, and map the reported Argos locations over the ensuing 24 or 48 hours. This will serve to flag "rogue" transmitters, as well as any which are not being received by the satellite. Some testing is performed at the factory, but quality control could be improved. It may be desirable to equip future drifters with PTTs set to a 60 second repetition rate. This may increase both the quality and frequency of location updates.

3. LCDs for simulation of oil slick drift should be manufactured in symmetric form, and ballasting should be performed around the circumference to avoid subsurface drag effects. Some additional design work will be necessary to accomplish this.

4. One out of three IKU drifters tracked the leading edge of the slick well throughout the experiment. The other two IKU drifters, although apparently identical in shape and weight, performed relatively poorly. The extreme asymmetry of this design may make it very sensitive to small variations in placement of ballast, angle of end-skirts, etc. Any small change in the attitude of the drifter relative to the direction of drift would significantly alter the drag induced by its keel.

5. The presence of a film of emulsified oil (i.e. oil containing up to 70% water) on the upper surface of drifters may significantly decrease signal strength. This will not be a problem in simulation of trajectories, but should be considered in future field tests with oil.

6. Data from this experiment would be useful in validating mass balance oil spill models, and in development of improved algorithms for surface spreading and transport.

This project appears to have been extremely successful, despite the usual array of problems endemic to complex oceanographic field experiments. The bottom line is that the Argospheres performed well and consistently through a range of environmental states, shadowing the oil slick until the slick dissipated after about four days. Unballasted LCDs also performed extremely well; subsurface ballasting of these latter drifters significantly degraded their behavior.

These results should be valid in other mid-to-high latitude, oceanographic environments which are dominated by wind and long period waves. Further tests will be necessary to derive equivalent results for other types of environments.

Results of this experiment suggest that the Ekman shear in the top 30 cm of the water column may be extremely strong. Where wind-driven currents dominate the physical oceanography, surface drifters must carry enough "sail" above the water surface to overcome this Ekman drag, especially when subsurface ballast weights, which increase subsurface drag, are used to achieve the proper balance of aerodynamic and hydrodynamic forcing. Where tidal or other non-wind forcing is important, previous work indicates that ballasting may have to be increased by as much as a factor of 5 (Reed, 1989).

The type of oil spilled will also affect drift rate. Oils such as Oseberg and Prudhoe Bay crudes, which rapidly emulsify to densities very close to seawater, and viscosities on the order of 10,000 cP, (about the same as roofing tar at room temperature), will behave differently from crudes and other petroleum products which do not form oil-in-water emulsions.

It is therefore essential that we accumulate further empirical information to produce transfer functions for other oceanographic regimes and petroleums. The necessary data can be gathered only in the presence of oil on the sea surface. MMS should therefore consider additional experimental oil spills, as well as the use of spills of opportunity to complete this work prior to large scale deployments of surface drifters. Widespread use of these drifters to simulate surface oil drift is not yet warranted, based on the single isolated event reported here.

This project has resulted in a unique data set focussing on transport of oil and surface drifters at the air-water interface. The drifters which best simulated the drift of the surface slick extended only about 20 cm above or below the interface. The review of surface transport field experiments performed during the first phase of this project (Reed et al., 1988) reflected relatively little previous work directly applicable to this problem, and certainly none with such a large number of drifters and detailed observations. The successful use of surface drifters in simulating trajectories of surface oil represents a significant advance in the credibility of input data for future OCS environmental impact statements, as well as a valuable data source for scientists interested in surface transport phenomena in the ocean.

5. ACKNOWLEDGEMENTS

Primary support for this project came from the U.S. Department of the Interior, Minerals Management Service, Atlantic Region. David Browne served as Contracting Officer's Technical Representative. James Shilkett was contracting officer. Other institutions which supported the project include:

- The Netherlands North Sea Directorate (NNSD)
- The Norwegian State Pollution Control Authority (SFT)
- The Norwegian Operators Committee for Oil Spill Contingency (NOFO)
- The Continental Shelf and Petroleum Technology Institute (IKU)
- Norwegian Institute for Nature Research (NIVA)
- Norwegian Fisheries Directorate (NFD)
- Norsk Hydro A/S (NH)

The data analysis and final report were planned with and reviewed by a technical review board consisting of

Dr. Scott McDowell, Battelle Memorial Institute;
Dr. P. Peter Niiler, Scripps Institute for Oceanography;
Dr. Thomas Rossby, Rhode Island Graduate School of Oceanography.

The authors gratefully acknowledge their contributions.

Word processing was performed by Liz Kard, Kate Sexton, and Jan Hopp of Applied Science Associates, Inc.

6. REFERENCES

Audunson, T., B. Fossum, J. Haldorson, P. Steinbekke, 1979. Drift of Satellite and DECCA Positioned Buoys During the Experimental Oil Spill on Tromsøflaket, September, 1978 (in Norwegian). Continental Shelf Institute, Report No. P195/3/79, Trondheim, Norway, 54 p.

Audunson, T., H. Celius, Ø. Johansen, P. Steinbekke, S. Sørstrøm, 1984. The experimental oil spill on Haltenbanken, 1982. Continental Shelf Institute Report No. 112, Trondheim, Norway. 109 p.

Daling, P. and Ø. Johansen, 1986. Effectiveness of dispersants on oil spills at sea - a handbook for national pollution authority (in Norwegian). Sintef-Gruppen, Trondheim, Norway. 60 p.

LaBelle, R.P. and C.M. Anderson, 1985. The application of oceanography to oil-spill modeling for the Outer Continental Shelf Oil and Gas Leasing Program. Marine Technology Society Journal, 19(2):19-26.

Reed, M., 1989. Observations of satellite-tracked surface drifters and spilled oil in Prince William Sound, Alaska. Report to U.S. Department of the Interior, Minerals Management Service, Herndon, VA. May, 1989. Requisition No. 9-4350-0161. 21 p.

Reed, M., C. Turner, M. Spaulding, K. Jayko, D. Dorson Ø. Johansen, 1988. Evaluation of satellite-tracked surface drifting buoys for simulating the movement of spilled oil in the marine environment. Final Report (Phase I) to U.S. Dept. of Interior, MMS, Herndon, VA, Contract No. 14-12-0001-30340, 2 Vols, 84 p. + appendices.

Smith, R.A., J.R. Slack, T.Wyant, K.J. Lanfear, 1982. The oil spill risk analysis model of the U.S. Geological Survey. Geological Survey Professional Paper 1227, 107 pp.

Sørstrom S.E. and O. Johansen, 1985. Experimental oil spill at Haltenbanken. Data Report No. 85.136. Oceanographic Center. Trondheim, Norway, 119 p.

REMOTE SENSING OF OIL SPILLS

Merv Fingas
Environmental Emergency Technology Division
Conservation and Protection
Environment Canada
Ottawa, Ontario

INTRODUCTION

Remote sensing has become an increasingly important part of oil spill countermeasures. Public expectations with respect to the environment are increasing, the minimum action for a spill is that the government or the spiller know the location and extent of the contamination. It is also being recognized by spill cleanup personnel that remote sensing can be used to increase spill cleanup efficiency. Furthermore, the advance in electronics has made the instrumentation much cheaper and capabilities which were only once dreamed of are now in reach.

The definition of remote sensing implies that a sensor, other than the eye, is used to detect the target of interest at a distance. The most common form of remote sensing as applied to oil spills is aerial remote sensing - that is using aircraft as a platform. Visual observation of oil spills is by definition, not remote sensing.

OPTICAL TECHNIQUES

The most common means of remote sensing is the use of optical techniques, particularly cameras, both still and television. Aerial mapping is very common and many companies are equipped with aircraft and cameras to perform this function. Many cameras have been commercially available over the past 10 years. Table 1 lists a number of these.[1,2] (It is important to note that this table and all others in this paper include sensors that were available in the past, those that are currently available and in some cases, those under development.) The large format cameras listed in Table 1 are largely used for mapping purposes, however are occasionally used for oil spills. The front cover of the proceedings are a reproduction from a 9X9 inch format RC-10 camera. The image is of the EXXON VALDEZ spill during the early part of April, 1989.

Oil has an increased surface reflectance above that of water in the visible, but also shows some specific absorption tendencies to allow use of the visible spectrum as an oil detection means. The visible spectrum is from approximately 400 to 700 nm (blue to red). Oil has several manifestations throughout the spectrum. Heavy oil appears brown, showing up in the 600 to 700 nm region. Mousse shows up in the red-brown or closer to 700 nm. Sheen shows up silvery and reflects light over a wide spectral region up to the blue. There is no strong information in the visible region from 500 to 600 nm, so often this region is filtered out, to give stronger contrast. Experimenters have found that one technique for giving high contrast to visible imagery is to set the camera at the Brewster angle (53 degrees from vertical) and use a horizontally-aligned polarizing filter which passes only that light reflected from the water surface. It is this component that contains the information on surface oil.[1] This technique is said to increase contrast by as much as 100%. Filters that have band-pass below 450 nm may also be used to improve contrast. Figure 1 illustrates the use of a photographic camera in a nadir mode (looking straight down). Figure 2 shows an oblique photograph and illustrates the sun glint that often interferes with this type of photography.

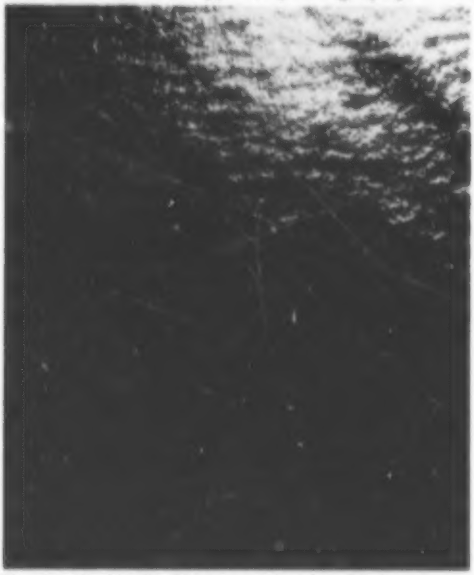

Figure 1 Nadir Photograph of a Slick

The use of visible techniques is largely restricted to that of documentation because the lack of a positive oil detection mechanism. Furthermore, many interferences exist. Sun glint and wind sheens can be mistaken for oil sheens. Biogenic material such as surface weeds or sunken kelp beds can be mistaken for oil. Oil on shoreline is difficult to positively identify because weeds can have similar appearance and oil on darker shorelines cannot be detected.

TABLE 1 **AERIAL CAMERAS**

MANUFACTURER	MODEL	FOCAL LENGTH (mm)	ANGLE COVER (deg.)	WEIGHT (kg.)	PRIME PURPOSE
9X9 in. OR 23X23 cm. FORMAT CAMERAS					
WILD HEERBRUGG	RC-10	90/150	74/104	78	MAPPING
JENA	MRB 15/2323	150	74	63	MAPPING
GALILEO	MODEL VI	150	74	36	MAPPING
CARL ZEISS	RMK A 8.5/23	85	107	60	MAPPING
CARL ZEISS	RMK A 15/23	150	74	57	MAPPING
CARL ZEISS	RMK A 60/23	610	23	54	MAPPING
FAIRCHILD	T11,T11A	150	74	39	MAPPING
FAIRCHILD	KC-6A	150	74	66	MAPPING
FAIRCHILD	F-639	150	74	45	MAPPING
FAIRCHILD	CA-3-2	150/300/600	74/41/20		RECON.
FAIRCHILD - GORD	CA-17	150/300	74/41		RECON.
HYCAN	K-22A	50/300/600/101	74/41/20/12		RECON.
AEROFLEX	KC-3	90	104		RECON.
9X18 in. OR 23X46 cm. FORMAT CAMERAS					
FAIRCHILD	CA-18	300/600/900	41/20/14		RECON.
4.5X4.5 in. OR 11X11 cm. FORMAT CAMERAS					
CAI	KA-30A	150	41		RECON.
CAI	KA-45A	150	41		RECON.
CAI	KA-50A	45	104		RECON.
CAI	KS-87A	75/150/300	74/41/21		RECON.
HYCAN	KS72C-1	75/150/300/450	74/41/21/14		RECON.
2.25X2.25 in. OR 6X6 cm. FORMAT CAMERAS					
FAIRCHILD	CAX-12	38/75/150/300	74/41/21/10		RECON.
VINTON	492	38/75	74/41	8	RECON.
0.69X0.87 in OR 1.5X2.2 cm. FORMAT CAMERAS					
MITCHELL	KF-8	50/100/150/250	18/9/6/3		RECON.
4.5 in. OR 11 cm. FORMAT STRIP CAMERAS (CONVERTIBLE TO 9 in.)					
CAI	CAS-2A	00/175/300/500	60/35/21/12		RECON.
CAI	KA-18A	75/150	41/74		RECON.
BILL JACK	S-11	89/150/500	69/74/12		RECON.
4.5X40 in. OR 11X100 cm. FORMAT PANORAMIC CAMERAS					
FAIRCHILD	KA-59A	300	12x180		RECON.
PERKIN ELMER	KA-58A	450	14X180		RECON.
4.5X9.4 in. OR 11X24 cm. FORMAT PANORAMIC CAMERAS					
FAIRCHILD	KA-56A,B	75	73X180		RECON.
FAIRCHILD	KB-78	75	81X180		RECON.
2.5X9.4in. OR 6X24 cm. FORMAT PANORAMIC CAMERAS					
PERKIN ELMER	KA-57A	75	41X180		RECON.
PERKIN ELMER	KA-73	75	41X180		RECON.
FAIRCHILD	KA-71A	75	40X180		RECON.
FAIRCHILD	KB-18A	75	40X180		RECON.

LEGEND RECON = RECONNAISSANCE

In addition to photographic cameras, television cameras are been used. Several systems use filters as noted for the photographic cameras, to improve the contrast. In the 1970's, when television cameras were not highly developed, low-light level television (L^3TV) was used to document spills and also as an inexpensive remote sensor. With the advent of charge-couple device (CDD) detectors in television with their high sensitivity, this technology has become obsolescent. An ordinary home video recorder has similar sensitivity to the former specially-purchased L^3TV. Some effort has been put into employing filters with television cameras to enhance their utility for oil spill remote sensing, but this technique has limited success, being still limited by poor contrast and lack of positive oil identification means.

Figure 2 Oblique Photograph of An Oil Slick

Another visible technique that has not been pursued in recent years is that of laser-illuminated television or active-gated television. The USCG had developed a prototype for their "Aireye" system. The purpose of the unit was to capture pictures of a ship's name. A laser pulse is used to illuminate the field of view and the television is gated to the pulsed laser. Unfortunately, a fully-functional unit was not completed.

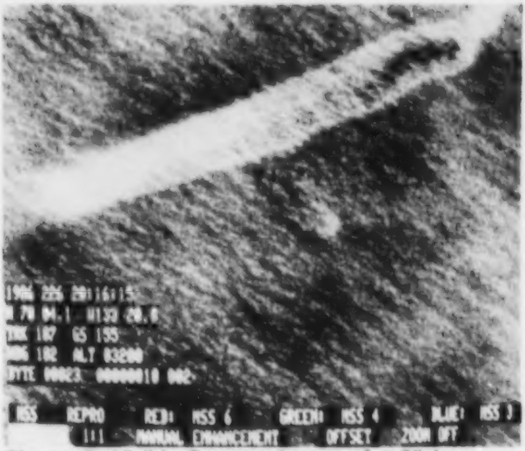
GS 155
ALT 03200
MSS REPRO RED: MSS 6 GREEN: MSS 4 BLUE: MSS 3
1:1 MANUAL ENHANCEMENT OFFSET ZOOM OFF

Figure 3 Visible Scanner Image of a Slick

Scanners are also used as sensors in the visible region of the spectrum. A rotating mirror or prism sweeps the field of view and directs the light to a detector. Before the advent of CCD detectors this method provided much more selectivity and sensitivity than a television camera. The other advantage of using scanners is that signals are digitized and can be processed before display. Figure 3 shows an scanner image of an oil slick. The advantage of using this type of sensor over a regular camera is readily apparent. In recent years, technology has evolved and similar digitization can be achieved without scanning by using a CCD imager and continually recording all elements, each of which is directed to a different field of view on the ground.This type of sensor is known as a push-broom scanner. The advantages of this technology over the older scanning types are many. Several types of abberations and errors can be overcome, units are more reliable than mechanical ones, and all data are collected simultaneously for a given line perpendicular to the direction of flight. Scanners and push broom devices are listed in Table 2. Of particular interest are the MEIS (Multi-spectral Electro-optical Imaging Scanner) devices. This series of push broom devices feature relatively narrow band widths and high resolutions. MEIS II has 1024 detector elements, and MEIS FM, currently under development, has 6000 elements, giving it near-photographic quality.

In summary, use of the visible spectrum for oil detection is limited,

TABLE 2 **LINE SCANNERS**

MANUFACTURER	MODEL	SCANNER	WIDTH (deg.)	RECORDER	WEIGHT (KG.)
INFRA-RED SCANNERS					
BENDIX	LM-3	45 deg. PRISM	120	TAPE,FILM	55
DAEDALUS	DE1-100	DBL. 45 MIRROR	120	TAPE,FILM	65
DAEDALUS	DS-1200	45 deg. MIRROR	77	TAPE,FILM	85
HRB SINGER	RECONOFAX VI	DBL. 45 MIRROR	120/140	FILM	75
HRB SINGER	RECONOFAX XIIIA	4-SIDE PRISM	120	FILM	135
TEXAS INSTRUMEN	RS-310	4-SIDE PRISM	90	FILM	97
TRW HAWKER		4-SIDE PRISM	90	FILM	25
MULTI-SPECTRAL SCANNERS					
ACTRUM	MMS-564K	CONICAL	51	TAPE	79
BENDIX	MMS	45 deg. MIRROR	60	HI-DEN. TAP	1300
DAEDALUS	1230	45 deg. MIRROR	77	TAPE	54
DAEDALUS	1260	45 deg. MIRROR	86	TAPE	129
TEXAS INSTRUMEN	RS-14	4-SIDE MIRROR	60	CRT. FILM	120
PUSH-BROOM MULTI-SPECTRAL DEVICES					
ITRUS	CASI	PUSH-BROOM	40	TAPE	30
CCRS	MEIS I	PUSH-BROOM	24	TAPE	46
MDA	MEIS II	PUSH-BROOM	45	TAPE	
MDA	MEIS FM	PUSH-BROOM	60	TAPE	

TABLE 3 **THERMAL INFRARED CAMERAS/SYSTEMS**

MANUFACTURER	MODEL	COOLING	WAVELG. (mic.)	WEIGHT(kg.)
FLIR OR FORWARD LOOKING INFRARED SYSTEMS				
FLIR SYSTEMS	L300 3	J-T CRY.	10.4	
FLIR SYSTEMS	L300 4	J-T CRY.	10.4	
FLIR SYSTEMS	L300 4A	J-T CRY.	10.4	
FLIR SYSTEMS	L300 4B	J-T CRY.	10.4	
HONEYWELL	WA8A17	J-T CRY.	7.5-11.5	
LOCKHEED	68-69	J-T CRY.	10	
AEROSYSTEMS	AEROFLIR	J-T CRY.	8.0-12.0	
GENERAL PURPOSE CAMERAS				
BARR & STROUD		J-T CRY. , AIR	8.0-14	10
SMALL GENERAL PURPOSE INDUSTRIAL CAMERAS				
GEN. ELECT.	EEV	NONE	7.-12	0.5
BOOTH	IND-R-SCOP	NONE	5.-12	0.7
AGEMA	HERMOVISIO	J-T CRY.	5.-13	1
HUGHES	ROBEYE 730	ELECTRIC	2-5.6	3
HUGHES	699	ELECTRIC	2-5.6	3
HUGHES	696	GAS	2-5.6	4
HUGHES	664	ELECTRIC	2-5.8	3
HUGHES	650	GAS	2-5.6	3

NOTE: J-T = JOULE-THOMPSON COOLING

it does, however, offer economical means of documenting spills and means of providing baseline data on shorelines or relative positions.

INFRARED SENSORS

Oil which is optically thick absorbs solar radiation and re-emits this radiation as thermal energy largely in the 8 to 14 micron (8000 to 14000 nm) region. This phenomenon lends itself to oil detect by infrared sensing. One part of the phenomenon that is not fully understood is the appearance of oil between thick layers and thin layers. This oil appears to be cool in the infrared. Thin oil, or sheens, are not detected by infrared. Thick oil appears hot or white in infrared data, middle thickness appear cool and black and thin oil is not detectable. The thicknesses at which these transitions occur are not known, but scientific evidence indicates that the transition between the heated and cooled layer lies between 50 and 150 microns and the minimum detectable layer lies between 10 and 70 microns. [3,4,5,6,7] The reason for the appearance of the "cool" slick is not fully understood.

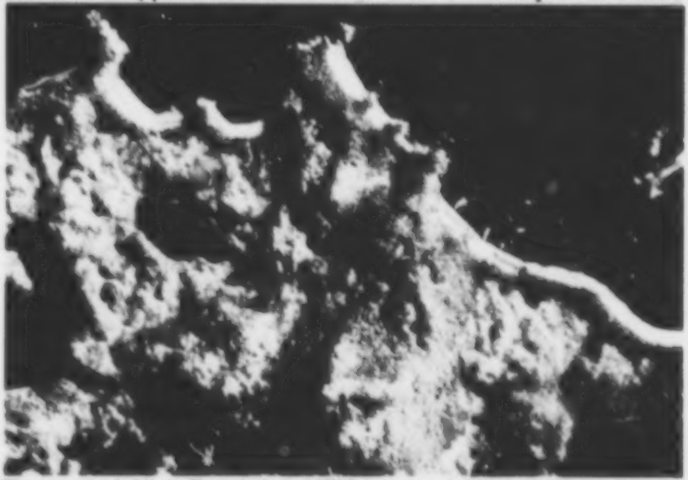

Figure 4 A High Resolution MEIS Image of Prince William Sound

One theory is that the evaporative cooling of the slick exceeds its radiative heating at a certain thickness and thus appears cool compared to the water. Another and more likely theory, is that a moderately thin layer of oil on the water surface causes destructive interference of the thermal radiation waves emitted by the water, or in some other way attenuates this signal, thereby reducing the amount of thermal radiation waves emitted by the water.[1]

Infrared cameras are very common now and several commercial units are available and are listed in table 3. In past years scanners with infrared detectors were largely used. Some of these units are detailed in Table 2. Infrared detectors of any type suffer from the disadvantage that their detectors require cooling to avoid thermal noise, which would in fact, destroy any useful signal. The traditional method of cooling the detector was by using liquid nitrogen. This generally gives about 4 hours of service. New, smaller sensors can use electric thermal coolers or Joule-Thompson coolers which use the cooling effect realized when a gas is expanded. This type of cooling implies that a gas cylinder or compressor be transported with the sensor but refills or servicing may not be required for days at a time.[8]

Most infrared sensing takes place at what is known as the thermal infrared at the wavelengths 8 to 14 microns. Figure 5 and 6 illustrate the usefulness of infrared imagery in oil spill work. Figure 8 shows the same slick as shown in Figure 7, but as a photographic image. One sensor which is designed as a fixed-mounted unit uses the differential reflectance of oil and water at 2.5 and 3.1 microns.[9]

The thickness indication of infrared is quite useful because it can be used to direct countermeasures equipment to thicker portions of the slick. The indication of oil is not positive, because a number of targets can interfere including weeds, shoreline, and oceanic fronts. Infrared is, however, relatively economical and is currently the prime tool used by the spill remote sensor.

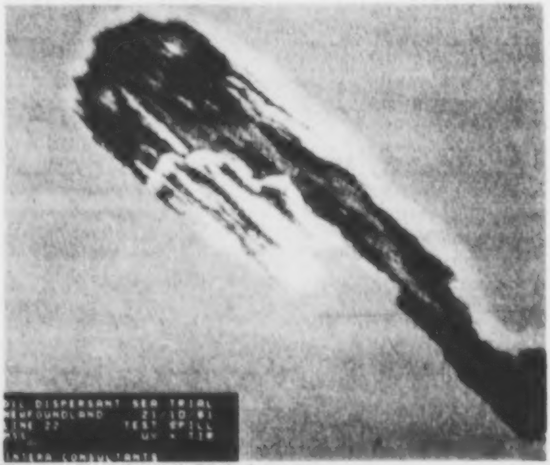

Figure 5 Infrared Slick Image

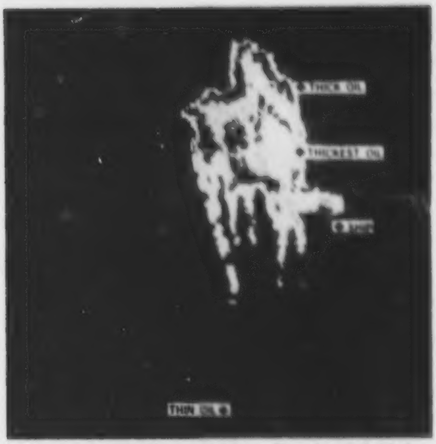

Figure 6 Thickness Map Produced Using IR and UV

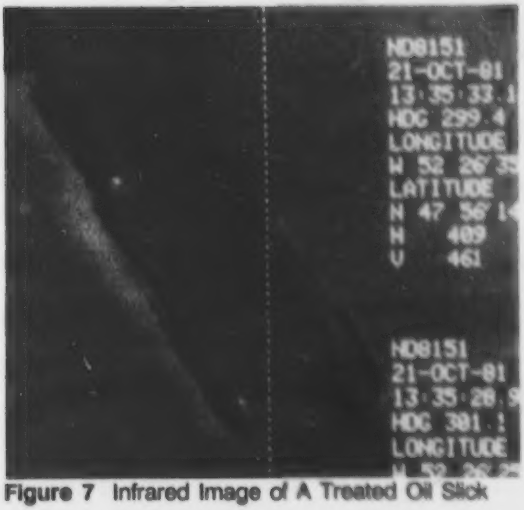

Figure 7 Infrared Image of A Treated Oil Slick

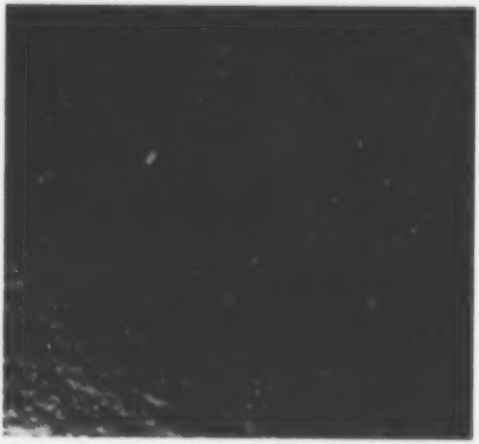

Figure 8 Photograph of The Same Slick as Shown Above

ULTRAVIOLET SENSORS

Oil displays high reflectivity of ultraviolet radiation even at thin layers (<0.01 microns). Ultraviolet sensors then can be used to map even thin sheens of oil. Overlapped ultraviolet and infrared images are often used to provide a relative thickness map of spills. Ultraviolet cameras, although inexpensive, are not used to a great extent because it is difficult to overlay camera images.[8] Scanner data and push-broom scanners allow for the easy superimposition of data and the production of IR/UV overlay maps. Ultraviolet data is also subject to a number of interferences such as wind slicks, sun glints, and biogenic material. Because these interferences are somewhat different than those for infrared sensing, the combination of IR and UV can provide a more positive indication of oil than the use of either technique alone.

FLUOROSENSORS

Fluorosensors employ the property that some compounds in the oil absorb light in the UV region and re-emit part of this energy in the visible region. Since very few other compounds show this tendency, fluorescence is a strong indication of oil presence. Natural fluorescing substances such as chlorophyll, fluoresce at sufficiently different wavelengths to avoid confusion. There is, however, a strong natural fluorescent material known as "gelbstoff" which consists of a broad spectrum of fluorescing materials. This background changes slowly over distance along the sensor path and thus can be compensated for rather easily. Different types of oil yield a slightly different fluorescent response. It is possible to differentiate between a heavy and a light oil under ideal conditions. This property is currently useful only as a scientific tool. Figures 9 and 10 shown signals from older instruments.

Most laser fluorosensors employ a laser operating in the ultraviolet region between 340 and 300 nm.[7,10] With this wavelength of activation, there exists a broad organic matter fluorescent return, centred at 420 nm. This is the Gelbstoff or yellow matter, which can be easily annulled. Chlorophyll yields a sharp peak at 685 nm. Oil fluorescent return is in the region between 400 to 550 nm with peak centres in the 480 nm region. There also exists a phenomenon known as Raman Scattering, which involves molecular reaction between the incident light and the water molecules on the surface. The water molecules can absorb some of the energy as rotational-vibrational energy and return the light as the incident energy less this energy of rotation or vibration. The water Raman signal occurs at 344 nm when the incident wavelength is 308 nm. The water Raman is useful for maintaining calibration of the fluorosensor in operation, but had also been used in a limited way to estimate oil thickness, because oil on the surface will suppress the water Raman signal in proportion to thickness.[11] The point at which the Raman signal is entirely suppressed is not known, and each oil type has a different absorption parameter. Therefore it is difficult to employ water Raman suppression as a thickness sensor.

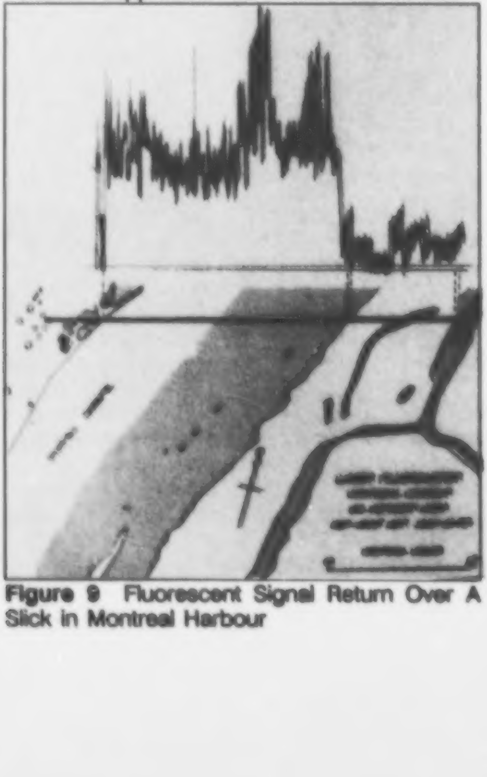

Figure 9 Fluorescent Signal Return Over A Slick in Montreal Harbour

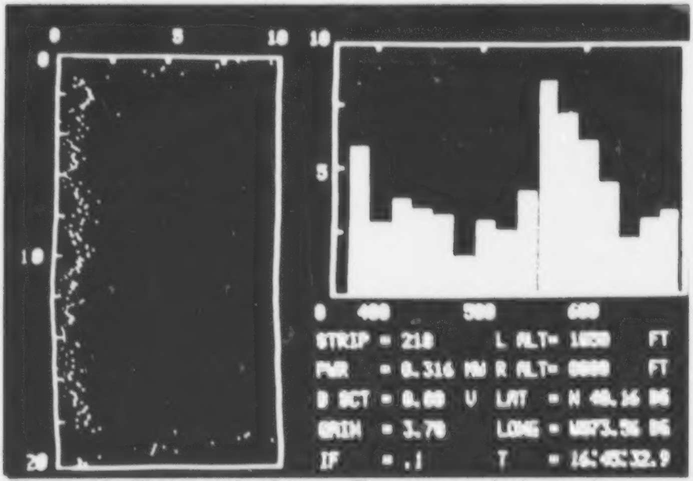

```
STRIP = 210       L ALT= 1050     FT
PWR   = 0.316 MW  R ALT= 0000     FT
B SCT = 0.00  V   LAT   = N 48.16 DG
GAIN  = 3.70      LONG  = W073.56 DG
IF    = .1        T     = 16:45:32.9
```

Figure 10 Photograph of Laser Fluorosensor Instrument Screen Showing Signal Strength and Spectrum

It is also possible to use the principle of oil fluorescence on a small scale. Work has been done to develop the use of a hand-held UV light to detect oil spills at night at short range.[12]

Another related instrument is the "Fraunhofer Line Discriminator" which is essentially a passive fluorosensor using solar irradiance instead of laser light.[1] This instrument did not achieve great success because of the limited discrimination and the poor signal-to-noise ratio.

Laser fluorosensors are thought to have significant potential for the future because they may be the only means to discriminate between oiled and un-oiled weeds on the sea surface and detecting oil on a variety of beach types. Additionally, the sensor offers the only means of detecting oil in certain ice and snow situations.

Development continues on laser fluorosensors, as the ideal instrument has still not been built. Table 4 provides details on some current and future instruments.

TABLE 4 **LASER FLUOROSENSORS**

MANUFACTURER	MODEL	LASER			NUMBER OF CHANNELS
		TYPE	WAVELENGTH (nm)	POWER (w)	
OLDENBURG	CURRENT	EXIMER	308	10	4/5
		DYE	450/533	1	4/5
OLDENBURG	PROPOSED	EXIMER	308	10	12
BARRINGER	MK III	NITROGEN	337	5	16
BARRINGER	LEAF	EXIMER	308	10	64
BARRINGER	PROPOSED	TRIP-YG	366	20	64

MICROWAVE AND RADAR

RADAR

Oil on a sea surface damps some of the small capillary waves. Since these capillary waves reflect radar energy producing a "bright" image known as sea clutter, the presence of an oil slick can be detected as a "cold" sea or one which has an absence of this sea clutter. Unfortunately oil slicks are not the only phenomenon which is detected in similar manner. Interferences are many and include fresh water slicks, wind slicks (calms), wave shadows behind land or structures, weed beds which calm the water just above them, glacial flour, biogenic oils, whale and fish sperm. Because of the number of these interferences, radar can be useless in situations such as in Prince William Sound where the hundreds of islands, fresh water inflows, ice, and other features yield literally hundreds of false targets. Radar is, despite these limitations, an important tool for oil spill remote sensing because it is the only useful sensor for large area searches, as will be demonstrated later, and because it is one of the few sensors that can "see" at night and through clouds or fog.

The usefulness of radars in conducting large-area searches is illustrated in Table 5. If one compares different sensor options in searching for lost-cargo-type spills. The scenarios given are real. A ship will upon rare occasions, reach its destination or a point in its journey and the crew discovers that it has lost a certain percentage of its cargo. A similar situation existed with the KURDISTAN tanker which broke in half, but due to the differential drift between the ship halves and the oil, the location of the lost cargo was unknown until found by remote sensing techniques. Table 5 illustrates that the only practical means of searching for this cargo is to use a wide-range radar and a jet airplane. Use of limited-range radars is not a practical means for performing this function.

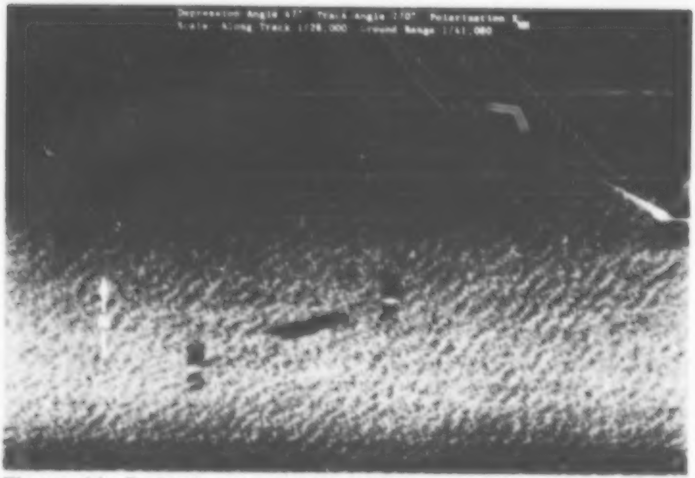
Depression Angle 47° Track Angle 270° Polarization
Scale: Along Track 1/28,000 Ground Range 1/41,000

Figure 11 Radar Image of A Test Slick

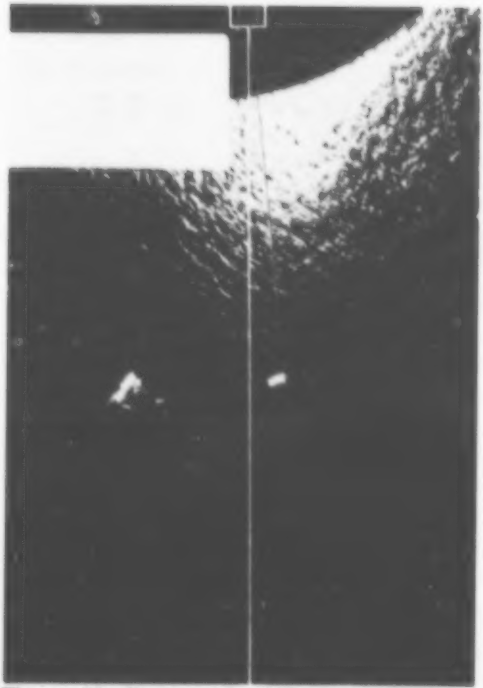

Figure 12 Photograph of The Same Slick

Table 5 Times to Cover Search Area Entirely For Three Historic Situations

Aircraft and Sensors	Time in Days to Cover Area		
	KURDISTAN	PETER STUYVESANT	Davis Strait
Propeller and UV/IR	2	60	110
Propeller and sm. radar	1	23	42
Jet and small radar	1/5	5	8
Jet and STAR radar	1/20	1	1

Two basic types of radars have application to oil spills and general environmental remote sensing, SARs or synthetic aperture radars and SLARs or Side-Looking Airborne radars. The latter are an older technology, however cheaper, and employ long antennae to try to improve spatial resolution. The synthetic aperture radars use the forward motion of the airplane to synthesize a very long antenna, thereby achieving very good spatial resolution at the expense of sophisticated electronic processing. SARs are more costly, but are capable of much more range and much greater resolution than SLARs. Some equipment that has been produced in the past as well as current equipment is listed in Table 6.

TABLE 6 RADARS/MICROWAVE DEVICES

MANUFACTURER	MODEL	BAND	POLARIZATION	POWER (PEAK, KW)	MAXIMUM RANGE (KM)	MAXIMUM RESOLUTION (m)	WEIGHT (kg)
SIDE-LOOKING REAL-APERTURE RADARS							
ERICKSON		X	V/V	10	20	7.5 X range	76
MOTOROLA	APS-94D	X	H or V	200	24-40,80	1.7Xrange	235
EMI	F391	X	H or V	100	15,30	3.5Xrange	196
CAL	SLAR-10	X	H/H		25,50,100		
WESTINGHOUSE	APD-7	C	H/H	50	8	1.7Xrange	225
SIDE-LOOKING SYNTHETIC -APERTURE RADARS							
ERIM		X,L,C	full polarimeter	250	24	1.5	1636
GOODYEAR	APQ-102	X	X	1-X,5-L	37	1.5xrange	232
JPL	DC-8	P,L,C	full polarimeter	60,67,61		4by11	
MDA	CCRS	C,X	H or V	-3.4,X-3.	62	0.8by6	1360
MDA	STAR I	X	V/V	500	70	4-30	250
MDA	STAR II	X	V/V	500	120	4-25	300
MDA	ENV	X	V/V	250	70	6-30	150
RADAR SCATTEROMETER					ANGLE		
RYAN	720	Ku	H or V	0.002	60 to + 6	20X20	16
MPB		C	H or V	0.005	60 to + 6	20X20	
PASSIVE MICROWAVE IMAGERS							
SWEDISH SPACE		35 GHz		-		2,4 deg.	29
AES	AIMR	37,90 G	H or V	-	60 to + 6	1 deg.	

Experimental work on oil spills has shown that X-band radar yields better data than L or C band radar. In addition, it has been shown that antenna polarizations of vertical for transmission and vertical for reception (VV) also yield better results than other configurations.[1,13,14] Radars are thought to be limited by sea state, too low sea states will not produce sufficient sea clutter in the surrounding sea to contrast to the oil and very high seas will scatter radar sufficiently to block detection inside the troughs. Detailed work on sea state limits has not been done but cases of both extremes have been documented in the literature.[1,15]

Search radars such as frequently employed by the military have little - if any - application to oil spills because they frequently remove the clutter signal. Thus, the primary signal of interest is deleted. Furthermore these radars have signal processing optimized to pinpoint small, hard(to radar signals) objects such as periscopes. This signal processing is very detrimental to oil spill detection.

Ship radars suffer from similar limitations and have the additional limitation of low altitude which restricts their theoretical range to between 8 to 30 km, depending on antenna height. Ship radars, however, can be adjusted to decrease the effect of sea clutter de-enhancement. Ship-borne radars were successfully used at 8 km to detect a surface slick in the Baltic and during a trial offshore Canada at a maximum range of 17 km.[16] The technique is highly limited by sea state and, in all cases where it was used, the presence and location of the slick was already known.

In summary, radars optimized for oil spills can provide useful application to spill remote sensing, in particular for large area searches and for night-time or foul weather work.

MICROWAVE SCATTEROMETER

A microwave scatterometer is a device that measures the scattering of microwave or radar waves by the target surface. The presence of oil reduces the scattering of the radar signals just as it does for the radar sensors and therefore suffers the large number of interfering factors noted above. One radar scatterometer was flown over several slicks and employed a low-power transmitter operating in the Ku band (13.3 GHz).[1] The advantage of this type of sensor is that it has a similar aerial coverage to optical sensors and has a nadir aspect (looks straight down). The disadvantages of the sensor include the lack of discrimination for oil and the lack of imaging capability.

MICROWAVE RADIOMETERS

The ocean is an emitter of microwave radiation. Oil on the ocean is a strong emitter of microwave radiation compared to water and thus appears as a bright object on a darker sea. Water has an emissivity factor of 0.4 compared to oil of 0.8.[1] A passive device can detect this emission and could provide a detection means for oil. Furthermore there is a signal change with thickness and, in theory, the device could give indication of thickness. This detection method has been tried over the years, but generally has not resulted in great success. First, the methodology depends on knowing a number of environmental and oil specific parameters and second, the signal return is dependant on signal strength but in a cyclical fashion. This is illustrated in Figure 13.[3] This figure shows that a given signal strength can imply any one of two or three signal film thicknesses within a given slick. Emission of microwaves is a maximum when the effective thickness equals an odd multiple of a quarter wavelength of the observed energy. The method suffers from other weaknesses as well. Biogenic materials also interfere and the signal-to-noise ratio is poor. The methodology does not appear to work at all on water-in-oil emulsions.[3] Scanning radiometers are necessary to produce a thickness map, but scanning with this device is difficult. The Swedish Space agency has done a great deal of work with different systems, primarily a dual band, 22.4 and 31 GHz, device, and also with a single band 37 GHz device.[17] Tests of the devices have achieved only mixed results.

In summary, passive microwave radiometry does not appear to offer potential as a useful oil sensor nor does it appear to offer a solution to reliable slick thickness measurements.

SLICK THICKNESS SENSORS

There exists a need to measure oil spill thickness. First, no reliable methods exists and the basic physics of oil spreading and behaviour are not well understood. The ability to measure slick thicknesses would, no doubt, result in significant advances in the understanding of spill behaviour and effects as well as improve our ability to deal with them. There does not exist a reliable laboratory method to measure thin slicks at this time. Second, there is strong motivation to develop a slick thickness sensor so that the effectiveness of certain countermeasures such as dispersants can be measured. The volume of oil remaining on the water cannot be measured without such a device.[18] Finally, there is strong motivation for determine the amount of oil in fugitive slicks. Aircraft surveillance of these often mistakes the amount of oil in these slicks. The variances of measuring slick thickness using a combination of sensor data and visual estimates, is illustrated in Table 7, the results of a field trial to assess oil slick volume using existing aerial techniques.

The use of the water Raman peak in laser fluorosensor data discussed above has not been exploited or tested fully.[11] This technique may work for thin slicks, but probably not for thick ones. Attempts to calibrate the thickness appearance of infrared imagery have been made, but also have not been successful.[5,6] It is suspected that the temperatures of the slick as seen in the IR are highly

VARIATION OF MICROWAVE BRIGHTNESS WITH OIL SLICK THICKNESS

FIGURE 13

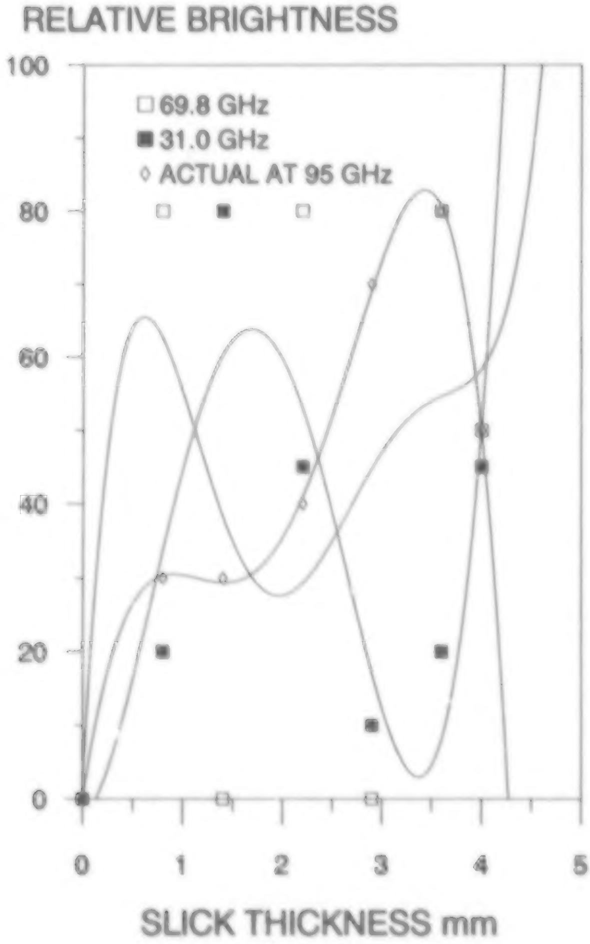

dependent on oil type, sun angle and weather conditions. If this is the case, it is not be possible to use IR as a calibrated thickness measurement tool. Surface methods do not exist, except for using micrometers on very thick slicks, so the calibration of existing equipment is very difficult.[19] The use of sorbent techniques to measure surface thickness is felt to yield highly variable results.[18] As noted in the discussion of the microwave radiometers above, the signal strength as measured by these instruments can imply one of several thicknesses. This methodology does not appear to hold promise for reliable oil thickness measurements.

A variety of electric, optical and acoustic techniques were investigated to measure oil thickness.[20] Two promising techniques were pursued to perform a series of laboratory measurements. The first technique is known as "thermal mapping".[21] A laser is used to heat a region of oil and the temperature profiles created over a small region near this heating is examined using an infrared camera. The temperature profiles created are dependant on the thickness. An even more promising technique is a "laser acoustic" one.[22] An infrared carbon dioxide laser is used to heat the oil layer. This sets up thermal and acoustic waves in the oil. The acoustic waves can be detected using another laser and an interferometer. The thickness can be determined from the time of propagation of the acoustic wave between the upper and lower surfaces of the oil slick. This is a very reliable means of studying oil thickness and offers great potential. A consortium of agencies including Esso Resources Canada, Environment Canada, the United States Minerals Management Service, and the American Petroleum Institute are pursuing the technology. Laboratory tests are planned to investigate the effect of waves and distance. If all goes well, the system will be flown to test it under real conditions.

REMOTE SENSING OF OIL UNDER UNIQUE CIRCUMSTANCES

OIL-IN-WATER

The only instrument to routinely measure oil in the water is the laser fluorosensor. One instrument, the Fluoroscan, was built specifically to perform this function. The system operates in a similar manner to that of a normal fluorosensor, except that only that signal derived from fluorescence in the water column is analyzed. The depth of penetration is thought to be a maximum of 6 metres. Because of the attenuation of the water column, sensitivity decreases logarithmically downwards from the water surface.

Another instrument that is thought to hold potential for detecting neutrally-buoyant oil is the Lidar bathymeter. This instrument uses a laser in the green region to map bottom contours. Presence of massive amounts of oil floating beneath the surface would, in theory, be detected.

OIL-ON-ICE

Oil has been detected on ice using visible techniques.[1] Oil appears to be black or brown against the white background of the ice. Sediment also has the same appearance and constitutes the major interference. Microwave techniques have been tried but were not successful because of the strong emissivity of the ice.[14] Microwave radiometry is, however, very useful in discriminating between first and multi-year ice. The best potential for positively identifying oil on ice resides in the laser fluorosensor.

OIL IN OR UNDER-ICE

Extensive work was done in this area by Esso Resources and Environment Canada. Examination of non-contact techniques such as the use of radar showed that this technique did not have potential.[23] A contact technique using acoustic means to detect the oil was however developed to the prototype testing stage.[24,25] The technique uses the phenomenon that oil appears to be a solid to an acoustic wave and propagates waves like a solid. Liquids propagate acoustic shear and pressure waves in a different manner. By examining the ratio of shear and pressure waves, one can ascertain if oil is present in or under the ice and even at what depth. The methodology requires further testing and development before proceeding to commercialization.

OIL-AMONGST-ICE

Oil amongst ice has been detected and mapped by both UV and IR techniques, however its location was already known.[1] This technique will work for situations where there is a lot of oil and a large amount of open water. In constricted situations, the best potential for detection is offered by the laser fluorosensor.

REAL TIME DISPLAYS AND PRINTERS

A very important aspect of remote sensing is the production of data so that operations people can quickly and directly use it. Real time displays are very important so that the remote sensor operators can adjust instruments directly in flight and so that they can provide information quickly on the location or state of the spill.

In 1980, the Canada Centre for Remote Sensing, with support from Environment Canada, developed the first generic real-time display (generic= compatibility with different sensors). The unit, known as the Norpak, provided a good deal of service displaying multispectral, IR and UV data. A series of devices under the trademark, ALICE, have been built by Knudsen Engineering. These devices are also used to display electro-optical data. A new device built by the same firm will allow the display of radar data along with optical data.

No printing devices are commercially-available for electro-optical data. Development work is required.

SATELLITE REMOTE SENSING

The use of satellite remote sensing for oil spills has been attempted several times. The slick from the IXTOC I well blowout in Mexico was detected using GOES and also by the AVHRR (Advanced Very High Resolution Radiometer) on the LANDSAT satellite.[1] Subsequently a blowout in the Persian Gulf was detected. The massive EXXON VALDEZ slick was detected on SPOT satellite data. Oiled ice in Gabarus Bay resulting from the KURDISTAN spill was detected using LANDSAT data.[26,27] It is significant to note that in all these cases the position of the oil was known and in all cases, data had to be processed to see the oil. Again, in all cases, this took several weeks.

A list of past, present and future satellite sensors are listed in Table 8.[28] Only SPOT and LANDSAT are active at this time.

There are several problems in reliance on satellite remote sensing. The first is the frequency with which overpasses occur. The second is the absolute reliance on clear skies to perform optical work. These two factors combined can give a very low probability of seeing a spill on satellite data. The case of the EXXON VALDEZ spill illustrates this clearly. Despite the fact that vast amounts of ocean were covered by the spill for over a month, only one clear day and a satellite overpass occurred, that on April 7. The third disadvantage of satellite remote sensing is the difficulty in developing algorithms to highlight the oil slicks and the long time to do so. It took over two months in the case of the EXXON VALDEZ spill before the first group managed to "see" the oil slick in the satellite imagery, despite the fact that its location was precisely known.

Optical satellite imagery does not offer a great deal of potential for oil spill remote sensing. The new Canadian RADARSAT may offer some potential for large offshore spills.

TABLE 8 **SATELLITE SYSTEMS**

SATELLITE	SENSOR	END OF LIFE (YEAR)	PERIOD (DAYS)	SWATH WIDTH (km)	MAXIMUM RESOLUTION (m)	BANDS/ CENTRE (nm)
NIMBUS	CZCS COASTAL ZONE COLOR SCANNER	1982	1		825	1--443 2-520 3-550 4-670 5-750 6-11500
	AVHRR ADVANCED VERY HIGH RESOLUTION RADIOMETER	199X	1	1600	1000/4000	5-580 to 12500
GOES	VISSR VISIBLE AND INFRARED SPIN SCAN SPECTROMETER	199X	STATIONARY		8000	1-630 2-11000
LANDSAT	MSS	1989	16 FULL REPEAT	185	80	1-550 2-650 3-750 4-925 5-11000
	TM THEMATIC MAPPER	1989	16 FULL REPEAT	185	30/120	1-4 from 450 to 900 5-1600 6-2200 7-11000
SPOT	SPOT	199X	2.5	60/117	10/20	1-550 2-650 3-840 P-620
SEASAT	SAR	1983	0.5	40	25	C RADAR
ERS-1	SAR	1991+	3	80	30	C RADAR
JERS-1	SAR	1992+		75	18	L RADAR
RADARSAT	SAR	1994+	3	60/500	8/100	C or L RADAR

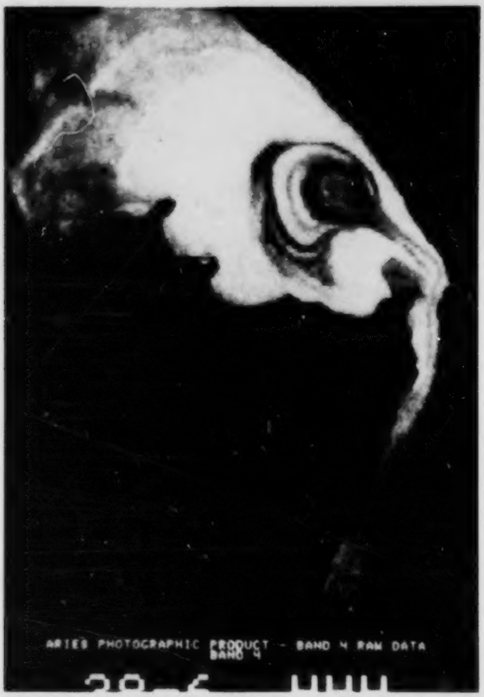

Figure 14 Satellite Image of Oil On Ice in Gabarus Bay, Streaks in Centre of White Ice Patch Are Oil, Outer Material is Sediment

SUMMARY RECOMMENDATIONS

The first sensor recommended for oil spill work is an infrared camera. This is the cheapest and most universal device. A camera and ancillary equipment can be purchased for under $100,000 and weighs less than 50 kg. This is the only piece of equipment that can be purchased off-the-shelf. All other require special order and in many cases, actual development. The second sensor recommended is a UV and visible device. These devices vary a good deal in price, size and state of development. The laser fluorosensor offers the only potential for discriminating between oiled weeds or shoreline and un-oiled ones, and for positively identifying oil pollution on ice, amongst ice and in a variety of other situations. This instrument however is large and expensive. A production unit could cost $500,000 and weigh 200 kg. Radar, although low in priority for purchase, offers the only potential for large area searches and foul weather remote sensing. SAR is recommended and a unit will cost about $1,000,000 and will require a dedicated aircraft. Most other sensors are experimental or do not offer good potential for oil detection or mapping.

Whatever sensor is purchased, the equipment package should always include a real time display and printer as well as a photographic camera for recording purposes.

ACKNOWLEDGEMENTS

Dr. Ron Goodman, Esso Resources, and Dr. Bob Neville of the Canada Centre For Remote Sensing are acknowledged for reviewing the manuscript and providing many helpful comments.

REFERENCES

1. O'Neil, R.A., R.A. Neville and V. Thompson, The Arctic Marine Oilspill Program (AMOP) Remote Sensing Study, Environment Canada Report Number EPS 4-EC-83-3, Ottawa, Ontario, 257 p., 1983.

2. Bercha, F.G. and Associates, Remote Sensing Equipment for Chronic Oil Discharges, Environment Canada Report Number EE-54, Ottawa, Ontario, 1984.

3. Hurford, N., "Review of Remote Sensing Technology", in The Remote Sensing of Oil Slicks, A.E. Lodge, Ed., John Wiley and Sons, Chichester, United Kingdom, p.7-16, 1989.

4. Goodman, R.H., "Application of The Technology in North America", in The Remote Sensing of Oil Slicks, A.E. Lodge, Ed., John Wiley and Sons, Chichester, United Kingdom, p.39-65, 1989.

5. Belore, R.C. Calibration of Infrared Imagery Using a Surface Sampling Device, Environment Canada unpublished report, 1983.

6. Belore, R.C., "A Device for Measuring Oil Slick Thickness", Spill Technology Newsletter, 7(2), p.44-47, 1982.

7. Neville, R.A., V. Thompson, K. Dagg and R.A. O'Neil, "An Analysis of Multispectral Line Scanner Imagery From Two Test Spills", in Proceedings of First Workshop Sponsored by Working Group I of the Pilot Study on The Use of Remote Sensing for the Control of Marine Pollution, NATO Challenges of Modern Society, Vol. 6, p.201-215, 1979.

8. Goodman, R.H., Simple Remote Sensing System For The Detection of Oil on Water, Environmental Studies Research Fund Report number 98, Ottawa, Ontario, 31 p., 1988.

9. Seakem Oceanography, Remote Sensing Chronic Oil Discharges, Environment Canada Report EE-108, 46 p., 1988.

10. Diebel, D., T. Hengstermann, R. Reuter and R. Willkomm, "Laser Fluorosensing of Mineral Oil Spirits", in The Remote Sensing of Oil Slicks, A.E. Lodge, Ed., John Wiley and Sons, Chichester, United Kingdom, p.127-142, 1989.

11. Hoge, F.F. and R.N. Swift, "Oil Film Thickness Measurement Using Airborne Laser-Induced Water Raman Backscatter", Applied Optics, 19(19), p. 3269-3281, 1980.

12. Fingas, M.F., "A Simple Night Time Oil Slick Detector", Spill Technology Newsletter, 7(1), p. 137-141, 1982.

13. Intera Technologies, Radar Surveillance in Support of the 1983 COATTF Oil Spill Trials, Environment Canada Report Number EE-51, 48 p., 1984.

14. C-CORE (Centre For Cold Ocean Resources Engineering), Microwave Systems for Detecting Oil Slicks in Ice-Infested Waters: Phase I - Literature Review and Feasibility Study, Environment Canada Report Number EPS 3-EC-81-3, 353 p., 1981.

15. Hielm, J.H., "NIFO Comparative Trials", in The Remote Sensing of Oil Slicks, A.E. Lodge, Ed., John Wiley and Sons, Chichester, United Kingdom, p.67-75, 1989.

16. Tennyson, E.J., "Shipborne Radar As An Oil Spill Tracking Tool", Proceedings of the Eleventh Arctic and Marine Oilspill Program Technical Seminar, Environment Canada, Ottawa, Ontario, p. 385-390, 1985.

17. Fast, O., "Remote Sensing of Oil on Water - Air and Space-Borne Systems", Proceedings of the DOOS Seminar, SINTEF, Trondheim, Norway, 1986.

18. Goodman, R.H. and M.F. Fingas, "The Use of Remote Sensing for The Determination of Dispersant Effectiveness", Proceedings of the Eleventh Arctic and Marine Oilspill Program Technical Seminar, Environment Canada, Ottawa, Ontario, p. 377-384, 1988.

19. Brown, H.M. and R.H. Goodman, "In-Situ Burning of Oil in Ice Leads", Proceedings of the Ninth Annual Arctic and Marine Oilspill Program Technical Seminar, Environment Canada, Ottawa, Ontario, p. 245-256, 1986.

20. Reimer, E.R. and J.R. Rossiter, Measurement of Oil Thickness on Water From Aircraft: A. Active Microwave Spectroscopy; B: Electromagnetic Thermoelastic Emission, Environmental Studies Revolving Fund Report Number 078, Ottawa, Ontario, 1987.

21. Aussel, J.D. and J.P. Monchalin, Laser-Ultrasonic Measurement of Oil Thickness on Water From Aircraft, Feasibility STudy, Industrial Materials Research Institute Report, Boucherville, Quebec, 1989.

22. Krapez, J.C. and P. Cielo, Laboratory Evaluation of Optothermal Techniques for Remote Oil Thickness Monitoring Applications, Industrial Materials Research Institute Report IGM-RT89-404-07-C, Boucherville, Quebec, 1989.

23. Tunaley, J.K.E. and D.R. Morrcraft, "Aspects of the Detection of Oil Under Ice Using Radar Methods", Proceedings of The Ninth Arctic and Marine Oilspill Program Technical Seminar, Environment Canada, Ottawa, Ontario, p. 463-474, 1986.

24. Jones, H.W., H.W. Kwan, T. Hayman and E.M. Yeatman, "The Detection of Crude Oil Under Seawater in The Arctic Ocean", Proceedings of the Sixth Arctic and Marine Oilspill Program Technical Seminar, Environment Canada, Ottawa, Ontario, p. 241-252, 1983.

25. Jones, H.W. and H.W. Kwan, "The Detection of Oil Under Ice by Ultrasound Using Multiple Element Phased Array", Proceedings of the Ninth Arctic and Marine Oilspill Program Technical Seminar, Environment Canada, Ottawa, Ontario, p. 475-484, 1986.

26. Dawe, B.R., S.K. Parashar, T.P. Ryan and R.O. Worsfold, The Use of Satellite Imagery For Tracking The KURDISTAN Oil Spill, Environment Canada Report Number EPS 4-EC-81-6, Ottawa, Ontario, 31 p., 1981.

27. Alfoldi, T.T. and N.A. Prout, The Use of Satellite Data For Monitoring Oil Spills in Canada, Environment Canada Report Number EPS 3-EC-82-5, Ottawa, Ontario, 1982.

28. Hord, R.M., Remote Sensing: Methods And Applications, John Wiley and Sons, New York, 1986.

BIOLOGICAL REMEDIATION OF SHORELINE OILY WASTE FROM MARINE SPILLS

by

Pierre Labrie
Ultramar Canada Inc.
Montreal, Qué

Benoît Cyr
Biogénie Inc.
Québec, Qué.

Introduction

On May the 8th 1988, the oil tanker Czantoria collided with Ultramar's dock located at the St.Romuald refinery in the Port of Quebec. One cargo tank was damage, resulting in a 2 to 3 thousand barrels spill of light crude oil in the St.Lawrence river. Subsequently two types of shoreline were affected. The first type consisted of beaches mostly composed of granular materials such as sand, rocks and silt. The second type consisted of marshes containing various types of weeds.

Oily waste was collected separately from those two types of shoreline for subsequent treatment and disposal. Material only slightly contaminated was landfilled in local sanitary landfill sites with the approval of the Quebec Ministry of the Environment. The remaining 300 m^3 was contaminated with up to 30 % oil, and could not be disposed of in landfill sites or local incinerators. The fastest and easiest way would have been to arrange transportation to the Tricil secure site in Sarnia. This was judged unacceptable for two reasons: first the cost of transportation and disposal is prohibitive; secondly, landfill of highly contaminated waste, even if it is done in a secure site, is not an environmentally sound solution. Bioremediation was judged a better solution because it could be done relatively cheaply, and provided proper control is used, it can yield very good results. During the project design and subsequent approval by the authorities, the oily waste was stored in secured containers on Ultramar's refinery site. The bioremediation site was ready to operate in November 1988. The site was closed in November 1989 after 170 days of actual operations.

By that time, the contamination level had been reduced to less than 1 % and the material was sent to 2 local landfill sites upon approval from the Ministry of the Environment.

Process

The parameters that affect efficiency of biodegradation of oily waste include:

1. Presence of active organisms (bacteria)
2. Oxygen supply
3. Nutrients addition
4. Use of surfactants
5. Presence of co-substrates
6. Temperature
7. Humidity
8. pH

The choice of the site design must take these parameters in account to allow maximum efficiency of the process. Figure 1 illustrates our design. First the site is constructed with a proper slope and lined with an impervious geomembrane in such fashion as to allow collection of drainage water. Then the oily waste is piled on a gravel bed inside which a series of perforated pipes linked to an air compressor are installed. This allows proper oxygenation of the pile. The compressor must be chosen to allow operation in suction mode as well as compressed mode, to give required control over air temperature and hydrocarbon vapors emission. An activated carbon filter system can be installed when the compressor operates in suction mode.

Irrigation is ensured with a surface system which is also used to deliver nutrients, surfactants and bacteria inoculates. Drainage water is also recirculated through this system. Analysis of phosphorus and nitrogen levels are used to optimize nutrients addition. The bacteria strain used was selected for its ability to degrade petroleum hydrocarbons. Incubation was done on site. A set of 23 thermocouples linked to a digital data collection system was used to monitor air and waste temperature. Temperature is the best indicator of biological activity.

This process design allows maximum control while eliminating the risk of contaminants migration to surrounding groundwater.

Figure 1

BIOTREATMENT PROCESS DIAGRAM

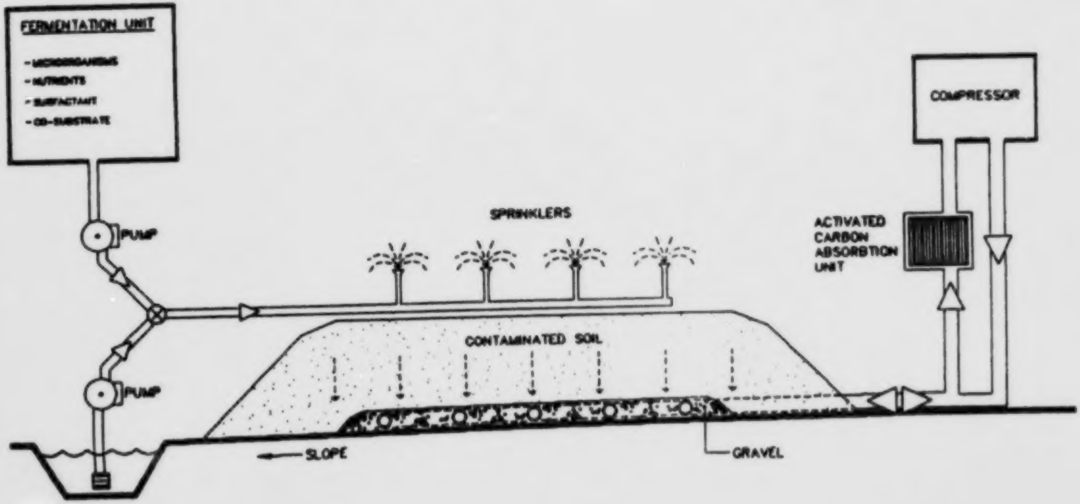

Operation

Operation was done in two phases. A first phase of 10 days in the Fall of 1988, and a second phase from May to November 1989.

During the first phase, two piles of waste were placed on the membrane. One pile of granular material (sand, soil, rocks and silt), and one pile of weeds and woody material. The site was operated for ten days from November 29/1988 to December 09/1988. Operation was ended because it was no longer possible to prevent water freeze-up.

The site was re-opened in May 1989. In June it became evident that water flow in the granular pile was no longer suitable for an efficient activity. The site was then redesigned to contain only one mixed pile. Mixing was done again in July and in September based on temperature variation analysis.

The site was closed in November 1989 when contamination level was down below 1 %.

Results

1 - Temperature

It is often said that bioremediation only works within a very narrow time window in our cold latitudes. This is probably very true for landfarming where a thin layer of waste is spread on a wide surface. Our design will work at much colder temperatures than what is considered the limit for landfarming. In fact the process works even at - 20°C.

Compressed air is warmer and the pile thickness generates friction that increases air temperature further more. Heat created by biological activity is less susceptible to dissipation in ambient air.

Figure 2 illustrates this phenomenon for the first ten days of operation. Sharp decreases in the pile temperature are caused by periodical addition of nutrient solution.

Figure 3 shows the temperature curves for the remainder of

Figure 2

TEMPERATURE PROFILE: Autumn 1988

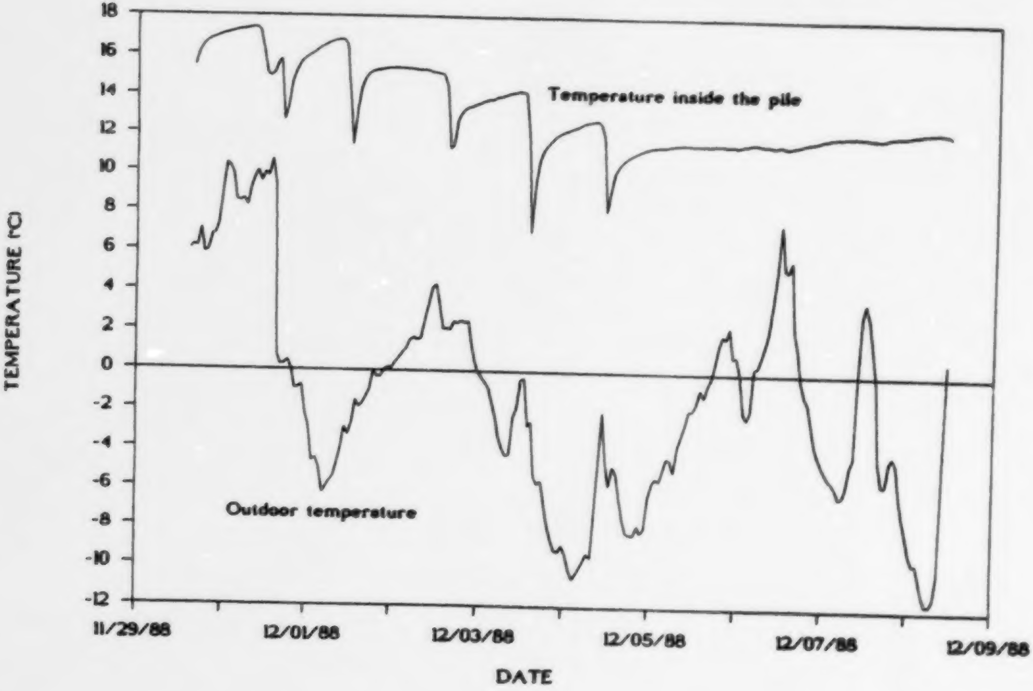

Figure 3 TEMPERATURE PROFILE: Summer 1989

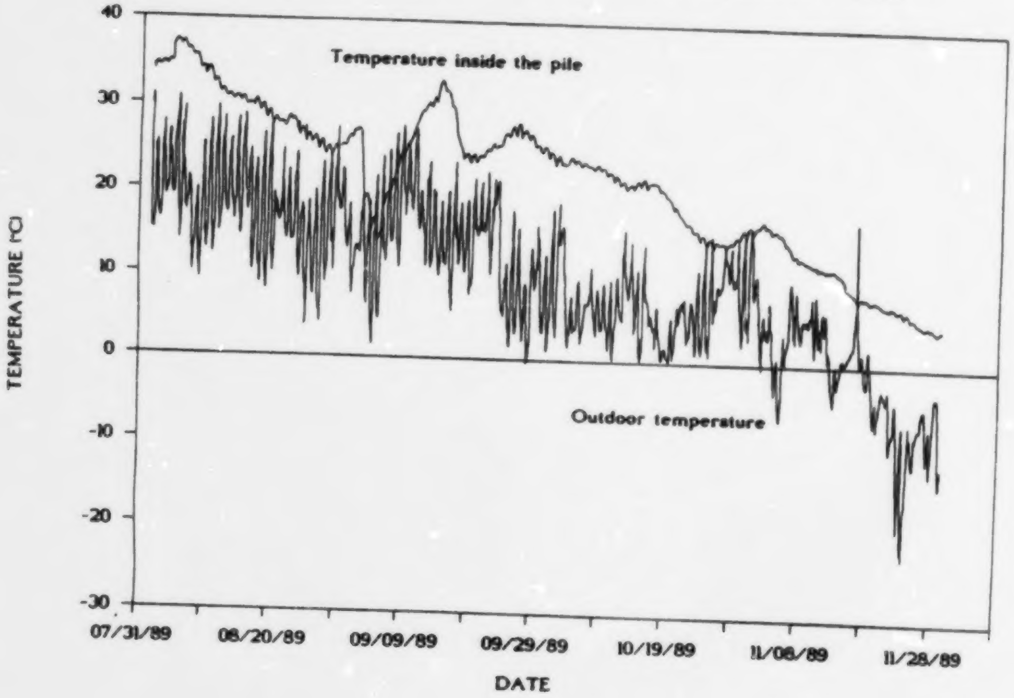

the operation. It is important to note that the pile temperature increases sharply right after each mixing operation. The decrease in September was caused by operating the compressor on suction mode. Figure 4 illustrates the temperature variations during the 13 days while the compressor was operated in this fashion. Although lower than during the compressed air mode, the pile temperature was always kept above ambient temperature.

One of the most important temperature feature of this bioremediation process is the stability of the pile temperature within diurnal cycles.

2 - Oil and Grease Degradation

Figure 5 shows the evolution of oil and grease concentration. The first ten days represent operation in the Fall of 1988, the remaining 160 days being related to the 1989 operation. Up to the 68th day two curves are shown, one for the granular material pile, the other for weeds. From the 69th day only one curve is shown representing the mixed pile oil and grease concentration.

Initial concentrations were respectively 30.5 and 3.9 % for weeds and granular material. Before mixing the two piles concentrations were down to 10.0 and 1.7 %. Average concentration of the mixed pile was 6.3 %, reduced to 1.1 % at the end of operations.

It must be pointed out however that oil and grease analysis is only performed on fine materials. Table 1 shows the breakdown of materials found in the combined waste pile. This was obtained by analyzing a representative sample of 20 kg. Rocks and large pieces of woody material were not tested for oil and grease. Since these can be considered very slightly contaminated - oil and grease % wt close to 0 - their relative contribution to the pile (50 %) allows a redistribution of the tested level of 1.1 % over the entire waste, bringing it closer to 0.52 %.

$$(0.473 \times 1.1) + (0.527 \times 0) = 0.52$$

Leachate test results indicated that the remaining material would not contaminate soil and groundwater. All tests showed 0 ppm

Figure 4

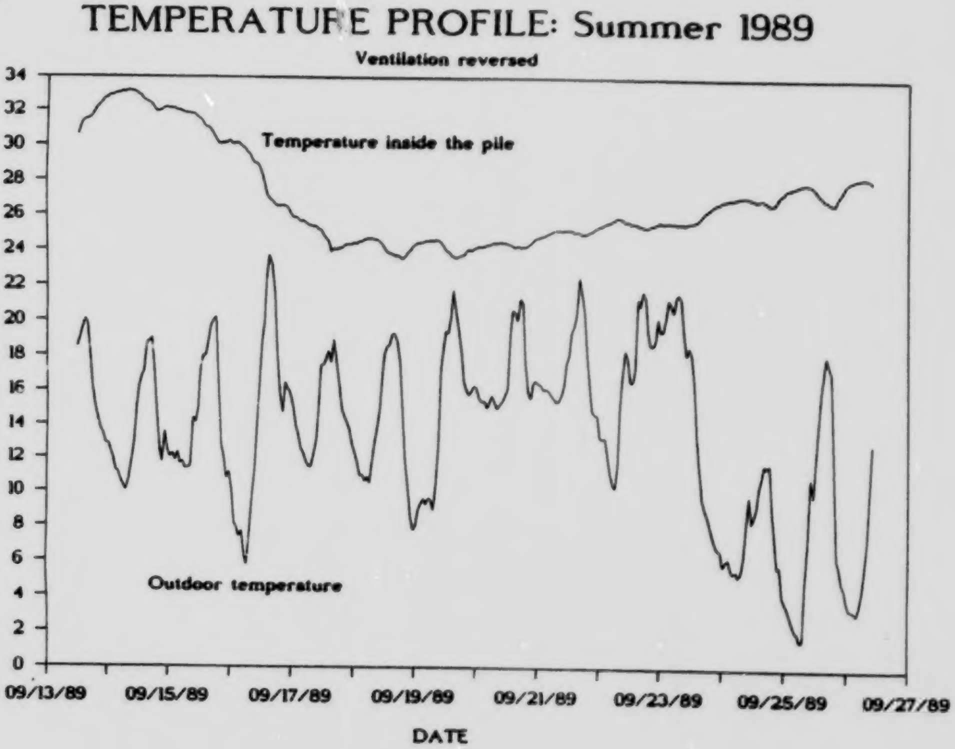

TEMPERATURE PROFILE: Summer 1989

Ventilation reversed

Figure 5

Mineral oil and grease degradation

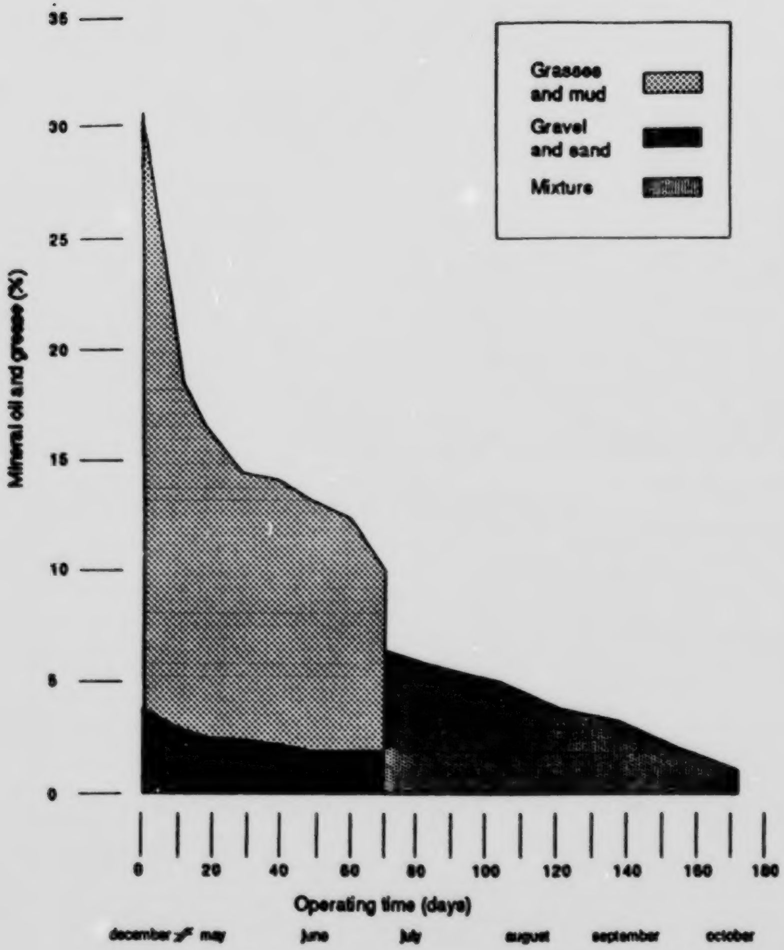

oil and grease; acceptable limit for sanitary landfill sites is 15 mg/kg.

Table 1 - MATERIAL BREAKDOWN FOR COMBINED WASTE PILE

Fine materials (weeds, clay, sand)	47.3 %
Large rocks (> 5 cm diam.) Small rocks (< 5 cm diam.)	15.4 % 31.4 %
Coarse woody material	5.9 %

3 - Polyaromatic Hydrocarbons (PAH's)

Figure 6 and Table 2 show the progression of PAH's degradation during the process. The chromatograms clearly show the disappearance of the characteristic PAH absorption peaks. No single PAH was found to be in excess of the regulated level for residential areas.

The low value for initial naphthalene concentration (3.8 ppm) is an indication that much of the original volatile PAH's were lost to the atmosphere during the first days of the spill.

Table 2 - PAH'S DEGRADATION

P.A.H.	**NOV. 88**	**JUNE 89**	**NOV. 89**
Naphthalene	3.8	n.d.	n.d.
Acenaphtylene	25.6	0.6	n.d.
Acenaphthene	20.7	3.4	0.4
Fluorene	45.8	3.1	1.4
Phenanthrene	97.6	14.5	1.8
Anthracene	27.7	----	0.8
Fluoranthene	6.5	0.6	1.2
Pyrene	34.2	18.0	1.0
Benzo(a)fluoranthene	15.5	.06	0.4
Benzo(b)fluoranthene	5.3	0.7	0.1
Benzo(k)fluoranthene	----	1.4	1.0
Benzo(a)pyrene	0.5	0.7	0.3
Total PAH	**283.2**	**44.0**	**8.5**

Figure 6

PAH's chromatograms

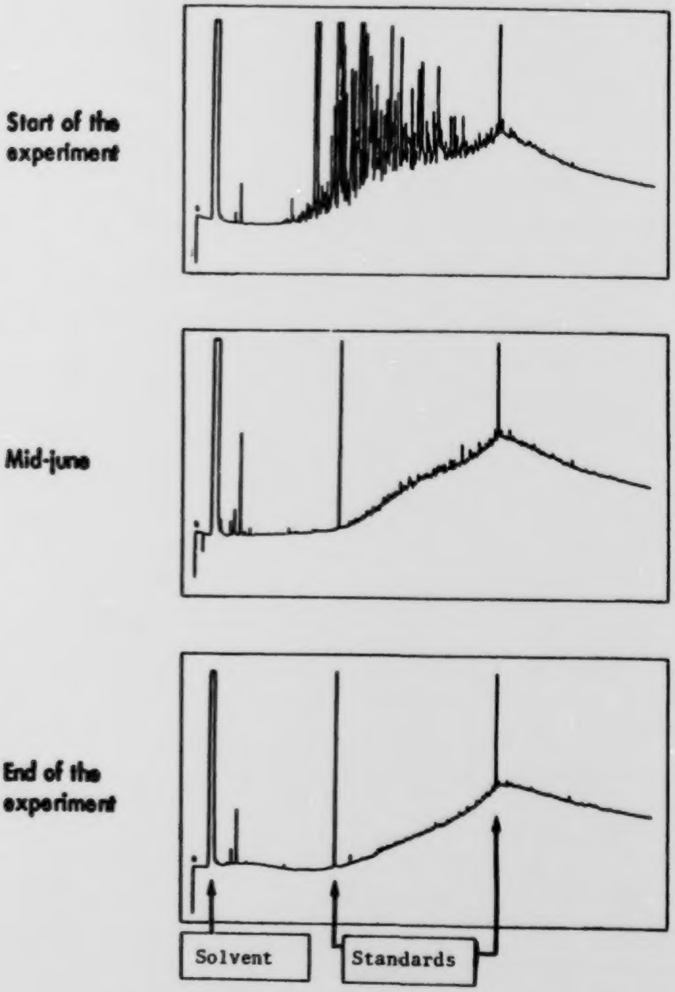

4 - Biological Activity

At various times during the operation biological activity was measured through bacteria count. At all times count was maintained above 1 X 10^7 units/g soil, with a peak count of 3.6 X 10^9 units/g in June 1989. Through growth analysis it was found that 100 % of the micro-organisms present in the soil had affinity for petroleum hydrocarbon substrates.

5 - Cost Benefits

The process described here had to be fine tuned during the course of the operation, thus precise bioremediation cost could not be accurately evaluated. However it is possible to draw a cost estimate for a future hypothetical case. The following cost figures are based on remediation of 500 m^3 of soil showing an average initial contamination of 30 % wt.

Membrane and other non-reusables	\$ 45 /m^3
operating cost	\$ 80 /m^3
Fixed assets amortization	\$ 20 /m^3

Total cost	\$ 145 /m^3

Disposal cost at the Tricil site in Sarnia for similar material varies from \$ 600 to \$ 1 000 per m^3 depending on the compaction of the material. Transportation cost to the nearest Tricil dispatching center must be added to the above.

DISCUSSION

The project has clearly shown that bioremediation can be a very efficient mean of degrading and disposing of oily waste from marine spill shoreline cleanup.

Content in oil and grease can be reduced to values under

1.0 % with leaching potential of close to 0 ppm. The actual requirements for sanitary landfill in Quebec are respectively 5 % and 15 mg/kg for oil and grease, and leaching.

Now that we have fine tuned the process we believe it could be implemented in a very short time in the event of another spill. We are also evaluating the feasibility of transposing it into a totally mobile system that could be used directly on the spill site. An oil and water separation unit could be added to reduce the initial volume of material.

Some of the key factors that were found during this project are:

1. Sound management practices and tight control are essential to achieve efficient bioremediation.
2. Good water drainage is essential to maintain low compaction and adequate air circulation.
3. Constant temperature measurement is necessary to accurately monitor biological activity.
4. Periodical mixing as indicated from temperature readings must be performed to maintain the system at its peak performance level.

We wish to thank The Quebec Ministry of the Environment for their support and cooperation. Their positive involvement was a key element in the success of this project.

STRANDED OIL PERSISTENCE IN COLD CLIMATES.

by

Blair Humphrey[1], Gary Sergy[2], Edward H. Owens[3]

1: Seakem Oceanography Ltd., Sidney, B.C.
2: Environment Canada, Edmonton, Alberta.
3: Woodward-Clyde Consultants, Seattle, WN.

ABSTRACT

Long term monitoring of an experimentally oiled beach has provided a consistent data base on changes of surface oil cover, the degree of oiling and the estimated volumes of oiled sediments and of oil at the BIOS site. After approximately eighteen months of open water, less than 10% of the original stranded oil remains. A comparison to other cold climate spill data is made. Measurement and use of the 'surface oil equivalent area' index is recommended. Total petroleum hydrocarbon data are considered to be highly variable and only should be used as general indicators. The observed trends are applicable to a range of spill situations. Monitoring and predicting stranded oil fate is still an artful science.

A WORSE CASE SCENARIO

A continuing program of monitoring the Bay 11 shoreline study component of the Baffin Island Oil Spill (BIOS) Project provides a consistent long-term data set against which other spills can be compared. The experimental site, at Cape Hatt on the northern tip if Baffin Island, is a sheltered, low energy bay set back from the main coastal trend. A narrow fetch window and light winds result in wave heights which rarely exceed 10 cm; the maximum tidal range is 2.5 m.

In August of 1981, 15 m^3 of Lago Medio crude oil were stranded on a 300 m section of beach (Sergy and Blackall, 1987). The poorly sorted sediments were subjected to a maximum oil loading as surplus oil which could not penetrate was removed by flooding tides. The stranded oil was not treated and was monitored at regular intervals from 1981 to 1989. The combination of low wave energy and oil loading represent a worse case scenario for a single oiling on a low permeability beach in a cold climate environment. Real world examples of similar situations include Black Duck Cove, Nova Scotia (**ARROW** spill), Espora Spit, Tierra del Fuego, (**METULA** spill), Ile Grande, Brittany (**AMOCO CADIZ** spill), Mayne Bay, Vancouver Island, British Columbia (**NESTUCCA** spill) and Herring Bay, Prince William Sound, Alaska (**EXXON VALDEZ** spill).

The bay in which the BIOS oil was stranded is covered by ice approximately 300 days per year; thus the study period represents only 18 months of open-water exposure over a period of nine years. There is no reworking of beach sediments during winter months as the movement of sea ice is not a littoral process on this beach. The stranded oil is protected by the in situ formation of an intertidal ice foot prior to freezeup.

INDICES OF CHANGE

Three indices of change were obtained over the period of the experiment. Surface oil volume was calculated by determining Total Petroleum Hydrocarbon (TPH) concentrations in beach sediments and scaling up to estimate the volume of oil on the beach, using surface oil equivalent area and the depth of the sampled surface (Owens et al, 1987).

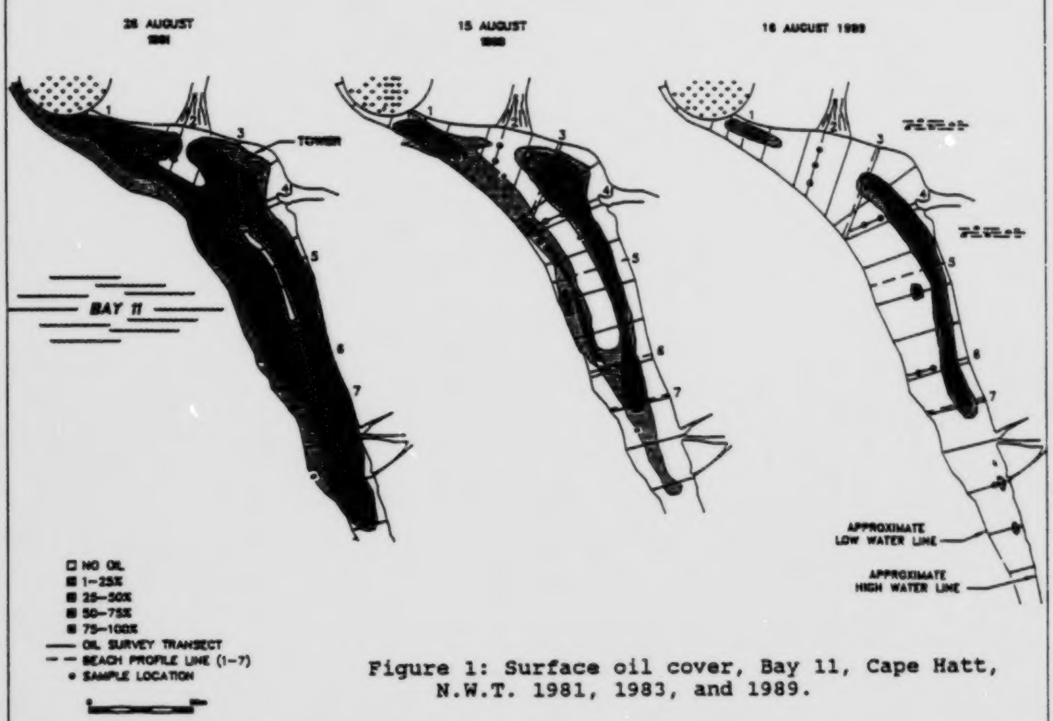

Figure 1: Surface oil cover, Bay 11, Cape Hatt, N.W.T. 1981, 1983, and 1989.

The surface oil equivalent area was determined by estimating percent cover for many transects on the beach, and adjusting the total area by the percent cover. Length of oiled beach was also measured.

Length was inappropriate as a measure of shoreline oiling as it did not consider the width or depth of oiling, or the oil concentration. Observed or measured total oiled area provided a useful value for identifying the total affected area, but did not represent the actual oil cover as it did not consider oil concentration or consider potential non-uniform oil cover. Equivalent area, obtained by integrating percent cover with total oiled area, was a more accurate measure of surface oil cover. The determination of oiled sediment volume or oil volume required a knowledge of oil penetration and concentration. Penetration and oil concentration were difficult to determine except at small scales. Although oiled volumes were the ideal measurements, when cost, effort and accuracy were considered, measured equivalent area was most beneficial.

The time series data show that computed oil volume (a three dimensional value) decreased faster than the observed oiled area (two dimensional) which in turn decreased faster than measured length of oiled beach (one dimensional) (Table 1).

The documented changes showed that the surface oil equivalent area was reduced by 87% (Humphrey and Owens, 1990). Rates of change were most rapid during the first six months of exposure (1981-1983). Given the lack of mechanical energy at the shoreline, the rate of natural removal was substantial. Most of the residual oil was concentrated in a narrow asphaltic band on the upper beach face slope Figure 1), whereas any remaining subsurface oil was fresh in appearance.

Table 1: Changes in shoreline oil.

BIOS - CHANGES IN SHORELINE OIL (%)						
Year	Open Water (Months)	Length of Oiled Shore	Total Oiled Area	Equiv. Oiled Area	Oil Volume	Oiled Sediment Volume
1981	0	100%	100%	100%	100%	100%
1982	3	90	113	68	67	112
1983	5	70	45	28	28	43
1985	9	67	51	25	25	51
1987	13	58	26	16	10	22
1989	17	58	19	13	5	19

OIL CONCENTRATION VARIABILITY

Early in the BIOS experiment, it was noted that the oil concentration data from sediment samples showed a wide range of values from single plots. The total petroleum hydrocarbon data from the BIOS T1 and T2 plots (Figure 2) demonstrate this variability. T1 and T2 were backshore plots of homogeneous sediments and were well protected. They were evenly oiled to maximum loading and were systematically sampled and analysed for ten years. The 105 values plotted in Figure 2 clearly illustrate the problems associated with describing overall oil concentration. The 8 samples collected and analysed in a single plot (T1) in 1980 had a range of 2.2% to 8.5% and the 11 samples collected and analysed from the same plot in 1989 range from 1.6% to 4.6% oil-in-sediment by weight. Indeed, t-tests applied to the between-year data from the T1 plot indicate that the oil concentration significantly decreased and

Figure 2: Total petroleum hydrocarbon concentrations, T1 and T2, BIOS project.

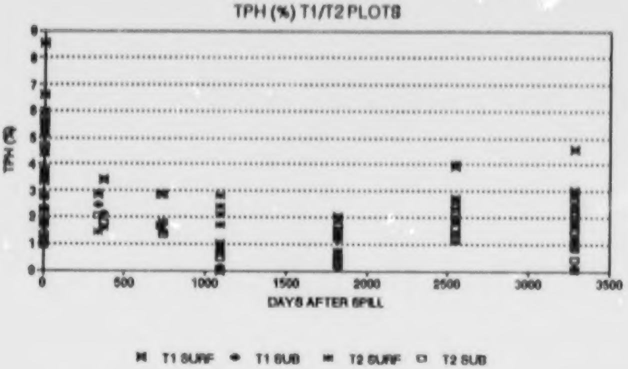

Figure 3: BIOS Changes in shoreline oil.

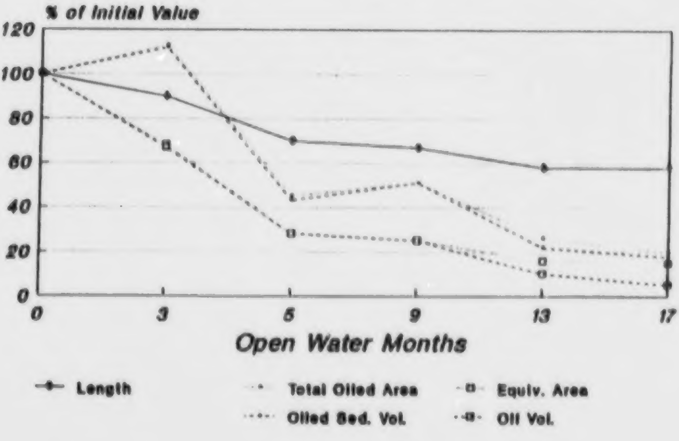

subsequently significantly increased, at 95% confidence or better. For the T2 plot, similar tests indicate no significant change over the study period because within-year variability was large. These data would result in a wide range of oil volumes.

TRENDS AND PROJECTIONS

The BIOS data provides trends of rates of change that can be applied to projections for real-world spills as a worse case boundary condition. For example, after approximately one year of exposure under low energy conditions, the oil volume was reduced to ten percent of the volume of original stranded oil. These changes, as depicted in Figure 3, can be used to project trends for other spills.

In attempting to define rates of change or trends of oil cover from previous large spills, we examined available data from some of those spills (Table 2). This review indicates that the **AMOCO CADIZ** spill was the first to provide a data set suitable for trend

Table 2: Systematic data sets.

INCIDENT	ARROW	METULA	AMOCO CADIZ	KURDISTAN	BIOS	NESTUCCA	EXXON VALDEZ
YEAR	1970	1976	1978	1979	1981	1989	1989
OIL TYPE	BUNKER C	LIGHT CRUDE	LIGHT CRUDE	BUNKER C	MEDIUM CRUDE	BUNKER	MEDIUM CRUDE
CLIMATE	TEMPERATE	SUB-POLAR	TEMPERATE	TEMPERATE	ARCTIC	TEMPERATE	SUB-POLAR
GLACIATED	YES	YES	YES	YES	YES	YES	YES
SEA ICE	YES	NO	NO	YES	YES	NO	NO
LENGTH DATA	YES	-	YES	YES	YES	-	YES
WIDTH DATA	-	-	-	-	YES	-	YES
EQUIV. AREA DATA	-	-	-	-	YES	-	YES
PENETRATION DATA	-	-	YES	-	YES	YES	YES
TPH DATA	-	YES	-	-	YES	YES	YES

analysis. That data set includes only length data over time. Therefore the development of a better case/worse case envelope for projecting oil removal rates is limited to length data, which is one of the weakest parameters (Figure 4)(Owens and Rashid, 1976, Gundlach et al, 1983, Humphrey and Owens 1989, Alaska Department of Environmental Conservation, 1990).

Figure 4: Changes in length of oiled shoreline. The **EXXON VALDEZ** data sources are ADEC, 1990 and Exxon, 1989, the **ARROW** data source is Owens et al, 1976, the **AMOCO CADIZ** data source is Gundlach et al, 1983.

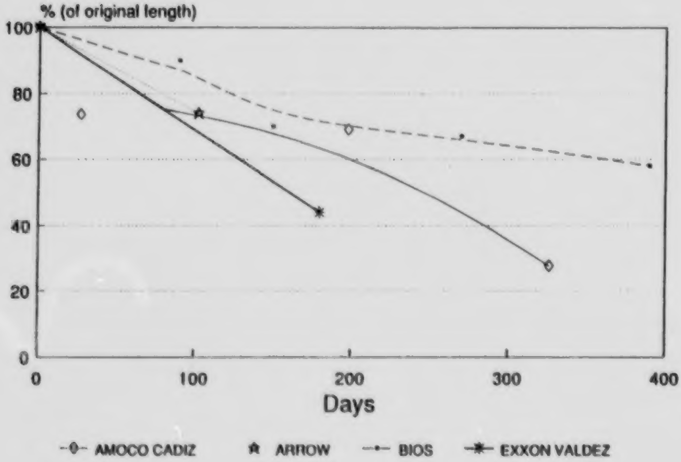

Only the BIOS project data and data being collected in Prince William Sound (Teal, 1989, Owens et al, 1990) provide the full suite of data from which trends may be determined.

CONCLUSION

An appropriate data base includes a consistent sampling and analytical protocol with replication and repetition. From our review, it is apparent that only the BIOS and the Prince William Sound data sets meet these criteria. The review also indicates that the two most commonly determined parameters are length and total petroleum hydrocarbon in sediment (TPH).

Length, as discussed above, does not account for the multidimensional distribution of oil. Total petroleum hydrocarbon data, used in the computation of oily sediment volume and oil volume, is discrete and rarely can be extended to describe large areas or volumes. These two parameters are the weakest of those available. Our experience permits confidence only in observed changes of at least one order of magnitude. We recommend using TPH data of one significant figure only, and we recommend that these data be expressed as percentages by weight, rather than as ppm or $mg \cdot kg^{-1}$. We put little credence in TPH data except as a general indicator of change, except for well sorted homogeneous sediments.

Our experience with BIOS and other spills has shown us that monitoring is not an exact science, and that considerable variability is to be expected. For example, equivalent or total oiled area may increase due to redistribution of oil through normal coastal processes. As we have seen, penetration and oil concentration data are very difficult to determine accurately, and these dramatically effect any attempt to calculate volumetric values. Equivalent area methods, however, are easy to do consistently and cheaply, and provide a good estimate of surface oil cover.

REFERENCES

Alaska Department of Environmental Conservation. Results of October Walkathon in Prince William Sound. Unpublished report. Anchorage, Alaska. 1990

Exxon. Shoreline Restoration Plan, 1 May 1989. Submitted to U.S. Coast Guard Federal On-Scene Coordinator, Valdez, Alaska. 39 pp. 1989.

Gundlach, E.R., P.D. Boehm, M. Marchand, R.M. Atlas, D.M. Ward, D.A. Wolfe. The fate of **AMOCO CADIZ** oil. Science. **221**: 122-129. 1983

Humphrey, B. and E.H. Owens. Fate and persistence of stranded oil from the BIOS project, Cape Hatt, N.W.T. An unpublished report to Environment Canada, Edmonton. 1990.

Owens, E.H. and M.A. Rashid. Coastal environments and oil spill residues in Chedabucto Bay, Nova Scotia. Can. J. Earth Sciences. **13**(7): 908-928. 1976.

Owens, E.H., J.R. Harper, W. Robson, P.D. Boehm. Fate and persistence of crude oil stranded on a sheltered beach. Arctic **40** (Supp. 1):109-123. 1987.

Owens, E.H., Initial results from a monitoring program of the oiled shorelines of Prince William Sound following the **EXXON VALDEZ** incident. This volume. 1990.

Sergy,G. and P.J. Blackall. Design and conclusions of the Baffin Island OIl Spill. Arctic **40** (Supp. 1): 1-9. 1987.

Teal, A. Proc. of the Cleanup Technology workshop. Anchorage, Alaska, November 28-30, 1989. Distributed by NOAA, Seattle, WA. 1989.

SHORELINE CLEANUP FOLLOWING THE *EXXON VALDEZ* OIL SPILL
Field Data Collection within the S.C.A.T. Program

Ed Owens
Woodward-Clyde Consultants
900 Fourth Ave., Seattle
WA 98164

Andrew Teal
Exxon USA, Alaska Operations
P.O. Box 240409, Anchorage
AK 99524

ABSTRACT

Systematic field data from ground and aerial videotape surveys were collected to assist the decision-making process for the treatment of shorelines oiled by the spill. Prior to the cleanup operations in 1989, the Exxon Shoreline Cleanup Advisory Team (S.C.A.T.) provided detailed field reports on the geomorphology, biology, cultural resources (archaeology) and oil conditions on a segment-by-segment basis. These reports were accompanied by treatment recommendations and submitted by Exxon to the Federal On-Scene Coordinator. Between April and September 1989 approximately 5500 km of coast in Prince William Sound and the Gulf of Alaska were surveyed on the ground and more than 8000 km were surveyed using low-altitude aerial VTR.

Following completion of the 1989 cleanup operations, 64 selected sites were monitored on a monthly basis throughout the winter to provide data on changes at representative shoreline locations. Further S.C.A.T. surveys were conducted in spring 1990 to define the distribution and character of remaining oil and to plan for the second-year shoreline treatment operations. Selected shoreline information from each segment report for each of the oil distribution surveys was stored on a relational database and mapped using AUTOCAD/GIS software.

INTRODUCTION

Following the spill that began in Valdez Arm on March 24, 1989 the oil was stranded along the shorelines of western Prince William Sound (PWS) and subsequently along the Gulf of Alaska (GOA) coast as far as Kodiak Island and the Alaskan Peninsula. This region has a topographically complex coastline and the distribution of oil on the shoreline was non-uniform. Information on the amount of stranded oil and on the character of the shoreline was needed initially to develop the strategies and the operational work plans for the cleanup activities. To collect this information and to provide technical support for the shoreline cleanup operation, Exxon established the Shoreline Cleanup Advisory Team (SCAT).

The major effort of the 1989 SCAT program involved teams of specialists who collected the field information on a segment-by-segment basis: the shoreline cleanup assessment teams. In addition, the SCAT group:

- set up a Geographical Information System (GIS) in the Command Center to archive the data collected by the field teams and to produce maps of the various data sets (oil distribution, shoreline character, etc.)
- carried out a low-altitude color videotape survey of the PWS and GOA coasts during the period May through August
- provided technical advice to the operations group
- established fate and persistence study sites for long-term monitoring of changes in oiling and of intertidal biology
- conducted a second aerial videotape survey of the PWS coasts in October
- established time-lapse photography locations to film shoreline dynamics during the winter of 1989-90

The SCAT program continues in 1990 with further field surveys and studies to evaluate the distribution and character of the remaining oil.

The key role of the SCAT program in 1989 involved the field assessment teams who carried out ground surveys to collect data and to evaluate the:

- distribution and character of the stranded oil,
- geomorphology/sedimentology of the shore zone,
- status of intertidal macro-species, and
- presence of cultural/archaeological resources.

Data collected by the field assessment teams was reviewed and treatment recommendations were developed in conjunction with the Exxon Operations group and then submitted to the Federal On-Scene Coordinator (FOSC) (Teal, 1990). The FOSC acted under the advisement of the Interagency Shoreline Cleanup Committee (ISCC) for the PWS area; outside of the Sound, three regional multi-agency committees (MACs) reviewed the submissions for the Seward, Homer, and Kodiak/Alaska Peninsula sub-regions, respectively. Each of these four shoreline cleanup committees was composed of representatives from Exxon and from each of the responsible federal and state agencies as well as other interested groups. The FOSC then approved the submitted or revised treatment plan which was then implemented by Exxon.

This procedure, based on frequent meetings of the cleanup committees, enabled each of the interested groups and/or agencies to be involved with the decision-making processes while not creating a cumbersome network that required continuing review and revision of documents. Data from the field teams could be processed and submitted to the FOSC within a matter of a few days and the submitted documents were usually returned from the Shoreline Cleanup Committees to the FOSC for signature within a further week's period. At times, when a more rapid turn around was required, this usually could be obtained so that the cleanup program was not hindered by the review procedure.

1989 SCAT PROGRAM

Each of the field assessment teams that was established to define the degree of oiling and the shore-zone character was composed of an oil spill/coastal geomorphologist (usually abbreviated to "o/g"), an ecologist, and an archaeologist. The first shoreline cleanup assessment team began surveying in PWS on April 13 and the procedure continued until the last segment report was completed on September 3, 1989. Over 5500 km of coastline were surveyed in detail by this method (Tables 1 and 2) and a total of 1149 separate segments of shoreline (549 in PWS and 600 in GOA) were defined and surveyed by ground teams. At one time as many as 9 field assessment teams worked simultaneously in the spill area. The logistics of this field program involved the use of small vessels with berthing facilities, float planes, and helicopters, as less than 10 km of the coastline affected by the spill could be accessed by road.

TABLE 1 SUMMARY OF SHORELINE SURVEY PROGRAMS

SCAT		April-September 1989	1611 km PWS 3922 km GOA
FASST		February-March 1990	170 km PWS 20 km GOA
SSAT	- phase 1	March-April 1990	687 km PWS 235 km GOA
	- total all 3 SSAT phases*		1043 km PWS 832 km GOA

*estimated

TABLE 2 SUMMARY OF SHORELINE DATA 1989

	REGIONAL COASTAL LENGTH (km)	SURVEYED BY SCAT	LENGTH WITH OIL
PWS	4926	1611	574
GOA	6345	3922	1270

The field assessment team subdivided the coast into segments based on geomorphology and/or oil conditions and used standard forms to describe the oil distribution and character, the substrate character, the biology and the archaeology of each segment of shoreline. The data that was collected by the field assessment teams was entered into database software using an FMS/AC program designed to interface between database systems and AUTOCAD, so that the information could be used on a GIS.

The field assessment reports were reviewed in Valdez and recommendations identified for shoreline treatment. The draft document was submitted to the State Historical Preservation Officer for review and signature, to ensure that the proposed activities would not affect existing or newly found cultural resources, and a group of segment reports and recommendations were combined to form a "block report" which was submitted to the FOSC. A block report was usually composed of a series of segments in an adjacent area that would form a reasonable shoreline package for one of the Exxon cleanup task forces.

FEATURES OF THE 1989 FIELD PROGRAM

(1) Consistent Reporting - Documentation A key element of this spill response was the consistency in the reporting of the degree of shoreline oiling. The procedures developed for the field assessment teams involved reporting the distribution and character of oil using standard forms and definitions so that each crew would be describing the location, amount, and type of oil using the same format and terminology. Crews were calibrated with each other as new team members arrived on the project so that the field observation techniques could be passed on directly in field situations.

(2) Data Handling The generation of large amounts of data involves the organization of the information so that it can be stored and retrieved efficiently. Computer-based systems that allow the data to be archived and also allow the production of maps that illustrate shoreline character, segment boundaries, and oil distribution are particularly useful. In this project an FMS/AC AUTOCAD-driven system was set up in Valdez simultaneously with the first field assessment surveys, so that no backlog developed for data entry. During a few peak periods data entry was a 24-hour operation.

(3) Field Maps The importance of good base maps for the field teams became evident when the published topographic maps were found to be out of date, due largely to the 1964 earthquake that effected the shorelines of this region considerably. Eventually, new maps from post-earthquake aerial photography were digitized by a

contractor and these were then used as the standard base maps by the field crews and the GIS team.

(4) Data Use The value of the data collected by the field teams was much greater than originally anticipated. The intention of the program was to collect information that could be used by the Exxon Operations Task Forces so that they would be able to respond in an appropriate manner. Throughout the incident the data was used by many of the federal and state agencies as well as by Exxon for a variety of purposes. The maps generated by the GIS from the data base were used extensively for operational planning and for tracking the progress of the cleanup task forces. The field sketches of shoreline features produced by the geologists frequently were used as a reference during discussions of treatment alternatives or of difficult sites.

(5) Aerial Video Tape Record/Mapping The 1989 SCAT program involved the use of a low-altitude, slow-airspeed, color video tape method to record the surface oil distribution on the shoreline. The video survey of PWS was conducted in May and then extended to the Kenai Peninsula-Alaskan Peninsula-Kodiak region during June - August and over 8000 km of shoreline were catalogued by this method. This proved to be an ideal technique for obtaining a reconnaissance-scale picture during the early stages of spill. When the results of this video survey were subsequently compared to the results of the ground surveys the agreement was found to be very close. The tapes were very useful also to identify shoreline subdivisions or segments which then could be surveyed by the ground crews. With time, the importance of ground surveys becomes greater as surface oil alone does not necessarily reflect the total degree of oiling due to burial and/or penetration of oil into the sub-surface of the sediments.

WINTER 1989-1990 SHORELINE MONITORING PROGRAM

Prior to completion of the summer 1989 field program a number of representative study sites were selected for monitoring on a systematic basis through the winter. Two separate types of surveys were carried out, with 28 detailed ("A" Program) and 36 reconnaissance ("B" Program) study locations. Six "A" and four "B" surveys were conducted during the period September 1989 to March 1990. The surveys were scheduled to coincide with low-tide during periods of daylight operation windows; the latter were as short as 5 hours in the middle of the winter. The overall success rate for site visits was high despite the winter conditions and the loss of 30% of the daylight/tidal windows due to weather downtime (Table 3). The number of actual site visits versus total possible number of visits for the "A" program was 70% for PWS and 80% for GOA, and for the "B" program was 80% for PWS and 55% for GOA.

TABLE 3 SUMMARY OF FIELD ACTIVITIES WINTER 1989-90

	TOTAL DAYS WORKED	WEATHER DOWN DAYS	MECHANICAL DOWN DAYS
PWS "A"	86	15.5	1
PWS "B"	21	7	0
GOA "A"	95	43	3
GOA "B"	26	4	0.5
Total	228	69.5	4.5
Total Person Days	650		

The "A" site program involved:

- surface oil cover observations on staked intertidal lines
- topographic surveys along selected staked profiles
- sediment sample collection for chemical analyses
- test pits to evaluate depth of oil penetration/burial
- biological measurements along selected transects
- still photography and a videotape record.

The number of transects varied depending upon the length of the shoreline at the study site, but most locations had 10 staked profiles for repetitive surveying. Data products included a surface oil cover map for each site, comparative values of Equivalent Oiled Area for sections on each transect where an overlap existed from surveys at different times, and summary spreadsheets of the relative abundances of all major macroscopic taxa. Preliminary results from this winter program are presented elsewhere in these Proceedings (Owens and Teal, 1990).

The "B" surveys involved a single transect that was photographed and videotaped, and along which surface oil cover estimates were recorded and pits were dug.

1990 SCAT PROGRAM

A reconnaissance survey was conducted in late-February/March to delineate sections of coast in PWS and GOA that might have "wide- band" amounts of stranded oil after the winter (Table 1). This Fast Assessment Shoreline Survey Team (FASST) program was conducted by an "o/g" accompanied by a representative from:

- Exxon Operations,
- the state (Alaska Department of Environmental Conservation (ADEC)), and from
- the federal government (United States Coast Guard (USCG) or National Oceanic and Atmospheric Administration (NOAA)).

The presence on each field team of a representative from the primary responsible agencies was intended to ensure that all parties could work from the same information base. An added benefit was that as many people as possible, who would be working on the subsequent treatment program either as decision makers or as field supervisors, could see and appreciate the condition of the oil on shoreline.

This survey was a precursor to a detailed program conducted in late-March/April that covered all PWS and GOA areas where oil had been reported during the fall ground survey. The 3-phase Spring Shoreline Assessment Team (SSAT) program involved 20 teams in the field simultaneously that were scheduled to survey over 1800 km of coast (Table 1). Each team comprised an "o/g" and an ecologist, accompanied by representatives from:

- Exxon Operations,
- USCG/NOAA,
- ADEC, and from
- the appropriate land manager.

The data from this survey was then used by Exxon Operations to prepare for the spring/summer 1990 treatment program. At the time of writing only phases 1 and 2 had been completed; this covered the area considered most likely to require treatment in 1990. The results from these first two phases are given in Table 4.

TABLE 4 SUMMARY OF 1990 SSAT PHASE 1 AND 2 DATA
(1194 km surveyed to 4/27/90)

LENGTH OF SHORELINE BY OIL BAND WIDTH CATEGORY (km)

	Wide > 6 m	Moderate 3-6 m	Narrow < 3 m	V. Light	No Oil
PWS	19.0	41.5	66.8	219.7	559.9
GOA	1.9	5.8	12.5	54.9	212.2

DISCUSSION

On the basis of experience gained on this incident, an ideal shoreline evaluation process might involve the following sequential stages:

- low-altitude video tape survey of coast
- initial oil distribution/shoreline-type map from video
- delineation from video of shoreline sections for ground surveys
- ground survey of the oiled sections of shoreline
- development of recommendations for shoreline treatment
- input of summary statistics to database files
- generation of oil distribution and other maps.

All of these stages were carried out in the "Exxon Valdez" response, although in the early stages the necessity to obtain information quickly for the operations teams required that some of the ground and video surveys be conducted concurrently.

Some of the highlights of the SCAT program were:

1) The collection of field information in a systematic manner was, on hindsight, a crucial element in the development of an information base that could be used for operational planning and to generate maps and statistics as the program proceeded.

2) The systematic shoreline descriptions enabled reliable comparisons to be made between surveys at different times to identify changes in the distribution of oil on the shoreline.

3) Low-altitude video taping proved to be very valuable in collecting information rapidly on the distribution of oil on the shoreline and also proved to be very accurate when compared to ground survey data, particularly during the early stages of the spill. A high level of agreement with ground data on surface oil cover was found even through the early winter months.

4) The winter monitoring program provided trend data on changes in surface oil cover and information on the changing character of the oil that remained on the shore. This data was used to project shoreline oil conditions for the following spring.

5) The cooperative nature of the spring FASST and SSAT field programs provided a single information base from which the responsible agencies could work and enabled a large number of people to gain first-hand knowledge of the shoreline oiling conditions.

REFERENCES

Owens, E.H. and Teal, A.R., 1990. A Brief Overview and Initial Results from the Winter Shoreline Monitoring Program following the "Exxon Valdez" Incident; Proc. Thirteenth Arctic Marine Oil Spill Program (AMOP) Tech. Seminar, Edmonton, Alberta, June 6-8.

Teal, A.R., 1990. Shoreline Cleanup Following the "Exxon Valdez" Oil Spill - The Decision Process for Cleanup Operations; Proc. Thirteenth Arctic Marine Oil Spill Program (AMOP) Tech. Seminar, Edmonton, Alberta, June 6-8.

SHORELINE CLEANUP FOLLOWING THE "EXXON VALDEZ" OIL SPILL - THE DECISION PROCESS FOR CLEANUP OPERATIONS

by

Andrew R. Teal
Exxon U.S.A., Alaska Operations
P. O. Box 240409
Anchorage, Alaska 99524

ABSTRACT

The shoreline response program presented a significant challenge for Exxon not only from an operational viewpoint but also in the involvement and communication with all of the responsible agencies and interested parties. Key environmental, economic, social and safety factors were identified and addressed throughout the planning and implementation process. Priorities were established so that the cleanup operations team could direct the movement of the resources to and from appropriate areas under the constraints imposed by the various factors under consideration. Exxon collected field data as part of the Shoreline Cleanup Advisory Team (SCAT) program and treatment proposals were developed for individual shoreline segments. Based on this and other available information, cleanup plans were submitted to the Federal On Scene Coordinator (FOSC). For the 1989 program a multiagency shoreline cleanup committee was established in each of the four operational regions to advise the FOSC on the treatment proposals. In 1990 this role was provided by a Resource Advisory Group (RAG) and a Technical Advisory Group (TAG). This interagency process provided a vehicle for agency and interest group input and could be used as a model for similar future response programs. The involvement of these groups early in the process and incorporation of their input was a key to a relatively smooth approval process.

INTRODUCTION

The 1989 shoreline cleanup program in Prince William Sound (PWS) and Gulf of Alaska (GOA) was the largest operation of its kind ever attempted. More than 11,000 people were mobilized in a region where boats and aircraft are the primary methods of transportation and access to the shoreline. An undertaking of this magnitude involved careful planning to ensure that cleanup activities could proceed with minimal disturbance, and adequate protection of the various resources present.

The development of the response strategy and the preparation of operational work plans required the information base which was generated as part of the SCAT program (described elsewhere in these Proceeding; Owens and Teal, 1990). The work plans were submitted to the FOSC, who acted under advisement through a procedure which allowed all of the responsible agencies and interested parties to have an opportunity to provide input to the decision process.

The procedures developed for this response program were designed to meet the particular needs of this operation. Every spill response is unique but some of the lessons learned, in terms of developing an appropriate data base and of developing a decision process that provides adequate communications between all parties involved, may be applicable to future incidents.

INFORMATION BASE FOR TREATMENT DECISIONS

Two different sets of information at different scales were required to develop a response program. Initially, at the strategy level, the identification of ecological and resource sensitivities indicated those locations or areas where treatment action needed to be focussed or constrained. The regional priorities for treatment were developed by inclusion of data on timing of the sensitivities, for example, the timing of seal or sea lion pupping on haul out sites, fish spawning, salmon fisheries, and subsistence resource use. The strategy for the location and movement of the Task Forces, of which the largest of the seven in the PWS comprised 100 vessels and 650 personnel, was based on these broad-scale considerations.

The second information set, provided by the SCAT program, involved a detailed segment-by-segment survey of (a) shoreline character and oiling conditions, and (b) physical, biological and archaeological factors that might constrain treatment activities or provide focus at a site. This level of information was used to develop the operations site specific work plans for each of the 1149 shoreline segments identified in the SCAT program. The following are the key factors assessed for each segment of shoreline and all influenced the treatment strategy in terms of timing and of applicable techniques.

BIOLOGICAL

FISH

- salmon outmigration
- salmon spawning in streams
- herring spawning areas

MAMMALS

- harbor seal and sea lion pupping and molting haul outs

BIRDS

- migrating waterfowl and shore birds staging areas
- seabird colonies
- bald eagle nests

RESOURCE USE

- salmon and finfish
- invertebrates
- seal and deer

COMMERCIAL

- fish hatcheries
- salmon fry nursery areas
- hatchery release areas
- gill net, purse seine and set net areas/sites

RECREATIONAL

- tent sites, cabins or lodges
- anchorages
- tour destinations
- wilderness parks

CULTURAL RESOURCES

- known and undiscovered archaeological and architectural sites

ENVIRONMENTAL/PHYSICAL

SAFETY

- wave exposure
- accessibility
- workability

DECISION PROCESS FOR TREATMENT PROPOSALS

Early in the spill it was recognized that the various regulatory/resource agencies, local fisherman and interest groups, could play a vital role in supplementing the existing resource information contained in the contingency plan. This wealth of regional and local knowledge, coupled with the detailed site specific SCAT reports, proved to be an effective means for developing prioritized treatment plans and appropriately addressing the site sensitivities. This resource group became known as the ISCC (Interagency Shoreline Cleanup Committee) and was comprised of 14 organizations for the PWS area. Similar organizations were set up for the Seward, Homer and Kodiak regions.

The information flow in the decision making process for 1989 is illustrated in Figure 1.

Step 1. The ISCC worked with Exxon representatives to identify and prioritize the key resources.

Step 2. Exxon SCAT catalogued the sensitivities and timing priorities to focus the field assessment teams.

Step 3. The Shoreline Cleanup Assessment Teams conducted site specific surveys to document site sensitivities and degree of oiling.

Step 4. The SCAT in conjunction with Operations developed the appropriate treatment approach for each shoreline segments.

Step 5. The State Historic Preservation Officer (SHPO) reviewed the proposed segment plan to ensure appropriate cultural resource protection measures were in place.

Step 6. Proposed site specific work plans were submitted to the Admiral (the Federal On Scene Coordinator FOSC) via the ISCC. The Admiral asked that the ISCC review the submitted packages and comment to him for his deliberations and decision.

Step 7. The work plan segment packages were reviewed within the ISCC's for completeness and accuracy then delivered to the Admiral for his approval.

Step 8. Exxon Operations implemented the work plan.

The decision-making procedure was developed quickly, so that by the time the first Task Force was deployed in PWS the priorities were set and the first treatment plans were approved by the SHPO and the FOSC. Thereafter, the process continued to work well through the 1989 program.

A slightly modified procedure developed for the 1990 season to streamline the decision process is also working smoothly. In this phase, the work plans are reviewed by TAG, prior to submittal to the SHPO and to the FOSC.

The 1990 decision flow diagram is shown in Figure 2. The main change from the 1989 process is the role of the ISCC. The RAG's, formerly known as the ISCC's, provide their input early in the process. The review, prior to the FOSC's approval is conducted by a tripartite group consisting of State, Federal, and Exxon representatives. The Federal Government is represented by a USCG and NOAA representative and the State of Alaska by Alaska Department of Environmental Conservation (ADEC). In addition the landowners are consulted by the FOSC immediately prior to his sign-off.

FIGURE 1

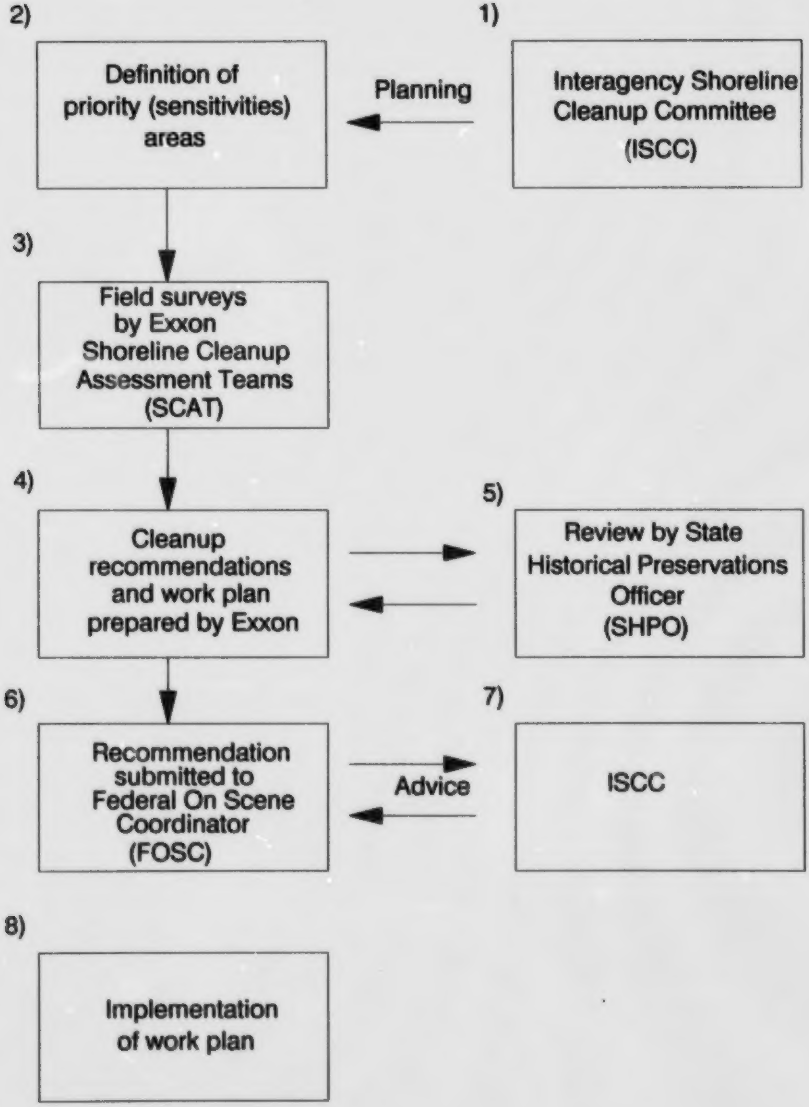
2)
1)
Definition of priority (sensitivities) areas
Planning
Interagency Shoreline Cleanup Committee (ISCC)
3)
Field surveys by Exxon Shoreline Cleanup Assessment Teams (SCAT)
4)
5)
Cleanup recommendations and work plan prepared by Exxon
Review by State Historical Preservations Officer (SHPO)
6)
7)
Recommendation submitted to Federal On Scene Coordinator (FOSC)
Advice
ISCC
8)
Implementation of work plan

Date: March 30, 1990

FIGURE 2 EXXON VALDEZ, Summer 1990

Shoreline Treatment Decision Chart

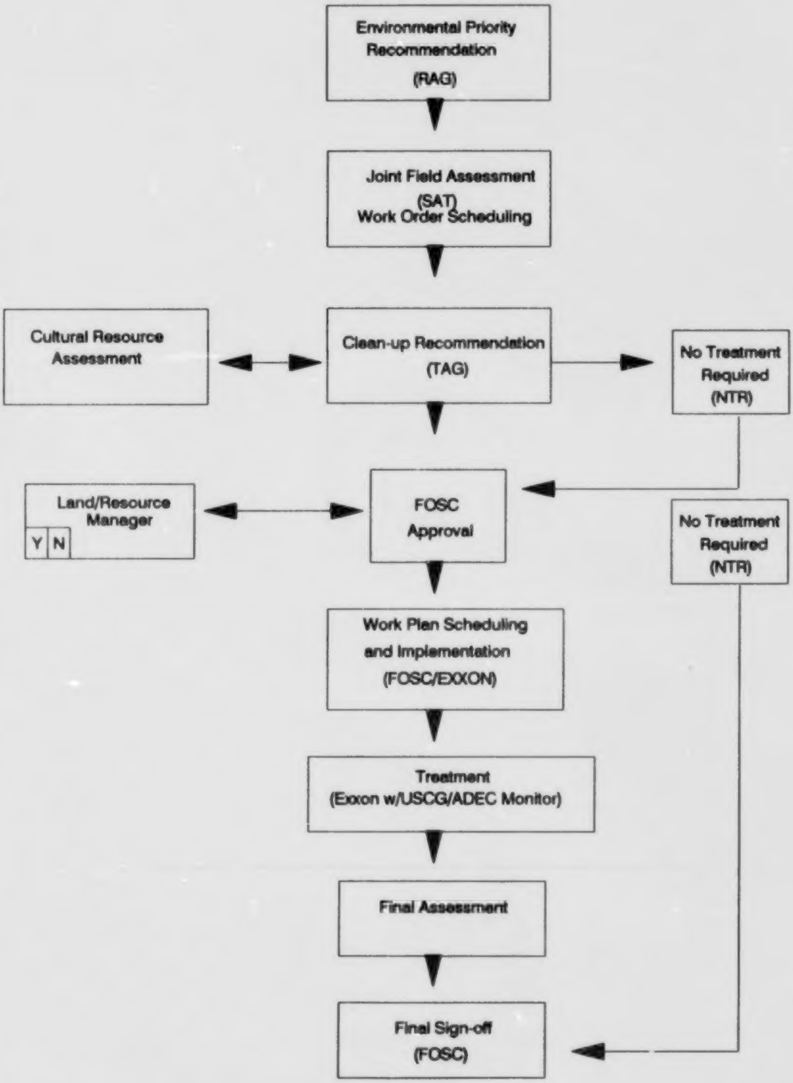
Environmental Priority Recommendation (RAG)
Joint Field Assessment (SAT) Work Order Scheduling
Cultural Resource Assessment
Clean-up Recommendation (TAG)
No Treatment Required (NTR)
Land/Resource Manager
Y
N
FOSC Approval
No Treatment Required (NTR)
Work Plan Scheduling and Implementation (FOSC/EXXON)
Treatment (Exxon w/USCG/ADEC Monitor)
Final Assessment
Final Sign-off (FOSC)

SUMMARY

Despite the enormous complexity of the 1989 shoreline response operations, the cleanup decision process that was developed was very straightforward:

1. Sensitive shoreline areas or locations were identified.
2. Timing constraints for field operations were reviewed.
3. Response priorities were set.
4. Detailed shoreline information was reviewed on a site specific basis.
5. A strategy for deployment of the Task Forces was developed.
6. Site specific work plans for each segment of shoreline were developed.
7. These plans were reviewed by the SHPO.
8. The approved plans were submitted to the FOSC.
9. The FOSC made a decision under advisement from an interagency committee.

The success of the method can be attributed to:

- the objectivity and scientific validity of the field team assessments.
- all of the cleanup decisions were made from the same information base.
- the involvement of agency and interest groups early in the decision process.

This latter point was even more important in the 1990 program as agency representatives participated directly in the field programs (FASST and SSAT; See Owens and Teal, this volume) that assessed the oiling conditions prior to the development of the operational strategy and work plans.

SHORELINE CLEAN-UP TECHNIQUES - EXXON VALDEZ OPERATIONS

by

Scott A. Nauman
Exxon Company, USA
3301 "C" Street
Anchorage AK 99503

The extreme diversity among impacted shoreline areas in Prince William Sound necessitated a variety of treatment techniques. Innovation produced equipment that was versatile and effective in the environment encountered. Rather than focus on a single concept, the tools developed represented an integration of techniques. This paper reviews some of the key shoreline treatment equipment used during the summer of 1989 - the cold water landing craft (LCV), the maxi-barge, the omni-barge and finally the hot water LCV. Also addressed in this text are the containment and collection methods used to support this treatment equipment.

COLD WATER LCV

Early in the shoreline cleanup, a priority was placed on flushing the still mobile oil off of the coastline to allow its containment and recovery. This flushing operation required pumps, hoses and auxiliary equipment. The lack of an infrastructure in the spill impacted area created a particular challenge in moving personnel and equipment to the jobsite. The rugged and rocky shoreline of Prince William Sound often dictated the use of shallow draft, maneuverable vessels. This challenge was met with military and civilian landing craft vessels (LCVs). These vessels varied in size and type, generally running 15' wide and ranging from 40-75' in length. The mission of the initial LCV's deployed was delivery of water to the shoreline. This was accomplished with a deluge system, augmented by workers with hoses and sprayers.

The deluge system, made up of pumps, hoses and manifolds, flushed large volumes of ambient temperature sea water down the face of the beach. The typical deluge system included a pair of diesel driven pumps onboard the vessel, supplying about 1000 gpm of water. Pumped from the vessel to shore, the water was moved to a flexible header line stretched high along the beach. Holes drilled in the header on a 12" spacing distributed the water across the face of the beach and down toward the waterline. Flexible header line was used as it matched the contours of the shoreline better than rigid pipe. This deluge system offered the advantage of simplicity in design and maintenance.

In addition to the deluge system, beach crews utilized hoses from the landing craft to assist in washing oil from the shore. The crews deployed across the face of the beach, working down slope. A crew of approximately 20 was typically used in conjunction with each landing craft. Water for the hoses was supplied to a distribution manifold from pumps on the landing craft. The manifold was equipped with multiple 2" take-off points. 2" fire hoses with standard brass nozzles were connected to the multiple takeoff points. This manifolding eliminated the need for multiple small pumps, one for each hose.

The cleaning options on the LCV were rounded out by self contained pressure wash units. These units provided low volume, high pressure water capability, with no external power supply needed. The unit typically consisted of a generator, pumps, a heater, hoses and a spray wand. Diesel driven industrial wash units eventually became the standard on the LCV.

The LCVs deployed in the summer of 1989 formed the backbone of Exxon's treatment program. Over 60 LCVs were ultimately deployed, supplying the means to reach coves, pocket beaches and various other impacted areas. While additional equipment evolved from this stage of the operation, the LCV remained an integral component throughout the summer.

MAXI BARGE

In an effort to increase the volume of water moved to the shoreline, the barge based "maxi" was developed. The development of the "maxi" barge went a step beyond the landing craft concepts. The maxi barge was designed specifically for use in Prince William Sound.

In order to pump more water onto the shoreline, a larger platform had to be established to hold the necessary equipment. Large ocean going barges met this need. The barges utilized were roughly 50' wide and ranged up to 180' in length. Beginning with bare-decked barges, equipment packages housed in shipping containers were set on deck. These enclosures provided protection from adverse weather.

Unlike the self-propelled landing craft, tugs were used to mobilize and demobilize the barges from the work site. The maxi barge required a crew of 25 per shift, with most operated on a two shift, 24 hour basis.

As an evolutionary step, the maxi barge added a few unique features not present on the landing craft. A schematic depicting the barge layout is shown in Figure 1. The size of the barge allowed incorporation of heat exchange units to provide added hot water capability. Two identical heat exchangers were incorporated into the maxi barge. Industrial heaters rated at 4.3 MBTU/hr each supplied hot fresh water to the shell side of the exchanger. Seawater was pumped through the tubes of the exchanger and heated by the circulating fresh water. The heat exchange concept was adopted to minimize the boiler's exposure to seawater corrosion and scaling.

The heated seawater was fed to a 4" manifold which ran the length of the barge. The manifold provided multiple 2' connections for hoses. Because of this configuration, the maxi barge was typically deployed parallel to the shoreline.

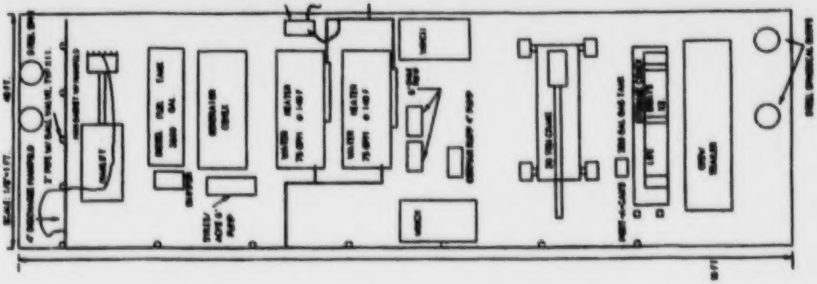

Figure 1 - Typical Maxi Barge Layout

Two new delivery systems were incorporated onto the maxi barge - fire monitors and a manlift platform. The fire monitors mounted on the barge provided a focused spray to those areas inaccessible to beach crews. The manlift concept was similar, with a platform like that often used in working on utility lines. The platform was capable of reaching 60-70 feet and was supplied with hot water from the 4" manifold. This water could be directed to a spray nozzle or hose connection. Again, this system allowed access to hard to reach areas. At the same time, the increased volume of hot water available from the maxi barge enhanced its ability to clean large stretches of beach. Thirteen of these maxi barges were deployed in Prince William Sound during the summer.

OMNI BARGE

The next generation of equipment in the cleanup focused on getting more hot water to the beach. As crude oil weathers, its viscosity increases, making it more difficult to mobilize. Heating the water used to flush the oil from the shoreline improves cleaning efficiency. The distinctive Omni barge provided this capability with a unique delivery system.

The development of the Omni barge vividly reflects the innovation inherent in the shoreline cleanup technology. A hydraulically operated articulating arm and spray head were installed on the deck of a barge. This articulating boom was adapted from the construction industry, where it is used to pump concrete. When equipped with a spray head and nozzles, the 100'+ boom became a valuable tool in cleaning the hard to access shoreline areas. The boom and spray head were manipulated remotely by an operator at the bow of the barge. The operator could move the boom up and down the beach, directing the high pressure spray at a variety of angles. The nozzles mounted on the spray head could be changed to alter the spray pattern. The head was designed to allow hose connection was well, reducing heat loss by lifting the hose above the ambient temperature seawater.

Efficiently heating the water available from the Omni barge was a key goal. Direct fired industrial heaters, arranged six abreast, became the standard on the Omni. Each heater was made up of a horizontal steel cylinder, flanged at both ends. Roughly three feet in diameter and twelve feet long, each unit was rated at 8 MMBTU/hr. "U" bend steel firetubes ran through the combustion chamber, providing heat to the circulating seawater. Water from the six heaters was commingled via overhead manifolding. The manifold was routed to the articulating boom for delivery of large volumes of heated water to the shoreline.

The Omni barge was similar in size to the maxi barge, but differed in key respects. Rather than a sea going barge, the Omnis were constructed from flexifloat components. These cube-shaped flotation cells were bound together to form a unit strong enough to carry the equipment load, yet flexible enough to accommodate the shifting sea states. Single or dual thrusters were installed at the rear of the barge, allowing the Omni to self position along the shoreline. A winch system was typically used along the shoreline to move the barge in and out with the tide.

Figure 2 displays the equipment layout on the Omni barge. Two 6" electrical submersible pumps, mounted on the side of the barge, fed seawater to the bank of six heaters. The heated seawater could be directed to the Omni boom, to hoses or to a bow mounted fire monitor. Supporting the massive fuel needs of the Omni barge were two 5000 gallon diesel tanks, typically straddling the boom. Mid barge, housed in containers, sat the warehouse and repair shops used to maintain the equipment on the barge. Toward the rear of the barge sat two diesel generator sets, each rated at 125 kw.

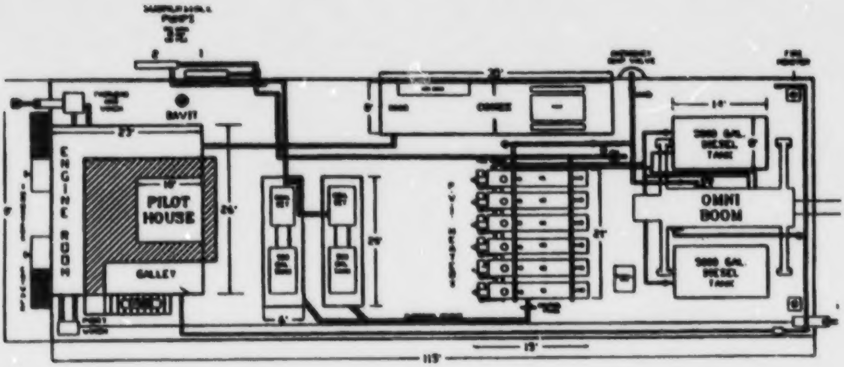

Figure 2 - Typical Omni Barge Layout

In normal operation, one of the submersible pumps supplied water for heating, one for back-up or cold water deluge. Four heaters were generally utilized, leaving 50% back-up to allow for maintenance. This operational mode supplied 500 gpm of 140 degrees F water which could be sent through the spray head. This high volume flush could be accomplished without the need for personnel on shore, making the Omni barge attractive in many hard to access areas. The reach of the boom could be applied to rocky outcrops as well as broad beaches. Thirteen Omni barges were placed in service, distributed throughout Prince William Sound.

HOT WATER LCV

The final major phase of development coupled the maneuverability of the landing craft with the hot water capability provided by industrial heaters. The hot water LCV became known as a 2-pac, as a pair of industrial heaters like those used in Omni service were mounted in the vessel. Figure 3 shows the hot water LCV layout. A 30-50 kw generator provided electrical power for the heaters and controls. A pair of 6" diesel driven centrifugal pumps supplied water for the heaters. A skid mounted fuel tank provided diesel for the heaters, pumps, and generator. Run in its typical configuration, with both heaters operating simultaneously, the hot water LCV produced about 250 gpm of 140 degree F water which could be distributed through hoses or bow mounted fire monitors.

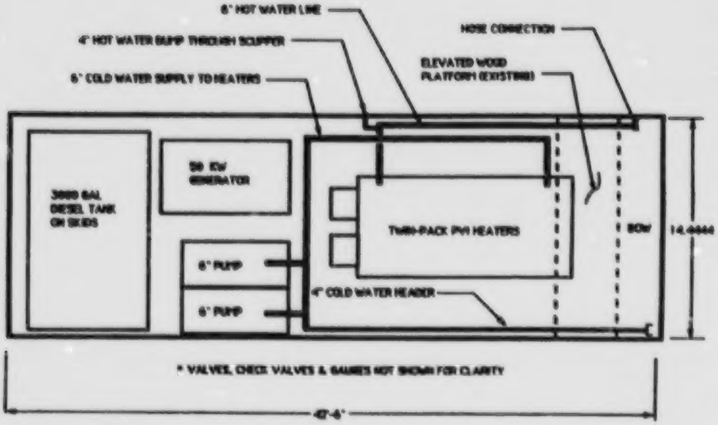
6" HOT WATER LINE
4" HOT WATER DUMP THROUGH SCUPPER
6" COLD WATER SUPPLY TO HEATERS
HOSE CONNECTION
ELEVATED WOOD PLATFORM (EXISTING)
3000 GAL DIESEL TANK ON SKIDS
50 KW GENERATOR
TWIN-PACK PVI HEATERS
6" PUMP
6" PUMP
4" COLD WATER HEADER
BOW
14.4444
* VALVES, CHECK VALVES & GAUGES NOT SHOWN FOR CLARITY
42'-6"

Figure 3 Typical Hot Water LCV Layout

The hot water LCV became particularly effective as the mobility of the treatment teams was increased to reach a wider geographic area. Nimble enough to move around rocks and near to shore on its own, the hot water LCV was able to generate more hot water than a maxi barge. Over a dozen hot water LCVs were commissioned during the clean-up.

CONTAINMENT

The array of equipment described above was designed to wash oil from the shoreline, using cold and/or hot water. The oil liberated from the shoreline had to next be contained once on the water. Regardless of the washing equipment, this containment was typically accomplished via booming.

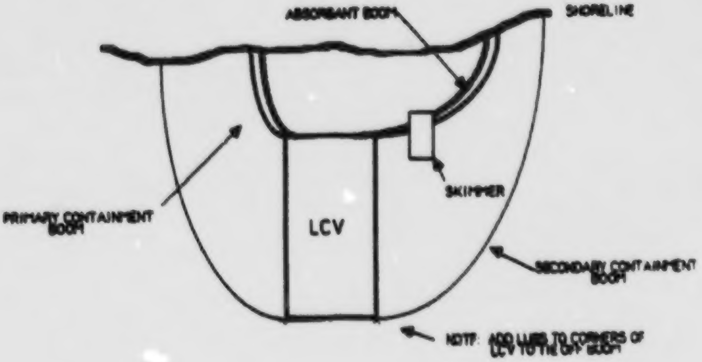
ABSORBANT BOOM
SHORELINE
SKIMMER
PRIMARY CONTAINMENT BOOM
LCV
SECONDARY CONTAINMENT BOOM
NOTE: ADD LINES TO CORNERS OF LCV TO THE OFF BOOM

Figure 4 - Typical LCV Booming Configuration

The standard booming configuration utilized a redundant system with primary and secondary containment. A schematic depicting a standard LCV booming pattern is shown in Figure 4. The primary boom was deployed off the front of the LCV, with the secondary looping behind. The purpose of the primary containment boom was to corral the oil as it was flushed from the shoreline. Once contained, the oil could then be collected off the water's surface of the water, typically using skimming devices.

The secondary containment boom was used to enclose the vessels and prevent the escape of sheen to the surrounding water. Absorbent boom was often used to reduce loss from the primary system and as a backup to oil collection via skimmers.

Deployment of the containment boom was an extremely labor intensive task, involving beach crews and skiffs for positioning. With tide cycles of 15' or greater, the boom had to be stretched high enough onshore to conform to the high tide, yet far enough into the water for low tide. Once the booms were in the place, the flushing operations would drive liberated oil within the primary containment system. The final step, collecting this oil, is described in the next section.

Sorbents supplemented the skimmers in the oil recovery process. Snare boom and pom-poms were effective in collecting oil on the face of the shoreline. Regardless of the skimming method used, the goal was to efficiently recover the liberated oil. In some cases, mechanical methods were applicable, in others the passive use of sorbents predominated.

COLLECTION

Once contained, skimming devices of various size and description were used to collect the waterborne oil. While skimmers were the primary means used in this recovery process, sorbent boom, snare boom and pom-poms were widely and effectively used.

The skimmers used included sorbent type skimmers, weir devices and suction devices. Rope mop skimmers, a sorbent type, utilized an absorbent rope which rotated around pulleys, contacting the water's surface. The rope was then squeezed through wringers to remove the absorbed oil. Belt skimmers, another sorbent type, found widespread utilization. These self propelled units could rove between sights along the shoreline, collecting oil from within the primary containment systems. The belt could be raised as the boom was approached, then lowered into the oil, leaving the containment intact. Once the oil had been skimmed from the primary, the unit would raise its belt and move to a new sight.

Disk skimmers were small devices suspended within the primary boom. The oil adhered to rotating disks, which deposit the oil in the skimmers' interior. Weir-type skimmers were also used. Suction devices, including vacuum trucks, were particularly effective where the layer of floating oil was fairly thick.

SUMMARY

The conditions encountered during shoreline cleanup can vary significantly, and dictate equipment that is flexible and effective. The mix of tools described in this paper was necessary to accomplish the task. No one piece of equipment could have matched all of the situations faced. Each played its own key role. The maxi and Omni barges provided vast quantities of hot water, delivered through a variety of systems. The cold and hot water LCVs provided maneuverable vehicles from which small segments of shoreline could be reached. In the end, all types described were in service, playing complimentary roles.

SUGGESTED IMPROVEMENTS TO OIL SPILL RESPONSE PLANNING FOLLOWING THE "NESTUCCA" AND "EXXON VALDEZ" INCIDENTS

E. H Owens
Woodward-Clyde Consultants
900 Fourth Avenue
Seattle, Washington 98164

ABSTRACT

The evaluation of shoreline oiling following the "Nestucca" and "Exxon Valdez" oil spills involved field teams that collected data in a systematic format. The involvement of responsible or interested agency representatives in this evaluation process can facilitate consensus for a response program. In addition, standardization of reporting, terminology and map bases increases the accuracy of data gathering and reduces confusing or conflicting information. Such reporting also provides documentation of the spill incident. Both spills affected extensive and remote coastal environments and field operations involved the delegation of responsibility to sub-bases or regional centers in order to effectively manage widespread activities. The practical experience gained from these two recent spills can be applied directly to contingency planning and response manuals.

Introduction

The purpose of this discussion is to suggest ways in which oil spill contingency plans and response manuals could be improved in the light of recent experience. This is not a critique of the spill response in either incident nor of the cleanup activities following the spills, and the elements of the "Nestucca" spill that are discussed here refer specifically and solely to the response on the Canadian side of the border.

Although the two incidents involved oil volumes that were orders of magnitude different, there were many similarities in terms of the spill evaluations and the response logistics. The remote and largely inaccessible character of the coastlines affected by both spills required a high level of effort, simply to assess the location and the extent of the oiling. Further, time and resources were needed to evaluate the appropriate response actions. Reporting by different agencies or individuals was not consistent, for example, with respect to descriptive terminology, map scales, and even location names. The logistics of shoreline treatment and of the disposal of oil/oiled material were complex and expensive. No doubt all of these topics will be further scrutinized and debated as we attempt to learn from our experiences. Some elements of the responses have an immediate and practical application to the preparation of oil spill contingency plans and response manuals worldwide and it is those topics which are addressed briefly in this discussion.

Geographical Subdivision of Effort

As oil from the "Nestucca" spread north along the west coast of Vancouver Island to Cape Scott, 300 kilometers from the Ucluelet command center, 'lines of supply' rapidly became longer and longer. Helicopter and vessel transit times increased and efficiency decreased. Fuel depots became a logistics factor. In order to gather information over a long coastal area a boat-ground based Shoreline Surveillance Team (SST) and a helicopter supported Shoreline Evaluation Team (SET) were established to locate oil on the shore. The role of the two teams changed over time but the basic function remained as a means of collecting data and information. Early in the response it became necessary to split the shoreline evaluation team (SET) (Figure 1) so that one team could cover the northern and central sectors of the affected coastal region while the second remained in the south, based at the Ucluelet command post. Similarly, the on-scene coordinator (OSC) set up operational sub-bases at Port Hardy on northern Vancouver Island and at Sandspit in the Queen Charlotte Islands. The subdivision of effort and responsibility was greatly magnified during the "Exxon Valdez" response with four regional command centers (Valdez, Seward, Homer, and Kodiak). The 1989 Exxon Shoreline Cleanup Assessment Team (SCAT) program began with one field team but rapidly grew and at one time 9 teams were operating simultaneously over a coastal region that extended for more than a thousand kilometers from the Valdez command center.

In both incidents an effort was made to regionalize assignments so that the same individuals were in the same areas rather than being rotated, thereby becoming fa-

Figure 1
Organization of "Nestucca" Environmental Response

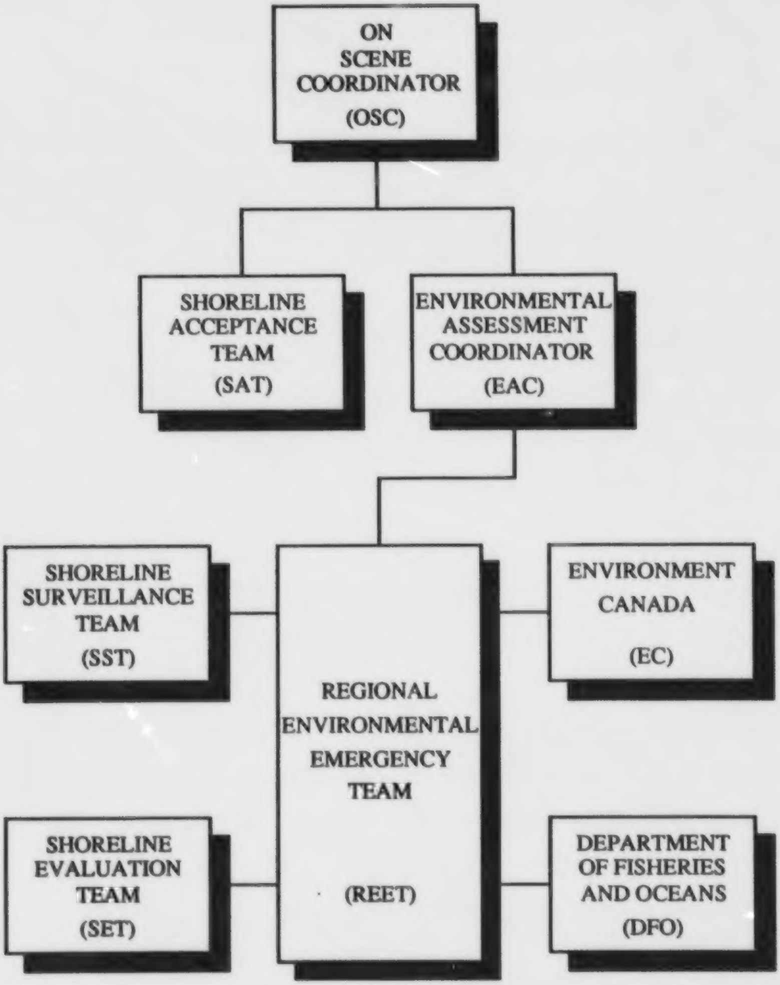
ON SCENE COORDINATOR (OSC)
SHORELINE ACCEPTANCE TEAM (SAT)
ENVIRONMENTAL ASSESSMENT COORDINATOR (EAC)
SHORELINE SURVEILLANCE TEAM (SST)
REGIONAL ENVIRONMENTAL EMERGENCY TEAM (REET)
ENVIRONMENT CANADA (EC)
SHORELINE EVALUATION TEAM (SET)
DEPARTMENT OF FISHERIES AND OCEANS (DFO)

miliar with the local geography and its particular problems. In the "Exxon Valdez" response this continues today (1990), with one set of field evaluation teams assigned to the Prince William Sound area and one group to the Kenai, Alaska Peninsula, Kodiak region. In March/April 1990, a total of 20 field teams were mobilized to reassess shoreline oiling and to provide data prior to the summer operations program.

Joint Response Evaluation

The "Nestucca" incident SST and SET teams that were established at the outset of the response included representatives from the OSC (the Canadian Coast Guard), the Regional Environmental Emergency Team (REET) (Environment Canada), and the land users (Nuu-Chah-Nulth Tribal Council (NTC)). These individuals observed together, conferred on-site together, and agreed together on what was there and what could be done. This joint evaluation was then presented to the REET and OSC each evening and greatly facilitated decisions for the subsequent response activities.

A similar program was instituted in Alaska during the 1989 operations, but as the number of responsible agencies and interested parties was more than a dozen, it was not possible to confer in the field. Discussions and decisions were a daily feature of the Valdez Interagency Shoreline Cleanup Committee (ISCC) and the regional Multi-Agency Committee (MAC) groups. A field assessment of shoreline oiling in spring 1990, prior to the second year of operations, involved a team comprised of a contract coastal geologist and ecologist to collect data, accompanied by a representative from Exxon, ADEC (Alaska Department of Environmental Conservation), USCG/NOAA and the land manager. This team represented the major responsible agencies involved with the program.

Standardized Reporting

Different or undefined terminology led to an inconsistent picture of the degree of shoreline oiling at the "Nestucca" spill on southern Vancouver Island. In particular, volunteers and local inhabitants reported volumes in a variety of terms ranging from 'truckloads' to 'complete fouling.' Such information was often provided without reference to a specific geographic location. An information check list and glossary to define the degree of oiling were included early in the shoreline evaluation, so that reports from different sources could be standardized. This system was not complex (Table 1, Figure 2) yet provided a consistent information base for the REET and the OSC.

The model for the checklists used on both spills is one developed for Environment Canada as a training tool. Such checklists area basically similar in format but are adapted to suit local coastal environments (e.g., Owens, 1979; IMO/UNEP, 1983).

The "Exxon Valdez" check list system used in 1989 provided for systematic information collection for (a) shoreline character/oiling (Figure 3), and (b) ecology, plus a form to document (c) the cultural and historical character of the shore zone. As the number of field teams and individuals who participated in the program increased, the value of this standardized system became greater. Although not perfect, once in place the forms continued to be used with no major modifications so that the information base could remain consistent geographically and through time. The 1990 resurvey teams again used checklists to describe the shoreline character, oiling conditions (Figure 4) and ecology (Exxon, 1990). A side benefit of standardized forms is that the information can be entered into an electronic data base and the files linked with CAD software to produce maps of the information. This GIS (Geographical Information System) approach was introduced early in the "Exxon Valdez" operation.

Table 1
"Nestucca" Shoreline Oil Classification (Owens, 1989)

1) OIL CHARACTER

Class 1	• no visible oil on surface of rock or beach • no visible oil in sub-surface sediments • no visible oil in or on logs
Class 2	• sheen (rainbow oil) on surface of rock or beach • no visible black oil on rock or beach • thin (< 2 cm) cover of oil on logs or rocks
Class 3	• sheen (rainbow oil) on surface AND brown or black oil • size of brown or black oil is 2 cm or less with • occasional 14-20 cm diameter blobs
Class 4	• surface oil cover on rocks and/or beach is thick (> 2.5 cm) • size of blobs is 25 cm or larger diameter • logs have blobs or oil cover > 2.5 cm thick
Class 5	• continuous oil cover, not blobs, > 5 cm thick

2) OIL COVER

Light	• 5 to 10% of the shore covered with sheen ("rainbow oil") • brown/black blobs no greater than nickel/dime size • no more than 10 blobs per square meter
Moderate	• brown/black oil blobs of plate or cow-patty size • more than 1 blob per square meter • greater than 10 meters of shore oiled
Heavy	• brown/black blobs of plate size or larger over more than 10 meters of shore but not continuous oil cover
Complete	• brown/black oil on surface covers more than 25% of the shore • more than 25 meters length of shore oiled

Figure 2
"Nestucca" Oil Spill Sighting Form (Owens, 1989)

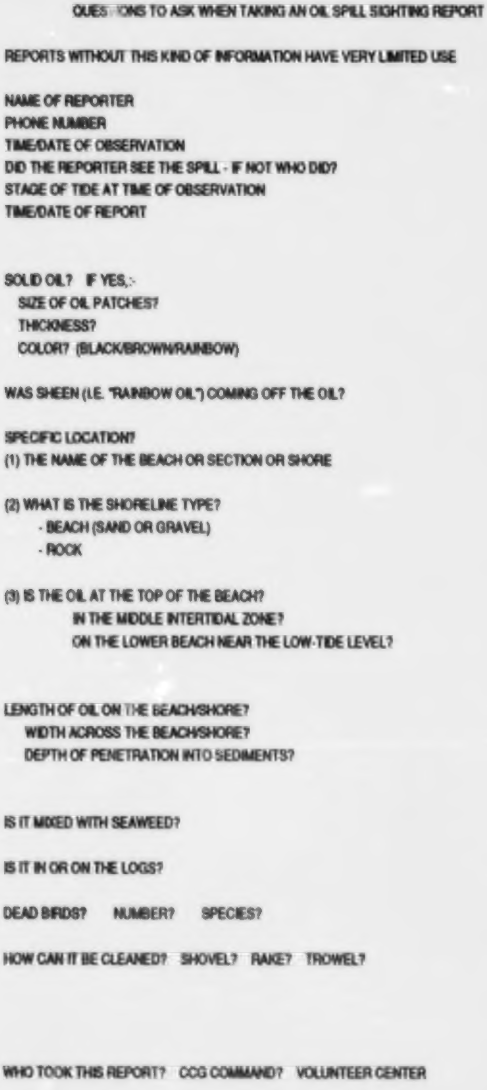

QUESTIONS TO ASK WHEN TAKING AN OIL SPILL SIGHTING REPORT

REPORTS WITHOUT THIS KIND OF INFORMATION HAVE VERY LIMITED USE

NAME OF REPORTER
PHONE NUMBER
TIME/DATE OF OBSERVATION
DID THE REPORTER SEE THE SPILL - IF NOT WHO DID?
STAGE OF TIDE AT TIME OF OBSERVATION
TIME/DATE OF REPORT

SOLID OIL? IF YES,:-
  SIZE OF OIL PATCHES?
  THICKNESS?
  COLOR? (BLACK/BROWN/RAINBOW)

WAS SHEEN (I.E. "RAINBOW OIL") COMING OFF THE OIL?

SPECIFIC LOCATION?
(1) THE NAME OF THE BEACH OR SECTION OR SHORE

(2) WHAT IS THE SHORELINE TYPE?
  - BEACH (SAND OR GRAVEL)
  - ROCK

(3) IS THE OIL AT THE TOP OF THE BEACH?
  IN THE MIDDLE INTERTIDAL ZONE?
  ON THE LOWER BEACH NEAR THE LOW-TIDE LEVEL?

LENGTH OF OIL ON THE BEACH/SHORE?
  WIDTH ACROSS THE BEACH/SHORE?
  DEPTH OF PENETRATION INTO SEDIMENTS?

IS IT MIXED WITH SEAWEED?

IS IT IN OR ON THE LOGS?

DEAD BIRDS? NUMBER? SPECIES?

HOW CAN IT BE CLEANED? SHOVEL? RAKE? TROWEL?

WHO TOOK THIS REPORT? CCG COMMAND? VOLUNTEER CENTER

Figure 3
"Exxon Valdez" 1989 S.C.A.T. Oil/Geomorphology Form

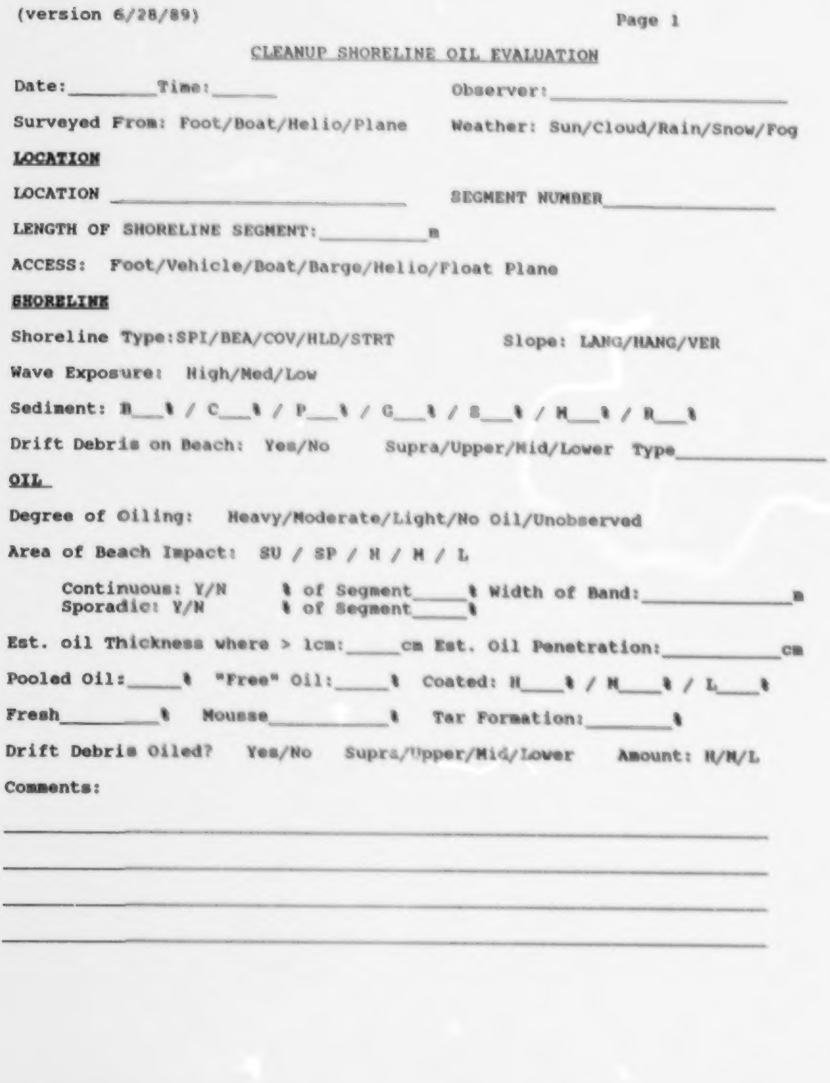

(version 6/28/89) Page 1

CLEANUP SHORELINE OIL EVALUATION

Date:________Time:______ Observer:________________________

Surveyed From: Foot/Boat/Helio/Plane Weather: Sun/Cloud/Rain/Snow/Fog

LOCATION

LOCATION ______________________________ SEGMENT NUMBER________________

LENGTH OF SHORELINE SEGMENT:__________m

ACCESS: Foot/Vehicle/Boat/Barge/Helio/Float Plane

SHORELINE

Shoreline Type:SPI/BEA/COV/HLD/STRT Slope: LANG/HANG/VER

Wave Exposure: High/Med/Low

Sediment: B___% / C___% / P___% / G___% / S___% / M___% / R___%

Drift Debris on Beach: Yes/No Supra/Upper/Mid/Lower Type_______________

OIL

Degree of Oiling: Heavy/Moderate/Light/No Oil/Unobserved

Area of Beach Impact: SU / SP / H / M / L

Continuous: Y/N % of Segment_____% Width of Band:_______________m
Sporadic: Y/N % of Segment_____%

Est. oil Thickness where > 1cm:_____cm Est. Oil Penetration:___________cm

Pooled Oil:_____% "Free" Oil:_____% Coated: H____% / M____% / L____%

Fresh_________% Mousse___________% Tar Formation:________%

Drift Debris Oiled? Yes/No Supra/Upper/Mid/Lower Amount: H/M/L

Comments:

Figure 4
"Exxon Valdez" 1990 S.S.A.T. Shoreline Oiling Form

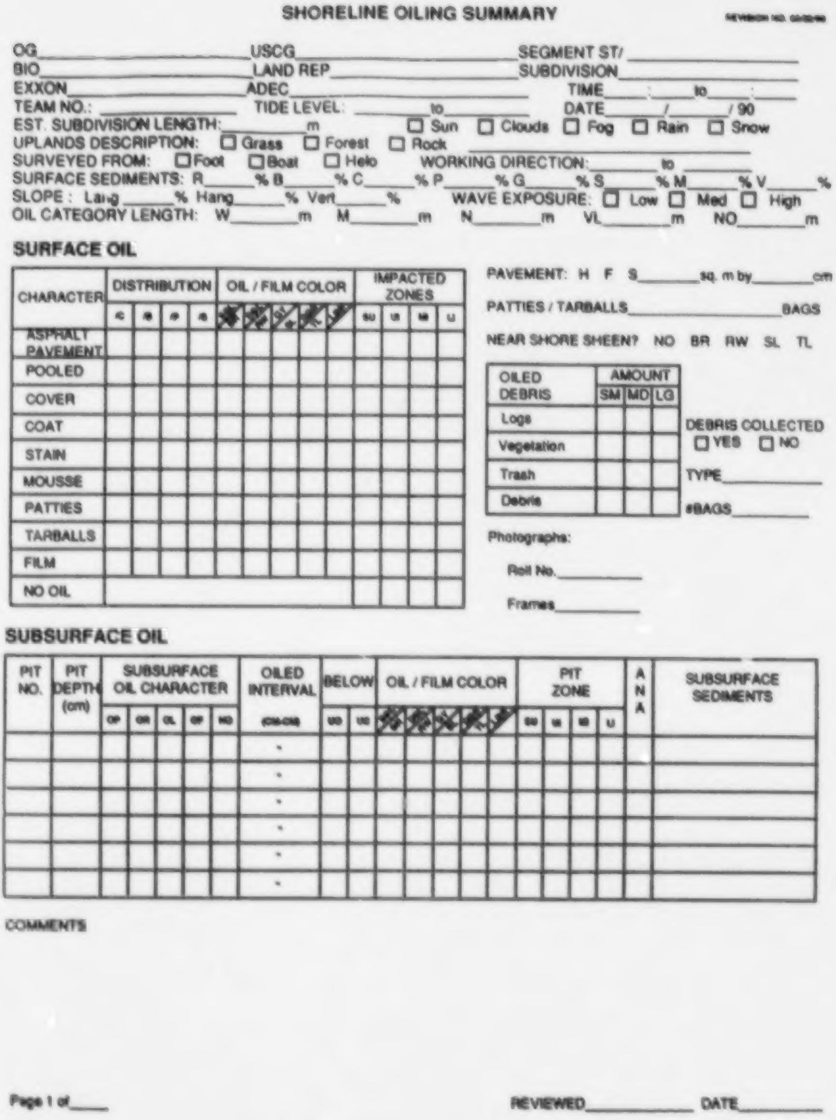

SHORELINE OILING SUMMARY

REVISION NO. [illegible]

OG__________ USCG__________ SEGMENT ST/ __________
BIO__________ LAND REP__________ SUBDIVISION__________
EXXON__________ ADEC__________ TIME____:____ to ____:____
TEAM NO.: __________ TIDE LEVEL: ______ to ______ DATE____/____/ 90
EST. SUBDIVISION LENGTH:______ m ☐ Sun ☐ Clouds ☐ Fog ☐ Rain ☐ Snow
UPLANDS DESCRIPTION: ☐ Grass ☐ Forest ☐ Rock __________
SURVEYED FROM: ☐ Foot ☐ Boat ☐ Helo WORKING DIRECTION:______ to ______
SURFACE SEDIMENTS: R____% B____% C____% P____% G____% S____% M____% V____%
SLOPE : Lang____% Hang____% Vert____% WAVE EXPOSURE: ☐ Low ☐ Med ☐ High
OIL CATEGORY LENGTH: W______m M______m N______m VL______m NO______m

SURFACE OIL

CHARACTER	DISTRIBUTION				OIL / FILM COLOR					IMPACTED ZONES			
	C	[illegible]	[illegible]	[illegible]	▨	▨	▨	▨	▨	SU	[illegible]	[illegible]	U
ASPHALT PAVEMENT													
POOLED													
COVER													
COAT													
STAIN													
MOUSSE													
PATTIES													
TARBALLS													
FILM													
NO OIL													

PAVEMENT: H F S______sq. m by______cm

PATTIES / TARBALLS__________BAGS

NEAR SHORE SHEEN? NO BR RW SL TL

OILED DEBRIS	AMOUNT		
	SM	MD	LG
Logs			
Vegetation			
Trash			
Debris			

DEBRIS COLLECTED
☐ YES ☐ NO

TYPE__________

#BAGS________

Photographs:

Roll No.________

Frames________

SUBSURFACE OIL

PIT NO.	PIT DEPTH (cm)	SUBSURFACE OIL CHARACTER					OILED INTERVAL	BELOW		OIL / FILM COLOR					PIT ZONE				ANA	SUBSURFACE SEDIMENTS
		OP	OR	OL	OF	NO	(cm-cm)	[illegible]	[illegible]	▨	▨	▨	▨	▨	[illegible]	[illegible]	[illegible]	U		
							-													
							-													
							-													
							-													
							-													
							-													

COMMENTS

Page 1 of____

REVIEWED__________ DATE________

Forms such as these may differ in appearance and length depending on the information requirements, the character of the coastal zone, and the need for data transfer to computer files. The basic concept would be similar for most plans or incidents, with the important element of geography modifying the details of the shore-zone geology and ecology reporting. Clearly, a system developed for the fjord coasts of the Pacific Northwest is not appropriate for east coast barrier beach environments.

A simple example that illustrates the need for standardization is the use of different map bases or scales by different parties. Agreement on the use of a specific map or chart system and scale for the collection and display of data can avoid the development of confusing or even conflicting information sets.

Standardized reporting techniques provide a simple yet effective method of documenting a spill incident. The method is useful for even small spills, but is particularly valuable when multiple field teams are required to collect information.

Environmental Sensitivity

In both incidents, pre-spill response planning had evaluated shoreline sensitivity in terms of ecology and of commercial/recreational activities. During the "Nestucca" response it was clear that shore-zone subsistence activities (food gathering) were a major feature of the life style of the coastal native population. In Alaska, the importance of historical (and prehistorical) cultural features in the coastal zone affected by the "Exxon Valdez" spill were not addressed by the environmental sensitivity index studies for Prince William Sound and the Gulf of Alaska. The response activities in both incidents were adapted quickly to include these previously unforeseen sensitivities and illustrate the need for a thorough understanding of local land/coastal use and of cultural resources as well as of the standard socioeconomic and ecological features that are included in most environmental sensitivity evaluations. Training check lists used by Environment Canada have included archaeological/cultural features, but prior to these two incidents these features had not been significant elements of coastal zone sensitivity affected by a spill nor had they been included in shoreline sensitivity analyses.

Summary and Recommendations

1. Spills that affect extensive and remote coastal areas may often require regional or sector subdivision for both evaluation and response operations.
2. Interagency or multi-agency field evaluations usually provide a mechanism to facilitate immediate on-site agreement between the main parties involved.
3. Standardized format and terminology for field observations greatly increase the accuracy of reporting, assist understanding of the problem, and facilitate agreement on response actions.
4. Pre-spill shoreline evaluations should be sufficiently broad to incorporate data/information on locally sensitive activities and resources or cultural resources; rather than a standard range of socioeconomic or ecological features.

References

Exxon, 1990. Joint Exxon/Agency Spring Shoreline Assessment Team (SSAT); Unpublished Operations Manual, Anchorage. 15 pp. + 16 attachments.

IMO/UNEP, 1983. Oil spills and Shoreline Cleanup in the Islands of the Wider Caribbean Region. Workshop Notes and Field Guide. Prepared for IMO, London, by Woodward-Clyde Consultants.

Owens, E. H., 1979. The Canadian Great Lakes: Coastal Environments and the Cleanup of Oil Spills. Environment Canada, Environmental Impact Control Directorate, Econ. and Tech. Review Rept. EPS 3-EC-79-2, 252 pp.

Owens, E. H., 1989. Preliminary Report on Shoreline Activities in British Columbia following the "Nestucca" Oil Spill Incident; Unpub. Report by Woodward-Clyde Consultants to Environment Canada, Vancouver, B.C., 14 pp.

A BRIEF OVERVIEW AND INITIAL RESULTS FROM THE WINTER SHORELINE MONITORING PROGRAM FOLLOWING THE *EXXON VALDEZ* INCIDENT

Ed Owens
Woodward-Clyde Consultants
900 Fourth Ave., Seattle
WA 98164

Andrew Teal
Exxon USA, Alaska Operations
P.O. Box 240409, Anchorage
AK 99524

ABSTRACT

Systematic measurements and observations were made monthly at 64 selected representative sites throughout Prince William Sound and the Gulf of Alaska following the "Exxon Valdez" spill in order to monitor changes in shoreline oil conditions. The Prince William Sound data show that after the 1989 treatment program the surface oil cover was reduced from an average of 27% to 4% over the period September 1989 to March 1990. Rates of change were similar on beaches characterized by widely varying wave-energy levels. By the end of the winter program the remaining oil was discontinuous or patchy and largely restricted to the upper intertidal zone. Subsurface oil was generally at depths less than 10-15 cm in low-energy environments and had been scoured out on the majority of high-energy beaches. Subsurface oil remains at a few exposed locations where sediment reworking was not as effective at depth. The 1989 shoreline treatment program significantly reduced the volume of oil, which in turn is believed to have accelerated winter removal rates. Also, few asphalt pavements had formed by spring 1990 as a result of the removal of mobile oil. The systematic data set generated by this field study program provides a major source of information against which future spills can be compared to better evaluate rates of natural change.

INTRODUCTION

Shoreline conditions in Prince William Sound (PWS) and the Gulf of Alaska (GOA) were monitored by Exxon through the winter months to (1) provide data on changes in the character of the stranded oil and (2) estimate the expected distribution of the remaining oil in the spring of 1990. This discussion is not a comprehensive review as much of the data base has yet to be fully analyzed. At this time it is possible to present only the obvious trends, a preliminary discussion of some of the results and to provide some examples of the data that has been obtained.

The field program continued throughout the winter and required a large commitment of resources in a cold and often stormy environment. Air support was provided by winterized twin-engine IFR Bell 212 helicopters, with winter survival equipment; vessel support involved 50-m supply boats with rigid inflatable skiffs for ship-to-shore transfer. All field personnel underwent a winter survival training program and minimum safe working conditions were observed at all times. Weather down-time resulted in a loss of 30% of the potential operating window (compared to a 2% loss due to helicopter/vessel mechanical reasons) and, despite the often inclement operating environment, there were no accidents or injuries during more than 650 field days.

The degree of oiling and the coastal environments of Prince William Sound (PWS) and of the Gulf of Alaska (GOA) coasts are so different that direct comparisons between these two geographic regions are not appropriate. Although this discussion focuses primarily on the data collected from the PWS surveys, similar oil and beach changes were observed at the GOA sites and considerably higher rates of change were observed on the high-energy exposed study sites in the Gulf. This discussion does not attempt to present any of the biological data generated by the study.

FIELD STUDY PROGRAM

The winter shoreline monitoring program was designed to make use of all available low-tide periods with water levels less than 1 m above lowest low water occurring during the restricted windows of daylight of the subarctic winter. Field studies were designed to obtain a systematic data set at representative locations during these operational windows. Two levels of effort were established in order to provide an optimal set of information. At the first level, 28 multi-profile detailed study sites, 18 in PWS and 10 in GOA, were to be monitored by 3-person teams, monthly from September 1989 to March 1990 ("A" program). As with most field projects, the program was sightly modified as it proceeded:

- one of the sites (AP-13) was subsequently split into 3 segments
- one survey window (February) was omitted due to reassignment of field priorities
- one site (AP-15) was visited only once due to access difficulties, and
- one site (AP-9) was dropped because of data redundancy.

Weather constraints limited operations and site access on some occasions. Nevertheless, in PWS 68 site visits were made during the winter "A" program out of a possible total of 96.

At a second level, 36 single-profile study sites, 18 each in PWS and GOA, were established for monthly surveys ("B" program). As other priorities developed during the winter months, this program was modified to conduct field surveys on 4 of the 7 low- tide/daylight windows. Despite one site (BP-16) which could not be reoccupied due to a change in the type of helicopters that were used for winter flying, visits in PWS were successful on 54 out of a possible total of 68 site visits.

A summary of the PWS site conditions in terms of general wave exposure and initial oil conditions is provided in Table 1. In the GOA, five "A" and ten "B" study sites were established on the Kenai Peninsula and five "A" and eight "B" sites in the Kodiak-Alaska Peninsula area.

In addition to the systematic studies at the "A" and "B" sites, information was obtained relative to shoreline oiling conditions from several activities. For example, time-lapse photography stations were set up to record shoreline dynamics and beach/oil changes. Site visits also were carried out specifically to obtain data on the distribution and character of surface and subsurface oil in PWS. These additional visits were made to a wide range of sites throughout the Sound in order to obtain as complete a picture as possible on beach and oil conditions.

FIELD METHODS

At each of the 28 detailed ("A") sites in PWS and GOA, the surface oil cover was visually estimated along a set of multiple, pre-established, cross-beach transects; beach elevation profiles were surveyed along selected transects; pits were dug to document

TABLE 1 PRINCE WILLIAM SOUND STUDY SITES

(a) Site Locations and Characteristics

SITE	LOCATION	ORIGINAL OIL BAND WIDTH	WAVE-ENERGY ENVIRONMENT
AP-1	Northeast Smith Is.	Wide	High
AP-2	Northwest Smith Is.	Wide	High
AP-3	NE Little Smith Is.	Wide	High
AP-4	Foul Pass, Ingot Is.	Wide	Low
AP-5	Passage Point, Knight Is.	Wide	Moderate
AP-6	East Herring Bay	Moderate	Low
AP-7	North Green Is.	Moderate	Moderate
AP-8	Northwest Green Is.	Wide	High
AP-9	North Point Helen	Wide	High
AP-10	South Point Helen	Wide	High
AP-11	Northeast Latouche Is. - S	Wide	High
AP-12	Northeast Latouche Is. - N	Wide	High
AP-13	Sleepy Bay, Latouche Is.	Wide	High
AP-14	Northwest Latouche Is.	Wide	High
AP-15	North Evans Island	Wide	Moderate
AP-16	East SW Elrington Is.	Moderate	Moderate
AP-17	North SW Elrington Is.	Moderate	Moderate
AP-18	South SW Elrington Is.	Moderate	Low
BP-1	East Perry Is.	Wide	Low
BP-2	South Perry Is.	Moderate	Moderate
BP-3	Outside Bay, Naked Is.	Narrow	Moderate
BP-4	East Applegate Is.	Moderate	Moderate
BP-5	Northwest Bay, East Arm	Wide	Low
BP-6	Northeast Block Is.	Wide	Low
BP-7	West Crafton Is.	Moderate	Low
BP-8	North Eshamy Bay	Moderate	Moderate
BP-9	West Herring Bay	Moderate	Low
BP-10	East Seal Is.	Wide	High
BP-11	Bay of Isles, West Arm	Moderate	Low
BP-12	Bay of Isles, South Arm	Wide	Low
BP-13	Northeast Chenega Is.	Moderate	Moderate
BP-14	North Applegate Rocks	Moderate	High
BP-15	Marsha Bay	Wide	Low
BP-16	Marsha Bay Lagoon	Moderate	Low
BP-17	Central Chenega Is.	Narrow	Moderate
BP-18	North Evans Is.	Moderate	Low

(b) Summary of PWS Site Characteristics (by number of sites)

		ORIGINAL OIL BAND WIDTH			
		Wide >6 m	Moderate 3 - 6 m	Narrow <3 m	Total Sites
	High	10	4	0	14
WAVE ENERGY:	Moderate	2	8	0	10
	Low	7	4	1	12

subsurface oil; and surface and subsurface sediment samples were collected for laboratory analysis of total petroleum hydrocarbons (TPH). The procedures for the oil cover and beach elevation surveys followed those used in the BIOS experiment (Owens et al., 1987). In PWS a total of 198 transect lines were established to monitor changes in the surface oil cover at the 18 sites and over the period September to March a total of 580 lines were surveyed. A biological survey was conducted along selected lines and this effort focused on recording macro-species abundance and general condition along or adjacent to the repeat profile transect. A photographic and 8-mm video record was obtained of site conditions. Each field team consisted of an experienced oil spill geomorphologist who carried out the beach and oil surveys, an ecologist who monitored intertidal biology transects, and a field technician. One team usually was able to survey one site per tidal/daylight window (3 to 4 hours). Consistency was maintained as the same observers were used at the same sites whenever possible throughout the program.

For the less detailed ("B") program, a two-person team observed and documented the surface oil cover along a single transect at each of the 36 sites. Pits were dug for subsurface evaluations and a complete photographic and video record of the site conditions was obtained.

DATA REDUCTION AND ANALYSIS

The data base that resulted from the field program is very large and as yet not fully reduced nor analyzed. In this discussion it is possible therefore to present only some examples of the data and a brief summary of the results obtained to date, rather than a comprehensive review of the changes that have been observed and measured. Data reduction priorities were assigned to those information sets that were needed for input into operations planning for 1990.

An important facet of the winter study was the separation of data reduction functions from the field data collection. This was designed from the outset to ensure that personnel could focus their attention on a specific role rather than have multiple assignments and possibly conflicting field/office schedules.

Initially, maps of the surface oil cover observations were produced manually and, subsequently, by a computer-aided drafting system (CAD) in order to illustrate changes in the distribution of the oil cover. Examples of the CAD surface oil cover maps for the beginning and end of the winter study at high, moderate and low wave-energy sites in PWS are given respectively in Figures 1, 2 and 3.

The description of the degree of surface oil cover and the comparisons of data sets use the Equivalent Oiled Area (EOA) as the preferred index of oiling (Humphrey et al., 1990). The EOA value is obtained by integrating the observed percentage of oil cover with the total observed area (Owens et al., 1987). The value is representative of the actual surface area that is oiled, relative to the total observed area, rather than the total area that has oil to one degree or another. All surface oil cover values reported in this discussion are EOA values, except for the data in Figures 1 through 4 which are plots of the actual observed values. The percentage values given in parentheses in the captions to these figures and the surface oil cover data reported in Table 5 are the EOA expressed as a percentage of the total observed area.

The oil cover and elevation data were compiled using Lotus™ 1-2-3 software. Single and superimposed oil cover and elevation profiles were plotted from these files. Figure 4 presents examples of the oil cover and elevation changes at high, moderate and low wave-energy sites in PWS for the beginning and end of the winter study period.

Not all profile lengths were the same from one survey to another, due to differing water levels at the times of the measurements, and several techniques were used to

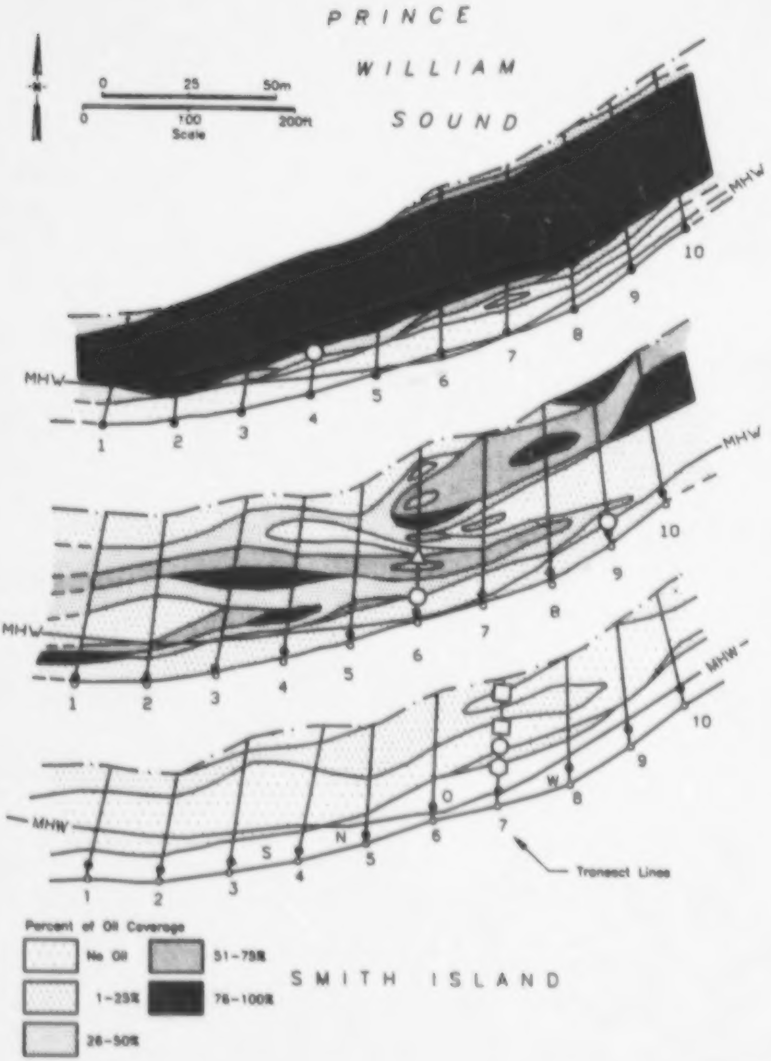

Figure 1 Surface Oil Cover Maps for Northeast Smith Island (AP-1), a high wave-energy location that was heavily oiled

top - 24 June 1989 (79 % oil cover)
middle - 16 September 1989 (28 %)
bottom - 9 March 1990 (1 %)

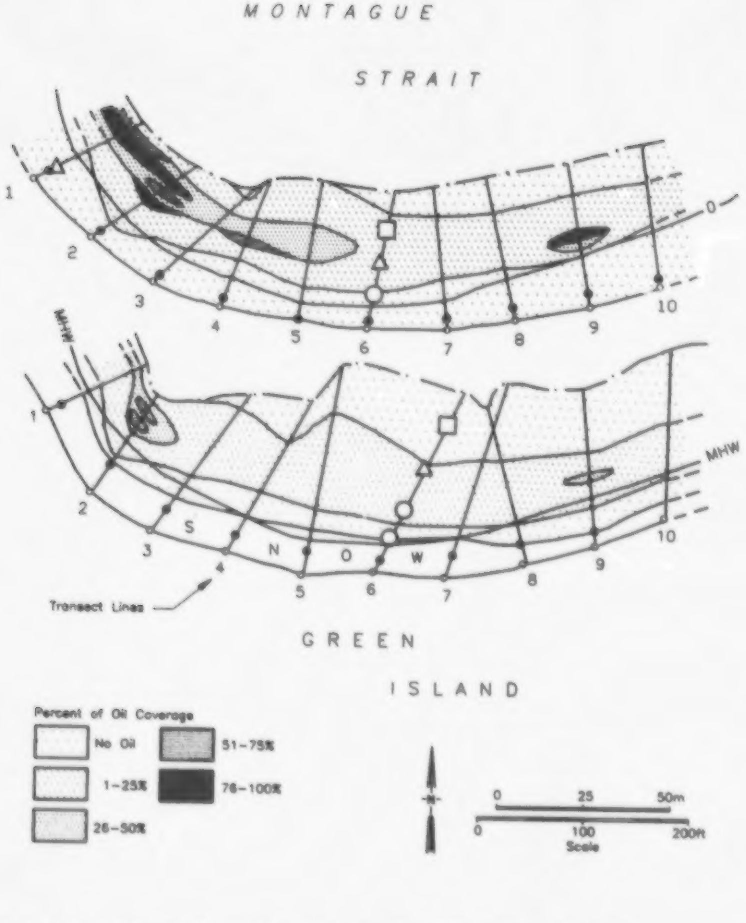

Figure 2 Surface Oil Cover Maps for Northeast Green Island (AP-7), a moderate wave-energy location that was moderately oiled
top - 20 September 1989 (11 %)
bottom - 6 March 1990 (4 %)

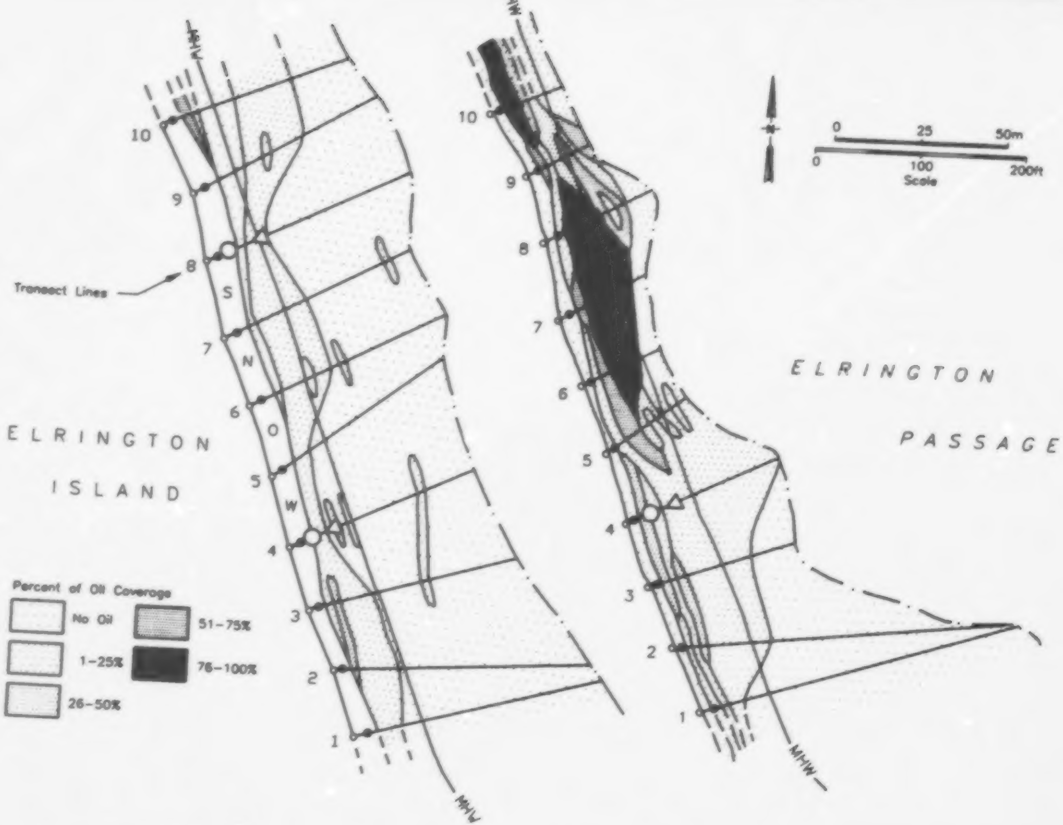

Figure 3 Surface Oil Cover Maps for South SW Elrington Island (AP-18), a low wave-energy location that was moderately oiled

right - 18 September 1989 (20 %)
left - 7 March 1990 (2 %)

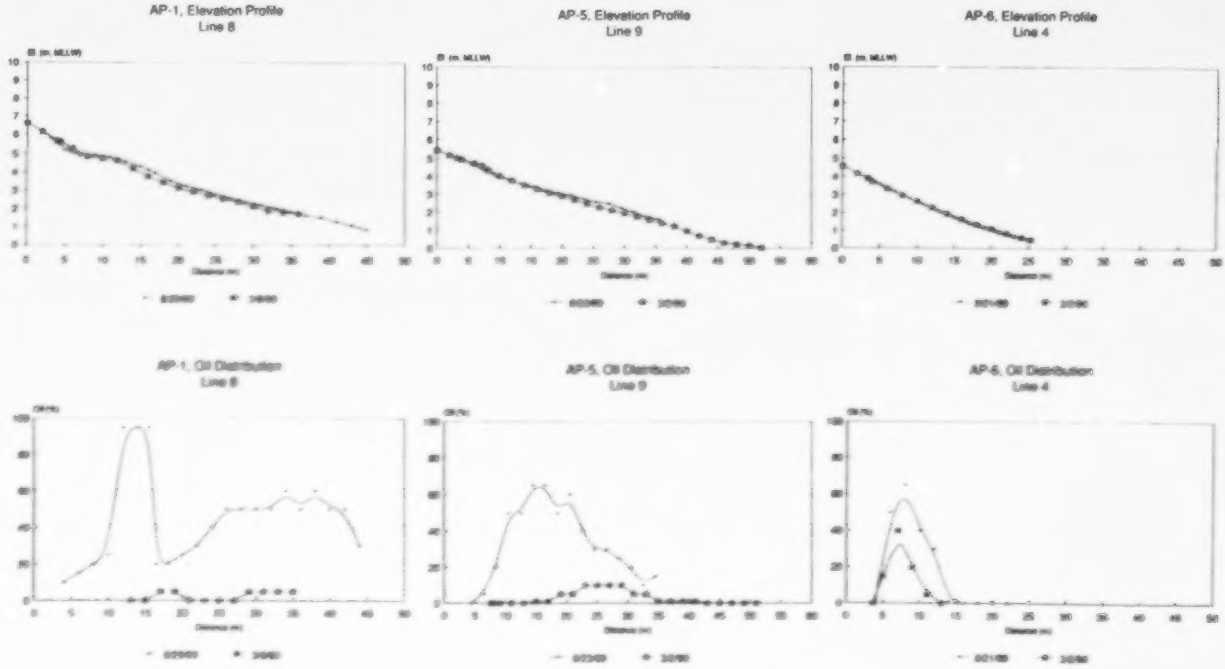

Figure 4 Examples of August 1989 and March 1990 Beach Elevation profiles (top) and Surface Oil Cover profiles (bottom) from

High (left; AP-1),
Moderate (center; AP-5) and
Low (right; AP-6) wave-energy sites

compare the profile data within and between sites. Profiles were subdivided according to cross-beach zones so that EOA data from a subdivision could be compared spatially or through time. These sections are termed "overlaps" when grouped for a single profile. A comparison of overlap profile and total profile EOA data combined from selected sites is given in Table 2a. As might be expected, this shows that total EOA values are almost always less than those for the overlaps. The difference between the two forms of data presentation becomes less through time as the degree of oiling decreases (Table 2b).

Another aspect that was evaluated concerned the variability of profile data within a study site. As the oil cover was non-uniform alongshore and across-beach, even over small areas (Figures 1, 2, and 3), it would be expected that one profile might not represent the overall oiling character of a beach. Table 3 presents the surface oil cover data from two surveys at AP-1, and illustrates the alongshore variability at this one study site. The observations at profile 6 on both of these occasions produced values 35 to 40% higher than the average surface oil cover for the site as a whole. Also, data from profile 7 showed an increase of nearly 50% between the two surveys, an increase that was observed also on two nearby profiles (9 and 10) at the eastern end of the study site. Data from the western half of the study beach showed a general decrease of surface oil (profiles 3, 4, and 5). The computed mean and standard deviation from that and additional data sets are summarized in Table 4. Similar variability occurs on all data sets that have been reviewed and point to the very limited value of single-line transects to record trends in the surface oil cover.

A summary of the surface oil cover data collected for the winter program and for the mid-summer (July-August) survey is given in Table 5, which also presents the all-site mean value for each monthly data set. GOA shores showed similar or even faster rates of reduction in surface oil cover.

TABLE 2 COMPARISON OF TOTAL SURFACE OIL COVER AND OVERLAP SURFACE OIL COVER (EOA values)

(a) Selected Data

SITE	MONTH	OVERLAP AREA EOA COVER (%)	TOTAL AREA EOA COVER (%)
AP-1	Oct	33	29
	Dec	16	14
AP-2	Sept	51	38
	Oct	71	54
	Dec	50	42
	Jan	24	22
AP-4	Oct	40	30
	Dec	37	33
	Jan	13	12
AP-12	Sept	78	58
	Oct	33	31
	Dec	33	31
	Jan	22	17
AP-16	Sept	17	12
	Oct	10	9
	Dec	11	10
	Jan	3	2
AP-18	Sept	37	20
	Oct	16	14
	Dec	12	8
	Jan	3	3

(b) Mean of Differences between Overlap and Total Cover - All Sites (%)

September	10
October	4
December	3
January	1.5

TABLE 3
SURFACE OIL COVER BY PROFILE FROM TWO SURVEYS AT SITE AP-1

(a) September

PROFILE LINE	OBSERVED INTERTIDAL AREA (m²)	EQUIVALENT OILED AREA (m²)	PER CENT COVER
1	190	66.6	35
2	200	49.5	25
3	110	33.8	31
4	110	32.0	29
5	110	39.5	36
6	120	45.5	38
7	140	43.5	31
8	140	42.5	30
9	130	20.5	16
10	110	12.3	11
Mean			28 %

(b) October

PROFILE LINE	OBSERVED INTERTIDAL AREA (m²)	EQUIVALENT OILED AREA (m²)	PER CENT COVER
1	70	22.6	32
2	90	28.6	32
3	100	17.8	18
4	100	22.0	22
5	100	27.6	28
6	120	49.6	41
7	180	82.1	46
8	200	32.1	16
9	140	34.0	24
10	120	40.5	34
Mean			29 %

TABLE 4
VARIABILITY OF SURFACE OIL COVER
(values used are EOA/TOA - %)

		MEAN %	StdDev %	DIST (m)
AP-1:	SEP	28	8.7	22-40
	OCT	29	9.7	14-40
	DEC	14	5.1	26-30
AP-12:	SEP	58	10	40-52
	OCT	34	22.5	28-44
	NOV	28	14.7	34-47
	DEC	29	19.8	36-46
	JAN	21	10	21-41
AP-13:	DEC	19	10.4	22-86

Mean % - The average percentage oil cover for all the lines on a given beach for that survey.
StdDev % - The standard deviation from the mean oil cover for all the lines on a beach.
Dist. - The length of the transect(s) surveyed.

TABLE 5
SUMMARY OF SURFACE OIL COVER (%) AT THE "A" STUDY SITES

(a) PWS

SITE	JUL/AUG	SEPT	OCT	NOV	DEC	JAN	MAR
AP- 1	44	28	29	15	14	-	1
2	72	38	54	-	42	22	-
3	23	26	-	0	-	-	-
4	34	29	30	-	33	12	6
5	30	-	11	-	8	-	2
6	13	12	8	-	-	8	5
7	8	11	11	-	-	4	4
8	41	40	24	24	-	14	9
9	58	-	-	-	-	-	-
10	39	37	24	-	-	19	-
11	61	48	17	-	-	-	1
12	70	58	31	28	31	17	7
13	70	-	38	7	23	0	10
14	24	24	-	-	12	4	3
15	44	-	-	-	-	-	7
16	25	12	9	-	10	2	1
17	16	15	12	-	3	2	-
18	32	20	14	-	8	3	2
Average PWS	39	27	22	(15)	18	9	4%
Total No. Transects	192	117	110	39	83	110	111

(b) GOA

SITE	JUL/AUG	SEPT	OCT	NOV	DEC	JAN	MAR
AH- 1	1	2	0	0	0	-	-
2	14	23	9	0	4	-	0
3	0	1	0	0	0	0	-
4	8	13	21	0	0	0	0
AK- 1	71	40	20	11	9	9	-
2	2	1	0	0	0	0	0
3	11	15	23	8	-	4	2
4	24	27	10	10	-	4	-
5	7	-	19	-	10	-	0
AS- 1	-	-	12	9	14	9	-
Average GOA	15	15	11	4	5	4	<1%
Total No. Transects	88	68	53	58	69	44	21

DISCUSSION OF PRELIMINARY RESULTS

The reduction and analysis of the large volume of data collected during this project is incomplete at the time of writing, nevertheless some preliminary trends and observations are evident.

The 1989 treatment program significantly reduced the volume of oil remaining on the shores of Prince William Sound and thereby accelerated the effectiveness of winter wave action to further remove stranded oil. Oil remains in greater concentrations at the few low or moderate wave-energy locations where no treatment occurred relative to comparable treated beaches.

It has been pointed out elsewhere (Humphrey et al., 1990 - these proceedings) that data collected on the length of oiled shoreline tends to overestimate the degree of oiling. At the time of writing sufficient data is available from the spring 1990 SSAT survey (Owens and Teal, 1990; these proceedings) in PWS to make a comparison with the same sections of coast that were surveyed in fall 1989. This comparison shows that the length of oiled shoreline in the surveyed sections was reduced from 457 to 274 km (Table 6), or respectively 62.5% and 38% of the shoreline surveyed. Systematic data sets from the long-term monitoring sites in PWS show that the average intertidal surface oil cover was reduced after cessation of the 1989 shoreline treatment program from 27% to 4% over the period September 1989 to March 1990 (Table 5a). The data shows that, although the length of oiled shoreline was reduced by almost half, by comparison the degree of oiling (expressed as surface area) changed more radically.

In the Gulf of Alaska the original distribution of oil on the shorelines was generally scattered and light, although with local concentrations, as individual slicks that had travelled from PWS were stranded. All of the study sites showed significant de-

TABLE 6
COMPARISON OF PWS FALL AND SPRING SHORELINE DATA
(for sections surveyed on both occasions) (km)

		October Ground Survey	Sprint SSAT Survey
OIL BAND WIDTH	Wide	63	14
	Moderate	55	35
	Narrow	98	48
	Very Light	241	177
	No Oil	273	455
	Total Oiled	457	274
	Total	730	729

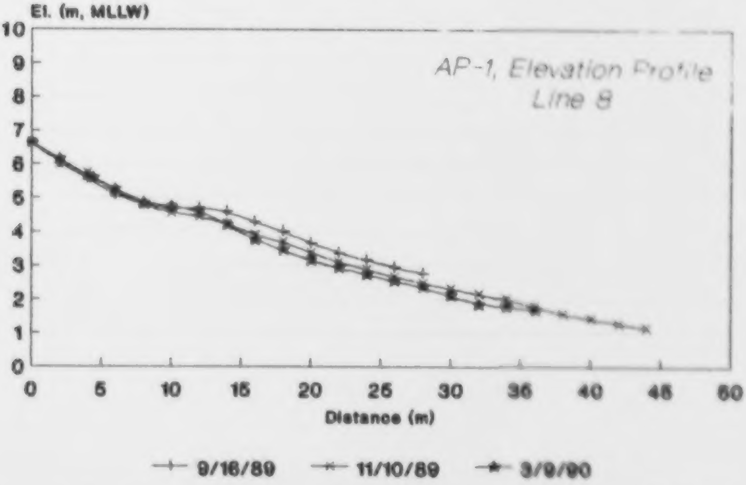

Figure 5 Beach Elevations changes along one profile at the high-energy Northeast Smith Island Study Site (AP-1); September 1989-March 1990

creases in surface oil cover, irrespective of shoreline wave-energy conditions, so that by early 1990 little surface oil remained (Table 5b).

There is no appreciable difference in rates of surface oil cover change on beaches in PWS and GOA categorized as having long-term high, moderate or low wave-energy levels. Changes were non-uniform in time and space depending upon very local wind directions (and therefore wave-energy levels at the shoreline) during periods of storm-wave activity. West- to northwest-facing beaches in PWS received lesser amounts of wave action than north- to southeast-facing beaches during the winter of 1989-90.

The majority of the oil that remains is observed predominantly as a coating or stain on coarse sediments, and is restricted largely to the upper sections of the intertidal zone. Where oil deposits occur, they are generally patchy and discontinuous. On some coarse sediment beaches, subsurface oil remains in the upper half of the intertidal zone; exceptions were noted on exposed coasts where reworking of oiled sediment by winter wave action occurred to depths of one meter or more. At profile 8 on AP-1, the heavily oiled intertidal zone had been eroded naturally to bedrock by the middle of November (Figure 5) resulting in the removal of all surface and subsurface oil. Subsurface oil depths were observed to be greater generally on higher energy beaches, partly because some of them were more heavily oiled but also presumably due to the coarse texture, better sorting, and the presence of larger and more open interstitial spaces on these coasts. On low and moderate energy beaches subsurface oil rarely exceeded 10-15 cm depths.

Widespread asphalt pavements appear not to have formed although scattered asphalt patches, usually less than a meter in diameter, have been observed on a few beaches.

It is believed that asphalt pavement or tar mat formation would have been much more widespread if removal of the mobile oil had not been carried out.

Data from total petroleum hydrocarbon (TPH) analyses shows large standard deviations. There is an evident bi-modal concentration of populations among samples, with low values for cleaned sediments and higher values from pavements or patches of oiled sediments. Values also tend to be higher from samples with finer sediments (sands and granules).

Evaluation of profile data indicates that surveys using only single profile lines may not accurately represent the total distribution of surface oil cover on a beach. This was particularly evident as the winter progressed and variability (or patchiness) became more common.

CONCLUSIONS

Considerable effort was required to obtain an appropriate information set that could be used to evaluate changes in shoreline oiling following the 1989 shoreline treatment program. The monitoring program was designed to collect accurate and representative data at regular intervals over the winter period with the primary purpose being to project, with a high degree of accuracy, the spring shoreline oil conditions for the 1990 operations program. This data base is also a valuable standard that can be applied to project rates of change for different spill scenarios.

ACKNOWLEDGMENTS

The Program Manager for this study was Andy Teal (Exxon USA) and the Project Manager was Ed Owens (Woodward-Clyde Consultants). The work was performed by WCC under contract to Exxon USA, who provided all air, vessel, and field logistic support.

The winter field data collection team members were:

> Sue Ban, Marty Cramer, Ken Critchlow, Mike Fawcett, Duncan Fitzgerald, John Harper, David Little, Dan Man, Graham MacDonald, Rich Marty, Debbie McCormick, Lindsay Nakashima, Doug Reimer, Jean-Marie Sempels, Sam Stoker, Bryan Trimm, Fred Wehrenberg, and Jerry Williams;

assisted by:

> Bill Barstow, William Ennis, Laurie Dilley, Cal Larson, William Reid, and Jim Renkert.

Data reduction and report preparation were carried out by:

> Ingrid Anderson, Holly Graham, Wade Guidry, David Little, Mike Lumpkin, Rich Marty, Melissa Nagan, John Putz, Marion Rideout, Doug Reimer, Doug Resnick, Amy Ritter, Kim Southam, Warren Stiles, Elliott Taylor, Bryan Trimm, Jerry Williams, and COMRIM.

The winter program would not have been as successful without the contribution of each and every one of these individuals, as well as the pilots, skippers, seamen, and mechanics who made the field work possible.

REFERENCES

Owens, E.H., Harper, J.R., Robson, W., and Boehm, P.D., 1987. Fate and Persistence of Crude Oil Stranded on a Sheltered Beach; Arctic, vol. 40, suppl., 1, 109-123.

Humphrey, B., Sergy, G.A., and Owens, E.H., 1990. Stranded Oil Persistence in Cold Climates; Proc. Thirteenth Arctic Marine Oil Spill Program (AMOP) Tech. Seminar, Edmonton, Alberta, June 6-8.

THE UNITED NATIONS "GESAMP" REVIEW OF IMPACT OF OIL ON THE MARINE ENVIRONMENT: CURRENT PROGRESS

by

Peter G. Wells
Environment Canada, Dartmouth, N.S.

GESAMP is the IMO/FAO/UNESCO/WMO/WHO/IAEA/UN/UNEP Joint Group of Experts on the Scientific Aspects of Marine Pollution. Oil is considered by UN member states to be a major marine pollutant, particularly in productive inshore waters. As a consequence, GESAMP is sponsoring the preparation of a synoptic review of the major new facts and principles pertaining to marine pollution by petroleum oils and individual hydrocarbons, used lubricating oils, chemicals used off-shore in oil exploration and exploitation, and oil-spill control agents, especially dispersants. This review is expeditiously updating the 1977 GESAMP report on oil for the UN agencies, concentrating on substantial new information on sources and inputs, chemical composition and physical properties, methods, fate, ecosystem effects, effects on human health and effects on man's use of the sea, for each of the four categories of "oil" and related compounds. Scientists from four countries (Canada, U.K., West Germany and the U.S.A.) comprise the review team. The paper describes the approaches taken to the review and some of the progress to date. A request is made for additional information useful to the review group's task. The final report is due in May 1991.

Note: Members of the Working Group are B. Ballantyne (USA), R. Blackman (UK), J.N. Butler (USA), M. Ehrhardt (FRG), R. Engelhardt (Canada), P. Howgate (UK), J. Payne (Canada), P.G. Wells (WG Chairman, Canada) and M. Nauke (IMO Technical Secretary, UK).

A STUDY OF THE UNDERWATER DISCHARGES OF CRUDE OIL AND GAS

by

R.J. Palczynski
School of Engineering, Acadia University
Wolfville, Nova Scotia, Canada

A potential major source of petroleum hydrocarbons released into the body of water is submarine blowout or failure (rupture) of an underwater pipeline which carries fresh crude oil under pressure from production wells to an oil terminal. In any such event, a large quantity of oil and natural gas is released at a certain depth in a relatively short period of time and slowly flows up to the water surface in the form of drops and bubbles. The discharge of oily, buoyant effluents into water bodies involves hydrodynamic relationships related to the dispersal and movement of one fluid in another. Increased complexity of the flow results in the sea from the substantial difference in fluid densities which cause the effluent to rise toward the surface of the water body.

In order to assess the influence of inertial, viscous, gravity, and surface tension forces on terminal velocity and trajectory of oily effluents, a series of laboratory experiments were conducted in which air and crude oil were simultaneously injected into a column of water at different depths, and measurements of the flow of bubbles and drops were taken. It was confirmed that the terminal velocity of the upward flow is proportional to the difference in specific gravity between oil and the surrounding water; currents cause oil to move in trajectories with a horizontal displacement proportional to the horizontal flow of water. Appropriate correlations concerning vertical motion of oil have been developed with the use of dimensional analysis which incorporates Reynolds, Strouhal, Eotvos, and Morton numbers. It has been revealed that internal circulation in the oil drops exists during motion in water with an attached wake. Two-phase (air-oil) bubbles usually separate upon release from the fluid outlet to form separate air bubbles and oil ellipsoidal drops. They rise towards the water surface with different velocities owing to the difference in density between air and oil and sea water. Bubbles and drops of intermediate size show two types of secondary motion: (i) rigid body type, e.g., rocking from side to side (wobbling motion), or following a zig-zag or spiral trajectory and (ii) shape dilations, usually referred to as oscillations. These two types of motion are often superimposed, so that the motion of intermediate size oil particles are particularly complex. Equations approximating this type of motion are proposed and graphs showing relationship between dimensionless numbers have been elaborated.

The Exxon Valdez Incident--One Year Later

by

R. H. Goodman
Esso Resources Canada Limited
Research and Technology Division
Calgary, Alberta
Canada

INTRODUCTION

The initial response to the grounding of the Exxon Valdez was reported at last years Arctic and Marine Oil Spill conference held in Calgary. That paper reviewed the recovery of oil from the water, and the initiation of the shoreline clean-up activities. This paper will give an overview of the clean-up activities during the summer months, and the design of the winter research and monitoring program.

Most of the oil on water containment and recovery activities had been completed by the end of May, and there was only a limited amount of additional oiling of the beaches occurring within Prince William Sound. One of the early activities in the response was planning for the shoreline clean-up which was to be initiated after most of the oil on water had been removed. The input to this planning process was data on the extent of shoreline oiling, its magnitude and the nature of the shoreline, combined with an assessment of the biological, cultural and economic resources of the site.

There are a number of papers at this conference on the shoreline evaluation methods developed by the SCAT (Shoreline Cleanup Assessment Teams) which discuss the methods developed and used in this process.

As a result of a detailed analysis of the winter climatic conditions in Prince William Sound, it became clear that clean-up activities on the scale of the summer operations would not be possible during the winter period. A winter program was developed which contained an extensive scientific program, combined with contingency plans and resources for responding in the event that oil slicks were observed in the region.

WINTER RESPONSE PROGRAM

There was in excess of 30,000 tons of equipment moved to Anchorage for storage after the completion of the summer program. This equipment was inventoried during the winter, and repaired or reconditioned in readiness for the spring. The winter response program consisted of a number of containerized response packages, situated at a variety of locations in the area including fish hatcheries and communities for immediate deployment should the need arise and the weather permit. The response activity was supported by four large vessels as well as a number of helicopters and fixed-wing aircraft. In order to ensure a high state of readiness, the emergency response teams routinely conduct drill and boom deployment tests.

WINTER SCIENCE PROGRAM

The logistical capabilities of the response system were also used to support a major scientific program and assisted in the collection of debris. The main purposes of the winter science studies were:

1. To determine the physical condition of the oil impacted shorelines.

2. To measure the level of hydrocarbons in the water and sediments.

3. To investigate the long term impact of the spill on the biological communities.

There are more than 450 people involved in the winter program. One of the main activities is a shoreline monitoring program at 36 predesignated sites in Prince William Sound and 38 sites in the Gulf of Alaska. These sites are a mixture of high and low energy beaches. The plan was to survey the beaches throughout the winter on a two week cycle, weather permitting. The survey teams took measurements and observations of surface oiling coverage, the depth of penetration of the oil, the beach erosion and deposition rate as well as macro-biological counts. This data is supported by extensive photographic records, as well as direct measurements. Both NOAA and ADEC (Alaska Department of Environmental Conservation) have similar programs in Prince William Sound and there is a data sharing agreement in place.

The survey data collected thus far indicated that there have been significant reductions in surface and subsurface oiling on shorelines exposed to winter storms and high wave energy. While the reduction is not uniform at all sites, the downward trend is clear. Reductions in oil concentrations at low energy sites is occurring, but at a lower rate. This data is consistant with the experience of other oil spills. On some beaches, isolated patches of asphalt have formed, especially in locations where there are fine glacial silt deposits.

Initial analysis of the water quality monitoring program shows that the hydrocarbon levels are in the parts per billion range, and that there is little difference between areas where the oil passed over and other areas. Since there is a significant circulation in the area the low levels of oil in the water column is to be expected and has been found in other spill monitoring programs.

HINDSIGHT OF THE SPILL

How does the spill of the Exxon Valdez compare with other spills that have occurred during the past two decades?

1.While the Valdez spill was the largest in the United States on a volume basis, it rates between 34th and 35th in international terms. The recent spill of the Kharg V was much larger than the Valdez spill, for example.

2.The percentage of oil removed using skimmers and booms was very high when compared to other large spills responses.

3. The occurrence and significance of a large number of archaeological sites in the spill area imposed another set of criteria on shoreline clean-up and oil removal activities.

4. The large area of the spill response activities and the associated logistic and communications problems were more significant than in many other spills.

5. The lack of adequate up to date maps for the area and the extensive shoreline change due to the 1964 earthquake presented some unique problems during the Valdez response.

6. The extensive length of shoreline impact due to the location of the spill and the local geography was greater than for the spills that occur in the open ocean.

7. The problems associated with permission to use in-situ burning and dispersants as response tools were more complex than in many other spills situations.

8. The magnitude of the response effort and its logistical support was much more

significant than in many other spills.

9. Each spill is different and requires its own technologies. During the Valdez spill, new shoreline treatment techniques ranging from hot water washing, chemical cleaning agents and bio-remediation methodology were developed and used successfully in some cases.

10. The lightering operation which removed 80% of the ships cargo in less than two weeks was an outstanding marine salvage activity.

11. The safety record of the Valdez response exceeded the injury levels for many other occupations, and was a significant achievement, especially considering the isolation of many of the operating sites.

As with most large spills, new technologies and understanding of the various options of responding to a spill situation have been developed. Many of these new methods are a direct result of the local peculiarities of the spill.

Remote Sensing--What do you really need?

R.H. Goodman
Esso Resources Canada Limited
Research and Technology Division
Calgary, Alberta
Canada

Abstract

This paper reviews the use of various remote sensing systems that were used during the Valdez response. The needs of the various clients are discussed, and the appropriate sensors and the associated data analysis is outlined. While most of the observations were made visually, an infrared/ultraviolet system was found to be useful in separating oil targets from other oceanographic and biological features.

No suitable system was found for the remote detection of oil on shorelines, nor for the identification of oiled kelp.

Introduction

One of the components of the response to the Exxon Valdez incident was the surveillance and tracking of the oil using a variety of remote sensing systems. These tasks were performed by both Exxon and NOAA using a variety of remote sensing systems including infrared, ultraviolet and radar imagery. The output of these systems was used to augment the visual mapping of the oil spill location and served to sort out oil from other visual targets. After most of the oil had been removed from the water, a number of remote sensing systems were used to measure oil on the shorelines and to detect the presence of oil on kelp. Each of these systems will be described.

The Need

During any large spill response, surveillance and tracking of the oil is a major support activity. There are a number of clients for this, each of whom has a different set of needs and expectations. These needs are summarized in Table 1.

Most of the needs shown in Table 1, with the exception of the trajectory work, are the direct products of surveillance and remote sensing flights. The data on the spill that is needed requires the measurement of several parameters. These include:

1. Location of the oil slick and a definition of its leading edge and spatial extremity. This is best presented on a map.

2. Total volume of oil on water and on shorelines, as well as the same data at a large number of sites.

3. Chemical composition of oil and its physical properties.

4. The volume and composition of oil in the water column.

TABLE I

Clients Needs

User or Client	Data Needed	Timing	Documentation
On-Scene Commander	Maps of Oil Location	Hours	Briefing Notes and Maps
	Oil Volumes	Hours	Tables and Maps
	Impacts	Daily	Maps and Text
	Mass Balance	Daily	Charts and Tables
	Trajectory	Twice Daily	Maps of Predicted Oil Motion
Operations	Maps of Oil Location and Volumes	Minutes to Hours	Briefing Notes and Maps
	Oil Properties	Twice Daily	Tables of Physical and Chemical Properties of Oil
	Trajectory	Twice Daily	Maps of Predicted Oil Motion
Long Range Planning	Shoreline Impact	Several Days	Maps and Tables
	Shoreline Oiling	Several Days	Maps and Text
	Shoreline Types	Several Days	Maps, Charts and Text
	Long Term Trajectory	Twice Weekly	Maps of Predicted Oil Motion
Public Affairs	Maps of Oil Location	Hours	Oil Position in a Simple Format
	Mass Balance	Daily	Simple Charts and Tables
	Trajectory	Daily	Simple Maps of Oil Motion
	Photographs	Hours	High Quality Photographs
Head Office	Maps of Oil Location	Daily	Maps of Oil Motion
	Mass Balance	Daily	Charts and Tables
	Trajectory	Daily	Maps of Predicted Oil Motion
	Photographs	Hours	High Quality Photographs
Historian or Archivist	Maps of Oil Location	Weekly	Oil Position on a Daily Basis
	Photographs	As Taken	High Quality Photographs
	Reports	Weekly	Text and Graphic Records

IR/UV system

The use of a combination of infrared and ultraviolet sensors to detect oil-on-water has been developed over the past few years, and was extensively used during the first two months on the Exxon Valdez response. The system used consists of an infrared camera operating in the 8-14 micron band, and a UV sensor operating in the near ultraviolet. The details of this system have been described by Goodman[1]. Two systems were used during the Valdez incident, as shown in Table 2.

TABLE 2

IR/UV Remote Sensing systems used during Valdez Response

Parameter	System 1	System 2
IR Camera	Barr and Stroud IR18	Barr and Stroud IR18
IR Lens	None	Wide Angle
High Pressure Air Source	QK-5 Electric Pump	Air Bottles
UV Camera	Cohu	None
UV Filter	HPMB	None
Aircraft	Piper Aztec Twin Otter	Twin Otter
Time Period	March 26 to May 15	April 4 to May 24

Both systems operated from the aircraft power supply, and used a standard television monitor and half-inch VHS video recorders. An attempt was made to integrate the navigational systems with the recorders but this was not found to be very reliable and was therefore not extensively used.

The mission profile for these sensors involved three flights a day, each of which performed a specific task. During the early days of the spill, the weather was clear and did not interfere with flying operations. The first flight of the day took off at dawn, and arrived over the observational area when the sun was a few degrees above the horizon. The "dawn patrol" concentrated on determining the location of the leading edge of the slick and changes in its position from day to day. This information was used in operational planning of the oil-on-water response efforts, and the results of these flights were used for the morning operational briefing. The second flight occurred at mid-day and was generally used to investigate reports of oil slicks in regions where oil had not been previously reported. In many cases these sightings were other floating material, such as plankton blooms, fresh water outflows and other oceanographic phenomena. The remote sensing equipment was very useful in identifying such "false" targets since it can uniquely distinguish the presence of hydrocarbons on the water surface. The third flight in the evening was used to determine the slick motion during the day, and to confirm reports from field observers and clean-up operations.

The data was recorded manually in the aircraft on composite maps of Prince William Sound. These maps were used for the briefing and then passed on to the NOAA group for entering into a computer system, which was used to produce maps for all interested parties.

As the spill area became larger, a second aircraft was moved along the Alaska coast to Seward and afterwards to Kodiak and Homer. The survey data from these sites was sent by FAX to Valdez, where it was integrated into the days surveillance reports. Active intensive airborne surveillance was continued until late May in Prince William Sound, and continued for another month in the Kodiak and Homer area.

The IR/UV system worked well. It was simple to use, and operators generally required only two days to become familiar with the system, its operation and the interpretation of the data. The system was reliable and apart from a few problems with cables, no failures were experienced in the electrical components. The compressor used to fill the air-bottles of system two was sometimes recalcitrant, and required occasional servicing.

One of the problems with the aircraft based observation systems for large area surveillance is the limited area that can be covered, which makes the production of a synoptic overview impossible. The dynamics of the slick have a shorter time period than the flight time required to produce a survey of the area.

Visual observations were used where possible, since a large area could be covered rapidly and comprehensively. The IR/UV system was the principal remote sensing system used by Exxon during this incident, and was used to augment the visual observations and provide positive identification of surface features.

Radar

The US Coast Guard operated a Desault Falcon with a side looking radar during the early period of the spill. The radar has the unique capability of all the sensors used of being able to penetrate cloud cover, and can survey large areas in a single flight. There were a number of unique oceanographic characteristics in Prince William Sound which resulted in a number of features which have radar signatures similar to the oil. These include fresh water overflows during the melt season, icebergs, wind shadowing on the lee side of cliffs as well as a number of biological sources such as plankton and algae blooms and kelp mats. Due to the variety of the targets, the radar was not useful in providing a unique identification of the location of oil spills. After a time, the slick formed into discontinuous windrows. Due to the spatial resolution of the radar, this discontinuous coverage could not be differentiated and thus the impression from the radar images was a more extensive pattern of oiling than was observed visually and using the IR/UV sensors.

The radar system has the advantage of being weather independent, but in Prince William Sound there were so many extraneous sources of damping of the capillary waves that the radar images were difficult of interpret. This would not be the case in an open offshore environment, and the radar would be much more useful under these conditions.

Satellite Imagery

There are a number of satellites that are routinely used to observe of a variety of earth features, and it would seem appropriate to use this capability to follow the oil spill. Many of the satellites have very discontinuous coverage of a given area, and thus they are not useful in providing tactical support for a spill response. An image was obtained on April 7, 1989 of Prince William Sound and this image was processed to enhance the observation of the oil slick. The initial attempt was not very successful, as the algorithms used were inadequate to uniquely define the existence of oil. The processing showed many areas where oil was known to exist, but also indicated the presence of oil in areas far removed from the spill and at large distances from the ocean shore. Further processing and algorithm development resulted in a dramatic improvement in the selection of oil areas, and produced a suitable map.

The advantage of satellite based imagery is its synoptic nature. However, there are a number of problems associated with the logistics of obtaining satellite images, and subsequently processing these into an oil location map. For tactical purposes, a turn-around time of a few hours is required. It is not clear that with existing downlink systems, communication capabilities and processing algorithms that this objective can be achieved in the required time scale. Some additional effort should probably be undertaken to identify the bottlenecks of the use of satellite imagery for detecting oil spills.

MEIS

The MEIS system is a multi-channel imaging system which uses narrow band filters to allow the discrimination between various features. As the result of a number of years of research, a set of suitable filters for the detection of oil had been developed and these were used for the Valdez surveys. The MEIS was mounted in a Desault Falcon, and two missions were undertaken in 1989. The first mission in April involved the rapid mapping of oil on the water. This was successful, but the MEIS as configured did not have a real time processing capability, and hence the images were not tactically useful.

The second mission of the MEIS was to detect oil on shorelines. The same filter set was used, and in order to achieve an adequate resolution, low flight altitudes had to be used. This resulted in an increased volume of data. There had been little experience in this area, and no proven and well developed algorithms were available for the analysis of this data. This required a significant amount of manual assistance in the processing. The large volumes of data combined with the need for manual assistance in processing resulted in long delays between the collection of the data and the production of the shore oiling maps.

A correlation of MEIS data with shoreline oiling information obtained from skilled observers was poor. There did not seem to be any trends of differences with respect to beach type, to degree of oiling or to illumination level. The MEIS data tended to miss oil on the shoreline, and thus could not be relied upon as a methodology for evaluating shoreline oiling. This is true of both the early and late missions of the aircraft.

Attempts to use the MEIS for the detection of isolated tar-balls and light shoreline oiling was equally unsuccessful.

The use of the visual range MEIS system in Prince William Sound was complicated by the nature of most of the shoreline which generally consists of dark materials. This resulted in a limited contrast between oiled and non-oiled beaches. The lack of a suitable, rapid image processing system meant that the data could not be used in a tactical sense, and the reliability of the data was not sufficiently high that it could be used for planning purposes.

CASI

The CASI system is a recently developed narrow band visual imaging system which uses a CCD detector and a grating spectro-graph. This system has similar capabilities to the MEIS, but was much more compact and could be mounted in a much smaller aircraft. The spectral bands could be readily changed, based on data obtained from real-time reflection spectra. The data was recorded on a video tape, and then analyzed using a ground based processing system. This processor was not available in Valdez due to shipping problems, and a substitute system was used. Some parts of the airborne system had to be used in the ground based system, and hence the collection of data and its analysis could not occur concurrently.

The CASI system was used for two different functions: the detection of oil on shorelines and the detection of the presence of oiled kelp. The CASI unit was mounted in a Cessna Skyknight, and flown over extensive lengths of shoreline and areas of oiled kelp. The shoreline areas had been previously surveyed by SCAT teams and the degree of oiling was well known. For the kelp beds, surface observations from ships and amphibious aircraft were used to verify the degree of oiling of the kelp.

The CASI system was successful in the detection of oil on water, but not successful in identifying oil on shorelines, or the presence of oil in kelp at sufficiently low levels to be used in identifying areas which could be opened to fishing. The oiled shoreline identification was frustrated by the character of the shoreline in Prince William Sound for the same reasons as the MEIS system was unsuccessful. The spectra of oiled kelp and non-oiled kelp was highly variable and seemed to depend strongly on the age and state of decay of the kelp. Since a wide range of kelp ages was present, this variation masked any effects of the presence of oil.

Near IR system

A near IR system, operating in the 2.5-3.5 micron range, was used to determine the existence of oil on the kelp. In this range, chlorophyll is strongly emissive and oil is absorptive. The theory behind this approach was that the kelp would generate a strong signal in the near IR and if oil was present at the surface, it would absorb the signal and the kelp would appear dark in this region of the spectral band.

As with the CASI system, the varying ages of the kelp and hence the variability of chlorophyll concentrations was greater than the differences between oiled and unoiled material. The oil on the kelp was present as a discontinuous film whose spatial variability was less than the resolution of the camera. This resulted in an average effect that further reduced the contrast between the oiled and unoiled kelp. The use of Near IR systems does not seem to have much potential in the detection of oil on vegetation.

Conclusions

What do you really need to conduct an adequate surveillance and tracking of a large oil spill? The answer to this question can be best derived from an examination of the clients needs.

The most important surveillance tool is an adequate number of skilled observers who have seen oil on the water, and have adequate experience to determine whether various features on the ocean surface or shoreline are oil or not. This would eliminate the reporting of cloud shadows, bottom features, biological entities and other features as oil, and hence reduce or eliminate the search and identification of false targets. In order to undertake an adequate surveillance program, two or three observers are needed to fly the surveillance flights and two briefer-interpreters are needed at the command centre to present the data, run the trajectory models and prepare maps. Skilled observers meet many of the needs of a surveillance and tracking activity.

In order to provide an estimate of oil thickness and hence volumes, an IR camera system should be used in conjunction with the visual observations. This sensor will allow for the determination of the location of thick oil patches, and provide useful ancillary information to the On-Scene Commander and Operations functions.

The use of a sensor operating in the ultra-violet will provide positive identification of the presence of hydrocarbons on the surface and will allow the elimination of false targets including features due to vegetation mats, plankton blooms and fresh water outflows.

With available technology, this is all you need. At the present time there is no reliable method of measuring oil thickness from the air and thus determining oil volumes from the air. There are a number of programs being undertaken to develop such technologies.

The most promising of these is a laser-acoustic method. In order to determine the physical and chemical characteristics of the oil, a laser-fluorosensor can be used. While there has been some development of these systems, no commercial unit is available and the research systems have been dismantled. A new laser-fluorosensor is being developed that will meet this need.

The observation and detection of oil on the water is an established response activity, and when trained observers and IR/UV equipment is available it becomes a routine operation. The detection of oil on shorelines and the characterization of shoreline using remote sensing is very much more difficult and no suitable system exists to undertake this function. The laser-fluorosensor and laser-acoustics systems have potential in this area, but their use and limitations for the detection of oil on shorelines is not well understood at this time.

Systems which allow the surveillance of oil, either on the shoreline or on water during periods of low lying cloud cover or darkness are limited in number. It is well known that radar can penetrate clouds and works in the dark, but there are problems in image interpretation and there are generally a number of false targets in a radar image, especially in the critical area near shore. The active laser-based sensors and IR detectors will work in darkness, but not cloud cover. At present there is no sensing package that has all weather capability that is useful for tactical support of an oil spill response.

References

1. Goodman, R.H." Application of the Technology in North America" in The Remote Sensing of Oil Slicks A.E. Lodge, Ed., John Wiley and Sons, Chichester, England, p39-65, 1989